ADVANCES IN SPINAL CORD EPIDURAL STIMULATION FOR MOTOR AND AUTONOMIC FUNCTIONS RECOVERY AFTER SEVERE SPINAL CORD INJURY

EDITED BY: Enrico Rejc, Ronaldo M. Ichiyama and Claudia A. Angeli
PUBLISHED IN: Frontiers in Systems Neuroscience and
Frontiers in Neuroscience

frontiers Research Topics

frontiers

ISSN 1664-8714
ISBN 978-2-88974-391-9
DOI 10.3389/978-2-88974-391-9

About Frontiers

Frontiers is more than just an open-access publisher of scholarly articles: it is a pioneering approach to the world of academia, radically improving the way scholarly research is managed. The grand vision of Frontiers is a world where all people have an equal opportunity to seek, share and generate knowledge. Frontiers provides immediate and permanent online open access to all its publications, but this alone is not enough to realize our grand goals.

Frontiers Journal Series

The Frontiers Journal Series is a multi-tier and interdisciplinary set of open-access, online journals, promising a paradigm shift from the current review, selection and dissemination processes in academic publishing. All Frontiers journals are driven by researchers for researchers; therefore, they constitute a service to the scholarly community. At the same time, the Frontiers Journal Series operates on a revolutionary invention, the tiered publishing system, initially addressing specific communities of scholars, and gradually climbing up to broader public understanding, thus serving the interests of the lay society, too.

Dedication to Quality

Each Frontiers article is a landmark of the highest quality, thanks to genuinely collaborative interactions between authors and review editors, who include some of the world's best academicians. Research must be certified by peers before entering a stream of knowledge that may eventually reach the public - and shape society; therefore, Frontiers only applies the most rigorous and unbiased reviews.
Frontiers revolutionizes research publishing by freely delivering the most outstanding research, evaluated with no bias from both the academic and social point of view. By applying the most advanced information technologies, Frontiers is catapulting scholarly publishing into a new generation.

What are Frontiers Research Topics?

Frontiers Research Topics are very popular trademarks of the Frontiers Journals Series: they are collections of at least ten articles, all centered on a particular subject. With their unique mix of varied contributions from Original Research to Review Articles, Frontiers Research Topics unify the most influential researchers, the latest key findings and historical advances in a hot research area! Find out more on how to host your own Frontiers Research Topic or contribute to one as an author by contacting the Frontiers Editorial Office: frontiersin.org/about/contact

ADVANCES IN SPINAL CORD EPIDURAL STIMULATION FOR MOTOR AND AUTONOMIC FUNCTIONS RECOVERY AFTER SEVERE SPINAL CORD INJURY

Topic Editors:
Enrico Rejc, University of Louisville, United States
Ronaldo M. Ichiyama, University of Leeds, United Kingdom
Claudia A. Angeli, University of Louisville, United States

Citation: Rejc, E., Ichiyama, R. M., Angeli, C. A., eds. (2022). Advances in Spinal Cord Epidural Stimulation for Motor and Autonomic Functions Recovery After Severe Spinal Cord Injury. Lausanne: Frontiers Media SA.
doi: 10.3389/978-2-88974-391-9

Table of Contents

frontiers in Systems Neuroscience

EDITORIAL
published: 06 January 2022
doi: 10.3389/fnsys.2021.820913

Editorial: Advances in Spinal Cord Epidural Stimulation for Motor and Autonomic Functions Recovery After Severe Spinal Cord Injury

Enrico Rejc[1,2]*, *Claudia A. Angeli*[1,3,4] *and Ronaldo M. Ichiyama*[5]

[1] Kentucky Spinal Cord Injury Research Center, University of Louisville, Louisville, KY, United States, [2] Department of Neurological Surgery, University of Louisville, Louisville, KY, United States, [3] Frazier Rehabilitation Institute, University of Louisville Health, Louisville, KY, United States, [4] Department of Bioengineering, University of Louisville, Louisville, KY, United States, [5] Faculty of Biological Sciences, School of Biomedical Sciences, University of Leeds, Leeds, United Kingdom

Keywords: spinal cord injury, motor function, autonomic function, bladder, locomotion, voluntary movement, cardiovascular, recovery

Editorial on the Research Topic

Advances in Spinal Cord Epidural Stimulation for Motor and Autonomic Functions Recovery After Severe Spinal Cord Injury

INTRODUCTION

Spinal cord injury (SCI) disrupts the communication within the nervous system, leading to loss of sensorimotor function caudal to the level of injury and loss of autonomic function. Individuals with more complete and chronic injuries have poor prognosis for neurological and functional recovery, and suffer from a significant decrease in quality of life. To date, standard of care for individuals with chronic, severe SCI is primarily focused on implementing compensatory strategies and managing SCI-related health complications. However, in the last decade, clinical studies implementing epidural electrical stimulation of the lumbosacral spinal cord (scES) in individuals with complete paralysis from SCI resulted in the unprecedented proof of principle that recovery of motor function, even at a chronic stage, is potentially available (Harkema et al., 2011; Angeli et al., 2014, 2018; Rejc et al., 2015; Gill et al., 2018; Wagner et al., 2018). More recent evidence also suggested that scES has the potential to regulate autonomic functions in this population (Harkema et al., 2018; Herrity et al., 2018; Squair et al., 2021). While these scientific findings have brought hope for recovery of lost functions to millions of individuals worldwide living with a SCI, further efforts are needed to achieve an effective clinical translation of this spinal cord stimulation technology.

The present Research Topic includes original human- and rat-model studies and a "hypothesis and theory" article focused on the mechanisms underlying spinal cord electrical stimulation and its positive multi-system effects targeting motor, bladder, cardiovascular, and immune functions. Of the 18 manuscripts that were initially submitted, 13 were accepted for publication. A total of 89 authors contributed to this Research Topic, the content of which has been viewed over 80,000 times since its launch in August 2019. When considering these numbers, themes and

OPEN ACCESS

Edited and reviewed by:
Olivia Gosseries, University of Liège, Belgium

***Correspondence:**
Enrico Rejc
enrico.rejc@louisville.edu

Received: *23 November 2021*
Accepted: *15 December 2021*
Published: *06 January 2022*

Citation:
Rejc E, Angeli CA and Ichiyama RM (2022) Editorial: Advances in Spinal Cord Epidural Stimulation for Motor and Autonomic Functions Recovery After Severe Spinal Cord Injury. Front. Syst. Neurosci. 15:820913. doi: 10.3389/fnsys.2021.820913

content of the manuscripts included in the present Research Topic, we believe that it can provide important perspectives to the field of spinal cord neuromodulation in SCI. So, we would like to thank our authors, referees, and above all our readers for having supported this project. The Topic contributions are summarized below in two thematic areas: (i) motor function and (ii) autonomic function.

MOTOR FUNCTION

To date, the prevailing view is that scES enhances motor function recovery after SCI by recruiting large dorsal root myelinated fibers associated with somatosensory information, and particularly proprioceptive information (Moraud et al., 2016), at their entry into the spinal cord as well as along the longitudinal portions of the fiber trajectories (Rattay et al., 2000; Capogrosso et al., 2013). This conceivably leads to altering the excitability of spinal circuits involved in motor patterns generation to a level that can enable sensory information and residual supraspinal inputs to become sources of motor control (Rejc and Angeli, 2019).

Militskova et al. proposed a structured approach that combines electrophysiological techniques with positional changes and participant-driven reinforcement maneuvers to assess the neurophysiological profile of individuals with clinically motor complete SCI, as well as the influence of weight bearing-related sensory information and supraspinal inputs on the excitability of the spinal circuitry caudal to the level of injury. This approach can be helpful to characterize the neurophysiological completeness of SCI, contributing to research participants' selection for upcoming scES clinical trials, and may also be implemented to assess the effects of activity-based training on neurophysiological profile. Gill M.L. et al. were also interested in investigating the effects of modulating afferent and supraspinal inputs on motor output in two individuals with motor complete SCI receiving scES. In particular, they demonstrated that the level of body weight support and the participant's intent to step on a treadmill modulated the stepping pattern facilitated by scES. In particular, lower body weight support (20% body weight) and the intent to step improved stepping independence and decreased clinician assistance. This research group (Gill M. et al.) also reported that scES improved aspects of sitting reaching performance in the same two SCI research participants, which is relevant to enhance the independent performance of activities of daily living. scES improved the forward reaching distance, while it had negligible effect on the lateral reach distances. Also, reach distances were larger when individuals were assessed from their wheelchair compared to sitting on a mat, emphasizing the importance of pelvic stabilization provided by the wheelchair cushion.

The recovery of volitional lower limb motor control promoted by scES in individuals with clinically motor complete SCI entails that residual supraspinal connectivity to the lumbosacral spinal circuitry still persists in these individuals. Rejc et al. aimed at exploring further the mechanisms underlying scES-promoted recovery of volitional lower limb motor control by investigating neuroimaging markers at the spinal cord lesion site via magnetic resonance imaging. Amount and location of spared spinal cord tissue at the lesion site were not related to the ability to generate volitional leg movements prior to any training with scES. On the other hand, spared tissue of specific cord regions significantly and importantly correlated with inhibitory and coordination aspects of motor control. Peña Pino et al. presented evidence for recovery of volitional lower limb movement in the absence of spinal stimulation following long-term application of scES. In particular, four out of seven participants with a chronic, clinically motor complete SCI developed the ability to voluntarily move their lower extremities without stimulation. Interestingly, the sub-group that was successful in generating movement without stimulation presented higher spasticity scores prior to the beginning of scES. This may suggest that the volitional movements generated with scES over a long period of time could result in motor re-learning that takes advantage of spasticity by modulating it to achieve the targeted motor outcomes. Spasticity is also often present in individuals with cerebral palsy, largely reflecting a functionally abnormal spinal-supraspinal connectivity. Edgerton et al. proposed a model of spinal cord stimulation in cerebral palsy, hypothesizing that spinal neuromodulation in combination with proprioceptive-activity based training can transform the dysfunctional spinal-supraspinal connections improving function.

Another area covered in this Research Topic is related to novel strategies aimed at optimizing neuromodulation outcomes. Taccola et al. explored the combination of scES and pharmacological interventions targeting adenosine A1 receptors as precursors to engage the sensorimotor networks and promote restoration of function in rats following chronic severe SCI. The different effects promoted by this combinatorial treatment in intact and injured animals support dedicated follow-up studies. Finally, Shkorbatova et al. presented a comparison of spinal stimulation methods that may be alternative to scES. In particular, a novel model of transvertebral stimulation was compared to transcutaneous spinal cord stimulation in rats, studying the muscle activation selectivity associated with these two neuromodulation approaches. Transvertebral stimulation had similar effects on the spinal sensorimotor networks compared to transcutaneous stimulation, and could be a viable neuromodulation strategy to be investigated in the future.

AUTONOMIC FUNCTION

Evidence to date suggests that spinal cord stimulation can target and regulate neural networks controlling multiple organ systems. Kreydin et al. evaluated the long-term effects of transcutaneous stimulation focused on bladder function in individuals with SCI, stroke, and multiple sclerosis. After the spinal cord stimulation period, positive outcomes including decreased detrusor overactivity, improved continence, and enhanced bladder sensation were found across the different subgroups. On the other hand, no changes in voiding efficiency were observed after the intervention when spinal stimulation was not applied. Herrity et al. provided evidence for improvements in bladder

function following motor- and/or cardiovascular-specific scES and activity-based training in individuals with chronic, motor complete SCI. Bladder capacity without stimulation improved post-intervention, and this adaptation was retained at the 1-year follow-up. Detrusor pressure and bladder compliance also improved following intervention, but returned to baseline levels at follow-up. Although showing successful bladder outcomes, activity-based interventions with scES did not attenuate the increases in systolic blood pressure as a result of bladder distention; this suggests the need of bladder-specific scES parameters that also include a component for blood pressure modulation. To this end, Sysoev et al. evaluated the effects of scES sites on detrusor and external sphincter muscles following a thoracic (T)8 lateral hemisection in a rat model. Results indicated that the activation of the detrusor and external sphincter were optimal at different stimulation sites, supporting the need for specific stimulation configurations to address bladder dysfunction following SCI.

The effects of scES on other organ systems were assessed in pilot human studies. Legg Ditterline et al. evaluated the cardiac structure and function adaptations following multiple scES interventions. Aortic root, left atrial and ventricular chamber dimensions and mass were all increased following scES interventions. These structural changes accompanied improved blood pressure regulation following scES interventions, and have implications for improved quality of life as well as reduction in cardiovascular morbidity. Finally, Bloom et al. evaluated the immune responses to long-term scES targeted to improve cardiovascular function. In a case study involving a chronic, cervical motor complete SCI individual, changes in whole-blood gene expression following the scES intervention suggested an improved immune system function. Inflammatory pathways were downregulated while adaptive immune pathways were upregulated. These findings provide additional evidence for holistic improvements associated with prolonged use of scES that might affect quality of life and reduce the burden of SCI in the affected individuals.

In conclusion, spinal cord neuromodulation in the form of epidural and transcutaneous electrical stimulation can provide a wide range of multi-system benefits for individuals with severe SCI and other neurological disorders. The exciting novel advances supporting recovery of motor, cardiovascular, and bladder functions by spinal cord electrical neuromodulation can provide real-world benefits to individuals that suffer from SCI. In the near future, parallel efforts by the scientific and clinical community to translate spinal cord electrical stimulation approaches to larger clinical trials, and to further improve their efficacy (i.e., by improved stimulation technology and/or combinatorial treatments) are warranted.

AUTHOR CONTRIBUTIONS

ER and CA wrote the first draft of the manuscript. All authors contributed to the conception of the manuscript, revised the manuscript, and approved its final version.

FUNDING

ER and CA were supported by Christopher & Dana Reeve Foundation, Kessler Foundation, the Leona M. and Harry B. Helmsley Charitable Trust, and Craig H. Nielsen Foundation. RI was supported by the International Spinal Research Trust (NMN007 and BBS003), and by Brain Research UK (WMCR P73576).

REFERENCES

Angeli, C. A., Boakye, M., Morton, R. A., Vogt, J., Benton, K., Chen, Y., et al. (2018). Recovery of over-ground walking after chronic motor complete spinal cord injury. *N. Engl. J. Med.* 379, 1244–1250. doi: 10.1056/NEJMoa1803588

Angeli, C. A., Edgerton, V. R., Gerasimenko, Y. P., and Harkema, S. J. (2014). Altering spinal cord excitability enables voluntary movements after chronic complete paralysis in humans. *Brain* 137(Pt 5), 1394–1409. doi: 10.1093/brain/awu038

Capogrosso, M., Wenger, N., Raspopovic, S., Musienko, P., Beauparlant, J., Bassi, L. L., et al. (2013). A computational model for epidural electrical stimulation of spinal sensorimotor circuits. *J. Neurosci.* 33, 19326–19340. doi: 10.1523/JNEUROSCI.1688-13.2013

Gill, M. L., Grahn, P. J., Calvert, J. S., Linde, M. B., Lavrov, I. A., Strommen, J. A., et al. (2018). Neuromodulation of lumbosacral spinal networks enables independent stepping after complete paraplegia. *Nat. Med.* 24, 1677–1682. doi: 10.1038/s41591-018-0175-7

Harkema, S., Gerasimenko, Y., Hodes, J., Burdick, J., Angeli, C., Chen, Y., et al. (2011). Effect of epidural stimulation of the lumbosacral spinal cord on voluntary movement, standing, and assisted stepping after motor complete paraplegia: a case study. *Lancet* 377, 1938–1947. doi: 10.1016/s0140-6736(11)60547-3

Harkema, S. J., Legg Ditterline, B., Wang, S., Aslan, S., Angeli, C. A., Ovechkin, A., et al. (2018). Epidural spinal cord stimulation training and sustained recovery of cardiovascular function in individuals with chronic cervical spinal cord injury. *JAMA Neurol.* 75, 1569–1571. doi: 10.1001/jamaneurol.2018.2617

Herrity, A., Williams, C., Angeli, C., Harkema, S., and Hubscher, C. (2018). Lumbosacral spinal cord epidural stimulation improves voiding function after human spinal cord injury. *Sci. Rep.* 8:8688. doi: 10.1038/s41598-018-26602-2

Moraud, E. M., Capogrosso, M., Formento, E., Wenger, N., DiGiovanna, J., Courtine, G., et al. (2016). Mechanisms underlying the neuromodulation of spinal circuits for correcting gait and balance deficits after spinal cord injury. *Neuron* 89, 814–828. doi: 10.1016/j.neuron.2016.01.009

Rattay, F., Minassian, K., and Dimitrijevic, M. R. (2000). Epidural electrical stimulation of posterior structures of the human lumbosacral cord: 2. Quantitative analysis by computer modeling. *Spinal Cord* 38, 473–489. doi: 10.1038/sj.sc.3101039

Rejc, E., Angeli, C., and Harkema, S. (2015). Effects of lumbosacral spinal cord epidural stimulation for standing after chronic complete paralysis in humans. *PLoS ONE* 10:e0133998. doi: 10.1371/journal.pone.0133998

Rejc, E., and Angeli, C. A. (2019). Spinal cord epidural stimulation for lower limb motor function recovery in individuals with motor complete spinal cord injury. *Phys. Med. Rehabil. Clin. N. Am.* 30, 337–354. doi: 10.1016/j.pmr.2018.12.009

Squair, J. W., Gautier, M., Mahe, L., Soriano, J. E., Rowald, A., Bichat, A., et al. (2021). Neuroprosthetic baroreflex controls haemodynamics after spinal cord injury. *Nature* 590, 308–314. doi: 10.1038/s41586-020-03180-w

Wagner, F. B., Mignardot, J. B., Le Goff-Mignardot, C. G., Demesmaeker, R., Komi, S., Capogrosso, M., et al. (2018). Targeted neurotechnology restores walking in

humans with spinal cord injury. *Nature* 563, 65–71. doi: 10.1038/s41586-018-0649-2

Conflict of Interest: The authors declare that the research was conducted in the absence of any commercial or financial relationships that could be construed as a potential conflict of interest.

Publisher's Note: All claims expressed in this article are solely those of the authors and do not necessarily represent those of their affiliated organizations, or those of the publisher, the editors and the reviewers. Any product that may be evaluated in this article, or claim that may be made by its manufacturer, is not guaranteed or endorsed by the publisher.

frontiers in Systems Neuroscience

ORIGINAL RESEARCH
published: 06 February 2020
doi: 10.3389/fnsys.2020.00001

Transcutaneous Electrical Spinal Cord Neuromodulator (TESCoN) Improves Symptoms of Overactive Bladder

*Evgeniy Kreydin[1,2], Hui Zhong[2,3], Kyle Latack[1,2], Shirley Ye[1,2], V. Reggie Edgerton[2,3,4,5,6,7,8] and Parag Gad[1,2,3,8]**

[1] Institute of Urology, Keck School of Medicine, University of Southern California, Los Angeles, CA, United States, [2] Rancho Research Institute, Rancho Los Amigos National Rehabilitation Center, Downey, CA, United States, [3] Department of Neurobiology, University of California, Los Angeles, Los Angeles, CA, United States, [4] Department of Integrative Biology and Physiology, University of California, Los Angeles, Los Angeles, CA, United States, [5] Department of Neurosurgery, University of California, Los Angeles, Los Angeles, CA, United States, [6] Brain Research Institute, University of California, Los Angeles, Los Angeles, CA, United States, [7] Institut Guttmann, Hospital de Neurorehabilitació, Institut Universitari adscrit a la Universitat Autònoma de Barcelona, Barcelona, Spain, [8] The Centre for Neuroscience and Regenerative Medicine, Faculty of Science, University of Technology Sydney, Ultimo, NSW, Australia

Neuromodulation is a therapeutic technique that is well-established in the treatment of idiopathic Lower urinary tract (LUT) dysfunction such as overactive bladder (OAB). We have recently developed a novel neuromodulation approach, Transcutaneous Electrical Spinal Cord Neuromodulation (TESCoN) and demonstrated its acute effects on LUT dysfunction after spinal cord injury (SCI) during urodynamic studies. We found that TESCoN can promote urinary storage and induce urinary voiding when delivered during urodynamic studies. The objective of this study was to determine whether TESCoN can retrain the spinal neural networks to induce chronic improvement in the LUT, such that positive changes can persist even in the absence of stimulation. In addition, we wished to examine the effect of TESCoN on LUT dysfunction due to multiple pathologies. To achieve this objective, 14 patients [SCI = 5, stroke = 5, multiple sclerosis (MS) = 3, and idiopathic OAB (iOAB) = 1] completed 24 sessions of TESCoN over the course of 8 weeks. Patients completed urodynamic studies before and after undergoing TESCoN therapy. Additionally, each subject completed a voiding diary and the Neurogenic Bladder Symptom Score questionnaire before and after receiving TESCoN therapy. We found that TESCoN led to decreased detrusor overactivity, improved continence, and enhanced LUT sensation across the different pathologies underlying LUT dysfunction. This study serves as a pilot in preparation for a rigorous randomized placebo-controlled trial designed to demonstrate the effect of TESCoN on LUT function in neurogenic and non-neurogenic conditions.

NEW AND NOTEWORTHY

Non-Surgical modality to reduce incidence of urinary incontinence and improve neurogenic bladder symptom scores (NBSS) in individuals with neurogenic bladder due to spinal cord injury or stroke.

Keywords: non-invasive spinal cord stimulation, spinal cord injury, stroke, multiple sclerosis, neurogenic bladder, over active bladder urodynamics

OPEN ACCESS

Edited by:
Ronaldo M. Ichiyama, University of Leeds, United Kingdom

Reviewed by:
Michelle Hook, Texas A&M University, United States
Kyle Baumbauer, University of Kansas Medical Center, United States

****Correspondence:***
Parag Gad
paraggad@ucla.edu

Received: *21 September 2019*
Accepted: *06 January 2020*
Published: *06 February 2020*

Citation:
Kreydin E, Zhong H, Latack K, Ye S, Edgerton VR and Gad P (2020) Transcutaneous Electrical Spinal Cord Neuromodulator (TESCoN) Improves Symptoms of Overactive Bladder. Front. Syst. Neurosci. 14:1. doi: 10.3389/fnsys.2020.00001

INTRODUCTION

The lower urinary tract (LUT, consisting of the bladder and bladder outlet) serves two main roles: to store and empty urine. LUT dysfunction occurs when either storage or voiding are impaired, resulting in urinary incontinence or retention. LUT dysfunction is common in patients with neurological disease and the general population (de Groat, 1997; Jeong et al., 2010). In the case of neurological disease, LUT dysfunction occurs because the normal pathways responsible for communication between the LUT and the neural micturition centers become disrupted. While the mechanism of idiopathic LUT dysfunction is not as obvious, the nervous system is thought to be at least partially implicated in the majority of cases. LUT dysfunction has profound effects which range from endangering patients' health [as the case of poorly managed LUT dysfunction after spinal cord injury (SCI)] to significantly impacting patients' quality of life [as in the case of idiopathic over active bladder (iOAB) and post-stroke LUT dysfunction].

While it is often assumed that paralyzed individuals prioritize recovery of ambulation, multiple studies have demonstrated that restoration of bladder function is ranked among the top 2–3 priorities, above goals such as regaining lower extremity function (Anderson, 2004). Likewise, urinary incontinence after stroke is a well-known risk factor for long-term disability, depression and institutionalization (Panfili et al., 2017). Current therapy for LUT focuses on managing these complications without addressing the underlying cause or attempting to normalize or restore function (Stohrer et al., 2009). Urinary incontinence, frequency and urgency present across diseases such as SCI, stroke, multiple sclerosis (MS) and iOAB. While the reasons for this may vary, detrusor overactivity (or uninhibited detrusor contractions) is a common physiologic phenomenon observed in these conditions. Multiple therapies exist for correcting urinary storage function; however, they are not always suitable populations (e.g., anticholinergic medications in patients with cognitive impairment; intravesical botulinum toxin in patients at risk for retention) and they do not attempt to restore normal LUT function. On the other hand, the premise of neuromodulation is to correct the underlying neurological deficit and thus restore function to an end organ. Some neuromodulation techniques are well-established in iOAB including sacral nerve stimulation (Dasgupta et al., 2005) and percutaneous tibial nerve stimulation (Peters et al., 2010). We have recently developed a novel neuromodulation approach, Transcutaneous Electrical Spinal Cord Neuromodulation (TESCoN) a novel non-invasive neuromodulation technique to facilitate functional restoration after neurological injury (Gad et al., 2019). This modality engages the automaticity and the feedforward (Gerasimenko et al., 2017) features of the spinal neural networks to activate the intrinsic control of the spinal networks that is sufficient to enable recovery of voluntary control. We have previously demonstrated that acute TESCoN facilitates urinary storage and promotes bladder emptying in individuals with SCI during urodynamic studies (Gad et al., 2018a). Patients experienced decreased detrusor overactivity, exhibited increased bladder capacity and improved detrusor-sphincter dyssynergia when stimulation was delivered at a high frequency; on the other hand, when stimulation was delivered at a low frequency subjects demonstrated improved voiding efficiency. These changes in LUT function were only noted during active stimulation. In this study we wished to determine whether repetitive stimulation over the course of several weeks can retrain the spinal neural networks to relearn timely storage and voiding. In addition, given the similarities in storage LUT symptoms and physiologic phenomena (e.g., detrusor overactivity) across multiple conditions, we wished to expand the application of TESCoN to LUT dysfunction due to stroke, MS and iOAB. Finally, our objective was to provide a clinical assessment of the effect of TESCoN on the LUT by examining changes in voiding diaries and validated clinical questionnaire following a course of the therapy.

MATERIALS AND METHODS

Patient Recruitment

This study was approved by the Institutional Review Board of Rancho Research Institute, the research arm of Rancho Los Amigos National Rehabilitation Center, Downey, CA, United States. All research participants signed an informed consent form before the start of the study and consented to their data being used in future publications and presentations. Five patients (four males and one female) with stable (greater than 1-year post diagnosis) SCI at T8 or above who used clean intermittent catheterization (CIC), five patients (three males and two females) with stable cortical stroke (greater than 1-year post diagnosis), three female patients with progressive MS symptoms for at least 1 year and one female patient with idiopathic OAB were recruited (**Table 1**). All patients experienced symptoms of urinary incontinence and sensate (i.e., non-SCI) patients reported urinary frequency and urgency.

Initial Assessment

Each patient underwent a detailed medical history and physical examination and completed an assessment of LUT symptoms using the Neurogenic Bladder Symptom Score (NBSS). A baseline urodynamic study was performed in SCI and stroke subjects according to International Continence Society (ICS) guidelines using a Goby Urodynamics System from Laborie (Ontario, Canada). In order to mimic a clinical setting where patients may not be evaluated with urodynamics prior to therapy, MS and idiopathic OAB subjects were assessed only with a detailed history and physical, a voiding diary, and the NBSS. Following the initial visit, each subject completed a 4-day voiding diary.

Delivery of Spinal Stimulation

Stimulation was delivered using a proprietary TESCoN device (spineX, Inc.) (Gad et al., 2019). The stimulation waveform consisted of two alternating pulses of opposite polarities separated by a 1 μS delay to form a delayed biphasic waveform. The pulses consisted of a high frequency biphasic carrier pulse (10 KHz) combined with a low frequency (30 Hz) burst pulse each with a pulse width of 1 ms. Stimulation was applied using

TABLE 1 | Table summarizing 14 patients, their pathology (n = 5 SCI, 5 Stroke, n = 3 MS and n = 1iOAB) location of injury, severity of injury, months post injury, current bladder management technique, LUT symptoms and current medications.

Pt#	Age (yrs)	Gender	Pathology	Location	Severity	Months post	Bladder management	Lower urinary tract symptoms	Lower urinary tract medications
P1	25–35	M	SCI	T4	AIS A	18 m	CIC	Incontinence	None
P2	25–35	F	SCI	T6	AIS A	29 m	CIC	Incontinence	Mirabegron 50 mg
P3	40–50	M	SCI	C4	AIS C	20 m	CIC	Urge Incontinence	None
P4	35–45	M	SCI	T5	AIS A	135 m	CIC	Urge Incontinence	Tolterodine LA 4 mg
P5	50–60	M	SCI	T9	AIS C	48 m	CIC	Urgency/Incontinence	Solifenacin 10 mg
P6	40–50	M	CVA	L Basal Ganglia		50 m	Volitional	Urgency/Nocturia	Tolterodine LA 4 mg
P7	40–50	M	CVA	R Basal Ganglia		36 m	Volitional	Urgency/urge incontinence	Tolterodine LA 4 mg
P8	55–65	F	CVA	L Centrum Semiovale		78 m	Volitional	Urge incontinence	Tolterodine LA 4 mg
P9	55–65	F	CVA	L Basal Ganglia		75 m	Volitional	Urge incontinence	Oxybutynin 5 mgTID
P10	55–65	M	CVA	LMCA		75 m	Volitional	Urgency/Frequency	None
P11	20–30	F	MS			48 m	Volitional	Urge incontinence	None
P12	55–65	F	MS			240 m	Volitional	Incontinence	None
P13	35–45	F	MS			24 m	Volitional	Urge incontinence	Tolterodine LA 4 mg, Tamsulosin 0.8 mg
P14	55–65	F	iOAB			48 m	Volitional	Urge Incontinence/Frequency	None

SCI, spinal cord injury; CVA, cerebral vascular accident; MS, multiple sclerosis; CIC, clean intermittent catheterization.

an adhesive electrode over the interspinous ligaments of T11 and L1 serving as the cathode and two adhesive electrodes over the iliac crests as the anodes. The frequencies were selected based on our previous findings demonstrating greatest reduction in incontinence and increase in bladder capacity (Gad et al., 2018a).

Identification of Stimulation Parameters

Patients with SCI and stroke underwent formal evaluation for selection of stimulation parameters as previously published (Gad et al., 2018a). In brief, a urodynamic two-port urethral catheter and a urodynamic rectal catheter were placed to measure intravesical (P_{ves}), external urethral sphincter (P_{ura}) and abdominal (P_{abd}) pressures, respectively. Stimulation was delivered as described above. Dose response curves were constructed for each parameter with incremental increase in stimulation intensity. The stimulation intensity that generated a noticeable change in P_{ura} with little to no change in P_{det} was selected (**Figure 1**). This stimulation intensity did not cause any discomfort to the patients. Urodynamic studies were then performed according to ICS guidelines with concurrent TESCoN stimulation. Again, to mimic a clinical setting which precludes such an assessment, subjects with MS and idiopathic OAB were stimulated at a preselected frequency (30 Hz) and location (T11 and L1). Stimulation intensity was set as the highest current that did not cause cutaneous discomfort or cause any muscle activation in pelvic floor muscles or lower extremity muscles.

TESCoN Therapy Course

Following the baseline evaluation, the patients were invited to return for an 8-week long course of TESCoN Subjects received stimulation for 90 min. Each subject completed three stimulation sessions a week.

Post-stimulation Assessment

Within 1 week after the last stimulation session, SCI and stroke patients completed another clinical urodynamic study in the absence of TESCoN. All patients also completed the NBSS at this time and submitted a voiding diary starting 4 days prior to the final assessment.

Data and Statistical Analysis

The following urodynamic variables were collected in SCI and stroke subjects: (1) Bladder capacity, (2) Voiding efficiency, (3) Maximum detrusor pressure during voiding contraction, (4) Change in urethral sphincter pressure during filling and voiding contraction, (5) volume at first sensation and (6) time between bladder capacity and beginning of voiding contraction. "ΔP_{ura} Filling" was defined as the change in pressure observed in P_{ura} during the filling cycle. "P_{ura} Baseline" was defined as the pressure in the P_{ura} prior to start of filling. "ΔP_{det} void" and "ΔP_{ura} void" were defined as the change in pressures observed in P_{det} and ΔP_{ura}, respectively, between bladder capacity and voiding. The paired t-test was used to determine the significance of differences in urodynamic parameters, NBSS scores of participants and number of daily voids and incontinence episodes with and without TESCoN and before and after therapy.

RESULTS

Urodynamic Assessment of SCI and Stroke Patients

During baseline urodynamics, SCI patients demonstrated detrusor overactivity at low volumes, low voiding efficiency and detrusor sphincter dyssynergia during voiding. Stroke patients demonstrated low bladder capacity, detrusor overactivity,

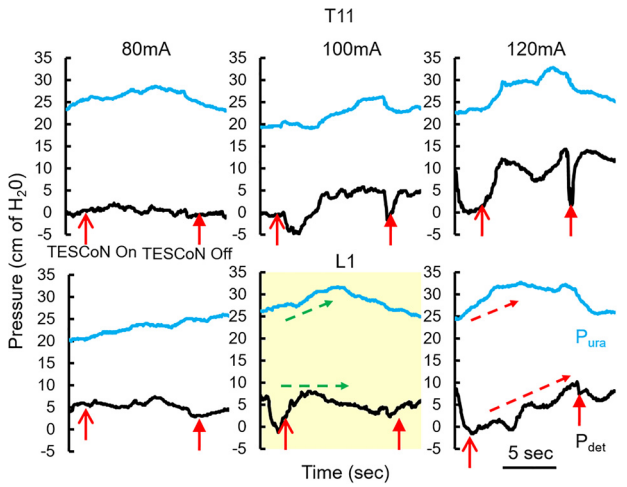

FIGURE 1 | Changes in detrusor and urethral pressures with changing parameters of TESCoN. Representative patient demonstrating the protocol to identify parameters of TESCoN that generates minimal change in Pdet along with a change in Pura. In this case stimulation at L1 at 100 mA (yellow box) generated no change in Pdet while Pura increased from ~25 to 32 cm of H20 (green arrows) between TESCoN On and TESCoN off. Note the increase in both the Pura and Pdet at L1 120 mA.

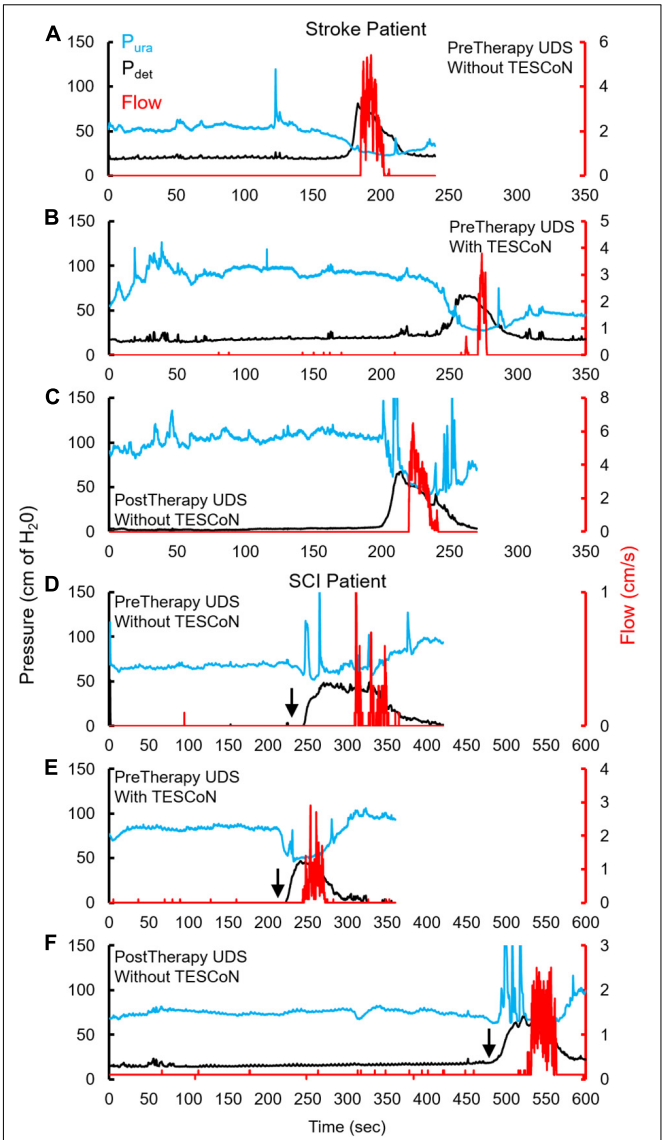

FIGURE 2 | Changes in urodynamic studies without and with TESCoN. Representative urodynamic study for a stroke patient, **(A)** before therapy (PreTherapy) without and **(B)** with TESCoN and **(C)** after therapy (PostTherapy) and spinal cord injured (SCI) **(D)** before therapy (PreTherapy) without and **(E)** with TESCoN and **(F)** after therapy (PostTherapy). Note the increased bladder capacity (time prior to detrusor contraction), improved flow, improved detrusor and sphincter coordination and increase in urethral pressure during filling both with TESCoN at PreTherapy and PostTherapy (without TESCoN). Black arrow marks the occurrence of detrusor overactivity.

and appropriate voiding efficiency (**Figure 2**; Weld and Dmochowski, 2000; Weld et al., 2000). Acute delivery of TESCoN in SCI patients reduced detrusor overactivity, increased bladder capacity, improved coordination between detrusor and the external urethral sphincter and increased voiding efficiency (**Figure 3**), consistent with our earlier observations (Gad et al., 2018a). In contrast, stroke patients did not demonstrate a change in bladder capacity or voiding efficiency. However, stroke patients exhibited an increase in the volume at first bladder sensation, and a significant increase in the ability to delay urination, as measured by the time between reaching bladder capacity and initiation of voiding ($P < 0.05$) (**Figure 4**). After completing the 8-week therapeutic intervention, both sets of patients ($n = 5$ Stroke and $n = 5$ SCI) demonstrated an increased bladder capacity ($P < 0.05$, **Figures 5A,F**) (without TESCoN); however, no change in voiding efficiency was observed in either group (**Figures 5B,G**). The average baseline pressure recorded at the urethral port (P_{ura}) and the change in P_{ura} during the filling phase of the urodynamic cycle were higher ($P < 0.05$) after compared to before therapy (**Figures 5C,D,H,I**). Detrusor pressure (P_{det}) during voiding did not change before vs. after therapy (**Figures 5E,J**).

Clinical Assessment of Patients

All patients underwent a clinical assessment in the form of a 4-day voiding diary and NBSS. Eleven ($n = 4$ SCI, $n = 5$ Stroke and $n = 2$ MS) out of thirteen neurogenic patients reported at least a five-point decrease (minimal clinically important difference, MCID) in the NBSS (Welk et al., 2018; **Figure 6A**). The mean score in the NBSS decreased from 35.9 ± 2.6 to 26.6 ± 3.1 ($P < 0.05$) with the highest change being 34 points and the lowest being 0 (**Figures 6C,D**). Note that significant decrease in NBSS scores were observed in all pathologies (**Figure 6E**). The distribution of NBSS decrease among the different underlying pathologies showed no obvious trends. All patients also reported a significant decrease in the number of incontinence episodes/day (~68% reduction in leaks, $P < 0.05$) (**Figure 7A**), a reduction (12%) in the

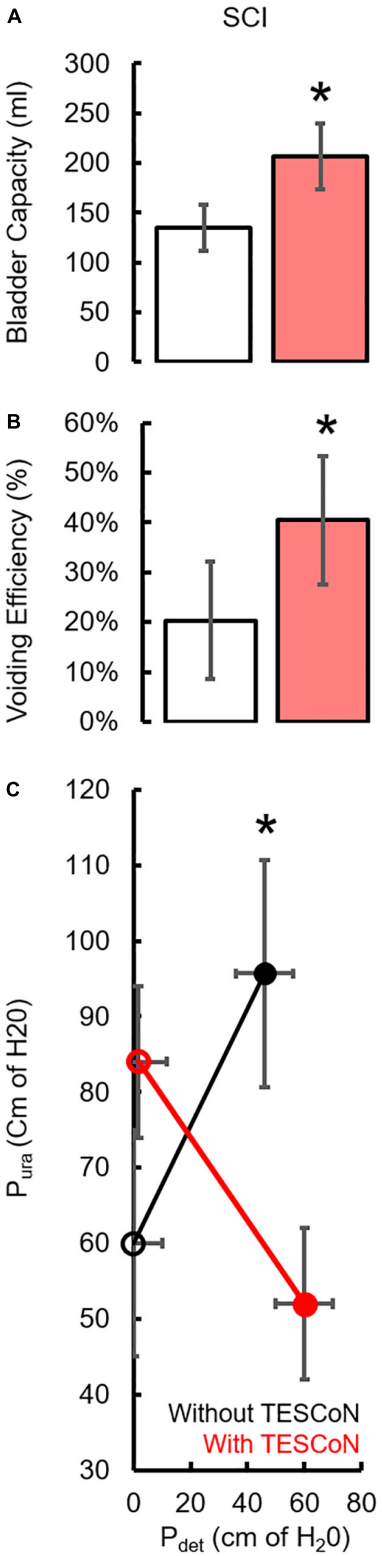

FIGURE 3 | Changes in urodynamic parameters during acute stimulation in SCI subjects. Mean ±SE (n = 5 SCI) without (white bar) and with (red bar) acute delivery of TESCoN. **(A)** bladder capacity, **(B)** Voiding efficiency, **(C)** changes in pressure during filling vs. voiding to demonstrate the improvement in Detrusor-Sphincter Dyssynergia (DSD) without (black) and with TESCoN (red). * statistically significant from without TESCoN at $P < 0.05$.

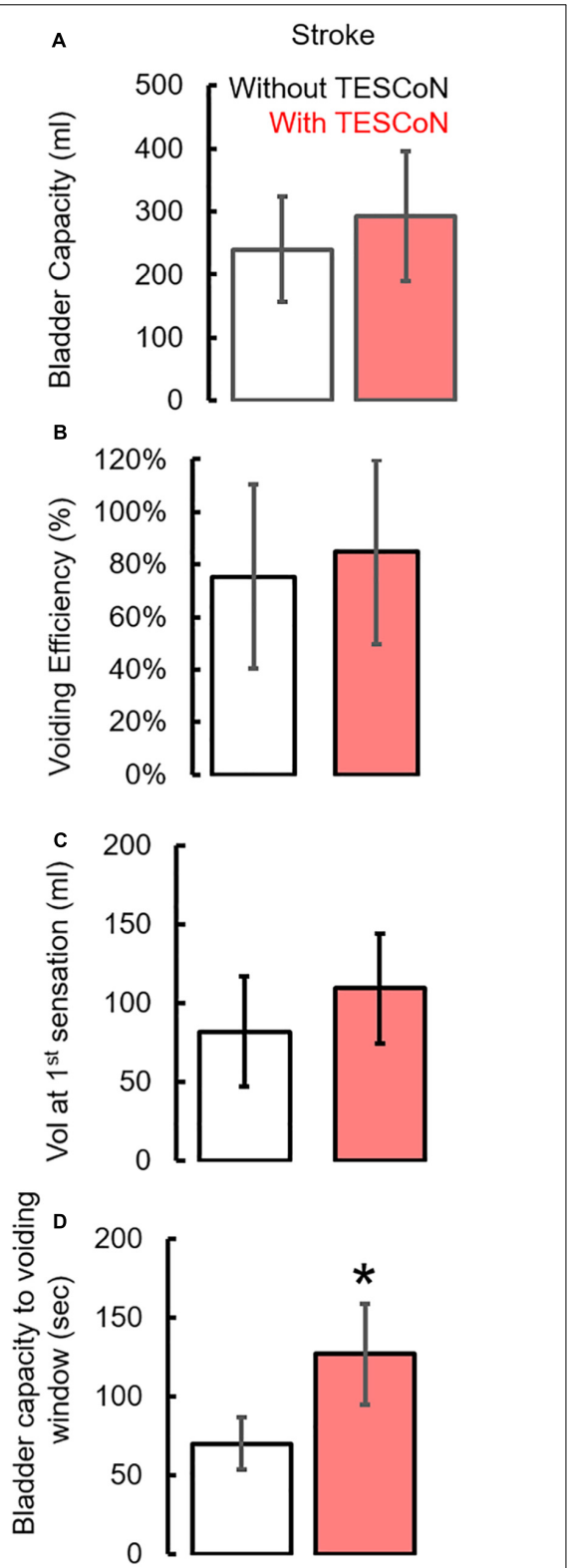

FIGURE 4 | Changes in urodynamic parameters during acute stimulation in stroke subjects. Mean ±SE (n = 5 Stroke) **(A)** bladder capacity, **(B)** Voiding efficiency, **(C)** volume at first sensation during urodynamic study without (white bar) and with (red bar) acute TESCoN and **(D)** time window between bladder capacity and voiding in stroke patients. * statistically significant from without TESCoN at $P < 0.05$.

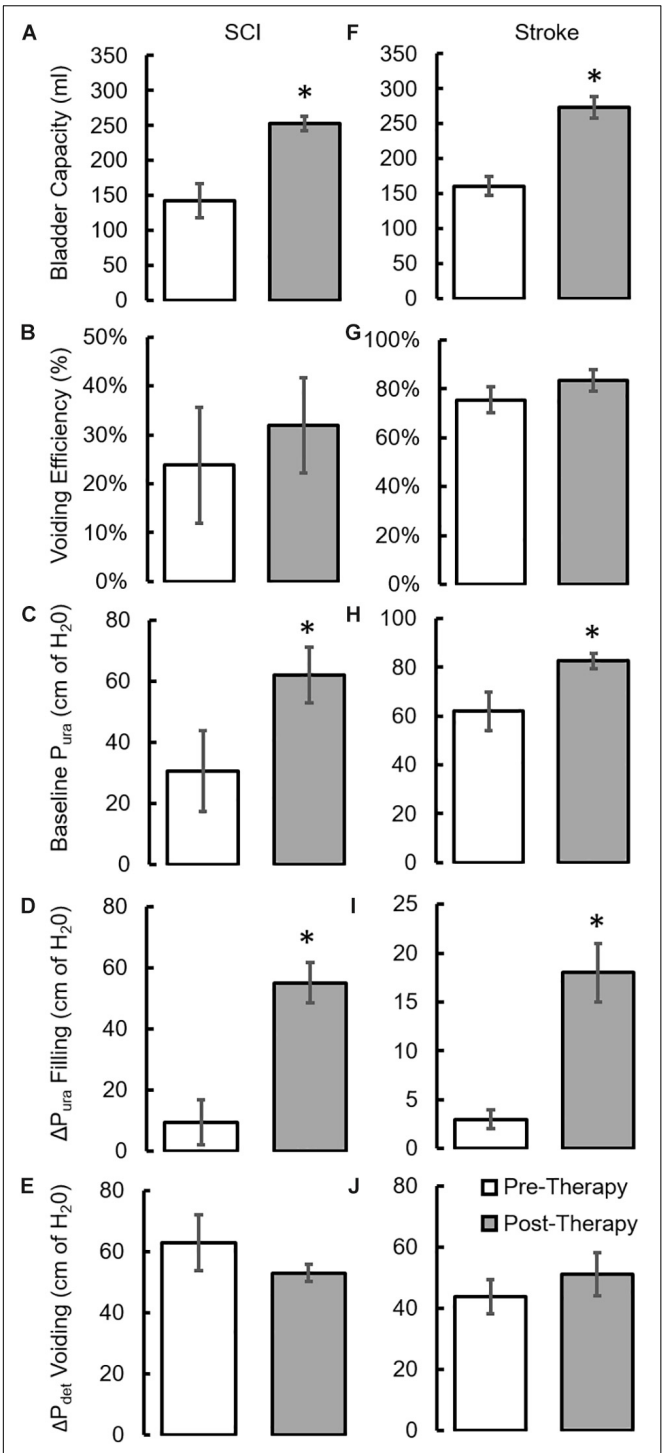

FIGURE 5 | Changes in urodynamic parameters after a 8-week course of stimulation. mean ±SE (n = 5 SCI patients) **(A)** bladder capacity, **(B)** Voiding efficiency **(C)** baseline Pura prior to filling, **(D)** ΔP_{ura} during bladder filling, **(E)** ΔP_{det} during voiding as observed during clinical urodynamic studies at Pre-Therapy and Post-Therapy without TESCoN. mean ±SE (n = 5 stroke patients) **(F)** bladder capacity, **(G)** Voiding efficiency **(H)** baseline Pura prior to filling, **(I)** ΔP_{ura} during bladder filling, **(J)** ΔP_{det} during voiding as observed during clinical urodynamic studies at Pre-Therapy and Post-Therapy without TESCoN. *Significantly different from Pre-Therapy at $P < 0.05$.

number of voiding/CIC episodes per day (**Figure 7B**) and a significant reduction (∼37%) in night time voiding/CIC episodes as recorded on the voiding diary (**Figure 7C**). No Adverse Events (AE) were reported. All patients reported to be satisfied with the therapy and would have continued beyond the 8 weeks if the therapy was offered.

DISCUSSION

Neuromodulation Enables Restoration of Sensation and Motor Control of LUT

Multiple components of the nervous system play a role in LUT control. Thus, when one or more components of the nervous system are affected by a disease, LUT dysfunction can ensue. Although modern management techniques have ensured that LUT dysfunction is rarely dangerous, it almost inevitably has a marked impact on patients' quality of life. Some current therapies for LUT dysfunction in neurogenic and idiopathic situations are effective for preventing incontinence (e.g., anticholinergics, beta-agonists, botulinum toxin injection) but they do not restore normal bladder sensation or voiding function and sometimes achieve continence at their expense. On the other hand, spinal neuromodulation is a technique whose premise is to restore neural control functions by delivering a sub-motor threshold electrical stimulus that can transform the controlling neural networks into more functional physiological states. After 8 weeks of non-invasive spinal cord stimulation, bladder capacity increased. SCI patients also demonstrated improved detrusor-sphincter dyssynergia during detrusor contractions. All patients reported an improved sensation of bladder fullness and an increased latency time between sensation of urgency and the first episode of detrusor overactivity (or volitional voiding contraction). These effects appeared to be durable as they were observed even 1 week after therapy was concluded.

A commons question in the field of neuromodulation is, how epidural and transcutaneous spinal stimulation compare? Some of the more Important comparisons are (1) the ability to deliver the desired stimulation parameters to the most functionally effective neuronal networks for a given target organ system, (2) patient acceptability and ease and accessibility of delivery of the intervention (3) cost of the intervention and (4) safety of the intervention. To date, there is insufficient knowledge to weigh the advantages, but it seems reasonably safe to conclude that both approaches should continue to be developed and tested. Given the data to date, it seems almost inevitable that the best choice of approach will be based on the net result of pros and cons for a given patient as judged by the patient, the physician and the caregivers.

To briefly expand on some of these points, it is obvious that using the transcutaneous approach, multiple organ systems can be targeted simply by moving the electrode along the length of the spinal cord (Gad et al., 2018a,b; Gad P. et al., 2018; Inanici et al., 2018; Phillips et al., 2018; Rath et al.,

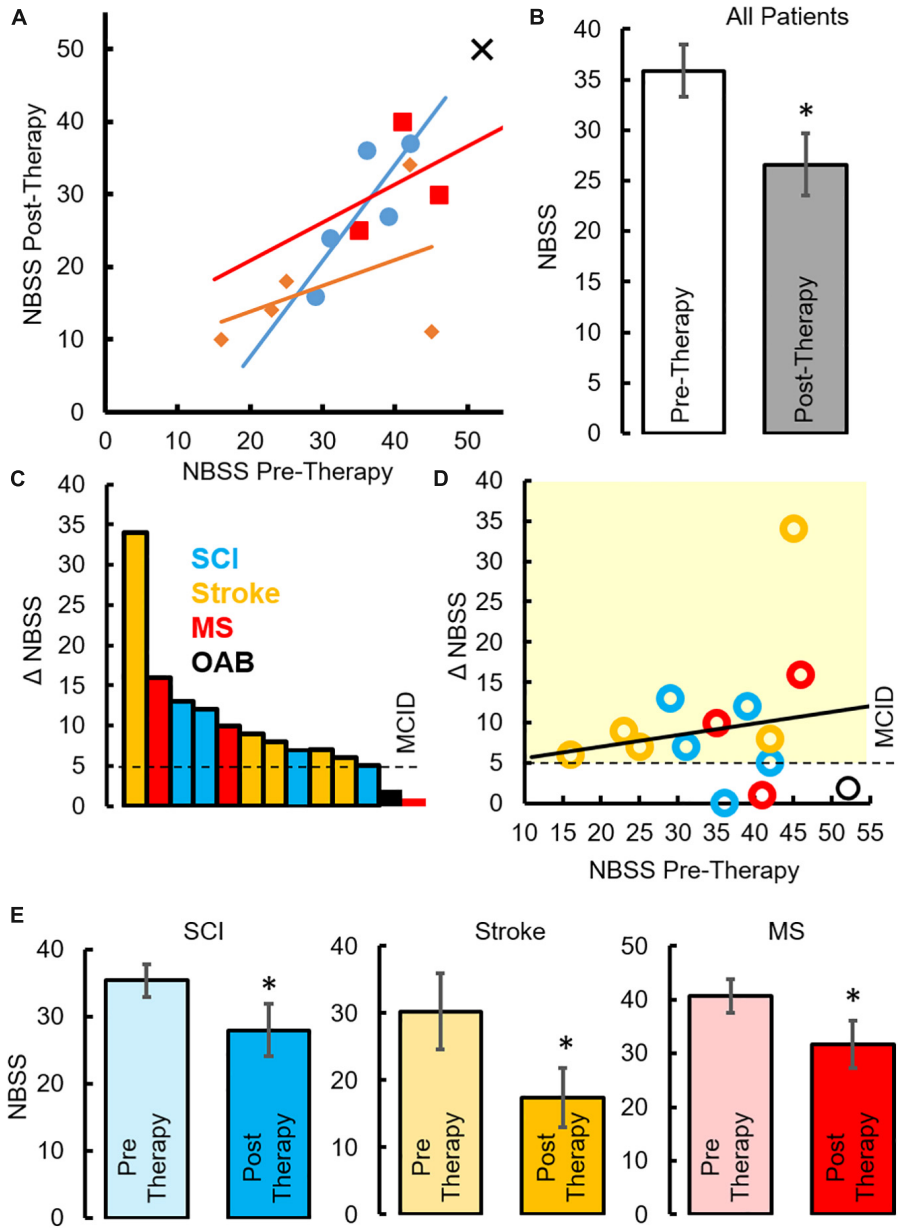

FIGURE 6 | Changes in NBSS parameters after TESCoN therapy **(A)** Neurogenic Bladder Symptom Score (NBSS) at Pre-Therapy and Post-Therapy for the 14 patients tested. **(B)** Mean ± SE (n = 14 patients) NBSS scores at Pre-Therapy and Post-Therapy. **(C)** Distribution of NBSS score decrease across the 14 patients tested, note only 5 SCI patients are plotted since 5th patient observed a change of 0, **(D)** decrease in NBSS scores relative to the initial NBSS scores, **(E)** mean ±SE (n = 5 SCI patients, n = 5 stroke and n = 3 MS) NBSS scores at Pre-Therapy and Post-Therapy. MCID, minimal clinically important difference. *statistically significant from Pre-therapy at $P < 0.05$.

2018; Hofstoetter et al., 2019; Sayenko et al., 2019). Epidural stimulation has been effective in treating both autonomic (Harkema et al., 2018; Herrity et al., 2018; Hubscher et al., 2018) and motor functions (Grahn et al., 2017; Angeli et al., 2018; Gill et al., 2018; Wagner et al., 2018) while maintaining the overall location of the implant even though the scope of the neural networks being neuromodulated may be more limited compared to transcutaneous stimulation. Evidence to date suggest that the transcutaneous approach in general has a greater advantage because of a more encompassing combination of networks that can be modulated to multiple organ systems. The activation of a broader network may enable multiple muscle groups and rely of the automaticity and feedforwardness of the spinal cord (Gerasimenko et al., 2017). A disadvantage of the transcutaneous approach is the inconvenience to frequently don and doff the electrodes and the lower spatial resolution compared to the epidural approach. While only a side-by-side comparison in the same

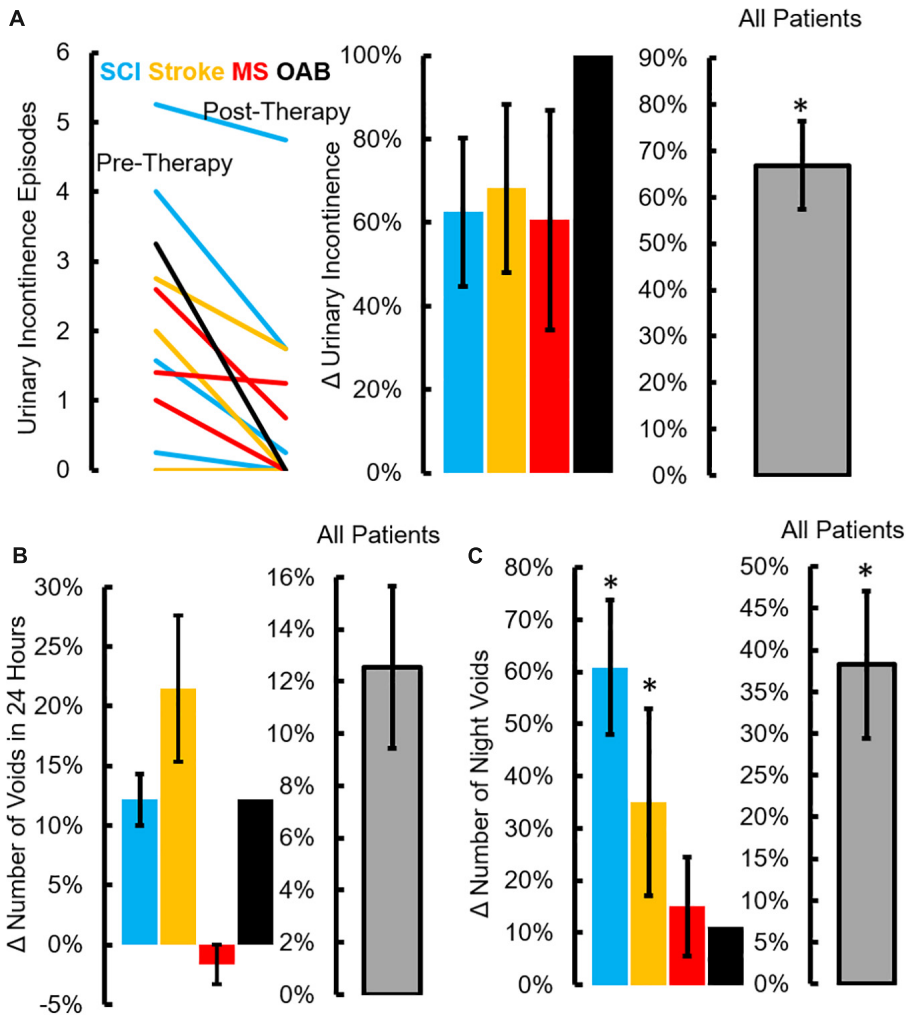

FIGURE 7 | Changes in voiding diary parameters after TESCoN therapy. **(A)** Number of urinary incontinence at Pre-Therapy and Post-Therapy for the 14 patients tested, mean ± SE percent decrease in incontinence episodes for the 4 patient groups and all patients (n = 14 patients) tested, **(B)** mean ± SE percent decrease in number of voids for the 4 patient groups and all patients (n = 14 patients) tested and **(C)** mean ±SE percent decrease in number of night time voiding/CIC episodes during the night (10pm to 6am) for the 4 patient groups and all patients (n = 14 patients) tested. *Significanatly different from pretherapy at $P < 0.05$.

patient may provide more definitive answers, the transcutaneous approach definitely can help screen potential responders and provide insights regarding effective sights for stimulation. One could proceed from the transcutaneous approach to the Implantation strategy if this would be viewed as a more long-term solution. The reverse approach, however, would be more problematic.

Clinically Significant Levels of LUT Function Can Be Restored

As important as the physiological changes observed on urodynamic testing were the clinical improvements assessed by the voiding diary and the NBSS. The NBSS is a validated questionnaire (Welk et al., 2018) that addresses common urological complaints in patients with neurological disease (e.g., incontinence, frequency, urgency and their impact on quality of life). The ability of NBSS to detect a meaningful clinical change has been recently shown in a pilot study of SCI and multiple sclerosis patients, receiving botulinum toxin injections for neurogenic urinary incontinence (Fragala et al., 2015). Over 85% of the neurogenic bladder patients in our study reported a statistically significant and clinically meaningful improvement in the overall NBSS score after TESCoN therapy was completed. Among the various domains of the questionnaire, there was improvement in the incidence of incontinence, quality of life and voiding/storage domains of the NBSS. As expected, there was no significant change in the consequences domain of the NBSS as the questions in this section of the questionnaire represent chronic problems related to the urinary tract (e.g., bladder and kidney stones), that would not be expected to improve immediately with positive change in LUT function. However, all patients also reported either a significant decrease in the number of urinary incontinence episodes per day or a decrease in the number of

night time voiding cycles. Similar to the responses observed in the NBSS scores, no obvious trends were observed across the pathologies.

Mechanistic Factors That Contribute to Restoration of LUT Functions

Although the mechanistic details of how spinal neuromodulation can improve bladder function is not known, multiple but highly linked mechanisms probably contribute to the observed improvements. We postulate that stimulation modulates both afferent and efferent spinal networks into a more functional state. Neuromodulation may alter the responsiveness of spinal networks to bladder filling and emptying and increase the conscious awareness of these states. After chronic TESCoN therapy, subjects reported improved bladder sensation and decreased urinary urgency. Together, these findings suggest that parts of the CNS responsible for conscious sensation in the brain may have been re-engaged along with re-activation and/or retraining of local spinal centers controlling the LUT, reflecting a highly significant level of functional neural plasticity. It is interesting to note that despite the varied pathology, location and severity of injury, the spinal control of detrusor and urethral sphincter muscles were intact and could be transformed using a non-invasive modality. Our finding that voiding efficiency after 8 weeks of treatments did not change when urodynamic test was repeated in absence TESCoN suggests that the parasympathetic system, that drives bladder emptying, may require ongoing stimulation in order to induce a functional change. On the other hand, it appears that TESCoN can induce long standing neuroplasticity in the sympathetic and somatic system, which drives bladder storage, as evidenced by our finding that bladder capacity and P_{ura} showed improvement even in the absence of stimulation.

Despite the potential shortcomings of the limited number of patients and lack of sham stimulation which will be addressed in future randomized controlled clinical trials, these data demonstrate the ability to transform the neural control of bladder function from a dysfunctional to a functional state using non-invasive spinal neuromodulation. Our previous results have demonstrated improvement in multiple functions (locomotion and autonomic function) with spinal neuromodulation during function rehabilitation (Gerasimenko et al., 2015; Gad et al., 2017; Gad P. et al., 2018). In this study, however, since the patients were seated while receiving TESCoN therapy, minimal improvements in locomotor function were observed. TESCoN could prove to be a critical component of in our clinical toolbox while designing rehabilitation therapies for patients that suffer from multiple organ dysfunction (autonomic and motor) due to paralysis. In addition, future studies will also identify potential chronic changes in the cortex during simultaneous functional MRI recordings during urodynamic studies. These data allow us to speculate about multiple neural mechanisms that can account for end-organ dysfunction in neurogenic and non-neurogenic states (e.g., loss of connectivity between centers responsible for end organ control, formation of aberrant neural connections resulting in abnormal function). However, the intrinsic spinal networks controlling the LUT seem to not only persist post injury, but also have the potential to undergo transformation to a more functional state. These observations are consistent with our studies of non-invasive spinal cord stimulation in other applications such as lower extremity (Gerasimenko et al., 2015; Gad et al., 2017), and upper extremity functional rehabilitation (Gad P. et al., 2018; Inanici et al., 2018), where we have consistently observed some restoration of voluntary control in individuals clinically diagnosed with complete motor and sensory paralysis. We hypothesize that neuromodulation enables activity-dependent mechanisms that transform functionally incompetent spinal and supraspinal networks to higher functional states. The idea that neuromodulation can affect a part of the CNS remote from the site of stimulation is supported by data from other groups. For example, sacral nerve stimulation (a peripheral nerve neuromodulation modality commonly employed for idiopathic overactive bladder) is known to generate changes in brain signaling even during acute delivery of stimulation (Dasgupta et al., 2005). The encouraging findings that TESCoN can improve LUT symptoms in a variety of disease states encourages the exploration of its use in other brain pathologies associated with LUT dysfunction (e.g., Parkinson's disease, cerebral palsy), thus expanding the potential impact of this technology to a wider range of diseases.

CONCLUSION

We have successfully demonstrated that TESCoN can (1) reduce detrusor overactivity, increase bladder capacity and reduce episodes of incontinence in patients with SCI, stroke, multiple sclerosis and idiopathic over active bladder, (2) functional transformation of the sensory component of bladder control to improve sensation of fullness bladder and awareness by delaying the time between reaching bladder capacity and initiation of voiding, and (3) significantly reduce the number of incontinence episodes and night time voids that also reflects in the changes in NBSS scores. These observations suggest that the level of functional autonomy that is intrinsic to the neural circuitry that controls bladder function. This is a highly attractive clinical target for regaining greater levels of function in SCI and other etiologies of neurogenic bladder because it is a non-invasive form of neuromodulation that can re-engage and restore, via activity-dependent mechanisms, the automaticity intrinsic to the autonomic control of the LUT.

DATA AVAILABILITY STATEMENT

All datasets generated for this study are included in the article/supplementary material.

ETHICS STATEMENT

The studies involving human participants were reviewed and approved by the Institutional Review Board

of Rancho Research Institute, the research arm of Rancho Los Amigos National Rehabilitation Center, Downey, CA, United States. The patients/participants provided their written informed consent to participate in this study.

AUTHOR CONTRIBUTIONS

EK, PG, and VE designed the study. EK performed the initial medical evaluation and performed the urodynamic study. HZ, KL, and SY performed the day to day stimulation. PG analyzed the data. EK and PG wrote the manuscript. All authors edited and approved the manuscript.

FUNDING

This research was funded in part by the Conquer Paralysis Now Challenge award, Walkabout Foundation, Dana and Albert R. Broccoli Charitable Foundation, Nanette and Burt Forester, including matching by PwC LLP, and International Foundation for Research in Paraplegia, Society of Urodynamics, Female Pelvic Medicine and Urogenital Reconstruction (SUFU), and Whittier Foundation. The authors declare that this study received funding from PwC LLP. The funder was not involved in the study design, collection, analysis, interpretation of data, the writing of this article, or the decision to submit it for publication.

REFERENCES

Anderson, K. D. (2004). Targeting recovery: priorities of the spinal cord-injured population. *J. Neurotrauma* 21, 1371–1383. doi: 10.1089/neu.2004.21.1371

Angeli, C. A., Boakye, M., Morton, R. A., Vogt, J., Benton, K., Chen, Y., et al. (2018). Recovery of over-ground walking after chronic motor complete spinal cord injury. *N. Engl. J. Med.* 379, 1244–1250. doi: 10.1056/NEJMoa1803588

Dasgupta, R., Critchley, H. D., Dolan, R. J., and Fowler, C. J. (2005). Changes in brain activity following sacral neuromodulation for urinary retention. *J. Urol.* 174, 2268–2272. doi: 10.1097/01.ju.0000181806.59363.d1

de Groat, W. C. (1997). A neurologic basis for the overactive bladder. *Urology* 50, 36–52. doi: 10.1016/s0090-4295(97)00587-6

Fragala, E., Russo, G. I., Di Rosa, A., Giardina, R., Privitera, S., Favilla, V., et al. (2015). Association between the neurogenic bladder symptom score and urodynamic examination in multiple sclerosis patients with lower urinary tract dysfunction. *Int. Neurourol. J.* 19, 272–277. doi: 10.5213/inj.2015.19.4.272

Gad, P., Gerasimenko, Y., Zdunowski, S., Turner, A., Sayenko, D., Lu, D. C., et al. (2017). Weight bearing over-ground stepping in an exoskeleton with non-invasive spinal cord neuromodulation after motor complete paraplegia. *Front. Neurosci.* 11:333. doi: 10.3389/fnins.2017.00333

Gad, P., Lee, S., Terrafranca, N., Zhong, H., Turner, A., Gerasimenko, Y., et al. (2018). Non-invasive activation of cervical spinal networks after severe paralysis. *J. Neurotrauma* 35, 2145–2158. doi: 10.1089/neu.2017.5461

Gad, P. N., Edgerton, V. R., Taccola, G., and Kreydin, E. I. (2019). *Transcutaneous Electrical Spinal Cord Neuromodulator and Uses Thereof*. Patent Pending.

Gad, P. N., Kreydin, E., Zhong, H., Latack, K., and Edgerton, V. R. (2018a). Non-invasive neuromodulation of spinal cord restores lower urinary tract function after paralysis. *Front. Neurosci.* 12:432. doi: 10.3389/fnins.2018.00432

Gad, P. N., Kokikian, N., Christe, K. L., Edgerton, V. R., and Havton, L. A. (2018b). Noninvasive neurophysiological mapping of the lower urinary tract in adult and aging rhesus macaques. *J. Neurophysiol.* 119, 1521–1527. doi: 10.1152/jn.00840.2017

Gerasimenko, Y., Sayenko, D., Gad, P., Liu, C. T., Tillakaratne, N. J. K., Roy, R. R., et al. (2017). Feed-forwardness of spinal networks in posture and locomotion. *Neuroscientist* 23, 441–453. doi: 10.1177/1073858416683681

Gerasimenko, Y. P., Lu, D. C., Modaber, M., Zdunowski, S., Gad, P., Sayenko, D. G., et al. (2015). Noninvasive reactivation of motor descending control after paralysis. *J. Neurotrauma* 32, 1968–1980. doi: 10.1089/neu.2015.4008

Gill, M. L., Grahn, P. J., Calvert, J. S., Linde, M. B., Lavrov, I. A., Strommen, J. A., et al. (2018). Publisher correction: neuromodulation of lumbosacral spinal networks enables independent stepping after complete paraplegia. *Nat. Med.* 24:1942. doi: 10.1038/s41591-018-0248-7

Grahn, P. J., Lavrov, I. A., Sayenko, D. G., Van Straaten, M. G., Gill, M. L., Strommen, J. A., et al. (2017). Enabling task-specific volitional motor functions via spinal cord neuromodulation in a human with paraplegia. *Mayo Clin. Proc.* 92, 544–554. doi: 10.1016/j.mayocp.2017.02.014

Harkema, S. J., Wang, S., Angeli, C. A., Chen, Y., Boakye, M., Ugiliweneza, B., et al. (2018). Normalization of blood pressure with spinal cord epidural stimulation after severe spinal cord injury. *Front. Huma. Neurosci.* 12:83. doi: 10.3389/fnhum.2018.00083

Herrity, A. N., Williams, C. S., Angeli, C. A., Harkema, S. J., and Hubscher, C. H. (2018). Lumbosacral spinal cord epidural stimulation improves voiding function after human spinal cord injury. *Sci. Rep.* 8:8688. doi: 10.1038/s41598-018-26602-2

Hofstoetter, U. S., Freundl, B., Danner, S. M., Krenn, M. J., Mayr, W., Binder, H., et al. (2019). Transcutaneous spinal cord stimulation induces temporary attenuation of spasticity in individuals with spinal cord injury. *J. Neurotrauma* doi: 10.1089/neu.2019.6588 [Epub ahead of print].

Hubscher, C. H., Herrity, A. N., Williams, C. S., Montgomery, L. R., Willhite, A. M., Angeli, C. A., et al. (2018). Improvements in bladder, bowel and sexual outcomes following task-specific locomotor training in human spinal cord injury. *PLoS One* 13:e0190998. doi: 10.1371/journal.pone.0190998

Inanici, F., Samejima, S., Gad, P., Edgerton, V. R., Hofstetter, C. P., and Moritz, C. T. (2018). Transcutaneous electrical spinal stimulation promotes long-term recovery of upper extremity function in chronic tetraplegia. *IEEE Trans. Neural Syst. Rehabil. Eng.* 26, 1272–1278. doi: 10.1109/TNSRE.2018.2834339

Jeong, S. J., Cho, S. Y., and Oh, S. J. (2010). Spinal cord/brain injury and the neurogenic bladder. *Urol. Clin. North Am.* 37, 537–546. doi: 10.1016/j.ucl.2010.06.005

Panfili, Z., Metcalf, M., and Griebling, T. L. (2017). Contemporary evaluation and treatment of poststroke lower urinary tract dysfunction. *Urol. Clin. North Am.* 44, 403–414. doi: 10.1016/j.ucl.2017.04.007

Peters, K. M., Carrico, D. J., Perez-Marrero, R. A., Khan, A. U., Wooldridge, L. S., Davis, G. L., et al. (2010). Randomized trial of percutaneous tibial nerve stimulation versus Sham efficacy in the treatment of overactive bladder syndrome: results from the SUmiT trial. *J. Urol.* 183, 1438–1443. doi: 10.1016/j.juro.2009.12.036

Phillips, A. A., Squair, J. W., Sayenko, D. G., Edgerton, V. R., Gerasimenko, Y., and Krassioukov, A. V. (2018). An autonomic neuroprosthesis: noninvasive electrical spinal cord stimulation restores autonomic cardiovascular function in individuals with spinal cord injury. *J. Neurotrauma* 35, 446–451. doi: 10.1089/neu.2017.5082

Rath, M., Vette, A. H., Ramasubramaniam, S., Li, K., Burdick, J., Edgerton, V. R., et al. (2018). Trunk stability enabled by noninvasive spinal electrical stimulation after spinal cord injury. *J. Neurotrauma* 35, 2540–2553. doi: 10.1089/neu.2017.5584

Sayenko, D. G., Rath, M., Ferguson, A. R., Burdick, J. W., Havton, L. A., Edgerton, V. R., et al. (2019). Self-assisted standing enabled by non-invasive spinal stimulation after spinal cord injury. *J. Neurotrauma* 36, 1435–1450. doi: 10.1089/neu.2018.5956

Stohrer, M., Blok, B., Castro-Diaz, D., Chartier-Kastler, E., Del Popolo, G., Kramer, G., et al. (2009). EAU guidelines on neurogenic lower urinary tract dysfunction. *Eur. Urol.* 56, 81–88. doi: 10.1016/j.eururo.2009.04.028

Wagner, F. B., Mignardot, J. B., Le Goff-Mignardot, C. G., Demesmaeker, R., Komi, S., Capogrosso, M., et al. (2018). Targeted neurotechnology restores walking in humans with spinal cord injury. *Nature* 563, 65–71. doi: 10.1038/s41586-018-0649-2

Weld, K. J., and Dmochowski, R. R. (2000). Association of level of injury and bladder behavior in patients with post-traumatic spinal cord injury. *Urology* 55, 490–494. doi: 10.1016/s0090-4295(99)00553-1

Weld, K. J., Graney, M. J., and Dmochowski, R. R. (2000). Clinical significance of detrusor sphincter dyssynergia type in patients with post-traumatic spinal cord injury. *Urology* 56, 565–568. doi: 10.1016/s0090-4295(00)00761-5

Welk, B., Lenherr, S., Elliott, S., Stoffel, J., Presson, A. P., Zhang, C., et al. (2018). The neurogenic bladder symptom score (NBSS): a secondary assessment of its validity, reliability among people with a spinal cord injury. *Spinal Cord* 56, 259–264. doi: 10.1038/s41393-017-0028-0

Conflict of Interest: VE holds shareholder interest in NeuroRecovery Technologies and hold certain inventorship rights on intellectual property licensed by The Regents of the University of California to NeuroRecovery Technologies and its subsidiaries. VE and PG holds shareholder interest in spineX Inc., and hold certain inventorship rights on intellectual property licensed by The Regents of the University of California to spineX Inc.

The remaining authors declare that the research was conducted in the absence of any commercial or financial relationships that could be construed as a potential conflict of interest.

frontiers in Neuroscience

CASE REPORT
published: 22 June 2020
doi: 10.3389/fnins.2020.00552

Supraspinal and Afferent Signaling Facilitate Spinal Sensorimotor Network Excitability After Discomplete Spinal Cord Injury: A Case Report

*Alena Militskova[1], Elvira Mukhametova[1], Elsa Fatykhova[2], Safar Sharifullin[3], Carlos A. Cuellar[4], Jonathan S. Calvert[5], Peter J. Grahn[5,6], Tatiana Baltina[1] and Igor Lavrov[1,7,8]**

[1] Institute of Fundamental Medicine and Biology, Kazan Federal University, Kazan, Russia, [2] Children's Republican Clinical Hospital of the Ministry of Health of the Republic of Tatarstan, Kazan, Russia, [3] Dicom Clinic, Kazan, Russia, [4] Centro de Investigación en Ciencias de la Salud, Universidad Anáhuac México, Huixquilucan, Mexico, [5] Department of Neurologic Surgery, Mayo Clinic, Rochester, MN, United States, [6] Department of Physical Medicine and Rehabilitation, Mayo Clinic, Rochester, MN, United States, [7] Department of Biomedical Engineering, Mayo Clinic, Rochester, MN, United States, [8] Department of Neurology, Mayo Clinic, Rochester, MN, United States

OPEN ACCESS

Edited by:
Enrico Rejc,
University of Louisville, United States

Reviewed by:
Karen Minassian,
Medical University of Vienna, Austria
Dimitry Sayenko,
Houston Methodist Research Institute, United States
Winfried Mayr,
Medical University of Vienna, Austria

***Correspondence:**
Igor Lavrov
Lavrov.igor@mayo.edu

Specialty section:
This article was submitted to Autonomic Neuroscience, a section of the journal Frontiers in Neuroscience

Received: 17 December 2019
Accepted: 04 May 2020
Published: 22 June 2020

Citation:
Militskova A, Mukhametova E, Fatykhova E, Sharifullin S, Cuellar CA, Calvert JS, Grahn PJ, Baltina T and Lavrov I (2020) Supraspinal and Afferent Signaling Facilitate Spinal Sensorimotor Network Excitability After Discomplete Spinal Cord Injury: A Case Report. Front. Neurosci. 14:552. doi: 10.3389/fnins.2020.00552

Objective: In this study, we evaluated the role of residual supraspinal and afferent signaling and their convergence on the sublesional spinal network in subject diagnosed with complete paralysis (AIS-A).

Methods: A combination of electrophysiologic techniques with positional changes and subject-driven reinforcement maneuvers was implemented in this study. Electrical stimulation was applied transcutaneously at the T9-L2 vertebra levels and the spinal cord motor evoked potentials (SEMP) were recorded from leg muscles. To test the influence of positional changes, the subject was placed in (i) supine, (ii) upright with partial body weight bearing and (iii) vertically suspended without body weight bearing positions.

Results: Increase in amplitude of SEMP was observed during transition from supine to upright position, supporting the role of sensory input in lumbosacral network excitability. Additionally, amplitudes of SEMP were facilitated during reinforcement maneuvers, indicating a supralesional influence on sub-lesional network. After initial assessment, subject underwent rehabilitation therapy with following electrophysiological testing that reviled facilitation of SEMP.

Conclusion: These results demonstrate that combination of electrophysiological techniques with positional and reinforcement maneuvers can add to the diagnostics of discomplete SCI. These findings also support an idea that integration of supraspinal and afferent information on sub-lesional circuitry plays a critical role in facilitation of spinal sensorimotor network in discomplete SCI.

Keywords: spinal cord injury, AIS-A, discomplete spinal cord injury, spinal cord stimulation, sub-lesional spinal circuitry

BACKGROUND

According to the World Health Organization, global estimate of up to 500,000 people sustain a SCI each year (Kumar et al., 2018). Disruption of neural connections between the brain and spinal cord after SCI leads to permanent functional impairment. The American Spinal Injury Association (ASIA) Impairment Scale (AIS) is a widely accepted diagnostic tool for assessment of SCI (Kirshblum et al., 2014). However, the AIS classification of "complete" or "incomplete" loss of function is not sensitive with respect to severity of tissue injury, nor does it indicate the presence of sub-functional connectivity across the injury in those diagnosed with complete AIS-A paralysis (Awad et al., 2015). Despite clinical diagnosis of complete absence of voluntary control after SCI, prior evidence suggests a majority of injuries contain sub-functional connections that are capable of transmitting supra-spinal influence on spinal circuitry excitability below the injury (Dimitrijevic et al., 1984, 1987). This injury profile is known as "discomplete SCI" (Dimitrijevic et al., 1987). Specifically, in a cohort of subjects diagnosed as motor complete (AIS-A or B), attempts to volitionally initiate foot movements resulted in 89% of muscles generating EMG activity, suggesting some level of voluntary control over muscle activity (Moss et al., 2011). Other studies reported anatomical and electrophysiological findings, indicating that some ascending and descending fibers remain intact across the damaged area of the spinal cord in AIS-A subjects (Kakulas, 1988). Unfortunately, currently available electrophysiological and imaging tools are insufficient in identifying discomplete SCI (Nicotra and Ellaway, 2006). Animal studies and clinical trials results indicate that spinal cord electrical stimulation alone (Dimitrijevic et al., 1998; Gerasimenko et al., 2001; Lavrov et al., 2006, 2008, 2015; Harkema et al., 2011; Cuellar et al., 2017; Grahn et al., 2017; Shah and Lavrov, 2017) and in combination with medications (Gerasimenko et al., 2015) or/and locomotor training (Gerasimenko et al., 2017), significantly improved sensorimotor and autonomic functions after SCI. These data suggest that advanced diagnostic tools need to be developed to identify functionally silent connections for targeted engagement of sub-lesional spinal circuitry via emerging neuromodulatory therapies (Minassian et al., 2016; Taccola et al., 2018; Islam et al., 2019). Here, we present a case report of the patient with an SCI classified as AIS-A with complete loss of motor and sensory function below the injury, who demonstrated the residual supraspinal and afferent signaling on the sublesional spinal network during combination of electrophysiologic techniques, changes in body position, and subject-driven reinforcement maneuvers (see **Supplementary Material**).

CASE PRESENTATION

The participant is a 21-year-old woman (163 cm, 55 kg) with no previous disease with Th12 vertebra fracture associated with spinal cord compression and spinal cord injury at the level Th11 (ASI A), multiple rib fractures, contused lung, traumatic hiatal hernia, kidney contusion, followed by paraplegia, sensory loss, loss of bladder and bowel control. Urgently, she underwent hepatorrhaphy, and 5 days after injury, the decompression spine surgery at the level Th12, followed by reduction spondylodesis Th11-L1 (**Figures 1A-1,2,3**). A computed tomography scan (CT) was performed before surgery and magnetic resonance imaging (MRI) was captured post-surgery, although, some distortion was apparent due to spinal fixation hardware (**Figures 1A-2,5**). Additionally, injury site was assessed with ultrasound (**Figure 1A-6**). One year after SCI, participant was enrolled into the study and underwent a re-evaluation of neurological functions below the lesion along with electrophysiologic assessment with positional changes and subject-driven reinforcement maneuvers. The neurological assessment was consistent with paraplegia with decreased muscle tone in proximal leg muscles and increased in distal muscles, neurological level of injury Th11. Light touch sensory loss from the level Th12 bilaterally, pinprick sensory loss from the level Th12 from the left side and L1 from the right side, joint position sense loss from the level Th12, loss of bladder control (uses clean intermittent catheterization, residual urine volume: 200–400 ml), loss of bowel control. **Figure 1B** summarizes tested in this report electrophysiological assessment: (I) examination of spinally evoked motor potentials (SEMP) to transcutaneous stimulation (tSCS) applied at Th9-10, Th10-11, Th11-12, Th12-L1, L1-2 levels; (II) the evaluation of the supraspinal influence and afferent signaling by assessment the effect of reinforcement maneuver (Jendrassik maneuver, JM) and positional changes. First, the effect of the JM was evaluated during testing H-reflex in supine position. Then, we investigated the combination of JM and afferent signaling with tSCS in supine and upright (less than 30% body weight support) positions (Apte et al., 2018). The visual assessment of the leg muscle activation during JM was evaluated in supine and in vertically suspended (100% body weight support) positions; (III) the impact of the motor rehabilitation on facilitation of the mono- and polysynaptic spinal cord circuitry. During the initial electrophysiological assessment, the subject with SCI was evaluated with techniques I and II (**Figures 1B,C**). After the initial assessment 65 rehabilitation sessions, approximately 45 min each, consisting of trainer-assisted standing and weight supported stepping were performed over 16 weeks, with the following electrophysiological assessment (**Figure 1C**; see **Supplementary Material**).

RESULTS

Electrophysiological Assessment of the Discomplete SCI

Evaluation of the Continuity of the Posterior Columns

The amplitude of the SSEP at popliteal region, L2-3, and at Th11-12 levels on the low extremities at each recording location is presented on **Figure 1** E and C. SSEPs were not detected at

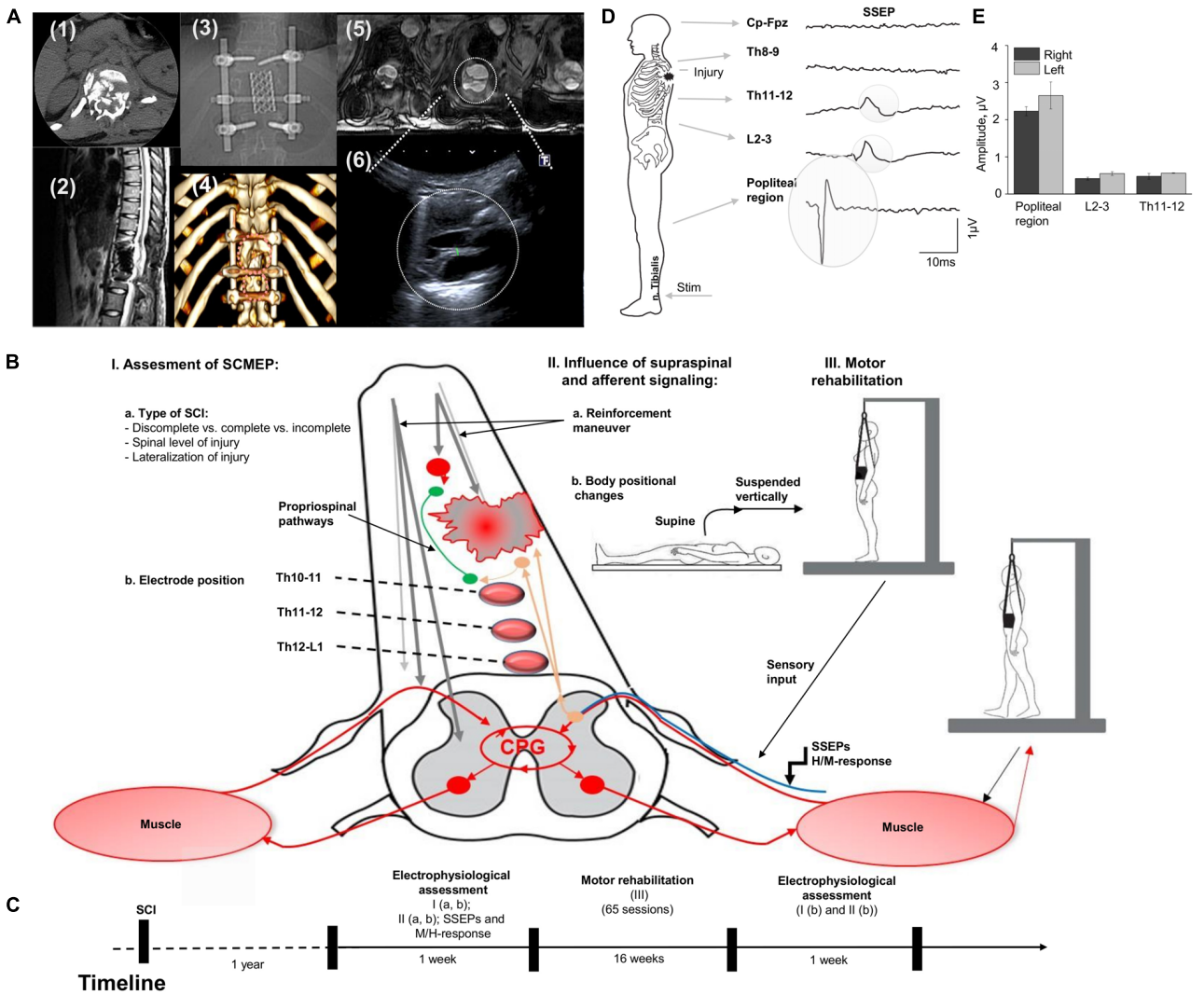

FIGURE 1 | (A) Initial evaluation with CT cross-section at injury level (1); the sagittal MRI view of the thoracic spine with the area of SCI; (3) X-ray view of the spine fixation structure; (4) 3D reconstruction of vertebras with areas of laminectomy and spine fixation structure, circles indicate position of the ultrasound sensor in the projection of laminectomy; (5) three transverse MRI sections of the spinal cord at the injury level (T1 weighted lesion); (6) visualization of the spinal cord at injury level with ultrasound technique. **(B)** Study design with approach of SCI evaluation in human. Assessment of SEMP (I) with the role of injury type (a) and electrode position (b); the influence of supraspinal and afferent information (II) tested with reinforcement maneuvers (a) and positional changes (b); and the role of motor rehabilitation (III). **(C)** Timeline of the study. **(D)** An example of somatosensory evoked potentials (SSEP) recorded with stimulation of the n. Tibialis with recording electrodes located at the Cz-Fpz, Th8-9, Th11-12, L2-3, and popliteal region. Average of 800 responses presented for each location. Gray circles indicate the SSEP at the Th11-12, L2-3, and popliteal region. **(E)** SSEP amplitude at popliteal region, L2-3, and Th11-12 level during stimulation on the right and left n. Tibialis (n = 3).

Th8-9 and Cz-Fpz levels located above the SCI (**Figure 1D**, two uppermost traces).

Evaluation of Spinally Evoked Motor Potentials at Different Spinal Levels

Figure 2 demonstrates examples of the SEMP in m. rectus femoris (RF) and m. tibialis anterior (TA) obtained at different stimulation intensities (**Figure 2A**) with threshold, amplitude values, and latency of the SEMP (**Figure 2B**) during tSCS at Th9-10, Th10-11, Th11-12, Th12-L1, and L1-2 levels (obtained at 100 mA). The order of activation of different muscles was dependent on the rostrocaudal location of stimulating electrodes. The stimulation intensity required to reach the motor threshold was gradually decreased from Th9-10 and Th10-11 to L1-2 in proximal and in distal muscles (n = 6, $p < 0.05$). In both distal and proximal muscles, the maximal amplitude of SEMP was gradually increased from T9-10 level reaching the highest value at T12-L1 and then decreased at the L1-2 level (n = 6, $p < 0.05$) (**Figure 2B**). The SEMP average latencies for the distal muscles were 14.90 ± 0.50 ms for the TA, 15.28 ± 0.52 ms for the SOL, 10.53 ± 0.43 ms for the RF and 10.27 ± 0.11 ms for the MH (n = 5). The SEMP latency was compatible with the distance between the stimulation level and the muscle and was larger in TA and m. soleus (SOL) and shorter in proximal muscles

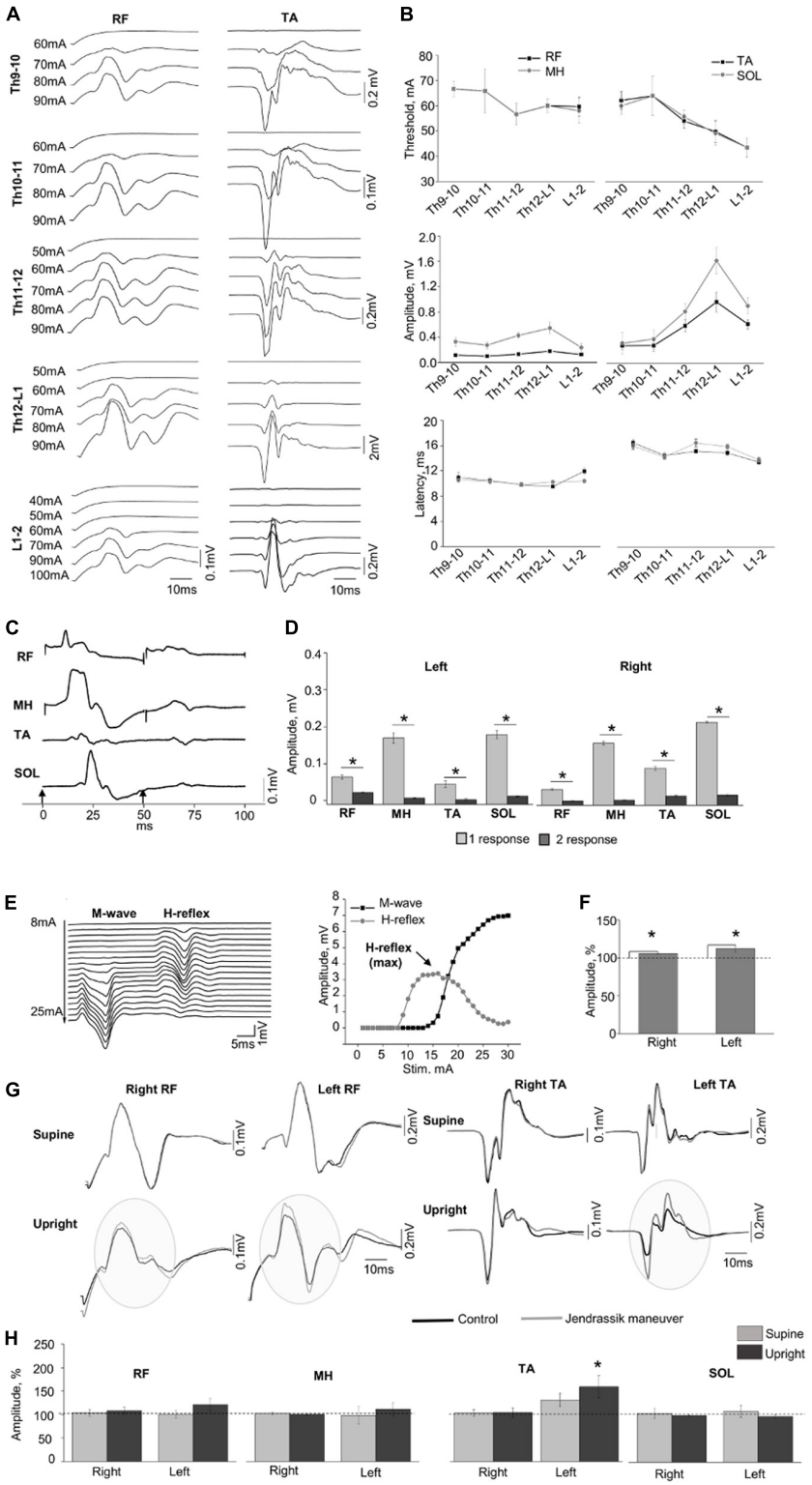

FIGURE 2 | (A) Examples of SEMP recorded from proximal (RF) and distal (TA) muscles during stimulation at Th9-10, Th10-11, Th11-12, Th12-L1, and L1-2 levels, in supine position. **(B)** Changes in the thresholds, maximal amplitudes, and the latency of the SEMP recorded from proximal (RF and MH) and distal (TA, SOL) muscles with stimulation applied at Th9-10, Th10-11, Th11-12, Th12-L1, and L1-2 levels. **(C)** Examples of the SEMP recorded from RF, MH, TA, and SOL with

(Continued)

FIGURE 2 | Continued
paired pulses stimulation (interstim interval of 50 ms) at Th11-12 level. Black arrow indicate the moment of the stim. **(D)** The amplitudes of the SEMP recorded from right and left side during paired stimulation at Th11-12 level. **(E)** Examples of M wave and H-reflex recorded form SOL muscle at stimulation intensity varied from 8 to 25 mA with increment of 1 mA. Recruitment curves of the M wave (black line) and the H-reflex (light gray line) presented on the right. **(F)** The amplitudes (%) of the H-reflex recorded from right and left side (n = 10) during performance of Jendrassik maneuver (gray bars). Dotted lines indicate the control values of the H-reflex (100%). **(G)** Examples of the SEMP recorded from RF and TA during stimulation at Th12-L1 without (black line) and with Jendrassik maneuver (gray line) in supine and in upright (less than 30% body weight support) positions. Gray circles indicate the facilitation of the SEMP bilaterally RF, and in left TA by Jendrassik maneuver. **(H)** The amplitudes (%) of the SEMP recorded from right and left proximal (RF and MH) and distal muscles (TA and SOL) with stimulation at Th12-L1 during performance of Jendrassik maneuver in supine (light gray) and upright (less than 30% body weight support) positions (dark gray) in subject with SCI (n = 4). Dotted lines indicate the control values of the SEMP (100%). Difference marked with an asterisk indicates significance (*$p < 0.05$).

RF and medial hamstring (MH) (**Figure 2B**). The maximal amplitudes of SEMP for proximal muscles were significantly lower compared to distal muscles ($n = 4$, $p < 0.05$). Examples of SEMPs recorded with paired tSCS at Th11-12 level are presented on **Figure 2C**. It is evident that the SEMPs were depressed with paired spinal cord stimulation (see more method details in **Supplementary Material**), supporting the reflex nature of the observed responses ($n = 6$, $p < 0.05$) (**Figure 2D**).

Evaluation of the Supraspinal-Spinal Connectivity

The M-wave and the H-reflex were recorded in SOL muscle (**Figure 2E**). During the JM the amplitude of H-reflex increased to 106.02 ± 0.94% and 111.43 ± 1.84% from control 100% values for the right and left leg, respectively ($n = 10$, $p < 0.05$) (**Figure 2F**). **Figure 2G** demonstrates examples of changes in the amplitude of SEMP recorded from RF and TA muscles without and with the JM, tested in supine and upright positions during the spinal cord stimulation at Th12-L1 level. Amplitude of the SEMP during JM was significantly facilitated in the left TA to 153.17 ± 22.45% from control 100% values only in upright position ($n = 4$, $p < 0.05$) (**Figures 2G,H**, Upright). In other muscles, JM did not change SEMP for either right or left leg (**Figure 2H**). Amplitudes of SEMP during JM with respect to the control condition were to 103.91 ± 7.14% (supine), and to 108.14 ± 7.79% (upright); in left RF to 101.09 ± 7.90% and to 121.10 ± 13.35%; in right MH to 102.83 ± 2.73% and to 100.87 ± 1.95%; in left MH to 98.53 ± 18.39% and to 111.43 ± 14.76%; in right TA to 102.65 ± 3.04% and 104.51 ± 8.64; in left TA to 129.16 ± 14.15% (supine); in right SOL to 104.28 ± 11.09% and to 99.67 ± 1.55%; in left SOL to 108.45 ± 12.70% and to 97.46 ± 3.81%; from control 100% values. In addition, delayed motor response with great toe extension was repeatedly observed on the right and left leg during JM only in vertically suspended (**Supplementary Video S1**).

The Effect of Rehabilitation Therapy on SEMP

Figure 3A shows examples of SEMP in TA muscle, evoked by stimulation of Th11-12 in supine position (supine) and immediately following the first verticalization (upright) before (gray lines) and after 16 weeks of rehabilitation therapy (black lines). Changes in SEMP (amplitude and threshold) before and after rehabilitation therapy in the supine position presented on **Figure 3C**. Maximum values of monosynaptic SEMP component in distal muscles before rehabilitation therapy were significantly lower compared to the amplitudes of SEMP after rehabilitation therapy ($n = 4$, $p < 0.05$) (**Figure 3C**). After subject with SCI underwent rehabilitation therapy, the thresholds of SEMP significantly decreased in all muscles ($n = 4$, $p < 0.05$) (**Figure 3C**). Polysynaptic components of the SEMP were found in TA muscle after rehabilitation therapy particularly in upright position. The cumulative analyses of latencies of LR demonstrated that the latencies of the polysynaptic components had wider distribution after rehabilitation therapy in upright position and mostly in TA (**Figure 3A**, Upright, and **Figure 3D**).

DISCUSSION

In this study we evaluated the influence of supraspinal and afferent information on sub-lesional spinal circuitry excitability in subject with AIS-A SCI. The results demonstrate: (1) body position can change the excitability of spinal circuitry and, in combination with reinforcement (Jendrassik) maneuvers, facilitate sub-functional connectivity, indicating the discompleteness of injury; (2) the effect of motor rehabilitation therapy on spinal circuitry excitability with respect to SEMP (**Figure 1A**).

Assessment of SEMP After SCI in Lumbosacral Level

Considering the importance of the functional state of sublesional circuitry in evaluation of spared subfunctional fibers, we hypothesized that the characteristics of SEMP with tSCS can indicate excitability across several spinal cord segments (Minassian et al., 2007; Dy et al., 2010) and, accordingly, provide detailed information on motoneuronal pools related to multiple muscles (Courtine et al., 2007). The results of this case report, combined with previous reports (Troni et al., 2011; Roy et al., 2012; Krenn et al., 2013; Sayenko et al., 2015) suggest that, the tSCS at different spinal levels can modulate the activation order of proximal and distal muscles. The different latency of proximal (RF and MH) and distal muscles (TA and SOL) can be explained by the difference in anatomical distribution of the motor pools and the distance between the place of stimulation and muscle. The amplitude of the SEMP with caudal shifting of the stimulation electrodes was gradually increased in distal muscles, meanwhile proximal muscled showed minimal changes in amplitude compared to the amplitude of response in distal muscles that can be explained by subject's injury level (Th11). Also, the activation order of proximal and distal muscles could be related to different localization of motoneuronal pools

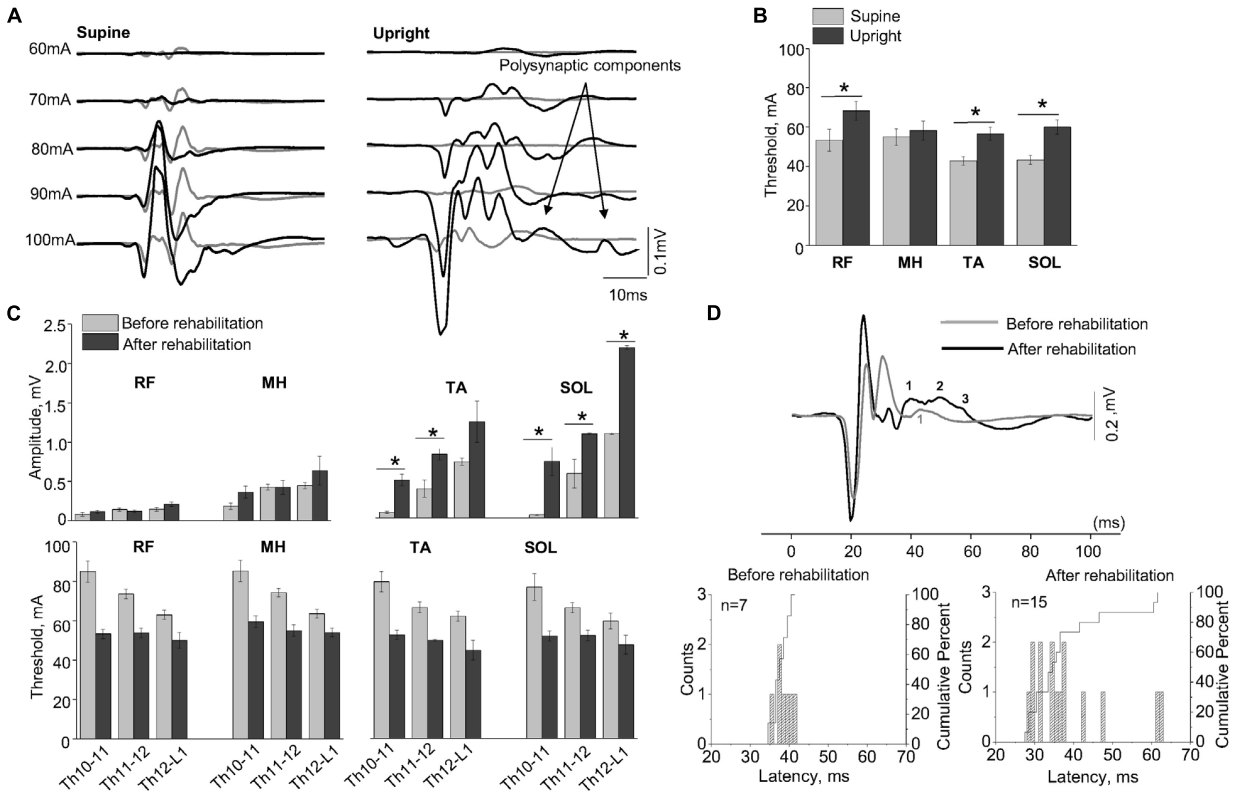

FIGURE 3 | (A) Examples of the SEMP recorded from TA muscle during stimulation at Th11-12 level in supine and upright (less than 30% body weight support) positions after the first verticalization before (gray lines) and after rehabilitation therapy (black lines). **(B)** The thresholds of the SEMP recorded in supine (gray lines) and upright (less than 30% body weight support) position after the first verticalization (black lines) in TA, SOL, RF, and MH (n = 6). **(C)** Changes in amplitude and threshold of SEMP recorded from RF, MH, TA, and SOL in supine position before (gray) and after (black) rehabilitation therapy (n = 4). **(D)** Example of the SEMP recorded from TA during stimulation at Th11-12 level in upright position (less than 30% body weight support) before (gray line) and after rehabilitation therapy (black line). The black and gray numbers indicate the number of polysynaptic components of the SEMP. Histograms and cumulative percentage of latencies (ms) of polysynaptic components of the SEMP recorded from TA before and after rehabilitation. Counts – frequency of occurrence of latencies of LR in interval of 1 ms. Cumulative percent – cumulative percentage of frequency of occurrence of latencies of LR in interval of 1 ms. Difference marked with an asterisk indicates significance (*$p < 0.05$).

(Phillips and Park, 1991) or current flow passage across several layers of back and spine tissues and anatomical curvatures (Hofstoetter et al., 2014).

The Role of the Supraspinal and Afferent Information in Assessment of SCI

The Influence of Reinforcement Maneuvers on H-Reflex and SEMP

Previous studies indicated that supraspinal influence may have different effect on motoneurons and interneurons (Sabatino et al., 1995) and, therefore, modulation of mono- and polysynaptic responses can be a sensitive assessment tool of the spinal cord circuitry functional state after SCI. Given the nature of the H-reflex and the reflex components of the SEMP, it can be expected that the JM contribute in activation of downstream effects on spinal neuronal circuit. JM (Jendrassik, 1883), was used as a reinforcement to study spinal cord evoked responses in control subjects and in subjects with SCI (Dimitrijevic et al., 1977). One of the possible mechanisms of the effect of JM on spinal cord excitability was related to reduction of segmental presynaptic inhibition (Zehr and Stein, 1999). Our results indicate that JM can alter the H-reflex in supine position and SEMP in upright positioning the subject with discomplete SCI. At the same time, SEMP were affected primary in the left TA. As opposed to the SOL H-reflex, which is a monosynaptic response in a single muscle, the SEMP evoked by tSCS is related to a complex spinal network. Thus, facilitation of SEMP during JM may reflect the results of complex intraspinal and intersegmental interaction compared to monosynaptic response related to a single motor pool during H-reflex.

The Influence of the Positional Changes on the SEMP

The SEMP were previously studied applying tSCS in healthy subjects and in subjects with SCI, tested in various positions: supine (Minassian et al., 2007; Hofstoetter et al., 2018), upright, and during gait modulation (Minassian et al., 2015). It was demonstrated that in individuals with AIS-A and-B positional changes (supine vs. standing) can provide different

modulation of SEMPs components (Sayenko et al., 2014). In this study, transition from supine to upright position facilitated the amplitude of SEMP components that could be related to changes in sensory information from mechanoreceptors affecting the spinal circuitry excitability (Harkema et al., 1997). Presynaptic inhibition of Ia afferents on the motoneuron is considered to be controlled by descending tracts and the level of presynaptic inhibition input in SCI subjects declines compared to control subjects, contributing to enhancement of spinal reflexes (Calancie et al., 1993). The body position could influence the activation of the afferent and efferent fibers by tSCS (Danner et al., 2016). In contrast to our results, Danner et al. (2016) showed that the thresholds of evoked responses in subjects with intact spinal cord were lowest in upright position and highest in the prone position (Danner et al., 2016). Variations in mono- and polysynaptic responses during tSCS can be related to motoneuronal excitability and also to complex convergence of sensory afferents on spinal reflex pathways (Schomburg, 1990; Sayenko et al., 2014). It was suggested that the afferent information can be integrated by spinal circuitry and result in elevation interneuronal excitability during standing (Harkema et al., 2011; Rejc et al., 2015). Also, Sayenko et al. (2019) demonstrated that tSCS can modulate the lumbosacral spinal networks to facilitate postural control after SCI (Sayenko et al., 2019). Therefore, the characteristics of SEMP cannot be attributed only to a certain motor pools related to the spinal cord circuitry, but rather to specific interplay of multiple peripheral sensory resources and related interneurons (Sayenko et al., 2014). These results indicate that positional changes can facilitate lumbosacral networks and increase the sensitivity of electrophysiological testing for the residual sub- functional connections after SCI.

Assessment of SEMP After Motor Rehabilitation Therapy

Complete paralysis of the lower extremities and ability to stand and perform coordinated motor activity could be improved with epidural electrical stimulation (Harkema et al., 2011; Grahn et al., 2017; Gill et al., 2018; Wagner et al., 2018). Our results demonstrate that rehabilitation therapy can facilitate SEMP components, observed after 16-week rehabilitation program in supine and upright positions. It is noteworthy that facilitation of the late response in calf muscles was found in upright position. Similar to animal studies, initiation of rhythmic activity after SCI in human was associated with appearance of late responses (Minassian et al., 2004). As it has been shown earlier, the task-specific training with epidural SCS may reactivate previously silent neural circuits or promote plasticity (Harkema et al., 2011). In addition, tSCS, as well as epidural SCS, can modulate spinal circuitry in humans after SCI that enables sensory inputs to serve as a primary source of neural control of posture and balance (Sayenko et al., 2019). Decreased threshold and increased reflex excitation may be indicative for an increased spasticity. The presence of spasticity below the level of injury in patients with SCI could indicate that related motor pools are relatively preserved (Harris et al., 2007; Gorgey and Dudley, 2008), at the same time, characteristics of SEMP cannot be attributed only to the level of the spinal circuitry excitation and could be a consequence of interplay of multiple peripheral afferent signals and related interneurons (Sayenko et al., 2014). Findings of multiple studies suggest that spinal reflexes increase in patients with SCI and cannot be evaluated unambiguously. Particularly in this study, an increase of the motoneurons' excitability was not clearly related to spasticity.

LIMITATIONS

The key limitation of this research is that data were collected from one research participant. Another factor that should be considered in this study, is the titanium construction implanted for vertebras fixations that could influence the electrical field and alter the physiological effects of the stimulation. There is a shortage of studies providing the evidence of influence the implanted materials on electrophysiological outcomes. Potential influence of the metal construction should be considered when using tSCS in SCI patients and further electrophysiological and computer simulation studies are required to investigate this in detail.

CONCLUSION

The results of this work demonstrate that the afferent flow during positional tests and rehabilitation therapy can provide necessary excitation of spinal cord circuitries, helping in identification of neural connections, which can be further enhanced with rehabilitation and neuromodulation therapy. Considering that up to 80–90% of patients with clinically complete SCI have discomplete injury (Moss et al., 2011), it is expected that results of this study will provide significant background for a larger SCI population. The results of this case report emphasize the importance of evaluation with positional changes and reinforcement maneuvers during the assessment of SCI and could be important for future clinical trials and for assessments of patients with clinically complete SCI.

DATA AVAILABILITY STATEMENT

All datasets generated for this study are included in the article/**Supplementary Material**.

ETHICS STATEMENT

The studies involving human participants were reviewed and approved by Kazan Federal University Institutional Review Board (Review board decision December 4th, 2017, protocol No. 7). The patients/participants provided their written informed consent to participate in this study. Written informed consent was obtained from the individual(s) for the publication of any potentially identifiable images or data included in this article.

AUTHOR CONTRIBUTIONS

AM and IL designed model framework. AM, EF, SS, and IL conducted the data collection and electrophysiology experiments. AM, EM, CC, JC, PG, TB, and IL analyzed the data and worked on the manuscript. IL approved the final version of the manuscript. All authors read and helped to improve the manuscript.

FUNDING

This work was performed according to the Russian Government Program of Competitive Growth of Kazan Federal University. Additional funding was provided by the subsidy allocated to Kazan Federal University for the state assignment in the sphere of scientific activities no. 7.9783.2017/8.9.

ACKNOWLEDGMENTS

The authors thank Dr. Gusel Yafarova and Dr. Dinara Silantyeva at the Kazan Federal University for providing valuable suggestions during the manuscript writing and proofreading process.

SUPPLEMENTARY MATERIAL

The Supplementary Material for this article can be found online at: https://www.frontiersin.org/articles/10.3389/fnins.2020.00552/full#supplementary-material

VIDEO S1 | Effect of Jendrassik maneuver on toes movements in supine and vertically suspended (100% body weight support).

REFERENCES

Apte, S., Plooij, M., and Vallery, H. (2018). Influence of body weight unloading on human gait characteristics: a systematic review. *J. Neuroeng. Rehabil.* 15:53. doi: 10.1186/s12984-018-0414-7

Awad, A., Levi, R., Lindgren, L., Hultling, C., Westling, G., Nyberg, L., et al. (2015). Preserved somatosensory conduction in a patient with complete cervical spinal cord injury. *J. Rehabil. Med.* 47, 426–431. doi: 10.2340/16501977-1955

Calancie, B., Broton, J. G., Klose, K. J., Traad, M., Difini, J., and Ayyar, D. R. (1993). Evidence that alterations in presynaptic inhibition contribute to segmental hypo- and hyperexcitability after spinal cord injury in man. *Electroencephalogr. Clin. Neurophysiol.* 89, 177–186. doi: 10.1016/0168-5597(93)90131-8

Courtine, G., Harkema, S. J., Dy, C. J., Gerasimenko, Y. P., and Dyhre-Poulsen, P. (2007). Modulation of multisegmental monosynaptic responses in a variety of leg muscles during walking and running in humans. *J. Physiol.* 582, 1125–1139. doi: 10.1113/jphysiol.2007.128447

Cuellar, C. A., Mendez, A. A., Islam, R., Calvert, J. S., Grahn, P. J., Knudsen, B., et al. (2017). The role of functional neuroanatomy of the lumbar spinal cord in effect of epidural stimulation. *Front. Neuroanat.* 11:82. doi: 10.3389/fnana.2017.00082

Danner, S. M., Krenn, M., Hofstoetter, U. S., Toth, A., Mayr, W., and Minassian, K. (2016). Body position influences which neural structures are recruited by lumbar transcutaneous spinal cord stimulation. *PLoS One* 11:e0147479. doi: 10.1371/journal.pone.0147479

Dimitrijevic, M. R., Dimitrijevic, M. M., Faganel, J., and Sherwood, A. M. (1984). Suprasegmentally induced motor activity in paralyzed muscles of patients with established spinal cord injury. *Ann. Neurol.* 16, 216–221. doi: 10.1002/ana.410160208

Dimitrijevic, M. R., Gerasimenko, Y., and Pinter, M. M. (1998). Evidence for a spinal central pattern generator in humans. *Ann. N. Y. Acad. Sci.* 860, 360–376. doi: 10.1111/j.1749-6632.1998.tb09062.x

Dimitrijevic, M. R., Halter, J. A., Sharkey, P. C., and Sherwood, A. M. (1987). Epidural spinal cord stimulation and carry-over effect in chronic spinal cord injury patients. *Appl. Neurophysiol.* 50, 449–450. doi: 10.1159/000100761

Dimitrijevic, M. R., Spencer, W. A., Trontelj, J. V., and Dimitrijevic, M. (1977). Reflex effects of vibration in patients with spinal cord lesions. *Neurology* 27, 1078–1086. doi: 10.1212/WNL.27.11.1078

Dy, C. J., Gerasimenko, Y. P., Edgerton, V. R., Dyhre-Poulsen, P., Courtine, G., and Harkema, S. J. (2010). Phase-dependent modulation of percutaneously elicited multisegmental muscle responses after spinal cord injury. *J. Neurophysiol.* 103, 2808–2820. doi: 10.1152/jn.00316.2009

Gerasimenko, Y. P., Avelev, V. D., Nikitin, O. A., and Lavrov, I. A. (2001). Initiation of locomotor activity in spinalized cats by epidural stimulation of the spinal cord. *Ross. Fiziol. Zh. Im. I M Sechenova.* 87, 1161–1170.

Gerasimenko, Y., Sayenko, D., Gad, P., Liu, C. T., Tillakaratne, N. J. K., Roy, R. R., et al. (2017). Feed-forwardness of spinal networks in posture and locomotion. *Neuroscientist* 23, 441–453. doi: 10.1177/1073858416683681

Gerasimenko, Y. P., Lu, D. C., Modaber, M., Zdunowski, S., Gad, P., Sayenko, D. G., et al. (2015). Noninvasive reactivation of motor descending control after paralysis. *J. Neurotrauma* 32, 1968–1980. doi: 10.1089/neu.2015.4008

Gill, M. L., Grahn, P. J., Calvert, J. S., Linde, M. B., Lavrov, I. A., Strommen, J. A., et al. (2018). Neuromodulation of lumbosacral spinal networks enables independent stepping after complete paraplegia. *Nat. Med.* 24, 1677–1682. doi: 10.1038/s41591-018-0175-7

Gorgey, A. S., and Dudley, G. A. (2008). Spasticity may defend skeletal muscle size and composition after incomplete spinal cord injury. *Spinal Cord* 46, 96–102. doi: 10.1038/sj.sc.3102087

Grahn, P. J., Lavrov, I. A., Sayenko, D. G., Van Straaten, M. G., Gill, M. L., Strommen, J. A., et al. (2017). Enabling task-specific volitional motor functions via spinal cord neuromodulation in a human with paraplegia. *Mayo Clin. Proc.* 92, 544–554. doi: 10.1016/j.mayocp.2017.02.014

Harkema, S., Gerasimenko, Y., Hodes, J., Burdick, J., Angeli, C., Chen, Y., et al. (2011). Effect of epidural stimulation of the lumbosacral spinal cord on voluntary movement, standing, and assisted stepping after motor complete paraplegia: a case study. *Lancet* 377, 1938–1947. doi: 10.1016/S0140-6736(11)60547-3

Harkema, S. J., Hurley, S. L., Patel, U. K., Requejo, P. S., Dobkin, B. H., and Edgerton, V. R. (1997). Human lumbosacral spinal cord interprets loading during stepping. *J. Neurophysiol.* 77, 797–811. doi: 10.1152/jn.1997.77.2.797

Harris, R. L. W., Putman, C. T., Rank, M., Sanelli, L., and Bennett, D. J. (2007). Spastic tail muscles recover from myofiber atrophy and myosin heavy chain transformations in chronic spinal rats. *J. Neurophysiol.* 97, 1040–1051. doi: 10.1152/jn.00622.2006

Hofstoetter, U. S., Danner, S. M., and Minassian, K. (2014). "Paraspinal magnetic and transcutaneous electrical stimulation," in *Encyclopedia of Computational Neuroscience*, eds D. Jaeger and R. Jung (New York, NY: Springer), 1–21. doi: 10.1007/978-1-4614-6675-8

Hofstoetter, U. S., Freundl, B., Binder, H., and Minassian, K. (2018). Common neural structures activated by epidural and transcutaneous lumbar spinal cord stimulation: elicitation of posterior root-muscle reflexes. *PLoS One* 13:e0192013. doi: 10.1371/journal.pone.0192013

Islam, R., Cuellar, C. A., Felmlee, B., Riccelli, T., Silvernail, J., Boschen, S. L., et al. (2019). Multifactorial motor behavior assessment for real-time evaluation of emerging therapeutics to treat neurologic impairments. *Sci. Rep.* 9, 1–16. doi: 10.1038/s41598-019-52806-1

Jendrassik, E. (1883). Beitrag, zur Lehre von den Sehnenreflexen. *Dtsch. Arch. Klin. Med.* 33, 177–199.

Kakulas, A. (1988). The applied neurobiology of human spinal cord injury: a review. *Paraplegia* 26, 371–379. doi: 10.1038/sc.1988.57

Kirshblum, S. C., Biering-Sørensen, F., Betz, R., Burns, S., Donovan, W., Graves, D. E., et al. (2014). International standards for neurological classification of spinal cord injury: cases with classification challenges.

Top. Spinal Cord Inj. Rehabil. 20, 81–89. doi: 10.1179/2045772314Y.0000000196

Krenn, M., Toth, A., Danner, S. M., Hofstoetter, U. S., Minassian, K., and Mayr, W. (2013). Selectivity of transcutaneous stimulation of lumbar posterior roots at different spinal levels in humans. *Biomed. Tech.* 58(Suppl. 1):1. doi: 10.1515/bmt-2013-4010

Kumar, R., Lim, J., Mekary, R. A., Rattani, A., Dewan, M. C., Sharif, S. Y., et al. (2018). Traumatic spinal injury: global epidemiology and worldwide volume. *World Neurosurg.* 113, 345–363. doi: 10.1016/j.wneu.2018.02.033

Lavrov, I., Dy, C. J., Fong, A. J., Gerasimenko, Y., Courtine, G., Zhong, H., et al. (2008). Epidural stimulation induced modulation of spinal locomotor networks in adult spinal rats. *J. Neurosci.* 28, 6022–6029. doi: 10.1523/JNEUROSCI.0080-08.2008

Lavrov, I., Gerasimenko, Y., Burdick, J., Zhong, H., Roy, R. R., and Edgerton V. R. (2015). Integrating multiple sensory systems to modulate neural networks controlling posture. *J. Neurophysiol.* 114, 3306–3314. doi: 10.1152/jn.00583.2015

Lavrov, I., Gerasimenko, Y. P., Ichiyama, R. M., Courtine, G., Zhong, H., Roy, R. R., et al. (2006). Plasticity of spinal cord reflexes after a complete transection in adult rats: relationship to stepping ability. *J. Neurophysiol.* 96, 1699–1710. doi: 10.1152/jn.00325.2006

Minassian, K., Hofstoetter, U. S., Danner, S. M., Mayr, W., Bruce, J. A., McKay, W. B., et al. (2015). Spinal rhythm generation by step-induced feedback and transcutaneous posterior root stimulation in complete spinal cord-injured individuals. *Neurorehabil. Neural Repair* 30, 233–243. doi: 10.1177/1545968315591706

Minassian, K., Jilge, B., Rattay, F., Pinter, M. M., Binder, H., Gerstenbrand, F., et al. (2004). Stepping-like movements in humans with complete spinal cord injury induced by epidural stimulation of the lumbar cord: electromyographic study of compound muscle action potentials. *Spinal Cord* 42, 401–416. doi: 10.1038/sj.sc.3101615

Minassian, K., McKay, W. B., Binder, H., and Hofstoetter, U. S. (2016). Targeting lumbar spinal neural circuitry by epidural stimulation to restore motor function after spinal cord injury. *Neurotherapeutics* 13, 284–294. doi: 10.1007/s13311-016-0421-y

Minassian, K., Persy, I., Rattay, F., Dimitrijevic, M. R., Hofer, C., and Kern, H. (2007). Posterior root–muscle reflexes elicited by transcutaneous stimulation of the human lumbosacral cord. *Muscle Nerve* 35, 327–336. doi: 10.1002/mus.20700

Moss, C. W., Kilgore, K. L., and Peckham, P. H. (2011). A novel command signal for motor neuroprosthetic control. *Neurorehabil. Neural Repair* 25, 847–854. doi: 10.1177/1545968311410067

Nicotra, A., and Ellaway, P. H. (2006). Thermal perception thresholds: assessing the level of human spinal cord injury. *Spinal Cord* 44, 617–624. doi: 10.1038/sj.sc.3101877

Phillips, L. H., and Park, T. S. (1991). Electrophysiologic mapping of the segmental anatomy of the muscles of the lower extremity. *Muscle Nerve* 14, 1213–1218. doi: 10.1002/mus.880141213

Rejc, E., Angeli, C., and Harkema, S. (2015). Effects of lumbosacral spinal cord epidural stimulation for standing after chronic complete paralysis in humans. *PLoS One*. 10:e0133998. doi: 10.1371/journal.pone.0133998

Roy, F. D., Gibson, G., and Stein, R. B. (2012). Effect of percutaneous stimulation at different spinal levels on the activation of sensory and motor roots. *Exp. Brain Res.* 223, 281–289. doi: 10.1007/s00221-012-3258-6

Sabatino, M., Sardo, P., Iurato, L., and La Grutta, V. (1995). Cortical stimulation and reflex excitability of spinal cord neurones in man. *J. Neural. Transm. Gen. Sect.* 101, 159–168. doi: 10.1007/BF01271553

Sayenko, D. G., Angeli, C., Harkema, S. J., Edgerton, V. R., and Gerasimenko, Y. P. (2014). Neuromodulation of evoked muscle potentials induced by epidural spinal-cord stimulation in paralyzed individuals. *J. Neurophysiol.* 111, 1088–1099. doi: 10.1152/jn.00489.2013

Sayenko, D. G., Atkinson, D. A., Dy, C. J., Gurley, K. M., Smith, V. L., Angeli, C., et al. (2015). Spinal segment-specific transcutaneous stimulation differentially shapes activation pattern among motor pools in humans. *J. Appl. Physiol.* 118, 1364–1374. doi: 10.1152/japplphysiol.01128.2014

Sayenko, D. G., Rath, M., Ferguson, A. R., Burdick, J. W., Havton, L. A., Edgerton, V. R., et al. (2019). Self-assisted standing enabled by non-invasive spinal stimulation after spinal cord injury. *J. Neurotrauma* 36, 1435–1450. doi: 10.1089/neu.2018.5956

Schomburg, E. D. (1990). Spinal sensorimotor systems and their supraspinal control. *Neurosci. Res.* 7, 265–340. doi: 10.1016/0168-0102(90)90008-3

Shah, P., and Lavrov, I. (2017). Spinal epidural stimulation strategies: clinical implications of locomotor studies in spinal rats. *Neuroscientist* 23, 664–680. doi: 10.1177/1073858417699554

Taccola, G., Sayenko, D., Gad, P., Gerasimenko, Y., and Edgerton, V. R. (2018). And yet it moves: recovery of volitional control after spinal cord injury. *Prog. Neurobiol.* 160, 64–81. doi: 10.1016/j.pneurobio.2017.10.004

Troni, W., Di Sapio, A., Berra, E., Duca, S., Merola, A., Sperli, F., et al. (2011). A methodological reappraisal of non-invasive high voltage electrical stimulation of lumbosacral nerve roots. *Clin. Neurophysiol.* 122, 2071–2080. doi: 10.1016/j.clinph.2011.03.002

Wagner, F. B., Mignardot, J. B., Le Goff-Mignardot, C. G., Demesmaeker, R., Komi, S., Capogrosso, M., et al. (2018). Targeted neurotechnology restores walking in humans with spinal cord injury. *Nature* 563, 65–71. doi: 10.1038/s41586-018-0649-2

Zehr, E. P., and Stein, R. B. (1999). Interaction of the Jendrassik maneuver with segmental presynaptic inhibition. *Exp. Brain Res.* 124, 474–480. doi: 10.1007/s002210050643

Conflict of Interest: The authors declare that the research was conducted in the absence of any commercial or financial relationships that could be construed as a potential conflict of interest.

frontiers in Systems Neuroscience

ORIGINAL RESEARCH
published: 30 June 2020
doi: 10.3389/fnsys.2020.00035

Long-Term Spinal Cord Stimulation After Chronic Complete Spinal Cord Injury Enables Volitional Movement in the Absence of Stimulation

*Isabela Peña Pino[1], Caleb Hoover[2], Shivani Venkatesh[2], Aliya Ahmadi[2], Dylan Sturtevant[2], Nick Patrick[1], David Freeman[2], Ann Parr[2], Uzma Samadani[3,4], David Balser[5], Andrei Krassioukov[5], Aaron Phillips[6], Theoden I. Netoff[1] and David Darrow[2,7]**

[1] Department of Biomedical Engineering, University of Minnesota, Minneapolis, MN, United States, [2] Department of Neurosurgery, University of Minnesota, Minneapolis, MN, United States, [3] Department of Bioinformatics and Computational Biology, University of Minnesota, Minneapolis, MN, United States, [4] Division of Neurosurgery, VA Healthcare System, Minneapolis, MN, United States, [5] International Collaboration on Repair Discoveries, Division of Physical Medicine and Rehabilitation, University of British Columbia, Vancouver, BC, Canada, [6] Department of Physiology and Pharmacology, Cumming School of Medicine, University of Calgary, Calgary, AB, Canada, [7] Division of Neurosurgery, Hennepin County Medical Center, Minneapolis, MN, United States

OPEN ACCESS

Edited by:
Ronaldo M. Ichiyama, University of Leeds, United Kingdom

Reviewed by:
Karen Minassian, Medical University of Vienna, Austria
Jamie Lynn Reed, Vanderbilt University Institute of Imaging Science, United States

***Correspondence:**
David Darrow
darro015@umn.edu

Received: *21 March 2020*
Accepted: *18 May 2020*
Published: *30 June 2020*

Citation:
Peña Pino I, Hoover C, Venkatesh S, Ahmadi A, Sturtevant D, Patrick N, Freeman D, Parr A, Samadani U, Balser D, Krassioukov A, Phillips A, Netoff TI and Darrow D (2020) Long-Term Spinal Cord Stimulation After Chronic Complete Spinal Cord Injury Enables Volitional Movement in the Absence of Stimulation. Front. Syst. Neurosci. 14:35. doi: 10.3389/fnsys.2020.00035

Background: Chronic spinal cord injury (SCI) portends a low probability of recovery, especially in the most severe subset of motor-complete injuries. Active spinal cord stimulation with or without intensive locomotor training has been reported to restore movement after traumatic SCI. Only three cases have been reported where participants developed restored volitional movement with active stimulation turned off after a period of chronic stimulation and only after intensive rehabilitation with locomotor training. It is unknown whether restoration of movement without stimulation is possible after stimulation alone.

Objective: We describe the development of spontaneous volitional movement (SVM) without active stimulation in a subset of participants in the Epidural Stimulation After Neurologic Damage (ESTAND) trial, in which locomotor training is not prescribed as part of the study protocol, and subject's rehabilitation therapies are not modified.

Methods: Volitional movement was evaluated with the Brain Motor Control Assessment using sEMG recordings and visual examination at baseline and at follow-up visits with and without stimulation. Additional functional assessment with a motor-assisted bicycle exercise at follow-up with and without stimulation identified generated work with and without effort.

Results: The first seven participants had ASIA Impairment Scale (AIS) A or B thoracic SCI, a mean age of 42 years, and 7.7 years post-injury on average. Four patients developed evidence of sustained volitional movement, even in the absence of active stimulation after undergoing chronic epidural spinal cord stimulation (eSCS). Significant increases in volitional power were found between those observed to spontaneously

move without stimulation and those unable ($p < 0.0005$). The likelihood of recovery of spontaneous volitional control was correlated with spasticity scores prior to the start of eSCS therapy ($p = 0.048$). Volitional power progressively improved over time ($p = 0.016$). Additionally, cycling was possible without stimulation ($p < 0.005$).

Conclusion: While some SVM after eSCS has been reported in the literature, this study demonstrates sustained restoration without active stimulation after long-term eSCS stimulation in chronic and complete SCI in a subset of participants. This finding supports previous studies suggesting that "complete" SCI is likely not as common as previously believed, if it exists at all in the absence of transection and that preserved pathways are substrates for eSCS-mediated recovery in clinically motor-complete SCI.

Clinical Trial Registration: www.ClinicalTrials.gov, identifier NCT03026816.

Keywords: spinal cord injury, spinal cord stimulation, volitional movement, traumatic spinal cord injury, neuromodulation, human

INTRODUCTION

Almost 800,000 people suffer from traumatic spinal cord injury (SCI) worldwide every year (Kumar et al., 2018). While some recovery is expected after acute SCI, chronic SCI carries a stable prognosis with low probability of recovery. After the first year of injury, less than 2% of patients with motor complete spinal injury will become incomplete by the fifth year after injury (Kirshblum et al., 2004). Interventions for chronic complete SCI generally focus on the medical management of SCI-related complications, therapies to prevent musculoskeletal deterioration, and to provide adaptive strategies. Currently, predictors of neurological recovery in the acute phase include initial neurological status, incomplete injuries, and presence of a zone of partial preservation on imaging studies in complete injuries (Wilson et al., 2012). Only intensive neurorehabilitative therapies, such as body weight-supported treadmill training, have level 3 evidence for improving functional ambulation in chronic SCI, and this likelihood is greater in motor incomplete injuries (Lam et al., 2007).

Epidural spinal cord stimulation (eSCS, SCS, or estim) has long been used for the treatment of chronic pain (Shealy et al., 1967) and is originally based on Melzack and Wall's (1965) gate control theory for peripheral neuromodulation of pain perception. As a neuromodulation platform capable of stimulating the central and peripheral nervous system, the therapeutic application of eSCS has been attempted on multiple fronts including Parkinson's disease, MS, and SCI (Illis et al., 1980; Barolat et al., 1995; de Andrade et al., 2016). Several small clinical reports of spinal cord stimulation after chronic SCI have documented a promising potential to restore volitional movement in an immediate and long-term fashion (Angeli et al., 2018; Gill et al., 2018; Wagner et al., 2018). However, these improvements are achieved only within the context of intensive locomotor training coupled with eSCS.

Abbreviations: BMCA, Brain Motor Control Assessment; eSCS, epidural spinal cord stimulation; ESTAND, Epidural Stimulation After Neurologic Damage; MAS, Modified Ashworth Scale; SVM, Spontaneous Volitional Movement.

The mechanisms by which electrical stimulation restores supraspinal control or modulates the function of the spinal cord remain unclear. Careful electrophysiology during motor-control tasks has revealed subtle supraspinal control in more than 80% of participants with clinically motor-complete injuries (Sherwood et al., 1992), which indicates the presence of clinically silent supraspinal tracts potentially amenable to electrical stimulation. Acutely, epidural electrical stimulation primarily activates monosynaptic reflexes and generates complex burst-like patterns initiated in the dorsal roots, identified as short-latency compound muscle action potentials (Minassian et al., 2004). At a minimum, by activating collateral dorsal root sensory projections, stimulation may modulate the excitability of local circuitry to allow for diminished and quiescent supraspinal activity to exert greater influence.

While the potential biological effects of *chronic* eSCS on the function of injured spinal cords remain unexplored, a few reports exist that highlight the possibility of the development of restored volitional movement even after eSCS is made inactive, usually after months of intensive rehabilitation and stimulation. The progressive development of improved function due to chronic neuromodulation would provide a potentially impactful therapeutic platform. However, it has not been reported without intensive rehabilitation, which requires significant additional cost and dedicated time (French et al., 2007).

The Epidural Stimulation After Neurologic Damage (ESTAND) trial tests the effect of eSCS after motor-complete thoracic SCI on volitional movement and autonomic function without implementing locomotor therapy (Darrow et al., 2019). After several participants unexpectedly began to exhibit clinical evidence of volitional movement *without* active eSCS, results were analyzed to further characterize this phenomenon. Here, we present preliminary analysis of the first seven patients in the trial across clinical observation, electrophysiology, and a functional bicycling task to characterize and compare those who did and did not develop volitional movement during periods without stimulation.

METHODS

Subject Description

All the procedures described in this study were approved by the Hennepin Healthcare Research Institute Institutional Review Board and with an Investigational Device Exemption from the United States Food and Drug Administration. Patients with chronic, traumatic SCI (more than 1 year since injury) were recruited if they met the following criteria: older than 22 years of age, ASIA Impairment Scale (AIS) classification A or B with a neurological level of injury between C6 and T10, full arm and hand strength and intact segmental reflexes below the level of injury. Participants were excluded if they had medical or psychological comorbidities that would significantly increase the risk of surgery, severe dysautonomia (systolic blood pressure fluctuation below 50 or above 200 mmHg) during autonomic testing, contractures, pressure ulcers, recurrent urinary tract infection, unhealed spinal fracture, recent botulinum toxin use, or pregnancy. Once enrolled, subjects were asked to suspend any medications used for spasticity, for example, baclofen and oxybutynin. This analysis includes seven participants that have completed 80% or more of the study. The six participants that have completed the study in its entirety were enrolled for a range of 1.26–1.47 years. Overall, participants had a mean age (±SD) of 42 ± 11.4 years, and a mean time since injury (±SD) of 7.7 ± 4.8 years ranging from 3 to 17 years (**Table 1**). Three of the participants were female, and four were male. Utilizing the International Standards for Neurological Classification of Spinal Cord Injury (ISNCSCI) (Kirshblum et al., 2011), six participants were classified as AIS A, motor and sensory complete, and one subject was classified as AIS B, motor complete, and sensory incomplete. Subclinical motor complete injuries were further confirmed to be electrophysiologically complete with a baseline Brain Motor Control Assessment (BMCA) (Sherwood et al., 1996). All injuries were in the thoracic spine, with two participants at the T4 level, three participants at the T5 level, and two participants at the T8 level. Mechanisms of injury included falls, sports injuries, and motor vehicle accidents (MVA) (**Table 1**). Modified Ashworth Scale (MAS) (Meseguer-Henarejos et al., 2018) scores were collected at baseline before continuous stimulation therapy. A score of 0 to 4 was assigned to four muscle groups of each leg: hamstrings, quadriceps, gastrocnemius, and soleus. These scores were then averaged for a mean lower extremity MAS score. All subjects included in this manuscript completed all 13 follow-up visits, for approximately 1 year, except for subject 7, who had completed 8 follow-up visits or approximately 9 months in the study.

Imaging

All participants provided thoracic spinal cord magnetic resonance imaging (MRI) at screening (**Figure 1**). Post-traumatic spinal cord changes observed on MRI included dorsal tethering, myelomalacia, syrinx, and cystic changes. In order to further categorize SCI severity and atrophy, spinal cord anteroposterior (AP) and transverse diameters were manually measured at C7–T1 (above the injury) and at T9 (below the injury) to assess for spinal cord atrophy (Freund et al., 2010). Both measures were matched to same-level normalized spinal cord diameters from healthy participants (Frostell et al., 2016) and their differences computed for statistical modeling. One subject's MRI (Subject 7) was excluded from statistical analysis because it was obtained during the acute SCI period.

Implantation and Follow-Up

All participants were implanted with an epidural stimulator upon enrollment after baseline data, including a detailed neurological exam and self-reported questionnaires, were collected. Participants underwent epidural placement of a three-column, 16-contact paddle lead through a T11–T12 laminectomy and subcutaneous placement of a primary cell internal pulse generator (IPG) (Tripole and Proclaim Elite, Abbott, Plano, TX, United States) in the lower lumbar area under general anesthesia (**Figure 2**). Intraoperative needle electromyogram (EMG) guided optimal paddle placement for symmetric and extended coverage of target spinal segments L2–S2. Starting 1 month after implantation, 13 follow-up assessments, 30–45 days apart, were conducted involving stimulator setting reprogramming and study assessments. Participants were provided with a patient programmer and allowed to utilize specific stimulation settings for different goals such as volitional movement, spasticity control, core strength, and autonomic functions. Participants could use the stimulation throughout each day (up to 24 h a day) after a month of gradual adjustment to time and amplitude. A detailed description of study methods can be found in a previous publication (Darrow et al., 2019). Observational

TABLE 1 | Demographic information: *ages are rounded to the closest decade.

Subject	SVM	Age*	Years post injury	AIS	Lowest injury site	Vertebral fracture level	Mechanism of injury	Implant level
1	No	50	10.96	A	T8	T8	Fall	T11
2	Yes	30	8.21	A	T4	T4 &T5	Sports injury	T12
3	Yes	40	16.83	A	T8	T7 &T8	MVA	T12-L1
4	No	40	5.36	B	T5	T5 &T6	Fall	T11-T12
5	Yes	50	5.44	A	T5	T5	MVA	L1
6	Yes	60	4.02	A	T5	T4-T5 dislocation fracture	MVA	L1-L2
7	No	30	3.05	A	T4	T4	Sports injury	T12-L1

Years post injury are set at the time of surgical implantation. Lowest site of injury is determined by the AIS neurological examination at screening. Spontaneous volitional movement (SVM): observed movement without stimulation. AIS, ASIA Impairment Scale; MVA, motor vehicle accident.

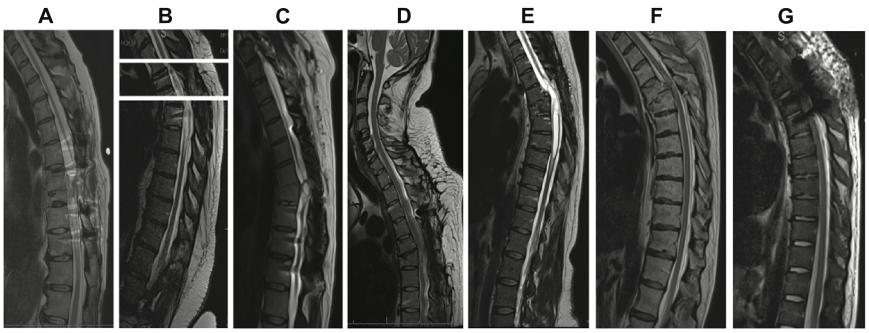

FIGURE 1 | T2 sagittal thoracic magnetic resonance imaging (MRI) obtained prior to enrollment. **(A)** Subject 1: spinal cord changes include dorsal tethering at T7 and syrinx from T8 to T10. **(B)** Subject 2: syrinx at T7. Owing to coronal scoliosis, a single sagittal image did not provide a full view of the spinal canal. A composite image of three different slices with the midline of the central canal kept as the axis is shown. **(C)** Subject 3: T8 cord injury with cystic changes at the same level. **(D)** Subject 4: T5 cord injury. **(E)** Subject 5: T5 cord injury and syrinx extending from T5 to T7. **(F)** Subject 6: T5 cord injury. **(G)** Subject 7: T4 cord injury.

data was collected using study personnel documentation from in-clinic follow-ups as well as subject self-reports.

Brain Motor Control Assessment

The BMCA was conducted during subject screening and twice at each follow-up visit, without and with eSCS. The eSCS program was selected based on participants' preferences during the previous month of eSCS use, as well as objective data on the current month's settings (Darrow et al., 2019). The BMCA is a neurophysiological assessment of voluntary motor function using surface EMG over a series of three phases in the supine position: relaxation, reinforcement maneuvers, and voluntary movements (Sherwood et al., 1996). At the beginning of the trial, participants are instructed to follow a two-toned auditory cue as the marker for the beginning and end of each task. The reinforcement maneuvers include deep breath, neck flexion, Jendrassik maneuver, and bilateral shoulder shrug. The first set of voluntary movements includes hip and knee flexion/extension with both legs, and then isolated left and right sides. The second set of voluntary movements are ankle dorsiflexion and plantar flexion bilaterally, and the isolated left and right sides. The participants are asked to attempt the movements even if they are unable to do so and even if the requested movements are not produced. Surface EMG is measured through 15 pairs of surface electrodes on the following muscles bilaterally: paraspinal, iliopsoas, rectus femoris, tibialis anterior, extensor hallucis longus, gastrocnemius, rectus abdominis, and intercostals. A Nicollet EDX, ECR-16, research EMG is used at a sampling rate of 600 Hz.

Electromyogram was pre-processed by removing 60-Hz noise with a Fourier filter and then power calculated in windows of time by average root mean square (RMS) (Darrow et al., 2019). Command start and end times were marked with labeled event timestamps in the EMG acquisition system. Baseline time windows for each trial started 3 s before the auditory cue and ended 1 s before the auditory cue for all six volitional tasks. An auditory cue was manually synchronized with the event timestamp. Muscle activity power during volitional task time windows was averaged across muscle groups and across all tasks.

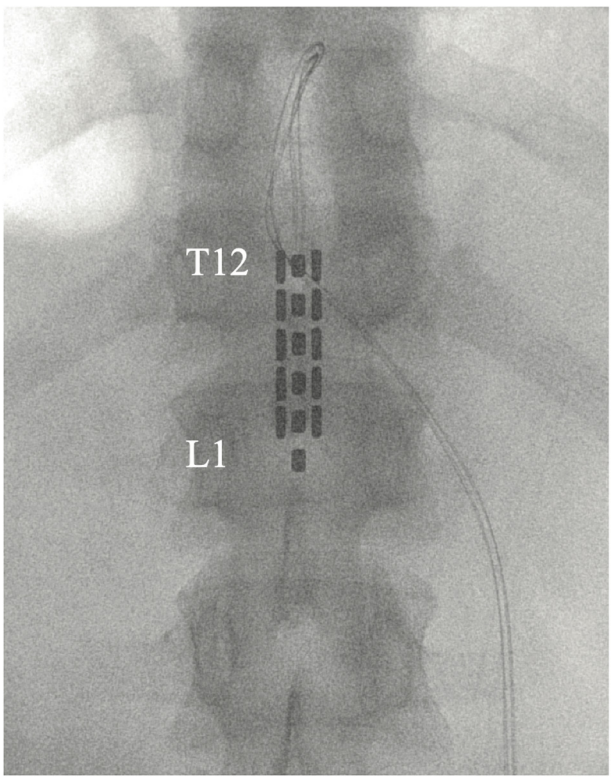

FIGURE 2 | Placement of 5-6-5 epidural paddle lead through a T12 laminectomy, overlying the T12–L1 epidural space. Final lead placement is guided by intraoperative electromyogram (EMG).

Similarly, muscle activity voltage at rest before each task was averaged. The ratio of average muscle power during volitional tasks to baseline preceding the command to start volitional movement was used to measure strength of volitional control and is represented in decibels [dB; $10\log_{10}\left(\frac{P_v}{P_b}\right)$, where P_v is the power during volitional control, and P_b is the power in the

immediately preceding window to the command to move] and will be referred to further on in this paper as volitional power.

Stationary Bike

The Muvi 300 cycle from MOTOmed was used to assess functional movement capabilities. The Muvi 300 includes a motor-assisted setting that facilitates training with minimal muscle strength by switching from passive to active training without strain. The active assist motor can vary in speed (rpm) and resistance. When the force sensitivity threshold is met, the motor ceases and the patients pedal on their own in the bike's active mode. The bicycle collects trial duration [seconds (s)], active and passive mode duration (s), active and passive distance traveled [meters (m)], active and passive speed [rotations per minute (rpm)], work done in active mode [kilojoules (kj)], and average and maximum energy produced during active phase [watts (W)].

The factorial design bicycling task was added after initial participants demonstrated enough movement capabilities with active eSCS to allow for more robust functional assessments during follow-up sessions. Therefore, the data capture window for each participant differs based on the relative enrollment date. If the bike was implemented after a subject initiated eSCS therapy, they did not undergo a baseline visit.

At the baseline visit, participants completed two motor-assisted bike trials: one passive trial where the subject was asked to relax and one active where the subject was asked to attempt to pedal. At each subsequent visit, the subject completed the same passive and active trials without stimulation and additional passive and active trials with selected preferred stimulation setting on. The duration of each trial was 2 min. As a result, there were two conditions without stimulation analyzed: (1) no effort, no stimulation and (2) maximal effort, no stimulation.

Statistical Analysis

RStudio (2015) software was used for statistical analyses. Mann–Whitney U tests were used as non-parametric testing of differences between Spontaneous Volitional Movement (SVM) group and non-Spontaneous Volitional Movement (non-SVM) group. Generalized linear models were used to assess linear relationships for BMCA volitional power without stimulation during each study visit. Fixed effects tested to fit the model included: subjects, follow-up visit (time), Modified Ashworth scores before and after the study visit and volitional power with the stimulation on. A second model was used to assess the effects of spinal cord atrophy on average BMCA volitional power. Fixed effects tested to fit the model included: transverse and anteroposterior spinal cord diameter changes above and below the injury. When testing models with the same response variable, the best-fit model was chosen based on the lowest Akaike information criterion (AIC). Biking data included an excess of zero counts and overdispersed counts. It was therefore analyzed with a zero-inflated negative binomial regression that was found to be significantly superior to a negative binomial generalized linear model with the Vuong Non-nested Hypothesis test ($p < 0.005$). For all statistical analyses, a p-value of less than 0.05 was considered to be statistically significant. p-values are summarized in figures as one star (*) for $p < 0.05$, two stars (**) for $p < 0.01$, three stars (***) for $p < 0.001$, and four stars (****) for $p < 0.0001$.

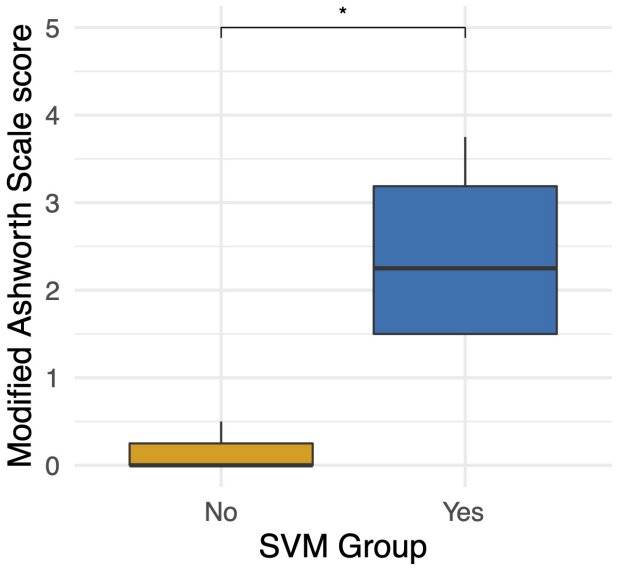

FIGURE 3 | Differences in baseline Modified Ashworth Scale scores between the spontaneous volitional movement (SVM) group (Yes) and non-SVM group (No). Participants in the SVM group had significantly higher spasticity MAS scores than those in the non-SVM group. These differences were present before the start of continuous eSCS therapy. *$p < 0.05$.

RESULTS

Study Population

Four participants unexpectedly developed sustained volitional movement with stimulation turned off, referred to as the SVM group. In order to ascertain group differences, participants from the SVM group were compared to the participants who only demonstrated movement with stimulation, referred to as the non-SVM group ($n = 3$) (**Supplementary Table S1**). Age ($p = 0.285$) and years post-injury ($p = 0.476$) were not significantly different between the SVM and non-SVM groups. The differences of anteroposterior ($p = 0.114$) and transverse ($p = 0.212$) spinal cord diameters from normal above the injury were not significantly different between SVM and non-SVM groups. The differences of anteroposterior ($p = 0.4$) and transverse ($p = 0.4$) spinal cord diameters from normal below the injury were not significantly different between SVM and non-SVM groups. Baseline spasticity scores (MAS) prior to continuous stimulation therapy were significantly higher at baseline in the SVM group (mean 2.44 ± 1.12) than in the non-SVM group (mean 0.17 ± 0.29; $p = 0.048$). This difference is depicted in **Figure 3**.

Across all participants, average daily stimulation use ranged from 5 to 21 h/day, with a mean of 13.7 ± 5.8 h/day. Total eSCS time at their final follow-up visit ranged from 101.2 to 454.5 days, with a mean of 255.3 ± 115.3 days. There were no statistically

significant differences in the total amount of stimulation used ($p = 0.629$) nor average daily stimulation ($p = 1$) between SVM and non-SVM groups. Within the SVM group, participants had undergone a range of 67.1–244.6 total days of stimulation at the time of their first observed movement, with a median of 87 days.

While this study does not involve an intensive rehabilitative therapy component, study personnel collected self-reported information in order to characterize modalities and hours of therapy undergone before and during the study. Six participants reported receiving rehabilitative therapy during acute care as well as general and specialized in-patient rehabilitation. Prior to the study, 57% (4/7) of the participants reported receiving specialized SCI out-patient therapy, 29% (2/7) reported receiving general out-patient therapy, and 43% (3/7) completed therapy at home. After implantation of the epidural stimulator, 43% (3/7) of the participants reported receiving specialized SCI out-patient therapy, 14% (1/7) reported receiving general out-patient therapy, and 43% (3/7) completed therapy at home. Out of the six participants who responded to retrospective surveys, three reported changing their exercise routine post-implantation.

Participants in the SVM group practiced a wide range of exercises spanning from range of motion, aerobic exercises, and general upper- and lower-body strength exercises up to specialized SCI out-patient therapy through adaptive gyms, clinic services with a physical therapist, and even activity-based locomotor exercise programs for core strength, leg strength, and balance. participants from the non-SVM group engaged in a similar range of exercise modalities. Of note, one subject in the non-SVM group participated in rehabilitative therapy that included using a standing frame, exoskeleton, and functional electrical stimulation to aid with stretching sessions. Intensity of rehabilitation therapy varied throughout the overall subject population (**Table 2**).

Observational Data

Volitional movement without epidural stimulation was observed among the four participants (two females, two males) in the SVM group as early as 3 months post-implantation. In three of the four participants, study personnel cited volitional movement without eSCS during the BMCA. A case report form (CRF) was implemented to document and characterize observed movements with and without stimulation (**Supplementary Video S1**). Of those three participants, 100% demonstrated hip flexion and extension as well as knee flexion without eSCS during at least one follow-up visit. Two out of the three exhibited knee extension as well as ankle dorsiflexion and plantar flexion during at least one follow-up visit (**Figure 4A**).

Subject 5 provided a self-report noting right hip adduction, knee flexion/extension, and plantar extension without eSCS at-home during month 13 (**Supplementary Video S2**). Volitional movement without eSCS was not observed during their in-clinic BMCA testing.

By comparison, movement with stimulation (**Figure 4B**) was observed to be more consistent across muscle groups and more prominent in range of motion than without stimulation. When stimulation was on, all participants from both the SVM and non-SVM groups achieved volitional movement to varying degrees of magnitude and extent. These results are observed early on in each subject's study enrollment time, and they can be observed as a direct effect of acute stimulation.

TABLE 2 | Weekly exercise schedule: reported exercises during study enrollment.

Subject	SVM	Exercises
1	No	Stretching and range of motion – 7× week, 30–45 min
2	Yes	Activity based locomotor exercise – 3× week, 60 min
3	Yes	Upper body exercises – 3× week, 60 min Leg exercises – 3× week, 20 min
4	No	Adaptive gym
5	Yes	Range of motion, strength training, aerobic exercise, in clinic rehabilitation with a physical therapist – 1× week, 120 min
6	Yes	Adaptive gym – 1–2× week, 60 min
7	No	Standing frame – 3–4× week, 40 min Exoskeleton – 1× week, 40 min Stretch sessions with electrodes – 2–3× week, 60 min

Subjects are assigned to SVM or non-SVM groups based on observational data.

Brain Motor Control Assessment

In order to characterize study observations, analysis of electrophysiological data from BMCA sessions without stimulation was performed. Sessions in which movement without stimulation was documented demonstrated increases in muscle activity specifically during volitional motor tasks compared to rest during baseline (**Figure 5**). The magnitude of volitional motor control is represented by volitional power, as this ratio corrects for any involuntary muscle activity at baseline related to spasticity or spasms. There was a significant difference in volitional power, controlling for involuntary movement at rest, when movement was recorded in BMCA CRFs ($p < 0.0005$) (**Figure 6**), meaning that clinical recognition of volitional movement is in agreement with EMG activity measured during the BMCA.

A generalized linear model was used to identify the effects of several variables on volitional power (dB) during volitional tasks without stimulation. Longitudinal explanatory variables tested included individual subject, follow-up visit, Modified Ashworth Scores during follow-up visits, and volitional power (dB) with stimulation on. When holding all other variables constant, there was a significant but weak effect of time ($p = 0.016$), a significant and strong positive effect from Subject 3 ($p = 0.0005$) who demonstrated the most significant improvement, a significant and moderate positive effect of spasticity before BMCA testing ($p = 0.002$) and a weak and trending toward significance positive effect of volitional power when stimulation was on ($p = 0.066$). To assess for SCI differences, a generalized linear model for average volitional power for each subject was tested with the difference between transverse and anteroposterior spinal cord diameters to normal spinal cord measures *above the injury* (C7, T1) as explanatory variables; there were no significant effects. In a generalized linear model for average volitional power for each subject with differences between transverse and anteroposterior spinal cord diameters to normal spinal cord measures *below the injury (T9)* as explanatory variables, there was a negative strong effect of the AP spinal cord diameter difference that

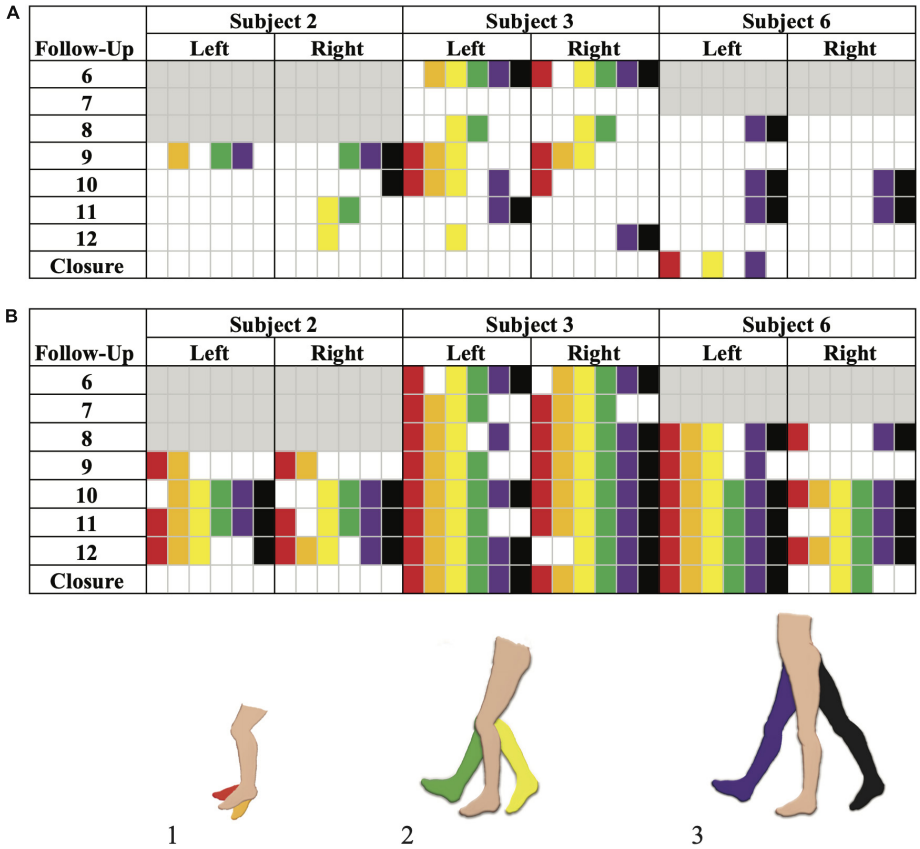

FIGURE 4 | Brain Motor Control Assessment (BMCA) documented muscle activation without stimulation **(A)** and with stimulation **(B)** in the SVM group. Joint movements are color coded as follows: (1) red, ankle dorsiflexion and orange, ankle plantarflexion. (2) Yellow, knee flexion and green, knee extension. (3) Purple, hip flexion and black, hip extension. Follow-up visits 1–5 and Subject 5 are not included as the BMCA CRF had not been implemented yet. Each subject's introduction of the CRF form is color-coded by gray boxes. Movements observed prior to the implementation of the BMCA CRF have not been included here. Recorded movements only occurred during the volitional task windows of the BMCA **(A)**. Recorded movements during BMCA in the *absence of stimulation*. Subject 3 demonstrated persistent movement in the absence of stimulation the earliest and across the most muscle groups among the SVM group. **(B)** Recorded movements during BMCA *with stimulation on* are included in order to exemplify how movement with stimulation is more prevalent earlier on in the study and across more muscle groups than movement without stimulation.

trended toward significance ($p = 0.071$). In other words, greater anteroposterior spinal cord atrophy had a negative effect on the amount of volitional power achieved.

When assessing for the independent effect of time, a trend is apparent as participants progress in follow-up visits (**Figure 7**), and the effect of time is significant when correcting for other fixed effects, as is mentioned above. With the exception of Subject 3's early volitional activity at follow-up visit 4, the rest of the subject's volitional power emerges later on in the study. While Subject 5 is included in the SVM group due to observed volitional movement outside of study assessments, these results are not reflected as volitional power that is apparent above baseline. On the other hand, while Subject 7 is included in the non-SVM group, they have not completed the study at the time of this manuscript submission, and the latest follow-up visits demonstrate a rise in volitional power above baseline. To correct for intersubject and between-visit variability, pooling observations between SVM and non-SVM groups during three different stages of the study allows for a clearer interpretation of the effect over time (**Figure 8**). Study periods were divided as follows: study period 1 corresponds to visits 1–5 (approximately 5 months), study period 2 corresponds to visits 6–9 (approximately 4 months), study period corresponds to visits 10–13 (approximately 4 months). In study period 2, greater volitional power in the SVM group than in the non-SVM group trends toward significance ($p = 0.087$), and in study period 3, there is significantly greater volitional power in the SVM group ($p < 0.001$). Furthermore, only within the SVM group is there a significant increase in volitional power from study period 1 to study period 2 ($p = 0.008$) and from study period 2 to study period 3 ($p = 0.03$).

Bike

Stationary bicycle trials proved complementary to electrophysiological measures as a functional assessment. During one participant's best bike trial, Subject 3 (**Supplementary Video S3**), they exerted 235 J of work that amounted to active pedaling without motor assistance for 94.2% of the trial time and 96.4% of the distance traveled. These results occurred after 6 months of

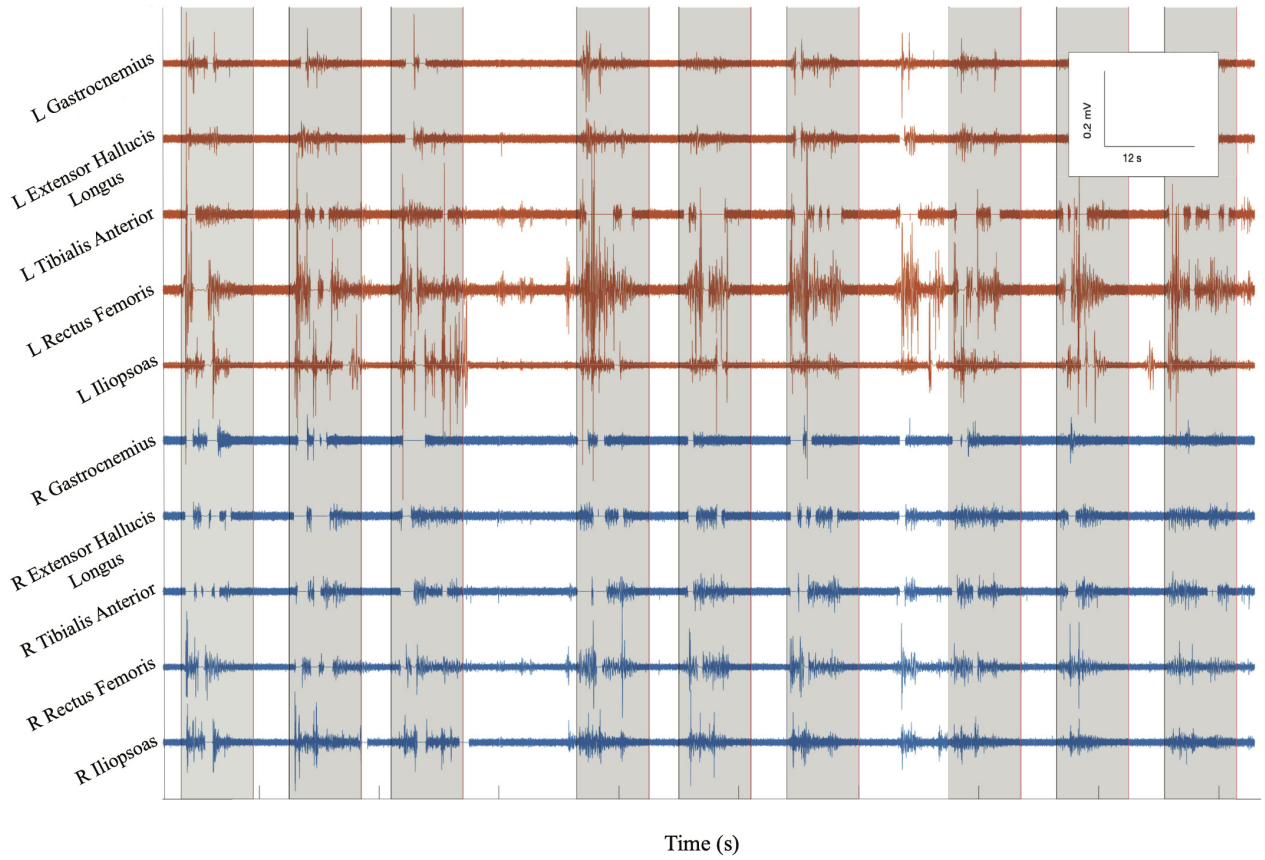

FIGURE 5 | BMCA at Subject 2's follow-up visit 13: surface EMG electrical activity recorded in volts over time for eight bilateral lower extremity muscle groups. Orange traces include left muscle groups and blue traces include right muscle groups. Gray boxes indicate volitional task events signaled by auditory cues. This subsample of EMG recording includes three cues for bilateral hip flexion, right hip flexion, and left hip flexion, respectively. EMG bursts can be seen to be synchronized with the auditory cue followed by silent periods at rest, demonstrating volitional activity.

chronic eSCS. In the SVM group, the earliest activity emerged at follow-up visit 6 and the latest at follow-up visit 10.

A zero-inflated negative binomial regression for two selected dependent variables, distance traveled and work, was constructed including the following independent variables: individual participants and the interaction between groups (SVM vs. non-SVM) and pedaling effort provided. When holding all other variables constant, there was a significantly strong positive effect on distance traveled ($p < 0.005$) and work ($p < 0.005$) only when participants from the SVM group attempted to pedal (**Figure 9**).

DISCUSSION

Preliminary data from the ESTAND trial suggests that long-term or chronic eSCS can induce plastic changes in chronic, severely injured spinal cords through restored volitional movement without stimulation and without significant intensive rehabilitation. More than half of the first seven patients were observed to exhibit volitional movement without stimulation, which agreed with the more sensitive electrophysiology, and resulted in marked improvements in a functional cycling task.

None of the participants included in this cohort demonstrated traditional signs of discomplete spinal cord injuries before eSCS therapy began (Sherwood et al., 1992). Despite the fact that all participants exhibited motor-complete traumatic spinal cord injuries confirmed with MRI, clinical testing, and electrophysiological testing at screening, more than half of the participants demonstrated the reported improvements in volitional movement capabilities with stimulation *inactive*. It is important to emphasize that before these improvements were apparent, there was no indication that study participants had different responses to long-term eSCS because, grossly, all participants demonstrated improvements in volitional muscle activity when epidural stimulation was *active*. When comparing researcher-observed movements during BMCA off and on stimulation, active stimulation allowed for volitional joint movements that spanned across more muscle groups and more consistently across study visits. However, joint movements observed off stimulation represented a subset of those facilitated by eSCS at similar time points. This finding might indicate that some of the same circuits that are potentiated by active stimulation are those responsive to chronic eSCS-facilitated plasticity.

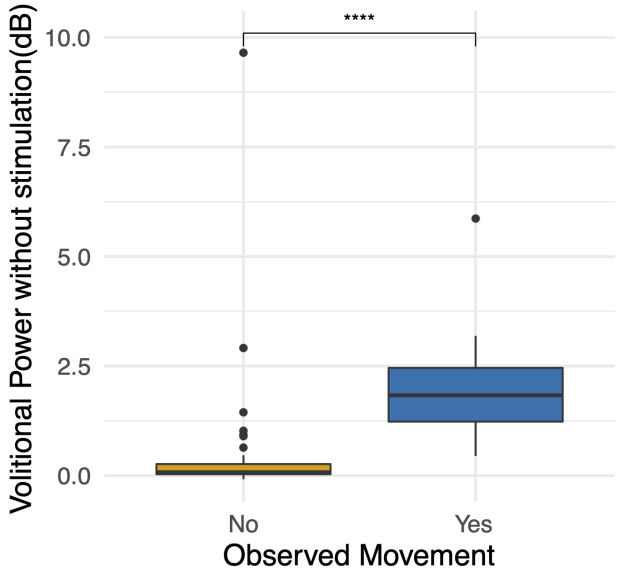

FIGURE 6 | Observations during BMCA. Differences in volitional power without stimulation (dB) when movement was observed and recorded on case report forms. *High volitional power outliers when movement was not observed demonstrate the lower sensitivity of researcher observations.* For reference, volitional power of 3 dB represents an increase in muscle activity during volitional tasks of two times (200%) that of muscle activity at baseline. Volitional power of 10 represents an increase in muscle activity during volitional tasks of 10 times (1000%) that of the muscle activity at baseline. ***$p < 0.001$.

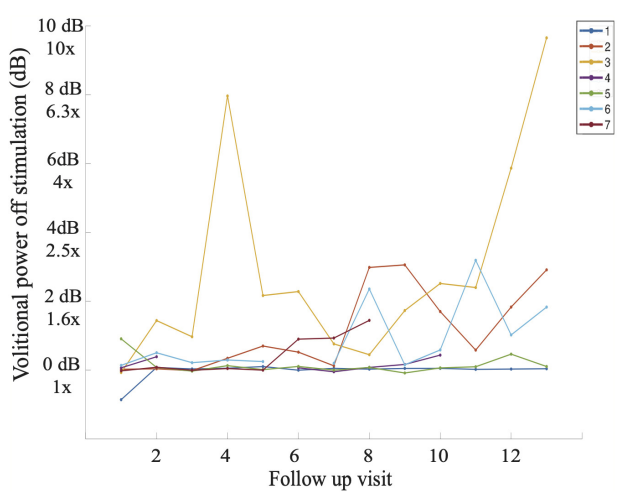

FIGURE 7 | Average volitional power without stimulation (dB) at each study follow-up visit including all seven participants. It is apparent that Subject 3 demonstrated volitional movement the earliest in the study (follow-up visit 4) and with the greatest magnitude on sEMG, reaching volitional muscle activity 10 times greater (1000%) than that at baseline on follow-up visit 13.

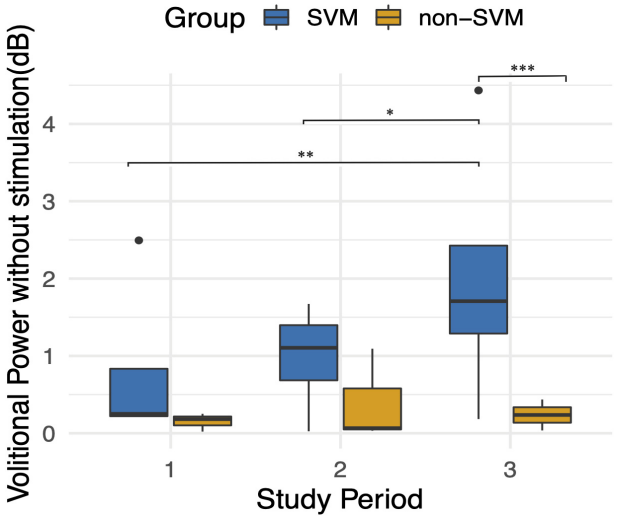

FIGURE 8 | Average volitional power without stimulation (dB) during three follow-up study periods. Study period 1 included follow-up visits 1–5. Study period 2 included follow-up visits 6–9. Study period 3 included follow-up visits 10–13. An improvement over time is apparent only in the SVM group and is statistically significant between study periods 1 and 3 ($p = 0.008$) and between study periods 2 and 3 ($p = 0.03$). Volitional power between SVM and non-SVM groups is significantly greater in study period 3 ($p < 0.001$). *$p < 0.05$, **$p < 0.01$, ***$p < 0.001$.

Predictors of Recovery

In an effort to characterize each subject's propensity for this type of recovery, several descriptive subject characteristics were included such as time since injury, mechanism of injury, injury level, vertebral fracture level, fusion level, and imaging studies. None of these factors were significant in determining if a subject would develop movement without stimulation. Overall, the heterogeneity between participants exemplifies how within the most severe subgroup of the AIS scale, there are no current adequate measures to characterize the functional capacity of the spinal cord. Adequate measures that reflect the degree of preserved and quiescent supraspinal tracts across the spinal cord lesion could allow for phenotyping those responsive to neuromodulation.

In our cohort, spasticity scores before initiating eSCS therapy were slightly greater in the SVM group than in the non-SVM group, which was statistically significant. Moreover, longitudinal spasticity scores before each BMCA session had a significant positive effect on volitional power. When assessing differences among motor-complete SCI participants, Sangari et al. (2019), compared spastic and non-spastic subgroups and reported that motor evoked potentials (MEP) were only present in the spastic subgroup, suggesting that spasticity might be a marker for preserved corticospinal tract axons (Sangari et al., 2019). Greater spasticity at baseline and during chronic eSCS therapy might reflect preserved but silent corticospinal tracts that served as substrates for the plastic effects of eSCS neuromodulation in the SVM group or may highlight the role that higher baseline spasticity may play in electrophysiology. Furthermore, high spasticity phenotypes might be more susceptible to the immediate depolarizing effects and long-term neuromodulation effects of eSCS that restore inhibition of uncontrolled spinal cord excitability and potentiate functional activation of the spinal

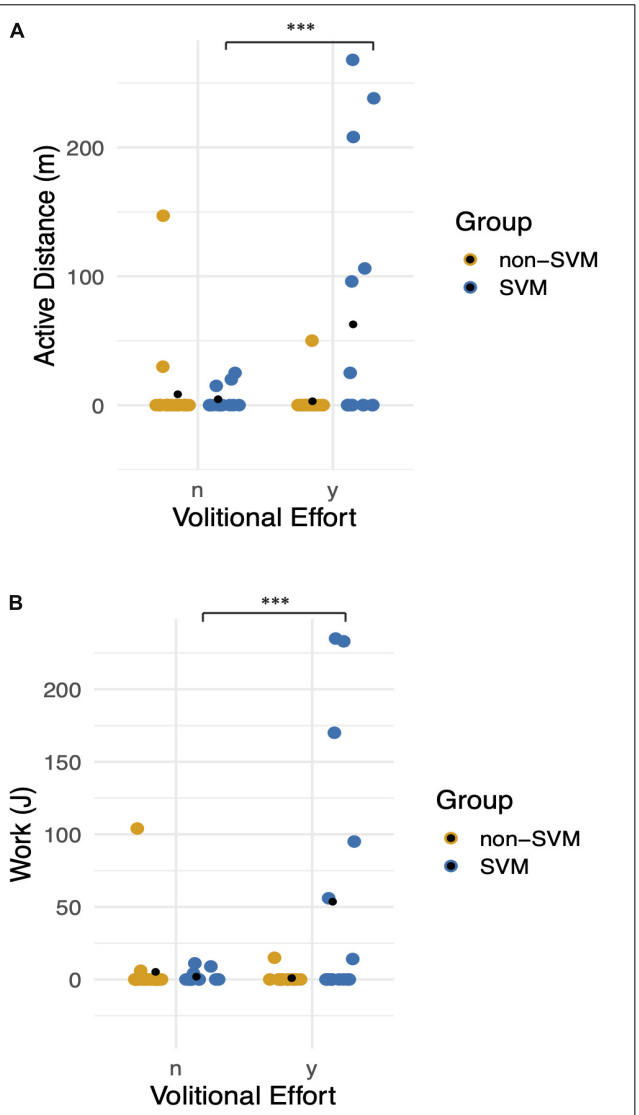

FIGURE 9 | Functional movement without stimulation: graphs demonstrate differences between Groups (0: non-SVM group and 1: SVM group) and between volitional effort (*n* = no effort, *y* = with effort). Means are symbolized by black points. **(A)** Distance traveled without assistance of the bicycle motor is plotted, when correcting for zero inflated data. There is a significant positive effect on distance when participants from the SVM group attempted to pedal. **(B)** Pedaling work exerted is plotted, when correcting for zero inflated data. Participants in the SVM group significantly achieved greater work when they provided effort compared to the non-SVM group. *** refers to a *p*-value of <0.001.

cord (D'Amico et al., 2014). Although the mechanisms might be unclear, spasticity should be further assessed as a predictor and biomarker for eSCS-mediated spontaneous recovery.

Measures of spinal cord atrophy were also assessed as a marker of injury severity. Only anteroposterior atrophy below the level of injury was found to have a strong effect on volitional power that did not quite meet our criteria for significance. In chronic motor complete spinal cord injuries, Sangari et al. (2019), reported MEP size to be positively correlated with the degree of spared tissue in lateral regions of the spinal cord above the injury. Our results should be interpreted with caution as spinal cord diameter changes have been reported as a measure of SCI severity only *above* the level of injury (Freund et al., 2010; Sangari et al., 2019), and the measurements in this cohort were limited by suboptimal MRI studies due to hardware artifacts and variability in SCI chronicity. As a result, imaging metrics did not prove to be useful predictors of recovery into the SVM group.

Most importantly, despite the large number of standard characteristics used to describe SCI, all but spasticity proved to be ineffective at predicting the variability in the development of movement without stimulation despite a uniform improvement with active stimulation. In other words, there are no major predictors of the development of movement without stimulation identified thus far that would restrict the potential future use of eSCS as a therapy.

Role of Concurrent Rehabilitation in eSCS Recovery

Since the first case of eSCS in SCI aiming to restore volitional movement was reported in 2004 (Carhart et al., 2004), there have been reports of three chronic SCI patients with eSCS therapy who have regained some level of volitional movement in the absence of stimulation after intensive locomotor therapy. Angeli et al. (2014), reported movement without eSCS in one 32-year-old male patient with an AIS B injury after 38 weeks of intensive locomotor training that included 80 sessions of full weight-bearing stand training and 80 sessions of step training with body weight support as well as home-based volitional training (Rejc et al., 2017). Wagner et al. (2018), also reported two participants, a 28-year-old male with AIS C injury and a 35-year-old male with AIS D injury both enrolled 6 years after injury, who demonstrated improvements in walking indices and motor scores without eSCS after participating in 5 months post-implantation of overground and treadmill locomotor training using a gravity assist device four to five times a week. In contrast, the ESTAND study did not prescribe the use of intensive locomotor training. In addition to their baseline rehabilitation therapies (described in **Table 2**), participation in this study involved a minimum of 10 min of daily visually cued flexion–extension tasks at home, 90 min of supine flexion–extension tasks during monthly BMCA, and 10 min of motor-assisted pedaling during monthly bike testing. Participants utilized eSCS in their daily activities according to their needs and preferences up to 24 h per day, and more independent rehabilitation therapy was not associated with any clear benefit.

Despite heterogeneity in daily time and effort dedicated to physical therapy among all participants, more than half of the participants (SVM group) demonstrated progressive statistically significant improvements in volitional movement in the off stimulation state during the study period. As a result, there were statistically significant improvements in the ability to cycle without assistance, providing the basis for cost-effective home-based therapies to provide incremental improvements in muscle mass, cardio-metabolic risk factors and activities of daily living

as well as a platform for activity-dependent plasticity (Shen et al., 2018; Gorgey et al., 2019).

While activity-based plasticity is often associated with rehabilitation therapies, there is a possibility that directly increasing volitional movement, increased use, and reliance on these improvements may facilitate more subtle and chronic activity-based plasticity in the sense that directed motor control during normal everyday life drives plastic changes. However, more intensive concurrent rehabilitation outside of the study did not drive further recovery, which is exemplified by the fact that the participant who underwent the most extensive specialized SCI therapy before and during the study did not develop spontaneous movement without stimulation. To our knowledge, this is the first report of eSCS-induced plasticity of volitional movement in the absence of concurrent prescribed intensive locomotor training therapy after motor-complete SCI. While the E-STAND trial remains generalizable by allowing for a wide range of independent therapy, careful data collection of previous therapy regimens may prove useful for assessing further contribution through modeling.

Limitations and Future Directions

One limitation in this study relates to an undefined off-stimulation time period. As our protocol allows participants to use as much stimulation as they require for their daily activities and comfort. As such, there was no established eSCS-weaning time beyond a minimum of 2 h when testing for off-stimulation activity. An important confounder to consider is whether the reported results might be related to stimulation carry-over effect, described as temporarily persisting changes in spinal cord circuit excitability. This has been described clinically in relation to spasticity modulation in SCI patients as lasting from hours to days (Cook, 1976; Dimitrijevic M. M. et al., 1986; Dimitrijevic M. R. et al., 1986; Barolat et al., 1988). Whether the effects in the absence of eSCS in the participants in this study are temporary or persistent over longer periods of time with stimulation off will have to be further assessed.

In this manuscript, the observed movements during the BMCA were not matched to the intended volitional task. Instead, pooling of observed movements was compared to pooled EMG muscle activation during all volitional tasks. In the future, a thorough analysis of the accuracy of muscle activation for each intended joint movement should be performed. The preliminary results at this stage were not sufficiently powered to assess these outcomes. Here we demonstrate the robust evidence of muscle activity magnitude. Muscle activity accuracy will have to be assessed in future larger studies.

Although this is the largest group reported of SCI patients treated with eSCS to restore volitional movement, results should be interpreted with caution due to the small number of participants. In the future, studies with larger cohorts might allow for adequate eSCS therapy phenotyping. In-depth analysis of stimulation usage might point to a dose–response relationship that was not apparent in this study. Furthermore, neurophysiological testing such as somatosensory evoked potentials, electroencephalogram, and transcranial magnetic stimulation motor-evoked potentials might allow for categorizing the effects of chronic eSCS on ascending pathways, cortical representation, and descending pathways, respectively. Correlating these results with high-resolution MRI at enrollment to detect spinal cord area differences might aid in further characterizing the heterogeneity of spinal cord injuries and identifying the degree of preserved pathways that may serve as substrates for recovery (Freund et al., 2010). With these results, we hope to further evidence the role of eSCS in SCI rehabilitation and exemplify how the effects of *chronic* eSCS are only starting to be apparent.

DATA AVAILABILITY STATEMENT

The datasets presented in this article are not readily available because the ESTAND trial is currently ongoing and datasets retain some identifiable information. A limited dataset may be made available. Requests to access the datasets should be directed to David P. Darrow, darro015@umn.edu.

ETHICS STATEMENT

The studies involving human participants were reviewed and approved by the Human Subjects Research Committee, Hennepin Healthcare System. The patients/participants provided their written informed consent to participate in this study. Written informed consent was obtained from the individuals for the publication of any potentially identifiable images or data included in this article.

AUTHOR CONTRIBUTIONS

DD provided all oversight for the study. DD, APa, AK, APh, US, and TN designed the study. DD, DF, APa, and US performed the critical surgical procedures of this study. CH, AA, SV, DS, DB, and DF performed the study procedures and data collection. DD, TN, NP, and IP analyzed the data. IP wrote the manuscript with support from DD, CH, AA, SV, and DS. All authors provided critical feedback and helped shape the research, analysis, and manuscript, and approved the final manuscript.

FUNDING

This study was funded by a MN State SCI/TBI grant from the Minnesota Office of Higher Education (grant number 159800).

ACKNOWLEDGMENTS

We would like to thank the Minnesota Office of Higher Education SCI/TBI Grant Program (grant number 159800) for the funding

to carry out this study and St. Jude/Abbott for a generous device donation.

SUPPLEMENTARY MATERIAL

The Supplementary Material for this article can be found online at: https://www.frontiersin.org/articles/10.3389/fnsys.2020.00035/full#supplementary-material

TABLE S1 | Summary of means and standard deviations *(SD)* for all variables used to assess differences between groups. *P*-values are obtained from single variable Mann-Whitney U tests. SVM: Spontaneous volitional movement. Non-SVM: No spontaneous volitional movement.

VIDEO S1 | BMCA video recording of subject 3 with stimulation off. Subjects lie supine with surface electromyography electrodes placed while they perform volitional tasks triggered by auditory cues. At follow up 6, the subject achieves bilateral but predominantly left hip internal rotation and flexion as well as left dorsiflexion of the toes. At follow up 9, he again achieves left hip internal rotation and flexion as well as left dorsiflexion of the toes.

VIDEO S2 | Home video recording of subject 4 demonstrates volitional right knee extension in the absence of stimulation.

VIDEO S3 | Stationary bike video recording of subject 3 at Follow-up visit 6. This trial involves 2 min when subjects intend to pedal with stimulation off. In this particular trial shown, the subject achieved active pedaling for 113 seconds (94% of trial time) for a distance of 268 meters (96% of trial distance).

REFERENCES

Angeli, C. A., Boakye, M., Morton, R. A., Vogt, J., Benton, K., Chen, Y., et al. (2018). Recovery of over-ground walking after chronic motor complete spinal cord injury. *N. Engl. J. Med.* 379, 1244–1250. doi: 10.1056/NEJMoa1803588

Angeli, C. A., Edgerton, V. R., Gerasimenko, Y. P., and Harkema, S. J. (2014). Altering spinal cord excitability enables voluntary movements after chronic complete paralysis in humans. *Brain J. Neurol.* 137(Pt 5), 1394–1409. doi: 10.1093/brain/awu038

Barolat, G., Myklebust, J. B., and Wenninger, W. (1988). Effects of spinal cord stimulation on spasticity and spasms secondary to myelopathy. *Appl. Neurophysiol.* 51, 29–44. doi: 10.1159/000099381

Barolat, G., Singh-Sahni, K., Staas, W. E. Jr., Shatin, D., Ketcik, B., and Allen, K. (1995). Epidural spinal cord stimulation in the management of spasms in spinal cord injury: a prospective study. *Stereotactic Funct. Neurosurg.* 64, 153–164.

Carhart, M. R., He, J., Herman, R., D'Luzansky, S., and Willis, W. T. (2004). Epidural spinal-cord stimulation facilitates recovery of functional walking following incomplete spinal-cord injury. *IEEE Trans. Neural Syst. Rehabil. Eng.* 12, 32–42. doi: 10.1109/TNSRE.2003.822763

Cook, A. W. (1976). Electrical stimulation in multiple sclerosis. *Hosp. Pract.* 11, 51–58. doi: 10.1080/21548331.1976.11706516

D'Amico, J. M., Condliffe, E. G., Martins, K. J. B., Bennett, D. J., and Gorassini, M. A. (2014). Recovery of neuronal and network excitability after spinal cord injury and implications for spasticity. *Front. Integr. Neurosci.* 8:36. doi: 10.3389/fnint.2014.00036

Darrow, D., Balser, D., Netoff, T. I., Krassioukov, A., Phillips, A., Parr, A., et al. (2019). Epidural spinal cord stimulation facilitates immediate restoration of dormant motor and autonomic supraspinal pathways after chronic neurologically complete spinal cord injury. *J. Neurotrauma* 36, 2325–2336. doi: 10.1089/neu.2018.6006

de Andrade, E. M., Ghilardi, M. G., Cury, R. G., Barbosa, E. R., Fuentes, R., Teixeira, M. J., et al. (2016). Spinal cord stimulation for Parkinson's disease: a systematic review. *Neurosurg. Rev.* 39, 27–35.

Dimitrijevic, M. M., Dimitrijevic, M. R., Illis, L. S., Nakajima, K., Sharkey, P. C., and Sherwood, A. M. (1986). Spinal cord stimulation for the control of spasticity in patients with chronic spinal cord injury: I. Clinical observations. *Centr. Nerv. Syst. Trauma* 3, 129–144. doi: 10.1089/cns.1986.3.129

Dimitrijevic, M. R., Illis, L. S., Nakajima, K., Sharkey, P. C., and Sherwood, A. M. (1986). Spinal cord stimulation for the control of spasticity in patients with chronic spinal cord injury: II. Neurophysiologic observations. *Centr. Nerv. Syst. Trauma* 3, 145–152. doi: 10.1089/cns.1986.3.145

French, D. D., Campbell, R. R., Sabharwal, S., Nelson, A. L., Palacios, P. A., and Gavin-Dreschnack, D. (2007). Health care costs for patients with chronic spinal cord injury in the Veterans Health Administration. *J. Spinal Cord Med.* 30, 477–481. doi: 10.1080/10790268.2007.11754581

Freund, P. A. B., Dalton, C., Wheeler-Kingshott, C. A. M., Glensman, J., Bradbury, D., Thompson, A. J., et al. (2010). Method for simultaneous voxel-based morphometry of the brain and cervical spinal cord area measurements using 3D-MDEFT. *J. Magn. Reson. Imaging JMRI* 32, 1242–1247.

Frostell, A., Hakim, R., Thelin, E. P., Mattsson, P., and Svensson, M. (2016). A review of the segmental diameter of the healthy human spinal cord. *Front. Neurol.* 7:238. doi: 10.3389/fneur.2016.00238

Gill, M. L., Grahn, P. J., Calvert, J. S., Linde, M. B., Lavrov, I. A., Strommen, J. A., et al. (2018). Neuromodulation of lumbosacral spinal networks enables independent stepping after complete paraplegia. *Nat. Med.* 24, 1677–1682. doi: 10.1038/s41591-018-0175-7

Gorgey, A. S., Khalil, R. E., Davis, J. C., Carter, W., Gill, R., Rivers, J., et al. (2019). Skeletal muscle hypertrophy and attenuation of cardio-metabolic risk factors (SHARC) using functional electrical stimulation-lower extremity cycling in persons with spinal cord injury: study protocol for a randomized clinical trial. *Trials* 20:526. doi: 10.1186/s13063-019-3560-8

Illis, L. S., Sedgwick, E. M., and Tallis, R. C. (1980). Spinal cord stimulation in multiple sclerosis: clinical results. *J. Neurol. Neurosurg. Psychiatry* 43, 1–14.

Kirshblum, S. C., Burns S. P., Biering-Sorensen F., Donovan W., Graves D. E., Jhan A., Johansen M., et al. (2011). International standards for neurological classification of spinal cord injury. *J. Spinal Cord Med.* 34, 535–546. doi: 10.1179/204577211x13207446293695

Kirshblum, S., Millis, S., McKinley, W., and Tulsky, D. (2004). Late neurologic recovery after traumatic spinal cord injury. *Arch. Phys. Med. Rehabil.* 85, 1811–1817. doi: 10.1016/j.apmr.2004.03.015

Kumar, R., Lim, J., Mekary, R. A., Rattani, A., Dewan, M. C., Sharif, S. Y., et al. (2018). Traumatic spinal injury: global epidemiology and worldwide volume. *World Neurosurg.* 113, e345–e363. doi: 10.1016/j.wneu.2018.02.033

Lam, T., Eng, J. J., Wolfe, D. L., Hsieh, J. T., Whittaker, M., and the Scire Research Team (2007). A systematic review of the efficacy of gait rehabilitation strategies for spinal cord injury. *Top. Spinal Cord Injury Rehabil.* 13, 32–57. doi: 10.1310/sci1301-32

Melzack, R., and Wall, P. D. (1965). Pain mechanisms: a new theory. *Science* 150, 971–979. doi: 10.1126/science.150.3699.971

Meseguer-Henarejos, A. B., Sanchez-Meca, J., Lopez-Pina, J. A., and Carles-Hernandez, R. (2018). Inter- and intra-rater reliability of the Modified Ashworth Scale: a systematic review and meta-analysis. *Eur. J. Phys. Rehabil. Med.* 54, 576–590. doi: 10.23736/S1973-9087.17.04796-7

Minassian, K., Jilge, B., Rattay, F., Pinter, M. M., Binder, H., Gerstenbrand, F., et al. (2004). Stepping-like movements in humans with complete spinal cord injury induced by epidural stimulation of the lumbar cord: electromyographic study of compound muscle action potentials. *Spinal Cord* 42, 401–416.

Rejc, E., Angeli, C. A., Atkinson, D., and Harkema, S. J. (2017). Motor recovery after activity-based training with spinal cord epidural stimulation in a chronic motor complete paraplegic. *Sci. Rep.* 7:13476. doi: 10.1038/s41598-017-14003-w

RStudio (2015). *RStudio: Integrated Development for R*. Boston, MA: RStudio, Inc.

Sangari, S., Lundell, H., Kirshblum, S., and Perez, M. A. (2019). Residual descending motor pathways influence spasticity after spinal cord injury. *Ann. Neurol.* 86, 28–41. doi: 10.1002/ana.25505

Shealy, C. N., Mortimer, J. T., and Reswick, J. B. (1967). Electrical inhibition of pain by stimulation of the dorsal columns: preliminary clinical report. *Anesth. Analg.* 46, 489–491.

Shen, C., Liu, F., Yao, L., Li, Z., Qiu, L., and Fang, S. (2018). Effects of MOTOmed movement therapy on the mobility and activities of daily living of stroke patients with hemiplegia: a systematic review and meta-analysis. *Clin. Rehabil.* 32, 1569–1580. doi: 10.1177/0269215518790782

Sherwood, A. M., Dimitrijevic, M. R., and McKay, W. B. (1992). Evidence of subclinical brain influence in clinically complete spinal cord injury: discomplete SCI. *J. Neurol. Sci.* 110, 90–98. doi: 10.1016/0022-510x(92)90014-c

Sherwood, A. M., McKay, W. B., and Dimitrijević, M. R. (1996). Motor control after spinal cord injury: assessment using surface EMG. *Muscle Nerve* 19, 966–979.

Wagner, F. B., Mignardot, J.-B., Le Goff-Mignardot, C. G., Demesmaeker, R., Komi, S., Capogrosso, M., et al. (2018). Targeted neurotechnology restores walking in humans with spinal cord injury. *Nature* 563, 65–71. doi: 10.1038/s41586-018-0649-2

Wilson, J. R., Cadotte, D. W., and Fehlings, M. G. (2012). Clinical predictors of neurological outcome, functional status, and survival after traumatic spinal cord injury: a systematic review. *J. Neurosurg.* 17(1 Suppl.), 11–26. doi: 10.3171/2012.4.AOSPINE1245

Conflict of Interest: US reports having no conflicts of interest relevant to this article. DD, AP, and TN report having several patents related to neuromodulation and are cofounders of a neuromodulation company.

The remaining authors declare that the research was conducted in the absence of any commercial or financial relationships that could be construed as a potential conflict of interest.

frontiers in Systems Neuroscience

ORIGINAL RESEARCH
published: 14 July 2020
doi: 10.3389/fnsys.2020.00044

Selective Antagonism of A1 Adenosinergic Receptors Strengthens the Neuromodulation of the Sensorimotor Network During Epidural Spinal Stimulation

Giuliano Taccola[1,2], Betsy Habeth Salazar[2], Rosamaria Apicella[1], Matthew Kevin Hogan[2], Philip John Horner[2] and Dimitry Sayenko[2]**

[1]*Department of Neuroscience, International School for Advanced Studies (SISSA), Trieste, Italy,* [2]*Department of Neurosurgery, Center for Neuroregeneration, Houston Methodist Research Institute, Houston, TX, United States*

Although epidural spinal stimulation (ESS) results in promising therapeutic effects in individuals with spinal cord injury (SCI), its potential to generate functional motor recovery varies between individuals and remains largely unclear. However, both preclinical and clinical studies indicate the capacity of electrical and pharmacological interventions to synergistically increase the engagement of spinal sensorimotor networks and regain motor function after SCI. This study explored whether selective pharmacological antagonism of the adenosine A1 receptor subtype synergizes with ESS, thereby increasing motor response. We hypothesized that selective pharmacological antagonism of A1 receptors during ESS would produce facilitatory effects in spinal sensorimotor networks detected as an increased amplitude of spinally-evoked motor potentials and sustained duration of ESS induced activity. Terminal experiments were performed in adult rats using trains of stereotyped pulses at 40 Hz delivered at L5 with the local administration to the cord of 8-cyclopentyl-1,3-dipropylxanthine (DPCPX). We demonstrated that ESS combined with the blockage of A1 receptors increased the magnitude of the endogenous modulation and postponed the decay of responses that occur during ESS alone. Although DPCPX significantly increased the yield of repetitive stimulation in intact spinal cords, the effects of A1 antagonism on motor evoked responses after an acute spinal transection was not detected. These studies support the future investigation of the optimal dosage, methods of delivery, and systemic effects of the synergistic application of A1 antagonists and spinal stimulation in the intact and injured spinal cord.

Keywords: motor control, spinal electrical stimulation, spinal reflexes, adenosine receptors, spinal transection, trains of pulses, terminal recordings

OPEN ACCESS

Edited by:
Enrico Rejc,
University of Louisville, United States

Reviewed by:
Amanda Pocratsky,
University College London, United Kingdom
Hui Zhong,
University of California, Los Angeles, United States
Prithvi Shah,
Stony Brook University, United States

****Correspondence:***
Giuliano Taccola
taccola@sissa.it
Dimitry Sayenko
dgsayenko@houstonmethodist.org

Received: *13 April 2020*
Accepted: *16 June 2020*
Published: *14 July 2020*

Citation:
Taccola G, Salazar BH, Apicella R, Hogan MK, Horner PJ and Sayenko D (2020) Selective Antagonism of A1 Adenosinergic Receptors Strengthens the Neuromodulation of the Sensorimotor Network During Epidural Spinal Stimulation. Front. Syst. Neurosci. 14:44. doi: 10.3389/fnsys.2020.00044

Abbreviations: ATP, adenosine triphosphate; ANOVA, analysis of variance; CNS, central nervous system; EMG, electromyogram; ESS, epidural spinal stimulation; GM, gastrocnemius; i.p., intraperitoneal; l, left; L, lumbar; SCI, spinal cord injury; SD, standard deviation; TA, tibialis anterior; Th, thoracic; DPCPX, 8-cyclopentyl-1,3-dipropylxanthine; DMPX, 3,7-dimethyl-1-propargylxanthine.

INTRODUCTION

Recent results from preclinical animal models and pilot phase clinical trials applying spinal neuromodulation have revealed that neural networks below the site of spinal cord injury (SCI) retain functional capabilities. Further, when electrically stimulated, neural networks can be reorganized to generate responses and motor activities previously thought to be permanently lost due to paralysis (Edgerton et al., 2008; Courtine et al., 2009; Fong et al., 2009; Rossignol and Frigon, 2011). Notably, epidural spinal stimulation (ESS) during activity-based rehabilitative therapy recovers previously paralyzed motor functions, improves autonomic nervous system functionality, and enhances well-being for those living with chronic paralysis due to SCI (Harkema et al., 2011; Angeli et al., 2014; Phillips and Krassioukov, 2015; Aslan et al., 2016, 2018; Grahn et al., 2017; Rejc et al., 2017; Herrity et al., 2018; Darrow et al., 2019). However, the level of functional performance regained following ESS therapy varies to a great extent, with the emergence of self-assisted stepping in a subset of trained individuals being the most advanced outcome to date (Angeli et al., 2018; Gill et al., 2018; Wagner et al., 2018). Variability in ESS efficacy likely results from unaccounted neurophysiological profiles among individuals, varying degrees of maladaptive neural plasticity, differences in training regimens, and/or high variation in spared neurologic function even within one grade of SCI severity. Given the variable effectiveness of ESS, studies that illuminate synergistic approaches (e.g., pharmacological agents) and mechanisms regulating the excitability of motor networks are needed to significantly impact the effectiveness of ESS therapy. Previous experiments in rats and cats have explored combination strategies, synergizing ESS with monoaminergic agents (e.g., clonidine, cyproheptadine, or levodopa; Courtine et al., 2009; Musienko et al., 2011) or non-competitive blockers (e.g., strychnine; de Leon et al., 1999). These works demonstrated that the spinal motor infrastructure is composed of a widely distributed and heterogeneous system of neural circuits and receptors that can generate a range of task-specific movements when recruited in different combinations (Tresch and Bizzi, 1999; Hochman et al., 2001; Courtine et al., 2009). However, researchers were unable to translate these results to the clinic, as the administration of buspirone, a serotonin agonist, produced mixed or moderate improvements (Gerasimenko et al., 2015; Gad et al., 2017; Freyvert et al., 2018). Therefore, there is a need to explore alternative pharmacological targets for more effective pharmacological neuromodulation, such as adenosine receptors (Bai et al., 2017). Adenosine is an endogenous purinergic autocoid with well-known vascular and anti-inflammatory effects (Layland et al., 2014). In the central nervous system (CNS), adenosine is synthesized by the hydrolysis of adenosine triphosphate (ATP) and then locally released by neurons and astrocytes in the synaptic cleft, where adenosine has a short half-life. Two receptors for adenosine (A1, A2) are reported in the CNS. While A1 is coupled to an inhibitory G*i* protein, A2s (A2A and A2B) are associated with a stimulating G*s* (Burnstock, 2007). The majority of A1 receptors are located presynaptically, mediating inhibition on neurotransmitter release (Fisone et al., 2004). Acting *via* A1 receptors, adenosine modulates ventral motoneurons (Witts et al., 2015) and acts on spinal motor networks as an intrinsic modulator, providing negative feedback that controls the activity generated by the spinal locomotor circuitry (Witts et al., 2011; Taccola et al., 2012; Acton and Miles, 2015). Moreover, primary afferents co-release ATP and glutamate on spinal synapses, where the resulting adenosine acts on presynaptic A1 autoreceptors to limit the flow of external input from the periphery (Burnstock and Wood, 1996). This endogenous neuromodulator inhibits afferent input from the periphery through A1 adenosine receptor subtypes, as indicated by modulation of nociceptive pathways with adenosinergic agents (Reeve and Dickenson, 1995).

An increase of endogenous adenosine during electrical stimulation has been reported arising from neuronal and glial cells (Caciagli et al., 1988; Tawfik et al., 2010). Peripheral stimulation of primary sensory afferents also releases adenosine in the spinal cord (Salter and Henry, 1987). During ESS, primary afferents are inevitably recruited and the released adenosine is a potential impediment to the yield of electrical stimulation. Indeed, A1 adenosine receptors may limit the inflow of electrical inputs, suggesting that the use of competitive antagonists for A1 adenosine receptors could facilitate the transit of electrical stimuli to neuronal networks in the spinal cord. As such, the effectiveness of electrical stimulation in recruiting a wider range of the spinal circuitry can be amplified, thus, maximizing plasticity and recovery of sensorimotor functions. Efficacy of A1 adenosine antagonists on spinal sensorimotor circuits has been studied on *in vitro* spinal cord preparations (Taccola et al., 2012), where it was demonstrated that activation of A1 adenosine receptors modulates the interneuronal networks responsible for the generation of locomotor behavior (Witts et al., 2011, 2015; Taccola et al., 2012; Acton and Miles, 2015). However, the effects of A1 adenosine antagonists on the modulation of spinally-evoked motor responses during ESS *in vivo* are currently unknown. The objective of this work is to explore whether the selective pharmacological antagonism of the subtype A1 adenosine receptors can synergize with ESS to increase spinal excitability and motor responses induced by spinal electrical stimulation. We hypothesized that the presence of A1 adenosine antagonists during spinal electrical stimulation would produce facilitatory effects in spinal sensorimotor networks, as revealed by increased amplitude of spinally-evoked motor potentials and sustained duration of the spinal electrical stimulation-induced activity. For this, we applied the A1 antagonist 8-cyclopentyl-1,3-dipropylxanthine (DPCPX) directly to the spinal cord of adult rats during supra-motor threshold ESS and assessed the neuromodulatory effects of DPCPX on spinally-evoked motor potentials. Although A2 receptors have been considered functionally marginal for the spinal sensorimotor circuits (Geiger et al., 1984), the A2 antagonist, 3,7-dimethyl-1-propargylxanthine (DMPX) was also tested in our study to explore any potential modulation of motor output evoked by ESS.

MATERIALS AND METHODS

Experimental Design

All procedures were approved by the Institutional Animal Care and Use Committee at Houston Methodist Research Institute. Further, they were in accordance with both the guidelines of the National Institutes of Health (NIH) Guide for the care and use of laboratory animals and the European Union directive on animal experimentation (2010/63/EU). Adult Long-Evans rats (female, 300–350 g body weight; Charles River Long-Evans, Houston, TX, USA) were anesthetized by intraperitoneal (i.p.) administration of ketamine (100 mg/Kg) and xylazine (5 mg/Kg) mix and terminal electrophysiological recordings were obtained. During each experiment, toe pinches were performed periodically to assess whether the anesthetic level was maintained. If animals exhibited a reflex, a booster of ketamine was administered, as needed. Additionally, animals were kept under anesthesia over a heating pad (37°C) throughout each experiment. Finally, at the end of all experiments (2–3 h), animals were euthanized by CO_2 followed by cervical dislocation or thoracotomy.

A cartoon schematizing the experimental design of the study is provided in **Figure 1A**. Briefly, two main experimental groups were included: rats with intact spinal cords (n = 8) and rats with transected spinal cords (n = 6). After collecting baseline recordings to serve as internal controls for each animal, the intact cord group was further split to explore the effects of DPCPX (n = 5) or DMPX (n = 3) applications. The transected group was also further divided into those exposed to DPCPX (n = 5, similar to the intact-DPCPX group) and sham control (n = 1). For the sham control animal, trains of pulses were regularly supplied as in the treated groups, albeit without the presence of any substances. The tests demonstrated the stability of baseline responses for the entire length of a recording session after acute spinal transection (50 min). This feature is illustrated in **Figure 1B**, as the unchanged main amplitude of spinal reflexes, pooled from bilateral tibialis anterior (TA) and left gastrocnemius (GM) muscles, in responses to the serial delivery of 40 Hz trains every 5 min, to mimic the stimulation rate provided during real experiments [P = 0.490, Friedman repeated-measures analysis of variance (ANOVA) on ranks, n = 3].

The prototypic experimental design is schematized in **Figure 1C**. After a 15 min wait for the full induction of anesthesia, surgical procedures were performed (lasting approximately 1 h) for laminectomy, as well as epidural and EMG electrode implantations. Where appropriate, a complete transection of the spinal cord was performed as soon as the cord was exposed (30 min). After surgery, the second injection of ketamine was administered followed by a rest period (15 min) that was required to achieve stable conditions. Then, electrophysiological recordings began by first placing EMG electrodes and exploring the threshold intensity of epidural stimulation and then by delivering three single rectangular pulses (100 μs, duration) at increasing intensities (0.1 mA increments) with an interstimulus interval of 5 s. Motor threshold intensity was defined in each animal as the lowest intensity to elicit consistent EMG responses in a given muscle, as revealed by visual inspection of waveforms on the computer monitor. The operative suprathreshold amplitude of stimulation (range of 0.4–2 mA) was selected for each animal to evoke responses in all recorded muscles during the experiments (usually equal to 0.1 mA over the threshold value). The stability of threshold responses was verified every 5 min, 2 min after each new application. After the threshold definition, the experiments started (40–45 min) by delivering a train of 2,000 pulses at 40 Hz every 5 min. To define baseline conditions, three trains (40 Hz) were firstly supplied before the local application of drugs on the cord. Then, chemicals (DPCPX or DMPX) were applied every 5 min at increasing concentrations (1–100 μM) and the trains were repeated every 5 min before a new concentration was applied.

Intramuscular Electromyogram (EMG) Electrode Implantation

EMG signals from bilateral TA and left GM muscles were derived from belly muscles using 13 mm paired subdermal needle electrodes (0.4 mm diameter, RLSND121-1.5, Rhythmlink Colombia, SC, USA) inserted through the shank skin. A ground electrode was placed subcutaneously on the left forearm. Before starting the experiment, proper placement of electrodes was confirmed by the motion artifact generated when tapping the muscle. EMG recordings were amplified (gain 1000, range 0.1 Hz to 1 kHz, and notched at 60 Hz) using a differential AC amplifier (DP-304A, Warner Instruments, Hamden, CT, USA) and subsequently digitalized at 40 kHz (PowerLab®, ADInstruments Pvt. Ltd., Bella Vista, NSW, Australia).

Epidural Electrode Implantation and Stimulating Protocol

After a partial laminectomy between thoracic (Th)12/Th13 and the complete removal of lumbar (L)1 lamina, two multistrand, Teflon-coated stainless-steel wires (AS 632, Cooner Wire Co, Chatsworth, CA, USA) was slid through the small opening at Th12/ Th13 up to L2. A small notch (0.5–1.0 mm) in each wire was deprived of insulation at L1 vertebral level (L5 spinal segment) to expose the conductor and form the electrodes, which were then placed on each side of the dorsal cord (1 mm laterally from the midline). The two wires were used as cathode and anode for bipolar stimulation. Single or repetitive current pulses (duration 100 μs) were supplied to the cord using a DS8R constant-current stimulator (Digitimer, UK). Trains of 2,000 stereotyped rectangular pulses at 40 Hz (interstimulus interval of 25 ms, the total time of the train of 50.2 s) were delivered every 5 min.

Experimental Spinal Cord Transection and Drug Application

An acute complete transection of the cord was performed in five animals at the upper thoracic level (vertebrae Th8 to Th11) using a pair of iridectomy scissors. The resulting gap was inspected by another expert surgeon and filled by a small cotton ball for the entire duration of the experiment. DPCPX (Cat. N. 0439/100, R&D Systems Inc., Minneapolis, MN, USA) and DMPX (Cat. N. D134, Sigma-Aldrich, St. Louis, MO, USA) were locally applied to the cord by diluting each drug in 500 μl of the saline medium. In four out of 14 experiments, before adding the two

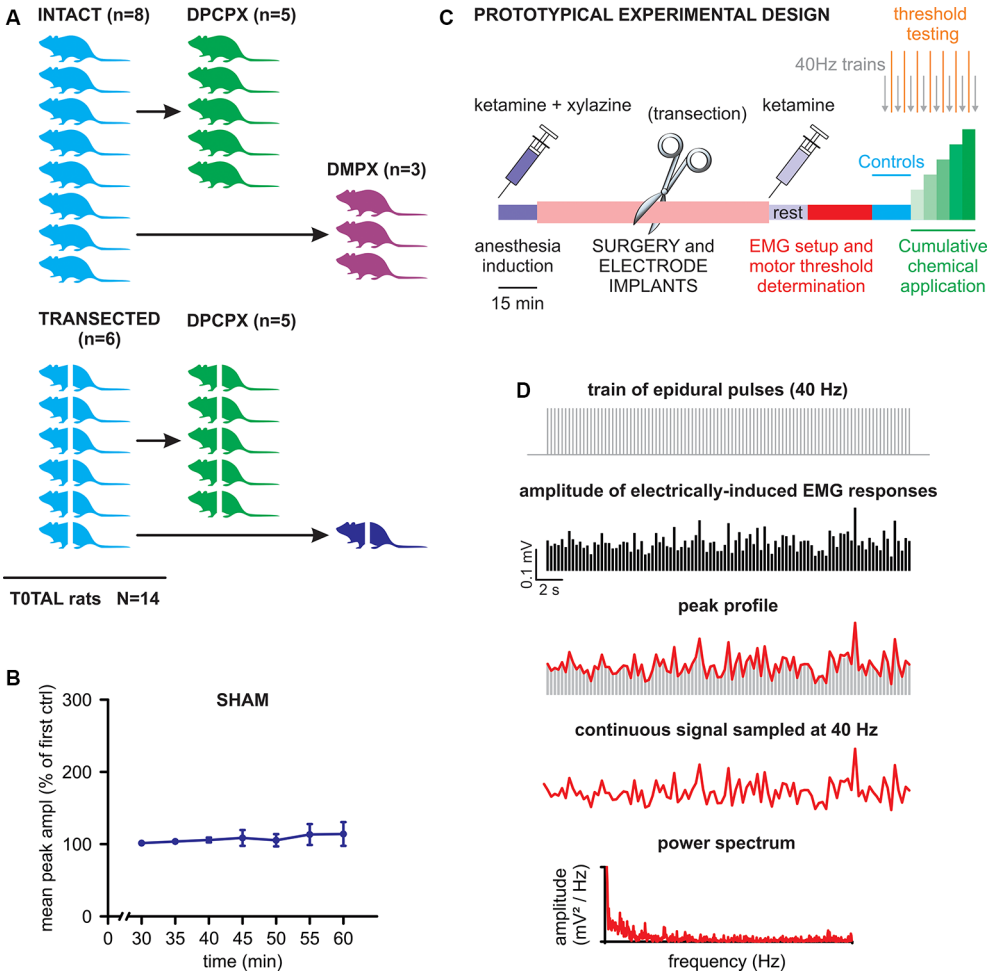

FIGURE 1 | Experimental design and analysis. **(A)** The cartoon schematizes the number of animals used in the study with the corresponding experimental protocols. Animals with transected spinal cords are represented by crossed bodies. **(B)** Mean peak amplitude, expressed as a percentage of the first delivered train, is shown in the graph for all consecutive trains applied for the whole duration of a standard experiment (one train per 5 min). The values of the amplitude of electromyogram (EMG) responses are averaged from three muscles of the same animal that received consecutive stimulations without any drug application (sham). Error bars represent standard deviation (SD). **(C)** A prototypical experiment is described in its different phases (see details in the "Materials and Methods" section). **(D)** The scheme draws the procedure to quantify the rhythmic pattern modulating the amplitude of electrically-induced EMG responses during the delivery of 40 Hz trains (see "Materials and Methods" for more details).

pharmacological agents, the dura was opened with a longitudinal incision along the midline of the entire spinal segment L5 (leaving the dura intact under the two electrodes). Given that no difference in drug effect was found when the dura remained intact compared to when it was not intact, data were pooled from both groups. This observation confirmed previous reports on the full permeability of the spinal dura to the substances used in the current study (Nantwi and Goshgarian, 2002). The effects of pharmacologic agents were determined by comparison with internal control for each animal. Specifically, responses in DPCPX or DMPX were compared to the baseline responses collected in the same animals before the application of drugs.

Data Analyses

Amplitude and latency (defined at the first deflection of baseline) of all EMG responses were determined using Labchart® version 8 (ADInstruments, Australia) and Clampfit® version 10.3 software (Molecular Devices, San Jose, CA, USA). The amplitude of all consecutive responses evoked by each train was plotted for each muscle as time-course graphs. In the animals in which simultaneous recordings were obtained from bilateral TA and left GM, all muscles showed equal responses as for latency (P = 0.567, one-way repeated measures ANOVA; n = 5) and peak to peak amplitude (P = 0.059, one-way repeated measures ANOVA; n = 5). The amplitude of suprathreshold responses in bilateral TAs and left GMs did not differ across muscle groups or among tested animals. Therefore, values were first averaged among different muscles in response to the same train, then averaged among repetitions from the same experiment, and finally pooled among different animals for statistical comparison between treatments. The sum of amplitude responses was calculated from raw values to obtain the mean cumulative

amplitude for each treatment. To identify whether spontaneous variations in the peaks of responses followed a rhythmic pattern of modulation, the procedure schematized in **Figure 1D** was performed. In brief, the linear profile connecting the peaks of the time-course of electrically induced EMG responses was handled as a continuous waveform, with the sampling period (25 ms) equal to the interstimulus interval at the frequency of stimulation (40 Hz). The intrinsic modulatory rhythm of the amplitude of EMG reflexes was quantified in terms of power spectrum magnitude and expressed as Root Mean Square (RMS; Deumens et al., 2013), measured with Clampex 10.3® (Molecular Devices Corporation, Downingtown, PA, USA). The analysis adopted a default rectangular windowing function, with data segments not overlapping, window length set at the largest value fitting within the data segments to be processed, and the first spectral bin of the periodogram excluded from RMS measurements. The magnitude of the resulting spectrum is the summed power of all rhythm frequencies. This statistical tool quantifies any increase in frequency and/or amplitude of EMG evoked-responses, expressed as a complex rhythm composed of multiple harmonics.

Statistical Analysis

Data are indicated as mean ± standard deviation (SD) values and n refers to the number of rats used. The normality of data distribution was determined based on a Kolmogorov–Smirnov normality test. Statistical analysis was performed using SigmaStat® version 3.5 software (Systat Software, San Jose, CA, USA) to compare the mean ± SD of different experimental conditions. All parametric values were analyzed using a two-tailed Student's *t*-test (paired or unpaired) to compare two groups of data or a one-way ANOVA for more than two groups. Nonparametric comparisons were performed using the Mann–Whitney rank-sum test (unpaired) and Wilcoxon signed-rank test (paired) for two groups and Kruskal–Wallis ANOVA for more than two groups. Friedman repeated-measures ANOVA on ranks was performed for multiple comparisons. Multiple comparisons were followed by *post hoc* tests (Dunn's Method). Results reached significance when $P < 0.05$.

RESULTS

Train Pulse Delivery Elicited EMG Responses That Were Spontaneously Modulated in Amplitude

In eight intact animals, electrical stimulation of the cord (intensity = 0.71 ± 0.26 mA) evoked control suprathreshold responses with a mean latency of 5.46 ± 0.77 ms and a mean peak to peak amplitude equal to 0.57 ± 0.45 mV. In **Figure 2A**, sample traces from three hindlimb muscles represent the first ten responses elicited by a train of rectangular pulses (100 μs) at 40 Hz applied to the cord at the L5 spinal segment (Th13/L1 vertebrae). The amplitude of consecutive motor reflexes varied from large to minimal (up to occasional abolishment) responses. A longer train of pulses (2,000 pulses at 40 Hz) elicited responses varying in amplitude throughout the entire protocol, as summarized by the average time-course of the peak amplitudes from five experiments (**Figure 2B**). Motor responses consistently faded away during the first 300 pulses (7.5 s of stimulation; **Figures 2B,C**) with a dramatic reduction occurring after the 1,800th pulse (45 s of stimulation) under continuous stimulation at a given intensity (**Figure 2D**). A brief rest was sufficient to reinstate full response, as evidenced by the equal values of the cumulative amplitude of all 2,000 motor reflexes evoked by two consecutive trains spaced 5 min apart (96.64 ± 16.77%; $P = 0.132$, paired *t*-test, $t = 1.703$; $n = 8$). To identify if the spontaneous variation of responses followed a particular rhythmic pattern of modulation, the mean time-course of peaks were analyzed using power spectral analysis (**Figure 2E**; $n = 5$). A rhythmic component centered around 1.41 ± 0.69 Hz and with an amplitude of 0.0017 ± 0.0011 mV/Hz^2 described the presence of a spontaneous rhythmic pattern of modulation with a power spectrum magnitude, expressed as RMS equal to 0.20 ± 0.13, $n = 5$.

These data indicate that continuous epidural stimulation with a train of pulses at 40 Hz produces EMG responses that are intrinsically modulated in amplitude by a spontaneous oscillatory rhythm of a lower frequency than the one supplied by the stimulating pattern.

The Selective A1 Competitive Antagonist, DPCPX, Maximizes Electrical Stimulation

To evaluate whether the selective pharmacological blockade of the A1 adenosine receptor subtype affects spinal cord stimulation, trains of 2,000 pulses (40 Hz) were serially delivered during increasing concentrations of the selective antagonist DPCPX (1–100 μM). The application of DPCPX at any dosage did not cause spontaneous activity in the muscles. The lowest concentration tested (1 μM) did not affect the cumulative amplitude of responses (DPCPX 1 μM = 134.46 ± 37.11% of control; $P = 0.080$, paired *t*-test, $t = -2.331$; $n = 5$). **Figure 3A** shows, from the same animal, reported in **Figure 2A**, the first 10 reflexes elicited in three hindlimb muscles by a train of rectangular pulses (100 μs) at 40 Hz. The cumulative amplitude of all 2,000 motor reflexes evoked from bilateral TA and left GM by electrical stimulation is significantly increased through the administration of 5 μM of DPCPX (**Figure 3E**; $P = 0.046$, paired *t*-test, $t = -2.861$; $n = 5$). **Figure 3F** illustrates that, in five animals, increasing concentrations of DPCPX (from 1 to 100 μM) further augments the cumulative amplitude of motor responses in a dose-response manner, reaching a plateau at the highest concentrations tested (263.36 ± 84.76% and 279.16 ± 119.08% to control, for 50 μM and 100 μM, respectively; $P = 0.044$, Kruskal–Wallis one-way ANOVA on ranks followed by *post hoc* multiple comparisons vs. DPCPX 1 μM group with Dunn's method, $n = 5, 5, 5, 5, 4$). Surprisingly, the first motor response evoked by a suprathreshold electrical stimulus applied to the spinal cord (duration = 0.1 ms; intensity = 0.78 ± 0.26 mA) was unaffected by 5 μM of DPCPX, as were the mean latency (5.44 ± 0.85 ms) and the mean peak to peak amplitude (0.50 ± 0.23 mV) of pooled data from five experiments. In the presence of DPCPX (5

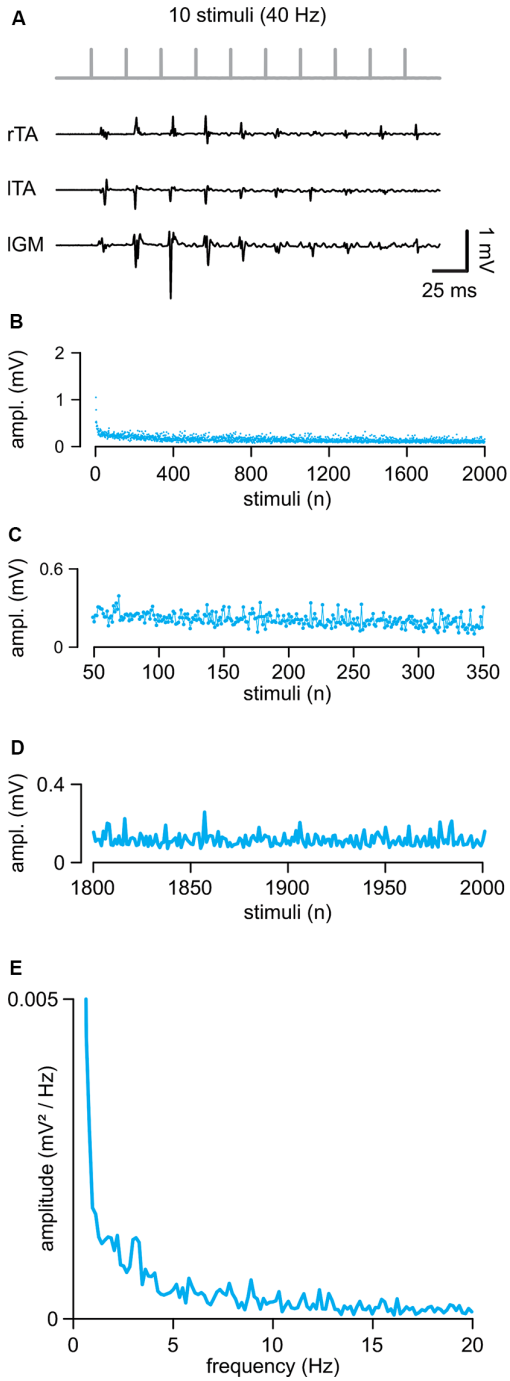

FIGURE 2 | Repetitive epidural stimuli elicit responses that are rhythmically modulated in amplitude. **(A)** A train of 10 stimuli applied to the cord (L5 spinal level) at 40 Hz evokes EMG reflexes from bilateral tibialis anterior (TA) and left gastrocnemius (GM) muscles. **(B)** The Mean time-course of the amplitude of responses over the entire length of a stimulation protocol (2,000 stimuli at 40 Hz) in five animals. **(C)** Magnification of the time-course in **(B)** draws responses to the first 300 stimuli (from the 50th to the 350th). **(D)** Magnification of the time-course in **(B)** shows the profile of peaks of the last 200 responses with their SD (from the 1,800th to the 2,000th). **(E)** The power spectrum of the mean time-course for five animals illustrates the rhythmic components of an oscillatory pattern of modulation of the peak amplitude throughout the entire stimulation protocol.

μM), the average time-course of peak amplitudes showed a trend of higher responses compared to control during the first 300 pulses from the beginning of stimulation (**Figures 3B,C** mean amplitude = 0.24 ± 0.04 mV in control vs. 0.33 ± 0.12 mV; P = 0.006, paired t-test, t = −5.240; n = 5). Moreover, with respect to control, multiple motor responses of higher amplitude appeared for the entire duration of the stimulation protocol (**Figures 3B,D**). Notably, the mean amplitude of the last two hundred responses in the presence of DPCPX (5 μM) was significantly higher than the last two hundred responses in control (181.77 ± 50.52%; P = 0.037, paired t-test, t = −3.088; n = 5). **Figure 3G** presents sample traces of recovering reflex responses evoked by the last ten stimuli of the train from the same experimental animal as in control and after administration of DPCPX (5 μM).

The power spectrum of the spontaneous amplitude of oscillations throughout the entire protocol demonstrated the presence of a rhythmic pattern of modulation with a frequency component equal to 1.29 ± 0.51 Hz, as reported in control (**Figure 3H**; P = 0.667, Paired t-test, t = 0.464; n = 5) and with an unchanged amplitude of 0.0036 ± 0.0031 mV/Hz^2 (Wilcoxon signed-rank test, P = 0.063; n = 5). However, following the administration of DPCPX (5 μM), the frequency spectrum was more populated by multiple harmonics at higher frequencies (around 3, 7, 13, and 19 Hz). Moreover, in the presence of DPCPX (5 μM), the power spectrum magnitude of rhythmic modulation significantly increased, as expressed by RMS equal to 0.32 ± 0.21 (P = 0.043, Paired t-test, t = 2.935; n = 5).

Overall, blockage of the adenosine A1 receptor subtype in combination with continuous electrical stimulation of the spinal cord increased the magnitude of the endogenous modulation pattern and postponed the decay of responses that, in fact, periodically appeared higher during the entire protocol.

In contrast, the selective A2 antagonist, DMPX, did not affect the amplitude of spinally-evoked EMG responses at any of the concentrations tested (from 1 to 100 μM; P = 0.995, Kruskal–Wallis one-way ANOVA on Ranks; n = 3).

An Acute Transection Reduced the Amplitude of EMG Responses to Trains of Consecutive Pulses

In five animals, an acute transection of the spinal cord at the low thoracic level did not affect motor responses to single epidural pulses applied below the lesion site (duration = 0.1 ms; intensity = 1.34 ± 0.44 mA). When compared to intact control responses, spinal reflexes elicited by single suprathreshold stimuli, after acute injury, showed unchanged mean latency (5.29 ± 1.04 ms; P = 0.738, t-test, t = 0.343; n = 8, 5) and mean amplitude (0.43 ± 0.26 mV; P = 0.549; t-test, t = 0.618; n = 8, 5). In **Figure 4A**, in a representative animal, the first ten reflexes elicited by a train at 40 Hz were derived from three muscles. Although spinal reflexes to the first pulse seemed unaffected by transection, they showed more frequent failures to the following nine stimuli (**Figure 4A**). To further explore responses to repetitive stimulation after an acute spinal transection, consecutive motor responses were induced by

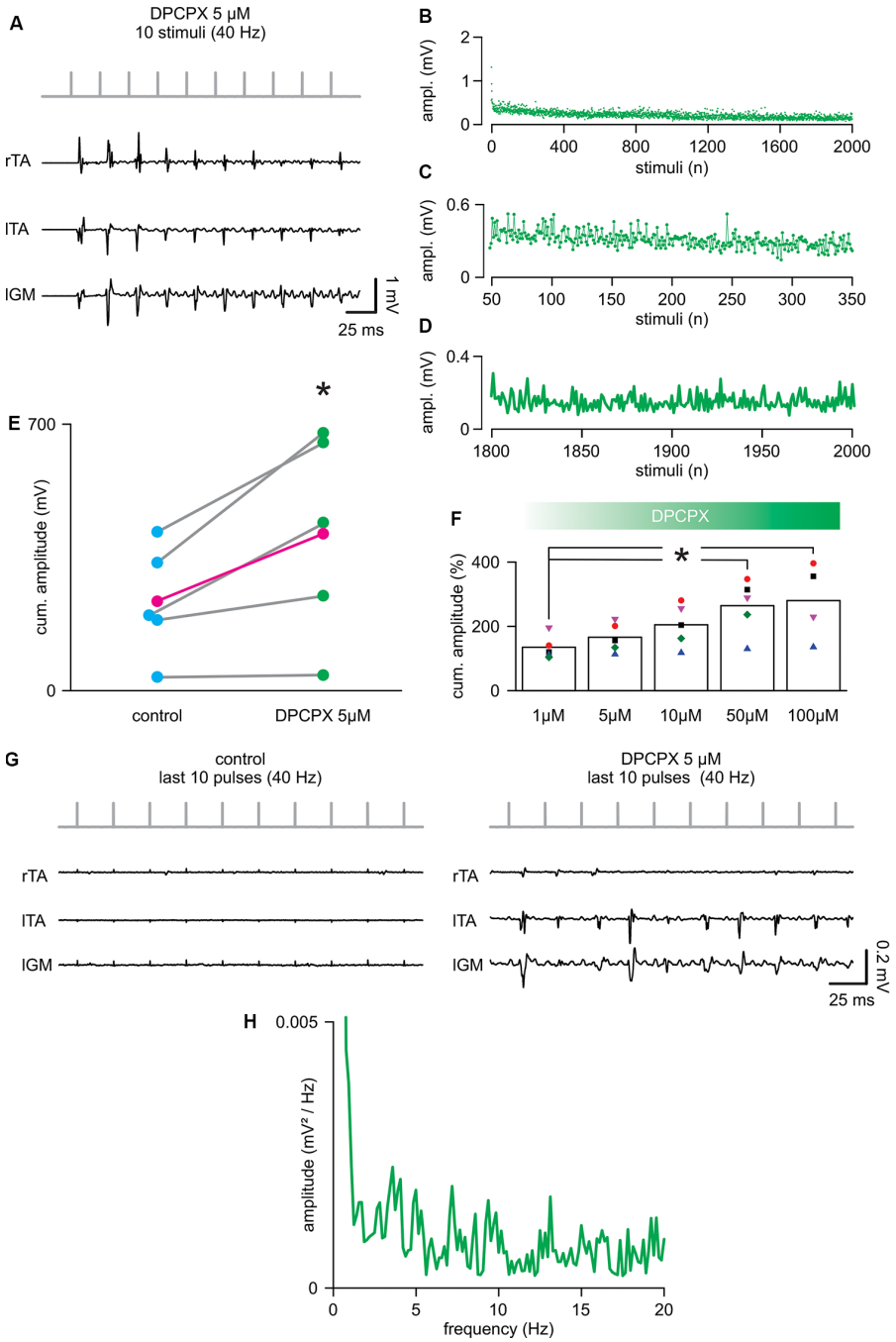

FIGURE 3 | 8-cyclopentyl-1,3-dipropylxanthine (DPCPX) augments reflex amplitude during repetitive stimulation. **(A)** For the same animal as in **Figure 1A**, DPCPX 5 µM increases the amplitude of reflexes elicited from bilateral tibialis anterior (TA) and left gastrocnemius (lGM) muscles by a train of 10 stimuli applied to the cord (L5 spinal level) at 40 Hz. **(B)** Mean time-course of the amplitude of responses over the entire length of a stimulation protocol (2,000 stimuli at 40 Hz) in combination with DPCPX (5 µM) in five animals (same animals of **Figure 2**). **(C)** Magnification of the time-course in **(B)** plots responses to the first 300 stimuli (from the 50th to the 350th). **(D)** Magnification of the time-course in **(B)** shows the profile of peaks of the last 200 responses (from the 1,800th to the 2,000th). **(E)** Scatter plot of paired data reports the statistical increase of the cumulative amplitude of EMG responses elicited in five experiments by DPCPX (5 µM) during the entire electrical stimulation protocol (*P = 0.046; each pair of dots represent a single animal, while the average values are in magenta; n = 5). **(F)** Cumulative dose-response of the effect of DPCPX (1–100 µM) in augmenting the cumulative amplitude of EMG reflexes elicited by 2,000 stimuli at 40 Hz. Data are pooled from five animals. Data are expressed as a percentage (%) of the respective untreated controls (*P = 0.044). **(G)** Sample traces from the same animal in **Figure 2A** comparing responses from bilateral TAs and lGM to the last 10 stimuli of the protocol (from 1,990th to 2,000th stimuli) in control (left) and DPCPX (5 µM; right). **(H)** The power spectrum of the mean time-course for five animals (as in **Figure 2**) illustrates the rhythmic components of the oscillatory pattern of modulation of the peak amplitude throughout the entire stimulation protocol.

delivering a train of pulses (2,000 stimuli, 40 Hz). In **Figure 4B**, the average time-course of peak amplitudes was traced from five experiments. Compared to intact animals, consecutive reflexes significantly faded away faster during the first 300 stimuli (7.5 s of stimulation; **Figures 4B,C**; 44.63 ± 22.57% to control; $P = 0.005$, t-test, $t = 3.810$; $n = 5$) and were completely abolished after approximately the 800th pulse (∼25 s of stimulation) under continuous stimulation at the same intensity (**Figures 4B,D**). Collectively, the mean cumulative amplitude of all 2,000 motor reflexes evoked by the stimulation protocol in injured spinal cords is significantly lower concerning intact control spinal cords (51% of intact controls; $P = 0.045$; Mann–Whitney rank-sum test; $n = 8, 5$).

The power spectrum of the mean time-course was largely suppressed (RMS = 0.077 ± 0.02; $n = 5$; **Figure 4E**), but still displayed a single principal component of modulation that is equal to intact controls (1.41 ± 0.33 Hz, $n = 5$), albeit of negligible amplitude (0.00002 ± 0.0002 mV/Hz^2; $n = 5$).

In summary, in contrast to intact animals, after an acute transection, the magnitude of motor response modulation to repeated ESS was abolished within the first few seconds (typically, less than 10 s) from stimulation onset, with the amplitude scarcely modulated by the endogenous rhythmic pattern.

The Selective A1 Competitive Antagonist, DPCPX Did Not Affect the Motor Output Induced by Electrical Stimulation Immediately Following Spinal Transection

In the current study, we reported that DPCPX augmented the amplitude of repetitive responses in intact animals. Moreover, we indicated that, after an acute spinal transection, the motor output elicited by a train of pulses was dramatically reduced. To verify whether the selective antagonism of A1 receptors could rescue motor reflexes immediately following spinal transection, increasing concentrations of DPCPX were applied to the lumbosacral cord below the level of transection. However, no differences were revealed in the cumulative amplitude of reflexes, even at higher DPCPX concentrations (50–100 μM; $P = 0.953$; Kruskal–Wallis one-way ANOVA on Ranks; $n = 5$), following transection when compared to baseline responses.

DISCUSSION

Despite the promise of ESS in subjects with SCI (Angeli et al., 2018; Gill et al., 2018; Wagner et al., 2018), variability in patient responses and sub-restorative levels of improvement indicate the need for the development of co-therapies to improve the clinical efficacy of ESS therapy. Combining spinal electrical neuromodulation with pharmacological approaches presents an appealing mechanism to augment the effectiveness of neurorehabilitation. Here, we demonstrate that selective pharmacological blockage of A1 subtype adenosine receptors during spinal electrical stimulation facilitates sensorimotor networks in the intact spinal cord. A1 inhibition results in an increased magnitude of an endogenous pattern that modulated

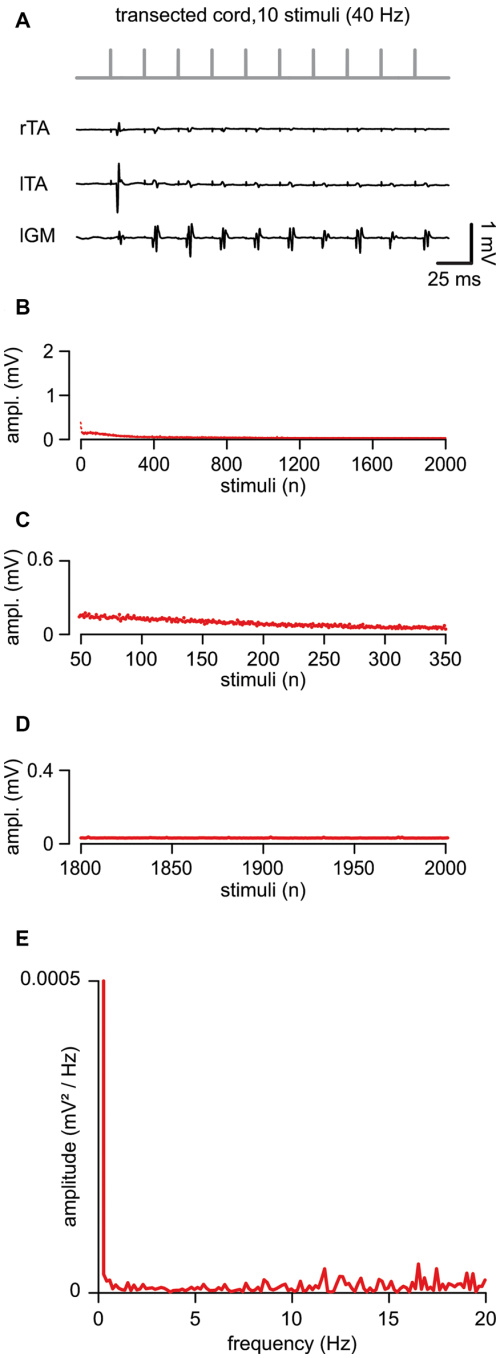

FIGURE 4 | An acute transection perturbs the peak amplitude of repetitive, spinally-induced reflexes. **(A)** After transection of the cord (Th 10/11), a train of 10 stimuli applied to the cord (L5 spinal level) at 40 Hz evokes EMG reflexes from bilateral tibialis anterior (TA) and left gastrocnemius (GM) muscles. **(B)** Mean time course of the amplitude of responses over the entire length of a stimulation protocol (2,000 stimuli at 40 Hz). Data pooled from five animals with a transected spinal cord. **(C)** Magnification of the time-course in **(B)** draws responses to the first 300 stimuli (from the 50th to the 350th). **(D)** Magnification of the time-course in **(B)** shows the profile of peaks of the last 200 responses (from the 1,800th to the 2,000th). **(E)** The power spectrum of the mean time-course for five animals illustrates the rhythmic components of an oscillatory pattern of modulation of the peak amplitude throughout the entire stimulation protocol.

spinally-evoked motor potentials and sustained duration of ESS-induced activity.

Motor Output to Epidural Stimulation Is Affected by an Endogenous Pattern of Modulation

In the clinic, repetitive ESS with a train of electrical pulses has been applied at different frequencies to elicit distinct types of motor recovery in select groups of young adults with chronic and complete SCI (Barolat et al., 1986; Jilge et al., 2004; Minassian et al., 2007; Harkema et al., 2011; Grahn et al., 2017). This pattern of stimulation elicits a series of spinally-evoked motor potentials, which are, in nature, similar to spinal reflexes from hindlimb muscles (Sayenko et al., 2014; Hofstoetter et al., 2018). However, the response to each delivered pulse can be periodically modulated during repetitive spinal stimulation of the same frequency and intensity (Hofstoetter et al., 2015; Sayenko et al., 2019). Similarly, here we demonstrate that the amplitude of spinally-induced reflexes can vary stochastically during repetitive epidural stimulation in fully anesthetized animals. These fluctuations of peak responses have also been observed previously in anesthetized animals that were continuously subjected to pulses train at a subthreshold intensity and lower frequency (i.e., 0.3 Hz) than those used in this study (Taccola et al., 2020a). Based on this evidence, we recently postulated that an endogenous pattern of modulation of the motor output originates from spinal networks (Taccola et al., 2020a). Present data corroborate that an endogenous pattern of modulation of spinally-induced reflexes occurs in response to a stimulation protocol that replicates the characteristics of a standard clinical ESS procedure (40 Hz, suprathreshold intensity). Moreover, power spectral density analysis of the reflex peaks' time-course shows that repetitive spinally-evoked motor potentials are rhythmically modulated. Indeed, we consistently observed that the main component of the periodic pattern of modulation was more pronounced in amplitude every ∼50 stimuli, which is at ∼0.8 Hz. A similar endogenous sinusoidal pattern originating from spinal circuits has been reported during rhythmic modulation of the amplitude of motor output in behaving cats (Cuellar et al., 2009).

It remains to be seen whether the optimal frequency of stimulation should be tuned to the intrinsic physiologic pattern of activity to maximize the effectiveness of neuromodulation.

In particular, it is yet to be explored whether spinal stimulation implemented by delivering trains of stimuli within the range shown to be physiologically effective and containing the principal components of the intrinsic physiological patterns of modulation (Gerasimenko et al., 2005; Lavrov et al., 2006), can modulate spinal networks to a more receptive state. Alternatively, it remains to be explored to what extent do the failures of stimulation to induce a response to contribute to the summation of the membrane potential of spinal neurons, thereby affecting spinal neuron thresholds at periodic higher frequencies.

Neurochemical Response to ESS

During training sessions in the presence of stimulation in humans, the motor output cannot be sustained at the same level and has been noticed to decline with the duration of the training and stimulation (Rejc et al., 2017; Gill et al., 2018; Sayenko et al., 2019). Multiple factors can contribute to this decline of a patient's performance, including cardiovascular and muscle fatigue which are proportionally dependent on the duration and amount of motor activity. However, this decline of performance must also be considered in the context of neurochemical responses to ESS. It is critical to note that spinal stimulation drives multiple responses. For example, spinal stimulation simultaneously facilitates the release of many neurotransmitters and neuromodulators because of the different synapses encountered by the electrical field in the spinal cord (Taccola et al., 2018). This increase of neurotransmitters and neuromodulators acts at the synaptic milieu of multiple network sites, including their release from the same Ia afferents that were involved during a continuous repetitive stimulation (Kuno, 1964; Hofstoetter et al., 2019). Through this release of multiple neurotransmitters and neuromodulators, ESS might mimic the physiological changes in the chemical environment of the spinal cord during rhythmic activities (e.g., locomotion) or lead to synaptic "fatigue" and induction of receptor sensitization (Taccola et al., 2018). In the current study, the amplitude of muscle responses to 40 Hz stimulation of suprathreshold intensity decreased until full response abolishment occurred after less than 45 s. This fact is reminiscent of the spontaneously decaying locomotor-like oscillations evoked by electrical stimulation in the isolated spinal cord, even during the continuous delivery of pulses (Marchetti et al., 2001b). This failure has been ascribed to presynaptic mechanisms associated with a diminished release of glutamate during prolonged stimulation. Besides, at the postsynaptic level, a membrane shunt determined by a local increase of potassium concentrations in the extracellular milieu should also be considered (Marchetti et al., 2001a). Further, the release of inhibitory neurotransmitters triggered by continuous stimulation can contribute to the decay of responses (Dale and Gilday, 1996). The present results indicate that, although a strong suppression of spinally-induced reflexes occurs after ∼45 s of the stimulation protocol, a brief 5-min rest was sufficient to promote the reemergence of suprathreshold motor responses between repetitions. This prompt recovery of the evoked motor output helps to explain the efficacy of burst spinal cord stimulation over the 40 Hz "gold standard" used for spinal stimulation protocols in experimental animal models (Taccola, 2011; Meuwissen et al., 2019; Taccola et al., 2020a). Indeed, when trains of stimuli (e.g. 60 s) were repetitively applied over a long time frame (e.g., 45 min) to spinal cords isolated from neonatal rats, 2-min pauses appeared necessary to equally activate spinal circuits for locomotion (Dingu et al., 2016). The self-limiting properties of the spinal circuits that process repetitive pulses indicate the need to include periodic pauses during continuous ESS to maximize the expression of motor responses.

The facilitatory effect of the A1 antagonist on the amplitude of motor output illustrated in the current study is explained by two tentative mechanisms. First, DPCPX selectively blocks inhibitory presynaptic receptors on primary afferents to maximize input

delivery. Second, the antagonism of postsynaptic A1 receptors depressing the activity of spinal networks (Witts et al., 2015) might increase the excitability of the spinal cord, in turn, maximizing the magnitude of motor output.

An Acute Spinal Transection Depresses the Response of Repetitive Spinal Cord Stimulation

In the present study, although DPCPX largely increased the yield of repetitive stimulation in intact cords, after a spinal transection the selective antagonism of A1 receptors appeared to be ineffective. This can be in line with the contrasting and paradoxical effects of adenosine agonists and antagonists reported in various neurodegenerative conditions (Stone et al., 2009). For instance, a previous study showed a massive release of adenosine right after a spinal lesion (McAdoo et al., 2000), and adenosine is putatively able to compete with DPCPX at A1 receptor sites. In our study, an acute spinal cord transection affected the amplitude of reflexes evoked by repetitive stimulation. Moreover, the endogenous pattern of modulation was largely silenced immediately after spinal transection, without the periodic appearance of higher peaks that occur in intact cords under the stimulation protocol. Following an acute SCI, a period of several hours to a few weeks has been reported both in humans and in animals (Lavrov et al., 2008), wherein electrophysiological signals, such as spinal reflexes, are depressed (Ditunno et al., 2004). The mechanisms of this reduced neural activity remain poorly understood. At the same time, although the existence of an acute period of spinal shock in rats has been reported after severe spinal contusions (Taccola et al., 2020b) it is rarely the case immediately after complete surgical transection of the cord conducted under full anesthesia (Coskun et al., 2010). Our study demonstrates that spinal reflexes in response to single epidural pulses remain unaffected by spinal transection, similar to what has been reported in awake rats (Lavrov et al., 2006). However, the responses to repetitive stimuli were reduced. We can speculate that the transection of descending and propriospinal projections reduces the extent of lumbar spinal circuits by interrupting reverberating polysynaptic pathways possibly involved in the modulation of repetitive responses. Still, whether similar effects are also present in chronic injuries needs to be demonstrated.

CONCLUSIONS

In the current study, we further explore how the amplitude of motor responses evoked by repetitive pulses applied to a rodent spinal cord is modulated by the endogenous spinal rhythm (Taccola et al., 2020b). This endogenous pattern of modulation is different from the central pattern generator for locomotion (Dimitrijevic et al., 1998) since it has not been able, *per se*, to generate any coordinated motor activity from hindlimb muscles. Rather, it can be speculated that the endogenous pattern of modulation represents an intrinsic and rhythmic tone able to set the subthreshold excitability of propriospinal circuits (Taccola et al., 2020a). At the cellular level, it should be viewed as synchronized spontaneous oscillations occurring in the resting potentials of circuit elements that do not reach the threshold for triggering an action potential, but which can still summate incoming external input. Synchronized subthreshold changes in membrane potentials spontaneously occur in microcircuits *in vitro* (Lampl and Yarom, 1993; Lefler et al., 2020). It seems imperative now to explore if a similar pattern of modulation can be found in the human spinal cord. This information will help better define the whole duration of each ESS session and tune the frequency of neuromodulating paradigms, thereby increasing the extent of motor recovery. Although in the current study, DPCPX was unable to facilitate neuromuscular response during spinal cord stimulation in acute spinal cord transected rats, this is likely due to temporary ionic disruption of spinal networks. Future research should include additional preclinical studies in chronically injured animals to elucidate a potential role of the selective pharmacological A1 antagonism in maximizing the recovery of motor output during ESS and compare the effects with previously used pharmacological neuromodulation agents within the same protocol. Also, spinal electrical neuromodulation has recently received great attention as an innovative rehabilitation tool for several neuromotor conditions that do not affect the spinal cord directly, such as multiple sclerosis (Illis et al., 1980), Parkinson's disease (Santana et al., 2014; de Andrade et al., 2016; Samotus et al., 2018; de Souza et al., 2018), and cerebellar ataxia (Solopova et al., 2017). For these pathologies, A1 antagonists are a potential new avenue for restoring sensorimotor functions in the presence of spinal stimulation. At the same time, more detailed and intensive preclinical studies are needed to investigate dosage, optimize methods of delivery, and potential systemic effects and precautions, before the synergistic application of A1 antagonists and spinal stimulation is translated to clinic.

DATA AVAILABILITY STATEMENT

The raw data supporting the conclusions of this article will be made available by the authors, without undue reservation.

ETHICS STATEMENT

The animal study was reviewed and approved by Institutional Animal Care and Use Committee at Houston Methodist Research Institute.

AUTHOR CONTRIBUTIONS

GT conceptualized the study. GT, DS, PJH, BHS, and MKH performed experiments. GT, RA, and DS analyzed data. GT prepared figures. GT and DS drafted the manuscript. All authors revised the manuscript and approved the final version. All authors agree to be accountable for all aspects of the work in ensuring that questions related to the accuracy or integrity of any part of the work are appropriately investigated and resolved.

FUNDING

GT was supported by the Leonardo da Vinci 2019 fellowship from The Conference of Italian University Rectors and the Ministry of Education, University and Research (Italy) and from the European Union's Horizon 2020 Research and Innovation Program under the Marie Skłodowska-Curie (grant agreement No. 661452). The authors declare that this study received philanthropic funding from Paula and Rusty Walter and Walter Oil and Gas Corp. The funder was not involved in the study design, collection, analysis, interpretation of data, the writing of this article or the decision to submit it for publication. MKH was supported by a fellowship from the Craig H. Neilsen Foundation and a Wings for Life grant to PJH.

ACKNOWLEDGMENTS

GT is grateful to Dr. Elisa Ius for her excellent assistance in preparing the manuscript. We thank Dr. Gillian Hamilton for reviewing and proofreading the manuscript.

REFERENCES

Acton, D., and Miles, G. B. (2015). Stimulation of glia reveals modulation of mammalian spinal motor networks by adenosine. *PLoS One* 10:e0134488. doi: 10.1371/journal.pone.0134488

Angeli, C. A., Boakye, M., Morton, R. A., Vogt, J., Benton, K., Chen, Y., et al. (2018). Recovery of over-ground walking after chronic motor complete spinal cord injury. *N. Engl. J. Med.* 379, 1244–1250. doi: 10.1056/NEJMoa1803588

Angeli, C. A., Edgerton, V. R., Gerasimenko, Y. P., and Harkema, S. J. (2014). Altering spinal cord excitability enables voluntary movements after chronic complete paralysis in humans. *Brain* 137, 1394–1409. doi: 10.1093/brain/awu038

Aslan, S. C., Legg Ditterline, B. E., Park, M. C., Angeli, C. A., Rejc, E., Chen, Y., et al. (2018). Epidural spinal cord stimulation of lumbosacral networks modulates arterial blood pressure in individuals with spinal cord injury-induced cardiovascular deficits. *Front. Physiol.* 9:565. doi: 10.3389/fphys.2018.00565

Aslan, S. C., Randall, D. C., Krassioukov, A. V., Phillips, A., and Ovechkin, A. V. (2016). Respiratory training improves blood pressure regulation in individuals with chronic spinal cord injury. *Arch. Phys. Med. Rehabil.* 97, 964–973. doi: 10.1016/j.apmr.2015.11.018

Bai, H.-H., Liu, J.-P., Yang, L., Zhao, J.-Y., Suo, Z.-W., Yang, X., et al. (2017). Adenosine A1 receptor potentiated glycinergic transmission in spinal cord dorsal horn of rats after peripheral inflammation. *Neuropharmacology* 126, 158–167. doi: 10.1016/j.neuropharm.2017.09.001

Barolat, G., Myklebust, J. B., and Wenninger, W. (1986). Enhancement of voluntary motor function following spinal cord stimulation—case study. *Appl. Neurophysiol.* 49, 307–314. doi: 10.1159/000100160

Burnstock, G. (2007). Physiology and pathophysiology of purinergic neurotransmission. *Physiol. Rev.* 87, 659–797. doi: 10.1152/physrev.00043.2006

Burnstock, G., and Wood, J. N. (1996). Purinergic receptors: their role in nociception and primary afferent neurotransmission. *Curr. Opin. Neurobiol.* 6, 526–532. doi: 10.1016/s0959-4388(96)80060-2

Caciagli, F., Ciccarelli, R., Di Iorio, P., Ballerini, P., and Tacconelli, L. (1988). Cultures of glial cells release purines under field electrical stimulation: the possible ionic mechanisms. *Pharmacol. Res. Commun.* 20, 935–947. doi: 10.1016/s0031-6989(88)80122-x

Coskun, C., Avci, B., Ocak, N., Yalcin, M., Dirican, M., and Savci, V. (2010). Effect of repeatedly given CDP-choline on cardiovascular and tissue injury in spinal shock conditions: investigation of the acute phase. *J. Pharm. Pharmacol.* 62, 497–506. doi: 10.1211/jpp.62.04.0013

Courtine, G., Gerasimenko, Y., van den Brand, R., Yew, A., Musienko, P., Zhong, H., et al. (2009). Transformation of nonfunctional spinal circuits into functional states after the loss of brain input. *Nat. Neurosci.* 12, 1333–1342. doi: 10.1038/nn.2401

Cuellar, C. A., Tapia, J. A., Juarez, V., Quevedo, J., Linares, P., Martinez, L., et al. (2009). Propagation of sinusoidal electrical waves along the spinal cord during a fictive motor task. *J. Neurosci.* 29, 798–810. doi: 10.1523/JNEUROSCI.3408-08.2009

Dale, N., and Gilday, D. (1996). Regulation of rhythmic movements by purinergic neurotransmitters in frog embryos. *Nature* 383, 259–263. doi: 10.1038/383259a0

Darrow, D., Balser, D., Netoff, T. I., Krassioukov, A., Phillips, A., Parr, A., et al. (2019). Epidural spinal cord stimulation facilitates immediate restoration of dormant motor and autonomic supraspinal pathways after chronic neurologically complete spinal cord injury. *J. Neurotrauma* 36, 2325–2336. doi: 10.1089/neu.2018.6006

de Andrade, E. M., Ghilardi, M. G., Cury, R. G., Barbosa, E. R., Fuentes, R., Teixeira, M. J., et al. (2016). Spinal cord stimulation for Parkinson's disease: a systematic review. *Neurosurg. Rev.* 39, 27–35. doi: 10.1007/s10143-015-0651-1

de Leon, R. D., Tamaki, H., Hodgson, J. A., Roy, R. R., and Edgerton, V. R. (1999). Hindlimb locomotor and postural training modulates glycinergic inhibition in the spinal cord of the adult spinal cat. *J. Neurophysiol.* 82, 359–369. doi: 10.1152/jn.1999.82.1.359

de Souza, C. P., Dos Santos, M. G. G., Hamani, C., and Fonoff, E. T. (2018). Spinal cord stimulation for gait dysfunction in Parkinson's disease: essential questions to discuss. *Mov. Disord.* 33, 1828–1829. doi: 10.1002/mds.27508

Deumens, R., Mazzone, G., and Taccola, G. (2013). Early spread of hyperexcitability to caudal dorsal horn networks after a chemically-induced lesion of the rat spinal cord *in vitro*. *Neuroscience* 229, 155–163. doi: 10.1016/j.neuroscience.2012.10.036

Dimitrijevic, M. R., Gerasimenko, Y., and Pinter, M. M. (1998). Evidence for a spinal central pattern generator in humans. *Ann. N Y Acad. Sci.* 860, 360–376. doi: 10.1111/j.1749-6632.1998.tb09062.x

Dingu, N., Deumens, R., and Taccola, G. (2016). Electrical stimulation able to trigger locomotor spinal circuits also induces dorsal horn activity. *Neuromodulation* 19, 38–46. doi: 10.1111/ner.12354

Ditunno, J., Little, J., Tessler, A., and Burns, A. (2004). Spinal shock revisited: a four-phase model. *Spinal Cord* 42, 383–395. doi: 10.1038/sj.sc.3101603

Edgerton, V. R., Courtine, G., Gerasimenko, Y. P., Lavrov, I., Ichiyama, R. M., Fong, A. J., et al. (2008). Training locomotor networks. *Brain Res. Rev.* 57, 241–254. doi: 10.1016/j.brainresrev.2007.09.002

Fisone, G., Borgkvist, A., and Usiello, A. (2004). Caffeine as a psychomotor stimulant: mechanism of action. *Cell. Mol. Life Sci.* 61, 857–872. doi: 10.1007/s00018-003-3269-3

Fong, A. J., Roy, R. R., Ichiyama, R. M., Lavrov, I., Courtine, G., Gerasimenko, Y., et al. (2009). Recovery of control of posture and locomotion after a spinal cord injury: solutions staring us in the face. *Prog. Brain Res.* 175, 393–418. doi: 10.1016/S0079-6123(09)17526-X

Freyvert, Y., Yong, N. A., Morikawa, E., Zdunowski, S., Sarino, M. E., Gerasimenko, Y., et al. (2018). Engaging cervical spinal circuitry with non-invasive spinal stimulation and buspirone to restore hand function in chronic motor complete patients. *Sci. Rep.* 8:15546. doi: 10.1038/s41598-018-33123-5

Gad, P., Gerasimenko, Y., Zdunowski, S., Turner, A., Sayenko, D., Lu, D. C., et al. (2017). Weight bearing over-ground stepping in an exoskeleton with non-invasive spinal cord neuromodulation after motor complete paraplegia. *Front. Neurosci.* 11:333. doi: 10.3389/fnins.2017.00333

Geiger, J., LaBella, F., and Nagy, J. (1984). Characterization and localization of adenosine receptors in rat spinal cord. *J. Neurosci.* 4, 2303–2310. doi: 10.1523/jneurosci.04-09-02303.1984

Gerasimenko, Y. P., Lavrov, I. A., Bogacheva, I. N., Shcherbakova, N. A., Kucher, V. I., and Musienko, P. E. (2005). Formation of locomotor patterns in decerebrate cats in conditions of epidural stimulation of the spinal cord. *Neurosci. Behav. Physiol.* 35, 291–298. doi: 10.1007/s11055-005-0059-4

Gerasimenko, Y. P., Lu, D. C., Modaber, M., Zdunowski, S., Gad, P., Sayenko, D. G., et al. (2015). Noninvasive reactivation of motor descending

control after paralysis. *J. Neurotrauma* 32, 1968–1980. doi: 10.1089/neu.2015.4008

Gill, M. L., Grahn, P. J., Calvert, J. S., Linde, M. B., Lavrov, I. A., Strommen, J. A., et al. (2018). Neuromodulation of lumbosacral spinal networks enables independent stepping after complete paraplegia. *Nat. Med.* 24, 1677–1682. doi: 10.1038/s41591-018-0175-7

Grahn, P. J., Lavrov, I. A., Sayenko, D. G., Van Straaten, M. G., Gill, M. L., Strommen, J. A., et al. (2017). Enabling task-specific volitional motor functions *via* spinal cord neuromodulation in a human with paraplegia. *Mayo Clin. Proc.* 92, 544–554. doi: 10.1016/j.mayocp.2017.02.014

Harkema, S., Gerasimenko, Y., Hodes, J., Burdick, J., Angeli, C., Chen, Y., et al. (2011). Effect of epidural stimulation of the lumbosacral spinal cord on voluntary movement, standing and assisted stepping after motor complete paraplegia: a case study. *Lancet* 377, 1938–1947. doi: 10.1016/S0140-6736(11)60547-3

Herrity, A. N., Williams, C. S., Angeli, C. A., Harkema, S. J., and Hubscher, C. H. (2018). Lumbosacral spinal cord epidural stimulation improves voiding function after human spinal cord injury. *Sci. Rep.* 8:8688. doi: 10.1038/s41598-018-26602-2

Hochman, S., Garraway, S. M., Machacek, D. W., and Shay, B. L. (2001). 5-HT receptors and the neuromodulatory control of spinal cord function. in *Motor Neurobiol. Spinal Cord*, eds Timothy C. Cope, (CRC Press), 47–87. ISBN: 978-0849300066.

Hofstoetter, U. S., Danner, S. M., Freundl, B., Binder, H., Mayr, W., Rattay, F., et al. (2015). Periodic modulation of repetitively elicited monosynaptic reflexes of the human lumbosacral spinal cord. *J. Neurophysiol.* 114, 400–410. doi: 10.1152/jn.00136.2015

Hofstoetter, U. S., Freundl, B., Binder, H., and Minassian, K. (2018). Common neural structures activated by epidural and transcutaneous lumbar spinal cord stimulation: elicitation of posterior root-muscle reflexes. *PLoS One* 13:e0192013. doi: 10.1371/journal.pone.0192013

Hofstoetter, U. S., Freundl, B., Binder, H., and Minassian, K. (2019). Recovery cycles of posterior root-muscle reflexes evoked by transcutaneous spinal cord stimulation and of the H reflex in individuals with intact and injured spinal cord. *PLoS One* 14:e0227057. doi: 10.1371/journal.pone.0227057

Illis, L. S., Sedgwick, E. M., and Tallis, R. C. (1980). Spinal cord stimulation in multiple sclerosis: clinical results. *J. Neurol. Neurosurg. Psychiatry* 43, 1–14. doi: 10.1136/jnnp.43.1.1

Jilge, B., Minassian, K., Rattay, F., Pinter, M. M., Gerstenbrand, F., Binder, H., et al. (2004). Initiating extension of the lower limbs in subjects with complete spinal cord injury by epidural lumbar cord stimulation. *Exp. Brain Res.* 154, 308–326. doi: 10.1007/s00221-003-1666-3

Kuno, M. (1964). Mechanism of facilitation and depression of the excitatory synaptic potential in spinal motoneurones. *J. Physiol.* 175, 100–112. doi: 10.1113/jphysiol.1964.sp007505

Lampl, I., and Yarom, Y. (1993). Subthreshold oscillations of the membrane potential: a functional synchronizing and timing device. *J. Neurophysiol.* 70, 2181–2186. doi: 10.1152/jn.1993.70.5.2181

Lavrov, I., Dy, C. J., Fong, A. J., Gerasimenko, Y., Courtine, G., Zhong, H., et al. (2008). Epidural stimulation induced modulation of spinal locomotor networks in adult spinal rats. *J. Neurosci.* 28, 6022–6029. doi: 10.1523/jneurosci.0080-08.2008

Lavrov, I., Gerasimenko, Y. P., Ichiyama, R. M., Courtine, G., Zhong, H., Roy, R. R., et al. (2006). Plasticity of spinal cord reflexes after a complete transection in adult rats: relationship to stepping ability. *J. Neurophysiol.* 96, 1699–1710. doi: 10.1152/jn.00325.2006

Layland, J., Carrick, D., Lee, M., Oldroyd, K., and Berry, C. (2014). Adenosine: physiology, pharmacology and clinical applications. *JACC Cardiovasc. Interv.* 7, 581–591. doi: 10.1016/j.jcin.2014.02.009

Lefler, Y., Amsalem, O., Vrieler, N., Segev, I., and Yarom, Y. (2020). Using subthreshold events to characterize the functional architecture of the electrically coupled inferior olive network. *Elife* 9:e43560. doi: 10.7554/elife.43560

Marchetti, C., Beato, M., and Nistri, A. (2001a). Alternating rhythmic activity induced by dorsal root stimulation in the neonatal rat spinal cord *in vitro*. *J. Physiol.* 530, 105–112. doi: 10.1111/j.1469-7793.2001.0105m.x

Marchetti, C., Beato, M., and Nistri, A. (2001b). Evidence for increased extracellular K^+ as an important mechanism for dorsal root induced alternating rhythmic activity in the neonatal rat spinal cord *in vitro*. *Neurosci. Lett.* 304, 77–80. doi: 10.1016/s0304-3940(01)01777-3

McAdoo, D. J., Robak, G., Xu, G.-Y., and Hughes, M. G. (2000). Adenosine release upon spinal cord injury. *Brain Res.* 854, 152–157. doi: 10.1016/s0006-8993(99)02333-1

Meuwissen, K. P., de Vries, L. E., Gu, J. W., Zhang, T. C., and Joosten, E. A. (2019). Burst and tonic spinal cord stimulation both activate spinal GABAergic mechanisms to attenuate pain in a rat model of chronic neuropathic pain. *Pain Pract.* 20, 75–87. doi: 10.1111/papr.12831

Minassian, K., Persy, I., Rattay, F., Pinter, M. M., Kern, H., and Dimitrijevic, M. R. (2007). Human lumbar cord circuitries can be activated by extrinsic tonic input to generate locomotor-like activity. *Hum. Mov. Sci.* 26, 275–295. doi: 10.1016/j.humov.2007.01.005

Musienko, P., van den Brand, R., Marzendorfer, O., Roy, R. R., Gerasimenko, Y., Edgerton, V. R., et al. (2011). Controlling specific locomotor behaviors through multidimensional monoaminergic modulation of spinal circuitries. *J. Neurosci.* 31, 9264–9278. doi: 10.1523/jneurosci.5796-10.2011

Nantwi, K. D., and Goshgarian, H. G. (2002). Actions of specific adenosine receptor A1 and A2 agonists and antagonists in recovery of phrenic motor output following upper cervical spinal cord injury in adult rats. *Clin. Exp. Pharmacol. Physiol.* 29, 915–923. doi: 10.1046/j.1440-1681.2002.03750.x

Phillips, A. A., and Krassioukov, A. V. (2015). Contemporary cardiovascular concerns after spinal cord injury: mechanisms, maladaptations and management. *J. Neurotrauma* 32, 1927–1942. doi: 10.1089/neu.2015.3903

Reeve, A. J., and Dickenson, A. H. (1995). The roles of spinal adenosine receptors in the control of acute and more persistent nociceptive responses of dorsal horn neurones in the anaesthetized rat. *Br. J. Pharmacol.* 116, 2221–2228. doi: 10.1111/j.1476-5381.1995.tb15057.x

Rejc, E., Angeli, C. A., Atkinson, D., and Harkema, S. J. (2017). Motor recovery after activity-based training with spinal cord epidural stimulation in a chronic motor complete paraplegic. *Sci. Rep.* 7:13476. doi: 10.1038/s41598-017-14003-w

Rossignol, S., and Frigon, A. (2011). Recovery of locomotion after spinal cord injury: some facts and mechanisms. *Annu. Rev. Neurosci.* 34, 413–440. doi: 10.1146/annurev-neuro-061010-113746

Salter, M., and Henry, J. (1987). Evidence that adenosine mediates the depression of spinal dorsal horn neurons induced by peripheral vibration in the cat. *Neuroscience* 22, 631–650. doi: 10.1016/0306-4522(87)90359-9

Samotus, O., Parrent, A., and Jog, M. (2018). Spinal cord stimulation therapy for gait dysfunction in advanced Parkinson's disease patients. *Mov. Disord.* 33, 783–792. doi: 10.1002/mds.27299

Santana, M. B., Halje, P., Simplício, H., Richter, U., Freire, M. A. M., Petersson, P., et al. (2014). Spinal cord stimulation alleviates motor deficits in a primate model of Parkinson disease. *Neuron* 84, 716–722. doi: 10.1016/j.neuron.2014.08.061

Sayenko, D. G., Angeli, C., Harkema, S. J., Edgerton, V. R., and Gerasimenko, Y. P. (2014). Neuromodulation of evoked muscle potentials induced by epidural spinal-cord stimulation in paralyzed individuals. *J. Neurophysiol.* 111, 1088–1099. doi: 10.1152/jn.00489.2013

Sayenko, D. G., Rath, M., Ferguson, A. R., Burdick, J. W., Havton, L. A., Edgerton, V. R., et al. (2019). Self-assisted standing enabled by non-invasive spinal stimulation after spinal cord injury. *J. Neurotrauma* 36, 1435–1450. doi: 10.1089/neu.2018.5956

Solopova, I., Sukhotina, I., Zhvansky, D., Ikoeva, G., Vissarionov, S., Baindurashvili, A., et al. (2017). Effects of spinal cord stimulation on motor functions in children with cerebral palsy. *Neurosci. Lett.* 639, 192–198. doi: 10.1016/j.neulet.2017.01.003

Stone, T. W., Ceruti, S., and Abbracchio, M. P. (2009). "Adenosine receptors and neurological disease: neuroprotection and neurodegeneration," in *Adenosine Receptors in Health and Disease*, eds C. Wilson and S. Mustafa (Berlin: Springer), 535–587.

Taccola, G. (2011). The locomotor central pattern generator of the rat spinal cord *in vitro* is optimally activated by noisy dorsal root waveforms. *J. Neurophysiol.* 106, 872–884. doi: 10.1152/jn.00170.2011

Taccola, G., Gad, P., Culaclii, S., Ichiyama, R. M., Liu, W., and Edgerton, V. R. (2020a). Using EMG to deliver lumbar dynamic electrical stimulation to facilitate cortico-spinal excitability. *Brain Stimul.* 13, 20–34. doi: 10.1016/j.brs.2019.09.013

Taccola, G., Gad, P., Culaclii, S., Wang, P.-M., Liu, W., and Edgerton, V. R. (2020b). Acute neuromodulation restores spinally-induced motor responses after severe spinal cord injury. *Exp. Neurol.* 327:113246. doi: 10.1016/j.expneurol.2020.113246

Taccola, G., Olivieri, D., D'Angelo, G., Blackburn, P., Secchia, L., and Ballanyi, K. (2012). A1 adenosine receptor modulation of chemically and electrically evoked lumbar locomotor network activity in isolated newborn rat spinal cords. *Neuroscience* 222, 191–204. doi: 10.1016/j.neuroscience.2012.07.030

Taccola, G., Sayenko, D., Gad, P., Gerasimenko, Y., and Edgerton, V. R. (2018). And yet it moves: recovery of volitional control after spinal cord injury. *Prog. Neurobiol.* 160, 64–81. doi: 10.1016/j.pneurobio.2017.10.004

Tawfik, V. L., Chang, S.-Y., Hitti, F. L., Roberts, D. W., Leiter, J. C., Jovanovic, S., et al. (2010). Deep brain stimulation results in local glutamate and adenosine release: investigation into the role of astrocytes. *Neurosurgery* 67, 367–375. doi: 10.1227/01.neu.0000371988.73620.4c

Tresch, M. C., and Bizzi, E. (1999). Responses to spinal microstimulation in the chronically spinalized rat and their relationship to spinal systems activated by low threshold cutaneous stimulation. *Exp. Brain Res.* 129, 401–416. doi: 10.1007/s002210050908

Wagner, F. B., Mignardot, J. B., Le Goff-Mignardot, C. G., Demesmaeker, R., Komi, S., Capogrosso, M., et al. (2018). Targeted neurotechnology restores walking in humans with spinal cord injury. *Nature* 563, 65–71. doi: 10.1038/s41586-018-0649-2

Witts, E. C., Nascimento, F., and Miles, G. B. (2015). Adenosine-mediated modulation of ventral horn interneurons and spinal motoneurons in neonatal mice. *J. Neurophysiol.* 114, 2305–2315. doi: 10.1152/jn.00574.2014

Witts, E. C., Panetta, K. M., and Miles, G. B. (2011). Glial-derived adenosine modulates spinal motor networks in mice. *J. Neurophysiol.* 107, 1925–1934. doi: 10.1152/jn.00513.2011

Conflict of Interest: The authors declare that the research was conducted in the absence of any commercial or financial relationships that could be construed as a potential conflict of interest.

frontiers in Systems Neuroscience

ORIGINAL RESEARCH
published: 22 July 2020
doi: 10.3389/fnsys.2020.00047

Site-Specific Neuromodulation of Detrusor and External Urethral Sphincter by Epidural Spinal Cord Stimulation

*Yuriy Sysoev[1,2†], Elena Bazhenova[1,3†], Vsevolod Lyakhovetskii[3,4], Gleb Kovalev[5], Polina Shkorbatova[3], Regina Islamova[6], Natalia Pavlova[1,3], Oleg Gorskii[1,3,4], Natalia Merkulyeva[1,3,4], Dmitry Shkarupa[5] and Pavel Musienko[1,3,4,7]**

[1]Institute of Translational Biomedicine, Saint-Petersburg State University, Saint-Petersburg, Russia, [2]Department of Pharmacology and Clinical Pharmacology, Saint-Petersburg State Chemical Pharmaceutical University, Saint-Petersburg, Russia, [3]Pavlov Institute of Physiology, Russian Academy of Sciences (RAS), Saint-Petersburg, Russia, [4]Granov Russian Research Center of Radiology and Surgical Technologies, Ministry of Healthcare of the Russian Federation, Saint-Petersburg, Russia, [5]Clinic of High Medical Technology named after N.I. Pirogov St. Petersburg State University, Saint-Petersburg, Russia, [6]Institute of Chemistry, Saint-Petersburg State University, Saint-Petersburg, Russia, [7]Saint-Petersburg State Research Institute of Phthisiopulmonology, Ministry of Healthcare of the Russian Federation, Saint-Petersburg, Russia

OPEN ACCESS

Edited by:
Enrico Rejc,
University of Louisville, United States

Reviewed by:
Parag Gad,
University of California, Los Angeles, United States
Casey Steadman,
Duke University, United States

***Correspondence:**
Pavel Musienko
pol-spb@mail.ru

†These authors have contributed equally to this work

Received: 20 March 2020
Accepted: 26 June 2020
Published: 22 July 2020

Citation:
Sysoev Y, Bazhenova E, Lyakhovetskii V, Kovalev G, Shkorbatova P, Islamova R, Pavlova N, Gorskii O, Merkulyeva N, Shkarupa D and Musienko P (2020) Site-Specific Neuromodulation of Detrusor and External Urethral Sphincter by Epidural Spinal Cord Stimulation. Front. Syst. Neurosci. 14:47. doi: 10.3389/fnsys.2020.00047

Impairments of the lower urinary tract function including urine storage and voiding are widely spread among patients with spinal cord injuries. The management of such patients includes bladder catheterization, surgical and pharmacological approaches, which reduce the morbidity from urinary tract-related complications. However, to date, there is no effective treatment of neurogenic bladder and restoration of urinary function. In the present study, we examined neuromodulation of detrusor (Detr) and external urethral sphincter by epidural electrical stimulation (EES) of lumbar and sacral regions of the spinal cord in chronic rats. To our knowledge, it is the first chronic study where detrusor and external urethral sphincter signals were recorded simultaneously to monitor their neuromodulation by site-specific spinal cord stimulation (SCS). The data obtained demonstrate that activation of detrusor muscle mainly occurs during the stimulation of the upper lumbar (L1) and lower lumbar (L5-L6) spinal segments whereas external urethral sphincter was activated predominantly by sacral stimulation. These findings can be used for the development of neurorehabilitation strategies based on spinal cord epidural stimulation for autonomic function recovery after severe spinal cord injury (SCI).

Keywords: epidural spinal cord electrical stimulation, low urinary tract, external urethral sphincter, detrusor, neuromodulation

INTRODUCTION

The abilities to store urine and control micturition are the principal functions of the lower urinary tract (LUT). LUT comprises two functionally different components: the bladder (detrusor) and urethra including internal and external urethral sphincters (EUS). In healthy rats, micturition involves simultaneous contraction of the detrusor (Detr), relaxation of the internal urethral sphincter (IUS), and bursting activity of EUS (Abud et al., 2015). These muscles work under the strict control of the cerebral cortex [right dorsolateral prefrontal cortex and the anterior cingulate

gyrus (Blok et al., 1997, 1998)], pontine micturition center [also known as Barrington's nucleus (Barrington, 1925)] and autonomic nervous system. Spinal cord injury (SCI) is often accompanied by disturbances of this hierarchy resulting in an overactive bladder, detrusor sphincter dyssynergia (DSD), or both (de Groat and Yoshimura, 2010).

Current treatments of neurogenic bladder and DSD may be divided into surgical and pharmacological approaches. The first one includes selective sacral rhizotomy which increases bladder capacity while preserving detrusor reflex and sphincter function (Rockswold et al., 1973) or a combination of sphincterotomy (Reynard et al., 2003) to decrease sphincter tone and enterocystoplasty, in which bladder capacity is increased by anastomosing a part of the ilium or ileocecal segment to the detrusor (Gurocak et al., 2007). However, sphincterotomy is largely supplanted by the use of botulinum toxin injections, medications, or urethral stents (Dorsher and McIntosh, 2012). Pharmacological treatments include anticholinergic (Wallis et al., 2016) or adrenergic medication (Welk et al., 2018) as a part of a comprehensive bladder management program. Despite the high prevalence of use, the beneficial effects of the above-mentioned options are limited due to low efficacy and side effects.

To date, several stimulation techniques, which can be used in combination with surgical and pharmacological approaches or alone, have been proposed. These include the direct stimulation of the bladder wall (Hald et al., 1967; Stenberg et al., 1967), stimulation of sacral (Li et al., 2016) or pudendal nerves (Vodušek et al., 1987; Previnaire et al., 1996; Hokanson et al., 2018; Li et al., 2018) and percutaneous (tibial) nerve stimulation (MacDiarmid et al., 2010; Peters et al., 2010, 2013). These approaches are quite effective in patients with LUT dysfunction, but there are several notable limitations. For example, direct bladder wall stimulation has had limited success in clinical practice due to a large number of electrodes and a high intensity of stimulation that is necessary. Clinical use has resulted in only local contractions of the bladder wall as well as unintended activation of the sphincter. Sacral nerve stimulation performed after the intradural approach is often associated with a high risk of mechanical damage (Rijkhoff et al., 1997). Tibial nerve stimulation requires intact supraspinal pathways and may not be suitable in patients with complete SCI, as was evidenced by animal studies (Xiao et al., 2014).

Future improvements for the treatment of LUT system disabilities might include neuromodulation of the spinal neuronal networks that contribute to the micturition control *via* epidural electrical stimulation (EES) of the spinal cord. Both animal and human studies have demonstrated that EES improves not only locomotor and postural functions (Minassian et al., 2004; Gerasimenko et al., 2008; Lavrov et al., 2015; Angeli et al., 2018; Gill et al., 2018) but also promotes the bladder control (Horst et al., 2011; Gad et al., 2014; Abud et al., 2015; Chang et al., 2018). However, the neuronal mechanisms underlying these effects have been poorly investigated. The main purpose of the present study was to reveal the effects of EES effects on the sympathetic, parasympathetic, and somatic networks that control the reflex activity of Detr and EUS. The obtained results expand our understanding of LUT spinal control and may result in the future development of rehabilitation algorithms for patients with SCI.

MATERIALS AND METHODS

The study was performed on four adult male Wistar rats (300–350 g body weight). All experimental procedures were approved by the Ethics Commission of the Pavlov Institute of Physiology. Experiments were performed in strong accordance with the requirements of Council Directive 2010/63EU of the European Parliament on the protection of animals used for experimental and other scientific purposes. The rats were housed in individual cages with free access to food and water. All surgical procedures were conducted under aseptic conditions under Isoflurane anesthesia (1%–2%;, mixed with Oxygen, a flow rate of 0.8 l/min).

The experiments were carried out with chronic implantation and testing during different time-points using the same EMG electrodes and electrodes for spinal cord stimulation (SCS). For chronic epidural electrodes implantation, partial laminectomies were performed and three Teflon-coated stainless steel wires (AS632, Cooner Wire, Chatsworth, CA, USA) from the Amphenol head connector cemented to the skull were passed under the vertebral arches inside the vertebral canal and above the dura mater of the remaining vertebrae between the partial laminectomy sites. Then the notch of insulation of 0.5 mm length was removed on each wire and the wires were sutured to the dura mater rostral and caudal to the exposed sites using 8.0 Ethilon suture. Then a midline lower abdominal incision was made to expose the bladder to implant the bladder catheter and stainless steel wire electrodes (AM-Systems, LLC, #793500) into the Detr, EUS (Scheepe et al., 1998; Merkulyeva et al., 2019). For surgical manipulations, the bladder was pulled out of the abdominal cavity, the access to the EUS was provided using a surgical dilator. The rostral portion of the pubic bone was partially removed using rongeurs to clearly expose the EUS muscle. The partially filled bladder was punctured by a needle (21G 0.8 × 40 mm) laterally on the left side and then a pre-marked catheter was inserted into the obtained hole so that its end was freely located in the cavity and did not touch the bladder walls. A plastic tube (Intramedic Polyethylene Tubing ID. 0.28 mm OD. 0.61 mm) conducted under the skin from the head to the bladder was used as a catheter that was implanted into the cavity of the bladder. The catheter was fixed in the bladder by using Ethilon 6.0 sutures. The further flow of fluid into the bladder through the catheter was provided using a cannula mounted on the free end of the catheter.

In addition to Detr and EUS, EMG electrodes were also implanted in gastrocnemius medialis (GM) and tibialis anterior (TA) muscles (Gerasimenko et al., 2006). In all cases, the needle and a small notch (∼0.5 mm) were removed from the insulation of each wire to expose the conductor and form the electrodes. EMG electrodes were fixed together with Ethylon 4 suture at the entrance and exit from the muscle. Two common ground (indifferent EMG and stimulation grounds) wires (1 cm of the Teflon removed distally) were inserted subcutaneously in the mid-back region. All wires (for both EMG and epidural

stimulation) were coiled in the back region to form a stress-release loop and were combined into one Amphenol head connector. The proper placement of the electrodes was verified during the surgery by stimulating through the head connector and post-mortem *via* dissection. Analgesia (ketorolac, 1 mg/kg, s/c) and antibiotic (enrofloxacin, 5 mg/kg, s/c) treatment were provided respectively 3 and 5 days after surgery. Bladder catheters were washed with distilled water once every two days during the experimental period.

After the testing of the reflex responses to SCS in 1 and 4 weeks after the initial bladder surgery, the lateral hemisection (van den Brand et al., 2012) at T8 spinal level was performed in each rat under gas anesthesia (isoflurane, 2–5%;). The spinal cord transection was verified by visual inspection under the microscope and then on the histological slices. Cut ends were exposed and separated by Gelfoam. An analgesic (ketorolac, 1 mg/kg, s/c) was given every 12 h for 48 h to relieve any post-operative pain. An antibiotic (enrofloxacin, 5 mg/kg, s/c) was given daily for 7 days to prevent urinary infection. Post-operatively, the bladder was manually expressed twice a day until the endpoint (1 week).

The main testing of the animals was performed in a chronic period (4 weeks) after bladder surgery. For supplementary experiments on the same group of animals, the additional analysis was done in an acute period (1 week) after the bladder surgery and soon (in 1 week) after the severe SCI (lateral hemisection). None of the implanted catheters or electrodes needed reimplantation. The reflex and urodynamic testing procedures were done on awake rats seated in the transparent plastic box with a cable from recording and stimulating equipment attached to the head plug. For urodynamic studies, the bladder catheters were connected to the infusion pump (ZooMed, SN-50C6). The infusion rate of the saline was 18 ml/h. In each rat, we analyzed the storage volume (volume of infused saline to start micturition) and the duration of the EUS bursting activity (Abud et al., 2015) during the micturition. For this, we performed 3–4 cycles of infusion/micturition. After the urodynamic recording, the motor evoked potentials were generated by EES (1 Hz frequency at stimulation intensities ranging from 50 μA to 800 μA in increments of 50 μA, 10 pulses for each stimulation amplitude, pulse duration of 0.2 ms) aiming to recruit various spinal pathways responsible for LUT and hindlimbs control (**Figures 1A–C**) in upper lumbar, lower lumbar and sacral spinal cord regions (Hou and Rabchevsky, 2014). The important criteria for the higher level of stimulation were to be in a painless range for the animals that was indicated by the calmness and immobility of the rats.

To trigger sympathetic pathways the upper stimulating electrode was implanted on the VT12 vertebral level and corresponded to L1, or border of L1–T13 spinal segments. The middle electrode was implanted on the VL1–2 vertebral level over the L5–L6 spinal region (Ishigooka et al., 2000) to stimulate a parasympathetic and somatic visceral network. The most caudal electrode was positioned on the VL2–VL3 vertebral level in relation to S3–S4 spinal segments, and spinal roots projecting afferent and efferent pathways from many overlying segments.

At the end of experiments, animals were deeply anesthetized with an overdose of tiletamine-zolazepam (Virbac, France, 100 mg/kg, i/m) and then perfused transcardially with 0.9%; NaCl (150 ml), followed by 4%; paraformaldehyde (300 ml) in 0.1 M PBS, pH 7.4. Then a detailed dissection of vertebrae, roots, and spinal cord was performed to determine the exact level of the spinal cord stimulation. The lumbosacral cord was divided into segments based upon the grouping of the dorsal rootlets (Shkorbatova et al., 2019). To define the exact position of the epidural electrode, the dura mater below the electrode was marked with a permanent marker. After removing the dura mater, this mark was carefully transferred to the pia mater. Then the lumbosacral spinal cord was removed from the spine and stored in 20 and 30%; sucrose until it sank. The segments under the stimulating electrodes were cut on a freezing microtome into 50 mm transverse sections, stained with 4.1%; cresyl violet (Sigma–Aldrich, St. Louis, MO, USA) and compared with the spinal cord atlas (Watson et al., 2009) to verify the spinal cord level (**Figures 2A–C**).

The EMG signals were differentially amplified (A-M Systems USA, model 1700, the bandwidth of 10 Hz–5 kHz) and digitized at 20 kHz with a National Instrument A/D board. The reflex responses to spinal cord stimulation were recorded from Detr (Craggs and Stephenson, 1976; Fry et al., 1998) and EUS (Merkulyeva et al., 2019) while the tested awake rat was sitting in the plastic box. Also, we recorded GM and TA EMG activity to control the triggering capacity of EES and specificity of this method in recruiting spinal reflex pathways (Gerasimenko et al., 2006). For each stimulation amplitude, 10 responses were chosen for further analysis. Custom scripts written in Matlab were used to measure evoked potentials from the selected muscles. We analyzed latency and peak-to-peak amplitude of responses at the maximum intensity of stimulation (**Figure 3**). Since the LUT system function normally depends on the reciprocal activity of the Detr and EUS muscles, we measured the ratio of the Detr/EUS activation level (**Figures 5B**, **7C–E**). The maximal amplitude of stimulation shown in (**Figures 3E,F**) was the same for both muscles in all stimulation points of one animal. Before averaging, each individual recruitment curve was normalized to the maximal response received in this animal either in the rostral or in medium or caudal stimulation points. All data are reported as mean ± SE. The hierarchical linear model with a constant slope and random intercept (Aarts et al., 2014) was used to compare latencies of Detr, EUS, GM and TA responses evoked by EES in rostral, medium and caudal points of the spinal cord stimulation, the volume and duration of voiding and the Detr/EUS and TA/GM activation level. The individual distributions of investigated values were normal in almost all cases by the Lilliefors test. The criterion level for the determination of statistical difference was set at $p < 0.05$.

RESULTS

We investigated the recruiting of different reflex pathways underlying Detr and EUS activity during EES of upper lumbar (L1), lower lumbar (L5–L6), and sacral spinal regions.

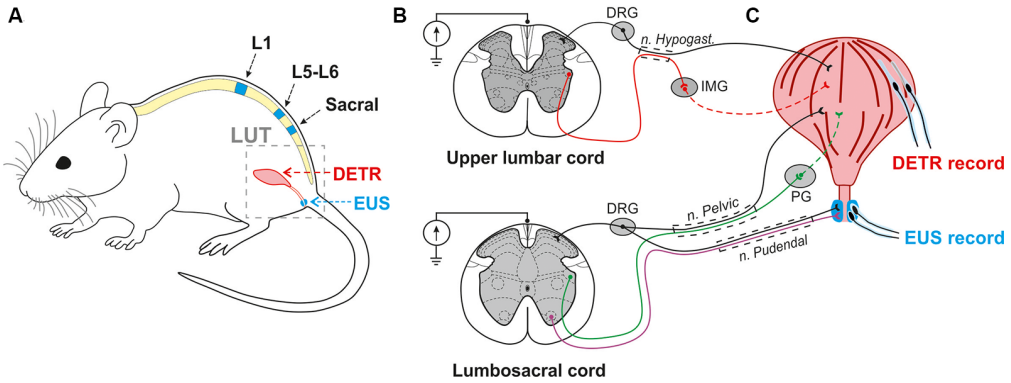

FIGURE 1 | Experimental model to investigate the effect of epidural electrical stimulation (EES) to the lower urinary tract (LUT) system. **(A)** EES electrodes were placed over the upper lumbar (L1), lower lumbar (L5-L6), and sacral regions of the spinal cord. EMG electrodes were implanted in the external urethral sphincters (EUS) and Detrusor (Detr) muscles. **(B,C)** Associated LUT neuronal pathways activated by EES at the upper lumbar and lumbosacral cord. Coordinated activity of EUS and Detr muscles is provided by sympathetic, parasympathetic, and somatic projections from upper lumbar and lumbosacral regions of the spinal cord. Sympathetic pathways (red) from the upper lumbar cord to detrusor muscle course through the hypogastric nerve, inferior mesenteric ganglia (IMG), and postganglionic projections. Parasympathetic innervation (green) from the lumbosacral level of the spinal cord occurs *via* the pelvic nerve which extends fibers onto the postganglionic nerves through the pelvic ganglion (PG). EUS contractions are under the control of motoneurons (violet) originating from the Onuf's nuclei situated in the ventral horns of spinal cord gray matter. Primary sensory neurons of dorsal root ganglia (DRG) carry sensory information from EUS and detrusor *via* hypogastric, pelvic, and pudendal nerves.

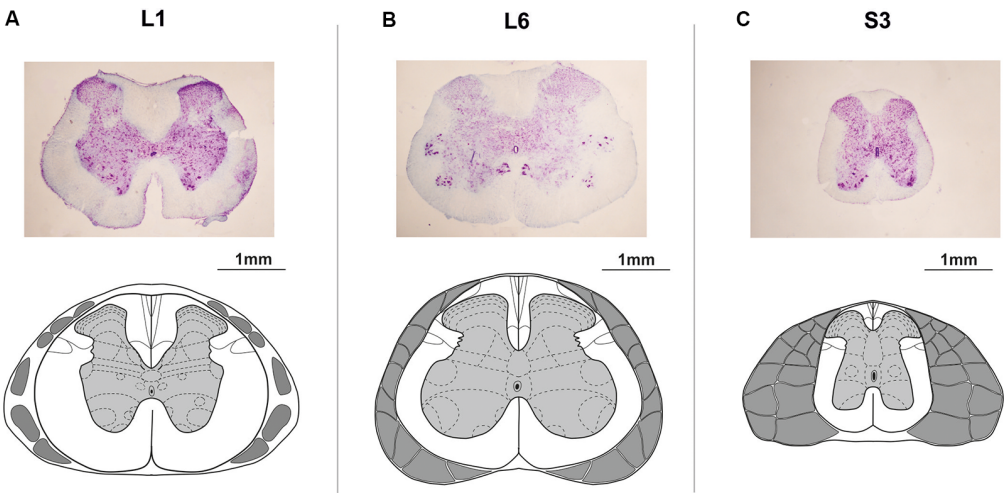

FIGURE 2 | Histological microphotographs and corresponding schemes under the **(A)** upper lumbar (L1), **(B)** lower lumbar (L6), and **(C)** sacral (S3) electrodes. The schemes of the spinal segments and adjacent roots adapted from Watson et al. (2009).

We aimed to affect the sympathetic, parasympathetic, and somatic neuronal circuitry participating in the control of the LUT system.

Effects of Upper Lumbar Spinal Stimulation on Detrusor and EUS Activity

Stimulation of the spinal cord in the upper lumbar region evoked responses in Detr and EUS muscles (**Figure 3**), whereas GM and TA responses were not present in all rats and were less prominent when extant. The latency of Detr responses was significantly longer ($p < 0.01$) than that of EUS (10.27 ± 0.50 and 3.77 ± 0.29 ms, respectively; **Figures 3A–D**, **4**). The evoked potential of Detr muscle was represented by a slow wave of 20–40 ms duration that consisted of positive and negative peaks. EUS responses were relatively faster and shorter and could contain several positive and negative waves. In both muscles, the observed responses were stable and their amplitude gradually increased with rising the magnitude of stimulation (**Figures 3E,F**).

Effects of Lower Lumbar Stimulation on Detrusor and EUS Activity

Unlike the upper lumbar region, the application of EES at the lower lumbar level-triggered responses in all recorded

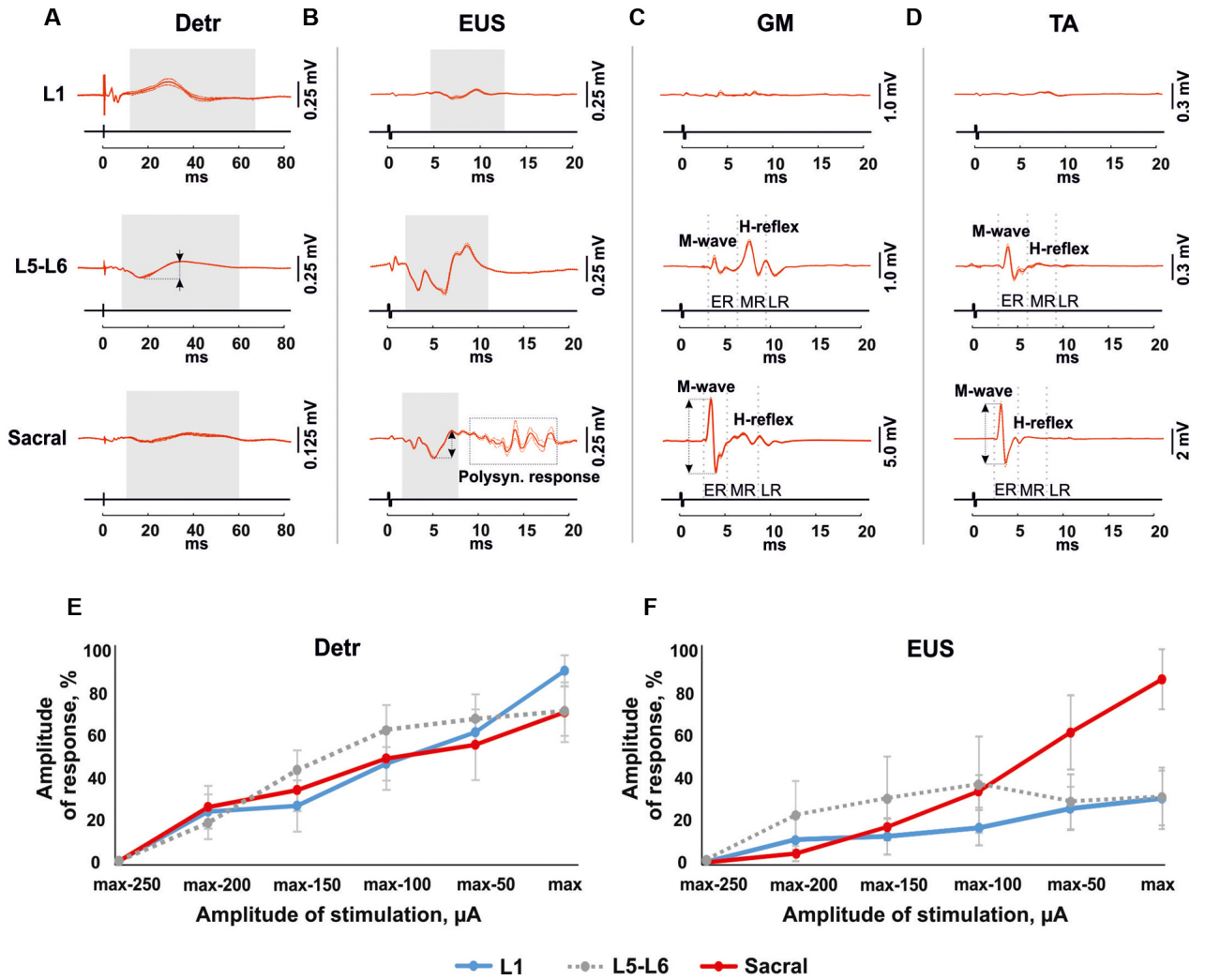

FIGURE 3 | Mean evoked potentials from Detr **(A)**, EUS **(B)**, gastrocnemius medialis (GM) **(C)** and tibialis anterior (TA; **D**; n = 10 stimulation pulses at 1 Hz) during the EES at the maximal intensity of upper lumbar (L1), lower lumbar (L5-L6) and sacral spinal cord in 4 weeks after the surgery. The gray areas show the evoked potentials in Detr, EUS during spinal cord stimulation. The reflex activity in GM and TA was divided into the early response (ER), medium response (MR), and late response (LR) by gray dotted lines. The calculated latency of the responses corresponds to the left edge of the gray area for Detr and EUS, and the gray dotted line for an ER and MR of GM and TA. The amplitude of the response indicated as a two-way arrow between dashed lines. **(E,F)** Recruitment curves of normalized (n = 4 rats, mean ± SE) Detr and EUS responses during the upper lumbar, lower lumbar, and sacral stimulation.

muscles. The Detr-evoked responses had the longest latency (7.21 ± 0.23 ms) and presented as a slow-wave composed of negative and positive components (**Figures 3A**, **4**). Significantly, in this region of the GM and TA muscles, there was a well-defined division of responses (**Figures 3C,D**): (1) Early response (ER), or a direct motor axone M-wave (2.96 ± 0.14 and 2.91 ± 0.18 ms, for GM and TA, respectively); and (2) medium response (MR), or a primary afferents H-wave (5.49 ± 0.56 and 5.32 ± 0.48 ms, for GM and TA, respectively). These responses illustrated classical recruiting dynamics; the H-wave was suppressed by the M-wave (Hoffman, 1910), as the amplitude of EES increased (Gerasimenko et al., 2006). We could also observe the late reflex component (LR) in some of the animals but it was not consistent. The latencies of EUS (1.71 ± 0.20 ms), GM, and TA reflexes were significantly shorter ($p < 0.01$) than the Detr responses (**Figures 3A–D**, **4**) and the general shape of EUS reflexes could contain several positive and negative peaks. Lower lumbar stimulation produced latencies in the Detr and EUS that were shorter ($p < 0.01$) than those observed during the upper lumbar stimulation (**Figure 4**). In the Detr and EUS muscles, the shape of the observed responses was rather stable, their amplitude increased as the stimulation magnitude rose until the submaximal level was saturated. Upon achievement of submaximal level, amplitude either reduced or remained unchanged up to the maximum level of EES (**Figures 3E,F**).

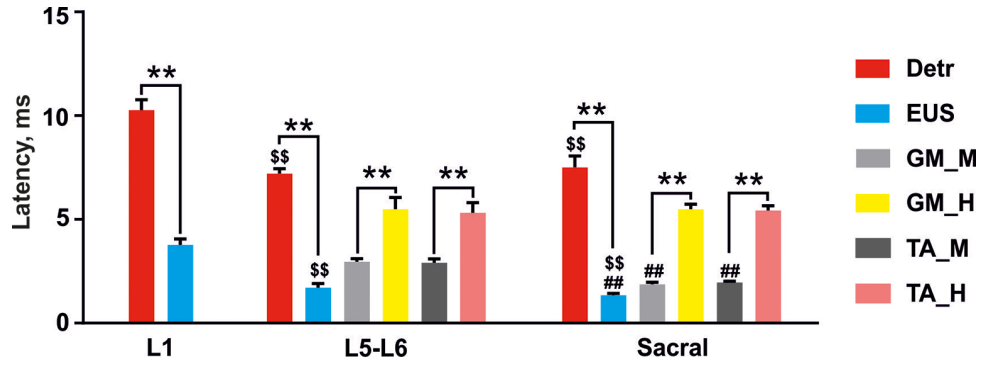

FIGURE 4 | Latencies of the reflex responses in Detr, EUS, GM, and TA to stimulation of upper lumbar (L1), lower lumbar (L5–L6), and sacral spinal cord. The data is presented as mean ± SE (n = 4 rats, 10 stimuli per rat, mean ± SE). For the lower lumbar and sacral region the responses in GM and TA were divided into M-wave (GM_M and TA_M, gray and dark gray, respectively) and H-reflex (GM_H and TA_H, yellow and pink, respectively). Indication of significance level: $^{**}p < 0.01$, $^{\$\$}p < 0.01$—vs. corresponding muscle response in upper lumbar region stimulation, $^{\#\#}p < 0.01$—vs. corresponding muscle response in lower lumbar region stimulation.

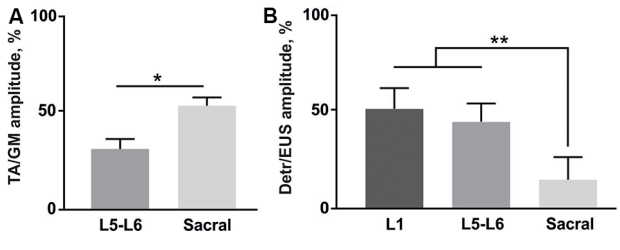

FIGURE 5 | (A) Amplitude ratio of TA and GM activity during the stimulation of lower lumbar (L5-L6) and sacral spinal regions (n = 4 rats, 10 stimuli per rat, mean ± SE). **(B)** Amplitude ratio of Detr and EUS activity during the stimulation of three different regions of the spinal cord (n = 4 rats, 10 stimuli per rat, mean ± SE). Indication of significance level: $^{*}p < 0.05$, $^{**}p < 0.01$.

Effects of Sacral Stimulation on Detrusor and EUS Activity

In contrast to the upper lumbar and lower lumbar regions, EES of the sacral level initially triggered responses only in the EUS, GM, and TA muscles. Only as stimulation intensity increased were responses also detected in the Detr muscle. The evoked potential in the Detr, similarly to other sites of EES, consisted of a slow wave with negative and positive peaks, whereas the EUS responses were fast and short, containing one or several positive and negative peaks. M-wave (1.87 ± 0.10 and 1.96 ± 0.06 ms, for GM and TA, respectively), and H-wave (5.49 ± 0.24 and 5.43 ± 0.23 ms, for GM and TA, respectively) for this region were similar to the lower lumbar (**Figures 3C,D**, **4**). The high intensity (∼from 450 μA and higher) stimulation-induced polysynaptic responses in EUS (∼7–10 ms) in all (n = 4) animals (**Figure 3B**). The Detr responses had significantly ($p < 0.01$) longer latency (7.50 ± 0.56 ms) than either the short-term EUS responses (1.34 ± 0.09 ms) or the GM or TA M- and H-waves (**Figure 4**). All recorded muscles had significantly shorter ($p < 0.01$) latencies during stimulation of the sacral region than those of the upper and lower lumbar regions (**Figure 4**).

An overall review of EES recruiting Detr and EUS activity is presented in (**Figures 3E,F**). For both LUT muscles, an increase in upper lumbar and sacral stimulation led to a stable linear increase of the evoked responses, and no response saturation, even at the highest current values, was obtained (**Figures 3E,F**). For the EUS, though notably not for the Detr, sacral EES led to a response with a more developed amplitude increase of the response (**Figure 3F**).

Finally, we analyzed the amplitude ratio of Detr vs. EUS and flexor (TA) vs. extensor (GM; **Figure 5**). The flexor/extensor ratio analysis was done as a supplementary condition and compared the site-specific effects of the stimulation in low lumbar and sacral locations ($p < 0.05$) which confirmed the reliability of our approach (**Figure 5A**). Stimulation of the L5-L6 segment induced higher activity in GM, as expected due to the closeness of their motoneuronal pools and in contrast to the TA motoneurones, which are located 1–2 segments above (Capogrosso et al., 2013; Wenger et al., 2016. The Detr/EUS ratio was significantly ($p < 0.01$) lower in the sacral region than in the upper lumbar segment (29 ± 7%;) and lower lumbar region (43 ± 20%; **Figure 5B**). Altogether, these findings confirm that the pattern of Detr and EUS activity can be modulated through EUS activation by the EES of the sacral region and more pronounced Detr activity can be activated by stimulation of the L1 and L5–L6 regions.

Relation of The Detr- and EUS-Evoked Potentials and The LUT Urodynamic Function

To show the functionality of the Detr- and EUS-evoked potentials (in the same group of rats, n = 4) we evaluated their relationship with the current functional state of the LUT system. To accomplish this, we performed two supplementary experiments with the impairments of the bladder, itself, and on supraspinal neuronal control.

First, we tested if detrusor and EUS reflex responses to EES related to the current condition of the LUT after bladder surgery. The reflex responses to stimulation of the different spinal cord regions 1 week after bladder surgery were compared with

those present in the stabilized chronic period (4 weeks after surgery). A urodynamic study was performed to calculate the volume of storage before voiding and duration of voiding as general characteristics of the LUT system (Abud et al., 2015). We found, soon after the bladder surgery, urinary incontinence (**Figures 6A,B**), a lower volume of storage (**Figure 6A**), and corresponding reduced voiding duration (**Figure 6B**) as a manifestation of postoperative cystitis (Chang et al., 2019). Accordingly, we observed reduced Detr and EUS reflex responses 1 week after the bladder surgery. Note that significant and pronounced differences were found for the Detr during upper and lower lumbar SCS (**Figures 6C–E**), while for EUS—in lower and sacral SCS (**Figures 6F–H**). These results additionally support the importance of spinal region stimulation specificity concerning Detr and EUS activity.

Second, we impaired the supraspinal regulation of bladder control. A severe but incomplete SCI, lateral hemisection, induced motor deficiency in the hind limbs (Friedli et al., 2015), which was accompanied by relatively pronounced excitability of the flexor muscles and an increased ratio of TA/GM reflex responses amplitudes (**Figures 7A–C**). In addition to the reduction of predominant extensor activity after the SCI, we observed suppression of reflexes in the Detr when site-specific stimulation in upper and low lumbar spinal regions was applied (**Figures 6C,D**). This makes sense in the acute period after injury and is related to the bladder atony evidenced by an increase of the voiding duration (**Figure 6B**). These results are evidence of the fact that the Detr and EUS in upper and lower spinal SCS, are changed in the direction of detrusor's excitability decrease (**Figures 7C,D**).

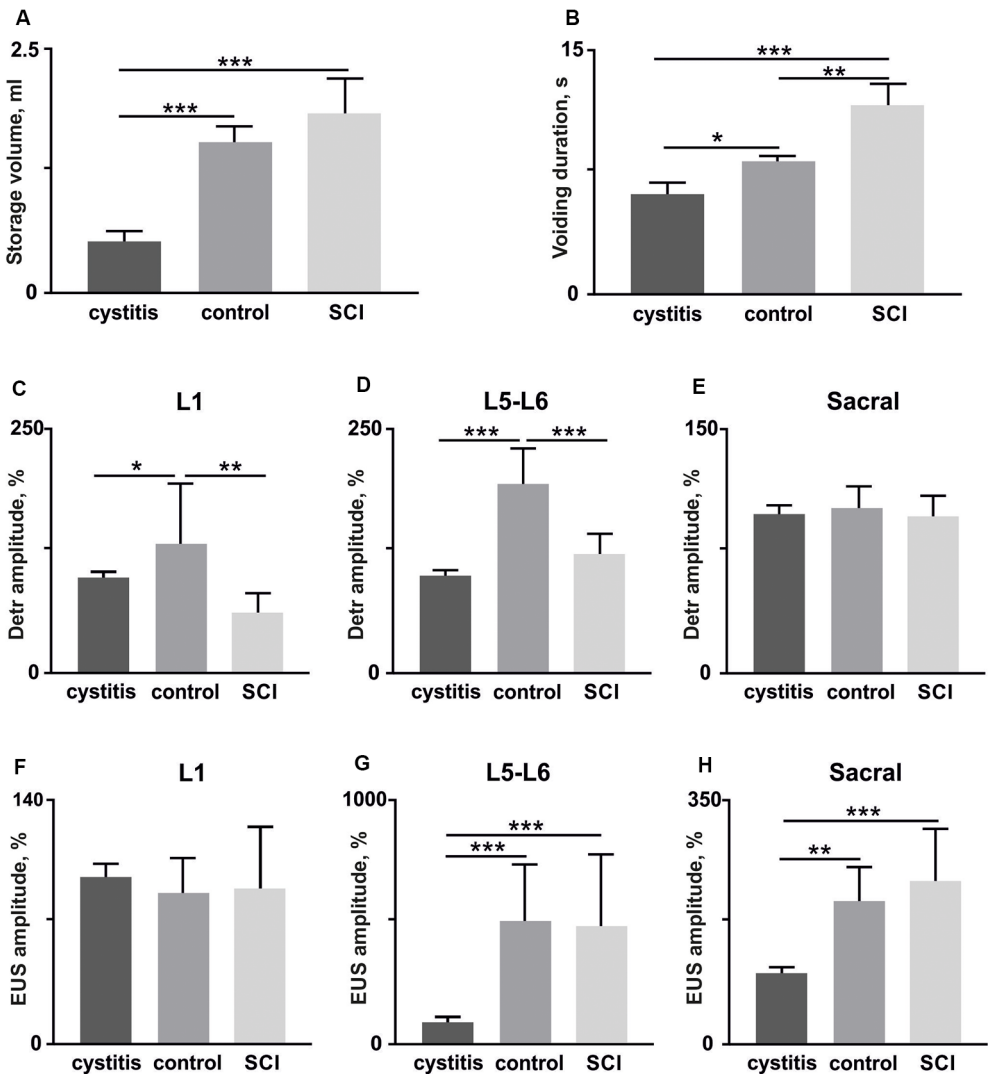

FIGURE 6 | The volume of storage before the voiding **(A)** and voiding duration **(B)** in rats ($n = 4$) soon after (1 week) the bladder surgery (cystitis), after 4 weeks (control) and soon after (1 week) hemisection (spinal cord injury, SCI). **(C–E)** amplitudes of Detr muscle in upper lumbar, lower lumbar, and sacral segments (10 stimuli per rat, mean ± SE). **(F–H)** amplitudes of EUS muscle in upper lumbar, lower lumbar, and sacral segments (10 stimuli per rat, mean ± SE). The normalization was done per rat basis using amplitude in the acute period as 100%. Indication of significance level: $^{*}p < 0.05$, $^{**}p < 0.01$, $^{***}p < 0.001$.

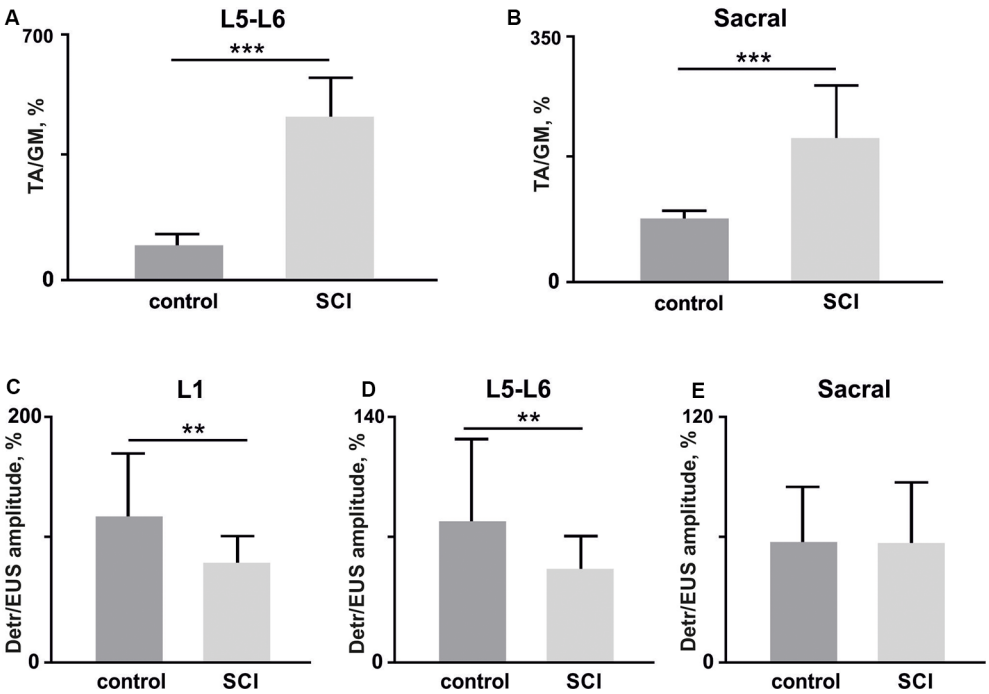

FIGURE 7 | (A,B) The amplitude ratio of TA and GM muscles in lower lumbar (L5–L6, **(A)** and sacral **(B)** spinal cord stimulation (10 stimuli per rat, mean ± SE) 4 weeks after bladder surgery (control) and soon after (1 week) hemisection (SCI). **(C–E)** Amplitude ratio of Detr and EUS muscles in upper lumbar (L1, **C**), lower lumbar (L5–L6, **D**), and sacral **(E)** regions of the spinal cord (10 stimuli per rat, mean ± SE) in control and after SCI. Indication of significance level: $^{**}p < 0.01$, $^{***}p < 0.001$.

In sum, both supplementary experiments directly supported the reliability of the Detr and EUS reflex testing approach, reflecting that the current functional state of the LUT system depends on the Detr and EUS neuronal network excitability level.

DISCUSSION

Neuromodulation of LUT System by Electrical Stimulation

Beneficial effects of EES to the LUT system, in combination with locomotor training after SCI, have previously been shown in both rats (Horst et al., 2011, 2013; Gad et al., 2014) and humans (Harkema et al., 2011). In the SCI rats study, it was observed that EES applied to the lumbosacral region of the spinal cord can facilitate the recovery of LUT function (Horst et al., 2011, 2013) and initiate micturition within seconds of stimulation onset (Gad et al., 2014). The authors proposed that EES enhances spinal neural networks excitability level (interneurons and motoneurons) and, when combined with motor training, increases the activation of the sensorimotor pathways that also control bladder function. In 2011, the first SCI patient exposed to EES demonstrated not only weight-bearing standing and some hindlimbs movements but also an ability to voluntarily void his bladder (Harkema et al., 2011). Further, recent studies have shown the efficiency of transcutaneous spinal cord stimulation in neuromodulation of LUT functions in rhesus monkeys (Gad et al., 2018a; Havton et al., 2019). Regarding SCI treatment in humans, it has been demonstrated that such non-invasive neuromodulatory techniques can normalize bladder and urethral sphincter function (Gad et al., 2018b; Herrity et al., 2018). However, while the proposed neuromodulatory treatments may be beneficial in some patients, in others it may be inefficient or cause unwanted side effects due to different integrity and excitability of spinal networks. Understanding the spatial distribution of neuronal projections that innervate the different LUT muscles can explain how best to apply SCS for maximal therapeutic efficacy.

In the present work, we show the site-specific effects of spinal cord stimulation to Detr and EUS activity and have proposed possible underlying reflex mechanisms of EES-mediated modulation of LUT functions. Testing the dynamics of Detr and EUS reflex activity in time after bladder surgery has shown that it was related to postoperative cystitis and recovery of the urodynamic function 4 weeks after. Moreover, we found the suppression of the evoked potentials in Detr muscle that matched bladder atony soon after the SCI. Therefore, similar to hindlimb motoneurons functional testing during EES (Lavrov et al., 2008), the evoked potentials in Detr and EUS muscles to spinal cord stimulation seems to reflect and can be used for the testing of LUT system functional state. Although future experiments that study the effects of different levels of EES to urodynamics are required, based on the data

obtained, we suppose that the site-specific stimulation of the rostrocaudal visceral and spinal network can be an efficient form of therapeutic neuromodulation after the SCI and other diseases inducing LUT disorders.

Neuronal Pathways Underlying The Reflex Activity of EUS and Detrusor Muscles Under EES

The data obtained show differences between detrusor and EUS activity in rats during the stimulation of three regions of the spinal cord. These results are in agreement with previous studies that proposed that the activity of detrusor and EUS occurs due to the activity of excitatory and inhibitory actions of a variety of segmental afferents, descending inputs, and sacral spinal actions (Shefchyk, 2001).

It is well known that detrusor muscle and EUS are controlled *via* parasympathetic, sympathetic, and somatic innervation in the lumbosacral regions of the spinal cord. In rats, parasympathetic nuclei situated in the lateral part of the spinal cord gray matter (L5-S1 level; Ishigooka et al., 2000; Hou and Rabchevsky, 2014) extend their axons to pelvic ganglia *via* the pelvic nerve (**Figures 1B,C**). The stimulatory action of acetylcholine (ACh), which is released from postganglionic nerve terminals on M3-muscarinic receptors induces bladder contraction (Lundberg, 1996) but causes simultaneous relaxation of urethral smooth muscles (IUS; Thornbury et al., 1992). Sympathetic nuclei of L1-L2 spinal cord level control LUT function through the hypogastric nerve and postganglionic projections. Norepinephrine released from postganglionic nerve terminals acts on β3-AR and causes bladder wall relaxation and, in direct contrast to ACh induces IUS contraction *via* α1-AR (de Groat et al., 1993; Andersson, 1999). Somatic innervation of EUS originating from the Onuf's nuclei (L6-S1 level) controls the striated muscle contractions *via* the pudendal nerves (Drake et al., 2010).

Epidural stimulation of the spinal cord sympathetic region located in the L1 segment predominantly activated the detrusor muscle but not EUS (**Figures 3E**, **4B**). This confirms the generally accepted view that hypogastric nerves and postganglionic projections innervate only the bladder wall and IUS, whereas EUS is controlled by the lower regions of the spinal cord (Hou and Rabchevsky, 2014). However, we also observed that stimulation of the upper lumbar region causes responses in the EUS with latency similar to GM (**Figure 4A**). It is plausible that the stimulation of the spinal cord upper lumbar region could trigger not only interneurons and motoneurons on this spinal level but also engage descending projections. These activities may be a part of propriospinal neuronal pathways or spinal-brainstem-spinal loop, for example, projections from L-region of Barrington's nucleus which innervate sacral EUS motor neurons originating from Onuf's nucleus (Morrison, 2008).

Independent of absolute amplitude values of EMG responses, the Detr and EUS ratios during L5–L6 stimulation were higher than during sacral stimulation (**Figure 4B**). This indicates that EES of the lower lumbar region had a more facilitating effect to detrusor muscle than did sacral EES. Since the stimulating electrode is positioned close to the detrusor parasympathetic preganglionic neurons and EUS motoneurons, the electrical current directly recruits two subsystems that have "competitive" reflex mechanisms (Shefchyk, 2001). Perhaps this causes the saturation effect, which we observed in Detr and EUS when stimulating lower lumbar segments at maximal magnitudes (**Figures 3D,E**).

Opposite results were obtained during the EES of the sacral region; we found higher activation of EUS than of the detrusor (**Figures 3D**, **4B**). Due to the anatomy of the spinal neuronal pathways under the sacral electrode, we recruited the roots from the majority of lumbar and sacral segments (**Figure 2C**). Most fibers of these roots carry sensorimotor information and form the peripheral nerves of the hind limbs. EUS activation during sacral stimulation can be associated with the somatovisceral integrative mechanisms (Merkulyeva et al., 2019). This effect is similar to tibial nerve stimulation, which is known to be effective in the clinical practice for EUS activation and treatment of the overactive bladder syndrome (Peters et al., 2010, 2013).

To confirm that the testing protocol of the reflex responses recruiting is well established, as a control experiment, we recorded an EES-evoked reflex activity of well studied GM and TA muscles. Similar to previous work (Gerasimenko et al., 2006), we obtained pronounced dynamics of H-reflex and M-wave on the recruitment curve of GM and TA muscles when the lower lumbar and sacral regions were stimulated. The H-reflex is associated with stimulation of group Ia afferents that project monosynaptically to motoneurons, whereas M-wave is a direct motor response due to stimulation of motor axons (Knikou, 2008) that project into the spinal roots from overlying segments (**Figure 2C**). It is worthwhile to note that, in some rats, we observed similar H/M-dynamic as in the EUS, but this phenomenon was not pronounced. It can be assumed that the EUS short-latency evoked potentials that have a similar nature with M-wave of GM and TA i.e., direct excitation of appropriate motor neurons. However, we do not deny that earlier recruiting responses of EUS with a latency of ∼4 ms can be an H-reflex, caused by activation of Ia afferents from muscle spindles. The existence of rare muscle spindles in human EUS was shown by Lassmann (1984). Significant differences between latencies of EUS and GM or TA responses (**Figure 4A**) may be related to different path lengths from the spinal cord stimulation area to EUS and GM or TA muscles, respectively.

Site-Specific Activation of The Spinal Network to Recover Visceral Function After SCI

Even though SCI disturbs spinal reflexes the lumbosacral mechanisms which remain intact provide an opportunity for restoration of LUT functions. In this article, we have shown that directly-applied EES can modulate EUS and detrusor reflex activity. Although further investigation of the EES effects on the urodynamic activity of the Detr and EUS is required, this may be a promising tool for the treatment of LUT disturbances manifesting as an inability to store and expel urine. Besides the short-latency reflex response, we have also observed polysynaptic

activity recruited by EES in Detr and EUS that is apparently due to activation of visceral and sensorimotor neuronal pathways underlying somatovisceral integrative mechanisms (Merkulyeva et al., 2019). Such mechanisms can be essential for the motor and autonomic functions recovery after SCI.

Site-specific modulation of EUS activity had previously been reported in rats with spinal cord and peripheral nerve injury (Abud et al., 2015; Chang et al., 2018). This is based on the evidence of the EUS-associated spinal neuronal network distribution in the thoracolumbar cord, the circuitry that controls tonic activity at L6–S1, and bursting activity between T8 and T9 and L3 and L4 (Chang et al., 2007). It was later confirmed that EES of predominantly caudal lumbar segments triggers EUS tonic contractions whereas stimulation of upper lumbar segments inhibits EUS tonic activity and elicited EUS bursting (Abud et al., 2015; Chang et al., 2018). Following our results, it was shown, in monkeys, that bladder pressure responses to spinal cord stimulation are mainly triggered by upper lumbar cord whereas EUS responses predominantly occurred due to lumbosacral enlargement of the lower regions (Gad et al., 2018a).

Recent clinical study of Kreydin et al. indicated that in patients with different pathologies (SCI, stroke, MS or idiopathic overactive bladder) stimulation of the spinal cord decreased detrusor overactivity, improved continence, and enhanced LUT sensation (Kreydin et al., 2020). Taken together with our data, these results provide a rationale for the development of spinal neuroprostheses that would enable to control LUT functions by the spatiotemporal neuromodulation approach (Wenger et al., 2016) that could be optimized to the specific clinical situation. In the recent study by Herrity et al. (2018), Medtronic implantable neurostimulation interface was used for bladder mapping. Effective configuration and stimulation parameters were successfully applied to improve reflex voiding efficiency in SCI patients. The bladder dysfunction caused by SCI often changes over the course of the injury. For instance, from bladder atonia to an overactive bladder (Cruz and Cruz, 2011). So, the possibility to change not only parameters of electrical current but also the site of stimulation is a very useful option. To date several neuroprosthetic arrays have been proposed (Borton et al., 2014; Hahnewald et al., 2016; Minev et al., 2015; Bareket et al., 2017); there are several existing design solutions (i.e., by Medtronic, Boston Scientific), including LUT spinal implants. Application of these spinal neuroprostheses is non restricted to SCI and may be suitable in patients with other neurological conditions that are accompanied by LUT dysfunction, for example, multiple sclerosis (Phé et al., 2016; Peyronnet et al., 2019) or Parkinson's disease (Winge, 2015; Hajebrahimi et al., 2019).

CONCLUSIONS

The data obtained demonstrate the neuromodulation of the LUT system by EES of lumbar and sacral regions of the spinal cord in chronic rats. The detrusor muscle activation mainly occurs during the stimulation of the upper L1 and lower lumbar (L5–L6) spinal segments whereas EUS was activated predominantly by sacral stimulation. These findings can be used for the development of neurorehabilitation strategies based on SCS for impaired autonomic function recovery.

DATA AVAILABILITY STATEMENT

The raw data supporting the conclusions of this article will be made available by the authors, without undue reservation.

ETHICS STATEMENT

The animal study was reviewed and approved by Ethics Commission of the Pavlov Institute of Physiology.

AUTHOR CONTRIBUTIONS

PM conceived the experiments. EB, YS, NP, GK, NM, OG and PM designed and performed the research. YS, VL, PS and PM analyzed the data. YS and PM wrote the article. YS, NM, PS, VL, DS, RI and PM edited the article. PM supervised the study.

FUNDING

This work was performed within project ID: 51134206 of the St. Petersburg State University, St. Petersburg, Russia (for YS, NM and OG), supported by the Russian Foundation for Basic Research [grant numbers 17-29-01034_ofi_m (for development of the experimental setup), 18-33-20062-mol-a-ved (for anatomical evaluation of the spinal cord stimulation), No. 20-015-00568-a (for electrophysiological testing and data analysis)].

REFERENCES

Aarts, E., Verhage, M., Veenvliet, J. V., Dolan, C. V., and Van Der Sluis, S. (2014). A solution to dependency: using multilevel analysis to accommodate nested data. *Nat. Neurosci.* 17, 491–496. doi: 10.1038/nn.3648

Abud, E. M., Ichiyama, R. M., Havton, L. A., and Chang, H. H. (2015). Spinal stimulation of the upper lumbar spinal cord modulates urethral sphincter activity in rats after spinal cord injury. *Am. J. Physiol. Ren. Physiol.* 308, 1032–1040. doi: 10.1152/ajprenal.00573.2014

Andersson, K. E. (1999). α1-adrenoceptors and bladder function. *Eur. Urol.* 36, 96–102.

Angeli, C. A., Boakye, M., Morton, R. A., Vogt, J., Benton, K., and Chen, Y., et al (2018). Recovery of over-ground walking after chronic motor complete spinal cord injury. *N. Engl. J. Med.* 379, 1244–1250. doi: 10.3410/f.734063095.793555382

Bareket, L., Barriga-Rivera, A., Zapf, M. P., Lovell, N. H., and Suaning, G. J. (2017). Progress in artificial vision through suprachoroidal retinal implants. *J. Neural Eng.* 14:045002. doi: 10.1088/1741-2552/aa6cbb

Barrington, F. J. F. (1925). The effect of lesions of the hind- and mid-brain on micturition in the cat. *Q. J. Exp. Physiol.* 15, 81–102. doi: 10.1113/expphysiol.1925.sp000345

Blok, B. F. M., Sturms, L. M., and Holstege, G. (1998). Brain activation during micturition in women. *Brain.* 121, 2033–2042. doi: 10.1093/brain/121.11.2033

Blok, B. F. M., Willemsen, A. T. M., and Holstege, G. (1997). A PET study on brain control of micturition in humans. *Brain.* 120, 111–121. doi: 10.1093/brain/120.1.111

Borton, D., Bonizzato, M., Beauparlant, J., DiGiovanna, J., Moraud, E. M., Wenger, N., et al (2014). Corticospinal neuroprostheses to restore locomotion after spinal cord injury. *Neurosci. Res.* 78, 21–29. doi: 10.3410/f.718535038.793498867

Capogrosso, M., Wenger, N., Raspopovic, S., Musienko, P., Beauparlant, J., Luciani, L. B., et al (2013). A computational model for epidural electrical stimulation of spinal sensorimotor circuits. *J. Neurosci.* 33, 19326–19340. doi: 10.1523/jneurosci.1688-13.2013

Chang, H. Y., Cheng, C. L., Chen, J. J., and de Groat, W. C. (2007). Serotonergic drugs and spinal cord transections indicate that different spinal circuits are involved in external urethral sphincter activity in rats. *Am. J. Physiol. Renal Physiol.* 292, F1044–F1053. doi: 10.1152/ajprenal.00175.2006

Chang, H. H., Jih-Chao, Y., Mao, J., Ginsberg, D. A., Ghoniem, G., and Rodriguez, L. V. (2019). Spinal cord stimulation ameliorates detrusor over-activity and visceromotor pain responses in rats with cystitis. *Neurourol. Urodyn.* 38, 116–122. doi: 10.1002/nau.23827

Chang, H. H., Yeh, J.-C., Ichiyama, R. M., Rodriguez, L. V., and Havton, L. A. (2018). Mapping and neuromodulation of lower urinary tract function using spinal cord stimulation in female rats. *Exp. Neurol.* 305, 26–32. doi: 10.1016/j.juro.2018.02.2627

Craggs, M. D., and Stephenson, J. D. (1976). The real bladder electromyogram. *Br. J. Urol.* 48, 443–451. doi: 10.1111/j.1464-410x.1976.tb06678.x

Cruz, C. D., and Cruz, F. (2011). Spinal cord injury and bladder dysfunction: new ideas about an old problem. *Scientific World Journal* 11, 214–234. doi: 10.1100/tsw.2011.26

de Groat, W. C., and Yoshimura, N. (2010). Changes in afferent activity after spinal cord injury. *Neurourol. Urodyn.* 29, 63–76. doi: 10.1002/nau.20761

de Groat, W. C., Booth, A. M., and Yoshimura, N. (1993). Neurophysiology of micturition and its modification in animal models of human disease. *Nerv. Cont. Urogenit. Syst.* 3, 227–289.

Dorsher, P. T., and McIntosh, P. M. (2012). Neurogenic bladder. *Adv. Urol.* 2012:816274. doi: 10.1155/2012/816274

Drake, M. J., Fowler, C. J., Griffiths, D., Mayer, E., Paton, J. F. R., and Birder, L. (2010). Neural control of the lower urinary and gastrointestinal tracts: supraspinal CNS mechanisms. *Neurourol. Urodyn.* 29, 119–127. doi: 10.1002/nau.20841

Friedli, L., Rosenzweig, E. S., Barraud, Q., Schubert, M., Dominici, N., Awai, L., et al (2015). Pronounced species divergence in corticospinal tract reorganization and functional recovery after lateralized spinal cord injury favors primates. *Sci. Transl. Med.* 7:302ra134. doi: 10.1126/scitranslmed.aac5811

Fry, C. H., Wu, C., and Sui, G. P. (1998). Electrophysiological properties of the bladder. *Int. Urogynecol. J. Pelvic Floor Dysfunct.* 9, 291–298. doi: 10.1007/BF01901509

Gad, P. N., Roy, R. R., Zhong, H., Lu, D. C., Gerasimenko, Y. P., and Edgerton, V. R. (2014). Initiation of bladder voiding with epidural stimulation in paralyzed, step trained rats. *PLoS One* 9:e108184. doi: 10.1371/journal.pone.0108184

Gad, P. N., Kokikian, N., Christe, K. L., Edgerton, V. R., and Havton, L. A. (2018a). Noninvasive neurophysiological mapping of the lower urinary tract in adult and aging rhesus macaques. *J. Neurophysiol.* 119, 1521–1527. doi: 10.1152/jn.00840.2017

Gad, P.N., Kreydin, E., Zhong, H., Latack, K., and Edgerton, V.R. (2018b). Non-invasive neuromodulation of spinal cord restores lower urinary tract function after paralysis. *Front. Neurosci.* 12:432. doi: 10.3389/fnins.2018.00432

Gerasimenko, Y. P., Lavrov, I. A., Courtine, G., Ichiyama, R. M., Dy, C. J., Zhong, H., et al (2006). Spinal cord reflexes induced by epidural spinal cord stimulation in normal awake rats. *J. Neurosci. Methods.* 157, 253–263. doi: 10.1016/j.jneumeth.2006.05.004

Gerasimenko, Y., Roy, R. R., and Edgerton, V. R. (2008). Epidural stimulation: comparison of the spinal circuits that generate and control locomotion in rats, cats and humans. *Exp. Neurol.* 209, 417–425. doi: 10.1016/j.expneurol.2007.07.015

Gill, M. L., Grahn, P. J., Calvert, J. S., Linde, M. B., Lavrov, I. A., and Strommen, J. A., et al (2018). Neuromodulation of lumbosacral spinal networks enables independent stepping after complete paraplegia. *Nat. Med.* 24, 1677–1682. doi: 10.1038/s41591-018-0175-7

Gurocak, S., Nuininga, J., Ure, I., De Gier, R. P. E., Tan, M. O., and Feitz, W. (2007). Bladder augmentation: review of the literature and recent advances. *Indian J. Urol.* 23, 452–457. doi: 10.4103/0970-1591.36721

Havton, L. A., Christe, K. L., Edgerton, V. R., and Gad, P. N. (2019). Noninvasive spinal neuromodulation to map and augment lower urinary tract function in rhesus macaques. *Exp. Neurol.* 322:113033. doi: 10.1016/j.expneurol.2019.113033

Hahnewald, S., Tscherter, A., Marconi, E., Streit, J., Widmer, H. R., Garnham, C., et al (2016). Response profiles of murine spiral ganglion neurons on multi-electrode arrays. *J. Neural Eng.* 13:016011. doi: 10.1088/1741-2560/13/1/016011

Hajebrahimi, S., Chapple, C. R., Pashazadeh, F., and Salehi-Pourmehr, H. (2019). Management of neurogenic bladder in patients with parkinson's disease: a systematic review. *Neurourol. Urodyn.* 38, 31–62. doi: 10.1002/nau.23869

Hald, T., Meier, W., Khalili, A., Agrawal, G., Benton, J. G., and Kantrowitz, A. (1967). Clinical experience with a radio-linked bladder stimulator. *J. Urol.* 97, 73–78. doi: 10.1016/s0022-5347(17)62982-3

Harkema, S., Gerasimenko, Y., Hodes, J., Burdick, J., Angeli, C., Chen, Y., et al (2011). Effect of epidural stimulation of the lumbosacral spinal cord on voluntary movement, standing and assisted stepping after motor complete paraplegia: a case study. *Lancet* 377, 1938–1947. doi: 10.1016/S0140-6736(11)60547-3

Herrity, A. N., Williams, C. S., Angeli, C. A., Harkema, S. J., and Hubscher, C. H. (2018). Lumbosacral spinal cord epidural stimulation improves voiding function after human spinal cord injury. *Sci Rep.* 8:8688. doi: 10.1038/s41598-018-26602-2

Hoffman, P. (1910). Beitrage zur kenntnis der menschlichen reflexe mit besonderer berucksichtigung der elektrischen erscheinungen. *Arch. F. Physiol.* 1, 223–256.

Hokanson, J. A., Langdale, C. L., Sridhar, A., and Grill, W. M. (2018). Stimulation of the sensory pudendal nerve increases bladder capacity in the rat. *Am. J. Physiol. Renal Physiol.* 314, F543–F550. doi: 10.1152/ajprenal.00373.2017

Horst, M., Heutschi, J., Van Den Brand, R., Andersson, K. E., Gobet, R., Sulser, T., et al (2013). Multisystem neuroprosthetic training improves bladder function after severe spinal cord injury. *J. Urol.* 189, 747–753. doi: 10.1016/j.juro.2012.08.200

Horst, M., Van den Brand, R., Heutschi, J., Musienko, P., Gobet, R., Sulser, T., et al (2011). Multi-systems neurorehabilitation improves bladder function after spinal cord injury. *J. Urol.* 185, E171–E171. doi: 10.1016/j.juro.2011.02.514

Hou, S., and Rabchevsky, A. G. (2014). Autonomic consequences of spinal cord injury. *Compr. Physiol.* 4, 1419–1453. doi: 10.1002/cphy.c130045

Ishigooka, M., Zermann, D. H., Doggweiler, R., and Schmidt, R. A. (2000). Similarity of distributions of spinal c-Fos and plasma extravasation after acute chemical irritation of the bladder and the prostate. *J. Urol.* 164, 1751–1756.

Knikou, M. (2008). The H-reflex as a probe: pathways and pitfalls. *J. Neurosci. Methods.* 171, 1–12. doi: 10.1016/j.jneumeth.2008.02.012

Kreydin, E., Zhong, H., Latack, K., Ye, S., Edgerton, V. R., and Gad, P. (2020). Transcutaneous electrical spinal cord neuromodulator (TESCoN) improves symptoms of overactive bladder. *Front. Syst. Neurosci.* 14, 1–11. doi: 10.3389/fnsys.2020.00001

Lassmann, G. (1984). Muskelspindeln und sensible endkörper in harnröhrenschließmuskel. *Acta. Neuropathol.* 63, 344–346. doi: 10.1007/bf00687343

Lavrov, I., Dy, C. J., Fong, A. J., Gerasimenko, Y., Courtine, G., and Zhong, H., et al (2008). Epidural stimulation induced modulation of spinal locomotor networks in adult spinal rats. *J. Neurosci.* 28, 6022–6029. doi: 10.1523/jneurosci.0080-08.2008

Lavrov, I., Musienko, P. E., Selionov, V. A., Zdunowski, S., Roy, R. R., Reggie Edgerton, V., et al (2015). Activation of spinal locomotor circuits in the decerebrated cat by spinal epidural and/or intraspinal electrical stimulation. *Brain Res.* 10, 84–92. doi: 10.1016/j.brainres.2014.11.003

Li, L. F., Ka-Kit Leung, G., and Lui, W. M. (2016). Sacral nerve stimulation for neurogenic bladder. *World Neurosurg.* 90, 236–243. doi: 10.1016/j.wneu.2016.02.108

Li, T., Feng, X., Lv, J., Cai, T., and Wang, S. (2018). Short-term clinical efficacy of electric pudendal nerve stimulation on neurogenic lower urinary tract disease: a pilot research. *Urology* 112, 69–73. doi: 10.1016/j.urology.2017.10.047

Lundberg, J. M. (1996). Pharmacology of cotransmission in the autonomic nervous system: Integrative aspects on amines, neuropeptides, adenosine triphosphate, amino acids and nitric oxide. *Pharmacol. Rev.* 48, 113–178.

MacDiarmid, S. A., Peters, K. M., Shobeiri, S. A., Wooldridge, L. S., Rovner, E. S., Leong, F. C., et al (2010). Long-term durability of percutaneous tibial nerve stimulation for the treatment of overactive bladder. *J. Urol.* 183, 234–240. doi: 10.1016/j.juro.2009.08.160

Merkulyeva, N., Lyakhovetskii, V., Veshchitskii, A., Bazhenova, E., Gorski, O., and Musienko, P. (2019). Activation of the spinal neuronal network responsible for visceral control during locomotion. *Exp. Neurol.* 320:112986. doi: 10.1016/j.expneurol.2019.112986

Minassian, K., Jilge, B., Rattay, F., Pinter, M. M., Binder, H., Gerstenbrand, F., et al (2004). Stepping-like movements in humans with complete spinal cord injury induced by epidural stimulation of the lumbar cord: electromyographic study of compound muscle action potentials. *Spinal Cord* 42, 401–416. doi: 10.1038/sj.sc.3101615

Minev, I. R., Musienko, P., Hirsch, A., Barraud, Q., Wenger, N., Moraud, E. M., et al (2015). Biomaterials: electronic dura mater for long-term multimodal neural interfaces. *Science* 347, 159–163. doi: 10.1126/science.1260318

Morrison, J. F. B. (2008). The discovery of the pontine micturition centre by F. J. F. barrington. *Exp. Physiol.* 93, 742–745. doi: 10.1113/expphysiol.2007.038976

Peters, K. M., Carrico, D. J., Perez-Marrero, R. A., Khan, A. U., Wooldridge, L. S., Davis, G. L., et al (2010). Randomized trial of percutaneous tibial nerve stimulation versus sham efficacy in the treatment of overactive bladder syndrome: results from the sumit trial. *J. Urol.* 183, 1438–1443. doi: 10.1016/j.juro.2009.12.036

Peters, K. M., Carrico, D. J., Wooldridge, L. S., Miller, C. J., and MacDiarmid, S. A. (2013). Percutaneous tibial nerve stimulation for the long-term treatment of overactive bladder: 3-year results of the STEP study. *J. Urol.* 189, 2194–2201. doi: 10.1016/j.juro.2012.11.175

Peyronnet, B., Krupp, L. B., Reynolds, W. S., Gamé, X., Amarenco, G., Cornu, J. N., et al (2019). Nocturia in patients with multiple sclerosis. *Rev. Urol.* 21, 63–73.

Phé, V., Chartier-Kastler, E., and Panicker, J. N. (2016). Management of neurogenic bladder in patients with multiple sclerosis. *Nat. Rev. Urol.* 13, 275–288. doi: 10.1038/nrurol.2016.53

Previnaire, J. G., Soler, J. M., Perrigot, M., Boileau, G., Delahaye, H., Schumacker, P., et al (1996). Short-term effect of pudendal nerve electrical stimulation on detrusor hyperreflexia in spinal cord injury patients: importance of current strength. *Paraplegia* 34, 95–99. doi: 10.1038/sc.1996.17

Reynard, J. M., Vass, J., Sullivan, M. E., and Mamas, M. (2003). Sphincterotomy and the treatment of detrusor-sphincter dyssynergia: current status, future prospects. *Spinal Cord* 41, 1–11. doi: 10.1038/sj/sc/3101378

Rijkhoff, N. J., Wijkstra, H., van Kerrebroeck, P. E., and Debruyne, F. M. (1997). Urinary bladder control by electrical stimulation: review of electrical stimulation techniques in spinal cord injury. *Neurourol. Urodyn.* 16, 39–53. doi: 10.1002/(sici)1520-6777(1997)16:1<39::aid-nau6>3.0.co;2-f

Rockswold, G. L., Bradley, W. E., and Chou, S. N. (1973). Differential sacral rhizotomy in the treatment of neurogenic bladder dysfunction. preliminary report of six cases. *J. Neurosurg.* 38, 748–754. doi: 10.3171/jns.1973.38.6.0748

Scheepe, J. R., Wipfler, G., Schumacher, S., Bross, S., Zendler, S., Jünemann, K.-P., et al (1998). Smooth muscle electromyography of the urinary bladder. *Neurourol. Urodyn.* 17, 71–80. doi: 10.1002/(sici)1520-6777(1998)17:1<71::aid-nau9>3.0.co;2-a

Shefchyk, S. J. (2001). Sacral spinal interneurones and the control of urinary bladder and urethral striated sphincter muscle function. *J. Physiol.* 533, 57–63. doi: 10.1111/j.1469-7793.2001.0057b.x

Shkorbatova, P. Y., Lyakhovetskii, V. A., Merkulyeva, N. S., Veshchitskii, A. A., Bazhenova, E. Y., Laurens, J., et al (2019). Prediction algorithm of the cat spinal segments lengths and positions in relation to the vertebrae. *Anat. Rec.* 302, 1628–1637. doi: 10.1002/ar.24054

Stenberg, C. C., Burnette, H. W., and Bunts, R. C. (1967). Electrical stimulation of human neurogenic bladders: experience with 4 patients. *J. Urol.* 97, 79–84. doi: 10.1016/s0022-5347(17)62983-5

Thornbury, K. D., Hollywood, M. A., and McHale, N. G. (1992). Mediation by nitric oxide of neurogenic relaxation of the urinary bladder neck muscle in sheep. *J. Physiol.* 451, 133–144. doi: 10.1113/jphysiol.1992.sp019157

van den Brand, R., Heutschi, J., Barraud, Q., DiGiovanna, J., Bartholdi, K., Huerlimann, M., et al (2012). Restoring voluntary control of locomotion after paralyzing spinal cord injury. *Science* 336, 1182–1185. doi: 10.1126/science.1217416

Vodušek, D. B., Plevnik, S., Vrtačnik, P., and Janež, J. (1987). Detrusor inhibition on selective pudendal nerve stimulation in the perineum. *Neurourol. Urodyn.* 6, 389–393. doi: 10.1002/nau.1930060506

Wallis, C. J. D., Lundeen, C., Golda, N., Brotherhood, H., Pommerville, P., and Carr, L. (2016). Anticholinergics for overactive bladder: temporal trends in prescription and treatment persistence. *Can. Urol. Assoc.* 10, 277–280. doi: 10.5489/cuaj.3526

Watson, C., Paxinos, G., and Kayalioglu, G. (Eds.) (2009). *The Spinal Cord. A Christopher and Dana Reeve Foundation Text and Atlas*. London: Academic Press/Elsevier. doi: 10.1016/C2009-0-01677-8.

Welk, B., Hickling, D., McKibbon, M., Radomski, S., and Ethans, K. (2018). A pilot randomized-controlled trial of the urodynamic efficacy of mirabegron for patients with neurogenic lower urinary tract dysfunction. *Neurourol. Urodyn.* 37, 2810–2817. doi: 10.1002/nau.23774

Wenger, N., Moraud, E. M., Gandar, J., Musienko, P., Capogrosso, M., Baud, L., et al (2016). Spatiotemporal neuromodulation therapies engaging muscle synergies improve motor control after spinal cord injury. *Nat. Med.* 22, 138–145. doi: 10.1038/nm.4025

Winge, K. (2015). Lower urinary tract dysfunction in patients with parkinsonism and other neurodegenerative disorders. *Handb. Clin. Neurol.* 130, 335–356. doi: 10.1016/B978-0-444-63247-0.00019-5

Xiao, Z., Rogers, M. J., Shen, B., Wang, J., Schwen, Z., Roppolo, J. R., et al (2014). Somatic modulation of spinal reflex bladder activity mediated by nociceptive bladder afferent nerve fibers in cats. *Am. J. Physiol. Renal Physiol.* 307, F673–F679. doi: 10.1152/ajprenal.00308.2014

Conflict of Interest: The authors declare that the research was conducted in the absence of any commercial or financial relationships that could be construed as a potential conflict of interest.

frontiers in Systems Neuroscience

ORIGINAL RESEARCH
published: 09 October 2020
doi: 10.3389/fnsys.2020.555593

Mapping of the Spinal Sensorimotor Network by Transvertebral and Transcutaneous Spinal Cord Stimulation

Polina Shkorbatova[1,2†], Vsevolod Lyakhovetskii[2,3†], Natalia Pavlova[1,2], Alexander Popov[2], Elena Bazhenova[1,2], Daria Kalinina[1], Oleg Gorskii[1,2,3] and Pavel Musienko[1,2,3,4]*

[1] Institute of Translational Biomedicine, Saint Petersburg State University, Saint Petersburg, Russia, [2] Pavlov Institute of Physiology Russian Academy of Sciences, Saint Petersburg, Russia, [3] Russian Research Center of Radiology and Surgical Technologies, Ministry of Health of the Russian Federation, Saint Petersburg, Russia, [4] Children's Surgery and Orthopedic Clinic, Department of Non-pulmonary Tuberculosis, Institute of Phthysiopulmonology, Saint Petersburg, Russia

Transcutaneous stimulation is a neuromodulation method that is efficiently used for recovery after spinal cord injury and other disorders that are accompanied by motor and sensory deficits. Multiple aspects of transcutaneous stimulation optimization still require testing in animal experiments including the use of pharmacological agents, spinal lesions, cell recording, etc. This need initially motivated us to develop a new approach of transvertebral spinal cord stimulation (SCS) and to test its feasibility in acute and chronic experiments on rats. The aims of the current work were to study the selectivity of muscle activation over the lower thoracic and lumbosacral spinal cord when the stimulating electrode was located intravertebrally and to compare its effectiveness to that of the clinically used transcutaneous stimulation. In decerebrated rats, electromyographic activity was recorded in the muscles of the back (m. longissimus dorsi), tail (m. abductor caudae dorsalis), and hindlimb (mm. iliacus, adductor magnus, vastus lateralis, semitendinosus, tibialis anterior, gastrocnemius medialis, soleus, and flexor hallucis longus) during SCS with an electrode placed alternately in one of the spinous processes of the VT12–VS1 vertebrae. The recruitment curves for motor and sensory components of the evoked potentials (separated from each other by means of double-pulse stimulation) were plotted for each muscle; their slopes characterized the effectiveness of the muscle activation. The electrophysiological mapping demonstrated that transvertebral SCS has specific effects to the rostrocaudally distributed sensorimotor network of the lower thoracic and lumbosacral cord, mainly by stimulation of the roots that carry the sensory and motor spinal pathways. These effects were compared in the same animals when mapping was performed by transcutaneous stimulation, and similar distribution of muscle activity and underlying neuroanatomical mechanisms were found. The experiments on chronic rats validated the feasibility of the proposed stimulation approach of transvertebral SCS for further studies.

Keywords: transvertebral spinal cord stimulation, transcutaneous stimulation, sensorimotor network, spinal cord, decerebrated rat, neuromodulation

OPEN ACCESS

Edited by:
Ronaldo M. Ichiyama, University of Leeds, United Kingdom

Reviewed by:
Jason Carmel, Columbia University, United States
David Magnuson, University of Louisville, United States

***Correspondence:**
Pavel Musienko
pol-spb@mail.ru

† These authors have contributed equally to this work

Received: *25 April 2020*
Accepted: *15 September 2020*
Published: *09 October 2020*

Citation:
Shkorbatova P, Lyakhovetskii V, Pavlova N, Popov A, Bazhenova E, Kalinina D, Gorskii O and Musienko P (2020) Mapping of the Spinal Sensorimotor Network by Transvertebral and Transcutaneous Spinal Cord Stimulation. Front. Syst. Neurosci. 14:555593. doi: 10.3389/fnsys.2020.555593

NEW AND NOTEWORTHY

Neuromodulation of the sensorimotor network distributed rostrocaudally over the lumbar and sacral spinal segments by transvertebral electrical stimulation.

INTRODUCTION

Spinal cord stimulation (SCS) is an effective method of recovery after spinal cord injury (SCI) and other disorders that are accompanied by motor and sensory deficits (Shapkova, 2004; Harkema et al., 2011; Zhong et al., 2019). Several approaches can be taken for electrode setting near the spinal cord: subdural (e.g., Minev et al., 2015; Capogrosso et al., 2018a), epidural (e.g., Musienko et al., 2005, 2009; Lavrov et al., 2006), transcutaneous (e.g., Minassian et al., 2007; Roy et al., 2012; Sayenko et al., 2015; Hofstoetter et al., 2018), or subcutaneous (Pavlova et al., 2019). In chronic studies (Schmidt et al., 1978) and intraoperative monitoring (e.g., Calancie et al., 1994), the target of stimulation may not be the spinal cord itself but a selective group of dorsal or ventral roots. Depending on the degree of invasiveness, the stimulation through electrodes located above the spinal cord can cause a certain selectivity of motor neuron pool activation, and this changes the effectiveness of the technique.

The least invasive transcutaneous SCS is now frequently used in studies on healthy humans aimed at central pattern generator research and central and peripheral neuronal control of locomotor activity (Gerasimenko et al., 2014, 2016; Gerasimenko Y. et al., 2015). This method has been efficiently applied and widely used in a clinical practice for neurorehabilitation of patients with severe SCI (Gerasimenko Y.P. et al., 2015; Gad et al., 2018a,b). However, further development of the method of transcutaneous stimulation requires suitable animal models. Unfortunately, in animals, the practical tasks of stable electrode fixation on the hairy and easily movable skin surface during longitudinal studies, as well as achieving identical electrode placement in several animals, are complicated and require considerable skill and patience (Peckham and Knutson, 2005). The transcutaneously induced locomotion in cats is more unstable and less coordinated than the epidurally induced locomotion, presumably due to instability of the electrode position (Musienko et al., 2013). Therefore, the method of non-invasive SCS is rarely used in these experiments although its effectiveness has been shown for recruiting spinal sensorimotor pathways and for initiation of the locomotor activity in acute decerebrate (Musienko et al., 2013) and chronic spinal cats (Edgerton et al., 2013; Musienko et al., 2013). In the current work, we have proposed a suitable approach for electrode implantation into the vertebral spinous processes for transvertebral SCS. This method has allowed us to quickly and stably fix the electrodes relative to the vertebral column and spinal cord segments in accordance with the skeletotopy relationships (Wenger et al., 2016; Shkorbatova et al., 2019). However, chronic transvertebral stimulation is still an experimental technique with significant differences compared to clinical protocols.

The neuronal mechanisms of either strongly invasive or less invasive SCS are not well defined, although some aspects have been investigated and discussed in a number of experimental papers (Gerasimenko et al., 2003; Musienko et al., 2005, 2012; Lavrov et al., 2006; Capogrosso et al., 2013). The consensus view is that the SCS effects are based on the recruiting of sensory inputs of the dorsal cord and roots lying under the stimulating electrodes, followed by polysynaptic activation of the sensorimotor neuronal circuits (Musienko et al., 2012). This underlying mechanism and anatomical spreading of the afferent fibers carrying the sensory input to the spinal network allowed the use of epidural SCS in a spatiotemporal neuromodulation mode that significantly improved the positive effects of stimulation after spinal sectioning (Musienko et al., 2009; Wenger et al., 2014, 2016). One of the important unanswered questions is whether it is possible to effectively recruit by surface SCS the specific neuronal pathways widely distributed rostrocaudal over the lumbar and sacral spinal segments (Merkulyeva et al., 2018).

We performed electrophysiological mapping of the spinal sensorimotor pathways by low thoracic and lumbosacral transvertebral SCS and recording of the activity of the multiple hindlimb and trunk muscles participating in normal locomotion and postural tasks.

The data obtained have shown that the muscle responses to stimulation are topical and reflect the rostrocaudal distribution of the corresponding motor neuron pools in the lumbosacral spinal cord. The received distribution of muscle activity was compared with the mapping performed by transcutaneous stimulation. The validity of the proposed stimulation approach was studied in a chronic experiment.

MATERIALS AND METHODS

Subjects

The study was performed on adult male Wistar rats (300–350 g body weight). All experimental procedures were approved by the Ethics Commission of the Pavlov Institute of Physiology. Experiments were performed in full accordance with the requirements of Council Directive 2010/63EU of the European Parliament on the protection of animals used for experimental and other scientific purposes. Before the experiments, the rats were housed with two to three animals per cage with free access to food and water. Eight rats were used for transvertebral mapping, and six rats were used for comparative study of transvertebral vs. subcutaneous mapping. Six rats were used in the chronic experiment to check the stability of muscle responses to transvertebral stimulation.

All surgical procedures were conducted under isoflurane anesthesia (4% for induction, 1–2% for maintenance, mixed with oxygen, flow rate 0.8 L/min). During surgery, the animals were placed on a heating pad at a temperature of 37°C and received injections of 2 ml of warm 0.9% NaCl subcutaneously every 2 h to prevent dehydration.

EMG Implantation

To record the EMGs, stainless steel wire electrodes (AS632, Cooner Wire, Chatsworth, CA, United States) were prepared by removing a small notch of insulation (0.5 mm) on each

wire to expose the conductor. The wires were inserted into the muscle through a 23G needle and positioned in the middle of the muscle in the most responsive part, which was identified by electrical stimulation ("hot spot"), then the wires were fixed together with Ethilon 4 suture at the entrance and exit from the muscle (Capogrosso et al., 2018b). The EMG signals were differentially amplified (A-M Systems United States, model 1700, bandwidth of 10 Hz–5 kHz) and digitized at 20 kHz with a National Instrument A/D board.

Muscle Set

In the acute experiment, the electrodes were implanted into the muscles of the back [m. longissimus dorsi (LD) near the VT13 vertebra], tail [m. abductor caudae dorsalis (ACD)], and hindlimb [m. iliacus (IL), m. adductor magnus (ADD), m. vastus lateralis (VL), m. semitendinosus (ST), m. tibialis anterior (TA), m. gastrocnemius medialis (GM), m. soleus (SOL), and m. flexor hallucis longus (FHL)]. The selected muscles had to meet at least one of three criteria. The first was that the muscles are widely used in studying locomotion (e.g., IL, VL, ST, GM, TA) or postural control (e.g., LD, ACD, SOL, ADD) (Siegel, 1970; Karayannidou et al., 2009; Musienko et al., 2014). The second was that they are the hindlimb muscles having the most rostral (ADD, IL) or the most caudal motoneuronal pools (FHL) in the spinal cord (Mohan et al., 2015; Wenger et al., 2016). The third was that they served as reference points with the most rostral (LD) or the most caudal (ACD) motoneuronal pools in our zone of interest.

For chronic muscle implantation, the TA and GM of one leg were chosen because they are most often used in chronic experiments as antagonist muscles to analyze a gait pattern.

Transcutaneous Mapping

The transcutaneous stimulation was conducted using a 5 × 5-mm electrode made of biocompatible self-adhesive conductive hydrogel (FDA 510(k) Premarket Notification K092546; CWN2505; GMDASZ Manufacturing Co., Ltd., Shenzhen, China) placed between the spinous processes of the VT12/VT13, VL1/VL2, and VS1/VS2 vertebrae. The vertebrae were carefully palpated and the VL6/VS1 vertebral junction was determined as the last movable joint before four sacral vertebrae, which were immobile relative to each other. The skin under the intervertebral spaces was then marked, but the exact position was checked every time before electrode placement. The 30 × 50-mm ground electrode (made of the same material) was fixed on the animal's abdomen.

Transvertebral Stimulation

Transvertebral mapping of the lower thoracic, lumbar, and sacral spinal segments was conducted in acute experiments after cutting the skin and the fascia on the back to expose the spinous processes of the vertebrae VT11–VS2 and separate them from the surrounding tissues. A hole (1 mm diameter) was drilled with a hand drill horizontally (**Figure 1B**) into each spinous process of vertebrae VT12–VS1 close to its basement.

For acute experiments, the wire electrode (2 mm of the Teflon insulation was removed around the wire, 2 cm from the wire tip) was placed alternately in one of the spinous processes of the VT12–VS1 vertebrae and fixed in the entrance and exit of the spinous process canal. For chronic experiments, the spinous process of the L2 vertebra was exposed through a minimal skin and muscle incision and drilled horizontally. The vertebral stimulation electrode was fixed inside the hole by tying a knot around the dorsal part of the spinous process. The skin was then closed with Ethilon 4. Two common ground (indifferent EMG and stimulation grounds) wires (with 1 cm of the Teflon removed distally) were inserted into the muscles near the right and left shoulders. The scheme of the stimulating electrode position in the VL2 spinous process is presented in **Figure 1B**.

For acute experiments after bilateral carotid artery ligation, the animal was decerebrated at the precollicular–postmammilar level (Dobson and Harris, 2012) and placed into a custom stereotaxic frame, where it was fixed with vertebral clamps for subsequent recordings as shown in **Figure 1A**. The head and the tail were supported with stripes of soft fabric. The hindlimbs were in the unsupported state. The anesthesia was turned off just after the decerebration.

For chronic animals, the recording electrodes were implanted into the muscles of one leg as described above and the wound was closed using Vicryl 5 for the fascia and Ethilon 4 for the skin. All wires were coiled in the back region to form a stress release loop and were combined into an Amphenol head connector, which was fixed on the animal's head. After surgery, the animal was let to recover from anesthesia in a warm box. Analgesic (ketorolac, 1 mg/kg, s.c.) and antibiotic (enrofloxacin, 5 mg/kg, s.c.) were administered during 3 and 5 days after surgery, respectively.

Electrical Stimulation and Recording

The recruiting was performed by stimulation with single pulses of 1 Hz frequency at stimulation intensities ranging from 1,500 to 4,500 μA for transcutaneous stimulation and from 500 to 3,300 μA for transvertebral stimulation in increments of 100 μA, with a pulse duration of 0.2 ms, interstimulus interval of 1 s, and 10 impulses for each current (example of response is in **Figure 1C**). Separation of the motor and sensory components of the muscle response was achieved using stimulation by double impulses with interpulse interval of 20 ms (Gerasimenko et al., 2006; Roy et al., 2012). Preliminary experiments confirmed that with submaximal currents the sensory components of the muscle response to the second part of a double impulse were suppressed (**Figure 1D**). However, in some cases, they reappeared in further current increases as described previously (Minassian et al., 2004). This is why the recruiting by itself was performed with a single impulse stimulation. The values of the latencies received by double-impulse stimulation were used to separate the early response component from the others during the single impulse stimulation.

Anatomical Verification of Spinal Pathways Under the Stimulating Electrodes

At the end of the experiment, the animal was perfused with 100 ml of 0.9% NaCl followed by 350 ml of 4% paraformaldehyde in 0.1 M phosphate buffered saline (PBS). A careful dissection was then performed to explore the lengths and the positions

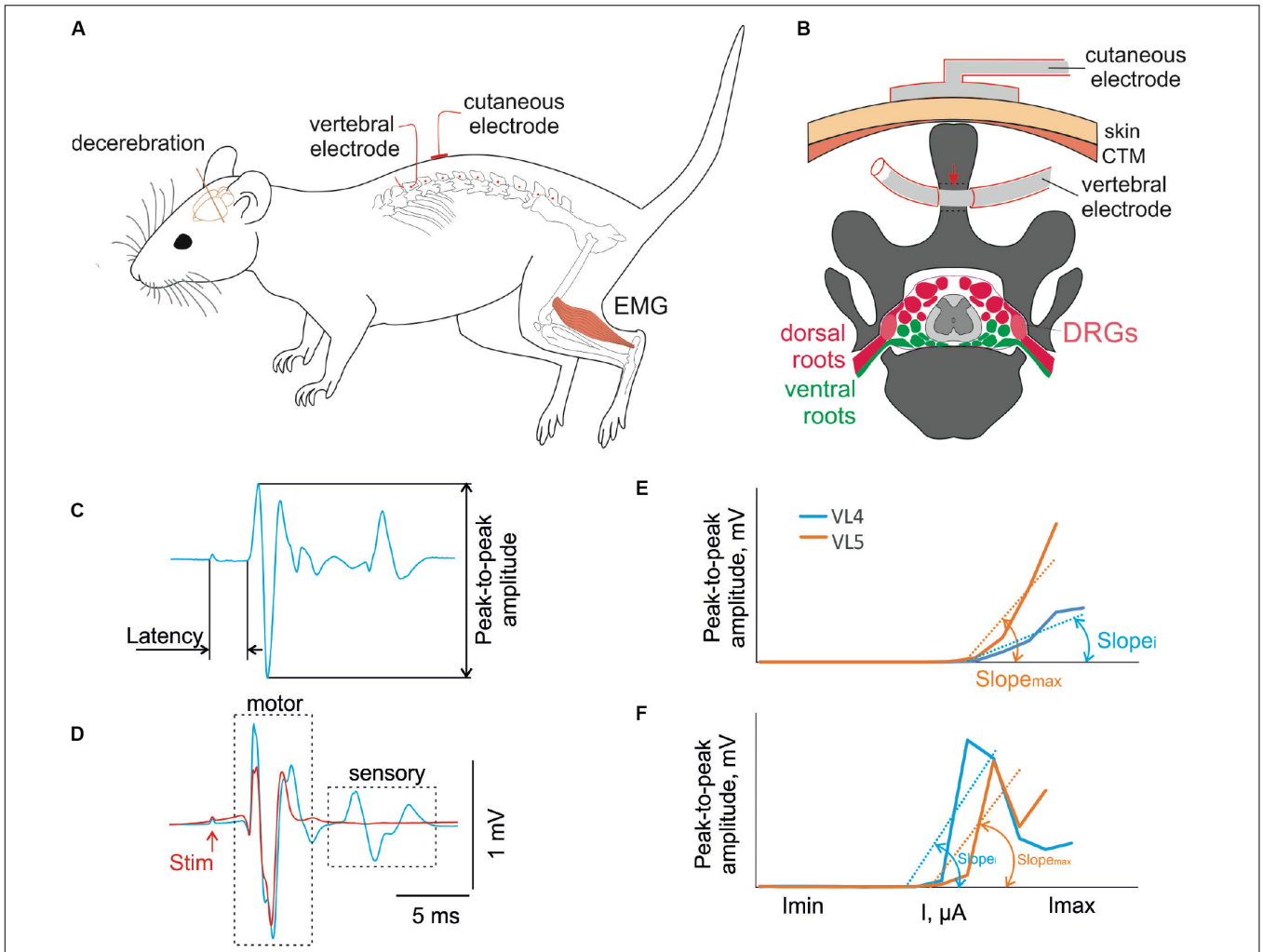

FIGURE 1 | (A) Design of the experiment. The decerebrate rat is fixed in the custom stereotaxic frame and the holes were drilled in the spinous processes of the VT12–VS1 (red dots) vertebrae. The stimulating vertebral electrode was placed alternately in the hole in each vertebra. The stimulating cutaneous electrode was placed in the zones between adjacent vertebrae. The intramuscular electrodes were implanted to record EMG signals. **(B)** The representative scheme of the frontal section of vertebra VL2 with the spinal cord, dorsal (red) and ventral (green) roots, and dorsal root ganglia (DRGs, pink) inside the vertebral canal. The position of the stimulating cutaneous electrode and vertebral electrode in the spinous process is shown. The contact insulation-free area of the vertebral electrode indicated with a red arrow. **(C)** An example of motor-evoked potential with the main characteristics measured. **(D)** An example of motor-evoked potential to first (blue) and second (red) pulse of double-pulse stimulation. **(E,F)** The recruitment curves of motor **(E)** and sensory **(F)** responses at stimulation of different vertebrae and their slopes (max, maximal slope; *i*, slope at stimulation of some other vertebra).

of the sT12–S1 spinal segments, the dorsal root ganglia (DRG) and the dorsal and ventral roots in relation to the VT12–VS1 vertebrae. The mean skeletotopy of the spinal segments was plotted based on these data.

Analysis and Statistics

Custom scripts written in MATLAB were used to measure the evoked potentials from the selected muscles. We analyzed the latency and peak-to-peak amplitude of the different response components in the 0.5 to 15 ms range after the stimulation impulse (**Figure 1C**). The "early" response (ER), which did not deteriorate during the double stimulation test (Gerasimenko et al., 2006) at submaximal current (**Figure 1D**), had the minimal latency. We attributed this to the motor response due to the direct activation of the motoneuronal axons. The "medium" response (MR) was second in terms of latency, just after the ER. The "late" response (LR) was third in terms of latency, just after the ER and MR. Both the MR and LR were deteriorated during the double stimulation test (Gerasimenko et al., 2006) as reflex (sensory) responses required time for recovery for synaptic transmission.

The recruitment curves for motor and sensory responses were constructed based on these values. For each muscle of each animal, the distribution of the recruitment curves was received over a range of stimulated vertebra. The slopes of the ascending parts of these curves were calculated by the least squares method (e.g., **Figures 1E,F**, $Slope_i$ and $Slope_{max}$), where the beginning value had to be greater than a 0.1-mV threshold. All slopes of the recruitment curve distributions were normalized to the maximal

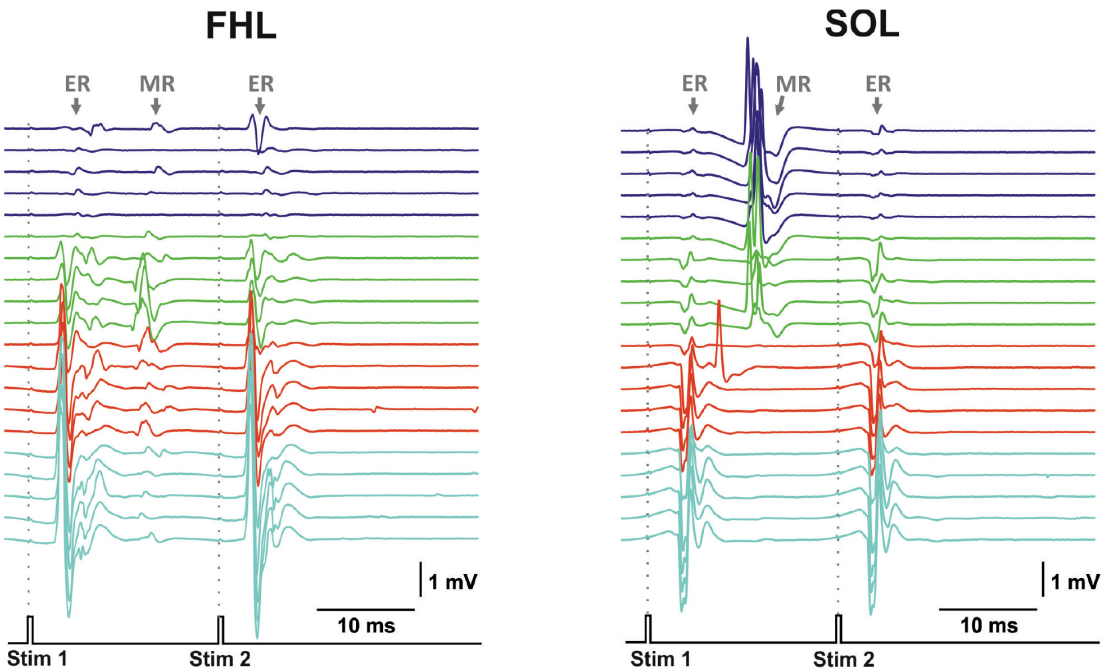

FIGURE 2 | The representative examples of evoked potential dynamics with increasing current for transvertebral double-pulse electrical stimulation (1,900–2,200 μA) delivered at VL5 vertebrae for mm. flexor hallucis longus (FHL) and soleus (SOL). Stim, stimulation impulse; ER, early response; MR, medium response.

slope value (**Figures 1E,F**, $Slope_{max}$). For transvertebral mapping, i = (VT12–VS1); for comparison of the transvertebral stimulation with the transcutaneous one, i = VT12, VL2, VL6.

The distributions of the normalized slopes of the recruitment curves of one muscle were averaged over all animals. The χ^2 two-sample Bonferroni-adjusted test (Press et al., 1992) was used when comparing these distributions for different muscles. The paired Wilcoxon criteria was applied to compare the normalized slopes of different muscles in one stimulation point when comparing transvertebral and transcutaneous stimulation. For each muscle, the latencies and threshold currents of the ERs for the recruitment curve that had maximal slope were averaged over animals. The Friedman test with *post hoc* Bonferroni adjustment was used to compare these values for the different muscles.

All data are reported as mean ± SE. The criterion level for the determination of statistical difference was set at $p < 0.05$.

RESULTS

Transvertebral Spinal Cord Stimulation

Transvertebral SCS over the VT12–VS1 vertebrae (**Figure 1**) of non-anesthetized decerebrated rats evoked site-specific EMG patterns of activity in the tested muscles. Examples of evoked potential dynamics with increasing current are presented in **Figure 2**. The sensory-evoked potentials (namely, MR on **Figure 2**), similar to the motor ones (ER, on **Figure 2**), appear at lower currents in response to the first impulse, but the sensory-evoked potentials are absent after the second impulse. The motor-evoked potentials increase similarly with further current increases in response to the first and to the second impulses, whereas the sensory-evoked potentials decay. Thus, the motor and sensory responses illustrated classical recruiting dynamics; the MR (H-wave) was suppressed by the ER (M-wave) as the amplitude of the stimulation increased (Hoffman, 1910; Gerasimenko et al., 2006). We also observed the late reflex component in some muscles, but this was not consistent (**Figure 3A**, ST). The latencies of ERs were almost equal to each other in all individual responses at one stimulation point, indicating reproducibility of the recorded motor-evoked potentials and the stability of the experimental model (**Figures 2**, **3**).

The examples of recruitment curves for individual muscles plotted for motor (early) and sensory responses of the same animal when the electrical stimulation was delivered at the VT12–VS1 vertebrae are presented in **Figure 4**. *For motor responses*, the saturation of peak-to-peak amplitudes was observed for some muscles (LD, VL, and ACD). For the different muscles, the "optimal" vertebrae where the stimulation causes a maximal recruitment curve slope were clearly different. For example, the set of LD recruitment curves had a maximum slope at the VT12 stimulation, the set of ACD recruitment curves had a maximum slope at the VS1 stimulation, and so on. When the vertebrae adjacent to the "optimal" one were stimulated, the recruitment curves had slopes close to the maximal value.

For sensory responses, the recruitment curves frequently had a typical inverted U-shape (e.g., FHL, SOL, GM, and VL) due to depression of the sensory responses by motor ones. Their threshold current was lower than the threshold current of the motor responses, as the sensory responses appear to arise due

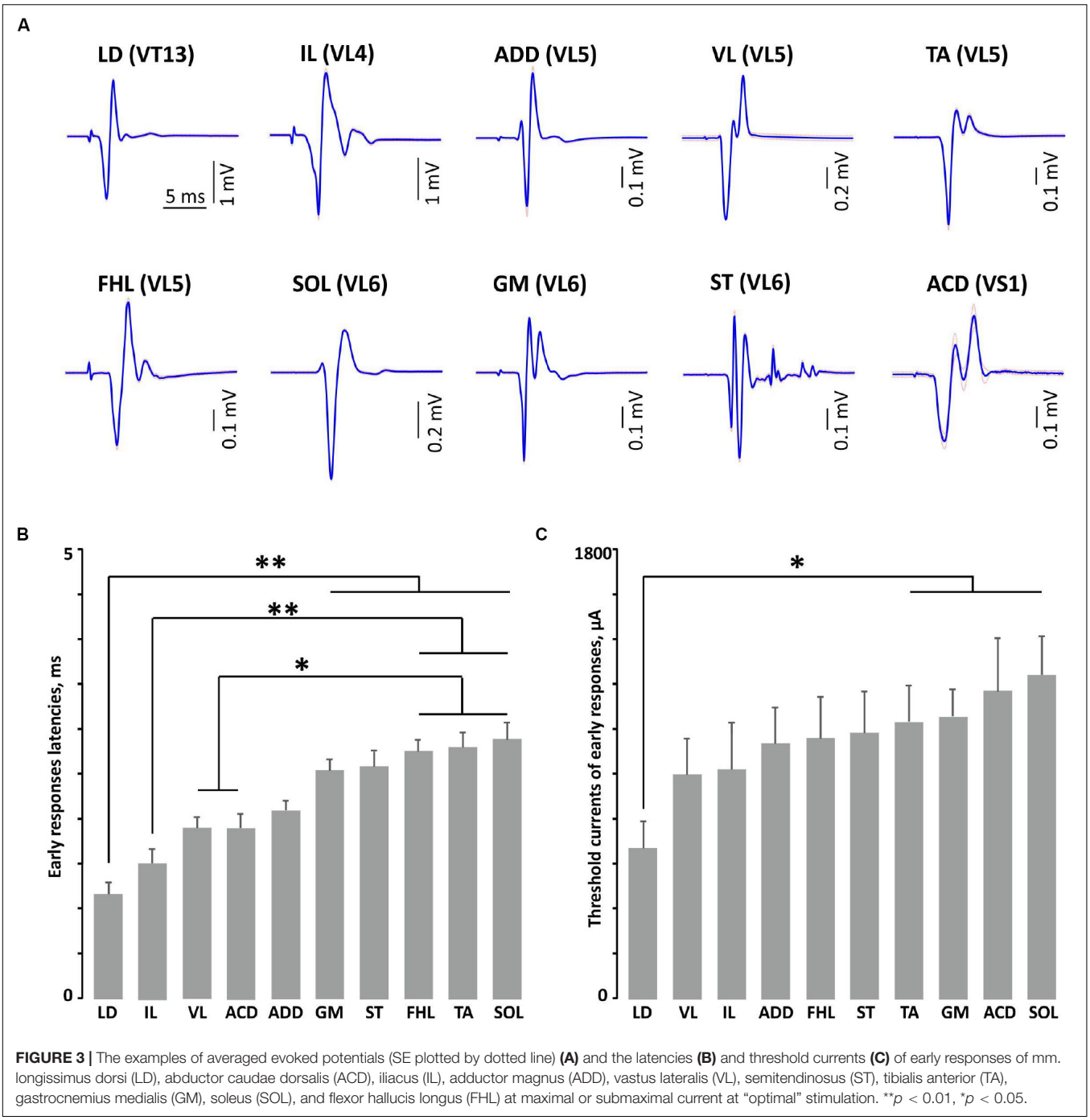

FIGURE 3 | The examples of averaged evoked potentials (SE plotted by dotted line) **(A)** and the latencies **(B)** and threshold currents **(C)** of early responses of mm. longissimus dorsi (LD), abductor caudae dorsalis (ACD), iliacus (IL), adductor magnus (ADD), vastus lateralis (VL), semitendinosus (ST), tibialis anterior (TA), gastrocnemius medialis (GM), soleus (SOL), and flexor hallucis longus (FHL) at maximal or submaximal current at "optimal" stimulation. $^{**}p < 0.01$, $^{*}p < 0.05$.

to activation of more excitable dorsal roots that are more closely situated to the stimulation electrode. The number of vertebrae where the stimulation caused a suprathreshold sensory response was greater than the number of vertebrae where the stimulation caused a motor response, in good agreement with previous findings (Roy et al., 2012).

The averaged distributions of the normalized slopes versus the mean skeletotopy of the VT12–VS1 region for motor and sensory responses are presented in **Figure 5**. The significance of the difference between each pair of distributions of *motor responses* is presented in **Table 1**. They are subdivided into five groups. The distribution for LD has a maximum at the VT12 stimulation; the distributions for IL, ADD, and VL have an inverted U-shape with a flat maximum at the VL2–VL4 stimulation (IL) or at VL4 (ADD and VL); the distributions for TA, FHL, and ST have maxima at the VL5 stimulation and additional submaxima at the VL2 stimulation; the distributions for SOL and GM have maxima at the VL6 stimulation and additional submaxima at the VL2 stimulation; and the distribution for ACD has a maximum at the VS1 stimulation. Notably, the VL1 and

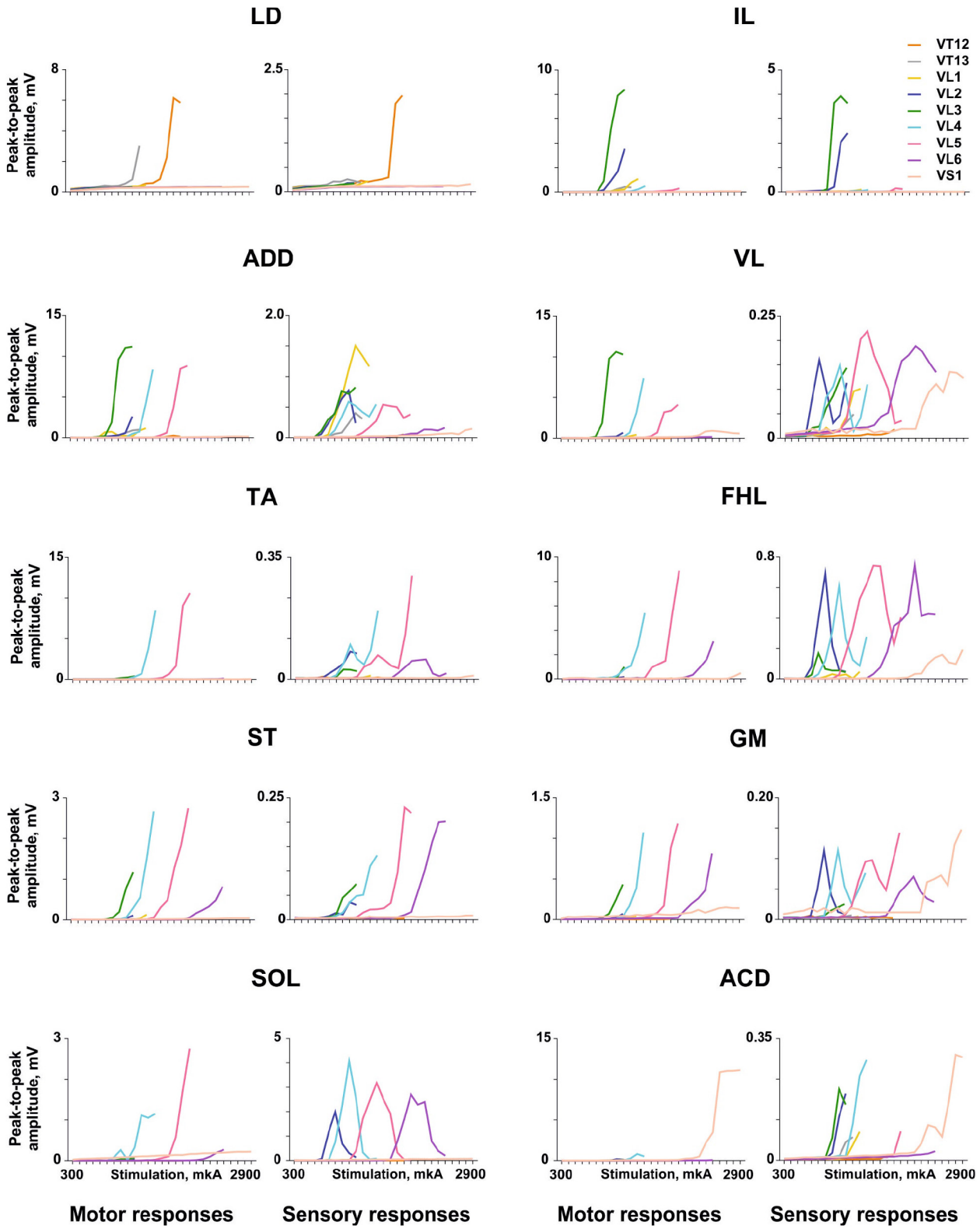

FIGURE 4 | Examples of the recruitment curves for mm. longissimus dorsi (LD), abductor caudae dorsalis (ACD), iliacus (IL), adductor magnus (ADD), vastus lateralis (VL), semitendinosus (ST), tibialis anterior (TA), gastrocnemius medialis (GM), soleus (SOL), and flexor hallucis longus (FHL) plotted for motor and sensory responses in the same animal when the electrical stimulation was delivered at the VT12–VS1 vertebrae.

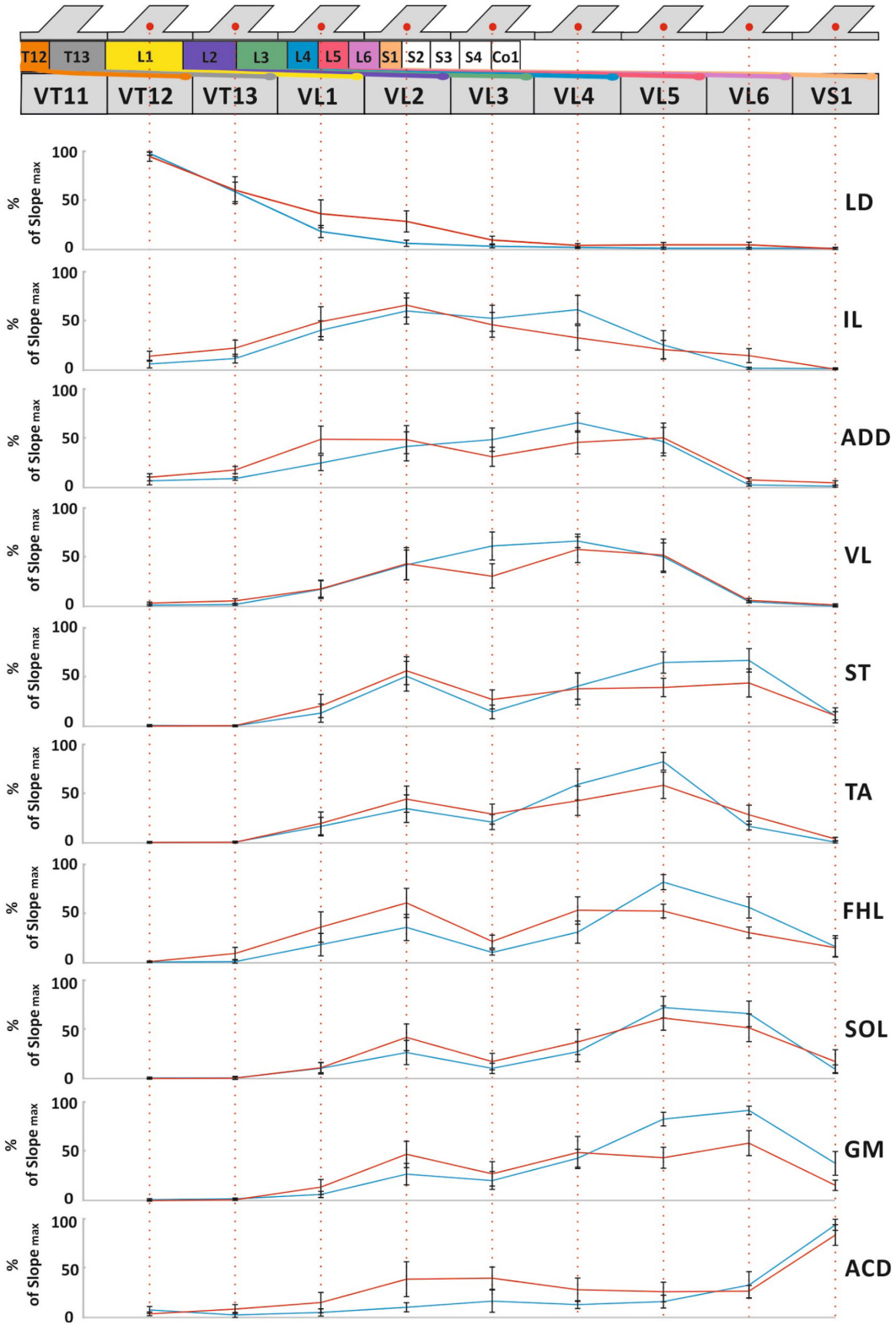

FIGURE 5 | The mean skeletotopy of spinal cord segments in relation to the VT12–VS1 vertebrae (the T11–S1 segments, their roots, and DRGs are marked by different colors corresponding to **Figure 2**) versus the averaged distributions of normalized slopes for mm. longissimus dorsi (LD), abductor caudae dorsalis (ACD), iliacus (IL), adductor magnus (ADD), vastus lateralis (VL), semitendinosus (ST), tibialis anterior (TA), gastrocnemius medialis (GM), soleus (SOL), and flexor hallucis longus (FHL) at the stimulation of these vertebrae. Motor responses (blue), sensory responses (red). The length of all vertebrae presented are equalized for simplicity.

TABLE 1 | The significance of the difference between distributions of slopes of motor responses (χ^2 two-sample Bonferroni-adjusted test, the significant differences on the $p < 0.05$ level are in boldface).

	IL	ADD	TA	FHL	VL	ST	GM	SOL	ACD
LD	**126.9**	**132.5**	**158.5**	**155.9**	**155.3**	**160.3**	**169.1**	**164.3**	**151.3**
IL		5.4	**35.9**	**61.6**	13.8	**54.6**	**79.4**	**73.6**	**98.2**
ADD			20.4	**48.8**	5.6	**44.7**	**63.9**	**58.5**	**93.3**
TA				19.8	15.2	19.1	**34.2**	**24.2**	**88.9**
FHL					**45.8**	3.9	8.7	3.4	**58.1**
VL						**39.9**	**57.4**	**52.7**	**95.4**
ST							10.6	4.2	**64.0**
GM								6.7	**42.2**
SOL									**65.0**

TABLE 2 | The significance of the difference between distributions of slopes of sensory responses (χ^2 two-sample Bonferroni-adjusted test, the significant differences on the $p < 0.05$ level are in boldface).

	IL	ADD	TA	FHL	VL	ST	GM	SOL	ACD
LD	**60.2**	**72.5**	**113.9**	**96.6**	**102.3**	**112.0**	**120.3**	**124.0**	**108.0**
IL		9.7	**31.9**	**23.2**	**23.8**	**31.6**	**42.5**	**51.7**	**45.3**
ADD			20.3	12.6	9.9	**26.7**	**34.3**	**37.4**	**44.0**
TA				8.5	11.5	5.2	8.2	9.0	**41.5**
FHL					14.4	7.1	10.9	12.4	**30.1**
VL						**22.6**	**26.7**	**29.7**	**47.2**
ST							2.5	5.9	**32.4**
GM								3.0	**31.3**
SOL									**34.1**

VL3 vertebrae are not optimal for any of the 10 muscles under consideration.

The distributions of *sensory responses* are wider than the distributions of motor responses. The significance of the difference between each pair of distributions is presented in **Table 2**. They can be subdivided into four less pronounced groups. The distribution for LD has a maximum at the VT12 stimulation; the distribution for IL has a maximum at VL2 stimulation; the distributions for ADD, VL, TA, FHL, ST, GM, and SOL have a complex form; and the distribution for ACD has maximum at the VS1 stimulation.

The distributions indirectly reflect the rostrocaudal distribution of the motoneuron pools in the rat spinal cord (Nicolopoulos-Stournaras and Iles, 1983; Mohan et al., 2015; Wenger et al., 2016). The S1 spinal cord segment is located in the VL2 vertebra due to spinal cord "ascension." Thus, the stimulation of the VL3–VS1 vertebrae does not affect the spinal cord itself. By contrast, the stimulation of the VL2 vertebra supposedly also activates the spinal cord, leading to the additional maxima in the distribution of the sensory and motor responses mentioned above.

The examples of averaged evoked potentials of all considered muscles at the maximal or submaximal current at the "optimal" stimulation are presented in **Figure 3A**. Again, the "optimal" stimulation of various muscles was carried out from different vertebrae. Most of the presented evoked potentials contain the high amplitude ER followed by MR of lower amplitude. The ER latencies in all the considered muscles at the maximal current applied to "optimal" stimulation sites are presented in **Figure 3B**. The LD latency is significantly lower than the latencies of GM, ST, FHL, TA, and SOL ($p < 0.01$); this corresponds to the LD anatomical location and the shorter motor axon path to this muscle. Following the same logic, the latencies are significantly lower for the proximal limb muscles (IL, VL, and ACD) than for the distal ones (FHL, TA, and SOL) (IL, $p < 0.01$; VL, ACD, $p < 0.05$). The SOL is the slow muscle; the rate of rise is lower for its action potential than for those of the extensor muscles (Albuquerque and Thesleff, 1968); the spectrum of its activity covers a region of lower frequencies than do the spectra of the fast muscles (Hodson-Tole and Wakeling, 2010). This is probably why the latency is higher for SOL responses than for GM responses. The ER threshold currents increased rostrocaudally (**Figures 3C**, **4**). The threshold current was significantly lower for LD that had optimal VT12 and VT13 stimulation vertebra ($p < 0.05$) than for TA, GM, SOL, and ACD that had optimal VL5, VL6, and VS1 stimulation vertebrae.

Chronic Experiments

The validity of the proposed approach of electrode implantation and the possibility of causing muscle responses to vertebral stimulation in chronic conditions were checked in a group of awake animals that had survived 1 week after all the implantation surgery. The typical pattern of the evoked response of the TA muscle is presented in **Figure 6A**. Similar to the acute experiments, the sensory responses were decaying and the motor responses were increasing as the current increased.

The recruitment curves plotted for the motor responses of the TA and GM of individual animals to the VL2 single-pulse stimulation are presented in **Figure 6B**. Presumably, the range of stimulation currents depends on the implantation peculiarities (e.g., variations in individual reactions to the electrodes as a foreign object, expressed by surrounding the wire with connective tissue, or a slightly different position of the wire inside the vertebral hole), whereas the slopes of the recruitment curves of different animals are rather similar.

Comparison of the Selectivity of Transcutaneous and Transvertebral Stimulation

The transcutaneous and transvertebral stimulation was compared at three stimulation points located on the edges and in the center of the zone of interest: the VT12, VL2, and VL6 vertebrae. The muscle responses to double-pulse transcutaneous stimulation were qualitatively similar to those of transvertebral stimulation (**Figure 7**). The motor-evoked potentials were elicited in response to both stimulation pulses, whereas the sensory-evoked potentials were elicited only in response to the first one. The sensory-evoked potentials decayed with the current increase. The motor responses were chosen for comparison of the selectivity, since their distributions were narrower than those of the sensory responses (**Figure 5**).

The pattern of the relative slopes for transvertebral stimulation is presented in **Figure 8A**. The VT12 stimulation activated the LD to a maximal degree and the VL, TA, SOL, FHL, GM, and ST to a minimal degree. The relative slopes of IL, ADD, and ACD were small but significantly higher than zero. The VL2 stimulation activated the LD to a minimal degree, whereas the differences between the relative slopes of other muscles were insignificant. The VL6 stimulation revealed a significant difference between the small relative slopes of LD, IL, ADD, and VL and the large relative slopes of TA, SOL, FHL, GM, ST, and ACD. Thus, the transvertebral stimulation of VT12 and VL6 allowed the selective stimulation of different muscle groups.

The pattern of relative slopes for transcutaneous stimulation (**Figure 8B**) had much in common with the transvertebral stimulation, although it had some peculiarities. The selectivity of stimulation of the cutaneous zones between VT12 and VT13 and between VL6 and VS1 was lower than the selectivity of transvertebral VT12 and VL6 stimulation, respectively. On the contrary, the stimulation of the cutaneous zone between VL2 and VL3 allowed selective recruitment of the muscles having more rostrally located motoneuronal pools.

DISCUSSION

In the present work, we performed detailed and thorough testing of the transvertebral stimulation of thoracic (VT12–VT13), lumbar (VL1–VL6), and sacral (VS1) vertebrae to recruit the motor-evoked potentials in 10 different muscles of the trunk and hindlimbs that participate in locomotion and postural activity. This electrophysiological mapping demonstrated that the transvertebral SCS, similar to the transcutaneous SCS, has substantially specific effects on the rostrocaudally distributed sensorimotor network of the lumbar and sacral spinal segments. These effects are mainly driven by stimulation of the roots carrying sensory and motor spinal pathways.

Site-Specific Recruitment of the Sensorimotor Pathways by Transvertebral Spinal Cord Stimulation

The spinal cord consists of rostrocaudally distributed neuronal pathways and cell groups. In particular, the lumbosacral spinal cord contains the motor pools of the trunk and hindlimb muscles (Romanes, 1951; Nicolopoulos-Stournaras and Iles, 1983; Vanderhorst and Holstege, 1997; Takahashi et al., 2010; Mohan et al., 2014, 2015), related interneuron populations (Carr et al., 1995; Dai et al., 2005; Merkulyeva et al., 2018), sensory inputs of different modalities from somatotopic regions (Rivero-Melián and Grant, 1990; Takahashi et al., 2003, 2006, 2007), and neuronal axons (Tani et al., 1994; Takahashi et al., 2010) that conduct motor commands to the musculoskeletal system during locomotor activity and postural tasks. Our aim in the present study was to use the method of transvertebral SCS to recruit specific neuronal pathways located under the thoracic, lumbar, and sacral vertebrae.

We chose ACD and LD (implanted near the VT13 vertebra) muscles as the reference points because they have the most caudal and rostral motor neuron pool localizations of all implanted muscles. In accordance, the ACD was found to be recruited at the most caudal stimulation point, namely VS1. Its motoneurons are distributed in the L5–Co1 segments with the maximum in the S1 segment (Grossman et al., 1982), where motoneurons of the hindlimb muscles are absent. The LD has multiple every-segment innervation by lateral branches of the dorsal rami of the lumbar spinal nerves (Brink and Pfaff, 1980). However, for the epaxial and hypaxial muscles, each segment of the spinal cord innervates a site located caudally; for example, a section of this muscle at the level of the VL5 vertebra is innervated by motor neurons located in the L2 and L3 segments (Takahashi et al., 2010) and the same segments receive its sensory inputs (Takahashi et al., 2003). Therefore, it makes sense that the LD implanted near the VT13 vertebra was recruited with a maximum slope during stimulation of the rostral VT12 vertebra.

A number of studies of the hindlimb motor neuron pools in various species, particularly in rats (Nicolopoulos-Stournaras and Iles, 1983; Mohan et al., 2015; Wenger et al., 2016), mice (Mohan et al., 2014), and cats (Romanes, 1951; Vanderhorst and Holstege, 1997), have shown that motor neurons innervating the proximal muscles are located more rostrally than are motor neurons innervating the distal muscles. A similar distribution pattern is well known and characteristic of the motor neurons innervating the muscles of the forelimb (McKenna et al., 2000). The proximodistal order of muscle activation has been shown in epidural (Lavrov et al., 2015) and transcutaneous (Roy et al., 2012; Gerasimenko Y. et al., 2015) stimulation experiments as the stimulation electrode moves from a rostral to a caudal direction.

However, some exceptions to this rule exist; for example, the neuronal pool for TA is rostral to the ones for GM and SOL

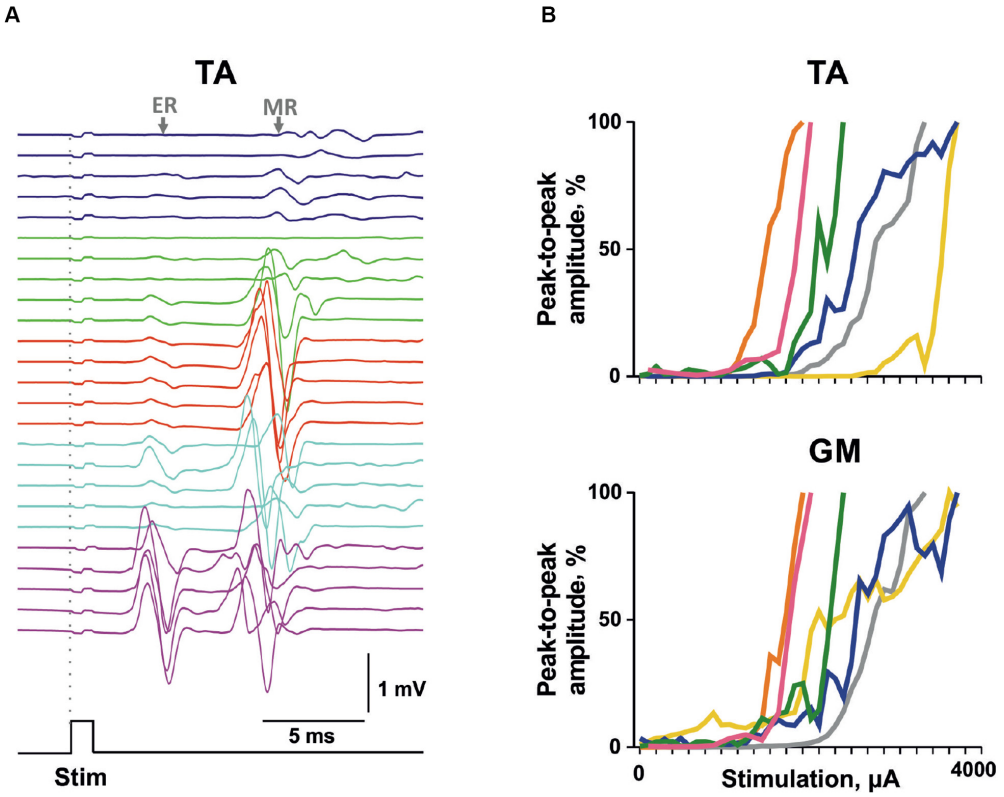

FIGURE 6 | The motor-evoked potentials triggered by transvertebral stimulation in chronic animals. **(A)** Example of evoked potential recruitment dynamics with increasing current (1,600–2,000 μA) for m. Tibialis anterior (TA). **(B)** The individual recruitment curves for mm. TA and gastrocnemius medialis (GM) of different chronic rats. Stim, stimulation impulse; ER, early response; MR, medium response.

although all these muscles are located on the shin and act to the ankle joint as a flexor and extensor, respectively (Nicolopoulos-Stournaras and Iles, 1983; Mohan et al., 2015; Wenger et al., 2016). A similar shift in motoneuron pools can be observed for the vastus and hamstrings groups (Watson et al., 2009; Mohan et al., 2015; Wenger et al., 2016) or for the forelimb biceps and triceps motoneurons (McKenna et al., 2000; Greiner et al., 2020). This may reflect the embryonic and phylogenetic origin of the TA and quadriceps group from the dorsal muscle mass and the origin of the SOL, GM, and hamstring group from the ventral one (Diogo et al., 2016).

The different maps of rat motoneuronal pools diverged in detail (Nicolopoulos-Stournaras and Iles, 1983 vs. Mohan et al., 2015 vs. Wenger et al., 2016). Furthermore, the response of a muscle to stimulation may depend indirectly on the location of its motoneuronal pool (due to root anastomosis, the peculiarities of current distribution over vertebrae, and so on). For example, Borrell et al. (2017) found a significant but partial coincidence of motoneuronal pools with intraspinal microstimulation-evoked movement patterns. This is why the following computational procedure was developed for each muscle. Initially, we calculated the maximal peak-to-peak amplitudes for sensory and motor responses at each stimulation point. We then constructed the recruitment curves based on those values and chose the recruitment curve with the maximal slope.

One of the outcomes of this study was the generation of maps of muscle-evoked potentials calculated on the basis of the averaged distributions of the normalized slopes of the recruitment curves. Our results are generally in good agreement with the data on the motoneuronal pool distribution, since the pattern of normalized slopes for proximal muscles has peaks in more rostral segments than for distal ones. The method of mapping is sufficiently sensitive even to reveal the abovementioned flexor–extensor shift of the motor neuron pool distribution. The aggregated map of the hindlimb muscles obtained is located more caudally than previously described (Nicolopoulos-Stournaras and Iles, 1983; Mohan et al., 2015) and is more similar to the data presented by Wenger et al. (2016); this requires further evaluation.

Neuroanatomical Mechanisms of the Transvertebral Spinal Cord Stimulation

The effects of epidural and transcutaneous stimulation on the hindlimb muscles are similar to each other in that they depend on the site of stimulation in a similar manner in the rat (Capogrosso et al., 2013), cat (Musienko et al., 2013), and human (Zhu et al., 1998; Minassian et al., 2007; Roy et al., 2012; Sayenko et al., 2015; Hofstoetter et al., 2018). The H-wave appears primarily upon stimulation of the upper lumbar segments of the spinal

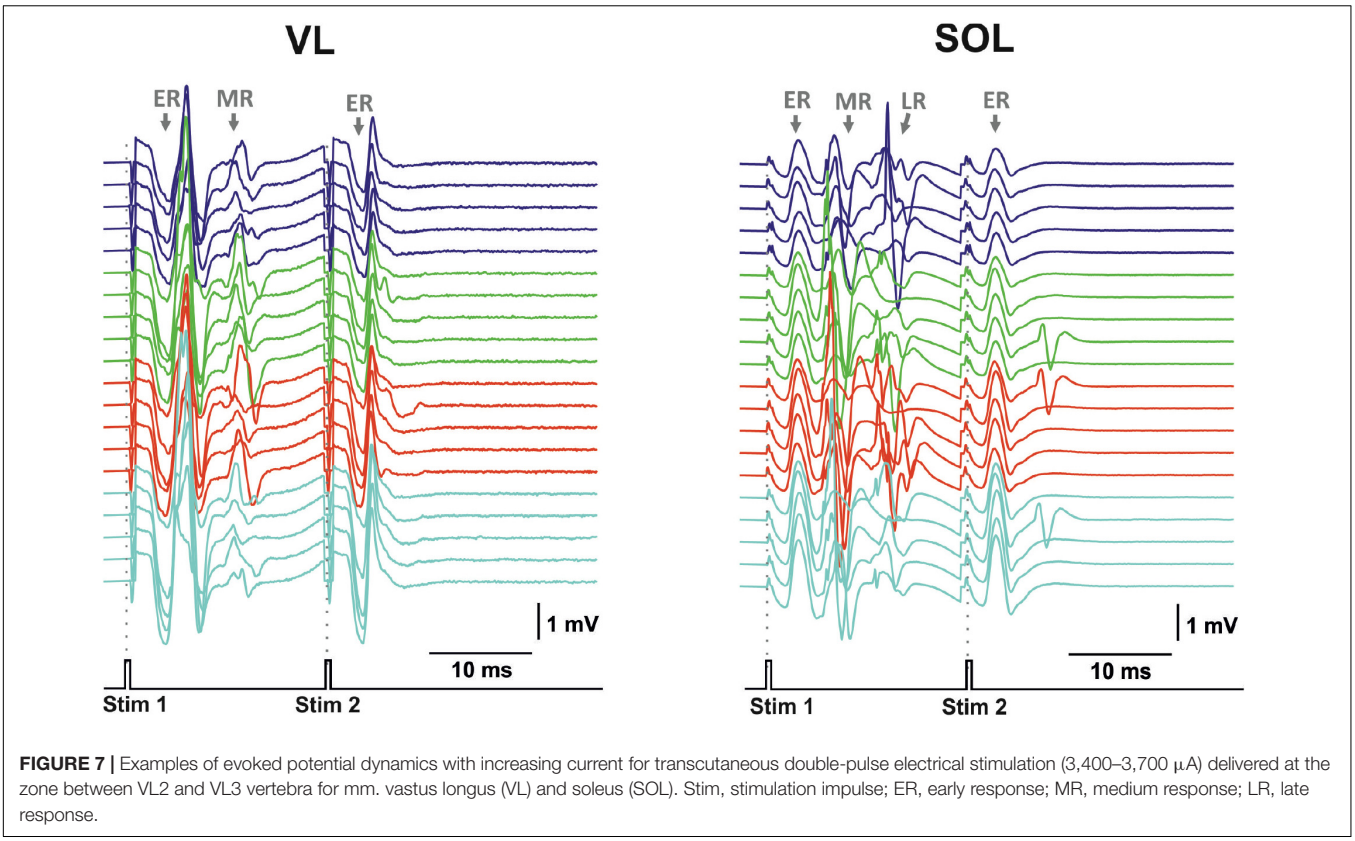

FIGURE 7 | Examples of evoked potential dynamics with increasing current for transcutaneous double-pulse electrical stimulation (3,400–3,700 μA) delivered at the zone between VL2 and VL3 vertebra for mm. vastus longus (VL) and soleus (SOL). Stim, stimulation impulse; ER, early response; MR, medium response; LR, late response.

cord or the vertebrae over them (Roy et al., 2012; Sayenko et al., 2015; Hofstoetter et al., 2018), since the dorsal root input zones into these segments are accessible for the electrical current first. The excitability is higher in the Ia afferents in the dorsal roots responsible for H-wave (Erlanger and Gasser, 1937; Lloyd and Chang, 1948) than in the low-threshold efferents in the ventral roots inducing the M-wave. The dorsal roots are anatomically much closer to the electrode and separated from the ventral roots due to the relatively large diameter of the spinal cord. The M-wave, however, may emerge with a further significant current increase. This sequence of wave appearance is also confirmed by simulation (Danner et al., 2011).

In the lower lumbar spinal cord, the dorsal and ventral roots are closer to each other (**Figure 1B**). In this case, the threshold currents of the M- and H-waves could be closer. Both the M- and H-waves can occur simultaneously with increasing current (Capogrosso et al., 2013). Similarly, in the lumbar vertebrae, the dorsal and ventral roots of the lower lumbar segments are located close to each other, especially in the areas near the intervertebral foramina that lead to the early appearance of the M-wave. However, in these vertebrae, the spinal cord in rats (Gelderd and Chopin, 1977; our data **Figure 5**), in cats (Shkorbatova et al., 2019), and in humans (Barson, 1970) may actually be absent. The M-wave may appear together with the H-wave (Zhu et al., 1998; Roy et al., 2012; Musienko et al., 2013) or at a slightly higher stimulation magnitude (Minassian et al., 2007).

The transvertebral SCS used in our work is similar to the transcutaneous one by its effects on spinal sensorimotor pathways. Firstly, the distributions are wider for the sensory-evoked potentials than for the motor ones, as was shown for transcutaneous stimulation of the human spinal cord (Roy et al., 2012). Potentially, the sensory responses may be elicited by stimulation of dorsal roots passing closer to dorsally located stimulating electrodes over the spinal cord. Therewith, the sensory pathways in the stimulating roots have wide projections and collateralization (Redett et al., 2005) while coming and switching at the spinal level. The motor responses are elicited more specifically by stimulation of the ventral roots of the segment, presumably, in their exit from the vertebral canal below the corresponding vertebra (Danner et al., 2011). Every segmental group of ventral root contains (with some individual variations) the particular set of motor axons running from motoneuron pools specific for the segment. Secondly, the responses to both types of stimulation indirectly reflect the rostrocaudal distributions of motoneuronal pools; that is, LD, IL, and ADD are active to a greater degree during the stimulation of the more rostral point (vertebrae VT12 or VT12–VT13 cutaneous zone), whereas SOL, FHL, and GM are active to a greater degree during the stimulation of the more caudal point (vertebrae VL6 or VL6–VS1 cutaneous zone). Therefore, taking into account a more superficial and distant location from the spinal canal and larger area of electrodes, the transcutaneous stimulation would appear to capture a wider zone of spinal pathways relative to the transvertebral stimulation.

Transvertebral intraoperative stimulation through the pedicle screws is widely used to monitor possible root trauma and

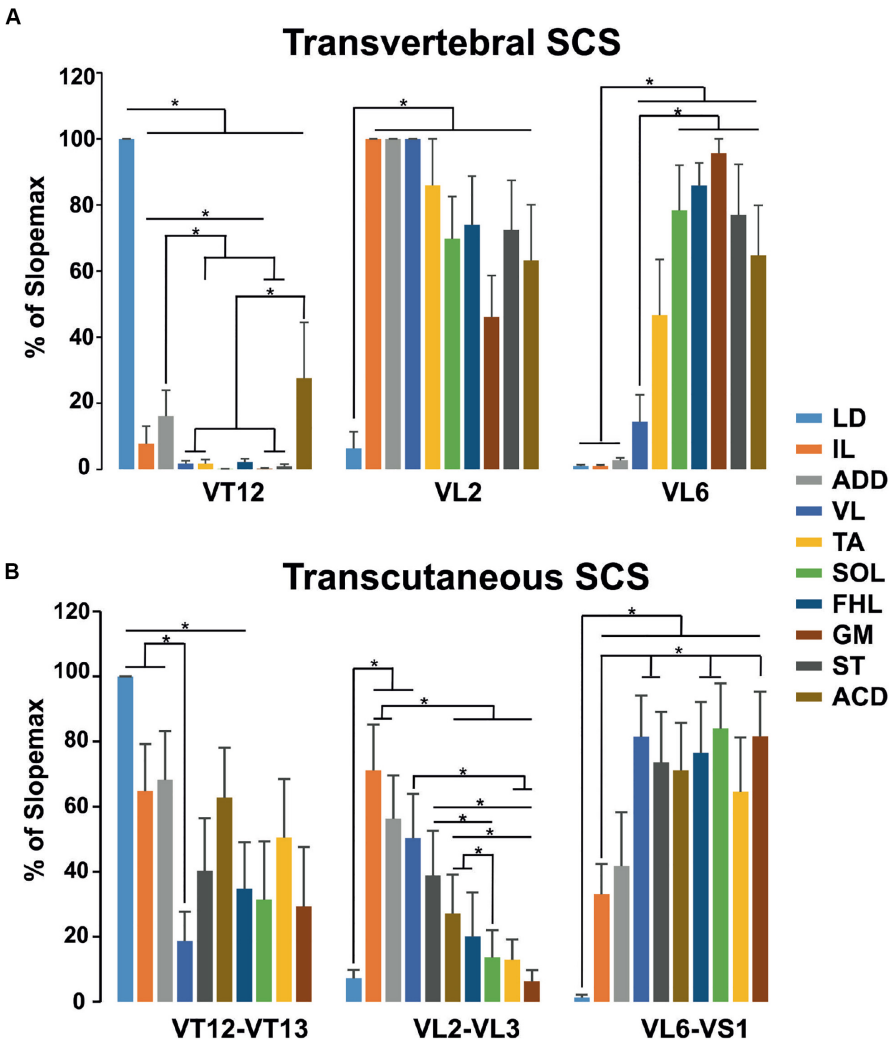

FIGURE 8 | The relative slopes of recruitment curves in **(A)** transvertebral stimulation of VT12, VL2, and VL6 and **(B)** transcutaneous stimulation of VT12–VT13, VL2–VL3, and VL6–VS1 zones of mm. longissimus dorsi (LD), abductor caudae dorsalis (ACD), iliacus (IL), adductor magnus (ADD), vastus lateralis (VL), semitendinosus (ST), tibialis anterior (TA), gastrocnemius medialis (GM), soleus (SOL), and flexor hallucis longus (FHL).

the quality of screw implantation (Calancie et al., 1992, 1994; Toleikis et al., 2000; Danesh-Clough et al., 2001). This technique is qualitatively similar to the one used in our work, except that it is lateralized, whereas we placed the electrode at the midline in the center of the spinous process. This stimulation in sheep (Danesh-Clough et al., 2001), pig (Lenke et al., 1995), and humans (Calancie et al., 1994) showed that the amplitude and latency of the EMG response in different muscles depend on the stimulated vertebra, again reflecting the rostrocaudal distribution of motoneuronal pools in the spinal cord. The EMG data presented previously (Calancie et al., 1994; Chansakul and Nair, 2012) allow us to suppose that, with this type of stimulation, the M-wave may appear already in the near threshold current.

The low values of all latencies obtained when the "optimal" vertebra is stimulated (**Figure 3B**) indicate the involvement of the ventral roots, resulting in the M-wave. The different latencies of the M-waves in different muscles are associated with the length of the motoneuron axons that innervate the particular muscle: the more proximal the muscle is in relation to the spinal cord, the shorter is its M-wave latency, and *vice versa*. The M-waves predominantly appeared in the threshold current in transvertebral stimulation. Interestingly, the early appearance of the M-wave was also observed by Pavlova et al. (2019) during deep subcutaneous stimulation of the intervertebral area. Presumably, the threshold currents for excitation of motor axons and Ia/Ib fibers are similar for stimulation of the caudal segments of the spinal cord (Capogrosso et al., 2013). In the case of SCS through pedicle screws, the threshold currents rise as the distance between the screw and the neural structures increases (Montes et al., 2012). The differences in threshold currents observed in our work (**Figure 3C**) may be associated with anatomical differences in the structure of the rat vertebrae. Supposedly, the rostrocaudal increase of the rat's spinous process height, calculated as Vd-VBd-SCd following Jaumard et al. (2015), leads to an increase in the

distance from the stimulation point to the stimulated structures of the spinal cord.

The Relevance of the Spinal Pathways Neuromodulation by Transvertebral Spinal Cord Stimulation

Although there are limitations in using a decerebrate preparation, our results show that transvertebral SCS can be further used in acute and chronic experiments on intact and injured animal models to access spinal pathways, such as the locomotor or visceral networks, and to investigate the neuronal control of the sensorimotor and autonomic functions. The relationship between spinal and vertebral levels are rather variable, especially for the more caudal segments (Needles, 1935; Shkorbatova et al., 2019). That is why the precise level for epidural SCS can only be well determined after a thorough neuroanatomical dissection and histology.

The important advantage of transvertebral stimulation is that it mostly affects the roots emerging from/entering into the spinal canal of the corresponding vertebra and containing sensory and motor fibers to the homologous segment. This has a special value when stimulating more caudal vertebrae where the cauda equina is formed by roots from ascending lumbosacral segments. The data obtained confirm that the transvertebral and transcutaneous stimulation approaches are selective in acting on the individual roots forming the cauda equina at the specific level from which they depart. Simply counting the vertebrae provides rather objective information about targeting the spinal cord region during the *in vivo* stage of the experiment.

One problem of transcutaneous stimulation is the difficulty in fixation of the stimulating electrode on the skin, as it is easily movable in the rat and, especially, in unanesthetized, freely behaving animals in chronic experiments. Moreover, animals have cutaneous trunk muscles that cover the back and sides of the animal body. Though the muscle is innervated from C7–T1 spinal segments (Theriault and Diamond, 1988), it responds to the stimulation of the dorsal aspects of the trunk skin by flicking or puckering the skin (Petruska et al., 2014). This causes movement of the cutaneously fixed sticky electrode during the stimulation. We also cannot exclude the direct influence of the electrical current, which may cause this muscle to contract. Possibly, for these reasons, the cutaneous stimulation was used in chronic rats in experiments where the exact position of the stimulation does not make much sense. For example, for management of neuropathic pain, relatively large (45 mm × 5 mm) adhesive electrodes were used, and they were repositioned on the dorsal rami of spinal nerves L1–L6 before the stimulation session (Somers and Clemente, 2006). However, this approach is not appropriate for more thorough examinations of the influence of stimulation points on the peculiarities of the muscle response or of locomotion.

The transcutaneous SCS may modulate corticospinal excitability and improve functional outcomes of rehabilitation (Powell et al., 2016). Possibly, the transvertebral SCS may be more selective than the transcutaneous one. There are clinical protocols using transvertebral stimulation intended to assess the functional state of spinal tracts and nerve roots after the operations that lead to potential risk of spinal cord damage, for example a simulation with the needle placed in the spinous process (Komanetsky et al., 1998; Wilson-Holden et al., 2000) or through pedicle screws (Calancie et al., 1992, 1994; Toleikis et al., 2000; Danesh-Clough et al., 2001). The latter allows an intraoperative monitoring of EMG activity of different muscle groups of human legs. This activity topically depends on the stimulation level (Chansakul and Nair, 2012). Meanwhile, the screws may be used for neuromodulation in further treatment procedures (Edidin, 2017). In addition to neurophysiological testing, the transvertebral SCS can be studied as a neurorehabilitation method in paralyzed animal models (Courtine et al., 2009) and in patients with vertebrospinal pathology (Gill et al., 2018; Wagner et al., 2018), as it is much simpler to apply, less invasive, and safer compared with epidural SCS. The value of the proposed approach to trigger rostrocaudally distributed spinal pathways is a crucial feature for neuromodulation treatments (Wenger et al., 2014, 2016).

Further experiments on chronic rats with severe SCI and daily stimulating sessions, independent of Ichiyama et al. (2005), Lavrov et al. (2006) or in combination with modulating pharmacological agents (Ichiyama et al., 2008; Musienko et al., 2011; Moshonkina et al., 2016), will test the clinical relevance of transvertebral SCS and the advisability of its translation to practical medicine.

DATA AVAILABILITY STATEMENT

The raw data supporting the conclusions of this article will be made available by the authors, without undue reservation.

ETHICS STATEMENT

The animal study was reviewed and approved by Ethics Commission of the Pavlov Institute of Physiology.

AUTHOR CONTRIBUTIONS

PS, VL, NP, and PM conceived the experiments. PS, VL, and PM wrote the manuscript. PS, VL, DK, AP, and PM edited the manuscript. PS, VL, OG, NP, DK, AP, and EB performed the research. PS and VL analyzed the data. MP supervised the study. All authors contributed to the article and approved the submitted version.

FUNDING

This work was performed within project ID: 51134206 of the Saint Petersburg State University, Saint Petersburg, Russia (for EB and OG), supported by the Russian Foundation for Basic Research [grant numbers 18-33-20062-mol-a-ved (for anatomical evaluation of the spinal cord stimulation), 19-015-00546-a (for electrophysiological testing and data analysis), and 20-015-00568-a (for development of the setup)].

REFERENCES

Albuquerque, E. X., and Thesleff, S. (1968). A comparative study of membrane properties of innervated and chronically denervated fast and slow skeletal muscles of the rat. *Acta Physiol. Scand.* 73, 471–480. doi: 10.1111/j.1365-201X.1968.tb10886.x

Barson, A. J. (1970). The vertebral level of termination of the spinal cord during normal and abnormal development. *J. Anat.* 106, 489–497.

Borrell, J. A., Frost, S., Peterson, J., and Nudo, R. J. (2017). A three-dimensional map of the hindlimb motor representation in the lumbar spinal cord in Sprague-Dawley rats. *J. Neural Eng.* 14:016007. doi: 10.1088/1741-2552/14/1/016007

Brink, E. E., and Pfaff, D. W. (1980). Vertebral muscles of the back and tail of the albino rat (*Rattus norvegicus* albinus). *Brain Behav. Evol.* 17, 1–47. doi: 10.1159/000121788

Calancie, B., Lebwohl, N., Madsen, P., and Klose, K. J. (1992). Intraoperative evoked EMG monitoring in an animal model. A new technique for evaluating pedicle screw placement. *Spine* 17, 1229–1235. doi: 10.1097/00007632-199210000-00017

Calancie, B., Madsen, P., and Lebwohl, N. (1994). Stimulus-evoked EMG monitoring during transpedicular lumbosacral spine instrumentation, Initial clinical results. *Spine* 19, 2780–2786. doi: 10.1097/00007632-199412150-00008

Capogrosso, M., Gandar, J., Greiner, N., Moraud, E. M., Wenger, N., Shkorbatova, P., et al. (2018a). Advantages of soft subdural implants for the delivery of electrochemical neuromodulation therapies to the spinal cord. *J. Neural Eng.* 15:026024. doi: 10.1088/1741-2552/aaa87a

Capogrosso, M., Wagner, F. B., Gandar, J., Moraud, E. M., Wenger, N., Milekovic, T., et al. (2018b). Configuration of electrical spinal cord stimulation through real-time processing of gait kinematics. *Nat. Protoc.* 13, 2031–2061. doi: 10.1038/s41596-018-0030-9

Capogrosso, M., Wenger, N., Raspopovic, S., Musienko, P., Beauparlant, J., Luciani, L. B., et al. (2013). A computational model for epidural electrical stimulation of spinal sensorimotor circuits. *J. Neurosci.* 33, 19326–19340. doi: 10.1523/JNEUROSCI.1688-13.2013

Carr, P. A., Huang, A., Noga, B. R., and Jordan, L. M. (1995). Cytochemical characteristics of cat spinal neurons activated during fictive locomotion. *Brain Res. Bull.* 37, 213–218. doi: 10.1016/0361-9230(94)00271-2

Chansakul, C., and Nair, D. R. (2012). "Evoked potential monitoring," in *Anesthesia for Spinal Surgery*, ed. E. Farag (Cambridge: Cambridge University Press), doi: 10.1017/CBO9780511793851.009

Courtine, G., Gerasimenko, Y., van den Brand, R., Yew, A., Musienko, P., Zhong, H., et al. (2009). Transformation of nonfunctional spinal circuits into functional states after the loss of brain input. *Nat. Neurosci.* 12, 1333–1342. doi: 10.1038/nn.2401

Dai, X., Douglas, J. R., and Jordan, L. M. (2005). Localization of spinal neurons activated during locomotion using the c-fos immunohistochemical method. *J. Neurophysiol.* 93, 3442–3452. doi: 10.1152/jn.00578.2004

Danesh-Clough, T., Taylor, P., Hodgson, B., and Walton, M. (2001). The use of evoked EMG in detecting misplaced thoracolumbar pedicle screws. *Spine* 26, 1313–1316. doi: 10.1097/00007632-200106150-00008

Danner, S. M., Hofstoetter, U. S., Ladenbauer, J., Rattay, F., and Minassian, K. (2011). Can the human lumbar posterior columns be stimulated by transcutaneous spinal cord stimulation? A modeling study. *Artif. Organs.* 35, 257–262. doi: 10.1111/j.1525-1594.2011.01213.x

Diogo, R., Bello-Hellegouarch, G., Kohlsdorf, T., Esteve-Altava, B., and Molnar, J. L. (2016). Comparative myology and evolution of marsupials and other vertebrates, with notes on complexity, bauplan, and "Scala Naturae". *Anat. Rec.* 299, 1224–1255. doi: 10.1002/ar.23390

Dobson, K. L., and Harris, J. (2012). A detailed surgical method for mechanical decerebration of the rat. *Exp. Physiol.* 97, 693–698. doi: 10.1113/expphysiol.2012.064840

Edgerton, V. R., Gerasimenko, Y., Roy, R., and Lu, D. C. (2013). The regents of the University of California, applicants. Transcutaneous spinal cord stimulation: noninvasive tool for activation of locomotor circuitry. International Patent Application WO2013/071309.

Edidin, A. A. (2017). Modulating nerves within bone using bone fasteners. U.S. Patent No: 9,724,151. Washington, DC: U.S. Patent and Trademark Office.

Erlanger, J., and Gasser, H. S. (1937). *Electrical Signs of Nervous Activity*. Philadelphia: University Pennsylvania Press.

Gad, P., Kreydin, E., Zhong, H., Latack, K., and Edgerton, V. R. (2018a). Non-invasive neuromodulation of spinal cord restores lower urinary tract function after paralysis. *Front. Neurosci.* 12:432. doi: 10.3389/fnins.2018.00432

Gad, P., Lee, S., Terrafranca, N., Zhong, H., Turner, A., Gerasimenko, Y., et al. (2018b). Non-invasive activation of cervical spinal networks after severe paralysis. *J. Neurotrauma* 35, 2145–2158. doi: 10.1089/neu.2017.5461

Gelderd, J. B., and Chopin, S. F. (1977). The vertebral level of origin of spinal nerves in the rat. *Anat. Rec.* 188, 45–48. doi: 10.1002/ar.1091880106

Gerasimenko, I. P., Lavrov, I. A., Bogacheva, I. N., Shcherbakova, N. A., Kucher, V. I, and Musienko, P. E. (2003). Features of stepping pattern formation in decerebrated cats under epidural spinal cord stimulation. *Ross Fiziol Zh Im I M Sechenova* 89, 1046–1057.

Gerasimenko, Y., Gorodnichev, R., Moshonkina, T., Sayenko, D., Gad, P., and Edgerton, V. R. (2015). Transcutaneous electrical spinal-cord stimulation in humans. *Ann. Phys. Rehabil. Med.* 58, 225–231. doi: 10.1016/j.rehab.2015.05.003

Gerasimenko, Y. P., Lu, D. C., Modaber, M., Zdunowski, S., Gad, P., Saenko, D., et al. (2015). Noninvasive reactivation of motor descending control after paralysis. *J. Neurotrauma* 32, 1968–1980. doi: 10.1089/neu.2015.4008

Gerasimenko, Y., Gorodnichev, R., Puhov, A., Moshonkina, T., Savochin, A., Selionov, V., et al. (2014). Initiation and modulation of locomotor circuitry output with multisite transcutaneous electrical stimulation of the spinal cord in non-injured humans. *J. Neurophysiol.* 113, 834–842. doi: 10.1152/jn.00609.2014

Gerasimenko, Y., Kozlovskaya, I., and Edgerton, V. R. (2016). Sensorimotor regulation of movements. *Fiziol Cheloveka* 42, 106–117. doi: 10.7868/s0131164616010094

Gerasimenko, Y. P., Lavrov, I. A., Courtine, G., Ichiyama, R. M., Dy, C. J., Zhong, H., et al. (2006). Spinal cord reflexes induced by epidural spinal cord stimulation in normal awake rats. *J. Neurosci. Methods* 157, 253–263. doi: 10.1016/j.jneumeth.2006.05.004

Gill, M. L., Grahn, P. J., Calvert, J. S., Linde, M. B., Lavrov, I. A., Strommen, J. A., et al. (2018). Neuromodulation of lumbosacral spinal networks enables independent stepping after complete paraplegia. *Nat. Med.* 24, 1677–1682. doi: 10.1038/s41591-018-0175-7

Greiner, N., Barra, B., Schiavone, G., James, N., Fallegger, F., Borgognon, S., et al. (2020). Recruitment of upper-limb motoneurons with epidural electrical stimulation of the primate cervical spinal cord. *bioRxiv* [Preprint]. doi: 10.1101/2020.02.17.952796

Grossman, M. L., Basbaum, A. I., and Fields, H. L. (1982). Afferent and efferent connections of the rat tail flick reflex (a model used to analyze pain control mechanisms). *J. Comp. Neurol.* 206, 9–16. doi: 10.1002/cne.902060103

Harkema, S., Gerasimenko, Y., Hodes, J., Burdick, J., Angeli, C., Chen, Y., et al. (2011). Effect of epidural stimulation of the lumbosacral spinal cord on voluntary movement, standing, and assisted stepping after motor complete paraplegia: a case study. *Lancet* 377, 1938–1947. doi: 10.1016/S0140-6736(11)60547-3

Hodson-Tole, E. F., and Wakeling, J. M. (2010). Variations in motor unit recruitment patterns occur within and between muscles in the running rat (*Rattus norvegicus*). *J. Exp. Biol.* 210, 2333–2345. doi: 10.1242/jeb.004457

Hoffman, P. (1910). Beitrage zur Kenntnis der menschlichen Reflexe mit besonderer Berucksichtigung der elektrischen Erscheinungen. *Arch. F. Physiol.* 1, 223–256.

Hofstoetter, U. S., Freundl, B., Binder, H., and Minassian, K. (2018). Common neural structures activated by epidural and transcutaneous lumbar spinal cord stimulation: elicitation of posterior root-muscle reflexes. *PLoS One* 13:e0192013. doi: 10.1371/journal.pone.0192013

Ichiyama, R. M., Gerasimenko, Y., Jindrich, D. L., Zhong, H., Roy, R. R., and Edgerton, V. R. (2008). Dose dependence of the 5-HT agonist quipazine in facilitating spinal stepping in the rat with epidural stimulation. *Neurosci. Lett.* 438, 281–285. doi: 10.1016/j.neulet.2008.04.080

Ichiyama, R. M., Gerasimenko, Y. P., Zhong, H., Roy, R. R., and Edgerton, V. R. (2005). Hindlimb stepping movements in complete spinal rats induced by epidural spinal cord stimulation. *Neurosci. Lett.* 383, 339–344. doi: 10.1016/j.neulet.2005.04.049

Jaumard, N. V., Leung, J., Gokhale, A. J., Guarino, B. B., Welch, W. C., and Winkelstein, B. A. (2015). Relevant anatomic and morphological measurements of the rat spine. *Spine* 40, E1084–E1092. doi: 10.1097/BRS.0000000000001021

Karayannidou, A., Zelenin, P. V., Orlovsky, G. N., Sirota, M. G., Beloozerova, I. N., and Deliagina, T. G. (2009). Maintenance of lateral stability during standing and walking in the cat. *J. Neurophysiol.* 101, 8–19. doi: 10.1152/jn.90934.2008

Komanetsky, R. M., Padberg, A. M., Lenke, L. G., Bridwell, K. H., Russo, M. H., Chapman, M. P., et al. (1998). Neurogenic motor evoked potentials: a prospective comparison of stimulation methods in spinal deformity surgery. *J. Spinal Disord.* 11, 21–28.

Lavrov, I., Gerasimenko, Y. P., Ichiyama, R. M., Courtine, G., Zhong, H., Roy, R. R., et al. (2006). Plasticity of spinal cord reflexes after a complete transection in adult tats: relationship to stepping ability. *J. Neurophysiol.* 96, 1699–1710. doi: 10.1152/jn.00325.2006

Lavrov, I., Musienko, P. E., Selionov, V. A., Zdunowski, S., Roy, R. R., Edgerton, V. R., et al. (2015). Activation of spinal locomotor circuits in the decerebrated cat by spinal epidural and/or intraspinal electrical stimulation. *Brain Res.* 1600, 84–92. doi: 10.1016/j.brainres.2014.11.003

Lenke, L. G., Padberg, A. M., Russo, M. H., Bridwell, K. H., and Gelb, D. E. (1995). Triggered electromyographic threshold for accuracy of pedicle screw placement. An animal model and clinical correlation. *Spine* 20, 1585–1591. doi: 10.1097/00007632-199507150-00006

Lloyd, D. P., and Chang, H. T. (1948). Afferent fibres in muscle nerves. *J. Neurophysiol.* 11, 199–227. doi: 10.1152/jn.1948.11.3.199

McKenna, J. E., Prusky, G. T., and Whishaw, I. Q. (2000). Cervical motoneuron topography reflects the proximodistal organization of muscles and movements of the rat forelimb: a retrograde carbocyanine dye analysis. *J. Comp. Neurol.* 419, 286–296. doi: 10.1002/(sici)1096-9861(20000410)419:3<286::aid-cne2>3.0.co;2-3

Merkulyeva, N., Veshchitskii, A., Gorsky, O., Pavlova, N., Zelenin, P. V., Gerasimenko, Y., et al. (2018). Distribution of spinal neuronal networks controlling forward and backward locomotion. *J. Neurosci.* 38, 4695–4707. doi: 10.1523/JNEUROSCI.2951-17.2018

Minassian, K., Jilge, B., Rattay, F., Pinter, M. M., Binder, H., Gerstenbrand, F., et al. (2004). Stepping-like movements in humans with complete spinal cord injury induced by epidural stimulation of the lumbar cord: electromyographic study of compound muscle action potentials. *Spinal Cord* 42, 401–416. doi: 10.1038/sj.sc.3101615

Minassian, K., Persy, I., Rattay, F., Dimitrijevic, M. R., Hofer, C., and Kern, H. (2007). Posterior root-muscle reflexes elicited by transcutaneous stimulation of the human lumbosacral cord. *Mus. Nerve* 35, 327–336. doi: 10.1002/mus.20700

Minev, I. R., Musienko, P., Hirsch, A., Barraud, Q., Wenger, N., Moraud, E. M., et al. (2015). Biomaterials. Electronic dura mater for long-term multimodal neural interfaces. *Science* 347, 159–163. doi: 10.1126/science.1260318

Mohan, R., Tosolini, A. P., and Morris, R. (2014). Targeting the motor end plates in the mouse hindlimb gives access to a greater number of spinal cord motor neurons: an approach to maximize retrograde transport. *Neuroscience* 274, 318–330. doi: 10.1016/j.neuroscience.2014.05.045

Mohan, R., Tosolini, A. P., and Morris, R. (2015). Segmental distribution of the motor neuron columns that supply the rat hindlimb: a muscle/motor neuron tract-tracing analysis targeting the motor end plates. *Neuroscience* 307, 98–108. doi: 10.1016/j.neuroscience.2015.08.030

Montes, E., De Blas, G., Regidor, I., Barrios, C., Burgos, J., Hevia, E., et al. (2012). Electromyographic thresholds after thoracic screw stimulation depend on the distance of the screw from the spinal cord and not on pedicle cortex integrity. *Spine* 12, 127–132. doi: 10.1016/j.spinee.2011.09.006

Moshonkina, T. R., Shapkova, E. Y., Sukhotina, I. A., Emeljannikov, D. V., and Gerasimenko, Y. P. (2016). Effect of combination of non-invasive spinal cord electrical stimulation and serotonin receptor activation in patients with chronic spinal cord lesion. *Bull. Exp. Biol. Med.* 161, 749–754. doi: 10.1007/s10517-016-3501-4

Musienko, P., Heutschi, J., Friedli, L., van den Brand, R., and Courtine, G. (2012). Multi-system neurorehabilitative strategies to restore motor functions following severe spinal cord injury. *Exp. Neurol.* 235, 100–109. doi: 10.1016/j.expneurol.2011.08.025

Musienko, P., van den Brand, R., Maerzendorfer, O., Larmagnac, A., and Courtine, G. (2009). Combinatory electrical and pharmacological neuroprosthetic interfaces to regain motor function after spinal cord injury. *IEEE Trans. Biomed. Eng.* 56, 2707–2711. doi: 10.1109/TBME.2009.2027226

Musienko, P., van den Brand, R., Märzendorfer, O., Roy, R. R., Gerasimenko, Y., Edgerton, V. R., et al. (2011). Controlling specific locomotor behaviors through multidimensional monoaminergic modulation of spinal circuitries. *J. Neurosci.* 31, 9264–9278. doi: 10.1523/JNEUROSCI.5796-10.2011

Musienko, P. E., Bogacheva, I. N., and Gerasimenko, I. P. (2005). Significance of peripheral feedback in stepping movement generation under epidural spinal cord stimulation. *Ross Fiziol Zh Im I M Sechenova* 91, 1407–1420.

Musienko, P. E., Bogacheva, I. N., Savochin, A. A., Kilimnik, V. A., Gorskii, O. V., Nikitin, O. A., et al. (2013). Non-invasive transcutaneous spinal cord stimulation facilitates locomotor activity in decerebrated and spinal cats. *Ross Fiziol Zh Im I M Sechenova* 99, 917–927.

Musienko, P. E., Deliagina, T. G., Gerasimenko, Y. P., Orlovsky, G. N., and Zelenin, P. V. (2014). Limb and trunk mechanisms for balance control during locomotion in quadrupeds. *J. Neurosci.* 34, 5704–5716. doi: 10.1523/JNEUROSCI.4663-13.2014

Needles, J. H. (1935). The caudal level of termination of the spinal cord in american whites and american negroes. *Anat. Rec.* 63, 417–424. doi: 10.1002/ar.1090630409C

Nicolopoulos-Stournaras, S., and Iles, J. F. (1983). Motor neuron columns in the lumbar spinal cord of the rat. *J. Comp. Neurol.* 217, 75–85. doi: 10.1002/cne.902170107

Pavlova, N. V., Bogacheva, I. N., Bazhenova, E. Yu, Gorsky, O. V., Moshonkina, T. R., and Gerasimenko, Y. P. (2019). Restoration of motor functions in spinal rats by electrical stimulation of the spinal cord and locomotor training. *Russia. J. Physiol.* 105, 565–577. doi: 10.1134/S086981391905008X

Peckham, P. H., and Knutson, J. S. (2005). Functional electrical stimulation for neuromuscular applications. *Annu. Rev. Biomed. Eng.* 7, 327–360. doi: 10.1146/annurev.bioeng.6.040803.140103

Petruska, J. C., Barker, D. F., Garraway, S. M., Trainer, R., Fransen, J. W., Seidman, P. A., et al. (2014). Organization of sensory input to the nociceptive-specific cutaneous trunk muscle reflex in rat, an effective experimental system for examining nociception and plasticity. *J. Compar. Neurol.* 522, 1048–1071. doi: 10.1002/cne.23461

Powell, E. S., Carrico, C., Raithatha, R., Salyers, E., Ward, A., and Sawaki, L. (2016). Transvertebral direct current stimulation paired with locomotor training in chronic spinal cord injury: a case study. *Neurorehabilitation* 38, 27–35. doi: 10.3233/NRE-151292

Press, W. H., Teukolsky, S. A., Vetterling, W. T., and Flannery, B. P. (1992). *Numerical Recipes in C: the Art of Scientific Computing*, 2nd Edn, Cambrigde: Cambrigde University Press.

Redett, R., Jari, R., Crawford, T., Chen, Y., Rohde, C., and Brushart, T. (2005). Peripheral pathways regulate motoneuron collateral dynamics. *J. Neurosci.* 25, 9406–9412. doi: 10.1523/JNEUROSCI.3105-05.2005

Rivero-Melián, C., and Grant, G. (1990). Distribution of lumbar dorsal root fibers in the lower thoracic and lumbosacral spinal cord of the rat studied with choleragenoid horseradish peroxidase conjugate. *J. Comp. Neurol.* 299, 470–481. doi: 10.1002/cne.902990407

Romanes, G. L. (1951). The motor cell columns of the lumbo-sacral spinal cord of the cat. *J. Comp. Neurol.* 94, 313–363. doi: 10.1002/cne.900940209

Roy, F. D., Gibson, G., and Stein, R. B. (2012). Effect of percutaneous stimulation at different spinal levels on the activation of sensory and motor roots. *Exp. Brain Res.* 223, 281–289. doi: 10.1007/s00221-012-3258-6

Sayenko, D. G., Atkinson, D. A., Floyd, T. C., Gorodnichev, R. M., Moshonkina, T. R., Harkema, S. J., et al. (2015). Effects of paired transcutaneous electrical stimulation delivered at single and dual sites over lumbosacral spinal cord. *Neurosci. Lett.* 609, 229–234. doi: 10.1016/j.neulet.2015.10.005

Schmidt, R. A., Bruschini, H., and Tanagho, E. A. (1978). Feasibility of inducing micturition through chronic stimulation of sacral roots. *Urology* 12, 471–477. doi: 10.1016/0090-4295(78)90309-6

Shapkova, E. Y. (2004). "Spinal locomotor capability revealed by electrical stimulation of the lumbar enlargement in paraplegic patients," in *Progress in Motor Control*, eds M. Latash and M. Levin (Champaign, IL: Human Kinetics), 253–289.

Shkorbatova, P. Y., Lyakhovetskii, V. A., Merkulyeva, N. S., Veshchitskii, A. A., Bazhenova, E. Y., Laurens, J., et al. (2019). Prediction algorithm of the cat spinal

segments lengths and positions in relation to the vertebrae. *Anat. Rec.* 302, 1628–1637. doi: 10.1002/ar.24054

Siegel, M. I. (1970). The tail, locomotion and balance in mice. *Am. J Phys. Anthropol.* 33, 101–102. doi: 10.1002/ajpa.1330330113

Somers, D. L., and Clemente, F. R. (2006). Transcutaneous electrical nerve stimulation for the management of neuropathic pain: the effects of frequency and electrode position on prevention of allodynia in a rat model of complex regional pain syndrome type II. *Phys. Ther.* 86, 698–709. doi: 10.1093/ptj/86.5.698

Takahashi, Y., Aoki, Y., Douya, H., Ohtori, S., and Kazuhisa, T. (2006). Projection field of primary afferent fibers innervating the ventral portion of the lumbar intervertebral disc in the spinal cord dorsal horn. *Anat. Sci. Int.* 81, 92–99. doi: 10.1111/j.1447-073X.2006.00137.x

Takahashi, Y., Aoki, Y., and Doya, H. (2007). Segmental somatotopic organization of cutaneous afferent fibers in the lumbar spinal cord dorsal horn in rats. *Anat. Sci. Int.* 82, 24–30. doi: 10.1111/j.1447-073x.2006.00164.x

Takahashi, Y., Chiba, T., Kurokawa, M., and Aoki, Y. (2003). Stereoscopic structure of sensory nerve fibers in the lumbar spine and related tissues. *Spine* 28, 871–880. doi: 10.1097/01.BRS.0000058717.43888.B9

Takahashi, Y., Ohtori, S., and Takahashi, K. (2010). Somatotopic organization of lumbar muscle-innervating neurons in the ventral horn of the rat spinal cord. *J. Anat.* 216, 489–495. doi: 10.1111/j.1469-7580.2009.01203.x

Tani, M., Kida, M. Y., and Akita, K. (1994). Relationship between the arrangement of motoneuron pools in the ventral horn and ramification pattern of the spinal nerve innervating trunk muscles in the cat (*Felis domestica*). *Exp. Neurol.* 128, 290–300. doi: 10.1006/exnr.1994.1139

Theriault, E., and Diamond, J. (1988). Intrinsic organization of the rat cutaneus trunci motor nucleus. *J. Neurophysiol.* 60, 463–477. doi: 10.1152/jn.1988.60.2.463

Toleikis, J. R., Skelly, J. P., Carlvin, A. O., Toleikis, S. C., Bernard, T. N., Burkus, J. K., et al. (2000). The usefulness of electrical stimulation for assessing pedicle screw placements. *J. Spinal Disord.* 13, 283–289. doi: 10.1097/00002517-200008000-00003

Vanderhorst, V. G., and Holstege, G. (1997). Organization of lumbosacral motoneuronal cell groups innervating hindlimb, pelvic floor, and axial muscles in the cat. *J. Comp. Neurol.* 382, 46–76. doi: 10.1002/(sici)1096-9861(19970526)382:1<46::aid-cne4>3.0.co;2-k

Wagner, F. B., Mignardot, J., Le Goff-Mignardot, C. G., Prior, J., Schurch, B., Rowald, A., et al. (2018). Targeted neurotechnology restores walking in humans with spinal cord injury. *Nature* 563, 65–71. doi: 10.1038/s41586-018-0649-2

Watson, C., Paxinos, G., and Kayalioglu, G. (2009). *The Spinal Cord*. Amsterdam: Elsevier.

Wenger, N., Moraud, E. M., Gandar, J., Musienko, P., Capogrosso, M., Baud, L., et al. (2016). Spatiotemporal neuromodulation therapies engaging muscle synergies improve motor control after spinal cord injury. *Nat. Med.* 22, 138–145. doi: 10.1038/nm.4025

Wenger, N., Moraud, E. M., Raspopovic, S., Bonizzato, M., Di Giovanna, J., Musienko, P., et al. (2014). Closed-loop neuromodulation of spinal sensorimotor circuits controls refined locomotion after complete spinal cord injury. *Sci. Transl. Med.* 6:255ra133. doi: 10.1126/scitranslmed.3008325

Wilson-Holden, T. J., Padberg, A. M., Parkinson, J. D., Bridwell, K. H., Lenke, L. G., and Bassett, G. S. (2000). A prospective comparison of neurogenic mixed evoked potential stimulation methods: utility of epidural elicitation during posterior spinal surgery. *Spine* 25, 2364–2371. doi: 10.1097/00007632-200009150-00016

Zhong, H., Zhu, C., Minegishi, Y., Richter, F., Zdunowski, S., Roy, R. R., et al. (2019). Epidural spinal cord stimulation improves motor function in rats with chemically induced parkinsonism. *Neurorehabil. Neural Repair.* 33, 1029–1039. doi: 10.1177/1545968319876891

Zhu, Y., Starr, A., Haldeman, S., Chu, J. K., and Sugerman, R. A. (1998). Soleus H-reflex to S1 nerve root stimulation. *Electroencephalogr. Clin. Neurophysiol.* 109, 10–14. doi: 10.1016/s0924-980x(97)00058-51

Conflict of Interest: The authors declare that the research was conducted in the absence of any commercial or financial relationships that could be construed as a potential conflict of interest.

frontiers in Systems Neuroscience

BRIEF RESEARCH REPORT
published: 15 October 2020
doi: 10.3389/fnsys.2020.571011

Prolonged Targeted Cardiovascular Epidural Stimulation Improves Immunological Molecular Profile: A Case Report in Chronic Severe Spinal Cord Injury

Ona Bloom[1,2,3], Jill M. Wecht[1,4,5], Bonnie E. Legg Ditterline[6,7], Siqi Wang[6,7], Alexander V. Ovechkin[6,7], Claudia A. Angeli[6,8], Anthony A. Arcese[2] and Susan J. Harkema[3,6,7,8]*

[1]VA RR&D National Center for the Medical Consequences of Spinal Cord Injury, James J. Peters VA Medical Center, Bronx, NY, United States, [2]Institute of Molecular Medicine, The Feinstein Institutes for Medical Research, Manhasset, NY, United States, [3]Departments of Molecular Medicine; Physical Medicine and Rehabilitation, Donald and Barbara Zucker School of Medicine at Hofstra-Northwell, Hempstead, NY, United States, [4]Department of Medicine, The Icahn School of Medicine, Mount Sinai, New York, NY, United States, [5]Rehabilitation Medicine, The Icahn School of Medicine, Mount Sinai, New York, NY, United States, [6]Kentucky Spinal Cord Injury Research Center, University of Louisville, Louisville, KY, United States, [7]Department of Neurosurgery, School of Medicine, University of Louisville, Louisville, KY, United States, [8]Department of Bioengineering, University of Louisville, Louisville, KY, United States

OPEN ACCESS

Edited by:
James W. Grau, Texas A&M University, United States

Reviewed by:
J. Russell Huie, University of California, San Francisco, United States
Veronica J. Tom, Drexel University, United States

***Correspondence:**
Ona Bloom
obloom@northwell.edu

Received: *09 June 2020*
Accepted: *09 September 2020*
Published: *15 October 2020*

Citation:
Bloom O, Wecht JM, Ditterline BEL, Wang S, Ovechkin AV, Angeli CA, Arcese AA and Harkema SJ (2020) Prolonged Targeted Cardiovascular Epidural Stimulation Improves Immunological Molecular Profile: A Case Report in Chronic Severe Spinal Cord Injury. Front. Syst. Neurosci. 14:571011. doi: 10.3389/fnsys.2020.571011

In individuals with severe spinal cord injury (SCI), the autonomic nervous system (ANS) is affected leading to cardiovascular deficits, which include significant blood pressure instability, with the prevalence of systemic hypotension and orthostatic intolerance resulting in an increased risk of stroke. Additionally, persons with SCI rostral to thoracic vertebral level 5 (T5), where sympathetic nervous system fibers exit the spinal cord and innervate the immune system, have clinically significant systemic inflammation and increased infection risk. Our recent studies show that lumbosacral spinal cord epidural stimulation (scES), applied at the lumbosacral level using targeted configurations that promote cardiovascular stability (CV-scES), can safely and effectively normalize blood pressure in persons with chronic SCI. Herein we present a case report in a female (age 27 years) with chronic clinically motor complete cervical SCI demonstrating that 97-sessions of CV-scES, which increased systemic blood pressure, improved orthostatic tolerance in association with increased cerebral blood flow velocity in the middle cerebral artery, also promoted positive immunological changes in whole-blood gene expression. Specifically, there was evidence of the down-regulation of inflammatory pathways and the up-regulation of adaptative immune pathways. The findings of this case report suggest that the autonomic effects of epidural stimulation, targeted to promote cardiovascular homeostasis, also improves immune system function, which has a significant benefit to long-term cardiovascular and immunologic health in individuals with long-standing SCI.

Clinical Trial Registration: www.ClinicalTrials.gov, identifier NCT02307565.

Keywords: spinal cord injury, epidural stimulation, neuromodulation, immune system, orthostatic hypotension, blood pressure regulation, cerebral blood flow velocity, cardiovascular regulation

INTRODUCTION

Severe cervical spinal cord injury (SCI) results in multi-organ system dysfunction that stems, in part, from impaired descending supraspinal control of the autonomic nervous system (ANS). As a result of ANS impairment, cardiovascular dysfunction is common and takes the form of blood pressure instability, which includes persistent hypotension, orthostatic hypotension, and autonomic dysreflexia. These blood pressure disorders have been implicated in an increased prevalence of cerebrovascular compromise (Saleem et al., 2018), cognitive deficits (Wecht et al., 2018), and stroke (Wu et al., 2012), which are independent of symptom reporting in the majority of individuals with SCI. It is thought that an additional consequence of ANS impairment is immune system dysfunction (Schwab et al., 2014; Herman and Bloom, 2018), which promotes systemic inflammation, and may also play a role in long-term cardiovascular morbidity and mortality following SCI.

The maladaptive reorganization of the ANS following SCI is independent of the level of injury as assessed by the International Standards for the Neurological Classification of SCI (ISNCSCI; Gimovsky et al., 1985; Currie and Krassioukov, 2015; Katzelnick et al., 2019). Although blood pressure instability appears to be more prevalent in individuals with cervical SCI (Claydon and Krassioukov, 2006; Wecht et al., 2013), it is not exclusive to this group because a critical proportion of thoracic sympathetic neurons integral to facilitating global vasomotor control are decentralized by spinal lesions occurring at or above thoracic vertebral level 1 (T1). Additionally, similar to astronauts returning from space flight (Convertino, 2009; Hargens and Richardson, 2009), blood pressure instability in individuals with SCI at any level may stem from reduced orthostatic pressure gradients due to the limited amount of time chronic wheelchair users spend in an upright standing position (Vaziri, 2003). Importantly, although most individuals with chronic cervical SCI do not report symptoms associated with cerebral hypoperfusion, mounting evidence suggests that asymptomatic daily fluctuations in blood pressure along with persistent hypotension are associated with reduced cerebral blood flow velocity in the middle cerebral artery (Phillips et al., 2014a,b, 2018; Wecht et al., 2017), and cognitive impairments (Jegede et al., 2010; Phillips et al., 2014b; Wecht et al., 2018). Individuals with SCI-induced blood pressure instability report that this condition restricts their participation in daily activities, and diminishes their independence, vitality, and quality of life (Weaver et al., 2007; Carlozzi et al., 2013).

After SCI, ANS impairment promotes immune system dysfunction *via* diminished descending supraspinal control and by damage to the sympathetic pre-ganglionic neurons that innervate immune organs at or below the thoracic level 5 (T5; Schwab et al., 2014; Herman and Bloom, 2018), which also corresponds to sympathetic neuronal innervation of cardiovascular targets. Two clinically relevant aspects of immune dysfunction after SCI are systemic inflammation and increased risk of infection. Chronic systemic inflammation, which promotes the risk of cardiovascular disease and stroke in all populations, is present in more than 75% of individuals living with SCI (Nash et al., 2016; Bloom et al., 2020) and is highest in individuals with the greatest neurological dysfunction and the least mobility (Morse et al., 2008; Bloom et al., 2020). Individuals with the greatest neurological dysfunction have the greatest risk for infection, and recent studies have demonstrated that the number of infections during the first year after injury correlates inversely with neurological recovery in individuals with cervical SCI (Failli et al., 2012; Brommer et al., 2016; Nash et al., 2016; Bloom et al., 2020). To better understand the molecular mechanisms contributing to increased systemic inflammation and infection risk after SCI, we recently analyzed gene expression changes in whole blood from individuals with chronic (>12-months post-injury) SCI and discovered broad upregulation of pro-inflammatory genes, in particular the Toll-like Receptor (TLR) pathway, a key signaling pathway for pathogen recognition and subsequent activation of innate immunity (Herman and Bloom, 2018; Herman et al., 2018). Also, we discovered the decreased expression of genes from natural killer (NK) cells, which are well-understood to be critical for fighting viral infections. Both of these molecular observations are significantly pronounced in individuals with SCI rostral to T5.

Recent findings that describe the use of targeted lumbosacral epidural stimulation to restore cardiovascular homeostasis (CV-scES) in individuals with chronic SCI indicate blood pressure can be immediately stabilized within a normotensive range for prolonged periods. Moreover, even when tested without active stimulation, the improved blood pressure regulation persists, and orthostatic hypotension is alleviated after 80-sessions of 2-h per day stimulation in a home setting (Harkema et al., 2018). Active epidural stimulation in the T11-L1 region in an individual with chronic C5, motor complete SCI has been reported to increase cerebral blood flow velocity during head-up tilt (West et al., 2018); however, the effects of a prolonged CV-scES intervention on cerebral blood flow velocity during a head-up tilt maneuver have not been reported. We explored here the effects of a prolonged CV-scES intervention on blood pressure and cerebral blood flow regulation and hypothesized that improved ANS function may also positively impact the immune system. The goals of this case study were to determine the effects of targeted CV-scES on orthostatic blood pressure and cerebral blood flow velocity responses during a head-up tilt maneuver and associated changes in whole blood gene expression in an individual with severe, chronic, cervical SCI.

MATERIALS AND METHODS

One individual (female, 26.9 years old, 3.1 years from initial SCI) with chronic cervical motor-complete (C4, AIS grade A) SCI who presented with significant cardiovascular dysfunction was implanted with a 16-electrode array epidural stimulator (RestoreAdvanced, Medtronic) on the dura between spinal segments L1–S1 at the T11-L1 vertebral level (**Figure 1**). Parameters for CV-scES, including electrode polarity, frequency, and pulse width (**Figure 1**), were optimized to maintain systolic blood pressure within a normative range of 110–120 mmHg (**Figure 1**) without eliciting lower extremity or core muscle activation (**Figure 1**). The participant was instructed to use

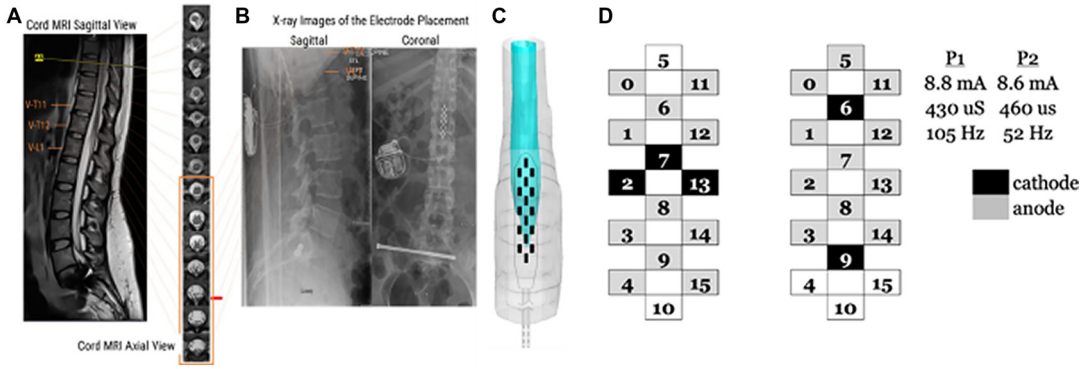

FIGURE 1 | Site of implantation of the electrode array and stimulating configuration for cardiovascular stability-spinal cord epidural stimulation (CV-scES). **(A)** Sagittal and Axial MRI sections of the lumbosacral cord were used to calculate the cross-sectional area of the spinal cord and cerebrospinal fluid to create a 3-D reconstruction of the spinal cord at the lumbosacral enlargement. **(B)** Sagittal x-rays indicating the final placement of the electrode array. **(C)** 3-D reconstruction of the electrode array relative to the lumbosacral enlargement. **(D)** Graphical representation of electrode configuration for CV-scES, configuration uses two programs (P1 and P2) running concurrently. Cathodes are represented in black and anodes in gray. Each program runs with an independent stimulating amplitude, pulse width, and frequency.

this electrode configuration at home throughout 97-sessions. Hemodynamic and immunological data were obtained before (pre) and after (post) the CV-scES intervention *without* active use of the stimulator during data collection. Data for the pre-CV-scES intervention were obtained before surgery. Data for the post-CV-scES intervention were obtained at least 24-h after the last stimulation session.

Medical History

The individual sustained a cervical SCI from a motor vehicle accident at 24 years of age. Hardware was implanted to fuse the C6 vertebrae after initial SCI and was later revised due to the hardware-related infection. Medication history before study enrollment included Gabapentin for neurological pain, Oxybutynin Chloride for neurogenic bladder, and Methenamine Hippurate for prophylactic urinary tract infection prevention; the individual was gradually weaned from Gabapentin before surgery with guidance from her physiatrist but was allowed to continue the use of Oxybutynin Chloride and Methenamine Hippurate. In her medical history, the individual reported antibiotic treatment for recurrent urinary tract infections, that occurred at an average rate of ten times per year. There was no history of cardiovascular or pulmonary disease unrelated to SCI, but she reported persistent low blood pressure, episodic orthostatic hypotension, and decreased respiratory functional performance. Three months post-surgery and after only 12 CV-scES training sessions, the individual was struck by an oncoming car and sustained an intertrochanteric fracture of the left femur; after which, participation in the research study was placed on medical hold. The femur fracture was surgically repaired with an intramedullary Gamma nail and hip screw. The individual was an inpatient for a total of 14 days and was discharged to a rehabilitation hospital with recommendations to add Eliquis to her daily medications after developing a pulmonary embolism after surgery. At the rehabilitation hospital, the individual participated in standard physical and occupational therapy, including bed mobility, upright sitting, and upper extremity exercises. After 15 days as an inpatient at the rehabilitation hospital, the individual expressed interest in continuing in the research study. After medical clearance by her physiatrist, the study-physician, and the Data Safety Monitoring Board, the individual resumed study participation 53-days after the accident occurred.

Hemodynamic Data Acquisition

Hemodynamic assessments were recorded in the morning in a quiet, temperature-controlled room. The participant was instructed to avoid consuming caffeine, alcohol, and nicotine products for at least 12-h and asked to empty her bladder upon arrival. Instrumentation was applied supine and included a three-lead ECG (Finapres Medical Systems, Amsterdam, Netherlands); beat-to-beat blood pressure recorded from the index finger, middle finger, or thumb using photoplethysmography (Finapres Medical Systems, Amsterdam, Netherlands); and transcranial Doppler (TCD) ultrasound of the middle cerebral artery (Terumo Cardiovascular Systems 1311 Valencia Avenue Tustin, CA 92780-6447, USA). Brachial blood pressure was recorded (GE Healthcare, Milwaukee, WI, USA) to calibrate beat-to-beat blood pressure offline (Bos et al., 1996).

The middle cerebral artery was insonated through the left temporal window at a frequency of 2.0 MHz. The middle cerebral artery was identified by the target depth (45–55 mm), sound and direction of flow (i.e., towards the probe), the characteristic spectral waveform, and relatively faster flow velocity compared with surrounding cerebral vessels. Once the middle cerebral artery was visualized, probe placement was secured for the duration of testing using a head-harness. Data output from the TCD was monitored in real-time and included systolic flow velocity, diastolic flow velocity, and mean flow velocities, recorded in centimeters per second (cm/s); quality control for TCD recordings was implemented by identifying a clear

waveform, characterized by an upstroke to systolic peak and gradual decline to diastolic trough.

Acute orthostatic stress was induced with a passive, head-up tilt to 70° using a Hi-Lo Tilt Table (Hausman Industries, Inc., Northvale, NJ, USA). The individual was strapped to the bed at the tibial tuberosity, iliac crest, and below the axilla with her feet against the footplate. The individual rested quietly for 5 min in the supine position and then the bed was tilted to 70°, during which time blood pressure, ECG, and cerebral blood flow velocity were recorded continuously. The individual remained in the head-up tilt position for 30-min or until symptom-limited, in which case the test was immediately terminated. The head-up tilt test was performed before implantation and after 97-sessions of the CV-scES intervention; both assessments were performed without active CV-scES.

Hemodynamic Data analysis

Digitized blood pressure and heart rate signals were analyzed with a custom program (MATLAB, The Mathworks, Natick, MA, USA) that performed R-peak detection of ECG, and peak and trough detection of the blood pressure waveform. Systemic mean arterial pressure (MAP) was calculated from the finger waveform as [systolic blood pressure + (2*diastolic blood pressure)]/3. Flow velocities of the middle cerebral artery were analyzed offline using a custom program written with LabVIEW graphical software (National Instruments, Austin TX, USA). Cerebral mean arterial pressure (cMAP) was estimated as the difference between systemic MAP and the hydrostatic pressure gradient calculated between the heart and the head (i.e., 17.8 mmHg). Mean cerebral blood flow velocity (mCBFv) was calculated from the integrated TCD signal over each cardiac cycle. The cerebrovascular conductance index was calculated as mCBFv/cMAP; cerebral autoregulatory function was estimated as the correlation coefficient between mCBFv and cMAP.

Immunological Acquisition and Analysis

Blood for gene expression analysis was drawn from a butterfly catheter inserted into an antecubital vein pre and post-CV-scES intervention. Up to 8 ml of whole blood were collected in PAXgene tubes and stored at −20°C until analysis. Total RNA was isolated by QIAcube, using the manufacturer's protocol (Qiagen, Venlo, Netherlands). RNA quality was determined on the Agilent Bioanalyzer, mRNA-Seq libraries were prepared (Illumina TruSeq Stranded Total RNA with RiboZero Globin, Catalog #20020612) and 100 bp paired-end reads were collected on the Illumina HiSeq 2500 platform (Yale Center for Genome Analysis). Using Partek Genomics Flow software (St. Louis, MO, USA), trimmed reads were aligned using STAR to the human genome (hg38 genome assembly), filtered for expression >50, normalized using the Trimmed Mean of *M*-values (TMM) method using the edgeR package embedded in Partek Genomics, and log2 transformed. For an initial comparison with a sample size of convenience, mRNA-Seq libraries were also prepared from three able-bodied individuals (N = 2 males, one female; ages 63, 64, and 66, respectively). Transcripts that were differentially expressed according to the between or within-participant(s) comparisons described below were identified with a fold change greater than 1.5, using the step-up method of the Benjamini–Hochberg method to correct p values with a false discovery rate (FDR) = 0.05 (Partek Genomics Flow). Principal components analysis (PCA) was performed using default parameters for the determination of the component number, with all components contributing equally (Partek Genomics Flow). Component loadings for each comparison examined can be found in **Supplementary Table 1**. For functional analysis of differentially expressed genes, if multiple transcripts for the same gene symbol were differentially expressed, then the transcript with the lowest p-value for that gene symbol by were included for further analyses. Lists of differentially expressed genes for each comparison examined can be found in **Supplementary Table 1**.

For functional analysis of differentially expressed genes, if multiple transcripts or RNA sequences for the same gene were differentially expressed, then the transcript with the lowest significant p-value was selected for directionality and further analyses.

Individual differentially expressed genes of interest are described below. Functional analysis of all differentially expressed genes (using unique gene symbols) in a particular comparison was performed using Enrichr (Chen et al., 2013), as we have done previously (Herman et al., 2018) to compare samples from able-bodied with samples from individuals with SCI (obtained before scES intervention), and within this research study to compare samples obtained pre and post-CV-scES intervention. Enrichr is an online platform that hosts independent gene-set libraries, or bioinformatics tools, that can be used to analyze functions of differentially expressed genes based on published scientific literature and publicly available data sets (Chen et al., 2013). Broadly speaking, the tools are divided into categories that characterize the function(s) of genes queried according to their known roles in signaling pathways, gene ontologies (GO; Ashburner et al., 2000; Carbon et al., 2019), cell types, or other functions such as transcription factors. While each bioinformatics tool may vary concerning specific naming of individual categories of enriched genes, biological meaning can be inferred when there is a thematic agreement across multiple independent platforms.

RESULTS

Hemodynamic Data

Application of 97-sessions of CV-scES targeted to increase systolic blood pressure resulted in substantially improved cardiovascular and cerebrovascular responses during the head-up tilt maneuver. Orthostatic tolerance to 70° head-up tilt improved dramatically: from 10-min pre-CV-scES intervention to the full 30-min post-CV-scES intervention. Compared to pre-CV-scES intervention, improved orthostatic tolerance during head-up tilt post-CV-scES intervention was associated with increased cMAP (from 48.1 ± 13.3 to 51.8 ± 14.6 mmHg, respectively; **Figure 2A**) and increased mCBFv (from 28.0 ± 3.8 to 30.5 ± 3.2 cm/s, respectively; **Figure 2B**). Indeed, the slope of the relationship between cMAP and mCBFv pre CV-scES

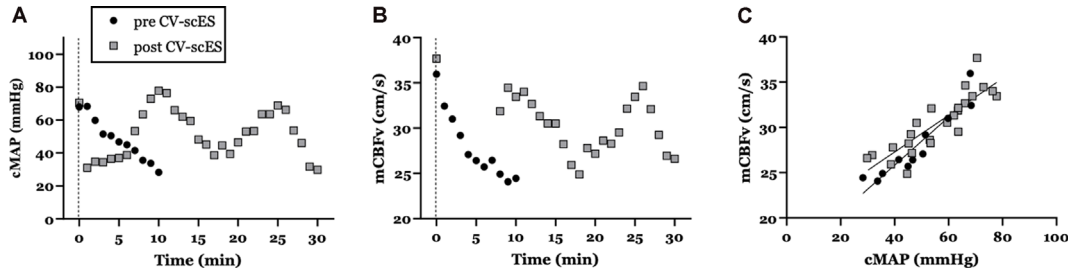

FIGURE 2 | Mean arterial pressure (MAP) and cerebral blood flow during the orthostatic challenge are improved with CV-scES. **(A)** Cerebral mean arterial pressure (cMAP), **(B)** mean cerebral blood flow (mCBFv) during the head-up tilt maneuver, and **(C)** relationship between cMAP and mCBFv pre CV-scES (black circles) and post CV-scES (gray squares). Note that the participant was only able to tolerate 10-min in the 70° head-up tilt position pre-CV-scES, but was able to tolerate 30-min post-CV-scES.

intervention (0.32 $cm^*s^{-1}*mmHg^{-1}$) was decreased compared with post CV-scES intervention (0.16 $cm^*s^{-1}*mmHg^{-1}$; **Figure 2C**). Changes to blood pressure while resting were minimal (pre-CV-scES: 112 ± 2.3/73 ± 2.3 mmHg; post-CV-scES: 114 ± 2.6/75 ± 1.6 mmHg).

Immunological Results and Discussion

We first analyzed major variations in whole blood gene expression in blood obtained pre CV-scES intervention from the individual with chronic SCI compared with able-bodied (AB) individuals. This is illustrated by principal component analysis (**Figure 3A**, **Supplementary Table 1**), where the first component explained 61.88% of the total variation in gene expression. Compared to uninjured individuals, in the sample obtained from the individual with SCI before CV-scES intervention, there were a total of 4019 differentially expressed unique genes (FDR = 0.05). Of these, there were 1,535 up- and 2,485 down-regulated genes in the individual with chronic SCI compared with able-bodied (AB) data (**Figure 3B**). We used multiple independent bioinformatics platforms to identify common functional themes among pathways enriched in the genes differentially expressed in the individual with SCI after usual care compared to the AB data. Interestingly, multiple bioinformatics platforms identified downregulated pathways that were related to adaptive immunity, antigen processing, and presentation, which is consistent with a clinical phenotype of immunosuppression (**Figure 3C**). By platform, these were: REACTOME = adaptive immune system (R-HSA-1280218), WIKI = B cell receptor signaling pathway (WP23), NCI-Nature = IL2-mediated signaling events (a2a1883c-6193-11e5-8ac5-06603eb7f303), KEGG = antigen processing and presentation, Panther = T cell activation (P00053), BioCarta = role of MEFD in T-cell Apoptosis. The Gene Ontology (GO) platform (Ashburner et al., 2000; Carbon et al., 2019), which categorizes known functions of biological molecules by drawing on data from many species, was used to analyze the enrichment of differentially expressed genes using the Biological Process ontology, which describes how genes contribute to multiple biological processes (geneontology.org). highlighted regulation of gene expression related to T cell receptor signaling (GO: 0050852), as enriched among downregulated transcripts. GO analysis using the Molecular Function platform, which describes gene-related activities at the molecular level, highlighted MHCII protein complex binding (GO: 0023026), which is part of the antigen presentation molecular machinery, as enriched among downregulated transcripts. Interestingly, cellular level analysis using the ARCHS4 tissues platform also identified the downregulation of genes enriched in NK Cells (2.45-Log10 *p*-value) of the innate immune system, which are critical for maintaining anti-viral immunity (**Figure 3D**). The Human Gene Atlas independently identified downregulated genes as highly enriched for CD56+ NK Cells transcripts (20.10, −Log10 *p*-value; **Figure 3D**). Multiple bioinformatics platforms identified pathways enriched among upregulated genes that were related to both eukaryote and viral transcription and translation, as well as cell cycle genes and pro-inflammatory genes (**Figure 3E**). By platform, these included: REACTOME = viral mRNA Translation (R-HSA-192823), WIKI = cytoplasmic ribosomal proteins (WP477), NCI-Nature = signaling events mediated by focal adhesion kinase (8fb80085-6195-11e5-8ac5-06603eb7f303), KEGG = Ribosome, Panther = *De novo* pyrimidine deoxynucleotide synthesis (P02739), BioCarta = Cyclin E destruction pathway. Gene Ontology (GO) analysis using the Biological Process platform highlighted viral gene expression (GO: 00190980), as enriched among downregulated transcripts. GO analysis using the Molecular Function platform highlighted RNA binding (GO: 0003723), which part of the antigen presentation machinery, as enriched among downregulated transcripts. Cellular level analysis using the ARCHS4 tissues platform also identified the upregulation of genes enriched in blood dendritic cells (**Figure 3F**), which are highly potent antigen-presenting cells that link the innate and adaptive immune system. The Human Gene Atlas identified upregulated genes as highly enriched for CD71+ (transferrin receptor) early erythroid progenitors (**Figure 4F**) and CD105+ endothelial cells (5.12 −Log10 *p*-value), among others.

We next analyzed changes in gene expression in the participant with SCI in response to CV-scES. After 97-sessions daily CV-scES, interestingly, 397 differentially expressed genes were observed compared with pre-CV-scES intervention, with 50 upregulated and 347 downregulated unique gene symbols (**Figures 4A,B**). At the gene level, several key pro-inflammatory genes of interest were downregulated, such as members of

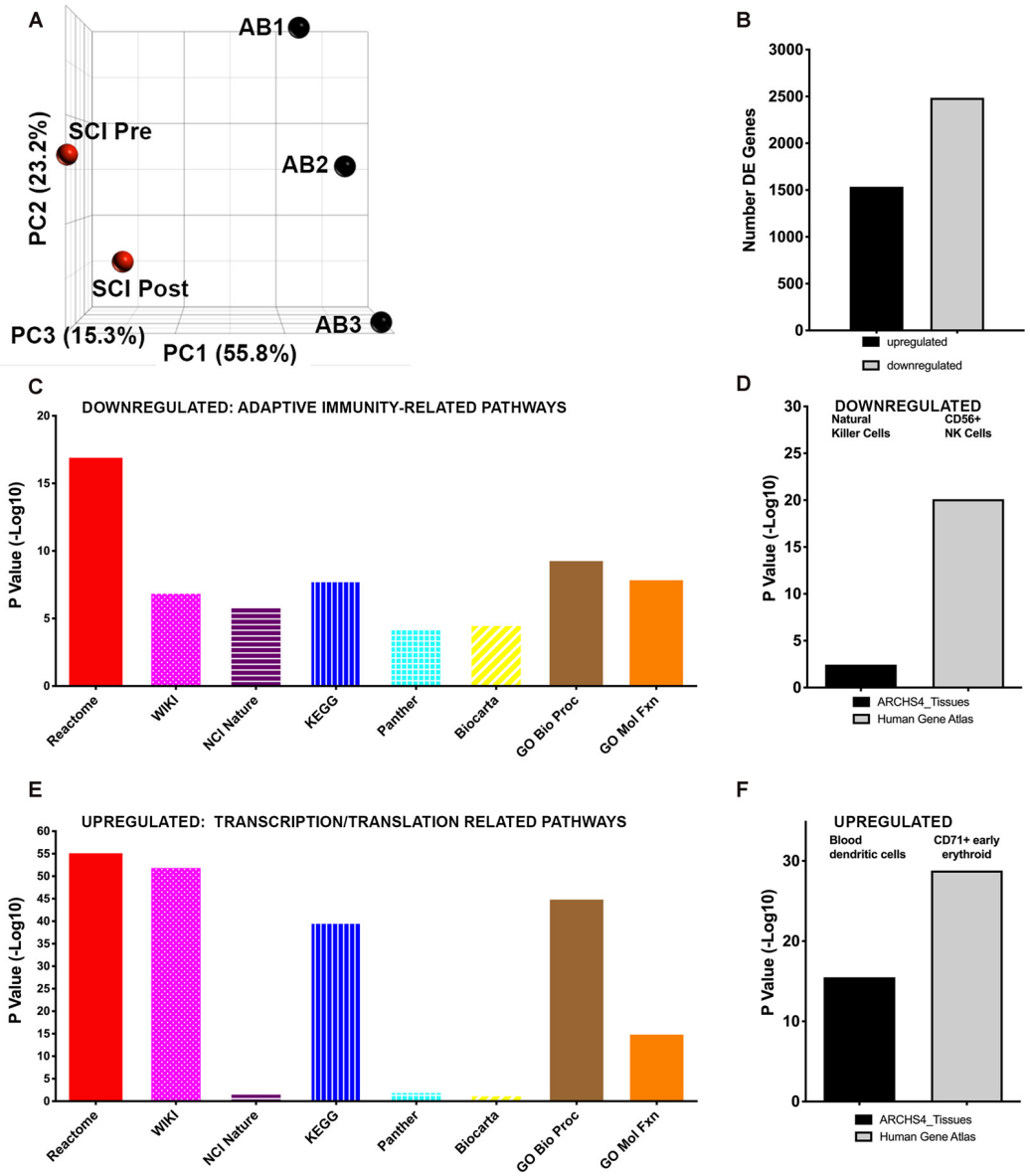

FIGURE 3 | Whole blood gene expression is profoundly changed in an individual with spinal cord injury (SCI) compared with able-bodied (AB) individuals. **(A)** Principal component analysis (PCA) shows patterns of gene expression. Black symbols represent data obtained from three AB individuals, each sampled once. Red symbols represent data obtained from the individual with chronic SCI, pre and post CVscES intervention. PCA gene expression in the individual with SCI is similar pre- and post-intervention along the *Y*-axis (PC2) and *X*-axis (PC1), but is different on the *Z*-axis (PC3) axis. **(B)** The number of differentially expressed genes (up- or down-regulated) is shown. **(C)** Downregulated genes: multiple bioinformatics platforms independently identified pathways enriched following usual care in the participant with SCI, which are related to adaptive immunity. **(D)** Two cell type bioinformatics platforms identified natural killer (NK) cell genes enriched among downregulated genes. **(E)** Upregulated genes: multiple bioinformatics platforms independently identified pathways enriched following usual care in the participant with SCI that are related to viral and eukaryotic transcription and translation. **(F)** Two cell type bioinformatics platforms identified dendritic cells and CD71+ early erythroid progenitor cells genes enriched among upregulated genes.

the MAP kinase family, TLRs-1, 2, and 4, and LY96, which interacts with TLR4 (**Figure 4A**). As with the analysis above, we used several independent bioinformatics platforms to identify pathways of genes that were differentially expressed post-CV-scES intervention compared with pre-CV-scES intervention within the individual with SCI. Interestingly, multiple bioinformatics platforms identified downregulated pathways related to the pro-inflammatory TLR signaling, which is critical for pathogen sensing by the innate immune system (**Figure 4C**). By platform, these were: REACTOME = Activated TLR signaling (R-HSA-166054), WIKI = SCI pathway (WP2431), NCI-Nature = endogenous TLR signaling (d8777e16-6191-11e5-8ac5-06603eb7f303), KEGG = tuberculosis, Panther = Toll receptor signaling pathway (P00054), BioCarta = Toll-like

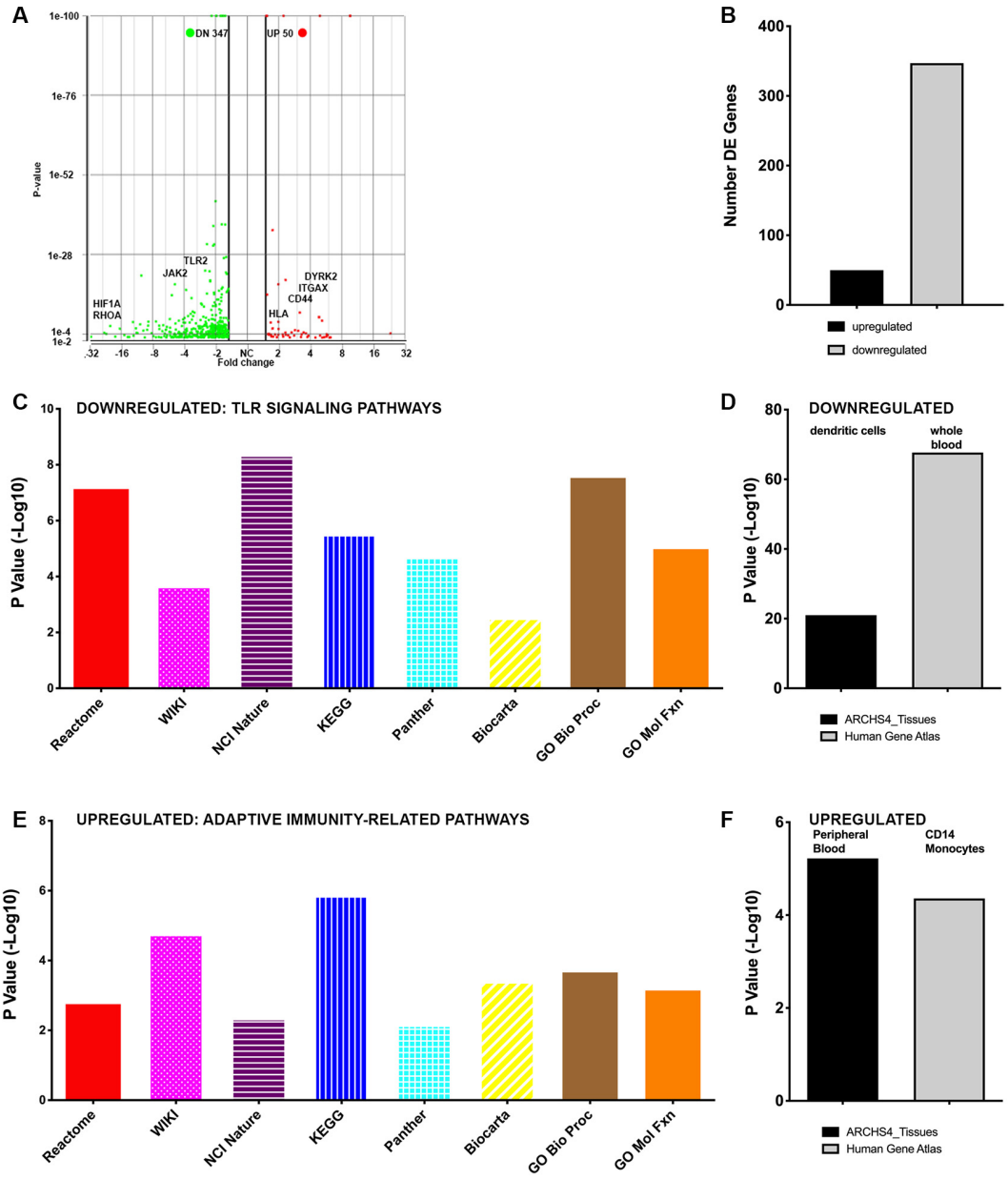

FIGURE 4 | Whole blood gene expression is profoundly changed within an individual with SCI after 80 sessions of CV scES. **(A)** The volcano plot shows several differentially expressed genes within the participant following 97-sessions of CV-scES. Downregulated genes (green) include pro-inflammatory genes of interest, such as JAK2, RHOA, and toll-like receptors (TLRs). Upregulated genes (red) include genes of interest related to adaptive immunity, e.g., CD44 and HLA related molecules (MHCI and MHCII). **(B)** The numbers of differentially expressed genes are shown. **(C)** Downregulated genes: multiple bioinformatics platforms independently identified pathways related to pro-inflammatory TLR signaling. **(D)** Cell type bioinformatics platforms identified whole blood and dendritic cells enriched among downregulated genes. **(E)** Upregulated genes: multiple bioinformatics platforms independently identified pathways related to adaptive immunity. **(F)** Two cell type bioinformatics platforms identified peripheral blood and CD14+ monocytes enriched among upregulated genes.

receptor pathway. Gene Ontology (GO) analysis using the Biological Process platform highlighted TLR signaling (GO: 0002224), as enriched among downregulated transcripts. GO analysis using the Molecular Function platform also highlighted TLR binding (GO: 003525), as enriched among downregulated transcripts. Also, cellular components analysis using the ARCHS4 tissues platform identified the downregulation of genes enriched in the potent antigen-presenting cells, dendritic cells (21.00 −Log10 *p*-value;). The Human Gene Atlas identified downregulated genes as highly enriched for whole blood transcripts (67.7, −Log10 *p*-value; **Figure 4D**). Multiple bioinformatics platforms identified pathways enriched among

upregulated genes that were related to adaptive immunity, including antigen processing and presentation (**Figure 4E**). By platform, these included: REACTOME = antigen presentation: folding, assembly and peptide loading of class I MHC (R-HSA-983170), WIKI = ebola virus pathway on the host (WP4217) which included the class I and II MHC molecules HLA-A, HLA-B and HLA-DR, NCI-Nature = integrin signaling (5d4f90b6-6188-11e5-8ac5-06603eb7f303), KEGG = antigen processing and presentation, Panther = integrin signaling pathway (P00034), BioCarta = antigen processing and presentation. GO analysis using the Biological Process platform highlighted the upregulation of gene expression related to antigen processing and presentation *via* MHCI (GO:0002480). GO analysis using the Molecular Function platform also highlighted antigen presentation *via* MHCII (GO: 0023026), as enriched among upregulated transcripts. Cellular components analysis using the ARCHS4 tissues platform also identified the upregulation of genes enriched in peripheral blood (**Figure 4F**), among others. The Human Gene Atlas identified upregulated genes as highly enriched in CD14+ monocytes, among others (**Figure 4F**). GO analysis using the Biological Process platform highlighted regulation of gene expression and cellular response to lipopolysaccharide (GO: 0071222), a major ligand for TLR4, as enriched among downregulated transcripts.

Self-reported Results

Following 97-sessions of the CV-scES intervention, the participant reported that her blood pressure no longer fell precipitously during daily activities and, as a result, her health and feelings of vitality improved. Because her blood pressure is stable and closer to a normotensive range, she reports that she has gained confidence, independence, and autonomy, allowing her to: participate in in social gatherings with friends and dating; return to college to finish a degree she started pre-injury; and feel a stronger connection within the community. Simple activities of daily life that previously required assistance have become a part of her daily routine, including brushing her teeth or her hair, washing alone in the shower, and applying her makeup without having to take breaks. Importantly, the participant was an avid singer before her accident, and she reports that she has regained the cardiovascular strength and stamina to allow her to return to singing loudly and to carry notes for an extended period. Finally, the participant reports significantly improved health such that she no longer feels "sick" and reported significantly reduced hospital and doctor's office visits for upper respiratory and urinary tract infections. Before the implant, the participant reported an annual incidence of ten urinary tract infections. In the 18 months, the individual has been using the stimulator, she has been diagnosed with and treated for three urinary tract infections without a change to her bladder maintenance program.

DISCUSSION

Findings of the current case report demonstrate that prolonged, targeted CV-scES intervention leads to improved blood pressure regulation, increased orthostatic tolerance, and improved cMAP and mCBFv responses during a head-up tilt maneuver even when assessed without stimulation during testing. There was also a reduction in the slope of the relationship cMAP and mCBFv during head-up tilt, suggesting improved cerebral autoregulation post-CV-scES intervention. Further, after the CV-scES intervention, genes related to adaptive immunity were upregulated, while genes related to TLR signaling were downregulated across multiple bioinformatics platforms, which would be consistent with improved immunity and reduced systemic inflammation, respectively. These improvements that persist post-CV-scES intervention without active stimulation suggest daily use of targeted CV-scES has a beneficial impact on multiple organ systems that are regulated by the ANS.

Spinal cord epidural stimulation has a long history for use in treating pain beginning in the 1960s (Shealy et al., 1967), which was FDA-approved in 1989, and has been shown to improve microvascular circulation in peripheral vascular disease (Jacobs et al., 1988). Epidural stimulation of the lumbosacral motor circuitry has been studied experimentally in animals (Gerasimenko, 2002) as well as in humans for spasticity and to understand network circuitry for locomotion following SCI (Dimitrijevic et al., 1998; Hargens and Richardson, 2009; Harkema et al., 2016; Grahn et al., 2017; Rejc et al., 2017a,b; Angeli et al., 2018). This approach takes advantage of sophisticated spinal networks below the level of injury to unexpectedly reactivate spared pathways, restoring supraspinal connectivity and resulting in functional recovery in those initially diagnosed clinically as motor complete (Rejc et al., 2017b, Calvert et al., 2019).

Investigators recently discovered that specific cardiovascular-targeted scES configurations (CV-scES, L1-S4/5 spinal cord), that did not elicit motor activity in individuals with SCI who report cardiovascular dysfunction, could increase and stabilize orthostatic blood pressure during the orthostatic challenge (Harkema et al., 2018; West et al., 2018; Darrow et al., 2019), and mitigate symptoms reporting associated with orthostatic intolerance. An interesting and novel finding from these studies was that orthostatic blood pressure was maintained after 80-sessions of CV-scES in 4 participants with chronic severe motor complete SCI, even with the stimulator turned off, which suggests that targeted CV-scES may facilitate adaptive neuroplasticity to restore endogenous ANS function (Harkema et al., 2018). Two recent case studies confirm the cardiovascular autonomic benefits following a single session of targeted scES in response to an orthostatic challenge (West et al., 2018; Darrow et al., 2019). Furthermore, improvement in cerebral blood flow velocity and cognitive function was reported during a 70° head-up tilt maneuver in a female participant with cardiovascular deficits in response to epidural stimulation of the thoracolumbar cord.

Profiling of whole blood gene expression in this individual pre-CV-scES intervention demonstrated molecular signatures consistent with reduced adaptive immune responses, as we saw previously in a larger cohort of individuals with chronic SCI (N = 31) vs. able-bodied persons (N = 26; Herman et al., 2018). For example, multiple pathway

analysis platforms identified genes related to T and B cell receptor signaling, required for antigen processing and presentation, as downregulated compared with able-bodied persons. Two independent cell type platforms identified genes enriched in NK cells, which are critical for killing virally infected cells, as downregulated, as well as general PBMC genes and other T and B cell genes. These findings of downregulated genes are consistent with a clinical phenotype of increased infection susceptibility. Pre CV-scES intervention, genes that were upregulated compared with able-bodied persons were related to eukaryotic and viral transcription and translation. In contrast, within the individual with SCI post-CV-scES intervention, genes related to adaptive immunity were upregulated across multiple bioinformatics platforms, which would be consistent with improved immunity. Interestingly, after CV-scES, downregulated genes were related to TLR signaling, a pathway that is critical for pathogen sensing by the innate immune system and promotes inflammation, which we previously identified as upregulated in individuals with chronic SCI (Herman et al., 2018). This would be consistent with reduced systemic inflammation.

There are several limitations to this proof-of-concept case report, including this is a report of effects in a single individual and therefore need to be validated in studies with a larger number of patients, the longer-term duration of effects is unknown, the optimal stimulation parameters for immune-related responses is unknown, and there may be unknown potential confounders that influence the observed effects. While defining the mechanisms that underlie this immune response to targeted epidural stimulation is beyond the scope of this case-report, this should be explored in future studies. Several pre-clinical studies in SCI have shown that an intact sympathetic nervous system is critical for proper immune function (Schwab et al., 2014). Furthermore, pre-clinical studies and clinical trials have shown that the parasympathetic nervous system is also critical for regulating inflammation and other aspects of immunity (Koopman et al., 2016; Pavlov and Tracey, 2017). Similarly, identifying the ANS changes that are responsible for the improved systemic and cerebral hemodynamics following prolonged application of CV-scES is essential and may impact (directly and indirectly) the observed effects on the immune system. As this is a single case study, additional efforts are ongoing to examine whether this effect is consistent in other participants receiving CV-scES and whether this effect is specific to a CV-targeted configuration. Despite these limitations, taken together, these data support the hypothesis that targeted CV-scES parameters that modulate blood pressure may elicit other improvements in ANS-regulated functions, including those that promote beneficial changes in the immune system.

DATA AVAILABILITY STATEMENT

The raw data supporting the conclusions of this article will be made available by the authors, without undue reservation.

ETHICS STATEMENT

The studies involving human participants were reviewed and approved by the local IRB of University of Louisville (NCT 03364660); the portion of the work performed at Northwell Health was reviewed by the local IRB and deemed exempt. The patients/participants provided their written informed consent to participate in this study. Written informed consent was obtained from the individual for the publication of any potentially identifiable images or data included in this article.

AUTHOR CONTRIBUTIONS

OB, JW, BD, SW, AO, CA, AA, and SH collected and analyzed data. OB, JW, BD, AO, and CA wrote the manuscript. SH and CA designed the clinical trial and the project. All authors contributed to the article and approved the submitted version.

FUNDING

This work was funded by the Christopher and Dana Reeve Foundation, Leona M. and Harry B. Helmsley Charitable Trust, Medtronic Plc., and the New York State Spinal Cord Injury Research Board. Northwell Health institutional funds were received for open access publication fees and to support RNA-Seq analysis.

ACKNOWLEDGMENTS

We thank the participant for her dedicated involvement in this study. We are indebted to the research participant for their courage, dedication, motivation, and perseverance that made these research findings possible. Dr. Maxwell Boakye performed surgical implantation and provided medical oversight. Dr. Glen Hirsch, Dr. Darryl Kaelin, and Dr. Sarah Wagers provided medical oversight. Yukisa Austin, Lynn Robbins, and Kristen Johnson provided medical management. We would like to thank Dr. Yangsheng Chen for engineering leadership and Taylor Blades for project management. We would like to thank Kristin Benton for her leadership in research interventions and the support of the research participant.

SUPPLEMENTARY MATERIAL

The Supplementary Material for this article can be found online at: https://www.frontiersin.org/articles/10.3389/fnsys.2020.571011/full#supplementary-material.

SUPPLEMENTARY TABLE 1 | Lists of differentially expressed genes. Gene symbols of differentially expressed genes (with redundant gene symbols removed as described in "Materials and Methods" section) are provided for each comparison as described in the text. Worksheets "SCI Pre CVscES vs. AB DE genes" lists the genes differentially expressed in the participant with SCI before CV-scES compared to able-bodied persons, "PCA Component loadings" shows the transcript loading components for each of five PCs in the PCA comparing the participant with SCI to the able-bodied persons, "SCI Post vs. Pre CVscES DE genes lists the genes differentially expressed in the participant with SCI after the 97 sessions compared to before the CV-scES.

REFERENCES

Angeli, C. A., Boakye, M., Morton, R. A., Vogt, J., Benton, K., Chen, Y., et al. (2018). Recovery of over-ground walking after chronic motor complete spinal cord injury. *N. Engl. J. Med.* 379, 1244–1250. doi: 10.1056/NEJMoa1803588

Ashburner, M., Ball, C. A., Blake, J. A., Botstein, D., Butler, H., Cherry, J. M., et al. (2000). Gene ontology: tool for the unification of biology. *Nat. Genet.* 25, 25–29. doi: 10.1038/75556

Bos, W. J. W., van Goudoever, J., van Montfrans, G. A., van den Meiracker, A. H. and Wesseling, K. H. (1996). Reconstruction of brachial artery pressure from noninvasive finger pressure measurements. *Circulation.* 94, 1870–1875. doi: 10.1161/01.CIR.94.8.1870

Bloom, O., Herman, P. E., and Spungen, A. M. (2020). Systemic inflammation in traumatic spinal cord injury. *Exp. Neurol.* 325, 1131–1143. doi: 10.1016/j.expneurol.2019.113143

Brommer, B., Engel, O., Kopp, M. A., Watzlawick, R., Muller, S., Pruss, H., et al. (2016). Spinal cord injury-induced immune deficiency syndrome enhances infection susceptibility dependent on lesion level. *Brain* 139, 692–707. doi: 10.1093/brain/awv375

Calvert, J. S., Grahn, P. J., Strommen, J. A., Lavrov, I. A., Beck, L. A., Gill, M. L., et al. (2019). Electrophysiological guidance of epidural electrode array implantation over the human lumbosacral spinal cord to enable motor function after chronic paralysis. *J. Neurotrauma* 36, 1451–1460. doi: 10.1089/neu.2018.5921

Carbon, S., Douglass, E., Dunn, N., Good, B., Harris, N. L., Lewis, S. E., et al. (2019). The gene ontology resource: 20 years and still GOing strong. *Nucleic Acids Res.* 47, D330–D338. doi: 10.1093/nar/gky1055

Carlozzi, N. E., Fyffe, D., Morin, K. G., Byrne, R., Tulsky Dimitrijevic, S., Victorson, D., et al. (2013). Impact of blood pressure dysregulation on health-related quality of life in persons with spinal cord injury: development of a conceptual model. *Arch. Phys. Med. Rehabil.* 94, 1721–1730. doi: 10.1016/j.apmr.2013.02.024

Chen, E. Y., Tan, C. M., Kou, Y., Duan, Q., Wang, Z., Meirelles, G. V., et al. (2013). Enrichr: interactive and collaborative HTML5 gene list enrichment analysis tool. *BMC Bioinformatics* 14:128. doi: 10.1186/1471-2105-14-128

Claydon, V. E., and Krassioukov, A. V. (2006). Orthostatic hypotension and autonomic pathways after spinal cord injury. *J. Neurotrauma* 23, 1713–1725. doi: 10.1089/neu.2006.23.1713

Convertino, V. A. (2009). Status of cardiovascular issues related to space flight: implications for future research directions. *Respir. Physiol. Neurobiol.* 169, S34–S37. doi: 10.1016/j.resp.2009.04.010

Currie, K. D., and Krassioukov, A. V. (2015). A walking disaster: a case of incomplete spinal cord injury with symptomatic orthostatic hypotension. *Clin. Auton. Res.* 25, 335–337. doi: 10.1007/s10286-015-0309-7

Darrow, D., Balser, D., Netoff, T. I., Krassioukov, A., Phillips, A., Parr, A., et al. (2019). Epidural spinal cord stimulation facilitates immediate restoration of dormant motor and autonomic supraspinal pathways after chronic neurologically complete spinal cord injury. *J. Neurotrauma* 36, 2325–2336. doi: 10.1089/neu.2018.6006

Dimitrijevic, M. R., Gerasimenko, Y., and Pinter, M. M. (1998). Evidence for a spinal central pattern generator in humans. *Ann. N Y Acad. Sci.* 860, 360–376. doi: 10.1111/j.1749-6632.1998.tb09062.x

Failli, V., Kopp, M. A., Gericke, C., Martus, P., Klingbeil, S., Brommer, B., et al. (2012). Functional neurological recovery after spinal cord injury is impaired in patients with infections. *Brain* 135, 3238–3250. doi: 10.1093/brain/aws267

Gerasimenko, I. P. (2002). Generators of walking movements in humans: spinal mechanisms of their activation. *Aviakosm. Ekolog. Med.* 36, 14–24.

Gimovsky, M. L., Ojeda, A., Ozaki, R., and Zerne, S. (1985). Management of autonomic hyperreflexia associated with a low thoracic spinal cord lesion. *Am. J. Obstet. Gynecol.* 153, 223–224. doi: 10.1016/0002-9378(85)90118-8

Grahn, P. J., Lavrov, I. A., Sayenko, D. G., Van Straaten, M. G., Gill, M. L., Strommen, J. A., et al. (2017). Enabling task-specific volitional motor functions *via* spinal cord neuromodulation in a human with paraplegia. *Mayo Clin. Proc.* 92, 544–554. doi: 10.1016/j.mayocp.2017.02.014

Hargens, A. R., and Richardson, S. (2009). Cardiovascular adaptations, fluid shifts, and countermeasures related to space flight. *Respir. Physiol. Neurobiol.* 169, S30–S33. doi: 10.1016/j.resp.2009.07.005

Harkema, S. J., Legg Ditterline, B., Wang, S., Aslan, S., Angeli, C. A., Ovechkin, A., et al. (2018). Epidural spinal cord stimulation training and sustained recovery of cardiovascular function in individuals with chronic cervical spinal cord injury. *JAMA Neurol.* 75, 1569–1571. doi: 10.1001/jamaneurol.2018.2617

Harkema, S. J., Shogren, C., Ardolino, E., and Lorenz, D. J. (2016). Assessment of functional improvement without compensation for human spinal cord injury: extending the neuromuscular recovery scale to the upper extremities. *J. Neurotrauma* 33, 2181–2190. doi: 10.1089/neu.2015.4213

Herman, P. E., and Bloom, O. (2018). Altered leukocyte gene expression after traumatic spinal cord injury: clinical implications. *Neural Regen. Res.* 13, 1524–1529. doi: 10.4103/1673-5374.237112

Herman, P., Stein, A., Gibbs, K., Korsunsky, I., Gregersen, P., and Bloom, O. (2018). Persons with chronic spinal cord injury have decreased natural killer cell and increased toll-like receptor/inflammatory gene expression. *J. Neurotrauma* 35, 1819–1829. doi: 10.1089/neu.2017.5519

Jacobs, M. J., Jörning, P. J., Joshi, S. R., Kitslaar, P. J., Slaaf, D. W., and Reneman, R. S. (1988). Epidural spinal cord electrical stimulation improves microvascular blood flow in severe limb ischemia. *Ann. Surg.* 207, 179–183. doi: 10.1097/00000658-198802000-00011

Jegede, A. B., Rosado-Rivera, D., Bauman, W. A., Cardozo, C. P., Sano, M. and Moyer, J. M. et al. (2010). Cognitive performance in hypotensive persons with spinal cord injury. *Clin. Auton. Res.* 20, 3–9. doi: 10.1007/s10286-009-0036-z

Katzelnick, C. G., Weir, J. P., Jones, A., Galea, M., Dyson-Hudson, T. A., Kirshblum, S. C., et al. (2019). Blood pressure instability in persons with SCI: evidence from a 30-day home monitoring observation. *Am. J. Hypertens.* 32, 938–944. doi: 10.1093/ajh/hpz089

Koopman, F. A., Chavan, S. S., Milijko, S., Grazio, S., Sokolovic, S., Schuurman, P. R., et al. (2016). Vagus nerve stimulation inhibits cytokine production and attenuates disease severity in rheumatoid arthritis. *Proc. Natl. Acad. Sci. U S A.* 113, 8284–8289. doi: 10.1073/pnas.1605635113

Morse, L. R., Stolzmann, K., Nguyen, H. P., Jain, N. B., Zayac, C., Gagnon, D. R., et al. (2008). Association between mobility mode and C-reactive protein levels in men with chronic spinal cord injury. *Arch. Phys. Med. Rehabil.* 89, 726–731. doi: 10.1016/j.apmr.2007.09.046

Nash, M. S., Tractenberg, R. E., Mendez, A. J., David, M., Ljungberg, I. H., Tinsley, E. A., et al. (2016). Cardiometabolic syndrome in people with spinal cord injury/disease: guideline-derived and nonguideline risk components in a pooled sample. *Arch. Phys. Med. Rehabil.* 97, 1696–1705. doi: 10.1016/j.apmr.2016.07.002

Pavlov, V. and Tracey, K. (2017). Neural regulation of immunity: molecular mechanisms and clinical translation. *Nature Neurosci.* 20, 156–166. doi: 10.1038/nn.4477

Phillips, A. A., Krassioukov, A. V., Ainslie, P. N., and Warburton, D. E. R. (2014a). Perturbed and spontaneous regional cerebral blood flow responses to changes in blood pressure after high-level spinal cord injury: the effect of midodrine. *J. Appl. Physiol.* 116, 645–653. doi: 10.1152/japplphysiol.01090.2013

Phillips, A. A., Warburton, D. E. R., Ainslie, P. N., and Krassioukov, A. V. (2014b). Regional neurovascular coupling and cognitive performance in those with low blood pressure secondary to high-level spinal cord injury: improved by α-1 agonist midodrine hydrochloride. *J. Cereb. Blood Flow Metab.* 34, 794–801. doi: 10.1038/jcbfm.2014.3

Phillips, A. A., Matin, N., Jia, M., Squair, J. W., Monga, A., Zheng, M. M. Z., et al. (2018). Transient hypertension after spinal cord injury leads to cerebrovascular endothelial dysfunction and fibrosis. *J. Neurotrauma* 35, 573–581. doi: 10.1089/neu.2017.5188

Rejc, E., Angeli, C. A., Atkinson, D., and Harkema, S. J. (2017a). Motor recovery after activity-based training with spinal cord epidural stimulation in a chronic motor complete paraplegic. *Sci. Rep.* 7:13476. doi: 10.1038/s41598-017-14003-w

Rejc, E., Angeli, C. A., Bryant, N., and Harkema, S. J. (2017b). Effects of stand step training with epidural stimulation on motor function for standing in chronic complete paraplegics. *J. Neurotrauma* 34, 1787–1802. doi: 10.1089/neu.2016.4516

Saleem, S., Vucina, D., Sarafis, Z., Lee, A. H. X., Squair, J. W., Barak, O. F., et al. (2018). Wavelet decomposition analysis is a clinically relevant strategy to evaluate cerebrovascular buffering of blood pressure after spinal cord injury.

Am. J. Physiol. Heart Circ. Physiol. 314, H1108–H1114. doi: 10.1152/ajpheart.00152.2017

Schwab, J. M., Zhang, Y., Kopp, M. A., Brommer, B., and Popovich, P. G. (2014). The paradox of chronic neuroinflammation, systemic immune suppression, autoimmunity after traumatic chronic spinal cord injury. *Exp. Neurol.* 258, 121–129. doi: 10.1016/j.expneurol.2014.04.023

Shealy, C. N., Mortimer, J. T., and Reswick, J. B. (1967). Electrical inhibition of pain by stimulation of the dorsal columns: preliminary clinical report. *Anesth. Analg.* 46, 489–491.

Vaziri, N. D. (2003). Nitric oxide in microgravity-induced orthostatic intolerance: relevance to spinal cord injury. *J. Spinal Cord Med.* 26, 5–11. doi: 10.1080/10790268.2003.11753653

Weaver, F. M., Collins, E. G., Kurichi, J., Miskevics, S., Smith, B., Rajan, S., et al. (2007). Prevalence of obesity and high blood pressure in veterans with spinal cord injuries and disorders: a retrospective review. *Am. J. Phys. Med. Rehabil.* 86, 22–29. doi: 10.1097/phm.0b013e31802b8937

Wecht, J. M., Weir, J. P., and Bauman, W. A. (2017). Inter-day reliability of blood pressure and cerebral blood flow velocities in persons with spinal cord injury and intact controls. *J. Spinal Cord Med.* 40, 159–169. doi: 10.1080/10790268.2015.1135556

Wecht, J. M., Weir, J. P., Katzelnick, C. G., Wylie, G., Eraifej, M., Nguyen, N., et al. (2018). Systemic and cerebral hemodynamic contribution to cognitive performance in spinal cord injury. *J. Neurotrauma* 35, 2957–2964. doi: 10.1089/neu.2018.5760

Wecht, J. M., Zhu, C., Weir, J. P., Yen, C., Renzi, C., and Galea, M. (2013). A prospective report on the prevalence of heart rate and blood pressure abnormalities in veterans with spinal cord injuries. *J. Spinal Cord Med.* 36, 454–462. doi: 10.1179/2045772313y.0000000109

West, C. R., Phillips, A. A., Squair, J. W., Williams, A. M., Walter, M., Lam, T., et al. (2018). Association of epidural stimulation with cardiovascular function in an individual with spinal cord injury. *JAMA Neurol.* 75, 630–632. doi: 10.1001/jamaneurol.2017.5055

Wu, J.-C., Chen, Y.-C., Liu, L., Chen, T.-J., Huang, W.-C., Cheng, H., et al. (2012). Increased risk of stroke after spinal cord injury. *Neurology* 78, 1051–1057. doi: 10.1212/WNL.0b013e31824e8eaa

Conflict of Interest: The authors declare that this study received funding from Medtronic Plc in the form of implantable devices. The funder was not involved in the study design, collection, analysis, interpretation of data, the writing of this article, or the decision to submit it for publication.

frontiers in Systems Neuroscience

ORIGINAL RESEARCH
published: 21 October 2020
doi: 10.3389/fnsys.2020.559313

Spinal Cord Imaging Markers and Recovery of Volitional Leg Movement With Spinal Cord Epidural Stimulation in Individuals With Clinically Motor Complete Spinal Cord Injury

Enrico Rejc[1,2], Andrew C. Smith[3], Kenneth A. Weber II[4], Beatrice Ugiliweneza[1,2], Robert J. Bert[5], Mohammadjavad Negahdar[5], Maxwell Boakye[1,2], Susan J. Harkema[1,2,6,7] and Claudia A. Angeli[1,6,7]*

[1] Kentucky Spinal Cord Injury Research Center, University of Louisville, Louisville, KY, United States, [2] Department of Neurological Surgery, University of Louisville, Louisville, KY, United States, [3] University of Colorado School of Medicine, Department of Physical Medicine and Rehabilitation, Physical Therapy Program, Aurora, CO, United States, [4] Department of Anethesiology, Perioperative and Pain Medicine, Stanford University School of Medicine, Palo Alto, CA, United States, [5] Department of Radiology, University of Louisville, Louisville, KY, United States, [6] Frazier Rehabilitation Institute, University of Louisville Health, Louisville, KY, United States, [7] Department of Bioengineering, University of Louisville, Louisville, KY, United States

OPEN ACCESS

Edited by:
James W. Grau,
Texas A&M University, United States

Reviewed by:
Igor Lavrov,
Mayo Clinic, United States
Keith E. Tansey,
Methodist Rehabilitation Center, United States

***Correspondence:**
Enrico Rejc
enrico.rejc@louisville.edu

Received: 05 May 2020
Accepted: 28 September 2020
Published: 21 October 2020

Citation:
Rejc E, Smith AC, Weber KA II, Ugiliweneza B, Bert RJ, Negahdar M, Boakye M, Harkema SJ and Angeli CA (2020) Spinal Cord Imaging Markers and Recovery of Volitional Leg Movement With Spinal Cord Epidural Stimulation in Individuals With Clinically Motor Complete Spinal Cord Injury. Front. Syst. Neurosci. 14:559313. doi: 10.3389/fnsys.2020.559313

Previous studies have shown that epidural stimulation of the lumbosacral spinal cord (scES) can re-enable lower limb volitional motor control in individuals with chronic, clinically motor complete spinal cord injury (SCI). This observation entails that residual supraspinal connectivity to the lumbosacral spinal circuitry still persisted after SCI, although it was non-detectable when scES was not provided. In the present study, we aimed at exploring further the mechanisms underlying scES-promoted recovery of volitional lower limb motor control by investigating neuroimaging markers at the spinal cord lesion site *via* magnetic resonance imaging (MRI). Spinal cord MRI was collected prior to epidural stimulator implantation in 13 individuals with chronic, clinically motor complete SCI, and the spared tissue of specific regions of the spinal cord (anterior, posterior, right, left, and total cord) was assessed. After epidural stimulator implantation, and prior to any training, volitional motor control was evaluated during left and right lower limb flexion and ankle dorsiflexion attempts. The ability to generate force exertion and movement was not correlated to any neuroimaging marker. On the other hand, spared tissue of specific cord regions significantly and importantly correlated with some aspects of motor control that include activation amplitude of antagonist (negative correlation) muscles during left ankle dorsiflexion, and electromyographic coordination patterns during right lower limb flexion. The fact that amount and location of spared spinal cord tissue at the lesion site were not related to the ability to

generate volitional lower limb movements may suggest that supraspinal inputs through spared spinal cord regions that differ across individuals can result in the generation of lower limb volitional motor output prior to any training when epidural stimulation is provided.

Keywords: epidural stimulation, spinal cord injury, voluntary movement, spinal cord MRI, spinal cord lesion, spinal tracts

INTRODUCTION

In an intact nervous system, supraspinal inputs to the spinal circuitry are primarily involved in volitional movement initiation and cessation, and fine motor control. Supraspinal inputs also provide a non-specific tonic drive that optimizes the spinal circuitry level of excitability to perform a motor task (i.e., walking or standing), thus capitalizing on spinal circuitry automatic properties for the control of posture and locomotion (Edgerton et al., 2004). After a severe spinal cord injury (SCI), the prevailing view is that the loss of supraspinal tonic drive to the spinal circuitry disrupts its state of excitability (Harkema, 2008; Cote et al., 2017); this fact, together with the disruption of inputs for fine motor control, leads to the inability to walk, stand and volitionally move the lower limbs. Recovery of lower limb voluntary movement in the presence of spinal cord epidural stimulation (scES) following motor complete and incomplete SCI has been demonstrated in a number of studies (Harkema et al., 2011; Angeli et al., 2014; Grahn et al., 2017; Wagner et al., 2018; Darrow et al., 2019). These findings provide evidence that the residual brain-spinal connectivity, not detectable by clinical means, can be enhanced by the scES-mediated modulation of excitability of the spinal circuitry, enabling the recovery of voluntary movement in individuals with motor paralysis.

Neuroimaging provides useful biomarkers to predict future outcomes and glean mechanistic insights following traumatic SCI (Freund et al., 2019). Magnetic resonance imaging (MRI), in particular, has been used to examine characteristics of the spinal cord and its corresponding lesion (Flanders et al., 1996; Miyanji et al., 2007; Huber et al., 2017; O'Dell et al., 2018; Vallotton et al., 2019). Both qualitative and quantitative approaches may be used to assess the severity of spinal cord damage to establish relationships with future neurological status (Miyanji et al., 2007; Talbott et al., 2015; Aarabi et al., 2017). Considering the spinal cord lesion in the axial plane, researchers are able to evaluate the extent of intramedullary cord damage in relationship to the surrounding spinal cord boundaries (Talbott et al., 2015; Smith et al., 2017). The open-source software, Spinal Cord Toolbox, allows for a standardized quantitative template-based approach to assess the integrity of white matter pathways and gray matter within the spinal cord (De Leener et al., 2017, 2018). Using this approach, spinal cord damage in the axial plane in the corresponding regions of the right and left lateral corticospinal tracts was associated with a decreased ability to generate voluntary torque in the lower extremities, in an ipsilesional manner (Smith et al., 2018). This is one example of how neuroimaging may elucidate mechanisms into recovery of motor function after SCI.

Improved mechanistic understanding of implanted spinal epidural stimulation to augment function after SCI is warranted (Rejc and Angeli, 2019), and neuroimaging is one potential approach to address this call. To the best of our knowledge, to date no studies have used quantitative MRI to investigate mechanisms involved with responsiveness to epidural stimulation after SCI.

MATERIALS AND METHODS

Participants

Thirteen individuals ($n = 9$ males and $n = 4$ females) with chronic, clinically motor complete and sensory complete or incomplete SCI are included in this study (**Table 1**). The research participants signed an informed consent for lumbosacral scES implantation, stimulation, activity-based training and physiological monitoring studies, which were conducted according to the standards set by the Declaration of Helsinki, and were approved by the University of Louisville Institutional Review Board (ClinicalTrials.gov identifiers NCT02037620, NCT02339233, and NCT03364660). Prior to epidural stimulator implantation, the International Standards for Neurological Classification of Spinal Cord Injury (Burns et al., 2012) was used for classifying the injury using the ASIA (American Spinal Injury Association) Impairment Scale (AIS). The research participants were implanted with a scES unit between 3.1 and 8.6 years after SCI, and were enrolled into interventional studies focused on either the facilitation of standing and stepping, the recovery of cardiovascular function, or the recovery of cardiovascular function as well as volitional leg movements and standing (Studies 1, 2 and 3, respectively; **Table 1**). However, the data presented in this study were collected prior to the beginning of any intervention with scES.

Spinal Cord MRI Collection

Prior to epidural stimulator implantation, 2-D magnetic resonance images from cervical-thoracic (C-T) and thoracic-lumbar (T-L) levels of the spinal cord in axial and sagittal views were collected. Images were obtained using a 3 Tesla system (Siemens Magnetom Skyra, Siemens Medical Solutions, Malvern, PA, United States) with Turbo Spin Echo T2-weighted pulse sequences.

Sagittal images were first obtained in two or three separate sequences to cover the spine from at least the foramen magnum to the mid lumbar or sacral regions with large field of view (FOV) images to screen patients for syringes, significant stenoses, scoliosis, levels of injury and stabilizing treatment-related surgical changes. Usually this was performed with two

TABLE 1 | Characteristics of the research participants.

Pub ID	Age range (years)	Time between injury and surgery (years)	Injury level	AIS	Approx. lesion center	Adhesions	Decom-pression	Wallerian Deg.	Study
B30	21–25	3.2	T1	B	C6–C7	None	A, P	P	1
B23	26–30	4.2	C7	B	C5	A	A, P	A, P	1
A80	31–35	7.9	C6	A	C6	A	A, P	P	2
B21	31–35	6.9	C4	B	C5	P	P	A, P	2
A41	21–25	7.2	C4	A	C5	P	A, P	P	2
A68	31–35	3.8	C5	A	C6	A, P	A, P	P	2
A99	16–20	2.8	C4	A	C4–C5	A, P	A, P	P, min	3
B32	61–65	7.4	C4	B	C6	A	A, P	A, P	3
A101	31–35	2.4	C2	A	C3–C4	None	A	P	3
A96	26–30	3.1	C4	A	C5	A, P	A, P	A, P min	3
A110	21–25	5.8	C5	A	C7	None	A, P	A, P	3
B41	26–30	8.6	C8	B	C7	None	A	A, P	3
B47	41–45	8.2	C4	B	C4–C5	A, P	A	A, P	3

Injury level: neurological level of the lesion by AIS (American Spinal Injury Association (ASIA) Impairment Scale; Burns et al., 2012). Approx. lesion center: vertebral level used for Spinal Cord Toolbox (De Leener et al., 2017) template registration based on the approximate lesion center. Clinical interpretation of Magnetic Resonance Imaging including presence of adhesions, type of decompression performed, and evidence for Wallerian degeneration (A, anterior; P, posterior). Each individual was enrolled in an interventional study focused on either the facilitation of standing and stepping (Study 1), the recovery of cardiovascular function (Study 2), or the recovery of cardiovascular function as well as volitional leg movements and standing (Study 3).

sequences but taller subjects required three separate sequences because of field of view limitations. Typical parameters were:

TR/TE/FA/Thick/ETL/Re_Matrix/PFOV/NSA/BW/Pixal/AQ_matrix/%samp/PE =

Upper sagittal:

3000/74/160/3 × 3.45/17/320 × 320/100%/2/600/1.125 × 1.125/320 × 240/75/442

Lower Sagittal:

3000/74/∼130/3 × 3.45/17/320 × 320/100/2/600/1.25 × 1.25/324 × 240/75/442

Where TR = repetition time, TE = echo time, ETL = echo train length, Re_Matrix = reconstruction matrix, PFOV = % phase field of view, NSA = number of signal averages, BW = bandwidth, Pixal = pixel dimensions, AQ_matrix = acquisition matrix, % samp = % sampling (or partial fourier) and PE = number of phase 3 encodes.

In a few cases, minor adjustments were made to the parameters for specific absorption rate (SAR) limitations, patient size or clinical factors. Tables with the exact values for each individual are given in **Supplementary Table 1**.

Additional sequential axial T2 Turbo spin echo images were obtained from the foramen magnum to the T3-4 level. In most cases, these images were obtained either with a 10% gap (standard) or no gap. Axial 5 mm images were obtained through thoracic and lumbar regions at 5 mm thickness with a 5 mm gap between images in order to reach sustainable imaging times that could be tolerated by the research participants. Example parameters are:

Cervical spine:

5190/74/160/3 × 3/26/512 × 512/100/2/610/0.35 × 0.35/256 × 179/70/260

Thoracic spine:

3690/82/121/5 × 10/28/512 × 512/100/2/610/0.35 × 0.35/256 × 179/70/252

Lumbar spine:

3280/82/121/5 × 10/28/512 × 512/100/2/610/0.35 × 0.35/256 × 179/70/252

Spinal Cord MRI Analysis

Clinical reports were provided for each research subject prior to their inclusion in the study by a subspecialty certified neuroradiologist (RJB). In addition to screening for exclusion criteria, clinical reports included evidence (T2 hyperintensity) for Wallerian degeneration along the anterior and posterior central cord (**Supplementary Figure 1**), type of decompression performed, and the presence of anterior or posterior adhesions.

The open-source Spinal Cord Toolbox (Version 4.3.0) was used to calculate the amount of spared white matter (De Leener et al., 2017). SCT contains a comprehensive set of tools for the processing of multi-modal spinal cord MRI datasets including the PAM50 spinal cord standard template (resolution = 0.5 × 0.5 × 0.5 mm^3) with a corresponding probabilistic atlas of 15 pairs (i.e., left and right side) of white matter tracts as well as functions for multi-modal registration and spatial normalization (Fonov et al., 2014; De Leener et al., 2017; Dupont et al., 2017). The individual white matter tracts within the anterior, posterior, right lateral, and left lateral spinal cord were combined to quantify the amount of spared tissue within these white matter regions (Cloney et al., 2018). Spatial normalization is the process of bringing the subject-level images into spatial agreement with a standard template. Once aligned, the subject-level images can be transformed to the template space, and the template atlases can then be used to identify corresponding anatomical regions in the subject-level images. Spatial normalization of pathological images has unique challenges (Crinion et al., 2007). In the case of spinal cord injury, the lesion appears hyperintense on T_2-weighted images, and the spinal cord injury can also lead to spatial distortions

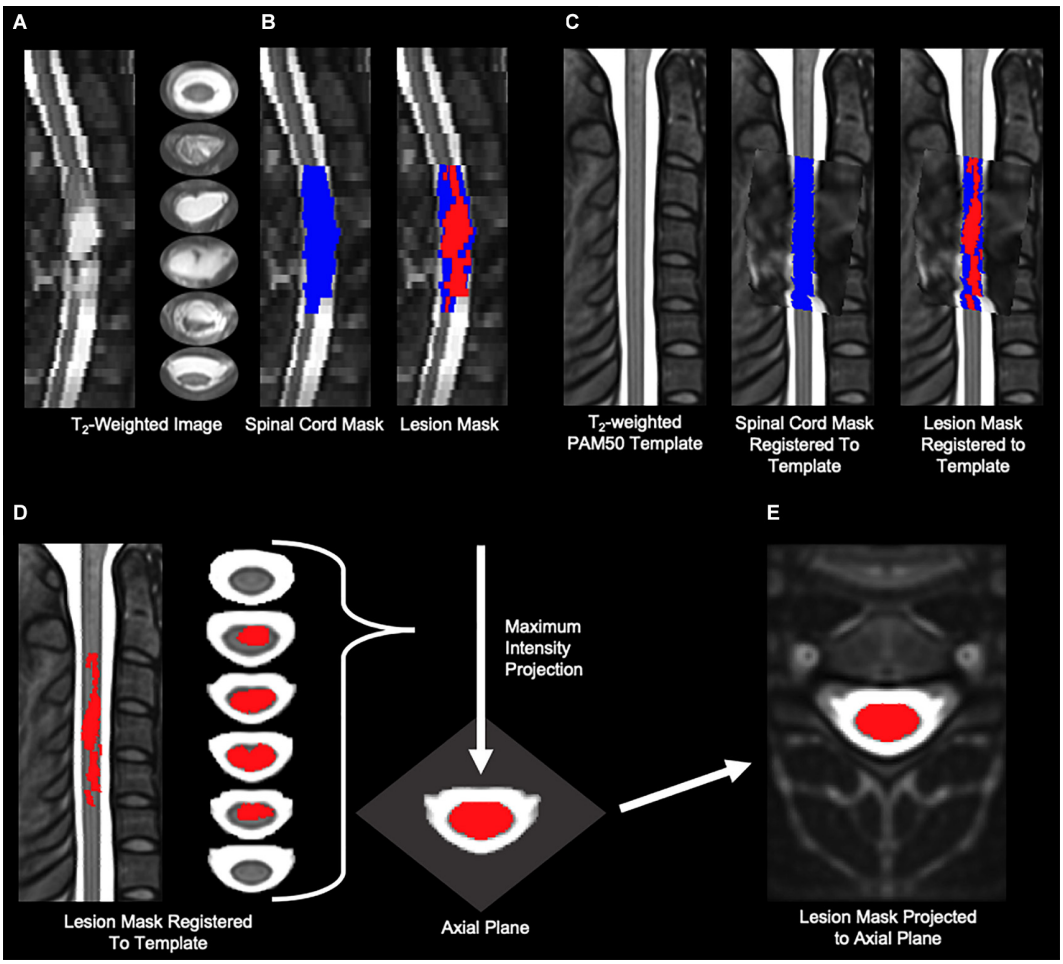

FIGURE 1 | Imaging analysis methods. **(A)** Sagittal and axial slices of the T2-weighted image of a representative participant with a severe lesion. The lesion is identified as the hyperintensity in the spinal cord. **(B)** A blinded experimenter manually segmented the spinal cord (blue) and lesion (red) from the T2-weighted image. **(C)** The PAM50 T2-weighted template was then registered to the T2-weighted image using the manually draw spinal cord mask. The transformation was then applied to lesion mask to bring the lesion into template space. The spinal cord mask and lesion mask from **(B)** are shown transformed to the PAM50 spinal cord template. **(D,E)** To quantify the axial extent of the spinal cord lesion, the lesion mask in template space was then projected onto the axial plane to create one projected axial image of the composite lesion.

of the lesioned and non-lesioned tissues in the cord (Talbott et al., 2019). To register the white matter atlas to the lesioned images, an experimenter blinded to the clinical history and experimental measures first manually segmented the images to generate binary spinal cord and spinal cord lesion masks. The spinal cord mask included the spinal cord lesion. The PAM50 T_2-weighted template was then registered to the T_2-weighted image (reference = subject) using the manually drawn spinal cord mask and PAM50 template spinal cord mask to perform the registration. The vertebral level at the center of the spinal cord lesion was used to localize the template along the superior-inferior axis. The spinal cord segmentations were then initially aligned using their center of mass, and then a series of non-linear deformations (bsplinesyn followed by columnwise) were performed to register the template spinal cord mask to the manually drawn spinal cord mask. The final registration step was performed separately for each slice (i.e., slicewise) allow for greater deformation in the warping process to account for spatial distortions in the spinal cord shape and fine-tune the registration to each slice. The utilization of the segmentation masks for spatial normalization prevented the registration from being influenced by the lesion hyperintensity. The corresponding spatial transformation was then applied to the spinal cord lesion mask to transform the lesion to template space. To quantify the spatial extent of the spinal cord lesion, the lesion mask was then projected to the axial plane, and the percentage of spared region volume (non-lesion) within the axial plane was calculated for each of the white matter regions, and these values were used for statistical analyses (**Figure 1**). The template registration was visually inspected at each step for quality control.

Spinal Cord Epidural Stimulation Implant

During the scES implantation procedure, a midline bilateral laminotomy was performed typically at the L1-L2 disc space.

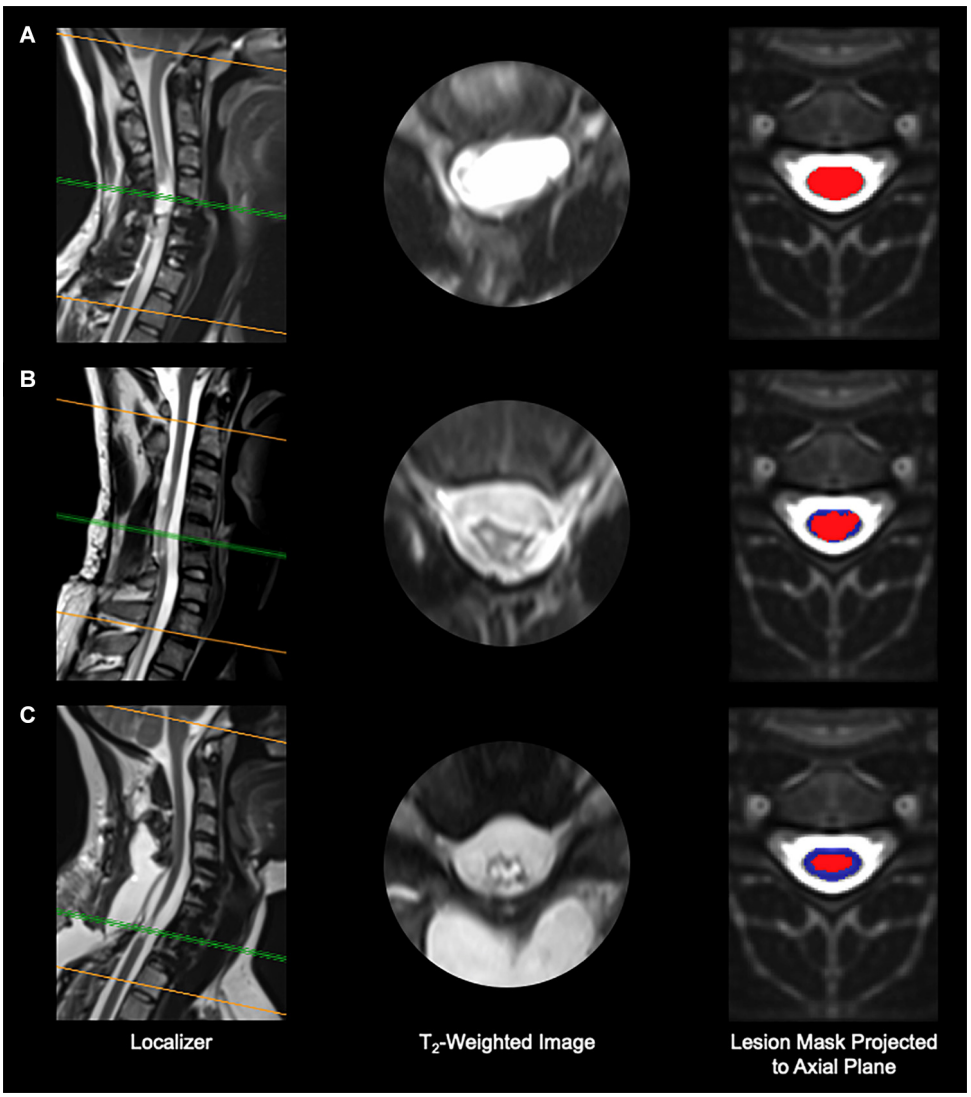

FIGURE 2 | Imaging results from three representative research participants. **(A)** Participant A99, with no spared tissue of the spinal cord remaining. **(B)** Participant B21, who shows minimal spared spinal cord tissue. **(C)** Participant A110, who presents considerable spared spinal cord tissue. Red, spinal cord damage; blue, spared spinal cord tissue.

The electrode array with 16 contacts (Medtronic Specify 5-6-5 lead) was placed into the epidural space at midline. Electrophysiological mapping was performed after initial placement to optimize the positioning of the paddle electrode based on the evoked responses recorded by surface EMG electrodes from representative lower limb muscles. After the final placement of the electrode array, the electrode lead was tunneled subcutaneously and connected to the neurostimulator.

Voluntary Movement Experimental Procedures and Analysis

Research participants began the experimental sessions in the laboratory approximately 2–3 weeks after the surgical implantation of the spinal cord epidural stimulation unit. Spatio-temporal mapping of the spinal cord motor evoked responses was performed with the individuals relaxed in supine position (Sayenko et al., 2014; Mesbah et al., 2017; Rejc et al., 2017b). Stimulation amplitude- and frequency-response curves were used as an initial guide for the selection of stimulation parameters to facilitate voluntary leg movement (voluntary movement mapping experiments). Voluntary movement mapping took place over 1–3 days of testing. For the present study, volitional movement patterns of the right and left lower limb were assessed for ankle dorsiflexion and lower limb flexion; these motor tasks were performed in supine or semi-reclined position. In all individuals, the left and right stimulation configurations were different. Stimulation intensity was sub-motor threshold for the prime movers of the selected motor task.

Once the stimulation parameters were optimized for each individual, range of motion and force generation were assessed

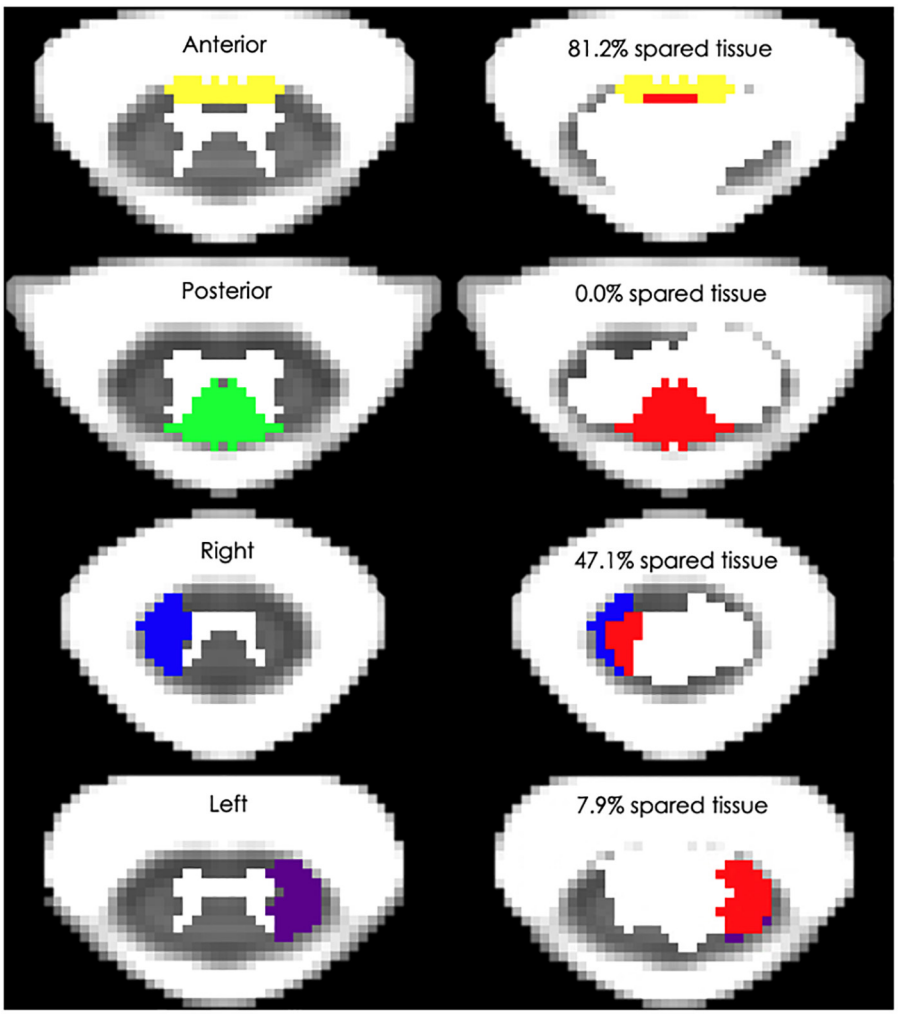

FIGURE 3 | Spinal cord white matter regions and exemplary percent spared tissue. The left column depicts the four white matter regions that were used to quantify the spared tissue correlated with motor outcomes. The right column shows four representative research subjects' spinal cord damage as well as the percentage of the corresponding white matter region that was spared. The red area indicates the lesioned tissue in each region.

using either a force transducer (Kistler Holding AG, Winterthur, Switzerland) attached to a custom-built frame (Angeli et al., 2014) (n = 6) or a Biodex dynamometer (Biodex Inc., Shirley, NY) (n = 7). Electromyography (EMG) was collected bilaterally from iliopsoas, rectus femoris, vastus lateralis, medial hamstrings, tibialis anterior, and soleus. EMG data were amplified and recorded at 2,000 Hz using a hard-wired AD board and a custom-written acquisition software (LabView, National Instruments, Austin, TX), as well as band pass-filtered (30–1,000 Hz). Force and position data were also acquired with the same system and synchronized with EMG.

The background (resting) root mean square (RMS) EMG amplitude recorded prior to each volitional attempt was subtracted to the RMS EMG amplitude detected during the attempt, which was then normalized by the largest evoked potential peak-peak amplitude detected for each investigated muscle. The evoked potentials to scES were assessed with the research participants relaxed in supine position, delivering stimulation (frequency: 2 Hz; pulse width: 450 μs; electrode configuration: the three most caudal contacts (number 1, 10, 15) set as cathodes, and the three more rostral contacts (number 0, 5, 11) set as anodes) at increasing amplitude (amplitude-response curve) until either the participant requested to stop due to discomfort, or the maximum stimulator amplitude was reached. Five stimuli were delivered at each of the stimulation intensities applied; the average peak-peak amplitude for each stimulation intensity was then calculated, and the largest value recorded from each investigated muscle was considered for normalization. Quantitative information about the coordination pattern between representative muscles during volitional movement attempts (iliopsoas *vs* medial hamstrings during lower limb flexion; tibialis anterior *vs* soleus during ankle dorsiflexion) have been obtained as reported by Rejc and colleagues (Rejc et al., 2017a). Briefly, each data point of the joint

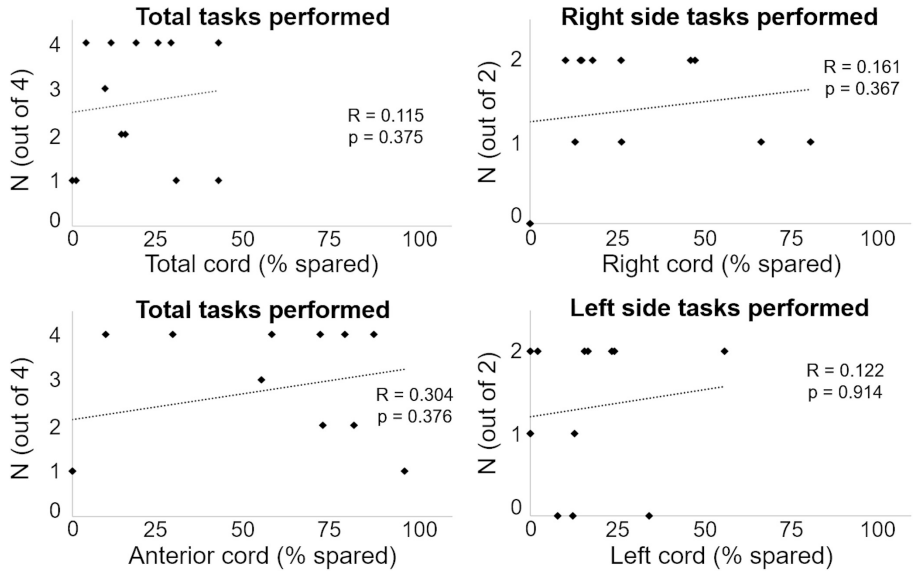

FIGURE 4 | Number of motor tasks successfully performed are plotted against the amount of spared tissue of representative cord regions.

probability density distribution (JPD) (Hutchison et al., 1989) represents the amplitude relationship of the EMG signals from the two muscles at a given time point. Ten percent of the largest amplitude detected during the attempt was set as threshold to define four areas of the plot representing the isolated activation of either muscle, or the co-contraction at lower or higher level of activation. The number of data points distributed in each of these four areas was finally expressed as a percentage of the total data points collected during a given attempt. Attempts with no activation detected for both muscles resulted in 100% co-contraction at low level of activation.

Statistical Analysis

Five MRI outcomes (spared tissue of total, anterior, posterior, right, and left spinal cord) and 39 motor outcomes (number of motor tasks successfully generated, EMG amplitude of primary agonist and antagonist muscles, electromyographic coordination pattern; **Supplementary Table 2**) were initially considered for each research participant. We then performed the following dimensionality reduction to include only informative outcomes and important predictors. Initially, variables with zero variability were excluded because no information can be learned from them. From the remaining independent variables, we retained those that were not weakly correlated with, or were found to be important predictors, of the remaining dependent variables. The correlations were evaluated with Spearman Correlation, and the variables importance was evaluated with the Boruta Variable Importance algorithm (Kursa and Rudnicki, 2010). Any MRI outcome that was found either correlated or important for at least one motor outcome was retained. Motor variables that were not correlated with any independent variable and had no important predictor were dropped.

For count outcomes [number of motor tasks (out of four) that were successfully generated, i.e., that resulted in force exertion and movement], we used Poisson regression; for binary variables (whether force exertion and movement were detected for a given motor task), we applied the logistic regression; and for the remaining continuous variables we used the linear regression. Statistically significant MRI outcomes were combined into a multivariable regression for each motor outcome, and the adjusted estimates and *p*-values were considered for analysis. To reduce variance resulting from the relatively small sample size, we performed bagged multiple linear regressions fitted on 1,000 bootstrap copies of the data (Hastie et al., 2009). Estimates, averaged from the ensemble, were presented as the change in outcome associated with 1-unit increase in MRI measure. Data analysis was performed in SAS 9.4 (SAS Inc., Cary, NC) and R 3.6.1 (R Core Team, 2019).

TABLE 2 | Statistically significant and important correlations between cord MRI and motor outcomes.

Motor outcome	MRI outcome	Adjusted	
		Estimate (SE)	*p*-value
L dorsiflexion—L SOL EMG RMS	Anterior cord spared	−0.02 (0.01)	0.017
R lower limb flexion—JPD R MH	Right cord spared	0.65 (0.22)	0.015
R lower limb flexion—JPD Co-co-Low	Total cord spared	−0.987 (0.34)	0.014

Estimated effect of the change in motor outcome associated with 1-unit increase in magnetic resonance imaging (MRI) outcome is reported, as well as the significance (p-value) of the correlation between motor and MRI outcomes. R, right side; L, left side; SOL, soleus; MH, medial hamstrings. RMS, root mean square; JPD, joint probability density distribution; JPD R MH, isolated activation of R MH; JPD Co-co-Low, co-contraction at lower level of activation between right MH and iliopsoas.

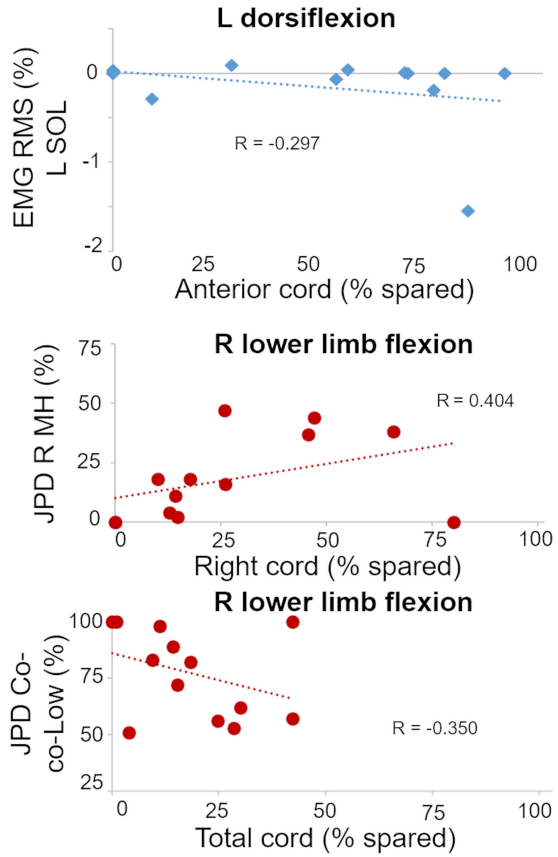

FIGURE 5 | Plots of statistically significant and important correlations between amount of spared tissue of specific cord regions and muscle activation outcomes. R, right side; L, left side; RMS, root mean square; SOL, soleus; JPD R MH, amount of isolated activation of R medial hamstrings; JPD Co-co-Low, amount of co-contraction at lower level of activation between right MH and iliopsoas.

RESULTS

Cord MRI analysis revealed that the amount of spared tissue varied substantially across individuals, as exemplified in **Figure 2**. Total cord spared tissue was on average 18.6 ± 14.2%, and ranged between 0 and 42.3%.

Also, **Figure 3** depicts the four white matter regions of interest as well as exemplary amounts of spared tissue. In particular, lateral cord spared tissue was on average 15.8 ± 16.1% (range: 0–55.9%) and 27.7 ± 24.8% (range: 0–80.0%) for the left and right side, respectively. Finally, the anterior cord spared tissue was on average 49.0 ± 36.4% (range: 0–95.8%), and the posterior 17.8 ± 17.9% (range: 0–53.2%).

On the other hand, motor responses (i.e., force generation and movement) were detected on average for 2.7 ± 1.4 motor tasks out of the four tested for each individual (range: 1–4) when scES optimized for volitional movement was applied. Conversely, no force generation and/or muscle activation was detected when research participants attempted to volitionally move the lower limb without scES.

We initially tested whether the total cord spared tissue as well as the spared tissue of the four cord regions assessed in this study were correlated with the ability to generate a motor response (i.e., force exertion and movement) in the right and left side during attempts to flex the lower limb and perform ankle dorsiflexion. As exemplified in **Figure 4**, no significant correlations (p-values ranging between 0.184 and 0.985) were found between these MRI and motor outcomes.

We then expanded this correlation analysis by considering the activation pattern as quantified by EMG amplitude and coordination of primary muscles involved in the attempted motor tasks, and three statistically significant and important correlations were found (**Table 2**). The plotting of individual data points for these three correlations between amount of spared tissue of specific cord portions and muscle activation characteristics is reported in **Figure 5**.

It is worth noting that these correlations appear meaningful from a functional perspective. For example, a negative correlation between spared tissue of the anterior cord and EMG amplitude of the left soleus muscle (ankle plantarflexor; antagonist) was observed during left ankle dorsiflexion attempts (p = 0.017). Also, the amount of isolated activation of the right medial hamstrings (i.e., without the concurrent activation of right iliopsoas) was directly related (p = 0.015) with the spared tissue of the lateral right cord during right lower limb flexion attempts. Finally, for the same motor task, the amount of co-contraction at lower level of activation between right medial hamstrings and iliopsoas was inversely related (p = 0.014) with the total cord spared tissue.

Figure 6 exemplifies the effects of scES during attempts to perform left ankle dorsiflexion in individuals that showed different amount of anterior cord spared tissue, which was found correlated with the activation amplitude of a key antagonist muscle (soleus, SOL) for this motor task. As expected, no movement or EMG modulation was observed in response to volitional attempts without scES (**Figure 6A**). Also, no force exertion was detected when scES was applied (**Figure 6B**). However, in this condition, the individual with greater amount of anterior cord spared tissue (A110) demonstrated a decrement in SOL EMG activity when attempting to dorsiflex the ankle joint, while a concurrent EMG burst of the tibialis anterior muscle (agonist) was also detected. Conversely, no EMG activity modulation was observed during the same motor task in the other individual (A80), who was diagnosed with no anterior cord spared tissue, while still demonstrating 30% of total cord spared.

Other two significant relationships between EMG activity modulation and cord spared tissue are exemplified in **Figure 7**, which focuses on right lower limb flexion. As expected, no movement or EMG modulation was observed in response to volitional attempts without scES (**Figure 7A**). On the other hand, when scES was applied, both research participants were able to volitionally flex the lower limb (**Figure 7B**). However, greater amount of isolated activation of right medial hamstrings as well as lower amount of co-contraction at low level of activation between right iliopsoas and medial hamstrings were found in participant A101, who showed greater right cord spared tissue (26 vs. 12%)

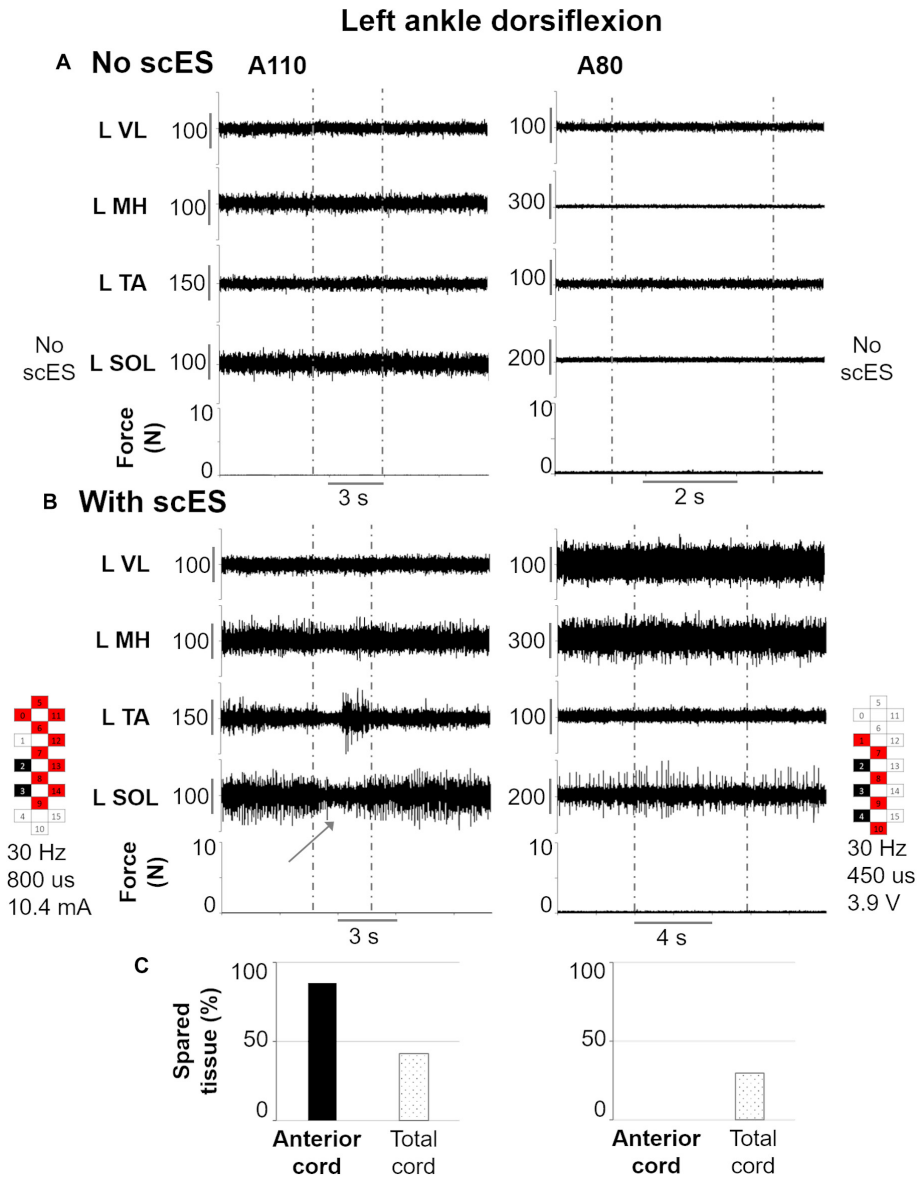

FIGURE 6 | Representative EMG activity modulation and force generation during isometric ankle dorsiflexion attempts performed without **(A)** and with **(B)** spinal cord epidural stimulation (scES) by two research participants (A110 and A80). Vertical gray dotted lines: attempt duration. **(C)** Spared tissue of the anterior cord, which was found inversely correlated with EMG amplitude of L SOL (antagonist muscle) during left ankle dorsiflexion attempts, and of the total cord for the same two participants. L, left side; VL, vastus lateralis; MH, medial hamstrings; TA, tibialis anterior; SOL, soleus. The gray arrow points out the decrease in L SOL EMG activity in response to the volitional attempt. Epidural stimulation electrode configuration (cathodes in black, anodes in red, inactive in white), frequency, pulse width and intensity are reported.

as well as total cord spared tissue (28 vs. 15%) as compared to participant B21.

DISCUSSION

A traumatic SCI diagnosed as chronic, clinically motor complete can manifest different neurophysiological and anatomical (**Figures 2**, **3**) profiles. For example, it is not uncommon to detect activation of paralyzed leg muscles in response to volitional movement attempts, with or without concurrent "reinforcement maneuvers" resulting from volitional activation of muscles above the level of injury (i.e., motor discomplete SCI) (Dimitrijevic et al., 1984; Dimitrijevic, 1988; McKay et al., 2004). Clinically motor complete SCI can also be characterized by the lack of these neurophysiological responses, while still presenting limited spared neural connectivity across the lesion; in fact, most of the clinically complete SCI are not anatomically complete (Kakulas, 2004). Interestingly, we have previously observed that 7 individuals with this profile of chronic SCI (clinically

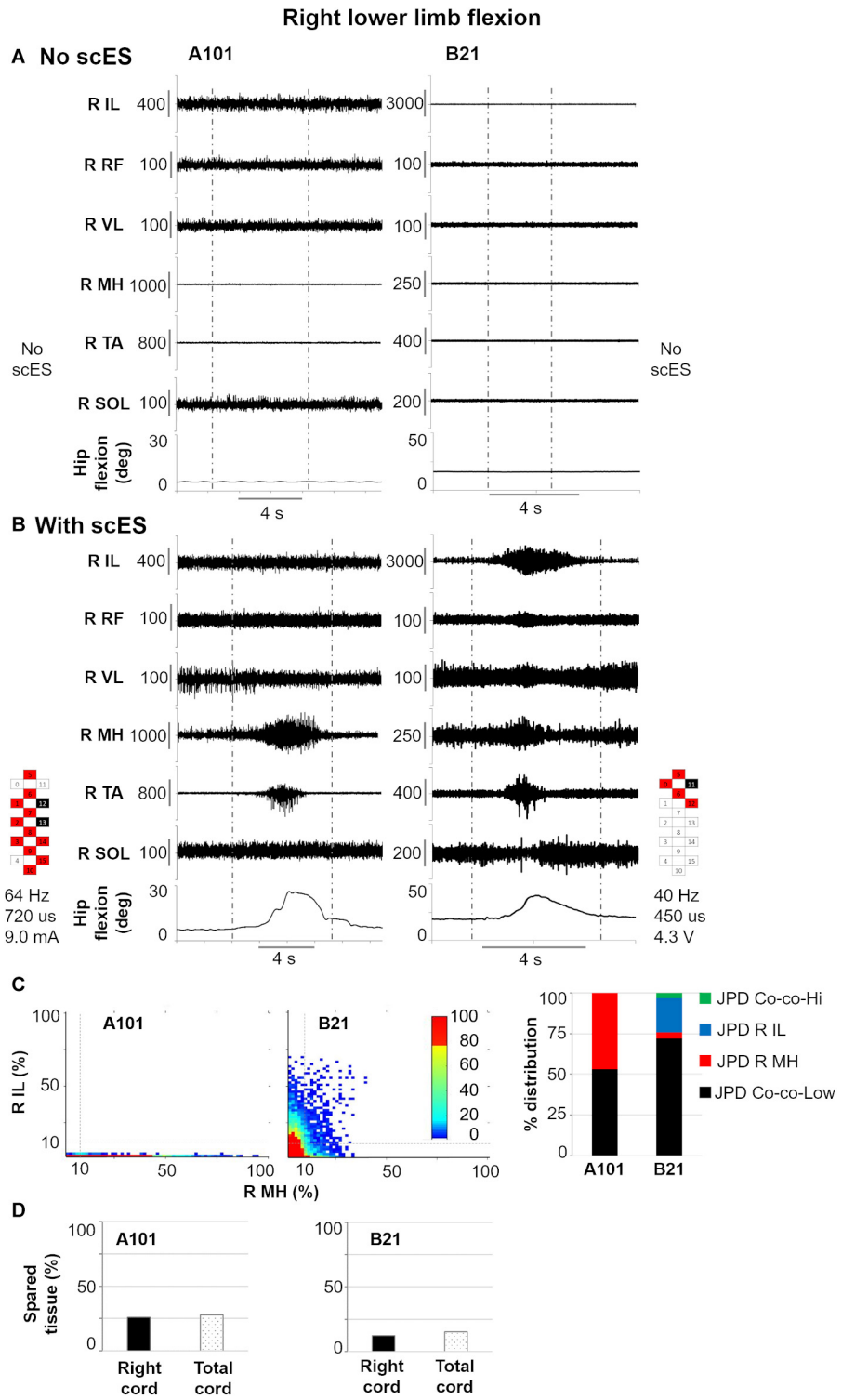

FIGURE 7 | Representative EMG activity modulation and hip joint movement during right lower limb flexion attempts performed without **(A)** and with **(B)** spinal cord epidural stimulation (scES) by two research participants (A101 and B21). Vertical gray dotted lines: attempt duration. **(C)** Probability density distribution (JPD) of normalized EMG amplitudes between right (R) iliopsoas (IL) and medial hamstrings (MH) calculated during the volitional attempts, and related data points distribution in each of the four identified areas [co-contraction at lower (JPD Co-co-Low) or higher (JPD Co-co-Hi) level of activation; isolated activation of R IL (JPD R IL) or R MH (JPD R MH)]. **(D)** Spared tissue of the right and total cord, which were found correlated with JPD R MH and JPD Co-co-Low, respectively, during right lower limb flexion attempts. RF, rectus femoris; VL, vastus lateralis; TA, tibialis anterior; SOL, soleus. Epidural stimulation electrode configuration (cathodes in black, anodes in red, inactive in white), frequency, pulse width and intensity are reported.

motor complete, without the ability to generate EMG activity in the paralyzed muscles during volitional attempts with and without reinforcement maneuvers) were able to volitionally generate meaningful leg muscles activation and movements in the presence of subthreshold levels of scES before the occurrence of any activity-based training with scES (Angeli et al., 2014, 2018).

In the present study, none of the research participants were able to modulate the baseline EMG activity of lower limb muscles by volitionally attempting to generate lower limb flexion or ankle dorsiflexion when scES was not present (**Figures 6A**, **7A**). Conversely, all individuals were able to generate meaningful volitional motor output (generation of force and movement, and/or activation of primary muscles involved in the movement attempt) when scES was present (i.e., **Figures 6B**, **7B**). The regaining of volitional lower limb muscle activation and movement has been interpreted as scES modulated the excitability of lumbosacral spinal circuitry, thus allowing the supraspinal input to travel across small and dormant spared fibers, engaging the appropriate spinal networks to generate the desired motor pattern. This perspective that low-intensity scES can "amplify" the residual supraspinal input is supported by experimental findings in a rat model, showing that the amplitude of motor potentials evoked from cortical stimulation was substantially increased in the presence of timed sub-motor threshold scES (Mishra et al., 2017). However, the volitional leg movement ability assessed in this study varied substantially across participants; in fact, volitional movement and force exertion was observed on average for 2.7 ± 1.4 motor tasks out of the 4 tested, ranging between 1 and 4 tasks for each individual. This inter-subject variability may suggest that individual-specific characteristics may play an important role in the extent of motor function recovery promoted by scES (Dietz, 1997; Hiersemenzel et al., 2000; Beauparlant et al., 2013). Herein, we have made an effort to explore this topic further, attempting to understand whether the amount of spared tissue of specific spinal cord regions is related to the recovery of lower limb volitional movement with scES.

In the present study we found that amount and location of spared spinal cord tissue at the lesion site were unrelated to the ability to generate volitional lower limb movements with scES (**Figure 4**). Residual descending inputs often undergo neuroplastic sprouting into intact pathways below the level of injury in order to communicate with their distal targets (Courtine et al., 2008; Rosenzweig et al., 2010; Asboth et al., 2018). For example, reorganization of the corticospinal system to propriospinal and brainstem pathways have been indicated in motor recovery (Courtine et al., 2008; Filli and Schwab, 2015; Asboth et al., 2018). Spinal cord sprouting of individual-specific spared tissue may have occurred in our participants, resulting in volitional lower limb motor recovery when scES is applied. Supraspinal reorganization has also been demonstrated to play a role in recovery of motor function after SCI (Winchester et al., 2005), and this is also a research avenue of interest in the context of scES. Furthermore, it is also important to acknowledge that factors other than the spared neural tissue across the lesion site play a critical role for the scES-promoted motor function recovery. For example, the appropriate selection of scES parameters, which are individual- and task-specific, crucially affects the extent and characteristics of motor recovery (Gad et al., 2013; Rejc et al., 2015; Mesbah et al., 2019; Rejc and Angeli, 2019). Additionally, recent findings also suggest that the position of the electrode array with respect to the conus tip as well as the amount of lumbosacral enlargement coverage by the electrode array concur to determine volitional lower limb movement ability in this population prior to any activity-based intervention (Ball et al., 2019).

On the other hand, we found MRI spinal cord measures related to some aspects of motor control. In primates, approximately 2% of corticospinal fibers descend ipsilaterally in the anterior corticospinal tract (Rosenzweig et al., 2009). Following SCI, lateral corticospinal tract fibers show capacity to project to this anterior column region (Steward et al., 2008), and this neuronal sprouting has been associated with functional recovery (Weidner et al., 2001). For our study, anterior spinal cord spared tissue was related to less antagonist muscle activation (i.e., lower soleus EMG amplitude) during volitional dorsiflexion attempts of the left ankle (**Table 2** and **Figure 6**), suggesting that residual descending inputs can access inhibitory pathways after severe SCI (McKay et al., 2004) when scES is applied for facilitating volitional leg movement. Neuroplastic changes of the lateral and anterior corticospinal systems may be involved in this finding; however, it is important to consider that both spinal cord MRI and volitional motor function were assessed prior to any training with scES. Hence, these potential neural adaptations would be the result of spontaneous plasticity following SCI, and/or would have been facilitated by standard rehabilitative approaches performed prior to epidural stimulation implantation. We also found the amount of isolated activation of the right medial hamstrings during lower limb flexion attempts to be significantly related to spared tissue of the ipsilateral spinal cord (**Table 2** and **Figures 5**, **7**). This result is in alignment with a previous study involving a cohort with less severe SCIs (motor incomplete), where integrity of the lateral corticospinal tract was related to ipsilateral lower limb torque production (Smith et al., 2018). For the same motor task, the amount of co-contraction at lower level of activation between right medial hamstrings and iliopsoas was inversely related with total spared tissue, suggesting that higher level of activation of either muscle, or both muscles concurrently, may be facilitated by overall greater spinal cord spared tissue. Interestingly, spared tissue in the posterior cord was not related to any motor outcome. This is in line with the anatomical perspective that the posterior column conveys light touch and non-noxious sensory afferent information. One future direction of this research is also to investigate the role of spared posterior cord tissue in sensory recovery when sES is applied. Overall, it is worth noting that spared spinal cord tissue characteristics at the lesion site were conceivably related to residual descending inputs that affected some aspects of motor coordination (i.e., inhibition of antagonist muscles; muscle activation synergies) rather than directly and solely affecting the level of excitability of motor pools primarily involved in the attempted motor task. This observation seems interesting in the context of motor recovery after SCI, as previous evidence suggests that improving intra- and inter-limb coordination of motor

pools is a primary adaptation in the process of re-learning to perform a motor task (Edgerton and Roy, 2009). For example, the progression from inability to achieve volitional muscle activation, to the co-activation of agonist, antagonist and distant muscles, to a more refined, task-specific activation pattern and movement generation has been observed following long-term activity based training with scES (Rejc et al., 2017a) as well as in individuals with incomplete SCI (McKay et al., 2011), suggesting the occurrence of neural reorganization involving inhibitory and excitatory interneurons. Locomotor training, which can promote significant motor recovery after incomplete SCI, also results in significant activity-dependent plasticity involving inhibitory interneurons (Knikou et al., 2015).

Limits of the Study

The imaging approach in the present study has been recently applied to an incomplete spinal cord injury cohort, with lateral corticospinal tract regions correlating with their corresponding lower extremity motor output, and a high level of reliability (Smith et al., 2018). Also, similar methods using the Spinal Cord Toolbox have been applied to a cohort of acute myelitis (McCoy et al., 2017). However, an intrinsic limitation of these imaging approaches is that they provide an *estimate* of spinal cord damage location based on MRI. MRI can provide high-resolution volumetric information with excellent visualization of the lesion hyperintensity. However, the spinal cord lesion itself distorts the spinal cord dimensions in the axial plane, and the majority of the participants had undergone spinal cord fusion with implanted metallic surgical hardware, which can also cause imaging artifacts (Hargreaves et al., 2011). Importantly, none of the participants of the present study had visible imaging artifacts extending into the spinal cord; nevertheless, cord distortions could influence the accuracy of the white matter atlas registration and the localization of the lesion to the respective white matter tracts (Talbott et al., 2019). Also, for this study we used available clinical scans which had moderate resolution yet may not be able to detect minute amounts of spared tissue, as we observed that one individual with estimated 0% spared tissue achieved one volitional movement out of the four attempted tasks. Future studies applying image acquisition methods with higher spatial resolution (<1 mm^3) and reduced susceptibility to metal as well as improved image analysis methods will further enhance our ability to localize and quantify the lesion after SCI with quantitative spinal cord MRI (Alley et al., 2018; Shi et al., 2019).

Additionally, the epidural stimulation implants utilized in this study are not 3T-MRI compatible. This does not allow the assessment of the same research participants longitudinally in order to investigate the effects of activity-based training with scES on the neural tissue at the lesion site, possibly elucidating which neural adaptations might be related to the training-induced improvements of lower limb volitional motor control.

As discussed above, the selection of stimulation parameters plays a critical role in characterizing the motor pattern promoted by scES. Each research participant underwent between 1 and 3 experimental sessions aimed at defining appropriate stimulation parameters prior to assessing volitional leg movement ability. While this procedure followed consistent guidelines and was performed by two operators with similar and extensive expertise in the field, it is possible that the level of optimization of scES parameters might have been slightly differed across participants.

In conclusion, the amount and location of spared spinal cord tissue at the lesion site were not related to the ability to generate epidural stimulation-promoted volitional joint movement and/or force exertion during attempts to flex the lower limb and dorsiflex the ankle in individuals with chronic motor complete SCI prior to any activity-based training. On the other hand, spared tissue of specific cord regions were related to some aspects of motor control. These findings may suggest that supraspinal inputs through spared spinal cord regions that differ across individuals can result in the generation of lower limb volitional movements prior to any training when epidural stimulation is provided. Future studies aimed at detailing the spared tissue of specific white matter pathways using higher resolution MRI, and pairing imaging and neurophysiology markers appear important to provide further mechanistic insights on the recovery of volitional leg movements as well as other motor functions (i.e., standing and stepping) promoted by epidural stimulation after severe spinal cord injury.

DATA AVAILABILITY STATEMENT

The raw data supporting the conclusions of this article will be made available by the authors, without undue reservation, to any qualified researcher.

ETHICS STATEMENT

The studies involving human participants were reviewed and approved by the Institutional Review Board at the University of Louisville. The patients/participants provided their written informed consent to participate in this study.

AUTHOR CONTRIBUTIONS

ER and AS contributed to the study conception. ER, AS, SH, and CA contributed to the study design. RB and MN contributed to spinal cord MRI collection. MB performed epidural stimulation implantation. CA, SH, and ER contributed to voluntary movement data collection and analysis. AS, KW, and RB contributed to spinal cord MRI analysis. BU contributed to the statistical analysis. ER, AS, KW, and RB created the figures. ER, AS, and KW wrote the first draft of the manuscript. All authors contributed to the interpretation of results, revised the manuscript and approved its final version.

FUNDING

This work was supported by the Christopher and Dana Reeve Foundation, the Leona M. and Harry B. Helmsley Charitable Trust, Craig H. Nielsen Foundation, University of Louisville Hospital; and Medtronic plc. AS and KW were

supported by the Eunice Kennedy Shriver National Institute of Child Health and Human Development under award number R03HD094577. KW was also supported by the National Institute of Neurological Disorders and Stroke under award nos. K23NS104211 and L30NS108301.

ACKNOWLEDGMENTS

We thank the research volunteers for their valuable contribution to this study. We also gratefully acknowledge our research staff for their contribution to the data collection, and our training staff for their support of the research volunteers; Drs. Sarah Wagers, Darryl Kaelin, Glenn Hirsh, Douglas Stevens, and Camilo Castillo for medical oversight; Yukishia Austin, Lynn Robbins, Kristen Johnson, Hye Conner, and Gretchen Carolan for medical management.

SUPPLEMENTARY MATERIAL

The Supplementary Material for this article can be found online at: https://www.frontiersin.org/articles/10.3389/fnsys.2020.559313/full#supplementary-material

Supplementary Table 1 | Spinal cord MRI collection parameters utilized for each research participant.

Supplementary Figure 1 | Wallerian degeneration. **(A,C)** Sagittal and axial T2 Turbo spin-echo images through the spinal cord at the C2 level (yellow line), above a long segment injury from C4 to C6. The arrow points to wedge-shaped T2 hyperintensity at the dorsal columns. The signal extends linearly slightly anterior to the center of the cord. **(B,D)**. Sagittal and axial T2 Turbo spin-echo images through the spinal cord at the C4-5 level in a different subject, above a T1–T2 injury. The dorsal column T2 hyperintensity is less wedge-shaped in this subject and linear T2 hyperintensity extends to the anterior surface of the cord.

Supplementary Table 2 | Motor outcomes considered for analysis.

REFERENCES

Aarabi, B., Sansur, C. A., Ibrahimi, D. M., Simard, J. M., Hersh, D. S., Le, E., et al. (2017). Intramedullary lesion length on postoperative magnetic resonance imaging is a strong predictor of ASIA impairment scale grade conversion following decompressive surgery in cervical spinal cord injury. *Neurosurgery* 80, 610–620. doi: 10.1093/neuros/nyw053

Alley, S., Gilbert, G., Wheeler-Kingshott, C. G., Samson, R. S., Grussu, F., Martin, A., et al. (2018). "Consensus acquisition protocol for quantitative MRI of the cervical spinal cord at 3T," in *Joint Annual Meeting International Society for Magnetic Resonance in Medicine – European Society for Magnetic Resonance in Medicine and Biology*, (Fira de Barcelona: ESMRMB).

Angeli, C. A., Boakye, M., Morton, R. A., Vogt, J., Benton, K., Chen, Y., et al. (2018). Recovery of over-ground walking after chronic motor complete spinal cord injury. *N. Engl. J. Med.* 379, 1244–1250. doi: 10.1056/NEJMoa1803588

Angeli, C. A., Edgerton, V. R., Gerasimenko, Y. P., and Harkema, S. J. (2014). Altering spinal cord excitability enables voluntary movements after chronic complete paralysis in humans. *Brain* 137(Pt 5), 1394–1409. doi: 10.1093/brain/awu038

Asboth, L., Friedli, L., Beauparlant, J., Martinez-Gonzalez, C., Anil, S., Rey, E., et al. (2018). Cortico-reticulo-spinal circuit reorganization enables functional recovery after severe spinal cord contusion. *Nat. Neurosci.* 21, 576–588. doi: 10.1038/s41593-018-0093-5

Ball, T., Angeli, C. A., Rejc, E., Mesbah, S., Harkema, S., and Boakye, M. (2019). "Correlation of radiographic spinal cord parameters with volitional movement after spinal cord epidural stimulation for chronic traumatic spinal cord injury," in *Proceedings of the Annual Meeting Society for Neuroscience*, (Chicago, IL: Society for Neuroscience).

Beauparlant, J., van den Brand, R., Barraud, Q., Friedli, L., Musienko, P., Dietz, V., et al. (2013). Undirected compensatory plasticity contributes to neuronal dysfunction after severe spinal cord injury. *Brain* 136(Pt 11), 3347–3361. doi: 10.1093/brain/awt204

Burns, S., Biering-Sorensen, F., Donovan, W., Graves, D. E., Jha, A., Johansen, M., et al. (2012). International standards for neurological classification of spinal cord injury, revised 2011. *Top. Spinal Cord Inj. Rehabil.* 18, 85–99. doi: 10.1310/sci1801-85

Cloney, M. B., Smith, Z. A., Weber, K. A. II, and Parrish, T. B. (2018). Quantitative magnetization transfer MRI measurements of the anterior spinal cord region are associated with clinical outcomes in cervical spondylotic myelopathy. *Spine (Phila Pa 1976)* 43, 675–680. doi: 10.1097/brs.0000000000002470

Cote, M. P., Murray, M., and Lemay, M. A. (2017). Rehabilitation strategies after spinal cord injury: inquiry into the mechanisms of success and failure. *J. Neurotrauma* 34, 1841–1857. doi: 10.1089/neu.2016.4577

Courtine, G., Song, B., Roy, R. R., Zhong, H., Herrmann, J. E., Ao, Y., et al. (2008). Recovery of supraspinal control of stepping via indirect propriospinal relay connections after spinal cord injury. *Nat. Med.* 14, 69–74. doi: 10.1038/nm1682

Crinion, J., Ashburner, J., Leff, A., Brett, M., Price, C., and Friston, K. (2007). Spatial normalization of lesioned brains: performance evaluation and impact on fMRI analyses. *Neuroimage* 37, 866–875. doi: 10.1016/j.neuroimage.2007.04.065

Darrow, D., Balser, D., Netoff, T. I., Krassioukov, A., Phillips, A., Parr, A., et al. (2019). Epidural spinal cord stimulation facilitates immediate restoration of dormant motor and autonomic supraspinal pathways after chronic neurologically complete spinal cord injury. *J. Neurotrauma* 36, 2325–2336. doi: 10.1089/neu.2018.6006

De Leener, B., Fonov, V. S., Collins, D. L., Callot, V., Stikov, N., and Cohen-Adad, J. (2018). PAM50: unbiased multimodal template of the brainstem and spinal cord aligned with the ICBM152 space. *Neuroimage* 165, 170–179. doi: 10.1016/j.neuroimage.2017.10.041

De Leener, B., Levy, S., Dupont, S. M., Fonov, V. S., Stikov, N., Louis Collins, D., et al. (2017). SCT: spinal cord toolbox, an open-source software for processing spinal cord MRI data. *Neuroimage* 145(Pt A), 24–43. doi: 10.1016/j.neuroimage.2016.10.009

Dietz, V. (1997). Neurophysiology of gait disorders: present and future applications. *Electroencephalogr. Clin. Neurophysiol.* 103, 333–355. doi: 10.1016/s0013-4694(97)00047-7

Dimitrijevic, M. R. (1988). Residual motor functions in spinal cord injury. *Adv. Neurol.* 47, 138–155.

Dimitrijevic, M. R., Dimitrijevic, M. M., Faganel, J., and Sherwood, A. M. (1984). Suprasegmentally induced motor unit activity in paralyzed muscles of patients with established spinal cord injury. *Ann. Neurol.* 16, 216–221. doi: 10.1002/ana.410160208

Dupont, S. M., De Leener, B., Taso, M., Le Troter, A., Nadeau, S., Stikov, N., et al. (2017). Fully-integrated framework for the segmentation and registration of the spinal cord white and gray matter. *Neuroimage* 150, 358–372. doi: 10.1016/j.neuroimage.2016.09.026

Edgerton, V. R., and Roy, R. R. (2009). Robotic training and spinal cord plasticity. *Brain Res. Bull.* 78, 4–12. doi: 10.1016/j.brainresbull.2008.09.018

Edgerton, V. R., Tillakaratne, N. J., Bigbee, A. J., de Leon, R. D., and Roy, R. R. (2004). Plasticity of the spinal neural circuitry after injury. *Annu. Rev. Neurosci.* 27, 145–167.

Filli, L., and Schwab, M. E. (2015). Structural and functional reorganization of propriospinal connections promotes functional recovery after spinal cord injury. *Neural Regen. Res.* 10, 509–513. doi: 10.4103/1673-5374.155425

Flanders, A. E., Spettell, C. M., Tartaglino, L. M., Friedman, D. P., and Herbison, G. J. (1996). Forecasting motor recovery after cervical spinal cord injury: value of MR imaging. *Radiology* 201, 649–655. doi: 10.1148/radiology.201.3.8939210

Fonov, V. S., Le Troter, A., Taso, M., De Leener, B., Leveque, G., Benhamou, M., et al. (2014). Framework for integrated MRI average of the spinal cord white and gray matter: the MNI-Poly-AMU template. *Neuroimage* 102(Pt 2), 817–827. doi: 10.1016/j.neuroimage.2014.08.057

Freund, P., Seif, M., Weiskopf, N., Friston, K., Fehlings, M. G., Thompson, A. J., et al. (2019). MRI in traumatic spinal cord injury: from clinical assessment to

neuroimaging biomarkers. *Lancet Neurol.* 18, 1123–1135. doi: 10.1016/s1474-4422(19)30138-3

Gad, P., Choe, J., Nandra, M. S., Zhong, H., Roy, R. R., Tai, Y. C., et al. (2013). Development of a multi-electrode array for spinal cord epidural stimulation to facilitate stepping and standing after a complete spinal cord injury in adult rats. *J. Neuroeng. Rehabil.* 10:2.

Grahn, P. J., Lavrov, I. A., Sayenko, D. G., Van Straaten, M. G., Gill, M. L., Strommen, J. A., et al. (2017). Enabling task-specific volitional motor functions via spinal cord neuromodulation in a human with paraplegia. *Mayo Clin. Proc.* 92, 544–554. doi: 10.1016/j.mayocp.2017.02.014

Hargreaves, B. A., Worters, P. W., Pauly, K. B., Pauly, J. M., Koch, K. M., and Gold, G. E. (2011). Metal-induced artifacts in MRI. *AJR Am. J. Roentgenol.* 197, 547–555. doi: 10.2214/ajr.11.7364

Harkema, S., Gerasimenko, Y., Hodes, J., Burdick, J., Angeli, C., Chen, Y., et al. (2011). Effect of epidural stimulation of the lumbosacral spinal cord on voluntary movement, standing, and assisted stepping after motor complete paraplegia: a case study. *Lancet* 377, 1938–1947. doi: 10.1016/S0140-6736(11)60547-3

Harkema, S. J. (2008). Plasticity of interneuronal networks of the functionally isolated human spinal cord. *Brain Res. Rev.* 57, 255–264. doi: 10.1016/j.brainresrev.2007.07.012

Hastie, T., Tibshirani, R. J., and Friedman, J. (2009). *The Elements of Statistical Learning*. Berlin: Springer Series in Statistics.

Hiersemenzel, L. P., Curt, A., and Dietz, V. (2000). From spinal shock to spasticity: neuronal adaptations to a spinal cord injury. *Neurology* 54, 1574–1582. doi: 10.1212/wnl.54.8.1574

Huber, E., Lachappelle, P., Sutter, R., Curt, A., and Freund, P. (2017). Are midsagittal tissue bridges predictive of outcome after cervical spinal cord injury? *Ann. Neurol.* 81, 740–748. doi: 10.1002/ana.24932

Hutchison, D. L., Roy, R. R., Bodine-Fowler, S. C., Hodgson, J. A., and Edgerton, V. R. (1989). Electromyographic (EMG) amplitude patterns in the proximal and distal compartments of the cats semitendinosus during various motor tasks. *Brain Res.* 479, 56–64. doi: 10.1016/0006-8993(89)91335-8

Kakulas, B. A. (2004). Neuropathology: the foundation for new treatments in spinal cord injury. *Spinal Cord* 42, 549–563. doi: 10.1038/sj.sc.3101670

Knikou, M., Smith, A. C., and Mummidisetty, C. K. (2015). Locomotor training improves reciprocal and nonreciprocal inhibitory control of soleus motoneurons in human spinal cord injury. *J. Neurophysiol.* 113, 2447–2460. doi: 10.1152/jn.00872.2014

Kursa, M. B., and Rudnicki, M. A. (2010). Feature selection with the boruta package. *J. Statis. Softw.* 36:30746.

McCoy, D. B., Talbott, J. F., Wilson, M., Mamlouk, M. D., Cohen-Adad, J., Wilson, M., et al. (2017). MRI atlas-based measurement of spinal cord injury predicts outcome in acute flaccid myelitis. *AJNR Am. J. Neuroradiol.* 38, 410–417. doi: 10.3174/ajnr.A5044

McKay, W. B., Lim, H. K., Priebe, M. M., Stokic, D. S., and Sherwood, A. M. (2004). Clinical neurophysiological assessment of residual motor control in post-spinal cord injury paralysis. *Neurorehabil. Neural Repair* 18, 144–153. doi: 10.1177/0888439004267674

McKay, W. B., Ovechkin, A. V., Vitaz, T. W., Terson de Paleville, D. G., and Harkema, S. J. (2011). Neurophysiological characterization of motor recovery in acute spinal cord injury. *Spinal Cord* 49, 421–429. doi: 10.1038/sc.2010.145

Mesbah, S., Angeli, C. A., Keynton, R. S., El-baz, A., and Harkema, S. J. (2017). A novel approach for automatic visualization and activation detection of evoked potentials induced by epidural spinal cord stimulation in individuals with spinal cord injury. *PLoS One* 12:e0185582. doi: 10.1371/journal.pone.0185582

Mesbah, S., Gonnelli, F., Angeli, C. A., El-Baz, A., Harkema, S. J., and Rejc, E. (2019). Neurophysiological markers predicting recovery of standing in humans with chronic motor complete spinal cord injury. *Sci. Rep.* 9:14474. doi: 10.1038/s41598-019-50938-y

Mishra, A. M., Pal, A., Gupta, D., and Carmel, J. B. (2017). Paired motor cortex and cervical epidural electrical stimulation timed to converge in the spinal cord promotes lasting increases in motor responses. *J. Physiol.* 595, 6953–6968. doi: 10.1113/jp274663

Miyanji, F., Furlan, J. C., Aarabi, B., Arnold, P. M., and Fehlings, M. G. (2007). Acute cervical traumatic spinal cord injury: MR imaging findings correlated with neurologic outcome–prospective study with 100 consecutive patients. *Radiology* 243, 820–827. doi: 10.1148/radiol.2433060583

O'Dell, D. R., Weber, K. A., Berliner, J. C., Elliott, J. M., Connor, J. R., Cummins, D. P., et al. (2018). Midsagittal tissue bridges are associated with walking ability in incomplete spinal cord injury: a magnetic resonance imaging case series. *J. Spinal Cord Med.* 43, 268–271. doi: 10.1080/10790268.2018.1527079

R Core Team, (2019). *R: A Language and Environment for Statistical Computing*. Vienna: R Foundation for Statistical Computing.

Rejc, E., Angeli, C., and Harkema, S. (2015). Effects of lumbosacral spinal cord epidural stimulation for standing after chronic complete paralysis in humans. *PLoS One* 10:e0133998. doi: 10.1371/journal.pone.0133998

Rejc, E., and Angeli, C. A. (2019). Spinal cord epidural stimulation for lower limb motor function recovery in individuals with motor complete spinal cord injury. *Phys. Med. Rehabil. Clin. N. Am.* 30, 337–354. doi: 10.1016/j.pmr.2018.12.009

Rejc, E., Angeli, C. A., Atkinson, D., and Harkema, S. J. (2017a). Motor recovery after activity-based training with spinal cord epidural stimulation in a chronic motor complete paraplegic. *Sci. Rep.* 7:13476. doi: 10.1038/s41598-017-14003-w

Rejc, E., Angeli, C. A., Bryant, N., and Harkema, S. J. (2017b). Effects of stand and step training with epidural stimulation on motor function for standing in chronic complete paraplegics. *J. Neurotrauma* 34, 1787–1802. doi: 10.1089/neu.2016.4516

Rosenzweig, E. S., Brock, J. H., Culbertson, M. D., Lu, P., Moseanko, R., Edgerton, V. R., et al. (2009). Extensive spinal decussation and bilateral termination of cervical corticospinal projections in rhesus monkeys. *J. Comp. Neurol.* 513, 151–163. doi: 10.1002/cne.21940

Rosenzweig, E. S., Courtine, G., Jindrich, D. L., Brock, J. H., Ferguson, A. R., Strand, S. C., et al. (2010). Extensive spontaneous plasticity of corticospinal projections after primate spinal cord injury. *Nat. Neurosci.* 13, 1505–1510. doi: 10.1038/nn.2691

Sayenko, D. G., Angeli, C., Harkema, S. J., Edgerton, V. R., and Gerasimenko, Y. P. (2014). Neuromodulation of evoked muscle potentials induced by epidural spinal-cord stimulation in paralyzed individuals. *J. Neurophysiol.* 111, 1088–1099. doi: 10.1152/jn.00489.2013

Shi, X., Levine, E., Weber, H., and Hargreaves, B. A. (2019). Accelerated imaging of metallic implants using model-based nonlinear reconstruction. *Magn. Reson. Med.* 81, 2247–2263. doi: 10.1002/mrm.27536

Smith, A. C., Weber, K. A. II, O'Dell, D. R., Parrish, T. B., Wasielewski, M., and Elliott, J. M. (2018). Lateral corticospinal tract damage correlates with motor output in incomplete spinal cord injury. *Arch. Phys. Med. Rehabil.* 99, 660–666. doi: 10.1016/j.apmr.2017.10.002

Smith, A. C., Weber, K. A., Parrish, T. B., Hornby, T. G., Tysseling, V. M., McPherson, J. G., et al. (2017). Ambulatory function in motor incomplete spinal cord injury: a magnetic resonance imaging study of spinal cord edema and lower extremity muscle morphometry. *Spinal Cord* 55, 672–678. doi: 10.1038/sc.2017.18

Steward, O., Zheng, B., Tessier-Lavigne, M., Hofstadter, M., Sharp, K., and Yee, K. M. (2008). Regenerative growth of corticospinal tract axons via the ventral column after spinal cord injury in mice. *J. Neurosci.* 28, 6836–6847. doi: 10.1523/jneurosci.5372-07.2008

Talbott, J. F., Huie, J. R., Ferguson, A. R., Bresnahan, J. C., Beattie, M. S., and Dhall, S. S. (2019). MR imaging for assessing injury severity and prognosis in acute traumatic spinal cord injury. *Radiol. Clin. N. Am.* 57, 319–339. doi: 10.1016/j.rcl.2018.09.004

Talbott, J. F., Whetstone, W. D., Readdy, W. J., Ferguson, A. R., Bresnahan, J. C., Saigal, R., et al. (2015). The brain and spinal injury center score: a novel, simple, and reproducible method for assessing the severity of acute cervical spinal cord injury with axial T2-weighted MRI findings. *J. Neurosurg. Spine* 23, 495–504. doi: 10.3171/2015.1.Spine141033

Vallotton, K., Huber, E., Sutter, R., Curt, A., Hupp, M., and Freund, P. (2019). Width and neurophysiologic properties of tissue bridges predict recovery after cervical injury. *Neurology* 92, e2793–e2802. doi: 10.1212/wnl.0000000000007642

Wagner, F. B., Mignardot, J. B., Le Goff-Mignardot, C. G., Demesmaeker, R., Komi, S., Capogrosso, M., et al. (2018). Targeted neurotechnology restores walking in

humans with spinal cord injury. *Nature* 563, 65–71. doi: 10.1038/s41586-018-0649-2

Weidner, N., Ner, A., Salimi, N., and Tuszynski, M. H. (2001). Spontaneous corticospinal axonal plasticity and functional recovery after adult central nervous system injury. *Proc. Natl. Acad. Sci. U.S.A.* 98, 3513–3518. doi: 10.1073/pnas.051626798

Winchester, P., McColl, R., Querry, R., Foreman, N., Mosby, J., Tansey, K., et al. (2005). Changes in supraspinal activation patterns following robotic locomotor therapy in motor-incomplete spinal cord injury. *Neurorehabil. Neural Repair* 19, 313–324. doi: 10.1177/1545968305281515

Conflict of Interest: The authors declare that the research was conducted in the absence of any commercial or financial relationships that could be construed as a potential conflict of interest.

frontiers in Neuroscience

ORIGINAL RESEARCH
published: 22 October 2020
doi: 10.3389/fnins.2020.554018

Beneficial Cardiac Structural and Functional Adaptations After Lumbosacral Spinal Cord Epidural Stimulation and Task-Specific Interventions: A Pilot Study

*Bonnie E. Legg Ditterline[1,2], Shelley Wade[1], Beatrice Ugiliweneza[1,2], Narayana Sarma Singam[3], Susan J. Harkema[1,2], Marcus F. Stoddard[3] and Glenn A. Hirsch[3,4]**

[1] Kentucky Spinal Cord Injury Research Center, University of Louisville, Louisville, KY, United States, [2] Department of NeuroSurgery, University of Louisville, Louisville, KY, United States, [3] Division of Cardiovascular Medicine, Department of Medicine, University of Louisville, Louisville, KY, United States, [4] Division of Cardiology, Department of Medicine, National Jewish Health, Denver, CO, United States

OPEN ACCESS

Edited by:
Ronaldo M. Ichiyama, University of Leeds, United Kingdom

Reviewed by:
Nobuhiro Watanabe, Tokyo Metropolitan Institute of Gerontology, Japan
Eberhard Weihe, Philipps-University of Marburg, Germany

***Correspondence:**
Glenn A. Hirsch
HirschG@NJHealth.org

Specialty section:
This article was submitted to Autonomic Neuroscience, a section of the journal Frontiers in Neuroscience

Received: *20 April 2020*
Accepted: *15 September 2020*
Published: *22 October 2020*

Citation:
Legg Ditterline BE, Wade S, Ugiliweneza B, Singam NS, Harkema SJ, Stoddard MF and Hirsch GA (2020) Beneficial Cardiac Structural and Functional Adaptations After Lumbosacral Spinal Cord Epidural Stimulation and Task-Specific Interventions: A Pilot Study. Front. Neurosci. 14:554018. doi: 10.3389/fnins.2020.554018

Cardiac myocyte atrophy and the resulting decreases to the left ventricular mass and dimensions are well documented in spinal cord injury. Therapeutic interventions that increase preload can increase the chamber size and improve the diastolic filling ratios; however, there are no data describing cardiac adaptation to chronic afterload increases. Research from our center has demonstrated that spinal cord epidural stimulation (scES) can normalize arterial blood pressure, so we decided to investigate the effects of scES on cardiac function using echocardiography. Four individuals with chronic, motor-complete cervical spinal cord injury were implanted with a stimulator over the lumbosacral enlargement. We assessed the cardiac structure and function at the following time points: (a) prior to implantation; (b) after scES targeted to increase systolic blood pressure; (c) after the addition of scES targeted to facilitate voluntary (i.e., with intent) movement of the trunk and lower extremities; and (d) after the addition of scES targeted to facilitate independent, overground standing. We found significant improvements to the cardiac structure (left ventricular mass = 10 ± 2 g, $p < 0.001$; internal dimension during diastole = 0.1 ± 0.04 cm, $p < 0.05$; internal dimension during systole = 0.06 ± 0.03 cm, $p < 0.05$; interventricular septum dimension = 0.04 ± 0.02 cm, $p < 0.05$), systolic function (ejection fraction = 1 ± 0.4%, $p < 0.05$; velocity time integral = 2 ± 0.4 cm, $p < 0.001$; stroke volume = 4.4 ± 1.5 ml, $p < 0.01$), and diastolic function (mitral valve deceleration time = -32 ± 11 ms, $p < 0.05$; mitral valve deceleration slope = 50 ± 25 cm s^{-1}, $p < 0.05$; isovolumic relaxation time = −6 ± 1.9 ms, $p < 0.05$) with each subsequent scES intervention. Despite the pilot nature of this study, statistically significant improvements to the cardiac structure, systolic function, and diastolic function demonstrate that scES combined with task-specific interventions led to beneficial cardiac remodeling, which can reverse

atrophic changes that result from spinal cord injury. Long-term improvements to cardiac function have implications for increased quality of life and improved cardiovascular health in individuals with spinal cord injury, decreasing the risk of cardiovascular morbidity and mortality.

Keywords: spinal cord injury, epidural stimulation, cardiac structure and function, systolic function, diastolic function, left ventricular structure

INTRODUCTION

Cardiac myocyte atrophy and the resulting decreases to the left ventricular mass and dimensions are well documented in spinal cord injury (Kessler et al., 1986; Eysmann et al., 1995; Gondim et al., 2004; Claydon et al., 2006; de Groot et al., 2006; Matos-Souza et al., 2011; Hostettler et al., 2012; Driussi et al., 2014; Williams et al., 2019). There is evidence that these reduced structural outcomes result from persistent decreases to preload and afterload: chronic skeletal muscle unloading can rapidly decrease the left ventricular volumes, mass, and contraction velocity in able-bodied and individuals with spinal cord injury (Arbeille et al., 2001; Meck et al., 2001; Martin et al., 2002; Summers et al., 2005; Giangregorio and McCartney, 2006; Platts et al., 2009; Moore et al., 2018). Decreased functional outcomes can be caused by sympathetic impairment, such that cardiac response during stress or exercise is significantly diminished in individuals with spinal cord injury when compared with able-bodied individuals (Teasell et al., 2000; Furlan et al., 2003; Grigorean et al., 2009; Theisen, 2012; Bartholdy et al., 2014; Wecht and Bauman, 2018). Therapeutic interventions that increase preload can increase the chamber size and improve the diastolic filling ratios in individuals with spinal cord injury, while athletes with spinal cord injury demonstrate greater left ventricle dimensions and improved relaxation velocities. This suggests that structural decreases in spinal cord injury are dynamic and can adapt to exercise interventions similar to non-injured individuals (Nash et al., 1991; Turiel et al., 2011; Maggioni et al., 2012; Guilherme et al., 2014). However, there are no data describing cardiac adaptation to interventions that lead to chronic afterload increases in individuals with spinal cord injury. Vascular stiffening and systemic inflammation are common in spinal cord injury, all of which can ultimately increase afterload and are implicated in diastolic dysfunction in able-bodied individuals (Bauman and Spungen, 2007, 2008; Gibson et al., 2008; West et al., 2013). Investigation of cardiac adaptation to increased afterload is therefore necessary, particularly as new research from our center has demonstrated that spinal cord epidural stimulation (scES) can normalize arterial blood pressure and mitigate orthostatic hypotension (Aslan et al., 2018; Harkema et al., 2018a; Legg Ditterline et al., 2020). Restoration of cardiovascular function at rest and during orthostatic stress would dramatically increase cardiac demand as individuals with spinal cord injury live with cardiac adaptation to persistent hypotension (Ditterline et al., 2020). Thus, we decided to investigate the effects of scES on cardiac structure and function. We hypothesized, first, that scES targeted to alleviate hypotension would lead to alterations in cardiac structure and function due to greater afterload from increased arterial blood pressure, reported previously (Aslan et al., 2018; Harkema et al., 2018a,b), and, second, that the addition of non-weight-bearing and weight-bearing motor interventions would alter the cardiac structure and function outcomes due to increased preload from the activation of the lower extremity and trunk muscles, with weight-bearing interventions eliciting the greatest improvements.

MATERIALS AND METHODS

Participants

Included in this study were four individuals (three males and one female) with chronic, cervical motor-complete spinal cord injury (**Table 1**). Individuals were clinically stable, presented with orthostatic hypotension, persistent low resting blood pressure, and periodic symptoms of autonomic dysreflexia without evidence of cardiovascular disease unrelated to spinal cord injury. This research study was approved by the University of Louisville Institutional Review Board in accordance with the Declaration of Helsinki. Individuals provided written informed consent in order to participate (NCT-02037620).

Echocardiography

Individuals lay in the left lateral decubitus position and were given sufficient time to acclimate prior to recording. Brachial blood pressure was recorded from the right arm. Individuals did not consume caffeine, alcohol, nicotine, or blood pressure medication the morning of the exam; they did not use scES for at least 12 h prior to acquisition to limit the residual effects of stimulation on the cardiovascular system. Assessments were repeated twice, with 2–4 days in between, to account for changes in volume related to variability in blood pressure. Registered diagnostic cardiac sonographers recorded images on a Philips EPIQ 7 ultrasound system with a Philips X5-1 MHz xMATRIX array transducer or a GE LOGIQ P6 ultrasound system with a GE 3Sp-D phased array transducer. Images were obtained in the parasternal long axis, parasternal short axis, and apical two-, three-, four-, and five-chamber views according to

TABLE 1 | Demographic characteristics of the individuals at implant.

ID	Age range (years)	Time since injury (years)	Level	AIS
A41	21–25	7.2	C4	A
A68	31–35	3.8	C5	A
A80	31–35	7.9	C6	A
B21	31–35	6.9	C4	B

AIS, American Spinal Injury Association impairment scale.

the standards and recommendations of the American Society of Echocardiography (Lang et al., 2015; Nagueh et al., 2016). Aortic, left ventricular, and left atrial dimensions were obtained using two-dimensional guided M-mode echocardiography. Left ventricular outflow velocities were measured using pulsed-wave Doppler recorded from the left ventricular outflow tract. Mitral inflow velocities during early (E-wave) and late (A-wave) diastole were recorded from the mitral valve leaflet tips using pulsed-wave Doppler. The isovolumic relaxation time was measured as the time between aortic valve closure and mitral valve opening. The myocardial peak systolic (s') and early diastolic (e') contraction velocities were measured using tissue Doppler imaging (TDI) in the lateral and septal annulus. Four consecutive cardiac cycles were recorded for off-line analysis.

Images were accepted for analysis according to the standards and recommendations of the American Society of Echocardiography (Lang et al., 2015; Nagueh et al., 2016). End-systolic volume, end-diastolic volume, and ejection fraction were calculated using Simpson's biplane method of discs from the apical two- and four-chamber views. Cardiac output and stroke volume were calculated from the left ventricular outflow tract diameter and the velocity time integral (VTI) of blood flow measured from the parasternal long axis and five-chamber views, respectively. Left ventricular mass was estimated from the internal diastolic diameter, posterior wall dimension, and septal dimension (Schiller et al., 1989). Relative wall thickness of the left ventricle is calculated as the ratio of twice the posterior wall dimension to the internal diastolic diameter. Left atrial filling pressure was calculated as ($1.24^{*}E/e'$ ratio) +1.9 (Nagueh et al., 1997). Global longitudinal strain was calculated from the apical two-, three-, and four-chamber views. Global circumferential strain was measured from the parasternal short-axis view at basal, mid-, and apical depths.

Implantation and Interventions

A 16-electrode array (5-6-5 Specify, Medtronic) was implanted under the T11-L1 vertebrae, spanning spinal cord segments L1–S1, as previously described (Harkema et al., 2011). Stimulation parameters, including electrode polarity, voltage, frequency, and pulse width, were unique to each individual and each intervention (below). We assessed the effects of scES interventions on cardiac function at the following time points (**Figure 1**): (a) prior to implantation; (b) after scES targeted to normalize systolic blood pressure (CV scES) (Harkema et al., 2018a,b); (c) after the addition of scES targeted to facilitate voluntary (i.e., with intent) movement of the trunk and lower extremities (Voluntary scES) (Angeli et al., 2014); and (d) after the addition of scES targeted to facilitate independent, overground standing (Stand scES) (Rejc et al., 2015). To prevent the reversal of functional gains between time points, interventions were added sequentially as individuals progressed through the study (**Table 2**). During the CV scES intervention, individuals trained only with CV scES. During the Voluntary scES intervention, individuals added in Voluntary scES and CV scES training sessions for a total of 4 h of stimulation each day. During the Stand scES intervention, individuals added Stand scES to Voluntary scES and CV scES training sessions, for a total of 5 h of stimulation each day. Individuals were given 1–4 h to rest in between scES sessions to minimize fatigue.

The stimulation parameters for CV scES were identified specifically to increase systolic blood pressure within a normative range (105–120 mmHg) without activation of the skeletal muscle, demonstrated by the absence of EMG activity (Harkema et al., 2018a,b). Individuals utilized CV scES in the sitting position for 2 h each day, during which time systolic blood pressure was maintained within the targeted range. Systolic blood pressure, diastolic blood pressure, and heart rate were monitored during each session to evaluate the effectiveness of the stimulation configuration and individual safety.

Stimulation configurations for the Voluntary scES interventions were selected to facilitate bilateral initiation, termination, and controlled movement of the trunk and lower extremities, including trunk flexion, extension, and rotation; isolated extension and flexion of the hip, knee, and ankle joints; and coordinated extension and/or flexion of the hip, knee, and ankle to move the lower extremities (Angeli et al., 2014). Individuals completed 2 h of daily Voluntary scES training while sitting or supine, alternating daily between trunk and lower extremity training sessions.

Stimulation configurations for Stand scES were selected to facilitate overground, independent, weight-bearing standing in a custom frame (Rejc et al., 2015). While the individual was seated, the stimulation amplitude was low to enable proprioception to coordinate the transition from sitting to standing; upon standing, the amplitude increased to the voltage optimized for each individual to stand fully weight-bearing. Manual assistance was provided at the hips or knees only if the joints moved outside the standing posture. Individuals were encouraged to stand as long as possible during the training sessions, up to a goal of 60 min. Individuals completed Stand scES each weekday.

Statistics

Data were analyzed with mixed linear models in which each measurement was the outcome. The only independent variable was the experimental time point (Pre CV scES, Post CV scES, Post Voluntary scES + CV scES, and Post Stand scES + Voluntary scES + CV scES). For each participant, a random intercept and random slope for time point were included. Assessments were repeated at each time point, but measurements were only included for analysis if the images met the standards established by the American Society of Echocardiography; to account for such variability, we included this in the linear model as a random effect nested within time point. To evaluate the improvements over time, linear contrasts were built to compare Post scES time points with Pre CV scES and evaluated with a t test. The significance level was set to 0.05 and all tests were two-sided. Statistical analyses were performed in SAS 9.4 (SAS Inc, Cary, NC, United States).

RESULTS

The mean age of individuals (n = 4) was 30.8 ± 2.7 years. At implant, the duration of injury was 6.5 ± 1.1 years. We found

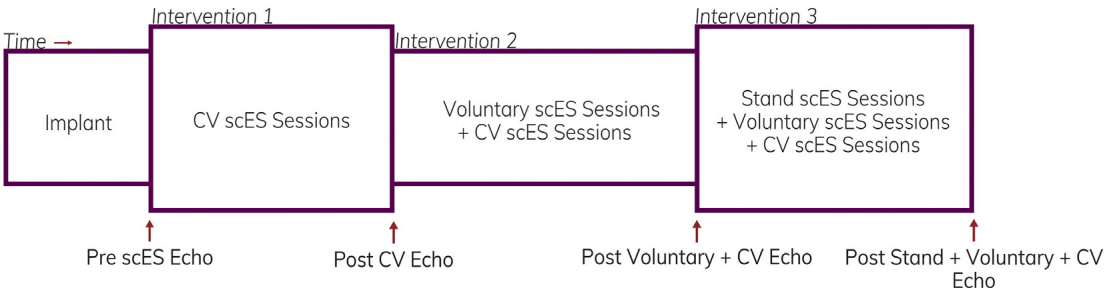

FIGURE 1 | Representation illustrating the timeline of assessments and interventions. Echocardiography assessments were obtained in four individuals prior to starting spinal cord epidural stimulation (scES) and after completion of each intervention.

TABLE 2 | Number of sessions that occurred during each intervention.

	Intervention 1	Intervention 2		Intervention 3		
	CV scES	**Voluntary scES**	**+ CV scES**	**Stand scES**	**+ Voluntary scES**	**+ CV scES**
Sessions (mean ± SD)	89 ± 13	95 ± 15	96 ± 52	80 ± 7	120 ± 31	102 ± 35

Data reported are the mean ± SD from four individuals. scES, spinal cord epidural stimulation; CV scES, scES targeted to normalize systolic blood pressure; Voluntary scES, scES targeted to facilitate voluntary movement of the trunk and lower extremities; Stand scES, scES targeted to facilitate independent, overground standing.

TABLE 3 | Left side chamber size, geometry, and mass before and after spinal cord epidural stimulation (scES) and task-specific interventions.

	Time points				Model results	
	Pre scES	**Post CV scES**	**Post Voluntary scES + CV scES**	**Post Stand scES + Voluntary scES + CV scES**	**Estimate (SE)**	***p*-value**
Left ventricle mass (g)	113 (10)	124 (11)	135 (11)*	142 (10)*	10 (2)	**<0.001**
Left ventricle internal diameter during diastole (cm)	4.71 (0.2)	4.84 (0.2)	4.86(0.2)	5.02(0.2)	0.1(0.04)	**0.011**
Left ventricle internal diameter during systole (cm)	3.33 (0.19)	3.32 (0.19)	3.33(0.19)	3.52(0.19)	0.06(0.03)	**0.040**
Interventricular septum dimension (cm)	0.57 (0.07)	0.63 (0.07)	0.73(0.07)*	0.67(0.07)	0.04(0.02)	**0.021**
Left ventricle posterior wall dimension during diastole (cm)	0.86 (0.05)	0.89 (0.05)	0.88(0.05)	0.93(0.05)	0.02(0.01)	0.177
Relative wall thickness	0.38 (0.02)	0.37 (0.03)	0.37(0.02)	0.38(0.03)	0 (0.01)	0.784
Aortic root diameter (cm)	2.87 (0.08)	2.88 (0.08)	2.98(0.08)*	2.99(0.08)*	0.04(0.01)	**<0.001**
LVOT diameter (cm)	2.15 (0.14)	2.11 (0.14)	2.16(0.14)	2.12(0.14)	−0.01(0.01)	0.585
Left atrial dimension (cm)	2.37 (0.31)	2.68 (0.32)	2.74(0.31)*	2.64(0.31)	0.1(0.04)	**0.046**

*Data are the estimate (SE) of the echocardiography data obtained from individuals with spinal cord injury (n = 4) before and after spinal cord epidural stimulation (scES) and task-specific interventions. Measurements from each intervention are compared to pre scES measurements (*p < 0.05). Changes associated with the addition of each subsequent scES intervention are presented as the estimated change (SE) and p value; significant changes are bolded. LVOT, left ventricular outflow tract; CV scES, scES targeted to normalize systolic blood pressure; Voluntary scES, scES targeted to facilitate voluntary movement of the trunk and lower extremities; Stand scES, scES targeted to facilitate independent, overground standing. Bolded values in the table correspond to p-values <0.05.*

significant increases to the aortic root, left atrial dimension, and left ventricular chamber dimension and mass after scES interventions, associated with statistically significant increases in systolic and diastolic function measurements. After the Voluntary scES intervention, the left ventricular mass ($\Delta 22 \pm 7$ g, $p < 0.05$), interventricular septum dimension ($\Delta 0.16 \pm 0.05$ cm, $p < 0.05$), aortic root diameter ($\Delta 0.11 \pm 0.03$ cm, $p < 0.01$), and left atrial dimension ($\Delta 0.37 \pm 0.14$ cm, $p < 0.05$) increased significantly compared with the Pre scES time point. Likewise, after the Stand scES intervention, the left ventricular mass ($\Delta 29 \pm 7$ g, $p < 0.01$) and the aortic root diameter ($\Delta 0.12 \pm 0.03$ cm, $p < 0.01$) increased significantly compared with the Pre scES time point (**Table 3**). With each subsequent scES intervention, the left ventricular mass (10 ± 2 g, $p < 0.001$), left ventricular internal dimension during diastole (0.1 ± 0.04 cm, $p < 0.05$), left ventricular internal dimension during systole (0.06 ± 0.03 cm, $p < 0.05$), and the interventricular septum dimension (0.04 ± 0.02 cm, $p < 0.05$) increased significantly (**Figure 2**). The aortic root diameter (0.04 ± 0.01 cm, $p < 0.001$) and left atrial dimension (0.10 ± 0.04 cm, $p < 0.05$) also increased significantly with each subsequent scES intervention.

The VTI of blood (i.e., distance traveled with each heartbeat, 4.4 ± 1.6 cm, $p < 0.05$) was significantly increased after the Stand scES intervention compared with the Pre scES time point

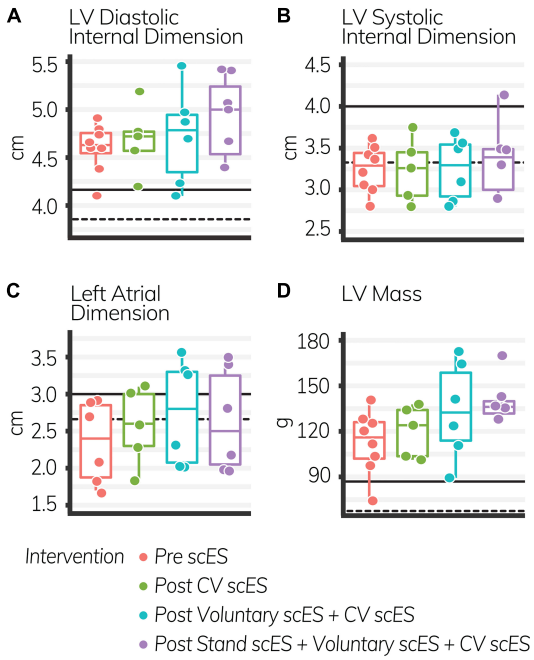

FIGURE 2 | The LV diastolic internal dimension **(A)**, left atrial dimension **(C)**, and LV mass **(D)** increased significantly with each subsequent intervention ($p < 0.05$); LV systolic internal dimension **(B)** did not change. *Black lines* indicate the healthy limit according to the American Society of Echocardiography guidelines. LV diastolic internal dimension: females (*dashed line*), 3.8 cm; males (*solid line*), 4.2 cm; LV systolic internal dimension: females (*dashed line*), 3.3 cm; males (*solid line*), 4.0 cm; left atrial dimension: females (*dashed line*), 2.8 cm; males (*solid line*), 3.0 cm; LV mass: females (*dashed line*), 67 g; males (*solid line*), 88 g. Each *circle* is an individual observation. *Box-and-whisker plots* illustrate the 5th, 25th, 50th, 75th, and 95th percentiles. Each individual ($n = 4$) had two echocardiography assessments at each time point, but data were only included for analysis if they met the image standards set by the American Society of Echocardiography.

(**Table 4**). With each subsequent scES intervention, the ejection fraction ($1 \pm 0.4\%$, $p < 0.05$) increased significantly without changes to the end-diastolic or end-systolic volume, but the VTI (2 ± 0.4 cm, $p < 0.001$) and stroke volume (4.4 ± 1.5 ml, $p < 0.01$) increased significantly without a change in heart rate (**Figure 3**). Diastolic blood pressure (4 ± 1.7 mmHg, $p < 0.05$) increased significantly with each subsequent scES intervention.

The isovolumic relaxation time decreased significantly (Δ-18 ± 7 ms, $p < 0.05$) after the Voluntary scES intervention compared with the pre scES time point. The mitral valve deceleration slope increased significantly ($\Delta 179 \pm 78$ cm s^{-1}, $p < 0.05$) and the mitral valve deceleration time decreased significantly ($\Delta -98 \pm 39$ ms, $p < 0.05$) after the Stand scES intervention compared with the Pre scES time point (**Table 5**). With each subsequent scES intervention, the mitral valve deceleration time (-32 ± 11 ms, $p < 0.05$) and the isovolumic relaxation time (-6 ± 1.9 ms, $p < 0.05$) decreased significantly and the mitral valve deceleration slope (50 ± 25 cm s^{-1}, $p < 0.05$) increased significantly (**Figure 4**). These changes were not associated with the changes to the E/A ratio, e' velocity, E/e' ratio, or left atrial filling pressure.

DISCUSSION

We found that significantly increased systolic function and diastolic function measures increased the left atrial and ventricular chamber and aortic root dimensions after scES interventions. With each subsequent scES intervention, the ejection fraction, stroke volume, and mitral valve deceleration slope increased significantly, while the isovolumic relaxation time and mitral valve deceleration time decreased significantly, suggestive of an improved systolic and diastolic function. The left ventricular mass, diastolic internal dimension, and systolic internal dimension also increased significantly. These statistically significant structural improvements suggest that scES interventions could lead to cardiac remodeling and reverse atrophic changes that result from spinal cord injury – the left ventricle dimensions and mass increased significantly, and all volume measurements were obtained without scES. The myocardial, systolic function, and diastolic function changes that occurred in four individuals with spinal cord injury (SCI) were thus adaptations to the scES interventions and not just residual effects of stimulation. Long-term improvements to cardiac function have implications for increased quality of life and improved cardiovascular health in individuals with spinal cord injury, decreasing the risk of cardiovascular morbidity and mortality.

Structural and Functional Myocardial Improvements

Measurement of the left ventricle dimensions illustrates preload and afterload within the left ventricle and its ability to generate sufficient force to open the aortic valves against the high-resistance systemic circulation. After scES interventions, the left ventricle dimensions and mass increased significantly in response to increased preload and afterload. Even though these increases were not accompanied by significant increases to the posterior wall thickness, the relative wall thickness did not change after scES interventions. There was therefore no evidence of eccentric (i.e., maladaptive) hypertrophy of the myocardium because the geometry of the left ventricle remained the same after each intervention. In four individuals, the myocardium was thus able to strengthen appropriately in response to increased cardiac demand and wall stress imposed by the scES interventions. These changes are similar to those reported by other groups that observed improved posterior wall (Δ1.5 mm), interventricular septum (Δ1.6 mm), and left ventricular diastolic (Δ3.2 mm) dimensions in individuals with SCI after functional electrical stimulation. These changes also mirror those observed in non-injured individuals after reversal of left ventricular atrophy (mass = Δ12.4 g) and left ventricular hypertrophy (posterior wall = Δ1.7 mm, interventricular septum = Δ1.2 mm) (Nash et al., 1991; Gaddam et al., 2010; Westby et al., 2016). This beneficial adaptation has implications for long-term cardiovascular health in individuals with spinal cord injury, especially in light of new interventions that lead to long-term increases in preload and afterload. Maladaptive thinning of the

TABLE 4 | Global systolic function and blood pressure outcomes before and after spinal cord epidural stimulation (scES) interventions.

	Timepoint				Model Results	
	Pre scES	**Post CV scES**	**Post Voluntary scES + CV scES**	**Post Stand scES + Voluntary scES + CV scES**	**Estimate (SE)**	**p-value**
Ejection fraction, %	57 (2)	58 (2)	58 (2)	60 (2)	1 (0.4)	**0.034**
End diastolic volume, mL	89 (7)	97 (7)	95 (8)	96 (7)	3 (2.0)	0.192
End systolic volume, mL	38 (4)	42 (4)	40 (4)	41 (4)	1 (0.7)	0.216
Velocity time integral, cm	20 (2)	21 (2)	23 (2)	25 (2)	2 (0.4)	**<0.001**
Cardiac output, L/min	3.8 (0.6)	4.1 (0.6)	4.2 (0.6)	4.2 (0.6)	0.2 (0.1)	0.051
Stroke volume, mL	73 (12)	77 (12)	84 (12)	84 (12)	4.4 (1.5)	**0.007**
Systolic blood pressure, mmHg	99 (10)	114 (12)	101 (11)	117 (11)	4 (3.1)	0.244
Diastolic blood pressure, mmHg	52 (5)	65 (6)	57 (6)	67 (6)	4 (1.7)	**0.034**
Heart rate, BPM	49 (3)	54 (3)	49 (4)	48 (4)	−1 (0.8)	0.378
s' contraction velocity, cm/s	9 (0.9)	8 (0.8)	8 (0.8)	9 (0.8)	−0.2 (0.2)	0.409
Global circumferential strain, %	−21 (2)	−23 (2)	−23 (2)	−23 (2)	0.4 (0.4)	0.291
Global longitudinal strain, %	−25 (3)	−26 (3)	−26 (3)	−27 (3)	0.5 (0.3)	0.066

*Data are the estimate (SE) of the echocardiography data obtained from individuals with spinal cord injury (n = 4) before and after scES and task-specific interventions. Measurements from each intervention are compared to pre scES measurements (*p < 0.05). Changes associated with the addition of each subsequent scES intervention are presented as the estimated change (SE) and p value. CV, cardiovascular; CV scES, scES targeted to normalize systolic blood pressure; Voluntary scES, scES targeted to facilitate voluntary movement of the trunk and lower extremities; Stand scES, scES targeted to facilitate independent, overground standing. Bolded values in the table correspond to p-values <0.05.*

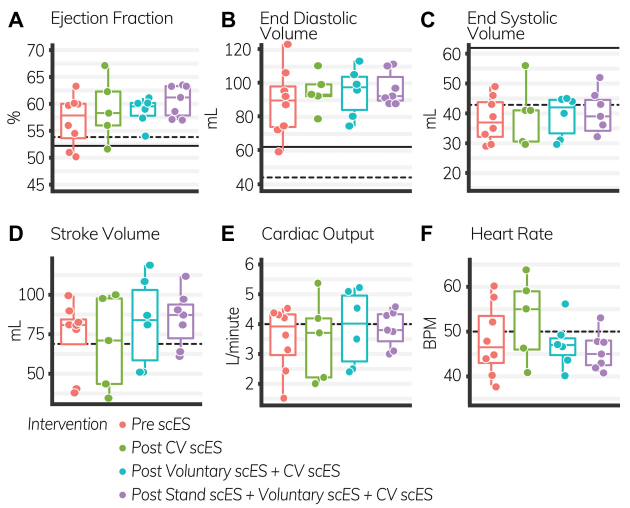

FIGURE 3 | Global systolic function outcomes before and after spinal cord epidural stimulation (scES) interventions. With each subsequent scES intervention, the ejection fraction **(A)** and stroke volume **(D)** increased significantly ($p < 0.05$). End diastolic volume **(B)**, end systolic volume **(C)**, cardiac output **(E)**, and heart rate **(F)** did not change. *Black lines* indicate the healthy limit according to the American Society of Echocardiography guidelines. Ejection fraction: females (*dashed line*), 54%; males (*solid line*), 52%; end-diastolic volume: females (*dashed line*), 46 ml; males (*solid line*), 62 ml; end-systolic volume: females (*dashed line*), 42 ml; males (*solid line*), 61 ml; stroke volume: females and males (*dashed line*), 70 ml; cardiac output: females and males (*dashed line*), 4.0 L/min; heart rate: females and males (*dashed line*), 50 bpm. Each *circle* is an individual observation. *Box-and-whisker plots* illustrate the 5th, 25th, 50th, 75th, and 95th percentiles. Each individual ($n = 4$) had two echocardiography assessments at each time point, but data were only included for analysis if they met the image standards set by the American Society of Echocardiography.

myocardium can ultimately lead to systolic and diastolic dysfunction whereby the weakened left ventricle cannot adequately pump blood to maintain homeostasis (Cwajg et al., 2000; Thygesen et al., 2012; Hoit, 2014). It is therefore possible that scES interventions not only lead to the recovery of cardiovascular and motor function but could reverse myocardial atrophy and improve cardiac health (Harkema et al., 2011, 2018a,b; Angeli et al., 2014, 2018; Rejc et al., 2017a,b; Aslan et al., 2018).

Systolic function outcomes illustrate the strength of the left ventricle as it pumps blood into the systemic circulation. We found significant increases to the ejection fraction and stroke volume with each subsequent scES intervention, suggesting a long-term adaptation to increased cardiac demand in four individuals with SCI. This observation is similar to other groups that report systolic function increases after body weight-supported treadmill training (Turiel et al., 2011). These functional increases persisted without active stimulation, and, unlike previous studies, we found significantly increased systolic function outcomes despite significant increases to arterial blood pressure. These significant increases were independent of load or heartbeat because they were not associated with increases in preload or filling time. Increased strength of the left ventricle is also illustrated by stable end-systolic volume with each scES intervention because, with each heartbeat, a greater amount of blood is pumped into the systemic circulation despite a dramatically increased afterload (Aslan et al., 2018; Harkema et al., 2018a,b). Each heartbeat thus removes a greater amount of blood from the compliant venous circulation, increasing oxygen delivery to and waste removal from metabolically active tissues. This is particularly beneficial to the brain and heart as they possess the greatest metabolic demand and

TABLE 5 | Diastolic function outcomes before and after spinal cord epidural stimulation (scES) interventions.

	Timepoint				Model Results	
	Pre scES	**Post CV scES**	**Post Voluntary scES + CV scES**	**Post Stand scES + Voluntary scES + CV scES**	**Estimate (SE)**	**p-value**
Mitral valve peak E-wave velocity, cm/s	80 (11)	91 (9)	89 (10)	93 (10)	3 (2.6)	0.229
Mitral valve peak A-wave velocity, cm/s	51 (4)	52 (5)	54 (5)	50 (5)	0 (1.3)	0.999
E/A ratio	1.6 (0.4)	1.8 (0.3)	1.6 (0.4)	1.9 (0.3)	0.08 (0.1)	0.370
Mitral valve deceleration time, ms	290 (24)	229 (27)	209 (24)	192 (30)	−32 (11)	**0.012**
Mitral valve deceleration slope, $cm*s^{-1}$	340 (50)	498 (54)	445 (50)	519 (60)	50 (25)	**0.048**
Isovolumic relaxation time, ms	104 (5)	104 (6)	85 (5)	89 (5)	−6 (1.9)	**0.008**
e' relaxation velocity, cm/s	13 (1)	13 (1)	12 (1)	13 (1)	−0.1 (0.3)	0.728
E/e' ratio	7.0 (1)	6.7 (1)	7.5 (1)	7.5 (1)	0.4 (0.3)	0.213
Left atrial filling pressure, mmHg	11 (1)	11 (1)	11 (1)	11 (1)	0.4 (0.3)	0.239

Data are the estimate (SE) of the echocardiography data obtained from individuals with spinal cord injury (n = 4) before and after scES and task-specific interventions. Measurements from each intervention are compared to pre scES measurements ($p < 0.05$). Changes associated with the addition of each subsequent scES intervention are presented as the estimated change (SE) and p value. CV, cardiovascular; CV scES, scES targeted to normalize systolic blood pressure; Voluntary scES, scES targeted to facilitate voluntary movement of the trunk and lower extremities; Stand scES, scES targeted to facilitate independent, overground standing. Bolded values in the table correspond to p-values <0.05.*

carry significant risk of adverse event when hypoperfused or oxygen-deprived (Yarkony et al., 1986; Bisharat et al., 2002; Dolinak and Balraj, 2007; Jegede et al., 2010; Wu et al., 2012; Wecht and Bauman, 2013; Phillips et al., 2014; Katz and Rolett, 2016; Wecht et al., 2018). Restoration of the ejection fraction and stroke volume in four individuals with spinal cord injury carries additional significance when considering the degree to which cardiovascular dysregulation decreases quality of life. Risk of syncope and persistent fatigue significantly delay therapeutic interventions, restrict independence and autonomy, and limit social engagement (Barrett-Connor and Palinkas, 1994; Blackmer, 1997; Illman et al., 2000; Furlan and Fehlings, 2008; Carlozzi et al., 2013; Guilcher et al., 2013; Piatt et al., 2016). Significant improvements to systolic function after scES interventions thus have the potential to improve the overall health, improve quality of life, and decrease the risk of cardiovascular disease in individuals with spinal cord injury.

Diastolic function outcomes quantify the elasticity of the ventricles and the degree to which the myocardium stretches during diastole to enable passive filling. With each subsequent scES intervention, we found significant increases to the left atrial dimension and mitral valve deceleration slope and associated decreases to the mitral valve deceleration time, illustrating greater preload and blood velocity through the mitral valve during early (i.e., passive) diastole (Stoddard et al., 1989). This was not associated with increased left atrial filling pressure or the E/e' ratio, nor with decreases to e' velocity. Therefore increased blood velocity through the mitral valve did not result from maladaptive increased left atrial pressure "pushing" blood into the left ventricle, but rather from stretch of the left ventricle "pulling" blood from the left atrium (Park and Marwick, 2011; Oliveira et al., 2014). Moreover, diastolic improvements in these four individuals persisted without active stimulation, suggesting an adaptation to scES interventions that led to long-term increases in venous return. Greater preload during early diastole provides a greater stroke volume without associated increases in pathologic metabolic demand, maintains left ventricular elasticity, and potentially decreases risk of heart failure (Redfield et al., 2003).

There were also significant decreases to the isovolumic relaxation time after scES interventions, similar to improvements observed after body weight-supported treadmill training, indicating improved coronary perfusion and cardiac health in these four individuals with SCI (Turiel et al., 2011). Prolonged isovolumic relaxation time precedes diastolic dysfunction and develops as increased afterload delays cross-bridge inactivation, preventing complete relaxation throughout the myocardium during diastole. Incomplete relaxation of the left ventricle during diastole, illustrated by increased isovolumic relaxation time and E/e' ratio, prevents the decrease in pressure required to open the mitral valve (Gillebert and Lew, 1991; Leite-Moreira et al., 1999; Cheng et al., 2009; Parikh et al., 2016; Taqueti et al., 2018). This decreases coronary perfusion in areas where cross-bridges remain active. Myocardial contraction during systole compresses the microvasculature such that coronary blood flow velocity is greatest during diastole (Galderisi et al., 2008; Altunkas et al., 2014). Significant decreases to the isovolumic relaxation time after scES suggest more rapid cross-bridge inactivation and more rapid onset of complete relaxation, which could increase coronary perfusion. It is therefore significant that we found significant improvements to the isovolumic relaxation time in these four individuals with SCI – despite significant increases to afterload – because significant improvements to coronary perfusion have serious implications for cardiac health. Increasing oxygen delivery to the myocardium decreases the maladaptive signaling pathways that cause concentric or eccentric hypertrophy and ultimately lead to heart failure (Ingwall, 2009; Katz and Rolett, 2016). This indicates that scES interventions may lead to beneficial improvements in

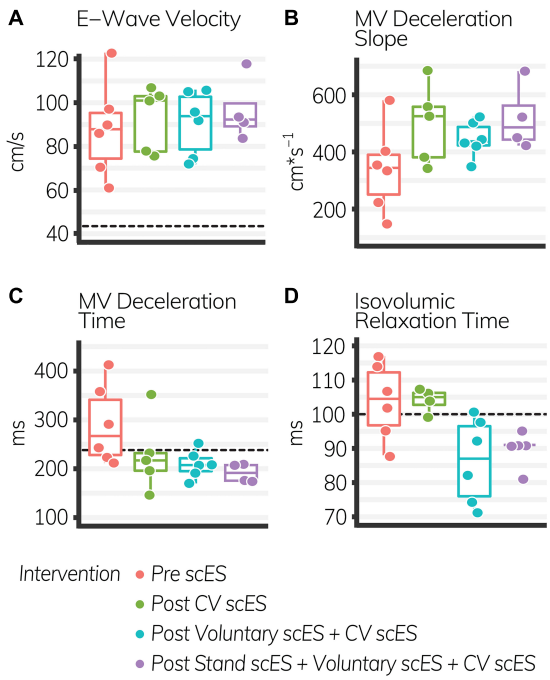

FIGURE 4 | Diastolic function outcomes before and after spinal cord epidural stimulation (scES) interventions. With each subsequent intervention, the mitral valve (*MV*) deceleration slope **(B)**, increased significantly ($p < 0.05$), while the MV deceleration time **(C)**, and isovolumic relaxation time **(D)** decreased significantly ($p < 0.05$). E-wave velocity **(A)** did not change. *Black dashed lines* indicate the healthy limit according to the American Society of Echocardiography guidelines. *E*-wave velocity: females and males, 42 cm s^{-1}; MV deceleration time: females and males, 140 ms; isovolumic relaxation time: females and males, 70 ms. The MV deceleration slope does not have a healthy range established by the American Society of Echocardiography. Each *circle* is an individual observation. *Box-and-whisker plots* illustrate the 5th, 25th, 50th, 75th, and 95th percentiles. Each individual ($n = 4$) had two echocardiography assessments at each time point, but data were only included for analysis if they met the image standards set by the American Society of Echocardiography.

coronary perfusion and could decrease the risk of developing myocardial ischemia.

Effects of Epidural Stimulation

While there was no investigation into the mechanism in this research study, animal models may lend insight into the hemodynamic changes that occur upon active stimulation. Research using anesthetized dog models demonstrate that electrical stimulation of the lumbar sympathetic ganglia elicits greater constriction of the hindlimb and splanchnic capacitance vessels than resistance vessels (Hainsworth and Karim, 1976; Karim and Hainsworth, 1976). Because the capacitance vessels function as a blood reservoir, their maximal constriction can dramatically increase preload and cardiac output and are thus a pharmacological target to maintaining blood pressure during anesthesia or septic shock (Hainsworth, 1990; De Backer et al., 2003; Sakka et al., 2007). This speculation is supported by the myocardial adaptations reported herein. Myocardial adaptations to exercise illustrate distinct differences between aerobic and isometric exercise. Aerobic exercise (e.g., swimming, running, etc.) dramatically increases preload and leads to increased left ventricle volumes, mass, and chamber dimensions as the myocardium adapts to volume loading (Morganroth et al., 1975; DeMaria et al., 1978; Maron, 1986). Isometric exercise (e.g., strength training, wrestling, etc.), however, increases afterload *via* vasopressor responses and results in increased wall thickness and mass of the left ventricle without any increase to the internal dimensions or preload – changes to the filling pressure and volume are minimal, but the myocardium thickens in order to generate sufficient force to overcome the increased afterload (Morganroth et al., 1975; DeMaria et al., 1978; Maron, 1986). Skeletal muscle contraction during voluntary lower extremity movement would decrease venous capacitance and increase venous return to the right atrium, thereby increasing preload similar to aerobic exercise. The significant increases to the left ventricle mass, stroke volume, and internal systolic and diastolic dimensions are thus more likely to result from repetitive increases in preload rather than afterload, despite significant increases to the arterial blood pressure observed previously (Aslan et al., 2018; Harkema et al., 2018a,b). And even though there were no significant increases to the end-diastolic volume after scES interventions, there were still significant changes to the diastolic function outcomes that indicate positive changes to the passive diastolic filling pressure (Stoddard et al., 1989).

Given the proximity of the stimulator to the lumbar sympathetic ganglia and that the significant increases we found indicate myocardial adaptation to increased preload, it is possible that scES removes blood from the compliant venous circulation to a greater degree than it elicits arterial vasoconstriction, which led to the significant changes in the cardiac structure, systolic function, and diastolic function after scES intervention. However, there were no significant differences between scES intervention, and in order to understand the effects of CV scES alone and compared with Voluntary and Stand scES, more research is needed. Additionally, investigation into catecholamine release, venous compliance, venous flow and velocity, and arterial diameter and stiffness would elucidate the mechanism by which scES increases preload and afterload.

LIMITATIONS

The data reported in this study were obtained from a heterogenous, young cohort of four individuals with severe cervical spinal cord injury without a statistical control since each participant served as their own control in this pre- and post-measurement study design. The clinically heterogenous injury characteristics make generalization inappropriate, while the small sample makes discrimination between the effects of each scES intervention difficult. However, the significant improvements are promising and justify expanding the research into a larger cohort

clinically representative of the SCI population. This would allow us to investigate the effects of scES interventions on cardiac function in lower-level injury, incomplete injury, and in relation to age-related declines in cardiac function.

CONCLUSION

We found significant improvements to the ejection fraction and stroke volume, diastolic filling times, and left ventricle dimensions after scES interventions, indicating that scES led to restorative cardiac remodeling in these four individuals with SCI. This has the potential to decrease the secondary health consequences of spinal cord injury and improve quality of life, with implications for improving cardiovascular health and attenuating immobility-related declines in cardiac function. Future studies should investigate this in a larger representative group of SCI participants.

DATA AVAILABILITY STATEMENT

The raw data supporting the conclusions of this article will be made available by the authors, without undue reservation.

ETHICS STATEMENT

The studies involving human participants were reviewed and approved by University of Louisville Institutional Review Board. The patients/participants provided their written informed consent to participate in this study.

AUTHOR CONTRIBUTIONS

BL: writing – original draft, methodology, visualization, and interpretation. SW: methodology, investigation, and writing – review and editing. BU: formal analysis and writing – review and editing. NS and MS: interpretation and writing – review and editing. SH: conceptualization, methodology, writing – review and editing, resources, and funding acquisition. GH: conceptualization, methodology, interpretation and writing – review and editing. All authors contributed to the article and approved the submitted version.

FUNDING

This work was supported by the Craig H. Neilsen Foundation: #ES2-CHN-2013 (SH). This work was supported by Christopher and Dana Reeve Foundation, Leona M. and Harry B. Helmsley Charitable Trust, University of Louisville Hospital, and Medtronic plc.

ACKNOWLEDGMENTS

We are indebted to our research participants for their courage, dedication, motivation, and perseverance that made these research findings possible. Dr. Maxwell Boakye performed surgical implantation and provided medical oversight. Drs. Glen Hirsch, Marcus Stoddard, Darryl Kaelin, Sarah Wagers, and Camilo Castillo provided medical oversight. Yukishia Austin, Lynn Robbins, and Kristen Johnson provided medical management. Kelly Ancel assisted with echocardiography aquisition and analysis. We would like to thank Dr. Yangsheng Chen for engineering leadership and Christie Ferreira for project management. Rebekah Morton, Sean Stills, Brittany Logdson, and Ricky Seither led research interventions and provided support to research participants.

SUPPLEMENTARY MATERIAL

The Supplementary Material for this article can be found online at: https://www.frontiersin.org/articles/10.3389/fnins.2020.554018/full#supplementary-material

REFERENCES

Altunkas, F., Koc, F., Ceyhan, K., Celik, A., Kadi, H., Karayakali, M., et al. (2014). The effect of slow coronary flow on right and left ventricular performance. *Med. Princ. Pract.* 23, 34–39. doi: 10.1159/000355471

Angeli, C. A., Boakye, M., Morton, R. A., Vogt, J., Benton, K., Chen, Y., et al. (2018). Recovery of over-ground walking after chronic motor complete spinal cord injury. *N. Engl. J. Med.* 379, 1244–1250. doi: 10.1056/NEJMoa1803588

Angeli, C. A., Edgerton, V. R., Gerasimenko, Y. P., and Harkema, S. J. (2014). Altering spinal cord excitability enables voluntary movements after chronic complete paralysis in humans. *Brain* 137(Pt 5), 1394–1409. doi: 10.1093/brain/awu038

Arbeille, P., Fomina, G., Roumy, J., Alferova, I., Tobal, N., and Herault, S. (2001). Adaptation of the left heart, cerebral and femoral arteries, and jugular and femoral veins during short- and long-term head-down tilt and spaceflights. *Eur. J. Appl. Physiol.* 86, 157–168. doi: 10.1007/s004210100473

Aslan, S. C., Legg Ditterline, B. E., Park, M. C., Angeli, C. A., Rejc, E., Chen, Y., et al. (2018). Epidural spinal cord stimulation of lumbosacral networks modulates arterial blood pressure in individuals with spinal cord injury-induced cardiovascular deficits. *Front. Physiol.* 2018:565. doi: 10.3389/fphys.00565

Barrett-Connor, E., and Palinkas, L. A. (1994). Low blood pressure and depression in older men: a population based study. *BMJ* 308, 446–449. doi: 10.1136/bmj.308.6926.446

Bartholdy, K., Biering-Sorensen, T., Malmqvist, L., Ballegaard, M., Krassioukov, A., Hansen, B., et al. (2014). Cardiac arrhythmias the first month after acute traumatic spinal cord injury. *J. Spinal Cord Med.* 37, 162–170. doi: 10.1179/2045772313Y.0000000181

Bauman, W., and Spungen, A. (2007). Risk assessment for coronary heart disease in a veteran population with spinal cord injury. *Top. Spinal Cord Injury Rehabil.* 12, 35–53. doi: 10.1310/sci1204-35

Bauman, W. A., and Spungen, A. M. (2008). Coronary heart disease in individuals with spinal cord injury: assessment of risk factors. *Spinal Cord* 46, 466–476. doi: 10.1038/sj.sc.3102161

Bisharat, N., Paz, E., Klimov, A., Friedberg, N., and Elias, M. (2002). Cerebral syncope in a patient with spinal cord injury. *Pac. Clin. Electrophysiol.* 25, 372–373. doi: 10.1046/j.1460-9592.2002.00372.x

Blackmer, J. (1997). Orthostatic hypotension in spinal cord injured patients. *J. Spinal Cord Med.* 20, 212–217. doi: 10.1080/10790268.1997.11719471

Carlozzi, N. E., Fyffe, D., Morin, K. G., Byrne, R., Tulsky, D. S., Victorson, D., et al. (2013). Impact of blood pressure dysregulation on health-related quality of life in persons with spinal cord injury: development of a conceptual model. *Archiv. Phys. Med. Rehabil.* 94, 1721–1730. doi: 10.1016/j.apmr.2013.02.024

Cheng, S., Fernandes, V. R., Bluemke, D. A., McClelland, R. L., Kronmal, R. A., and Lima, J. A. (2009). Age-related left ventricular remodeling and associated risk for cardiovascular outcomes: the multi-ethnic study of atherosclerosis. *Circ. Cardiov. Imag.* 2, 191–198. doi: 10.1161/CIRCIMAGING.108.819938

Claydon, V. E., Hol, A. T., Eng, J. J., and Krassioukov, A. V. (2006). Cardiovascular responses and postexercise hypotension after arm cycling exercise in subjects with spinal cord injury. *Arch. Phys. Med. Rehabil.* 87, 1106–1114. doi: 10.1016/j.apmr.2006.05.011

Cwajg, J. M., Cwajg, E., Nagueh, S. F., He, Z. X., Qureshi, U., Olmos, L. I., et al. (2000). End-diastolic wall thickness as a predictor of recovery of function in myocardial hibernation: relation to rest-redistribution T1-201 tomography and dobutamine stress echocardiography. *J. Am. Coll. Cardiol.* 35, 1152–1161. doi: 10.1016/s0735-1097(00)00525-8

De Backer, D., Creteur, J., Silva, E., and Vincent, J. L. (2003). Effects of dopamine, norepinephrine, and epinephrine on the splanchnic circulation in septic shock: which is best? *Crit. Care Med.* 31, 1659–1667. doi: 10.1097/01.CCM.0000063045.77339.B6

de Groot, P. C., van Dijk, A., Dijk, E., and Hopman, M. T. (2006). Preserved cardiac function after chronic spinal cord injury. *Arch. Phys. Med. Rehabil.* 87, 1195–1200. doi: 10.1016/j.apmr.2006.05.023

DeMaria, A. N., Neumann, A., Lee, G., Fowler, W., and Mason, D. T. (1978). Alterations in ventricular mass and performance induced by exercise training in man evaluated by echocardiography. *Circulation* 57, 237–244. doi: 10.1161/01.cir.57.2.237

Ditterline, B. L., Wade, S., Ugiliweneza, B., Singam, N. S. V., Harkema, S. J., Stoddard, M. F., et al. (2020). Systolic and diastolic function in chronic spinal cord injury. *PLoS One* 15:e0236490. doi: 10.1371/journal.pone.0236490

Dolinak, D., and Balraj, E. (2007). Autonomic dysreflexia and sudden death in people with traumatic spinal cord injury. *Am. J. Forensic. Med. Pathol.* 28, 95–98. doi: 10.1097/PAF.0b013e3180600f99

Driussi, C., Ius, A., Bizzarini, E., Antonini-Canterin, F., d'Andrea, A., Bossone, E., et al. (2014). Structural and functional left ventricular impairment in subjects with chronic spinal cord injury and no overt cardiovascular disease. *J. Spinal Cord Med.* 37, 85–92. doi: 10.1179/2045772313Y.0000000161

Eysmann, S. B., Douglas, P. S., Katz, S. E., Sarkarati, M., and Wei, J. Y. (1995). Left ventricular mass and diastolic filling patterns in quadriplegia and implications for effects of normal aging on the heart. *Am. J. Cardiol.* 75, 201–203. doi: 10.1016/s0002-9149(00)80082-x

Furlan, J. C., and Fehlings, M. G. (2008). Cardiovascular complications after acute spinal cord injury: pathophysiology, diagnosis, and management. *Neurosurg. Focus* 25:E13. doi: 10.3171/foc.2008.25.11.e13

Furlan, J. C., Fehlings, M. G., Shannon, P., Norenberg, M. D., and Krassioukov, A. V. (2003). Descending vasomotor pathways in humans: correlation between axonal preservation and cardiovascular dysfunction after spinal cord injury. *J. Neurotrauma* 20, 1351–1363. doi: 10.1089/089771503322686148

Gaddam, K., Corros, C., Pimenta, E., Ahmed, M., Denney, T., Aban, I., et al. (2010). Rapid reversal of left ventricular hypertrophy and intracardiac volume overload in patients with resistant hypertension and *Hyperaldosteronism*. *Hypertension* 55, 1137–1142. doi: 10.1161/HYPERTENSIONAHA.109.141531

Galderisi, M., de Simone, G., D'Errico, A., Sidiropulos, M., Viceconti, R., Chinali, M., et al. (2008). Independent association of coronary flow reserve with left ventricular relaxation and filling pressure in arterial hypertension. *Am. J. Hypertens.* 21, 1040–1046. doi: 10.1038/ajh.2008.226

Giangregorio, L., and McCartney, N. (2006). Bone loss and muscle atrophy in spinal cord injury: epidemiology, fracture prediction, and rehabilitation strategies. *J. Spinal Cord Med.* 29, 489–500. doi: 10.1080/10790268.2006.11753898

Gibson, A. E., Buchholz, A. C., Martin Ginis, K. A., and Group, S.-S. R. (2008). C-Reactive protein in adults with chronic spinal cord injury: increased chronic inflammation in tetraplegia vs paraplegia. *Spinal Cord* 46, 616–621. doi: 10.1038/sc.2008.32

Gillebert, T. C., and Lew, W. Y. (1991). Influence of systolic pressure profile on rate of left ventricular pressure fall. *Am. J. Physiol.* 261(3 Pt 2), H805–H813. doi: 10.1152/ajpheart.1991.261.3.H805

Gondim, F. A., Lopes, A. C. Jr., Oliveira, G. R., Rodrigues, C. L., Leal, P. R., Santos, A. A., et al. (2004). Cardiovascular control after spinal cord injury. *Curr. Vasc. Pharmacol.* 2, 71–79.

Grigorean, V. T., Sandu, A. M., Popescu, M., Iacobini, M. A., Stoian, R., Neascu, C., et al. (2009). Cardiac dysfunctions following spinal cord injury. *J. Med. Life* 2, 133–145.

Guilcher, S. J., Craven, B. C., Lemieux-Charles, L., Casciaro, T., McColl, M. A., and Jaglal, S. B. (2013). Secondary health conditions and spinal cord injury: an uphill battle in the journey of care. *Disabil. Rehabil.* 35, 894–906. doi: 10.3109/09638288.2012.721048

Guilherme, D. R., Matos-Souza, J. R., Costa, E. S. A. D., Campos, L. F., Santos, L. G., Azevedo, E. R., et al. (2014). Physical activity and improved diastolic function in spinal cord-injured subjects. *Med. Sci. Sports Exerc.* 46, 887–892. doi: 10.1249/MSS.0000000000000187

Hainsworth, R. (1990). The importance of vascular capacitance in cardiovascular control. *Physiology* 5, 250–254. doi: 10.1152/physiologyonline.1990.5.6.250

Hainsworth, R., and Karim, F. (1976). Responses of abdominal vascular capacitance in the anaesthetized dog to changes in carotid sinus pressure. *J. Physiol.* 262, 659–677. doi: 10.1113/jphysiol.1976.sp011614

Harkema, S., Gerasimenko, Y., Hodes, J., Burdick, J., Angeli, C., Chen, Y., et al. (2011). Effect of epidural stimulation of the lumbosacral spinal cord on voluntary movement, standing, and assisted stepping after motor complete paraplegia: a case study. *Lancet* 377, 1938–1947. doi: 10.1016/S0140-6736(11)60547-3

Harkema, S. J., Legg Ditterline, B., Wang, S., Aslan, S., Angeli, C. A., Ovechkin, A., et al. (2018a). Epidural Spinal cord stimulation training and sustained recovery of cardiovascular function in individuals with chronic cervical spinal cord injury. *JAMA Neurol.* 75, 1569–1571. doi: 10.1001/jamaneurol.2018.2617

Harkema, S. J., Wang, S., Angeli, C. A., Chen, Y., Boayke, M., Ugiliweneza, B., et al. (2018b). Normalization of blood pressure with spinal cord epidural stimulation after severe spinal cord injury. *Front. Hum. Neurosci.* 12:83. doi: 10.3389/fphys.00083

Hoit, B. D. (2014). Left atrial size and function: role in prognosis. *J. Am. Coll. Cardiol.* 63, 493–505. doi: 10.1016/j.jacc.2013.10.055

Hostettler, S., Leuthold, L., Brechbuhl, J., Mueller, G., Illi, S. K., and Spengler, C. M. (2012). Maximal cardiac output during arm exercise in the sitting position after cervical spinal cord injury. *J. Rehabil. Med.* 44, 131–136. doi: 10.2340/16501977-0913

Illman, A., Stiller, K., and Williams, M. (2000). The prevalence of orthostatic hypotension during physiotherapy treatment in patients with an acute spinal cord injury. *Spinal Cord* 38, 741–747. doi: 10.1038/sj.sc.3101089

Ingwall, J. S. (2009). Energy metabolism in heart failure and remodelling. *Cardiovasc. Res.* 81, 412–419. doi: 10.1093/cvr/cvn301

Jegede, A. B., Rosado-Rivera, D., Bauman, W. A., Cardozo, C. P., Sano, M., Moyer, J. M., et al. (2010). Cognitive performance in hypotensive persons with spinal cord injury. *Clin. Auton. Res.* 20, 3–9. doi: 10.1007/s10286-009-0036-z

Karim, F., and Hainsworth, R. (1976). Responses of abdominal vascular capacitance to stimulation of splachnic nerves. *Am. J. Physiol.* 231, 434–440. doi: 10.1152/ajplegacy.1976.231.2.434

Katz, A. M., and Rolett, E. L. (2016). Heart failure: when form fails to follow function. *Eur. Heart J.* 37, 449–454. doi: 10.1093/eurheartj/ehv548

Kessler, K. M., Pina, I., Green, B., Burnett, B., Laighold, M., Bilsker, M., et al. (1986). Cardiovascular findings in quadriplegic and paraplegic patients and in normal subjects. *Am. J. Cardiol.* 58, 525–530. doi: 10.1016/0002-9149(86)90027-5

Lang, R. M., Badano, L. P., Mor-Avi, V., Afilalo, J., Armstrong, A., Ernande, L., et al. (2015). Recommendations for cardiac chamber quantification by echocardiography in adults: an update from the American Society of Echocardiography and the European Association of Cardiovascular Imaging. *Eur. Heart J. Cardiovasc. Imaging* 16, 233–270. doi: 10.1093/ehjci/jev014

Legg Ditterline, B. E., Aslan, S. C., Wang, S., Ugiliweneza, B., Hirsch, G. A., Wecht, J. M., et al. (2020). Restoration of autonomic cardiovascular regulation in spinal cord injury with epidural stimulation: a case series. *Clin. Auton. Res.* doi: 10.1007/s10286-020-00693-2 [Epub ahead of print].

Leite-Moreira, A. F., Correia-Pinto, J., and Gillebert, T. C. (1999). Afterload induced changes in myocardial relaxation: a mechanism for diastolic dysfunction. *Cardiovasc. Res.* 43, 344–353. doi: 10.1016/s0008-6363(99)00099-1

Maggioni, M. A., Ferratini, M., Pezzano, A., Heyman, J. E., Agnello, L., Veicsteinas, A., et al. (2012). Heart adaptations to long-term aerobic training in paraplegic subjects: an echocardiographic study. *Spinal Cord* 50, 538–542. doi: 10.1038/sc.2011.189

Maron, B. J. (1986). Structural features of the athlete heart as defined by echocardiography. *J. Am. Coll. Cardiol.* 7, 190–203. doi: 10.1016/s0735-1097(86)80282-0

Martin, D. S., South, D. A., Wood, M. L., Bungo, M. W., and Meck, J. V. (2002). Comparison of echocardiographic changes after short- and long-duration spaceflight. *Aviat. Space Environ. Med.* 73, 532–536.

Matos-Souza, J. R., Pithon, K. R., Oliveira, R. T., Teo, F. H., Blotta, M. H., Cliquet, A. Jr., et al. (2011). Altered left ventricular diastolic function in subjects with spinal cord injury. *Spinal Cord* 49, 65–69. doi: 10.1038/sc.2010.88

Meck, J. V., Reyes, C. J., Perez, S. A., Goldberger, A. L., and Ziegler, M. G. (2001). Marked exacerbation of orthostatic intolerance after long- vs. short-duration spaceflight in veteran astronauts. *Psychosom. Med.* 63, 865–873. doi: 10.1097/00006842-200111000-00003

Moore, C. D., Craven, B. C., Thabane, L., Papaioannou, A., Adachi, J. D., and Giangregorio, L. M. (2018). Does muscle atrophy and fatty infiltration plateau or persist in chronic spinal cord injury? *J. Clin. Densitom.* 21, 329–337. doi: 10.1016/j.jocd.2017.06.001

Morganroth, J., Maron, B. J., Henry, W. L., and Epstein, S. E. (1975). Comparative left ventricular dimensions in trained athletes. *Ann. Intern. Med.* 82, 521–524. doi: 10.7326/0003-4819-82-4-521

Nagueh, S. F., Middleton, K. J., Kopelen, H. A., Zoghbi, W. A., and Quinones, M. A. (1997). Doppler tissue imaging: a noninvasive technique for evaluation of left ventricular relaxation and estimation of filling pressures. *J. Am. Coll. Cardiol.* 30, 1527–1533. doi: 10.1016/s0735-1097(97)00344-6

Nagueh, S. F., Smiseth, O. A., Appleton, C. P., Byrd, B. F. III, Dokainish, H., Edvardsen, T., et al. (2016). Recommendations for the evaluation of left ventricular diastolic function by echocardiography: an update from the american society of echocardiography and the european association of cardiovascular imaging. *J. Am. Soc. Echocardiogr.* 29, 277–314. doi: 10.1016/j.echo.2016.01.011

Nash, M. S., Bilsker, S., Marcillo, A. E., Isaac, S. M., Botelho, L. A., Klose, K. J., et al. (1991). Reversal of adaptive left ventricular atrophy following electrically-stimulated exercise training in human tetraplegics. *Paraplegia* 29, 590–599. doi: 10.1038/sc.1991.87

Oliveira, R. K., Ferreira, E. V., Ramos, R. P., Messina, C. M., Kapins, C. E., Silva, C. M., et al. (2014). Usefulness of pulmonary capillary wedge pressure as a correlate of left ventricular filling pressures in pulmonary arterial hypertension. *J. Heart Lung Transpl.* 33, 157–162. doi: 10.1016/j.healun.2013.10.008

Parikh, J. D., Hollingsworth, K. G., Wallace, D., Blamire, A. M., and MacGowan, G. A. (2016). Normal age-related changes in left ventricular function: role of afterload and subendocardial dysfunction. *Intern. J. Cardiol.* 223, 306–312. doi: 10.1016/j.ijcard.2016.07.252

Park, J. H., and Marwick, T. H. (2011). Use and limitations of E/e' to assess left ventricular filling pressure by echocardiography. *J. Cardiovasc. Ultrasound* 19, 169–173. doi: 10.4250/jcu.2011.19.4.169

Phillips, A. A., Warburton, D. E., Ainslie, P. N., and Krassioukov, A. V. (2014). Regional neurovascular coupling and cognitive performance in those with low blood pressure secondary to high-level spinal cord injury: improved by alpha-1 agonist midodrine hydrochloride. *J. Cereb. Blood Flow Metab.* 34, 794–801. doi: 10.1038/jcbfm.2014.3

Piatt, J. A., Nagata, S., Zahl, M., Li, J., and Rosenbluth, J. P. (2016). Problematic secondary health conditions among adults with spinal cord injury and its impact on social participation and daily life. *J. Spinal Cord Med.* 39, 693–698. doi: 10.1080/10790268.2015.1123845

Platts, S. H., Martin, D. S., Stenger, M. B., Perez, S. A., Ribeiro, L. C., Summers, R., et al. (2009). Cardiovascular adaptations to long-duration head-down bed rest. *Aviat. Space Environ. Med.* 80(5 Suppl.), A29–A36.

Redfield, M. M., Jacobsen, S. J., Burnett, J. C. Jr., Mahoney, D. W., Bailey, K. R., and Rodeheffer, R. J. (2003). Burden of systolic and diastolic ventricular dysfunction in the community: appreciating the scope of the heart failure epidemic. *JAMA* 289, 194–202. doi: 10.1001/jama.289.2.194

Rejc, E., Angeli, C., and Harkema, S. (2015). Effects of lumbosacral spinal cord epidural stimulation for standing after chronic complete paralysis in humans. *PLoS One* 10:e0133998. doi: 10.1371/journal.pone.0133998

Rejc, E., Angeli, C. A., Atkinson, D., and Harkema, S. J. (2017a). Motor recovery after activity-based training with spinal cord epidural stimulation in a chronic motor complete paraplegic. *Sci. Rep.* 7:13476. doi: 10.1038/s41598-017-14003-w

Rejc, E., Angeli, C. A., Bryant, N., and Harkema, S. J. (2017b). Effects of stand and step training with epidural stimulation on motor function for standing in chronic complete paraplegics. *J. Neurotrauma* 34, 1787–1802. doi: 10.1089/neu.2016.4516

Sakka, S. G., Hofmann, D., Thuemer, O., Schelenz, C., and van Hout, N. (2007). Increasing cardiac output by epinephrine after cardiac surgery: effects on indocyanine green plasma disappearance rate and splanchnic microcirculation. *J. Cardiothorac. Vasc. Anesth.* 21, 351–356. doi: 10.1053/j.jvca.2006.02.031

Schiller, N. B., Shah, P. M., Crawford, M., DeMaria, A., Devereux, R., Feigenbaum, H., et al. (1989). Recommendations for quantitation of the left ventricle by two-dimensional echocardiography. American society of echocardiography committee on standards, subcommittee on quantitation of two-dimensional echocardiograms. *J. Am. Soc. Echocardiogr.* 2, 358–367. doi: 10.1016/s0894-7317(89)80014-8

Stoddard, M. F., Pearson, A. C., Kern, M. J., Ratcliff, J., Mrosek, D. G., and Labovitz, A. J. (1989). Influence of alteration in preload on the pattern of left ventricular diastolic filling as assessed by Doppler echocardiography in humans. *Circulation* 79, 1226–1236. doi: 10.1161/01.cir.79.6.1226

Summers, R. L., Martin, D. S., Meck, J. V., and Coleman, T. G. (2005). Mechanism of spaceflight-induced changes in left ventricular mass. *Am. J. Cardiol.* 95, 1128–1130. doi: 10.1016/j.amjcard.2005.01.033

Taqueti, V. R., Solomon, S. D., Shah, A. M., Desai, A. S., Groarke, J. D., Osborne, M. T., et al. (2018). Coronary microvascular dysfunction and future risk of heart failure with preserved ejection fraction. *Eur. Heart J.* 39, 840–849. doi: 10.1093/eurheartj/ehx721

Teasell, R. W., Arnold, J. M., Krassioukov, A., and Delaney, G. A. (2000). Cardiovascular consequences of loss of supraspinal control of the sympathetic nervous system after spinal cord injury. *Arch. Phys. Med. Rehabil.* 81, 506–516. doi: 10.1053/mr.2000.3848

Theisen, D. (2012). Cardiovascular determinants of exercise capacity in the Paralympic athlete with spinal cord injury. *Exp. Physiol.* 97, 319–324. doi: 10.1113/expphysiol.2011.063016

Thygesen, K., Alpert, J. S., Jaffe, A. S., Simoons, M. L., Chaitman, B. R., White, H. D., et al. (2012). Third universal definition of myocardial infarction. *Circulation* 126, 2020–2035. doi: 10.1161/CIR.0b013e31826e1058

Turiel, M., Sitia, S., Cicala, S., Magagnin, V., Bo, I., Porta, A., et al. (2011). Robotic treadmill training improves cardiovascular function in spinal cord injury patients. *Int. J. Cardiol.* 149, 323–329. doi: 10.1016/j.ijcard.2010.02.010

Wecht, J. M., and Bauman, W. A. (2013). Decentralized cardiovascular autonomic control and cognitive deficits in persons with spinal cord injury. *J. Spinal Cord Med.* 36, 74–81. doi: 10.1179/2045772312y.0000000056

Wecht, J. M., and Bauman, W. A. (2018). Implication of altered autonomic control for orthostatic tolerance in SCI. *Auton. Neurosci.* 209, 51–58. doi: 10.1016/j.autneu.2017.04.004

Wecht, J. M., Weir, J. P., Katzelnick, C. G., Wylie, G., Eraifej, M., Nguyen, N., et al. (2018). Systemic and cerebral hemodynamic contribution to cognitive performance in spinal cord injury. *J. Neurotrauma* 35, 2957–2964. doi: 10.1089/neu.2018.5760

West, C. R., Alyahya, A., Laher, I., and Krassioukov, A. (2013). Peripheral vascular function in spinal cord injury: a systematic review. *Spinal Cord* 51, 10–19. doi: 10.1038/sc.2012.136

Westby, C. M., Martin, D. S., Lee, S. M., Stenger, M. B., and Platts, S. H. (2016). Left ventricular remodeling during and after 60 days of sedentary head-down bed rest. *J. Appl. Physiol.* 120, 956–964. doi: 10.1152/japplphysiol.00676.2015

Williams, A. M., Gee, C. M., Voss, C., and West, C. R. (2019). Cardiac consequences of spinal cord injury: systematic review and meta-analysis. *Heart* 105, 217–225. doi: 10.1136/heartjnl-2018-313585

Wu, J. C., Chen, Y. C., Liu, L., Chen, T. J., Huang, W. C., Cheng, H., et al. (2012). Increased risk of stroke after spinal cord injury: a nationwide 4-year follow-up cohort study. *Neurology* 78, 1051–1057. doi: 10.1212/WNL.0b013e31824e8eaa

Yarkony, G. M., Katz, R. T., and Wu, Y. C. (1986). Seizures secondary to autonomic dysreflexia. *Arch. Phys. Med. Rehabil.* 67, 834–835.

Conflict of Interest: The authors declare that the research was conducted in the absence of any commercial or financial relationships that could be construed as a potential conflict of interest.

frontiers in Systems Neuroscience

ORIGINAL RESEARCH
published: 19 November 2020
doi: 10.3389/fnsys.2020.569337

Epidural Electrical Stimulation of the Lumbosacral Spinal Cord Improves Trunk Stability During Seated Reaching in Two Humans With Severe Thoracic Spinal Cord Injury

*Megan Gill[1], Margaux Linde[1], Kalli Fautsch[1], Rena Hale[1], Cesar Lopez[1], Daniel Veith[1], Jonathan Calvert[2], Lisa Beck[1], Kristin Garlanger[1], Reggie Edgerton[3,4], Dimitry Sayenko[5], Igor Lavrov[6,7], Andrew Thoreson[1], Peter Grahn[1,8] and Kristin Zhao[1,9]**

[1]Assistive and Restorative Technology Laboratory, Department of Physical Medicine and Rehabilitation, Rehabilitation Medicine Research Center, Mayo Clinic, Rochester, MN, United States, [2]Mayo Clinic Graduate School of Biomedical Sciences, Mayo Clinic, Rochester, MN, United States, [3]Department of Neurobiology, University of California, Los Angeles, Los Angeles, CA, United States, [4]The Centre for Neuroscience and Regenerative Medicine, Faculty of Science, University of Technology Sydney, Ultimo, NSW, Australia, [5]Department of Neurosurgery, Center for Neuroregeneration, Houston Methodist Hospital, Houston, TX, United States, [6]Department of Neurology, Mayo Clinic, Rochester, MN, United States, [7]Institute of Fundamental Medicine and Biology, Kazan Federal University, Kazan, Russia, [8]Department of Neurologic Surgery, Mayo Clinic, Rochester, MN, United States, [9]Department of Physiology and Biomedical Engineering, Mayo Clinic, Rochester, MN, United States

OPEN ACCESS

Edited by:
Enrico Rejc,
University of Louisville, United States

Reviewed by:
Matthias J. Krenn,
University of Mississippi Medical Center, United States
Lisa Lombardo,
Louis Stokes Cleveland VA Medical Center, United States

***Correspondence:**
Kristin D. Zhao
zhao.kristin@mayo.edu

Received: 03 June 2020
Accepted: 06 October 2020
Published: 19 November 2020

Citation:
Gill M, Linde M, Fautsch K, Hale R, Lopez C, Veith D, Calvert J, Beck L, Garlanger K, Edgerton R, Sayenko D, Lavrov I, Thoreson A, Grahn P and Zhao K (2020) Epidural Electrical Stimulation of the Lumbosacral Spinal Cord Improves Trunk Stability During Seated Reaching in Two Humans With Severe Thoracic Spinal Cord Injury. Front. Syst. Neurosci. 14:569337. doi: 10.3389/fnsys.2020.569337

Background: Quality of life measurements indicate that independent performance of activities of daily living, such as reaching to manipulate objects, is a high priority of individuals living with motor impairments due to spinal cord injury (SCI). In a small number of research participants with SCI, electrical stimulation applied to the dorsal epidural surface of the spinal cord, termed epidural spinal electrical stimulation (ES), has been shown to improve motor functions, such as standing and stepping. However, the impact of ES on seated reaching performance, as well as the approach to identifying stimulation parameters that improve reaching ability, have yet to be described.

Objective: Herein, we characterize the effects of ES on seated reaching performance in two participants with chronic, complete loss of motor and sensory functions below thoracic-level SCI. Additionally, we report the effects of delivering stimulation to discrete cathode/anode locations on a 16-contact electrode array spanning the lumbosacral spinal segments on reach distance while participants were seated on a mat and/or in their wheelchair.

Methods: Two males with mid-thoracic SCI due to trauma, each of which occurred more than 3 years prior to study participation, were enrolled in a clinical trial at Mayo Clinic, Rochester, MN, USA. Reaching performance was assessed, with and without ES, at several time points throughout the study using the modified functional reach test (mFRT). Altogether, participant 1 performed 1,164 reach tests over 26-time points. Participant 2 performed 480 reach tests over 17-time points.

Results: Median reach distances during ES were higher for both participants compared to without ES. Forward reach distances were greater than lateral reach distances in all environments, mat or wheelchair, for both participants. Stimulation delivered in the caudal region of the array resulted in improved forward reach distance compared to stimulation in the rostral region. For both participants, when stimulation was turned off, no significant changes in reach distance were observed throughout the study.

Conclusion: ES enhanced seated reaching-performance of individuals with chronic SCI. Additionally, electrode configurations delivering stimulation in caudal regions of the lumbosacral spinal segments may improve reaching ability compared to rostral regions.

Keywords: spinal cord injury, epidural spinal electrical stimulation, modified functional reach test, reach distance, trunk stability, neuromodulation, neurorehabilitation, paralysis

INTRODUCTION

Traumatic spinal cord injury (SCI) can drastically disrupt mobility and change the way individuals interact with their surroundings, prompting adaptations to maximize the independent performance of activities of daily living (ADLs). While in a seated position, impairment of trunk and leg muscle activation after SCI leads to an inability to maintain the position of the spine, pelvis, and hips when challenged against gravity. Thus, individuals with SCI have a significantly diminished ability to reach forward, or laterally, from a seated position, as well as a reduced capability to perform movements that are dependent upon motor control of the trunk and postural muscles (Chen et al., 2003).

Sensorimotor functional impairment in individuals with SCI inevitably leads to increased risk of fall-related injuries when performing ADLs, and results in a poor posture that compromises shoulder stability (Cloud et al., 2017) and skin integrity (King et al., 2008). Undoubtedly, individuals with tetraplegia struggle with postural instability more than individuals with paraplegia due to a greater dysfunction of trunk musculature (Chen et al., 2003; Milosevic et al., 2015). Regaining trunk stability, which is one of the top priorities identified by those living with SCI, would reduce the risk of fall-related injury and increase the independent performance of ADLs (Brown-Triolo et al., 2002; Anderson, 2004). Therapeutic approaches to address trunk stability typically focus on neuromuscular re-education of the trunk and hip muscles through task-specific balance training (Boswell-Ruys et al., 2010; Tse et al., 2018). Trunk stability can also be gained through compensatory mechanisms such as complex seating systems that are tailored to fit the individual and attach to their wheelchair (Curtis et al., 1995).

Neuromuscular electrical stimulation (NMES) is an intervention that induces motor activation patterns that mimic neurologically intact functional performance with an overarching goal of leveraging intrinsic neuroplasticity to retrain impaired neurocircuitry and improve function in individuals with upper motor neuron damage. Over the past several decades, NMES has been identified as a reliable intervention to improve trunk stability and is suggested as a standard of care along with therapeutic exercise after SCI (Ho et al., 2014; Bergmann et al., 2019). The application of NMES during functional tasks *via* skin surface or implanted stimulating electrodes, described as functional electrical stimulation (FES), has been shown to improve trunk stability and seated posture during reaching tasks for individuals with SCI (Kukke and Triolo, 2004; Triolo et al., 2013a; Bergmann et al., 2019). However, the magnitude of electrically stimulated muscle activation is modest compared to that of the non-injured population under typical physiological conditions (Collins, 2007; Triolo et al., 2013a). Additionally, the efficacy of FES is limited by neurophysiological properties of directly activating peripheral components of neuromuscular circuitry, which is thought to preferentially activate fatigable motor units at lower stimulus intensities than fatigue-resistant motor units (Henneman et al., 1965; Boom et al., 1993; Riess and Abbas, 2001; Godfrey et al., 2002; Popovic et al., 2002). Consideration of spinal cord stimulation could minimize the issue of muscle fatigue of direct NMES allowing longer durations of stimulation enabled functions.

Over the last decade, transcutaneous spinal electrical stimulation and epidural spinal electrical stimulation (ES) have emerged as promising approaches that facilitate spinal sensorimotor circuits in a manner that produces a more physiological activation pattern compared to FES (Sayenko et al., 2014, 2015; Gerasimenko et al., 2008, 2015a,b; Minassian et al., 2016a; Grahn et al., 2017; Hofstoetter et al., 2018). Additionally, in contrast to the use of FES as a neuroprosthetic technology, evidence suggests spinal stimulation engages spared sub-functional connections that span the injury site to restore volitional control over stimulation-enabled motor activity (Minassian et al., 2016b; Ievins and Moritz, 2017; Calvert et al., 2019a; Cho et al., 2019). For example, postural stability and ability to regain balance during self-initiated perturbations within a single session have been described through the use of transcutaneous spinal electrical stimulation in humans with motor complete ($N = 6$), as well as motor incomplete ($N = 2$), SCI (Rath et al., 2018); however, ES-enabled trunk stability and reaching ability while seated have not been described in detail. The underlying mechanisms through which ES, as well as transcutaneous spinal electrical stimulation, enables functional gains are thought to involve the facilitation of a "central state of excitability" within spinal networks that reside below the level of SCI (Taccola et al., 2018). Following the described

theory, ES could potentially result in similar improvements in trunk stability to those described during transcutaneous electrical spinal stimulation. Optimizing stimulation parameters for task-specific activities relies on multiple different variables, including electrode location and voltage intensity. Localized activation of the rostral electrodes primarily activates proximal muscles, whereas localized activation of caudal electrodes activates predominately distal muscles (Sayenko et al., 2014; Calvert et al., 2019a).

We previously demonstrated that ES in combination with task-specific training, which we defined as multimodal rehabilitation (MMR), likely facilitates reorganization of the supraspinal-spinal connectome to recover lost functions following SCI (Gill et al., 2018). Similarly, multiple reports have shown that over several months of MMR sessions, performed multiple days per week, individuals with SCI achieved improvements in standing performance in the presence of ES (Harkema et al., 2011b; Rejc et al., 2015, 2017; Grahn et al., 2017) as well as restoration of independent weight-bearing stepping activity (Angeli et al., 2018; Gill et al., 2018; Wagner et al., 2018) and trunk stability (Angeli et al., 2018). Here, we describe the effects of ES on seated reaching ability in two individuals with chronic motor and sensory complete paraplegia following SCI. Secondly, we describe seated reaching outcomes produced by localizing active electrode configurations within the rostral, and caudal regions of the implanted electrode array.

MATERIALS AND METHODS

Participant Descriptions

At the time of study enrollment, participant 1 was a 26-year-old male who sustained a traumatic SCI at the T6 vertebral level 3 years prior and was diagnosed as American Spinal Injury Association Impairment Scale-A (AIS-A; i.e., complete loss of motor, sensory, and autonomic functions below the level of injury). We previously reported lower extremity motor functions that were restored using ES, such as standing and stepping, in participant 1 (Grahn et al., 2017; Gill et al., 2018; Calvert et al., 2019a).

At the time of enrollment, participant 2 was a 37-year-old male who sustained a traumatic SCI at the T3 vertebral level 6 years prior and was diagnosed as AIS-A. Together with data generated by participant 1, we previously reported that the participant achieved a step-like movement of his lower extremity using ES while positioned side-lying with his leg suspended in a gravity-neutral position (Calvert et al., 2019a).

Both participants provided written informed consent to conduct experiments described within a study protocol that was approved by the FDA for an investigational device exemption as well as approved by Mayo Clinic's IRB. For mobility in their personal lives, both participants used rigid frame, self-propelled wheelchairs that were custom-fit to maximize comfort, appropriate posture, and trunk stability.

ES System and Rehabilitation Paradigm

Both participants underwent 6 months of locomotor training (Harkema et al., 2011a; **Figure 1A**) followed by surgical implantation of a 16-contact epidural spinal electrical stimulation electrode array (Specify 5-6-5, Medtronic, Fridley, MN, USA) at the T11-L1 vertebral region. To refine electrode array alignment to the lumbosacral spinal cord enlargement (i.e., spinal segments L2-S1), intraoperative electromyography was used to record ES-evoked motor potentials from several muscles of the lower extremities, bilaterally (Calvert et al., 2019a). After 3 weeks of rest, each participant performed approximately three sessions of MMR per week for the next 12 months. MMR sessions were comprised of ES parameter adjustment to enable maximum independence during stand, step, and reach training. During the 12 months of MMR, participants were allowed to use a subset of ES parameters outside the laboratory, only if deemed safe by study staff, to perform tasks, such as supine or seated volitional leg movements and standing with appropriate assistive devices (Gill et al., 2018). After 12 months of MMR, each participant took a 3-month break from study-related activities. Then, they performed 12 additional months of MMR sessions and testing, during which they attended two days of laboratory-based activities twice a month, which focused on examining ES-enabled trunk stability and reaching functions.

Modified Functional Reach Test to Assess ES-Enabled Performance

The modified functional reach test (mFRT) is a clinical assessment used to evaluate reaching performance and provide immediate feedback to participants and study staff (Lynch, 1995). The mFRT was performed 1–2 times per month throughout the study while participants were seated either on a padded, height-adjustable mat or while positioned in their wheelchair. At each recording session, the mFRT was performed with, and without ES, while the participants' feet were positioned flat on the floor or the footrest of their wheelchair. For safety purposes, a trainer was located in front of the participant to prevent falls if a loss of balance occurred. At the start of each recording, they were instructed to raise one arm to 90 degrees of either shoulder flexion (forward reach) or abduction (lateral reach) with their elbow joint fully extended while maintaining a neutral wrist position and extended fingers (**Figure 1B**). A meter stick was held horizontally by study staff in proximity to the participant's finger. Zero distance marked the starting point and maximum reach distance was captured when the participant reached forward or laterally as far as possible while retaining the ability to independently return to their initial, upright seated position. The participant's uninvolved arm could be used for counterbalance, but not for support while reaching. If the uninvolved arm was used for support, or if trainer assistance was required to return to the initial position, the attempt was not recorded for data analysis, and a subsequent attempt was performed. Three independent reaches were collected for each condition: ES ON and NO ES (e.g., left arm forward, right arm forward, left arm lateral, right arm lateral). The sequence of these four conditions was not standardized across sessions or participants. ES pulse amplitude, width, and frequency, as well as anode/cathode configurations, were adjusted during each testing session with a focus on improving trunk stability. Rostral ES and Caudal ES were defined as localized programs increasing

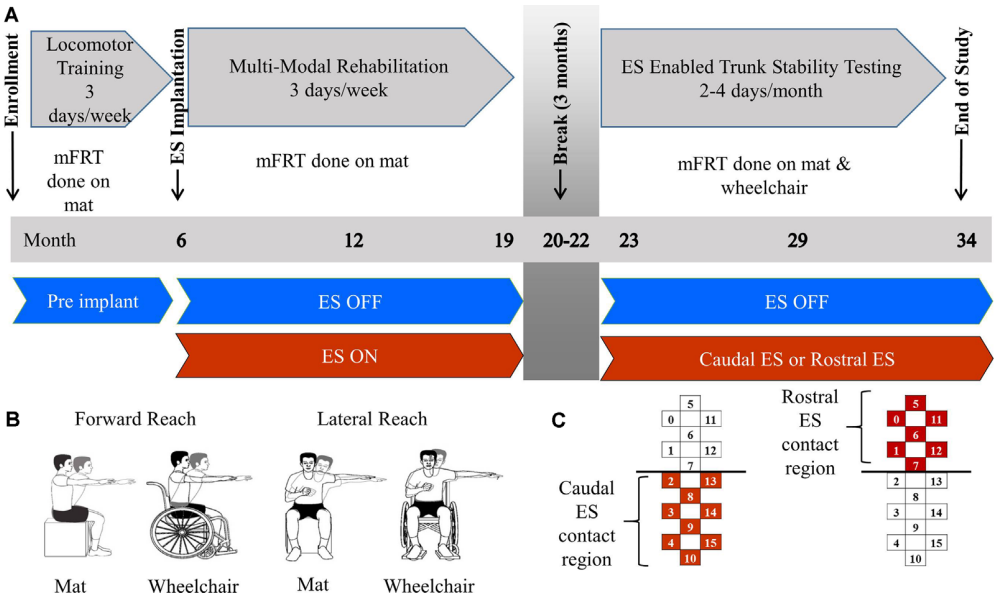

FIGURE 1 | Methods description. Panel **(A)** describes clinical trial timeline including enrollment, time of electrical stimulation (ES) implantation, 3 month break, and end of study. Training focus is described for each phase of the study as well as the environment of each modified functional reach test (mFRT). Panel **(B)** is a pictorial of forward and lateral reaching tasks performed on the mat or wheelchair. Panel **(C)** demonstrates the active electrodes used on the stimulating array for Caudal ES and Rostral ES.

stimulation intensity to facilitate the greatest reaching distance possible. Regional descriptions of the electrodes used (anodes and cathodes) for Rostral ES and Caudal ES are visually provided in **Figure 1C**. The parameters used for this study were a subset of the ranges that are defined by the ES device manufacturer, which were approved for use in this study by the Mayo Clinic IRB after obtaining an IDE from the FDA. For comparison purposes, Caudal ES and Rostral ES parameters were tracked over months 23–34. During Caudal ES, stimulation intensity and frequency ranges for participant 1 were 2.0–6.5 V and 20–25 Hz with a 210 μs pulse width and during Rostral ES, the same parameter ranges were 4.4–7.8 V and 20 Hz with a 420 μs pulse width. During Caudal ES, the stimulation intensity range for participant 2 was 2.9–3.0 V with a frequency of 20 Hz and pulse width range of 200–400 μs, while during Rostral ES, the stimulation intensity range was 3.8–5.0 V with a frequency of 25 Hz and pulse width of 450 μs.

Reach Distances Across Clinical Trial Time Points

Participant 1

For all conditions tested, a total of 1,164 successful reaches were recorded using the mFRT across 26-time points resulting in 388 averaged data points (**Figure 2**). Out of the 388 averaged data points, 208 represent reaching performance without ES and 180 represent reaching performance with ES.

Participant 2

A total of 480 mFRT recordings were collected across 17-time points of the clinical trial. From those recordings, 60 represent reaching performance without ES and 100 represent reaching performance with ES (**Figure 6**). All mFRT were performed while seated on a mat. During month 22, the participant was withdrawn from the clinical trial due to personal commitments, not due to study-related complications or adverse events.

Data Analysis

Reach distance recordings from three successful, independent reaches were averaged. Averaged reach distances were categorized by reaching limb (right or left), reaching direction (forward or lateral), environment (mat or wheelchair), and ES and NO ES conditions. To evaluate the repeatability of reach distances within each trial, the coefficient of variation (CV) was calculated for each condition tested. The NO ES condition was then subdivided into pre-implant (months 0–6) and ES OFF (months 6–34). The ES condition was then subdivided into Rostral and Caudal ES (months 23–34; **Figure 1**). Due to non-normal distribution, data were summarized and presented descriptively as median values and interquartile ranges (IQR) calculated using JMP statistical software (SAS, Cary, NC, USA). One group's value was considered to be notably larger than that of another if medians were different and if more than two-thirds of the data points in the stated lesser-valued group fell below the median of the greater-valued group. Reach distances were calculated and plotted across time according to when mFRT recordings were gathered during the clinical trial. The timing of mFRT recordings is shown as a test date minus enrollment date. For pictorial analysis only, a spline fit was generated for median values across time. Data from participant 1 was analyzed independently from participant 2.

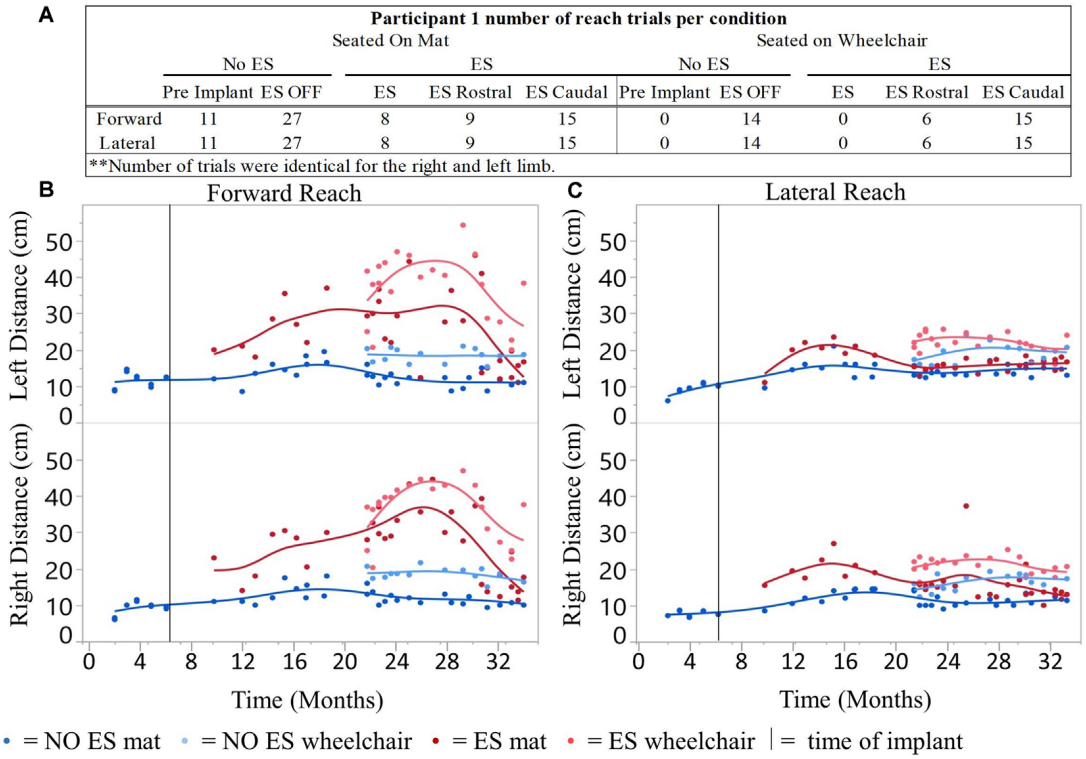

FIGURE 2 | Participant 1 reach distances for all conditions recorded over time. Number of mFRT trials recorded throughout the study demonstrating forward and lateral (right and left equally), through all ES conditions: NO ES and ES. Numbers display trials performed on mat and on wheelchair **(A)**. The average of three trials per day for forward **(B)** and lateral reach **(C)** on mat and wheelchair. Solid vertical line indicates epidural stimulator implantation time point.

RESULTS

Participant 1

Variability of Reaching Performance Across Experimental Conditions

Left median forward reach CV values for the mat and wheelchair conditions were higher during the NO ES condition when compared to the ES condition. A small difference in CV was noted for the lateral reaching task (**Figure 3**). While seated on the mat, median forward reach distance variability was 1.9% higher for the right arm and 1.5% higher for the left arm; while median lateral reach distance variability was 0.9% higher for the right arm and 1.7% lower for the left when comparing the NO ES condition to ES conditions. While seated in the wheelchair, median forward reach distance variability was 3.5% lower for the right arm and 2.6% higher for the left arm while median lateral reach variability was 0.2% higher for the right arm and 0.6% lower for the left arm when comparing the NO ES condition to ES condition. During ES conditions, median forward reach distance variability was 1.2% lower for the right arm and 2.4% higher for the left arm, while median lateral reaching distance variability was 1.5% higher for the right arm and 4.0% higher for the left arm when comparing the mat to wheelchair environment. During the NO ES condition, the median forward reach distance variability was 4.2% higher for the right arm and 1.3% higher for the left arm, while median lateral reaching was 2.2% higher for the right arm and 2.9% higher for the left arm when comparing the mat to the wheelchair environment.

Reaching With ES Compared to NO ES

Participant 1 consistently had a higher median forward and lateral reach distance with ES compared to NO ES condition when seated on the mat as well as in the wheelchair. While seated on the mat, ES resulted in greater median forward reaching distances by 17.4 cm (right) and 12.7 cm (left) than NO ES. Additionally, median lateral reaching distances with ES increased by 5.1 cm (right) and 3.3 cm (left), respectively. While seated in the wheelchair, ES resulted in median forward reaching distances that were 19.0 cm (right) and 19.6 cm (left) greater than NO ES, as well as median lateral reaching distances that were 4.2 cm (right) and 2.0 cm (left) greater (**Figure 4**). In the mat and wheelchair environments, improvements in reach distances, specifically in forward but not lateral reach, resulted in an instantaneous effect when utilizing ES.

Reaching While Seated on the Mat Compared to Seated on the Wheelchair

Participant 1 consistently reached farther (forward and laterally) in the wheelchair than on the mat in both ES and NO ES conditions (**Figure 4**). Reaching with ES while seated in the wheelchair resulted in median forward reaching distances that were 9.3 cm (right) and 13.3 cm (left) greater than reaching while

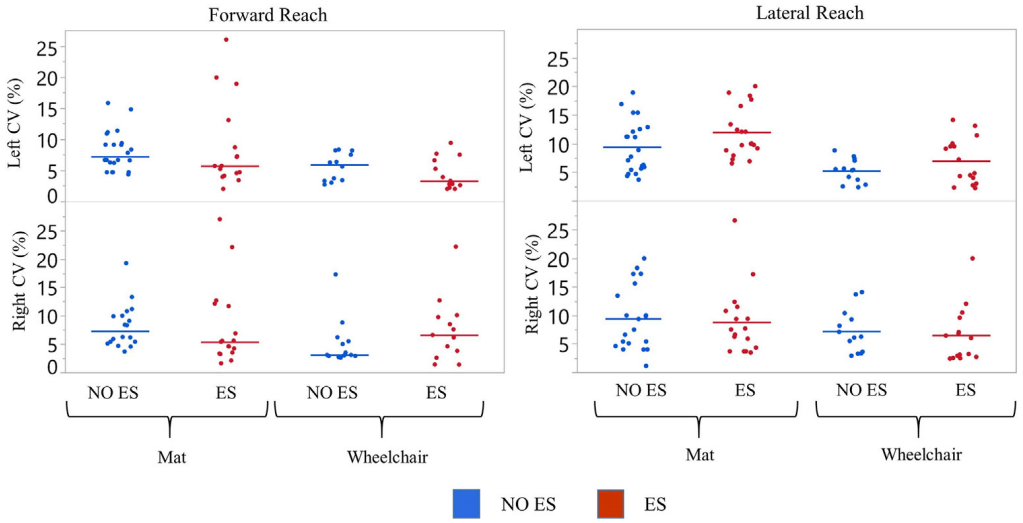

FIGURE 3 | Participant 1 coefficient of variation (CV) of reach scores. The CV was calculated for all reach distances of NO ES (Blue) and ES (Red) for the right and left arm while seated on a mat or a wheelchair. Data represented in a scatter plot with line at the median value.

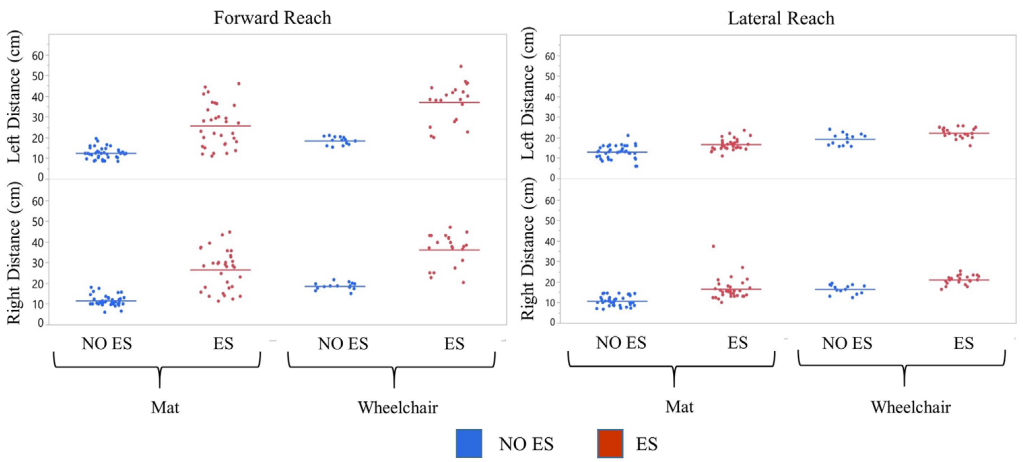

FIGURE 4 | Participant 1 comparison of No ES to ES reach distances. Forward and lateral reach distances during No ES and ES conditions were compared for right and left sides while seated on the mat or the wheelchair. Dots represent the average of three trials for forward and lateral reach and solid horizontal line represents the median of all trials combined.

seated on the mat. Similarly, median lateral reaching distances were 5.6 cm (right) and 5.7 cm (left) greater from the wheelchair compared to the mat. Reaching from the wheelchair during NO ES resulted in median forward reach distances that were 7.7 cm (right) and 6.4 cm (left) greater than reaching from the mat. Likewise, median lateral reach distances were 6.5 cm (right) and 7.0 cm (left) greater during NO ES when reaching from the wheelchair as compared to NO ES reaching from the mat.

Comparison of Rostral ES, Caudal ES, and ES OFF Conditions

Participant 1 consistently reached farther during forward reach, using Caudal ES, compared to Rostral ES, and ES OFF conditions. Additionally, superior reaching performance during Caudal ES was observed when seated on the mat as well as when seated in the wheelchair (**Figure 5**).

Mat Environment

While seated on the mat, there was a greater difference in reaching distances during forward reaching as compared to lateral reaching. Compared to ES OFF, Rostral ES generated an increase in median forward reach distance of 4.0 cm (right) and 2.7 cm (left), as well as an increase in median lateral reach distance of 2.3 cm (right) and 3.4 cm (left). Compared to ES OFF, Caudal ES resulted in median forward reach distances that were 22.3 cm (right) and 17.7 cm (left) greater and median lateral reach distances that were 5.0 cm (right) and 2.0 cm (left) greater. Compared to Rostral

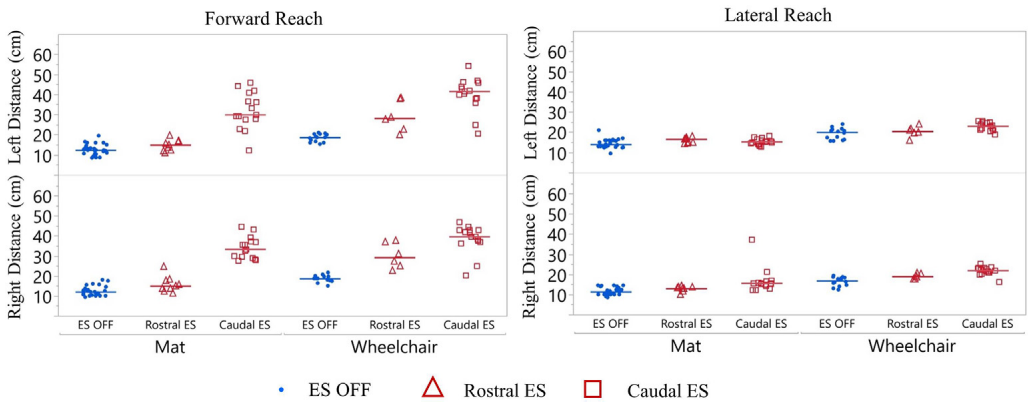

FIGURE 5 | Participant 1 reach distance during three conditions (ES OFF, ES Rostral and ES Caudal) on mat and wheelchair. ES conditions for forward and lateral reach distances reported for right and left sides. Each data point indicates the average of three trials at each test date, blue represents ES off, red triangles represent Rostral ES usage, and red squares represent Caudal ES usage. Each reach direction, forward, lateral, right, and left were performed and reported for mat and wheelchair environments.

A

Participant 2 number of reach trials per condition

	Seated on Mat					Seated on Wheelchair				
	No ES		ES			No ES		ES		
	Pre Implant	ES OFF	ES	ES Rostral	ES Caudal	Pre Implant	ES OFF	ES	ES Rostral	ES Caudal
Forward	13	12	10	4	1	0	0	0	0	0
Lateral	13	12	10	4	1	0	0	0	0	0

**Number of trials were identical for the right and left limb.

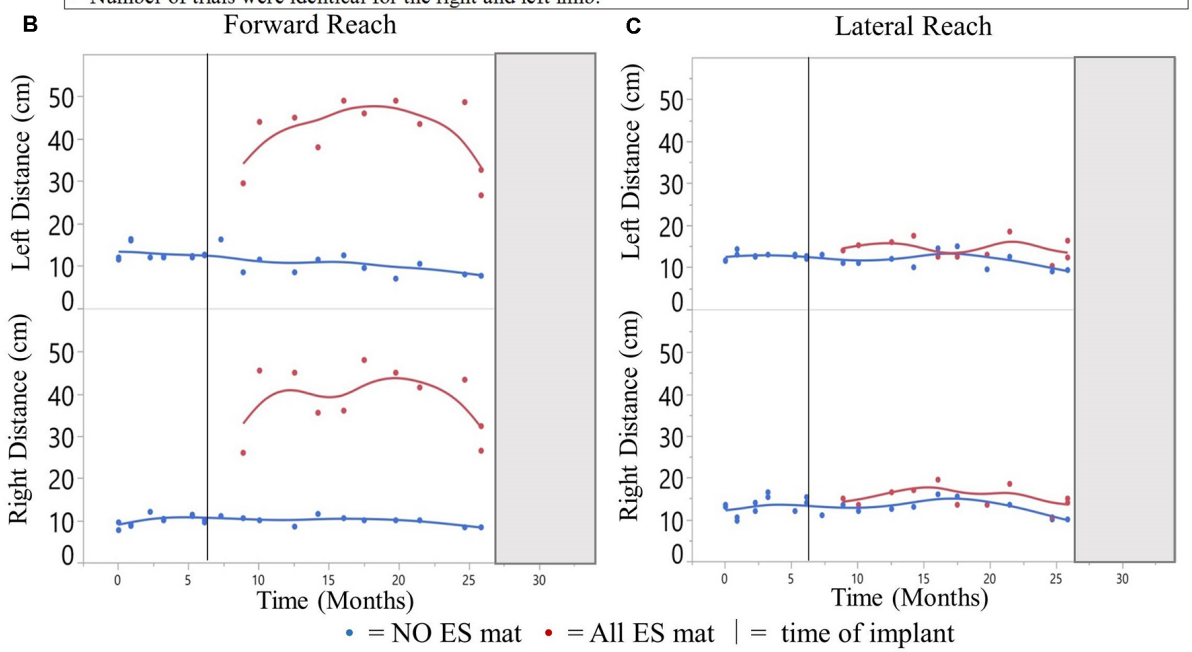

FIGURE 6 | Participant 2 reach distances for all conditions recorded over time. Number of mFRT trials recorded throughout the study demonstrating forward and lateral (right and leftarm), through all ES conditions: NO ES and ES. Numbers display trials performed on mat **(A)**. The average of three trials per day for forward **(B)** and lateral reach **(C)**. Solid vertical line indicates ES implantation time point. Gray box represents when the participant exited the study.

ES, the Caudal ES electrode configuration enabled greater median reach distances of 18.3 cm (right) and 15.0 cm (left) during forward reaching. Rostral ES enabled greater median lateral reaching for the left arm (1.4 cm) whereas Caudal ES enabled greater lateral reaching for the right arm (2.7 cm).

Wheelchair Environment

While seated on the wheelchair, the difference in median reach distance was greatest between ES OFF and Caudal ES. Compared to ES OFF, Rostral ES resulted in median forward reach distances that increased by 10.5 cm (right) and 9.5 cm (left), and median lateral reach distances that increased by 2.2 cm (right) and 0.5 cm (left). Compared to ES OFF, Caudal electrode configurations lead to median increases of 21.0 cm (right) and 23.0 cm (left) during forward reaching as well as increases of 5.2 cm (right) and 3.0 cm (left) during lateral reaching. We found that during Caudal ES forward reaching distances were 10.5 cm (right) and 13.5 cm (left) greater than during Rostral ES. Similarly, median lateral reaching distances were 3.0 cm (right) and 2.5 cm (left) greater during Caudal ES compared to Rostral ES.

Comparison of Seated Position (Wheelchair vs. Mat)

For all ES conditions, median reach distances from the wheelchair were greater than those performed while seated on the mat (**Figure 5**). Sitting in the wheelchair, compared to the mat, led to increases in median forward reaching distances of 7.7 cm (right) and 6.4 cm (left) during ES OFF; 14.2 cm (right) and 13.2 cm (left) during Rostral ES, and 6.4 cm (right) and 11.7 cm (left) during Caudal ES. Similarly, median lateral reach distances while seated in the wheelchair were greater than when seated on the mat: 6.1 cm (right) and 6.7 cm (left) during NO ES; 6.0 cm (right) and 3.8 cm (left) during Rostral ES; and 6.3 cm (right) and 7.7 cm (left) during Caudal ES.

Participant 2

Variability of Reaching Performance Across Experimental Conditions

The NO ES condition had slightly higher median CV values when compared to the ES condition during forward reach with the right and left arms and during lateral reach with the right arm (**Figure 7**). Specifically, the median forward reach distance variability was 4.9% higher for the right arm and 4.5% higher for the left arm when comparing the NO ES condition to the ES conditions. Median lateral reach distance variability during NO ES was 7.6% higher than ES when reaching to the right and 4.8% lower than ES when reaching to the left.

Reaching With ES Compared to NO ES While Seated on the Mat

Participant 2 demonstrated greater median forward and lateral reach distances with ES compared to NO ES (**Figure 8**). While seated on the mat, the use of ES resulted in median forward reach distances that were 26.0 cm (right) and 31.5 cm (left) greater than during NO ES. Median lateral reach distances from the mat were 1.5 cm (right) and 0.5 cm (left) greater with ES compared to NO ES. Similar to participant 1, improvement in reach distances, specifically forward, resulted in an instantaneous effect when utilizing ES.

Comparison of Rostral ES, Caudal ES, and ES OFF Conditions While Seated on the Mat

Similar to participant 1, participant 2 reached farther forward, with Caudal ES compared to Rostral ES, as well as ES OFF, in the mat environment (**Figure 9**). Rostral ES resulted in median forward reach distances that were 8.1 cm (right) and 7.7 cm (left) greater than ES OFF. However, during Rostral ES, the median lateral reach distance to the right was 1.3 cm less than ES OFF, and lateral reach distance to the left was 1.0 cm less than ES OFF. Similarly, when compared to ES OFF, Caudal ES median forward reach distances increased by 33.3 cm (right) and 37.2 cm (left) while median lateral reach distances decreased by 3.0 cm (right) and 2.2 cm (left). Likewise, Caudal ES, when compared to Rostral ES, resulted in median forward reach distances that were 25.2 cm (right) and 29.5 cm (left) higher, while median lateral reach distances were 1.7 cm (right) and 1.2 cm (left) lower.

DISCUSSION

Results from this study demonstrate the feasibility of enhancing trunk stability during seated reaching tasks using lumbosacral ES in humans with chronic SCI. Data from the CV analysis suggests

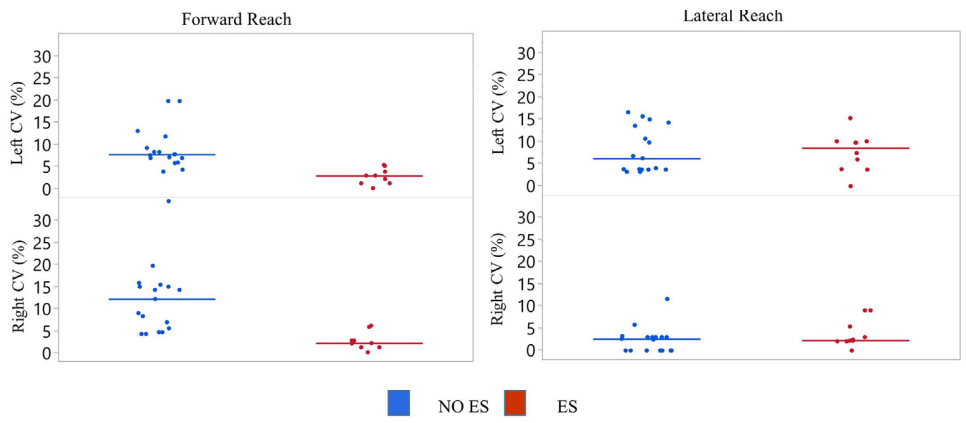

FIGURE 7 | Participant 2 coefficient of variation (CV) of reach scores. The CV was calculated for all reach distances of NO ES (Blue) and ES (Red) for the right and left arm while seated on a mat. Data represented in a scatter plot with line at the median value.

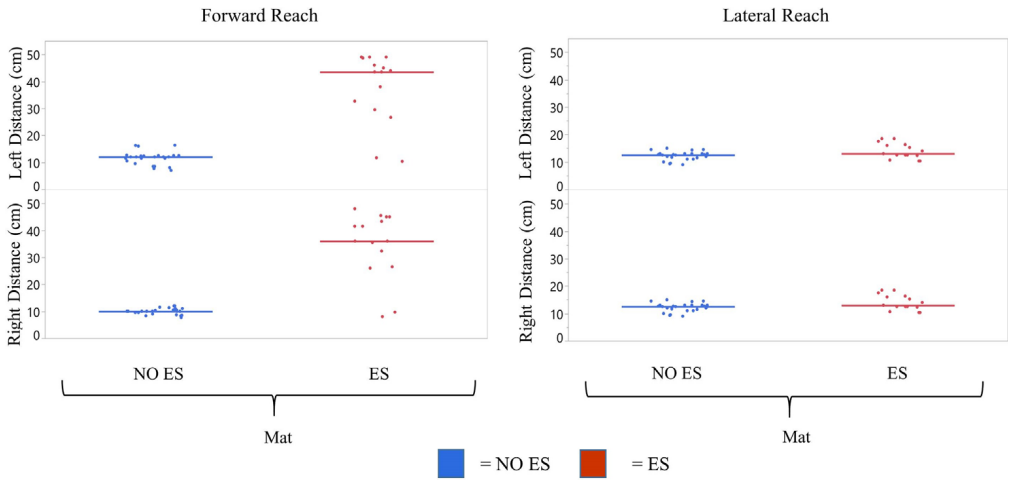

FIGURE 8 | Participant 2 comparison of No ES to ES reach scores. mFRT scores for forward and lateral reach distances in No ES conditions were compared for right and left sides while seated on the mat. Dots represent average of three trials for forward and lateral reach and solid horizontal line represents the median of all trials combined.

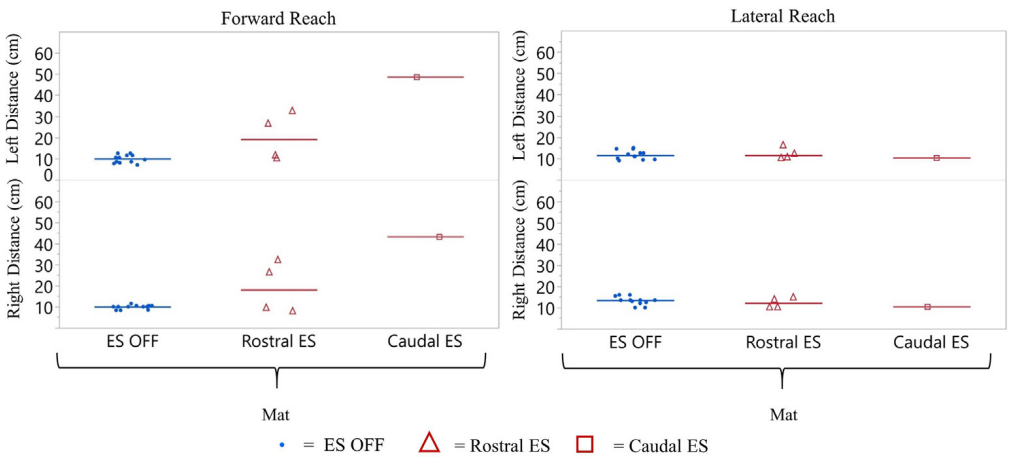

FIGURE 9 | Participant 2 reach distance during three conditions (ES OFF, Rostral ES and Caudal ES contacts) while seated on the mat. ES conditions for forward and lateral reach distances reported for right and left side. Each data point indicates the average of three trials at each test date, blue representing ES off, red triangles represent Rostral ES usage, and red squares represent Caudal ES usage.

that patients with SCI are repeatable in their forward and lateral reach tests, and reach distances are affected by the ES ON and ES OFF conditions. Results indicate that when ES is enabled, forward reach distances increase, and lateral reach distances remains unchanged. Within the ES condition, caudal stimulation was more effective in improving forward reach distance than rostral stimulation.

Epidural Spinal Electrical Stimulation Enables Increased Reach Distance

The act of reaching forward or laterally, from a stable seated position to the limit of stability, followed by a return to an upright sitting position can be significantly impaired after a SCI. Impaired reaching ability results in a drastic loss of independence as well as an increase in the risk of injury due to loss of balance and falling. Here, we objectively demonstrated that reach distances instantaneously improved in individuals with SCI in the presence of ES. During ES both participants were able to reach farther in the forward direction using either arm when compared to without ES.

Reach distance variability was dependent upon: (1) the seated environment; (2) the range and direction of mFRT recordings; and (3) the presence of ES compared to NO ES. Results from CV analysis demonstrate that reach distance scores were more repeatable when the participants were sitting in their wheelchair while ES was enabled compared to sitting on the mat with NO ES. Customized manual wheelchair seating

systems enhance seated stability by providing individualized support for appropriate pelvic and trunk positioning during ADLs. Although the confidence in reaching ability was subjectively reported by both participants to be greater with ES, the reach distance measurement range was wider, especially during forward reach. When ES was not enabled, reaching ability returned to its original functional state for both participants.

For both participants, ES-enabled improvements in the forward reach distance were notably greater than those observed in lateral reach distance. Forward and lateral reaching requires activation of different muscle groups to achieve direction-specific movement patterns. Factors that typically affect seated posture and could potentially impact lateral reach include pelvic obliquity, presence of scoliosis, and SCI motor asymmetry. We demonstrated that rostral and caudal ES configurations enabled reaching abilities differently. Our findings suggest unique ES configurations may be needed to enable maximum reaching performance in all directions, which may be a critical feature of next-generation ES technologies to successfully translate ES use for ADL performance by individuals with SCI. Additionally, continued investigation of lower extremity activation patterns during reaching and returning to the upright sitting position may provide new insight that can be leveraged during ES configuration optimization to facilitate similar patterns of activation, and in turn, achieve optimal reaching performance with ES. Our results show that the use of ES, specifically caudal ES configurations designed to engage distal leg muscles, generally resulted in greater reach distances when compared to rostral ES configurations outlined in Calvert et al. (2019b).

Therapeutic Potential of ES

Both participants' forward reaching ability improved instantaneously with ES compared to without. Of equal importance, these improved reaching abilities with ES were repeatable throughout the study. Our findings suggest that ES provides a therapeutic option for restoring functional trunk stability which is currently untreatable, or at best, marginally improved by long-term, strenuous exercise paradigms (Sliwinski et al., 2020). In addition to enabling supraspinal control over motor functions, ES-enabled motor functions are thought to facilitate a more physiological pattern of motor unit recruitment when compared to currently-available NMES systems (Henneman, 1957; Henneman et al., 1965; Maffiuletti, 2010; Bickel et al., 2011). Furthermore, the magnitude of forward reaching we observed during ES was considerably greater than absolute reach distances reported by others during NMES (Triolo et al., 2013b).

When delivering electrical stimulation to the skin over the spine, which has recently emerged as a promising approach to modulate spinal networks after SCI, direct activation of trunk musculature likely occurs, in a similar manner as FES, in addition to previously described spinal network activation (Hofstoetter et al., 2018; Rath et al., 2018; Sayenko et al., 2019). However, during ES, focal activation occurs within spinal networks, rather than directly activating peripheral components of trunk neuro-musculature. Therefore, the improvements in the seated function we observed may have been achieved engaging multi-segmental spinal networks that span rostrally from the lumbosacral implantation site of the electrode array, which in turn, enabled coordinated activation of muscle synergies across the trunk, hip, and lower limbs to improve the reaching ability.

The evidence presented here demonstrates a critical step toward the restoration of functional motor activity using ES to enhance ADLs in individuals with SCI. Future studies should incorporate full-body biomechanical assessments (e.g., motion capture, electrophysiology, etc.) to better understand dynamic interactions that occur across spinal sensorimotor networks during ES, and the extent to which ES-facilitated spinal networks integrate supraspinal motor control signals across the site of SCI, necessary to generate functional motor outputs, such as improved seated reaching performance. Future studies investigating ES-enabled reaching abilities should include individuals with different classifications of SCI to determine the generalizability of our results. Additionally, we recognize the study reported herein has limitations that challenge generalizing these results, given the heterogeneity of the severity of SCI and limited sample size. In conclusion, our results demonstrate that ES generated instantaneous improvements in seated reaching performance in two individuals with severe, motor, and sensory complete thoracic SCI. Additionally, stimulation delivered in the caudal region of the array resulted in improved forward reach distance compared to stimulation in the rostral region.

DATA AVAILABILITY STATEMENT

The raw data supporting the conclusions of this article will be made available by the authors, without undue reservation.

ETHICS STATEMENT

The studies involving human participants were reviewed and approved by Mayo Clinic Institutional Review Board (IRB). The participants provided their written informed consent to participate in this study. Written informed consent was obtained from the individual(s) for the publication of any potentially identifiable images or data included in this article.

AUTHOR CONTRIBUTIONS

PG, MG, RE, DS, and KZ initiated the project. LB, JC, MG, PG, ML, and DV designed the experiments with contributions from all authors, performed clinical assessments and designed and performed rehabilitation. LB, JC, MG, PG, ML, IL, and DV contributed to stimulation setting refinement. LB, JC, KF, PG, MG, ML, CL, RH, AT, DV, and KZ contributed to data collection, analysis, and interpretation. KF, MG, ML, and RH drafted the manuscript with subsequent contributions from all authors. KZ supervised all aspects of the work. All authors contributed to the article and approved the submitted version.

FUNDING

This work was supported by multiple foundations and entities, including: The Grainger Foundation, Regenerative Medicine Minnesota, The Jack Jablonski Bel13ve in Miracles Foundation, Mayo Clinic Graduate School of Biomedical Sciences, Mayo Clinic Center for Regenerative Medicine, Mayo Clinic Rehabilitation Medicine Research Center, Mayo Clinic Transform the Practice, Minnesota Office of Higher Education's Spinal Cord Injury and Traumatic Brain Injury Research Grant, and Craig H. Neilsen Foundation. Individual team members were also supported by Regenerative Medicine Minnesota, Mayo Clinic Center for Regenerative Medicine, and Mayo Clinic Graduate School of Biomedical Sciences.

ACKNOWLEDGMENTS

We thank the participants for their time and dedication to this study. We also thank K. Lee, C. Blaha, J. Chen, B. Cloud, T. Gardner, D. Hare, Y. Li, A. Mendez, C. Mitrovich, A. Schmeling, T. Scrabeck, M. Shaft, C. Stoppel, J. Strommen, M. Van Straaten, B. Wessel, and L. Zoecklein, as well as the surgical team for their support during device implantation.

REFERENCES

Anderson, K. D. (2004). Targeting recovery: priorities of the spinal cord-injured population. *J. Neurotrauma* 21, 1371–1383. doi: 10.1089/neu.2004.21.1371

Angeli, C. A., Boakye, M., Morton, R. A., Vogt, J., Benton, K., Chen, Y., et al. (2018). Recovery of over-ground walking after chronic motor complete spinal cord injury. *N. Engl. J. Med.* 379, 1244–1250. doi: 10.1056/NEJMoa1803588

Bergmann, M., Zahharova, A., Reinvee, M., Asser, T., Gapeyeva, H., and Vahtrik, D. (2019). The effect of functional electrical stimulation and therapeutic exercises on trunk muscle tone and dynamic sitting balance in persons with chronic spinal cord injury: a crossover trial. *Medicina* 55:619. doi: 10.3390/medicina55100619

Bickel, C. S., Gregory, C. M., and Dean, J. C. (2011). Motor unit recruitment during neuromuscular electrical stimulation: a critical appraisal. *Eur. J. Appl. Physiol.* 111, 2399–2407. doi: 10.1007/s00421-011-2128-4

Boom, H. B. K., Mulder, A. J., and Veltink, P. H. (1993). Fatigue during functional neuromuscular stimulation. *Prog. Brain Res.* 97, 409–418. doi: 10.1016/s0079-6123(08)62300-6

Boswell-Ruys, C. L., Harvey, L. A., Barker, J. J., Ben, M., Middleton, J. W., and Lord, S. R. (2010). Training unsupported sitting in people with chronic spinal cord injuries: a randomized controlled trial. *Spinal Cord* 48, 138–143. doi: 10.1038/sc.2009.88

Brown-Triolo, D. L., Roach, M. J., Nelson, K., and Triolo, R. J. (2002). Consumer perspectives on mobility: implications for neuroprosthesis design. *J. Rehabil. Res. Dev.* 39, 659–669.

Calvert, J. S., Grahn, P. J., Strommen, J. A., Lavrov, I. A., Beck, L. A., Gill, M. L., et al. (2019a). Electrophysiological guidance of epidural electrode array implantation over the human lumbosacral spinal cord to enable motor function after chronic paralysis. *J. Neurotrauma* 36, 1451–1460. doi: 10.1089/neu.2018.5921

Calvert, J. S., Grahn, P. J., Zhao, K. D., and Lee, K. H. (2019b). Emergence of epidural electrical stimulation to facilitate sensorimotor network functionality after spinal cord injury. *Neuromodulation* 22, 244–252. doi: 10.1111/ner.12938

Chen, C. L., Yeung, K. T., Bih, L. I., Wang, C. H., Chen, M. I., and Chien, J. C. (2003). The relationship between sitting stability and functional performance in patients with paraplegia. *Arch. Phys. Med. Rehabil.* 84, 1276–1281. doi: 10.1016/s0003-9993(03)00200-4

Cho, N., Squair, J. W., Bloch, J., and Courtine, G. (2019). Neurorestorative interventions involving bioelectronic implants after spinal cord injury. *Bioelectron. Med.* 5:10. doi: 10.1186/s42234-019-0027-x

Cloud, B. A., Zhao, K. D., Ellingson, A. M., Nassr, A., Windebank, A. J., and An, K.-N. (2017). Increased seat dump angle in a manual wheelchair is associated with changes in thoracolumbar lordosis and scapular kinematics during propulsion. *Arch. Phys. Med. Rehabil.* 98, 2021.e2–2027.e2. doi: 10.1016/j.apmr.2017.02.014

Collins, D. F. (2007). Central contributions to contractions evoked by tetanic neuromuscular electrical stimulation. *Exerc. Sport Sci. Rev.* 35, 102–109. doi: 10.1097/jes.0b013e3180a0321b

Curtis, K. A., Kindlin, C. M., Reich, K. M., and White, D. E. (1995). Functional reach in wheelchair users: The effects of trunk and lower extremity stabilization. *Arch. Phys. Med. Rehabil.* 76, 360–367. doi: 10.1016/s0003-9993(95)80662-8

Gerasimenko, Y. P., Lu, D. C., Modaber, M., Zdunowski, S., Gad, P., Sayenko, D. G., et al. (2015a). Noninvasive reactivation of motor descending control after paralysis. *J. Neurotrauma* 32, 1968–1980. doi: 10.1089/neu.2015.4008

Gerasimenko, Y., Gorodnichev, R., Moshonkina, T., Sayenko, D., Gad, P., and Reggie Edgerton, V. (2015b). Transcutaneous electrical spinal-cord stimulation in humans. *Ann. Phys. Rehabil. Med.* 58, 225–231. doi: 10.1016/j.rehab.2015.05.003

Gerasimenko, Y., Roy, R. R., and Edgerton, V. R. (2008). Epidural stimulation: comparison of the spinal circuits that generate and control locomotion in rats, cats and humans. *Exp. Neurol.* 209, 417–425. doi: 10.1016/j.expneurol.2007.07.015

Gill, M. L., Grahn, P. J., Calvert, J. S., Linde, M. B., Lavrov, I. A., Strommen, J. A., et al. (2018). Neuromodulation of lumbosacral spinal networks enables independent stepping after complete paraplegia. *Nat. Med.* 24, 1677–1682. doi: 10.1038/s41591-018-0175-7

Godfrey, S., Butler, J. E., Griffin, L., and Thomas, C. K. (2002). Differential fatigue of paralyzed thenar muscles by stimuli of different intensities. *Muscle Nerve* 26, 122–131. doi: 10.1002/mus.10173

Grahn, P. J., Lavrov, I. A., Sayenko, D. G., Van Straaten, M. G., Gill, M. L., Strommen, J. A., et al. (2017). Enabling task-specific volitional motor functions *via* spinal cord neuromodulation in a human with paraplegia. *Mayo Clin. Proc.* 92, 544–554. doi: 10.1016/j.mayocp.2017.02.014

Harkema, S., Gerasimenko, Y., Hodes, J., Burdick, J., Angeli, C., Chen, Y., et al. (2011a). Effect of epidural stimulation of the lumbosacral spinal cord on voluntary movement, standing and assisted stepping after motor complete paraplegia: a case study. *Lancet* 377, 1938–1947. doi: 10.1016/S0140-6736(11)60547-3

Harkema, S. J., Behrman, A. L., Barbeau, H. (2011b). *Locomotor Training: Principles and Practice.* Oxford: Oxford University Press.

Henneman, E. (1957). Relation between size of neurons and their susceptibility to discharge. *Science* 126, 1345–1347. doi: 10.1126/science.126.3287.1345

Henneman, E., Somjen, G., and Carpenter, D. O. (1965). Excitability and inhibitibility of motoneurons of different sizes. *J. Neurophysiol.* 28, 599–620. doi: 10.1152/jn.1965.28.3.599

Ho, C. H., Triolo, R. J., Elias, A. L., Kilgore, K. L., DiMarco, A. F., Bogie, K., et al. (2014). Functional electrical stimulation and Spinal Cord Injury. *Phys. Med. Rehabil. Clin. N. Am.* 25, 631–654. doi: 10.1016/j.pmr.2014.05.001

Hofstoetter, U. S., Freundl, B., Binder, H., and Minassian, K. (2018). Common neural structures activated by epidural and transcutaneous lumbar spinal cord stimulation: elicitation of posterior root-muscle reflexes. *PLoS One* 13:e0192013. doi: 10.1371/journal.pone.0192013

Ievins, A., and Moritz, C. T. (2017). Therapeutic stimulation for restoration of function after spinal cord injury. *Physiology* 32, 391–398. doi: 10.1152/physiol.00010.2017

King, R. B., Porter, S. L., and Vertiz, K. B. (2008). Preventive skin care beliefs of people with spinal cord injury. *Rehabil. Nurs.* 33, 154–162. doi: 10.1002/j.2048-7940.2008.tb00221.x

Kukke, S. N., and Triolo, R. J. (2004). The effects of trunk stimulation on bimanual seated workspace, *IEEE Trans. Neural Syst. Rehabil. Eng.* 177–185. doi: 10.1109/TNSRE.2004.827222

Lynch, S. M. (1995). The reliability and validity of the modified functional reach test in subjects with spinal cord injury. *Neurol. Rep.* 19, 19–20.

Maffiuletti, N. A. (2010). Physiological and methodological considerations for the use of neuromuscular electrical stimulation. *Eur. J. Appl. Physiol.* 110, 223–234. doi: 10.1007/s00421-010-1502-y

Milosevic, M., Masani, K., Kuipers, M. J., Rahouni, H., Verrier, M. C., McConville, K. M. V., et al. (2015). Trunk control impairment is responsible for postural instability during quiet sitting in individuals with cervical spinal cord injury. *Clin. Biomech.* 30, 507–512. doi: 10.1016/j.clinbiomech.2015.03.002

Minassian, K., Hofstoetter, U. S., Danner, S. M., Mayr, W., Bruce, J. A., McKay, W. B., et al. (2016a). Spinal rhythm generation by step-induced feedback and transcutaneous posterior root stimulation in complete spinal cord-injured individuals. *Neurorehabil. Neural Repair* 30, 233–243. doi: 10.1177/1545968315591706

Minassian, K., Mckay, W. B., Binder, H., and Hofstoetter, U. S. (2016b). Targeting lumbar spinal neural circuitry by epidural stimulation to restore motor function after spinal cord injury. *Neurotherapeutics* 13, 284–294. doi: 10.1007/s13311-016-0421-y

Popovic, M. R., Popovic, D. B., and Keller, T. (2002). Neuroprostheses for grasping. *Neurol. Res.* 24, 443–452. doi: 10.1179/016164102101200311

Rath, M., Vette, A. H., Ramasubramaniam, S., Li, K., Burdick, J., Edgerton, V. R., et al. (2018). Trunk stability enabled by noninvasive spinal electrical stimulation after spinal cord injury. *J. Neurotrauma* 35, 2540–2553. doi: 10.1089/neu.2017.5584

Rejc, E., Angeli, C. A., Atkinson, D., and Harkema, S. J. (2017). Motor recovery after activity-based training with spinal cord epidural stimulation in a chronic motor complete paraplegic. *Sci. Rep.* 7:13476. doi: 10.1038/s41598-017-14003-w

Rejc, E., Angeli, C., and Harkema, S. (2015). Effects of lumbosacral spinal cord epidural stimulation for standing after chronic complete paralysis in humans. *PLoS One* 10:e0133998. doi: 10.1371/journal.pone.0133998

Riess, J. A., and Abbas, J. J. (2001). Adaptive control of cyclic movements as muscles fatigue using functional neuromuscular stimulation. *IEEE Trans. Neural. Syst. Rehabil. Eng.* 9, 326–330. doi: 10.1109/7333.948462

Sayenko, D. G., Angeli, C., Harkema, S. J., Reggie Edgerton, V., and Gerasimenko, Y. P. (2014). Neuromodulation of evoked muscle potentials induced by epidural spinal-cord stimulation in paralyzed individuals. *J. Neurophysiol.* 111, 1088–1099. doi: 10.1152/jn.00489.2013

Sayenko, D. G., Atkinson, D. A., Floyd, T. C., Gorodnichev, R. M., Moshonkina, T. R., Harkema, S. J., et al. (2015). Effects of paired transcutaneous electrical stimulation delivered at single and dual sites over lumbosacral spinal cord. *Neurosci. Lett.* 609, 229–234. doi: 10.1016/j.neulet.2015.10.005

Sayenko, D. G., Rath, M., Ferguson, A. R., Burdick, J. W., Havton, L. A., Edgerton, V. R., et al. (2019). Self-assisted standing enabled by non-invasive spinal stimulation after spinal cord injury. *J. Neurotrauma* 36, 1435–1450. doi: 10.1089/neu.2018.5956

Sliwinski, M. M., Akselrad, G., Alla, V., Buan, V., and Kaemmerlen, E. (2020). Community exercise programing and its potential influence on quality of life and functional reach for individuals with spinal cord injury. *J. Spinal Cord Med.* 43, 358–363. doi: 10.1080/10790268.2018.1543104

Taccola, G., Sayenko, D., Gad, P., Gerasimenko, Y., and Edgerton, V. R. (2018). And yet it moves: recovery of volitional control after spinal cord injury. *Prog. Neurobiol.* 160, 64–81. doi: 10.1016/j.pneurobio.2017.10.004

Triolo, R. J., Bailey, S. N., Lombardo, L. M., Miller, M. E., Foglyano, K., and Audu, M. L. (2013a). Effects of intramuscular trunk stimulation on manual wheelchair propulsion mechanics in 6 subjects with spinal cord injury. *Arch. Phys. Med. Rehabil.* 94, 1997–2005. doi: 10.1016/j.apmr.2013.04.010

Triolo, R. J., Bailey, S. N., Miller, M. E., Lombardo, L. M., and Audu, M. L. (2013b). Effects of stimulating hip and trunk muscles on seated stability, posture and reach after spinal cord injury. *Arch. Phys. Med. Rehabil.* 94, 1766–1775. doi: 10.1016/j.apmr.2013.02.023

Tse, C. M., Chisholm, A. E., Lam, T., and Eng, J. J. (2018). A systematic review of the effectiveness of task-specific rehabilitation interventions for improving independent sitting and standing function in spinal cord injury. *J. Spinal Cord Med.* 41, 254–266. doi: 10.1080/10790268.2017.1350340

Wagner, F. B., Mignardot, J. B., Le Goff-Mignardot, C. G., Demesmaeker, R., Komi, S., Capogrosso, M., et al. (2018). Targeted neurotechnology restores walking in humans with spinal cord injury. *Nature* 563, 65–71. doi: 10.1038/s41586-018-0649-2

Conflict of Interest: RE holds shareholder interest in NeuroRecovery Technologies and holds certain inventorship rights on intellectual property licensed by the Regents of the University of California to NeuroRecovery Technologies. RE holds shareholder interest in spineX Inc. and holds certain inventorship rights on intellectual property licensed by the Regents of the University of California to spineX Inc. RE serves on the scientific advisory board of *in vivo* Therapeutics and ArianRF, and serves as the Chair of the Scientific Advisory board at spineX.

The remaining authors declare that the research was conducted in the absence of any commercial or financial relationships that could be construed as a potential conflict of interest.

frontiers in Systems Neuroscience

ORIGINAL RESEARCH
published: 05 January 2021
doi: 10.3389/fnsys.2020.614691

Improvements in Bladder Function Following Activity-Based Recovery Training With Epidural Stimulation After Chronic Spinal Cord Injury

April N. Herrity[1,2], Sevda C. Aslan[1,2], Beatrice Ugiliweneza[1,2], Ahmad Z. Mohamed[3], Charles H. Hubscher[1,4] and Susan J. Harkema[1,2]*

[1]Kentucky Spinal Cord Injury Research Center, University of Louisville, Louisville, KY, United States, [2]Department of Neurological Surgery, University of Louisville, Louisville, KY, United States, [3]Department of Urology, University of Louisville, Louisville, KY, United States, [4]Department of Anatomical Sciences and Neurobiology, University of Louisville, Louisville, KY, United States

Spinal cord injury (SCI) results in profound neurologic impairment with widespread deficits in sensorimotor and autonomic systems. Voluntary and autonomic control of bladder function is disrupted resulting in possible detrusor overactivity, low compliance, and uncoordinated bladder and external urethral sphincter contractions impairing storage and/or voiding. Conservative treatments managing neurogenic bladder post-injury, such as oral pharmacotherapy and catheterization, are important components of urological surveillance and clinical care. However, as urinary complications continue to impact long-term morbidity in this population, additional therapeutic and rehabilitative approaches are needed that aim to improve function by targeting the recovery of underlying impairments. Several human and animal studies, including our previously published reports, have documented gains in bladder function due to activity-based recovery strategies, such as locomotor training. Furthermore, epidural stimulation of the spinal cord (scES) combined with intense activity-based recovery training has been shown to produce volitional lower extremity movement, standing, as well as improve the regulation of cardiovascular function. In our center, several participants anecdotally reported improvements in bladder function as a result of training with epidural stimulation configured for motor systems. Thus, in this study, the effects of activity-based recovery training in combination with scES were tested on bladder function, resulting in improvements in overall bladder storage parameters relative to a control cohort (no intervention). However, elevated blood pressure elicited during bladder distention, characteristic of autonomic dysreflexia, was not attenuated with training. We then examined, in a separate, large cross-sectional cohort, the interaction between detrusor pressure and blood pressure at maximum capacity, and found that the functional relationship between urinary bladder distention and blood pressure regulation is disrupted. Regardless of one's bladder emptying method (indwelling suprapubic catheter vs. intermittent catheterization), autonomic instability can play a critical role in

OPEN ACCESS

Edited by:
James W. Grau,
Texas A&M University, United States

Reviewed by:
Michelle Hook,
Texas A&M University, United States
Jamie Lynn Reed,
Vanderbilt University, United States

***Correspondence:**
April N. Herrity
april.herrity@louisville.edu

Received: *06 October 2020*
Accepted: *03 December 2020*
Published: *05 January 2021*

Citation:
Herrity AN, Aslan SC, Ugiliweneza B, Mohamed AZ, Hubscher CH and Harkema SJ (2021) Improvements in Bladder Function Following Activity-Based Recovery Training With Epidural Stimulation After Chronic Spinal Cord Injury. Front. Syst. Neurosci. 14:614691. doi: 10.3389/fnsys.2020.614691

the ability to improve bladder storage, with SCI enhancing the vesico-vascular reflex. These results support the role of intersystem stimulation, integrating scES for both bladder and cardiovascular function to further improve bladder storage.

Keywords: lower urinary tract, urodynamics, neurogenic bladder, neuromodulation, locomotor training, cardiovascular

INTRODUCTION

Over 1.4 million Americans have a spinal cord injury (SCI; Armour et al., 2016), with 70–84% having at least some degree of bladder dysfunction (Hamid et al., 2018). Injury above the sacral cord results in a loss of volitional control of micturition consistent with an upper motor neuron-type injury. The resulting neurogenic bladder is characterized by detrusor overactivity and detrusor-sphincter dyssynergia, where simultaneous detrusor and urinary sphincter contractions lead to high bladder pressure and insufficient emptying (de Groat and Yoshimura, 2010). Functional impairments of the lower urinary tract (LUT) is an area of highest priority, as it has a dramatic negative impact on overall health and quality of life (Anderson, 2004; Ditunno et al., 2008; Piatt et al., 2016). Major urological concerns contributing to increased morbidity and mortality include repeated LUT infections that can lead to sepsis, chronic vesicoureteral reflux and hydronephrosis with progression to renal failure as a result of high-intravesical pressures, and inter-related cardiovascular complications such as autonomic dysreflexia (Van Kerrebroeck et al., 1993; Zeilig et al., 2000; Hagen et al., 2011) that limits bladder storage (Hubscher et al., 2018). Standard management of LUT dysfunction post-SCI includes a combination of pharmacological approaches to reduce bladder over-activity and pressure and catheter-based management to empty the bladder. While these approaches can decrease urinary complications in those who can tolerate medications as well as perform urethral catheterizations, many individuals performing intermittent catheterization do not remain on this method long-term, with some having surgical urinary diversion, either continent or to a stoma device, and most transitioning to an indwelling catheter, a management strategy associated with a high degree of medical complications and hospitalizations (Cameron et al., 2010, 2011). There is a critical need for a successful intervention that aims to restore function, as even though the standard of care manages the many limitations attributed to secondary complications after injury, it does not access the inherent ability of the nervous system to recover function. Current bladder management approaches commonly require life-long maintenance, and have adverse side effects leading to recurring illness and reduced quality of life (Benevento and Sipski, 2002).

Activity-based recovery therapy, such as locomotor training, which engages lumbosacral spinal networks below the level of injury to retrain the nervous system to recover a specific motor task, is an effective rehabilitation strategy for improving post-SCI motor outcomes (Dietz and Harkema, 2004; Behrman et al., 2005; Harkema et al., 2012; Jones et al., 2014; Kaiser et al., 2020), as well as improving autonomic responses (Harkema et al., 2008; Terson de Paleville et al., 2013; Onushko et al., 2019), including bladder, bowel, and sexual function (Hubscher et al., 2018; Morrison et al., 2018). Previous work in animal models (Gad et al., 2014; Ward et al., 2014, 2016) and human SCI (Hubscher et al., 2018) indicate that sufficient excitation of the nervous system and/or residual supraspinal input, driven by repetitive stepping and appropriate sensory cues, resulted in improvements in multiple urological outcomes. Furthermore, the combination of locomotor training (step and stand training) plus spinal cord epidural stimulation (scES) has not only enhanced coordinated and controlled voluntary motor behavior, including walking over-ground in clinically motor complete SCI individuals (Grahn et al., 2017; Rejc et al., 2017; Angeli et al., 2018; Gill et al., 2018; Wagner et al., 2018; Darrow et al., 2019), but was also reported by individuals to improve physiologic outcomes such as cardiovascular function (Aslan et al., 2018; Harkema et al., 2018a,b; West et al., 2018) temperature regulation, bladder, and sexual function (Harkema et al., 2011; Darrow et al., 2019). Additional improvements in bladder storage and voiding have been reported with neuromodulation of the lumbosacral circuitry using scES following both motor complete (Herrity et al., 2018; Walter et al., 2018) and rodent models (Abud et al., 2015; Gad et al., 2016) of SCI. As the central state of excitability of the lumbosacral spinal cord is an important factor in promoting recovery of function (Angeli et al., 2014, 2018), the objective of this study was to test the effects of activity-dependent scES on bladder function in participants enrolled in scES training studies (activity-based recovery training, ABRT-scES) in our center relative to those participants in usual care who continued their typical daily lives without any study-related change in routine (no intervention). To further our understanding of the interaction between critical inter-dependent autonomic systems after SCI, the urological profiles in response to filling/emptying and cardiovascular-associated effects were also examined in a separate, large cross-sectional cohort.

MATERIALS AND METHODS

Participants

A total of 85 individuals, 35 ± 11 years of age (71% male, 29% female), with chronic SCI are included in this study (**Table 1**). Study participant groups include a cross-sectional cohort (n = 65), a usual care cohort (n = 10), and an interventional cohort (n = 10). Participants in the cross-sectional cohort (n = 65) were enrolled in a research study (IRB#16.0179, NCT03364660, Task and Physiological Specific Stimulation for Recovery of Autonomic Function, Voluntary Movement and Standing using Epidural Stimulation and Training after Severe SCI) that was conducted between the years of 2017–2019 (**Table 2**). However,

TABLE 1 | Usual care and ABRT-scES participant characteristics.

Group	Participant	Age	Sex	Years post injury	Neuro level	AIS grade	Anal sensation	Bladder emptying method
Usual Care	A101	31	Male	2	C3	A	No	SP
	A100	51	Male	15	C3	A	No	SP
	A105	33	Male	9	C4	A	No	SP
	A109	41	Male	14	C4	A	No	CIC
	B38	20	Male	1	C4	B	Yes	CIC
	A123	28	Male	7	C4	B	Yes	CIC
	A119	24	Female	9	C5	A	No	CIC
	A110	21	Female	5	C5	A	No	SP
	B24	21	Male	2	C7	B	Yes	CIC
	B41	26	Male	8	C8	B	Yes	CIC
ABRT-scES	A68	35	Male	4	C2	A	No	CIC
	A80	33	Female	8	C3	A	No	SP
	A41	24	Male	7	C5	A	No	SP
	B21	31	Male	7	C5	B	Yes	CIC
	B23	33	Male	4	C6	B	Yes	SP
	B13	33	Male	4	C7	B	Yes	CIC
	B30	22	Female	3	T1	B	Yes	CIC
	A45	24	Male	2	T4	A	No	CIC
	A53	28	Male	2	T4	A	No	CIC
	A60	23	Male	3	T4	A	No	CIC

ABRT, Activity-based recovery training; scES, spinal cord epidural stimulation; AIS, American Spinal Injury Association Impairment Scale; CIC, clean intermittent catheterization; SP, suprapubic catheter.

TABLE 2 | Cross-sectional participant characteristics.

		Bladder emptying method	
Number of participants	All *n* = 65	CIC *n* = 41	SP *n* = 24
Sex			
Female	21 (32%)	8 (20%)	13 (54%)
Male	44 (68%)	33 (80%)	11 (46%)
Age (years)	37 ± 12	37 ± 12	36 ± 12
Years Post Injury	7 ± 6	7 ± 5	8 ± 6
Neuro Level			
Cervical	45 (69%)	23 (56%)	22 (92%)
Thoracic	20 (31%)	18 (44%)	2 (8%)
AIS Grade			
A	38 (58%)	22 (54%)	16 (67%)
B	20 (31%)	14 (34%)	6 (25%)
C	5 (8%)	3 (7%)	2 (8%)
D	2 (3%)	2 (5%)	0 (0%)

AIS, American Spinal Injury Association Impairment Scale; CIC, clean intermittent catheterization; SP, suprapubic catheter.

these individuals only participated in screening, including a urodynamic assessment, and did not continue into the next stage of the study which was usual care. Thus, cross-sectional and usual care cohorts are comprised of different individuals.

Ten participants in the usual care cohort were enrolled in a research study conducted at the University of Louisville (IRB#16.0179, NCT03364660, *Task and Physiological Specific Stimulation for Recovery of Autonomic Function, Voluntary Movement and Standing using Epidural Stimulation and Training after Severe SCI*) between the years of 2017–2019. As part of that study, all participants received 2 Urodynamic assessments at least 5 months apart. This period was termed "usual care," as the participants continued their typical daily lives without any study-related change in routine (no intervention). This phase addresses whether there would be any inherent variability between two Urodynamic measurements within the same time interval as the interventional cohort receiving scES and training.

Ten participants in the interventional cohort were enrolled for the current bladder study (IRB# 14.0062, NCT03036527 - R01) from other ongoing research studies at the University of Louisville investigating the effects of ABRT-scES on lower limb motor function (IRB #07.0066, NCT02339233, *Spinal Epidural Electrode Array to Facilitate Standing and Stepping in SCI*) and cardiovascular function (IRB #13.0625, NCT02037620, *Recovery of Cardiovascular Function with Epidural Stimulation after Human SCI*) between the years of 2010–2018. As part of the interventional studies, a 16-electrode array (5-6-5 Specify, Medtronic, Minneapolis, MN, USA) was surgically implanted at the T11-L1 vertebral levels over spinal cord segments L1-S1 as previously described (Harkema et al., 2011; Angeli et al., 2014). The electrode lead was tunneled subcutaneously and connected to the pulse generator (RestoreADVANCED, Medtronic, Minneapolis, MN, USA) placed ventrally in the abdomen. All research participants provided written, informed consent and the research was approved by the Institutional Review Board (University of Louisville, Louisville, KY, USA).

Clinical Evaluation

All research participants received a clinical evaluation before study participation to assess motor and sensory status. Two clinicians independently performed the International Standards for Neurological Classification of SCI (Marino et al., 2003; Waring et al., 2010) to classify participants' injuries using the ASIA (American Spinal Injury Association) Impairment Scale (AIS; **Table 1**). A physical examination also was performed by a clinician for medical clearance, ensuring

participation safety using the following inclusion criteria: (1) stable medical condition; (2) no painful musculoskeletal dysfunction, unhealed fracture, contracture, pressure sore, or urinary tract infection that might interfere with training; (3) no untreated psychiatric disorders or ongoing drug abuse; (4) clear indications that the period of spinal shock is concluded determined by the presence of muscle tone, deep tendon reflexes or muscle spasms and discharged from standard inpatient rehabilitation; (5) non-progressive supra-sacral SCI; (6) bladder dysfunction as a result of SCI; and (7) epidural stimulator implanted at the lumbosacral spinal cord. None of the participants had ever received Botox injections for management of bladder dysfunction and all participants were off anti-spasticity medication (e.g., Baclofen). Note that all research participants refrained from taking any bladder medication at least 24 h before urodynamic testing [i.e., elimination half-life of oral oxybutynin, commonly used anticholinergic, is approximately 2 h and about 11 h to be eliminated from the body (Douchamps et al., 1988)] to rule out any pharmacologic impact on the clinical outcomes. Each participant also received a bladder/kidney Ultrasound at the time of enrollment and was medically cleared by both the study Urologist and study physician to participate in the research studies. None of the participants altered their method of bladder emptying throughout the study.

Activity-Based Recovery Training

After implantation of the stimulator, 10 participants underwent a total of 160 sessions of activity-based recovery training (ABRT-scES). Six of those participants received alternating stand and step recovery-based training with scES. Stand training over-ground lasted 1 h per session (five sessions per week) and was always performed with spinal cord epidural stimulation using a custom-designed standing apparatus comprised of horizontal bars anterior and lateral to the individual to provide upper extremity assistance and balance support. The individual was encouraged to stand for as long as possible throughout the training session, with the goal of standing for 60 min with the least amount of assistance. Seated resting periods occurred when requested by the individual. If during standing, the participant's knees or hips flexed beyond the normal standing posture, external assistance to facilitate hip and knee extension was provided either manually by a trainer or by elastic cords, which were attached between the two vertical bars of the standing frame. Step training (1 h, five sessions per week) was performed with bodyweight support (Innoventor, St. Louis, MO, USA) on a treadmill and always with spinal cord epidural stimulation. Research participants stepped at body-weight load and speed adapted to achieve appropriate stepping kinematics and trainers provided manual assistance only when needed following standard locomotor training principles (Harkema et al., 2012). Body-weight support was continuously reduced throughout the training sessions as the ability to bear weight on the weight-bearing limbs improved and manual facilitation was reduced as the ability to step independently improved. Four participants also underwent 160 sessions of cardiovascular training with scES which consisted of resting in a seated position for 2 h with continuous blood pressure and heart rate monitoring. Cardiovascular-scES configurations (anode and cathode electrode selection, voltage, frequency, and pulse width) were identified to maintain systolic blood pressure within a relatively stable blood pressure within non-injured defined normal ranges without eliciting motor activity (Harkema et al., 2018b). Participants in the cardiovascular-scES group also received 80 sessions of voluntary training with scES (included in the 160 sessions) which consisted of practicing, in the supine position, unilateral leg flexion, ankle dorsiflexion, and toe extension exercises with task-specific scES configurations daily (about 1 h per session, five sessions per week; Rejc et al., 2017). Note that use of scES at home during the 1-year before the follow-up assessment was variable and differed based upon sub-group (stand-scES only for locomotor training or cardiovascular-scES alone).

Urodynamics

As described previously (Herrity et al., 2018; Hubscher et al., 2018), all data were obtained from standard urodynamic evaluations with recommendations from the International Continence Society (Blaivas et al., 1982; Schafer et al., 2002; Winters et al., 2012; Gammie et al., 2014). All assessments were conducted in the same manner, using the same equipment, and by a single research nurse. Using the Aquarius® LT system (Laborie, Williston, VT, USA), cystometry was performed in the supine position *via* a single sensor, dual-channel catheter (7 Fr, T-DOC® Air-Charged™, Laborie, Williston, VT, USA) with a continuous filling of sterile, body-temperature water (37°C) at a fixed slow rate of 20 ml/min. Abdominal pressure was measured *via* a rectal catheter (7 Fr, T-DOC® Air-Charged™, Laborie, Williston, VT, USA). External anal sphincter electromyography (EMG; Neotrode II, Laborie, Williston, VT, USA) was recorded using surface patch EMG electrodes and a grounding pad was placed on a bony prominence, usually the hip or knee. Detrusor pressures were calculated by subtracting the intra-abdominal pressure from the intra-vesical pressure. Research participants were asked to cough to verify catheter positions and instructed to communicate sensations of a full bladder (first sensation), the desire to urinate (first urge to void), and strong desire to void, and the feeling that voiding/leaking cannot be delayed (maximum capacity; Wyndaele, 1998; Wyndaele and De Wachter, 2002). The volume of water and bladder pressure were recorded. Uninhibited bladder contractions also were identified. During the emptying phase, voluntary voiding events were generated from a low-pressure filling pressure and a proper detrusor contraction, distinguished from a reflexive leak, which often occurred in response to an elevation in detrusor pressure overriding the pressure generated at the bladder outlet. Participants were instructed to communicate bladder sensations (first sensation, desire, urgency) and any symptoms of autonomic dysreflexia (e.g., headache and/or chills). At the end of the filling, the was bladder drained with a catheter for measurement of residual volume. In the ABRT-scES group, filling cystometry was conducted post-implantation and before training, repeated after completion of 160 sessions of training, and at the 1-year follow-up time point. Stimulation was used

only during daily ABRT and was not used during any of the cystometrogram evaluations.

Blood pressure and heart rate were obtained from the brachial artery, measured by the oscillometric technique (Carescape V100, GE Healthcare, Milwaukee, WI, USA), throughout the urodynamic session. As previously described (Aslan et al., 2018; Harkema et al., 2018b), noninvasive continuous blood pressure was also measured from a finger cuff by plethysmographic technique (ADInstruments). Brachial blood pressure was recorded at multiple time points during the study: (1) in the seated position when the participant presented to the lab; (2) supine position before catheter placement; (3) reclined position before filling with catheters in place; (4) continuously during testing; (5) post-filling to ensure blood pressure values returned to baseline; and (6) post-testing, once catheters were removed and the participant returned to his or her wheelchair. Any signs and self-reported symptoms of autonomic dysreflexia were documented and observed throughout testing. Bladder filling was ceased if any of the following conditions were observed: (1) spontaneous urine leakage; (2) filling $\geq$600 ml or reaching maximum bladder capacity as evidenced by a rise in the compliance curve; (3) high intravesical pressure $\geq$40 cmH_2O or; (4) autonomic dysreflexia as evidenced by a sustained systolic blood pressure recording of $\geq$20 mm Hg from baseline and/or intolerable symptoms. If autonomic dysreflexia persisted beyond emptying, established guidelines were followed (Krassioukov et al., 2009). None of the research participants required the use of an antihypertensive agent to control autonomic dysreflexia after the assessment.

Data Analysis

Bladder capacity was calculated as the volume of leaked or voided fluid plus any residual amount removed from the bladder. Note that the total volume also includes the excess amount produced through diuresis and not solely infused volume. Voiding efficiency (VE) was calculated as: VE = [volume voided/(volume voided + residual volume) $\times$ 100]. Compliance was calculated by dividing the volume change (ΔV) by the change in detrusor pressure (ΔPdet) during that change in bladder volume and was expressed in ml/cm H_2O (Abrams et al., 2002). Compliance is considered low below 20 cm/H_2O (Stöhrer et al., 1999; Pannek et al., 2018). The intravesical pressure (Pves) at which involuntary expulsion of water/urine from the urethral meatus was observed was considered the detrusor leak point pressure (DLPP). Maximum detrusor pressure (MDP) was identified as the peak detrusor pressure during the voiding phase of the cystometrogram. Detrusor pressures were calculated by subtracting the intra-abdominal pressure from the intra-vesical pressure. All analyses were performed with customized software in MATLAB (MathWorks, Natick, MA, USA).

Statistical Analysis

Continuous participant descriptors and bladder outcomes were tested for normality using the Kolmogorov–Simonov test. Variables that were found normally distributed were compared with two-sample *t*-test for two group comparisons or paired t-test for pre-post evaluations. Variables that failed the normality test compared with either the Rank Sum Test or the Signed Rank Test. Categorical variables were summarized with frequency count with associated percentage and compared with Chi-square tests or Fisher's exact test as appropriate. Note that sample sizes were accounted for in all analyses, as 1 participant was not available for baseline Urodynamics and another participant was lost to follow-up. Both were in the ABRT-scES group. Blood pressure was also not available for 3 participants in the ABRT-scES group. All tests were 2-sided with a significance level of 0.05. Statistical analyses were performed in SAS 9.4 (SAS Inc., Cary, NC, USA).

RESULTS

Clinical Characteristics

The clinical characteristics of the 20 research participants, all having motor complete SCI, are provided in **Table 1**. Features represented in the table were determined from the time at which each participant presented for either the post-implant/pre-training or pre-usual care Urodynamic assessment. The research participants' mean age in the usual care and scES groups was 30 $\pm$ 10 and 29 $\pm$ 5 years, respectively, at the start of training. The usual care group included individuals having a cervical level of injuries, with a range of C3-C8 and a mean time since the injury of 7 $\pm$ 5 years. Individuals in the scES group had both cervical and upper thoracic level of injuries with a range of C2-T4 and a mean time since the injury of 4 $\pm$ 2 years. In the overall cohort, 80% of the participants were male, while 20% were female, closely representing the national statistical report of sex prevalence in SCI (National Spinal Cord Injury Statistical Center, 2020). Seven out of ten participants performed clean intermittent catheterization for bladder emptying, while the other three received a suprapubic cystostomy for bladder drainage. Note that suprapubic cystostomy in each of the three participants was performed at in-patient discharge and thus, each participant chronically utilized this method as the primary means of bladder emptying at study enrollment.

The clinical characteristics of the 65 participants in the cross-sectional cohort are provided in **Table 2**. The average age (37 $\pm$ 12 years) is more closely aligned with the national statistical report of the age at the time of injury (National Spinal Cord Injury Statistical Center, 2020). The mean time since injury (7 $\pm$ 6 years) was similar to those in usual care. About one-third of the population was female. The majority of individuals sustained a cervical level of injury and were motor and sensory complete, per AIS standards. The cohort was represented by 41 individuals performing intermittent catheterization and 24 with suprapubic cystostomy.

Lower Urinary Tract Function—Storage Phase

Baseline bladder capacity values were not statistically different between usual care and ABRT-scES groups (276 $\pm$ 174 ml and 231 $\pm$ 134 ml, respectively; **Figure 1**). Within the non-interventional usual care cohort alone, there were no significant changes in capacity at the post-usual care

time point (281 ± 171 ml) relative to baseline. Following ABRT-scES, there was a significant improvement in bladder capacity relative to baseline ($p < 0.05$) that maintained significance at follow-up ($p < 0.05$; Baseline, 231 ± 134 ml; Post-training, 313 ± 166 ml; Follow-up, 324 ± 201 ml; **Figure 1**). Capacity values for 60% of the participants reached ranges within clinically recommended guidelines for bladder storage (range from 300–600 ml; Gray, 2001; Lukacz et al., 2011; Rosier et al., 2013) at both post-training and follow-up time points. There was also a significant improvement change in bladder capacity at post-training (70 ± 83 ml, $p < 0.05$) and at follow-up (102 ± 120 ml, $p < 0.05$) in the ABRT-scES group compared to post-usual care (5 ± 70 ml).

Baseline detrusor pressure values were not statistically different between usual care and ABRT-scES groups (53 ± 38 cmH_2O and 53 ± 30 cmH_2O, respectively; **Figure 2**). Within the non-interventional usual care cohort alone, there were no significant changes in detrusor pressure at the post-usual care time point (57 ± 38 cmH_2O) relative to baseline. In contrast, detrusor pressure was significantly decreased post-training (Baseline, 53 ± 30 cmH_2O; Post-training, 29 ± 20 cmH_2O; $p < 0.01$), with the majority of participants (80%) having detrusor leak point pressure below 40 cmH_2O (**Figure 2**). There was also a significant improvement change (reduction) in detrusor pressure at post-training (−22 ± 14 cmH_2O, $p < 0.006$) in the ABRT-scES group compared to post-usual care (4 ± 21 cmH_2O). However, at follow-up, detrusor pressure was significantly elevated relative to post-training values (49 ± 20 cmH_2O, $p < 0.01$), and comparable to pre-training baseline ($p > 0.05$) in the ABRT-scES group.

Similar to the post-training improvements in bladder capacity and pressure, bladder compliance significantly improved post-training (9 ± 11 ml/cmH_2O vs. 20 ± 25 ml/cmH_2O, $p < 0.01$; **Figure 3**), but reverted to baseline values by the follow-up (8 ± 11 ml/cmH_2O). There were no changes in bladder compliance from baseline to post-usual care (12 ± 8 ml/cmH_2O and 9 ± 11 ml/cmH_2O).

Lower Urinary Tract Function—Emptying Phase

The emptying phase of bladder function was assessed at the end of filling or when participants indicated a strong desire to void, typically reported as fullness in the lower abdominal region. In total, 4 participants (2 AIS A, 2 AIS B) receiving ABRT-scES demonstrated the ability to voluntarily void with intent during this study. One participant (AIS B) was able to partially empty her bladder at all three time points and thus, a uroflow was conducted before catheter placement and filling, and flow was captured during the voiding phase once the participant reached maximum capacity. At post-training, the maximum flow rate (Qmax) during emptying was 2.0 ml/s (12% voiding efficiency, VE). Note that the expected value for Qmax in females younger than 40 years of age is >22.0 ml/s (Walsh et al., 2002). Another participant (AIS B) partially voided post-training (11% VE) and at follow-up (36% VE). In two other participants (both AIS A), one voided post-training (9% VE), and the other at follow-up (17% VE). All four participants identified distinct sensations of bladder fullness (first sensation of filling, first desire, strong desire) guiding their report of the need to empty and their intent during the void attempt. In the ABRT-scES group, there were no significant changes in total voiding efficiency from

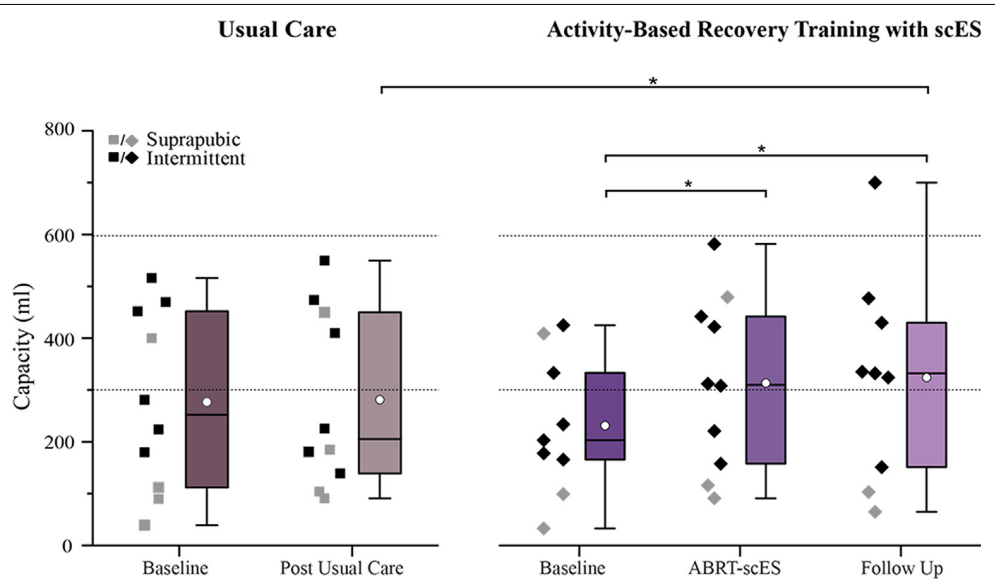

FIGURE 1 | Impact of usual care (left) and activity-based recovery training (ABRT) with spinal cord epidural stimulation (scES; right) on bladder capacity. Bladder capacity significantly improved following ABRT-scES relative to baseline ($p < 0.05$). Capacity remained significant at the 1-year follow-up time point ($p < 0.05$) with a significant change from post-usual care ($p < 0.01$). Dashed horizontal lines represent the clinical reference range for bladder capacity (300–600 ml). Box plot represents the 25th percentile, the median, the 75th percentile, and the mean (white circle). ml, milliliters. *Indicates significance.

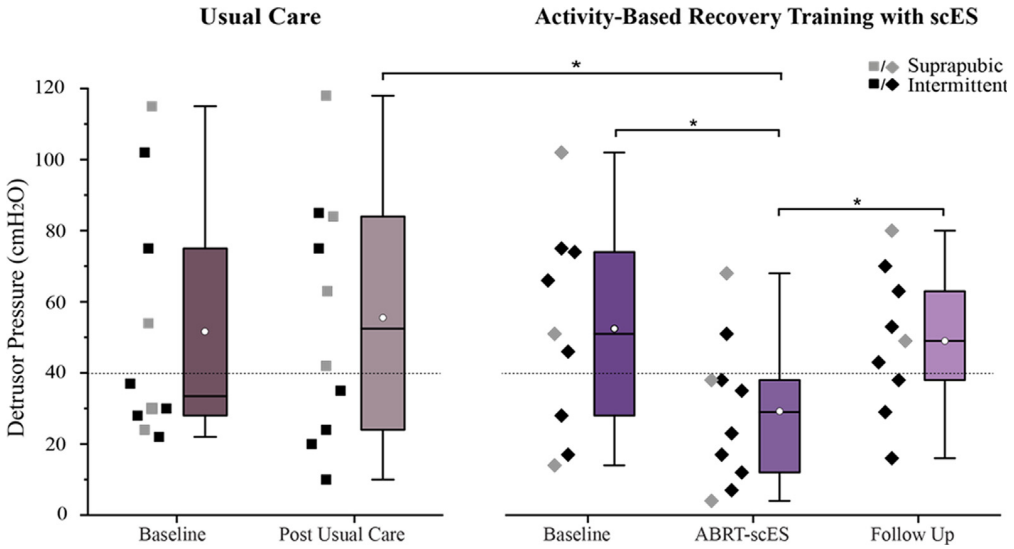

FIGURE 2 | Reduction in detrusor pressure following activity-based recovery training with spinal cord epidural stimulation (ABRT-scES). The distribution of detrusor pressure values for each participant is presented for the usual care group (left) and the ABRT-scES group (right). Detrusor pressure was significantly improved (reduced) from baseline ($p < 0.01$) and the change in detrusor pressure was significantly improved relative to the post-usual care change ($p < 0.05$) following ABRT-scES. While detrusor pressure was significantly elevated at the 1-year follow-up time point ($p < 0.01$), it was unchanged from baseline values. There were no significant changes in detrusor pressure values in the usual care group. The dashed horizontal line (at 40 cmH_2O) represents the critical cut-off value between high and low detrusor leak point pressure (DLPP). Box plot represents the 25th percentile, the median, the 75th percentile, and the mean (white circle). cmH_2O, centimeters of water. *Indicates significance.

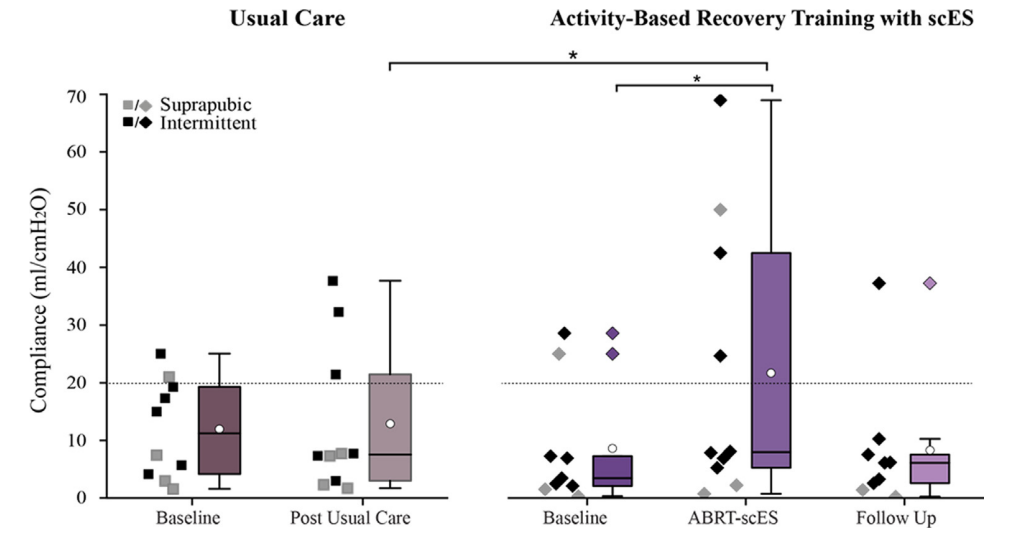

FIGURE 3 | Comparison of bladder compliance values in participants receiving usual care (left) vs. activity-based recovery training with spinal cord epidural stimulation (ABRT-scES; right). Bladder compliance was significantly improved from baseline ($p < 0.01$) in the ABRT-scES group and the change in compliance was significantly improved relative to the post-usual care change ($p < 0.05$). Bladder compliance is compromised if it is below 20 ml/cmH_2O (indicated by the dashed horizontal line). Box plot represents the 25th percentile, the median, the 75th percentile, and the mean (white circle). cmH_2O, centimeters of water; ml, milliliters. *Indicates significance.

pre-training (23 ± 27% VE) to post-training (28 ± 33% VE) nor from post-training to follow-up (24 ± 24% VE). None of the individuals in the usual care group were able to void voluntarily during testing. Voiding efficiency was also unchanged in the usual care group (10 ± 16% VE vs. 13 ± 29% VE).

Blood Pressure Responses to Bladder Distention

In the interventional group, systolic blood pressure responses to bladder distention did not differ following ABRT-scES (Pre-training, 131 ± 15 mmHg; Post-training, 140 ± 13 mmHg), nor

were there significant changes at follow-up (149 ± 26 mmHg) compared to baseline or post-training. Furthermore, the change in systolic blood pressure from pre-fill values (catheters in place) to values captured at the point of maximum cystometric capacity during the study indicates that ABRT-scES did not attenuate bladder-distention associated increases in systolic blood pressure (Pre-training change, 22 ± 20 mmHg; Post-training change, 25 ± 11 mmHg). However, concerning the usual care cohort, participants receiving ABRT-scES had significantly lower systolic blood pressure responses to bladder distention post-training (140 ± 13 mmHg, $p < 0.05$) compared to those in usual care (157 ± 18 mmHg; **Figure 4**). ABRT-scES sub-group (locomotor vs. cardiovascular + voluntary) training effects in relation to bladder outcomes were also evaluated. All pre-training bladder and blood pressure outcome measures between these two sub-groups were similar and there were no significant differences in these measures at pre-training, post-training, or follow-up.

Cross-sectional Cohort—Urological Profiles in Chronic SCI

Filling cystometry conducted on 65 research participants [$n = 41$ (63%), intermittent catheterization; $n = 24$ (37%) suprapubic catheter] revealed the majority of participants ($n = 37$, 57%) had low bladder capacity with values falling below normative ranges (300 ml; Gray, 2001; Lukacz et al., 2011; Rosier et al., 2013; **Figure 5A**). Within this sub-cohort ($n = 23$, 62%; 13 suprapubic catheters; 10 intermittent catheterizations), also had high detrusor pressure [>40 cmH_2O; values above which are associated with upper tract deterioration (Rosier et al., 2013)]. The greatest blood pressure responses (>150 mmHg) were present in those using suprapubic catheters and having bladder capacity less than 300 ml [$n = 17$, (26%) of all participants]. The percentage of individuals from the cross-sectional cohort having the capacity and detrusor pressure within the recommended ranges (gray shaded region of **Figure 5A**) was only 20%, yet the vast majority (86%) still presented with elevated blood pressure responses (>120 mmHg). Conversely, a subset of participants (12%), all utilizing intermittent catheterization, had large bladder volumes above the upper limit of the normal capacity range (>600 ml).

In the overall cohort, those using intermittent catheterization had significantly greater capacity relative to those using suprapubic catheters (425 ± 266 ml vs. 186 ± 105 ml, respectively, $p < 0.0001$; **Figure 5B**). Yet, many using intermittent catheterization still had volumes below and above the recommended capacity values as well as elevated detrusor pressure. While there were no significant differences in detrusor pressure values between catheter groups (intermittent catheter, 49 ± 32 cmH_2O; suprapubic catheter, 49 ± 29 cmH_2O), both were higher than recommended safety values (**Figure 5C**). In the intermittent catheter group alone, despite the lower ratio of females ($n = 8$) to males ($n = 33$), females had significantly lower detrusor pressure than males (24 ± 11 cmH_2O vs. 55 ± 35 cmH_2O, $p < 0.005$; **Figure 5C**). No additional sex differences related to the urodynamic measures were identified in the overall cohort as well as within each catheter sub-type. Bladder compliance was significantly greater in the intermittent catheter group relative to the suprapubic group (27 ± 24 ml/cmH_2O vs. 12 ± 8 ml/cmH_2O, $p = 0.002$; **Figure 5D**). Total voiding efficiency for the entire cross-sectional cohort was low (20 ± 27%) and there were no differences between catheter groups (intermittent, 15 ± 24%; suprapubic, 28 ± 30%; **Figure 5E**). Blood pressure responses at maximum capacity were similar between those performing intermittent catheterization vs. those with suprapubic catheters (148 ± 25 mmHg vs. 159 ± 18 mmHg, respectively).

DISCUSSION

Regardless of bladder management type (indwelling vs. intermittent catheterization) the urologic presentation of individuals in the usual care cohort, the baseline profile of the ABRT-scES group, and the majority of participants in the cross-sectional cohort were similar and largely characterized by low bladder capacity, high detrusor pressure at maximum capacity, and ubiquitous high blood pressure elicited by bladder distention. Decreased bladder volumes and high pressures are associated with urinary over-activity, frequency, incontinence, and places one at risk for upper urinary tract deterioration. Furthermore, in susceptible individuals with uncontrolled sympathetic hyperactivity (injury above the mid-thoracic level), bladder distention is one of the primary triggers of autonomic dysreflexia. Episodes of autonomic dysreflexia have been reported to occur up to 40 times a day, dramatically increasing one's risk for stroke by 300–400% (Cragg et al., 2013).

Despite the baseline presentation, we found that ABRT-scES positively influenced the storage phase, with improvements in bladder capacity, detrusor pressure, and overall compliance by the post-training time point. The increase in bladder capacity also persisted a year after training. Even though scES was not directly configured for bladder, nor was stimulation "on" during cystometry, sufficient excitation of neural networks, comprised of overlapping motor and autonomic networks, during training may have led to improved adaptations in detrusor activity and reciprocal somatic facilitation of the sphincter during bladder storage. While the ABRT-scES cohort demonstrated improved attenuation of blood pressure at maximum capacity relative to usual care, blood pressure was not entirely stabilized in response to bladder distention. We demonstrated that such elevations in blood pressure at maximum capacity were ubiquitous in a large cross-sectional cohort, indicating greater inter-connectedness of both the urinary and cardiovascular systems.

With the standard of care bladder management in the usual cohort, we did not see any change in bladder function across a similar time interval as those receiving the scES training intervention. While noted that all ten participants in the usual care cohort had a cervical level of injuries relative to the 60% with cervical injuries in the intervention group, there were no differences in baseline bladder outcome values across these two cohorts. Bladder management catheter usage was similar across the two groups (40% suprapubic—usual care; 30% suprapubic—ABRT-scES), and in fact, both cohorts had an equivalent percentage of participants with bladder capacity below 300 ml at baseline. In evaluating the impact of scES as an

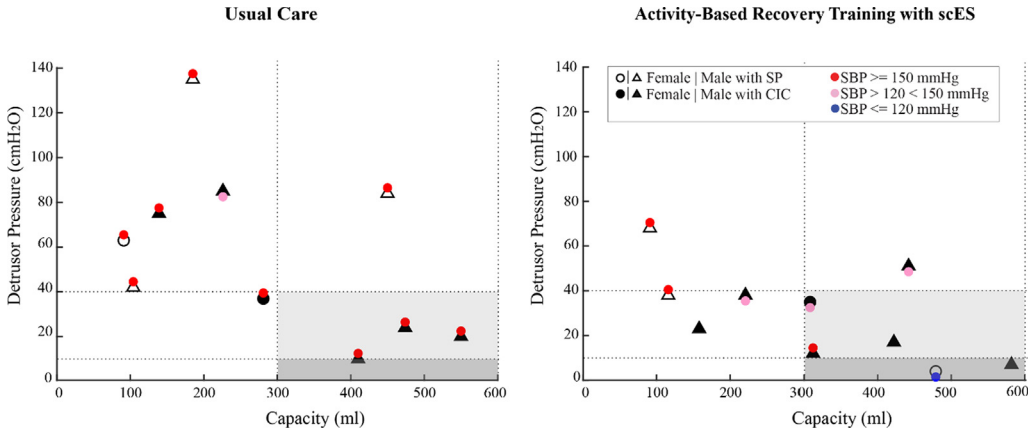

FIGURE 4 | Bladder pressure-volume relationship and distention associated blood pressure responses in the usual care group (left) and the activity-based recovery training with spinal cord epidural stimulation (ABRT-scES) group (right) at post-usual care and post-training. While the ABRT-scES group experienced significantly lower blood pressure responses to bladder distention after training relative to usual care ($p < 0.05$), the majority of participants still responded with increased systolic blood pressure to bladder distention regardless of their bladder function (small or normal capacity and low or high detrusor pressure). The dashed horizontal line at 40 cmH_2O represents the clinical upper threshold of high detrusor leak point pressure and the dashed horizontal line at 10 cmH_2O represents the upper limit of detrusor filling pressure. The dashed vertical lines represent the clinical reference range for bladder capacity (300–600 ml). Blood pressure at maximum capacity was not available in three participants in the ABRT-scES group. CIC, clean intermittent catheterization; cmH_2O, centimeters of water; ml, milliliters; mmHg, millimeters of mercury; SBP, systolic blood pressure; SP, suprapubic catheter.

intervention, the ability to harness existing spinal neural control mechanisms with devices for bladder control has continued to evolve over time, as the lumbosacral circuitry controlling the bladder remains intact after most SCI's. Some of the primary electrical stimulation approaches aimed at modulating bladder function have included stimulation of the spinal cord, select peripheral and sacral nerves, indirectly through the skin, as well as the bladder itself (McGee et al., 2015). Developed in the early 1980s, one of the more widely accepted treatments for refractory LUT dysfunction (i.e., urge urinary continence in those with bladder over-activity and non-obstructive urinary retention), chronic pelvic pain, as well as fecal incontinence, is sacral nerve stimulation with the Medtronic InterStim® device (Tanagho and Schmidt, 1982; Schmidt, 1988). Within the SCI population, the utility of sacral nerve therapy has been moderately effective, primarily improving storage and emptying for those with chronic incomplete injuries (Lombardi and Del Popolo, 2009; Kessler et al., 2010). In complete SCI, however, implantation of bilateral sacral nerve stimulators acutely after injury was shown to prevent detrusor-over-activity and incontinence, suggesting early intervention may prevent irreversible effects attributed to LUT dysfunction (Sievert et al., 2010). While this approach appears to modulate micturition reflexes through peripheral afferent signaling mechanisms, based on the direct interaction between urinary and cardiovascular systems that is enhanced after SCI, neuromodulation of spinal cord networks with scES may provide an enhanced communication bridge between descending signals and residual circuits below the level of injury, thereby promoting coordinated autonomic responses that improve bladder function while stabilizing blood pressure. A sufficient central state of excitability may also be necessary so that afferent input and cues related to bladder filling as well as signals from supraspinal centers can drive efficient on-demand voiding.

In our center, the use of scES initially focused on modulating the excitability of spinal neural networks to enhance stepping, standing, and voluntary movement in response to provided task-specific sensory cues in both complete and incomplete SCI (Harkema et al., 2011; Angeli et al., 2014). The integration of somatosensory and residual descending inputs to the spinal circuitry further contributed to unexpected gains in other physiological systems such as the bladder, sexual function, and temperature regulation (Harkema et al., 2011). Even though stimulation parameters were aimed at influencing the motor system and the execution of specific motor patterns, multiple autonomic improvements occurred. With the activation of lumbosacral spinal networks through ABRT-scES, significant improvements in bladder capacity, and detrusor pressure (reduction) were achieved. The finding that capacity remained significantly increased from baseline at follow-up may likely be due to participant clearance for community integration and independent home-training after completion of the intervention phase, whereby they utilize scES for standing or cardiovascular function consistently, and thus continue to activate these overlapping circuits. Other factors related to urological care that cannot be controlled outside the research environment, such as the method of bladder emptying (indwelling vs. intermittent catheterization) or medication usage impacting detrusor contractility, may be associated with the long-term changes in detrusor pressure at follow-up. Importantly, however, detrusor pressure never worsened (increased) in any of the research participants in response to scES, which has previously been suggested (Beck et al., 2020). Our results support the effect of adaptive scES training-induced plasticity in the nervous

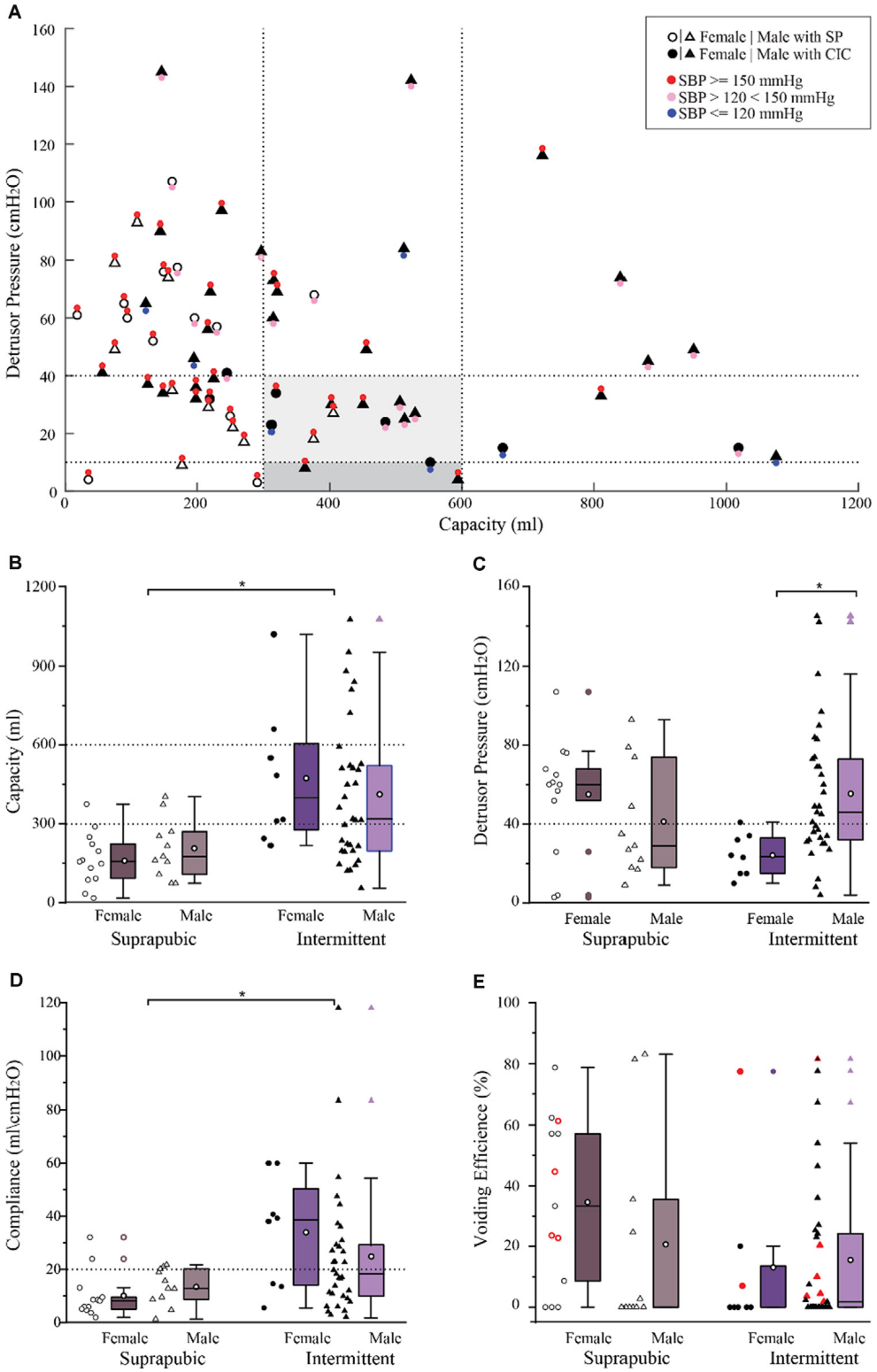

FIGURE 5 | Bladder pressure-volume relationship with associated blood pressure responses and urodynamic outcomes in a large cross-sectional cohort (n = 65). **(A)** The bladder pressure-volume relationship and distention-associated cardiovascular interactions indicate that systolic blood pressure was above 150 mmHg (red circles) in 40 (62%) participants, less than 150 mmHg but higher than 120 mmHg (pink circles) in 18 (28%) participants, and within the normative range in only in seven (11%) participants (blue circles). **(B)** Bladder capacity overall was significantly lower in those with suprapubic catheters relative to those performing intermittent

(Continued)

FIGURE 5 | Continued
catheterization ($p < 0.05$). **(C)** Detrusor pressure was comparable between the suprapubic and intermittent groups showing that 34 (52%) participants had clinically high detrusor pressure associated with bladder filling. In those performing intermittent catheterization, detrusor pressure was significantly lower in female relative to male participants ($p < 0.01$). **(D)** Compliance was significantly lower in the suprapubic group compared to the intermittent catheterization group ($p < 0.01$). **(E)** Total voiding efficiency was variable between participants and includes both uncontrolled reflex voiding (leak) and voluntary voiding. Participants who were able to void voluntarily were indicated in red ($n = 11$) 17%. Box plot black horizontal lower, mid and upper lines represent the 25th percentile, the median, and the 75th percentile respectively. The white circle in the middle of the box represents the mean. CIC, clean intermittent catheterization; cmH_2O, centimeters of water; ml, milliliters; mmHg, millimeters of mercury; SBP, systolic blood pressure; SP, suprapubic catheter.

system and the ability of the spinal cord to interpret and integrate distinct somatosensory cues associated with loading and/or autonomic inputs (Wolpaw and Tennissen, 2001). A vesico-somatic interaction between the circuitries controlling bladder and locomotor function is also anticipated, as we have previously demonstrated that locomotor training alone was sufficient to induce significant improvements in multiple bladder parameters (Hubscher et al., 2018). In the ABRT-scES group, there were improvements in blood pressure responses elicited from bladder distention relative to the usual care cohort, albeit, still not within normative ranges (i.e., 110–120 mmHg). It is important to note that a great deal of hemodynamic instability occurs after SCI, independent of level and severity of injury, and thus, understanding variations in blood pressure and heart rate responses among individuals with SCI will improve the characterization and overall clinical care of autonomic dysfunction (Wang et al., 2020). Potential factors contributing to the scES training-induced reduction of autonomic dysreflexia associated with bladder distention may be indirectly linked with central suppression of C-fiber mediated bladder reflex activity (de Groat, 1995) as the detrusor smooth muscle becomes more compliant in response to mechanical stimuli and scES with long-term training. In a rodent model of SCI, such C-fiber bladder afferents (capsaicin-sensitive) have been implicated in the generation of detrusor overactivity and non-voiding contractions (primary triggers of autonomic dysreflexia) during the filling phase (Cheng et al., 1995).

The study of a large cohort of individuals with chronic SCI revealed that the vast majority of participants had an altered relationship between bladder volume and bladder pressure. Similar to the urological profiles in the usual care group and baseline ABRT-scES values, these participants also demonstrated storage capacity and detrusor pressure abnormalities, ranging from very small volumes to large distended bladders, as well as ubiquitous high blood pressures regardless of bladder management type. Critical to ensuring the long-term safety of the upper and LUT is the ability to achieve and maintain safe storage pressures. The use of indwelling suprapubic catheters as a method to continuously drain the bladder is an alternative method of emptying the bladder if self-intermittent catheterization poses a challenge. While suprapubic catheters are regarded by many consumers as a convenient, effortless alternative to a more demanding urethral catheterization management protocol (Ahluwalia et al., 2006), constant bladder drainage through an open tube to an external storage bag impairs the physiological cyclic pattern of storage and emptying, resulting in possible histological changes and poor functional compliance (Pannek et al., 2010). As a result, minor increases in bladder volume may illicit high blood pressure. As expected, there was greater cardiovascular responsiveness to bladder distention during cystometry in this population. The rapid increase in systolic blood pressure is likely more dramatic in those utilizing suprapubic catheters, as these individuals represent a majority having cervical or high thoracic SCI, resulting in the loss of supraspinal regulation of spinal sympathetic activity and disrupted cardiovascular regulation (Garstang and Miller-Smith, 2007). Bladder distention is one of the primary triggers of autonomic dysreflexia and such severe fluctuations in blood pressure pose a major limitation in the ability to recover bladder function long-term and place these individuals at cardiovascular risk. Overall bladder self-care and hygiene, including routine suprapubic catheter replacement, caregiver availability to assist with catheter maintenance, and the incidence of LUT comorbidities (e.g., urinary tract infections) may also be contributing factors in diverse urological outcomes evident in those using suprapubic catheters.

A select group of individuals was also found to have over-distended bladders, with high bladder volumes, characterized as areflexic (low detrusor tone). Oftentimes, a reduction in the standard frequency of daily and/or nightly catheterizations as a means to curtail emptying can contribute to bladder over-distention long-term (Consortium for Spinal Cord, Medicine, 2006). One such contributing factor is altered diurnal secretion of antidiuretic hormone after SCI (Szollar et al., 1997; Kilinc et al., 1999), resulting in the incidence of polyuria (overproduction and/or passage of urine). Excessive urine production can further exacerbate an already demanding catheterization schedule and disrupt daily life. We have found that the mechanisms underlying SCI-induced polyuria are multifactorial, including an interplay of various peptides involved in the physiological regulation of fluid balance, plasma volume, and overall urine output (Ward and Hubscher, 2012; Montgomery and Hubscher, 2018; Gumbel et al., 2020).

Given that the consequences of SCI affect multiple systems, scES as an intervention has the potential to benefit autonomic systems and organ function, dramatically impacting quality of life. Further gains in bladder control may be achieved by accessing these highly integrated networks using scES parameters directly targeted for optimizing storage and emptying while regulating cardiovascular function, as bladder distention is a major trigger for autonomic dysreflexia. A multi-pronged neurorehabilitative approach that builds upon the principles of task-specific training provides an avenue to facilitate the recruitment of both spinal circuitries and spared supraspinal connections important for recovering function after chronic SCI (Rejc and Angeli, 2019). Further research on the mechanisms driving the effects of scES on bladder function will significantly

advance the technology and therapeutic approaches for bladder management, dramatically improving the quality of life for people with SCI.

DATA AVAILABILITY STATEMENT

The raw data supporting the conclusions of this article will be made available by the authors, without undue reservation.

ETHICS STATEMENT

The studies involving human participants were reviewed and approved by The University of Louisville Institutional Review Board. The participants provided their written informed consent to participate in this study.

AUTHOR CONTRIBUTIONS

AH, CH, and SA contributed to the acquisition of data. AH, SA, and BU contributed to the analysis of data. AH drafted the manuscript. SA developed programming tools, including acquisition software and coding for cystometry analyses and data visualization. BU conducted the statistical analyses. AM contributed to medical oversight and provided the clinical interpretation of data. AH, SA, CH, and SH contributed to concept development, design, and data interpretation. CH and SH obtained funding and supervised the research. All authors critically reviewed and revised the manuscript. All authors contributed to the article and approved the submitted version.

FUNDING

Data collection and dissemination of the data presented in this manuscript was supported by the National Institutes of Health R01HD080205 (Drs. Hubscher and Harkema Co-PIs) and 1R01EB007615 (Dr. Harkema PI), the Craig H. Neilsen Foundation (ES2-CHN-2013, Dr. Harkema PI), the Leona M. and Harry B. Helmsley Charitable Trust (2011PG-MED011 and 2016PG-MED001), the Christopher & Dana Reeve Foundation (ES1-2011, ES_BI-2017, and ES_BI-2017), Kessler Foundation, and UofL Health—University of Louisville Hospital and Medtronic PLc.

ACKNOWLEDGMENTS

We would like to thank the research volunteers for their valuable contributions to this study. We also gratefully acknowledge Susan Dougherty, M.S., Anthony Gallahar, Jessica Hargitt, Erin Wyles, M.S., Lynnette Montgomery, Ph.D., and Andrea Willhite for their contribution to the data collection; Claudia Angeli, Ph.D., Enrico Rejc, Ph.D., Brittany Logsdon, and Rebekah Morton for their contribution to the epidural stimulation training and support of the research volunteers; Taylor Blades, Blair Cade, Shannon Martin, and Alice Kennedy for regulatory support; Nurses Carolyn Williams, Kristen Johnson, Yukishia Austin, Lynn Robbins, and Hye Conner for medical care; Jonathan Hodes and Maxwell Boakye for surgical procedures and Camilo Castillo and Sarah Wagers for clinical evaluations; Drs. Jonathan Hodes and Maxwell Boakye for surgical procedures and Drs. Douglas Stevens, Darryl Kaelin, Camilo Castillo, and Sarah Wagers for clinical evaluations.

REFERENCES

Abrams, P., Cardozo, L., Fall, M., Griffiths, D., Rosier, P., Ulmsten, U., et al. (2002). The standardisation of terminology of lower urinary tract function: report from the standardisation sub-committee of the international continence society. *Am. J. Obstet. Gynecol.* 187, 116–126. doi: 10.1067/mob.2002.125704

Abud, E. M., Ichiyama, R. M., Havton, L. A., and Chang, H. H. (2015). Spinal stimulation of the upper lumbar spinal cord modulates urethral sphincter activity in rats after spinal cord injury. *Am. J. Physiol. Renal. Physiol.* 308, F1032–F1040. doi: 10.1152/ajprenal.00573.2014

Ahluwalia, R. S., Johal, N., Kouriefs, C., Kooiman, G., Montgomery, B. S., and Plail, R. O. (2006). The surgical risk of suprapubic catheter insertion and long-term sequelae. *Ann. R. Coll. Surg. Engl.* 88, 210–213. doi: 10.1308/003588406X95101

Anderson, K. D. (2004). Targeting recovery: priorities of the spinal cord-injured population. *J. Neurotrauma* 21, 1371–1383. doi: 10.1089/neu.2004.21.1371

Angeli, C. A., Boakye, M., Morton, R. A., Vogt, J., Benton, K., Chen, Y., et al. (2018). Recovery of over-ground walking after chronic motor complete spinal cord injury. *N. Engl. J. Med.* 379, 1244–1250. doi: 10.1056/NEJMoa1803588

Angeli, C. A., Edgerton, V. R., Gerasimenko, Y. P., and Harkema, S. J. (2014). Altering spinal cord excitability enables voluntary movements after chronic complete paralysis in humans. *Brain* 137, 1394–1409. doi: 10.1093/brain/awu038

Armour, B. S., Courtney-Long, E. A., Fox, M. H., Fredine, H., and Cahill, A. (2016). Prevalence and causes of Paralysis-United States, 2013. *Am. J. Public Health* 106, 1855–1857. doi: 10.2105/AJPH.2016.303270

Aslan, S. C., Legg Ditterline, B. E., Park, M. C., Angeli, C. A., Rejc, E., Chen, Y., et al. (2018). Epidural spinal cord stimulation of lumbosacral networks modulates arterial blood pressure in individuals with spinal cord injury-induced cardiovascular deficits. *Front. Physiol.* 9:565. doi: 10.3389/fphys.2018.00565

Beck, L., Veith, D., Linde, M., Gill, M., Calvert, J., Grahn, P., et al. (2020). Impact of long-term epidural electrical stimulation enabled task-specific training on secondary conditions of chronic paraplegia in two humans. *J. Spinal Cord Med.* doi: 10.1080/10790268.2020.1739894. [Epub ahead of print].

Behrman, A. L., Lawless-Dixon, A. R., Davis, S. B., Bowden, M. G., Nair, P., Phadke, C., et al. (2005). Locomotor training progression and outcomes after incomplete spinal cord injury. *Phys. Ther.* 85, 1356–1371. doi: 10.1093/ptj/85.12.1356

Benevento, B. T., and Sipski, M. L. (2002). Neurogenic bladder, neurogenic bowel and sexual dysfunction in people with spinal cord injury. *Phys. Ther.* 82, 601–612. doi: 10.1093/ptj/82.6.601

Blaivas, J. G., Awad, S. A., Bissada, N., Khanna, O. P., Krane, R. J., Wein, A. J., et al. (1982). Urodynamic procedures: recommendations of the urodynamic society. I. Procedures that should be available for routine urologic practice. *Neurourol. Urodynamics* 1, 51–55. doi: 10.1002/nau.1930010104

Cameron, A. P., Lauren Wallner, P., Denise Tate, G., Aruna Sarma, V., Gianna Rodriguez, M., and Quentin Clemens, J. (2010). Bladder management after spinal cord injury in the United States 1972 to 2005. *J. Urol.* 184, 213–217. doi: 10.1016/j.juro.2010.03.008

Cameron, A. P., Wallner, L. P., Forchheimer, M. B., Clemens, J. Q., Dunn, R. L., Rodriguez, G., et al. (2011). Medical and psychosocial complications associated with method of bladder management after traumatic spinal cord injury. *Arch. Phys. Med. Rehabil.* 92, 449–456. doi: 10.1016/j.apmr.2010.06.028

National Spinal Cord Injury Statistical Center (2020). Spinal cord injury facts and figures at a glance. National institute on disability and rehabilitation research. Available online at: https://www.nscisc.uab.edu/Public/Facts%20and%20Figures%202020.pdf.

Cheng, C.-L., Ma, C.-P., and de Groat, W. C. (1995). Effect of capsaicin on micturition and associated reflexes in chronic spinal rats. *Brain Res.* 678, 40–48. doi: 10.1016/0006-8993(95)00212-9

Consortium for Spinal Cord, Medicine (2006). Bladder management for adults with spinal cord injury: a clinical practice guideline for health-care providers. *J. Spinal Cord Med.* 29, 527–573. doi: 10.1080/10790268.2006.11753903

Cragg, J. J., Noonan, V. K., Krassioukov, A., and Borisoff, J. (2013). Cardiovascular disease and spinal cord injury: results from a national population health survey. *Neurology* 81, 723–728. doi: 10.1212/WNL.0b013e3182a1aa68

Darrow, D., Balser, D., Netoff, T. I., Krassioukov, A., Phillips, A., Parr, A., et al. (2019). Epidural spinal cord stimulation facilitates immediate restoration of dormant motor and autonomic supraspinal pathways after chronic neurologically complete spinal cord injury. *J. Neurotrauma* 36, 2325–2336. doi: 10.1089/neu.2018.6006

de Groat, W. C. (1995). Mechanisms underlying the recovery of lower urinary tract function following spinal cord injury. *Paraplegia* 33, 493–505. doi: 10.1038/sc.1995.109

de Groat, W. C., and Yoshimura, N. (2010). Changes in afferent activity after spinal cord injury. *Neurourol. Urodyn.* 29, 63–76. doi: 10.1002/nau.20761

Dietz, V., and Harkema, S. J. (2004). Locomotor activity in spinal cord-injured persons. *J. Appl. Physiol. (1985)* 96, 1954–1960. doi: 10.1152/japplphysiol.00942.2003

Ditunno, P. L., Patrick, M., Stineman, M., and Ditunno, J. F. (2008). Who wants to walk? Preferences for recovery after SCI: a longitudinal and cross-sectional study. *Spinal Cord* 46, 500–506. doi: 10.1038/sj.sc.3102172

Douchamps, J., Derenne, F., Stockis, A., Gangji, D., Juvent, M., and Herchuelz, A. (1988). The pharmacokinetics of oxybutynin in man. *Eur. J. Clin. Pharmacol.* 35, 515–520. doi: 10.1007/BF00558247

Gad, P. N., Roy, R. R., Zhong, H., Gerasimenko, Y. P., Taccola, G., and Edgerton, R. V. (2016). Neuromodulation of the neural circuits controlling the lower urinary tract. *Exp. Neurol.* 285, 182–189. doi: 10.1016/j.expneurol.2016.06.034

Gad, P. N., Roy, R. R., Zhong, H., Lu, D. C., Gerasimenko, Y. P., and Edgerton, R. V. (2014). Initiation of bladder voiding with epidural stimulation in paralyzed, step trained rats. *PLoS One* 9:e108184. doi: 10.1371/journal.pone.0108184

Gammie, A., Clarkson, B., Constantinou, C., Damaser, M., Drinnan, M., Geleijnse, G., et al. (2014). International continence society guidelines on urodynamic equipment performance. *Neurourol. Urodyn.* 33, 370–379. doi: 10.1002/nau.22546

Garstang, S. V., and Miller-Smith, S. A. (2007). Autonomic nervous system dysfunction after spinal cord injury. *Phys. Med. Rehabil. Clin. N. Am.* 18:275296. doi: 10.1016/j.pmr.2007.02.003

Gill, M. L., Grahn, P. J., Calvert, J. S., Linde, M. B., Lavrov, I. A., Strommen, J. A., et al. (2018). Neuromodulation of lumbosacral spinal networks enables independent stepping after complete paraplegia. *Nat. Med.* 24, 1677–1682. doi: 10.1038/s41591-018-0175-7

Grahn, P. J., Lavrov, I. A., Sayenko, D. G., Van Straaten, M. G., Gill, M. L., Strommen, J. A., et al. (2017). Enabling task-specific volitional motor functions *via* spinal cord neuromodulation in a human with paraplegia. *Mayo Clin. Proc.* 92, 544–554. doi: 10.1016/j.mayocp.2017.02.014

Gray, M. (2001). *Urologic Nursing: A Study Guide Urodynamics.* 2nd Edn. Pitman, NJ: Society of Urological Nurses and Associates.

Gumbel, J. H., Montgomery, L. R., Yang, C. B., and Hubscher, C. H. (2020). Activity-based training reverses spinal cord injury-induced changes in kidney receptor densities and membrane proteins. *J. Neurotrauma* 37, 555–563. doi: 10.1089/neu.2019.6670

Hagen, E. M., Faerestrand, S., Hoff, J. M., Rekand, T., and Gronning, M. (2011). Cardiovascular and urological dysfunction in spinal cord injury. *Acta Neurol. Scand. Suppl.* 191, 71–78. doi: 10.1111/j.1600-0404.2011.01547.x

Hamid, R., Augusto Averbeck, M., Chiang, H., Garcia, A., Al Mousa, R. T., Oh, S.-J., et al. (2018). Epidemiology and pathophysiology of neurogenic bladder after spinal cord injury. *World J. Urol.* 36, 1517–1527. doi: 10.1007/s00345-018-2301-z

Harkema, S. J., Legg Ditterline, B., Wang, S., Aslan, S., Angeli, C. A., Ovechkin, A., et al. (2018a). Epidural spinal cord stimulation training and sustained recovery of cardiovascular function in individuals with chronic cervical spinal cord injury. *JAMA Neurol.* 75, 1569–1571. doi: 10.1001/jamaneurol.2018.2617

Harkema, S. J., Ferreira, C. K., van den Brand, R. J., and Krassioukov, A. V. (2008). Improvements in orthostatic instability with stand locomotor training in individuals with spinal cord injury. *J. Neurotrauma* 25, 1467–1475. doi: 10.1089/neu.2008.0572

Harkema, S., Gerasimenko, Y., Hodes, J., Burdick, J., Angeli, C., Chen, Y., et al. (2011). Effect of epidural stimulation of the lumbosacral spinal cord on voluntary movement, standing and assisted stepping after motor complete paraplegia: a case study. *Lancet* 377, 1938–1947. doi: 10.1016/S0140-6736(11)60547-3

Harkema, S. J., Hillyer, J., Schmidt-Read, M., Ardolino, E., Sisto, S. A., and Behrman, A. L. (2012). Locomotor training: as a treatment of spinal cord injury and in the progression of neurologic rehabilitation. *Arch. Phys. Med. Rehabil.* 93, 1588–1597. doi: 10.1016/j.apmr.2012.04.032

Harkema, S. J., Wang, S., Angeli, C. A., Chen, Y., Boakye, M., Ugiliweneza, B., et al. (2018b). Normalization of blood pressure with spinal cord epidural stimulation after severe spinal cord injury. *Front. Hum. Neurosci.* 12:83. doi: 10.3389/fnhum.2018.00083

Herrity, A. N., Williams, C. S., Angeli, C. A., Harkema, S. J., and Hubscher, C. H. (2018). Lumbosacral spinal cord epidural stimulation improves voiding function after human spinal cord injury. *Sci. Rep.* 8:8688. doi: 10.1038/s41598-018-26602-2

Hubscher, C. H., Herrity, A. N., Williams, C. S., Montgomery, L. R., Willhite, A. M., Angeli, C. A., et al. (2018). Improvements in bladder, bowel and sexual outcomes following task-specific locomotor training in human spinal cord injury. *PLoS One* 13:e0190998. doi: 10.1371/journal.pone.0190998

Jones, M. L., Evans, N., Tefertiller, C., Backus, D., Sweatman, M., Tansey, K., et al. (2014). Activity-based therapy for recovery of walking in individuals with chronic spinal cord injury: results from a randomized clinical trial. *Arch. Phys. Med. Rehabil.* 95, 2239.e2–2246.e2.doi: 10.1016/j.apmr.2014.07.400

Kaiser, A., Chan, K., Pakosh, M., and Musselman, K. E. (2020). Characteristics of activity-based therapy interventions for people living with spinal cord injury or disease across the continuum of care: a scoping review protocol. *BMJ Open* 10:e040014. doi: 10.1136/bmjopen-2020-040014

Kessler, T. M., La Framboise, D., Trelle, S., Fowler, C. J., Kiss, G., Pannek, J., et al. (2010). Sacral neuromodulation for neurogenic lower urinary tract dysfunction: systematic review and meta-analysis. *Eur. Urol.* 58, 865–874. doi: 10.1016/j.eururo.2010.09.024

Kilinc, S., Akman, M. N., Levendoglu, F., and Ozker, R. (1999). Diurnal variation of antidiuretic hormone and urinary output in spinal cord injury. *Spinal Cord* 37, 332–335. doi: 10.1038/sj.sc.3100814

Krassioukov, A., Eng, J. J., Warburton, D. E., and Teasell, R. (2009). A systematic review of the management of orthostatic hypotension after spinal cord injury. *Arch. Phys. Med. Rehabil.* 90, 876–885. doi: 10.1016/j.apmr.2009.01.009

Lombardi, G., and Del Popolo, G. (2009). Clinical outcome of sacral neuromodulation in incomplete spinal cord injured patients suffering from neurogenic lower urinary tract symptoms. *Spinal Cord* 47, 486–491. doi: 10.1038/sc.2008.172

Lukacz, E. S., Sampselle, C., Gray, M., Macdiarmid, S., Rosenberg, M., Ellsworth, P., et al. (2011). A healthy bladder: a consensus statement. *Int. J. Clin. Pract.* 65, 1026–1036. doi: 10.1111/j.1742-1241.2011.02763.x

Marino, R. J., Barros, T., Biering-Sorensen, F., Burns, S. P., Donovan, W. H., Graves, D. E., et al. (2003). International standards for neurological classification of spinal cord injury. *J. Spinal Cord Med.* 26, S50–S56. doi: 10.1080/10790268.2003.11754575

McGee, M. J., Amundsen, C. L., and Grill, W. M. (2015). Electrical stimulation for the treatment of lower urinary tract dysfunction after spinal cord injury. *J. Spinal Cord Med.* 38, 135–146. doi: 10.1179/2045772314Y.0000000299

Montgomery, L. R., and Hubscher, C. H. (2018). Altered vasopressin and natriuretic peptide levels in a rat model of spinal cord injury: implications for the development of polyuria. *Am. J. Physiol. Renal Physiol.* 314, F58–F66. doi: 10.1152/ajprenal.00229.2017

Morrison, S. A., Lorenz, D., Eskay, C. P., Forrest, G. F., and Basso, D. M. (2018). Longitudinal recovery and reduced costs after 120 sessions of locomotor

training for motor incomplete spinal cord injury. *Arch. Phys. Med. Rehabil.* 99, 555–562. doi: 10.1016/j.apmr.2017.10.003

Onushko, T., Mahtani, G. B., Brazg, G., Hornby, T. G., and Schmit, B. D. (2019). Exercise-induced alterations in sympathetic-somatomotor coupling in incomplete spinal cord injury. *J. Neurotrauma* 36, 2688–2697. doi: 10.1089/neu.2018.5719

Pannek, J., Gocking, K., and Bersch, U. (2010). To clamp or not to clamp? Bladder management by suprapubic catheterization in patients with neurogenic bladder dysfunction. *World J. Urol.* 28, 637–641. doi: 10.1007/s00345-009-0501-2

Pannek, J., Kennelly, M., Kessler, T. M., Linsenmeyer, T., Wyndaele, J.-J., and Biering-Sørensen, F. (2018). International spinal cord injury urodynamic basic data set (version 2.0). *Spinal Cord Series Cases* 4:98. doi: 10.1038/s41394-018-0133-0

Piatt, J. A., Nagata, S., Zahl, M., Li, J., and Rosenbluth, J. P. (2016). Problematic secondary health conditions among adults with spinal cord injury and its impact on social participation and daily life. *J. Spinal Cord Med.* 39, 693–698. doi: 10.1080/10790268.2015.1123845

Rejc, E., and Angeli, C. A. (2019). Spinal cord epidural stimulation for lower limb motor function recovery in individuals with motor complete spinal cord injury. *Phys. Med. Rehabil. Clin. N. Am.* 30, 337–354. doi: 10.1016/j.pmr.2018.12.009

Rejc, E., Angeli, C. A., Atkinson, D., and Harkema, S. J. (2017). Motor recovery after activity-based training with spinal cord epidural stimulation in a chronic motor complete paraplegic. *Sci. Rep.* 7:13476. doi: 10.1038/s41598-017-14003-w

Rosier, P., Kuo, H., De Gennaro, M., Kakizaki, H., Van meel, T., and Hobson, P. (2013). *5th International Consultation on Incontinence: Recommendations of the International Scientific Committee: Urodynamics Testing*, Incontinence, Paris.

Schafer, W., Abrams, P., Liao, L., Mattiasson, A., Pesce, F., Spangberg, A., et al. (2002). Good urodynamic practices: uroflowmetry, filling cystometry and pressure-flow studies. *Neurourol. Urodyn.* 21, 261–274. doi: 10.1002/nau.10066

Schmidt, R. A. (1988). Applications of neurostimulation in urology. *Neurourol. Urodyn.* 7, 585–592. doi: 10.1002/nau.1930070607

Sievert, K. D., Amend, B., Gakis, G., Toomey, P., Badke, A., Kaps, H. P., et al. (2010). Early sacral neuromodulation prevents urinary incontinence after complete spinal cord injury. *Ann. Neurol.* 67, 74–84. doi: 10.1002/ana.21814

Stöhrer, M., Goepel, M., Kondo, A., Kramer, G., Madersbacher, H., Millard, R., et al. (1999). The standardization of terminology in neurogenic lower urinary tract dysfunction: with suggestions for diagnostic procedures. International continence society standardization committee. *Neurourol. Urodyn.* 18, 139–158. doi: 10.1002/(sici)1520-6777(1999)18:2<139::aid-nau9>3.0.co;2-u

Szollar, S. M., Dunn, K. L., Brandt, S., and Fincher, J. (1997). Nocturnal polyuria and antidiuretic hormone levels in spinal cord injury. *Arch. Phys. Med. Rehabil.* 78, 455–458. doi: 10.1016/s0003-9993(97)90155-6

Tanagho, E. A., and Schmidt, R. A. (1982). Bladder pacemaker: scientific basis and clinical future. *Urology* 20, 614–619. doi: 10.1016/0090-4295(82)90312-0

Terson de Paleville, D., McKay, W., Aslan, S., Folz, R., Sayenko, D., and Ovechkin, A. (2013). Locomotor step training with body weight support improves respiratory motor function in individuals with chronic spinal cord injury. *Respir. Physiol. Neurobiol.* 189, 491–497. doi: 10.1016/j.resp.2013.08.018

Van Kerrebroeck, P. E., Koldewijn, E. L., Scherpenhuizen, S., and Debruyne, F. M. (1993). The morbidity due to lower urinary tract function in spinal cord injury patients. *Paraplegia* 31, 320–329. doi: 10.1038/sc.1993.56

Wagner, F. B., Mignardot, J. B., Le Goff-Mignardot, C. G., Demesmaeker, R., Komi, S., Capogrosso, M., et al. (2018). Targeted neurotechnology restores walking in humans with spinal cord injury. *Nature* 563, 65–71. doi: 10.1038/s41586-018-0649-2

Walsh, P. C., Retik, A. B., Vaughan, E. D., and Wein, A. J. (2002). *Campbell's Urology*. 8th Edn. Philadelphia, PA: W.B. Saunders.

Walter, M., Lee, A. H. X., Kavanagh, A., Phillips, A. A., and Krassioukov, A. V. (2018). Epidural spinal cord stimulation acutely modulates lower urinary tract and bowel function following spinal cord injury: a case report. *Front. Physiol.* 9:1816. doi: 10.3389/fphys.2018.01816

Wang, S., Wecht, J. M., Legg Ditterline, B., Ugiliweneza, B., Maher, M. T., Lombard, A. T., et al. (2020). Heart rate and blood pressure response improve the prediction of orthostatic cardiovascular dysregulation in persons with chronic spinal cord injury. *Physiol. Rep.* 8:e14617. doi: 10.14814/phy2.14617

Ward, P. J., Herrity, A. N., Harkema, S. J., and Hubscher, C. H. (2016). Training-induced functional gains following SCI. *Neural Plast.* 2016:4307694. doi: 10.1155/2016/4307694

Ward, P. J., Herrity, A. N., Smith, R. R., Willhite, A., Harrison, B. J., Petruska, J. C., et al. (2014). Novel multi-system functional gains *via* task specific training in spinal cord injured male rats. *J. Neurotrauma* 31, 819–833. doi: 10.1089/neu.2013.3082

Ward, P. J., and Hubscher, C. H. (2012). Persistent polyuria in a rat spinal contusion model. *J. Neurotrauma* 29, 2490–2498. doi: 10.1089/neu.2012.2402

Waring, W. P., 3rd, Biering-Sorensen, F., Burns, S., Donovan, W., Graves, D., Jha, A., et al. (2010). 2009 review and revisions of the international standards for the neurological classification of spinal cord injury. *J. Spinal Cord Med.* 33, 346–352. doi: 10.1080/10790268.2010.11689712

West, C. R., Phillips, A. A., Squair, J. W., Williams, A. M., Walter, M., Lam, T., et al. (2018). Association of epidural stimulation with cardiovascular function in an individual with spinal cord injury. *JAMA Neurol.* 75, 630–632. doi: 10.1001/jamaneurol.2017.5055

Winters, J. C., Dmochowski, R. R., Goldman, H. B., Herndon, C. D., Kobashi, K. C., Kraus, S. R., et al. (2012). Urodynamic studies in adults: AUA/SUFU guideline. *J. Urol.* 188, 2464–2472. doi: 10.1016/j.juro.2012.09.081

Wolpaw, J. R., and Tennissen, A. M. (2001). Activity-dependent spinal cord plasticity in health and disease. *Annu. Rev. Neurosci.* 24, 807–843. doi: 10.1146/annurev.neuro.24.1.807

Wyndaele, J. J. (1998). The normal pattern of perception of bladder filling during cystometry studied in 38 young healthy volunteers. *J. Urol.* 160, 479–481.

Wyndaele, J. J., and De Wachter, S. (2002). Cystometrical sensory data from a normal population: comparison of two groups of young healthy volunteers examined with 5 years interval. *Eur. Urol.* 42, 34–38. doi: 10.1016/s0302-2838(02)00221-x

Zeilig, G., Dolev, M., Weingarden, H., Blumen, N., Shemesh, Y., and Ohry, A. (2000). Long-term morbidity and mortality after spinal cord injury: 50 years of follow-up. *Spinal Cord* 38:563. doi: 10.1038/sj.sc.3101043

Conflict of Interest: The authors declare that the research was conducted in the absence of any commercial or financial relationships that could be construed as a potential conflict of interest.

frontiers in Systems Neuroscience

CLINICAL TRIAL
published: 28 January 2021
doi: 10.3389/fnsys.2020.590231

Alterations of Spinal Epidural Stimulation-Enabled Stepping by Descending Intentional Motor Commands and Proprioceptive Inputs in Humans With Spinal Cord Injury

Megan L. Gill[1], Margaux B. Linde[1], Rena F. Hale[1], Cesar Lopez[1], Kalli J. Fautsch[1], Jonathan S. Calvert[2], Daniel D. Veith[1], Lisa A. Beck[1], Kristin L. Garlanger[1], Dimitry G. Sayenko[3], Igor A. Lavrov[4,5], Andrew R. Thoreson[1], Peter J. Grahn[1,6,7] and Kristin D. Zhao[1,8]**

[1] Assistive and Restorative Technology Laboratory, Department of Physical Medicine and Rehabilitation, Rehabilitation Medicine Research Center, Mayo Clinic, Rochester, MN, United States, [2] Mayo Clinic Graduate School of Biomedical Sciences, Mayo Clinic, Rochester, MN, United States, [3] Department of Neurosurgery, Center for Neuroregeneration, Houston Methodist Hospital, Houston, TX, United States, [4] Department of Neurology, Mayo Clinic, Rochester, MN, United States, [5] Institute of Fundamental Medicine and Biology, Kazan Federal University, Kazan, Russia, [6] Department of Neurosurgery, Mayo Clinic, Rochester, MN, United States, [7] Office for Education Diversity, Equity and Inclusion, Mayo Clinic, Rochester, MN, United States, [8] Department of Physiology and Biomedical Engineering, Mayo Clinic, Rochester, MN, United States

OPEN ACCESS

Edited by:
Enrico Rejc,
University of Louisville, United States

Reviewed by:
Keith Gordon,
Northwestern University, United States
Ursula Hofstoetter,
Medical University of Vienna, Austria
Keith E. Tansey,
Methodist Rehabilitation Center, United States

***Correspondence:**
Peter J. Grahn
grahn.peter@mayo.edu
Kristin D. Zhao
zhao.kristin@mayo.edu

Received: 31 July 2020
Accepted: 11 December 2020
Published: 28 January 2021

Citation:
Gill ML, Linde MB, Hale RF, Lopez C, Fautsch KJ, Calvert JS, Veith DD, Beck LA, Garlanger KL, Sayenko DG, Lavrov IA, Thoreson AR, Grahn PJ and Zhao KD (2021) Alterations of Spinal Epidural Stimulation-Enabled Stepping by Descending Intentional Motor Commands and Proprioceptive Inputs in Humans With Spinal Cord Injury. Front. Syst. Neurosci. 14:590231. doi: 10.3389/fnsys.2020.590231

Background: Regaining control of movement following a spinal cord injury (SCI) requires utilization and/or functional reorganization of residual descending, and likely ascending, supraspinal sensorimotor pathways, which may be facilitated via task-specific training through body weight supported treadmill (BWST) training. Recently, epidural electrical stimulation (ES) combined with task-specific training demonstrated independence of standing and stepping functions in individuals with clinically complete SCI. The restoration of these functions may be dependent upon variables such as manipulation of proprioceptive input, ES parameter adjustments, and participant intent during step training. However, the impact of each variable on the degree of independence achieved during BWST stepping remains unknown.

Objective: To describe the effects of descending intentional commands and proprioceptive inputs, specifically body weight support (BWS), on lower extremity motor activity and vertical ground reaction forces (vGRF) during ES-enabled BWST stepping in humans with chronic sensorimotor complete SCI. Furthermore, we describe perceived changes in the level of assistance provided by clinicians when intent and BWS are modified.

Methods: Two individuals with chronic, mid thoracic, clinically complete SCI, enrolled in an IRB and FDA (IDE G150167) approved clinical trial. A 16-contact electrode array was implanted in the epidural space between the T11-L1 vertebral regions. Lower extremity motor output and vertical ground reaction forces were obtained during clinician-assisted ES-enabled treadmill stepping with BWS. Consecutive steps were achieved

during various experimentally-controlled conditions, including intentional participation and varied BWS (60% and 20%) while ES parameters remain unchanged.

Results: During ES-enabled BWST stepping, the knee extensors exhibited an increase in motor activation during trials in which stepping was passive compared to active or during trials in which 60% BWS was provided compared to 20% BWS. As a result of this increased motor activation, perceived clinician assistance increased during the transition from stance to swing. Intentional participation and 20% BWS resulted in timely and purposeful activation of the lower extremities muscles, which improved independence and decreased clinician assistance.

Conclusion: Maximizing participant intention and optimizing proprioceptive inputs through BWS during ES-enabled BWST stepping may facilitate greater independence during BWST stepping for individuals with clinically complete SCI.

Clinical Trial Registration: ClinicalTrials.gov identifier: NCT02592668.

Keywords: paralysis, spinal cord injury, task-specific training, multi- modal rehabilitation, body weight supported stepping, spinal neuromodulation, epidural spinal stimulation

INTRODUCTION

A spinal cord injury (SCI) causes disruption of communication between spinal circuitries and supraspinal centers often resulting in permanent motor and sensory deficits. Advanced rehabilitation approaches, such as task-specific training, focus on re-engaging spinal circuitries below the level of injury to gain recovery of lost motor and sensory functions with a goal of increasing independence for individuals with spared motor or sensory function (Behrman et al., 2017). Regaining control of goal directed intentional movement following SCI requires utilization and/or functional reorganization of residual descending, and likely ascending, supraspinal sensorimotor pathways (Winstein et al., 1994; Winchester et al., 2005; Cai et al., 2006; Field-Fote and Roach, 2011; Petersen et al., 2012; Barthélemy et al., 2015; Huie et al., 2017). More specifically, body weight supported treadmill (BWST) training is used by clinicians to facilitate spinal circuitry influencing afferent proprioceptive input in a task-specific manner, which has been demonstrated to improve locomotor functions in individuals with motor incomplete SCI (Thomas et al., 2005). However, BWST training has not been shown to sufficiently facilitate functional residual connections in individuals with motor complete SCI (Forrest et al., 2008; Scivoletto et al., 2014).

During BWST training, spinal circuitries below the injury site are capable of interpreting afferent proprioceptive inputs in order to coordinate downstream motor outputs during activities such as standing and stepping (Harkema et al., 1997; Dietz et al., 2002; Beres-Jones and Harkema, 2004; Edgerton et al., 2008). Activation of proprioceptive inputs can be achieved during BWST training through lower extremity loading, clinician-assisted joint manipulation and tactile facilitation (Harkema et al., 2011a). Specifically, lower extremity loading has been shown to increase extensor muscle activity in individuals with SCI during stepping, even those with motor complete SCI, despite no return of clinically detectable function (Dietz et al., 1995; Dobkin et al., 1995; Harkema et al., 1997; Wirz et al., 2001; Apte et al., 2018).

Traditionally in the field of rehabilitation, patient progress is measured through the level of perceived independence determined by the amount of physical assistance needed to complete activities of daily living such as walking. Quantitative measures to describe performance during a dynamic task such as BWST stepping in the motor complete SCI population is challenging. The level of clinician assistance for joint manipulation and tactile facilitation are constantly changing, determined by the success of generating flexion or extension movements necessary for each phase of gait. Galvez et al. (2011) quantified trainer/clinician variability of manual skills during BWST step training while identifying key phases of gait with the greatest amount of variability.

Over the last decade, investigations of task-specific training combined with epidural electrical stimulation (ES) applied to the dorsal surface of the spinal cord, below the level of SCI, have demonstrated the restoration of standing and stepping functions in individuals diagnosed as motor complete SCI (Rejc et al., 2015, 2017; Grahn et al., 2017; Angeli et al., 2018; Gill et al., 2018). Functional improvements enabled by ES and task-specific training are thought to be achieved by facilitating activity across spinal circuitries in order to re-establish states of excitability that enable robust, coordinated motor outputs necessary to perform standing and stepping tasks (Dimitrijevic et al., 1998; Minassian et al., 2004; Danner et al., 2015). Our team previously reported the use of multi-modal rehabilitation, a combined approach of task-specific training with continuous ES, in an individual with a sensorimotor complete SCI, which resulted in the ability to step over ground with the aid of a walker and minimal assistance at the hips for balance and no assistance at the knees (Gill et al., 2018). In the presence of ES, improvements of motor functions were observed over 12 months of BWST training. These improvements

were dependent upon several variables such as optimization of proprioceptive input during training, ES parameters and the degree to which participants attempted to intentionally control motor activity during each step cycle. However, the impact of each variable on the degree of independence achieved during BWST stepping remains unknown.

Herein, we describe lower extremity motor activity and vertical ground reaction forces (vGRF) during various experimentally-controlled conditions of ES-enabled BWST stepping in two individuals with chronic, complete loss of function below the level of SCI. Furthermore, we describe qualitative features of perceived changes in the level of assistance provided by clinicians during ES-enabled BWST stepping.

METHODS

Participants

Two participants diagnosed with an American Spinal Injury Association (ASIA) Impairment Scale Grade A (AIS-A) sensorimotor complete SCI (Burns et al., 2012) were enrolled in this clinical trial. Participant 1, 26 years of age, sustained traumatic T6 SCI 3 years prior to enrollment. Participant 2, age 37 years of age, sustained traumatic T3 SCI 6 years prior to enrollment. Both participants presented with absent lower extremity motor evoked potentials and scalp somatosensory evoked potentials. Both participants demonstrated evidence of spared connections of lower extremity non-specific electromyography (EMG) during Jendrassik maneuver described in the literature as a discomplete SCI profile (Dimitrijevic, 1988; Sherwood et al., 1992). Participants provided written, informed consent to all procedures which were performed under the approval of the Mayo Clinic Institutional Review Board with a US Food and Drug Administration Investigational Device Exemption (IDE G150167).

Clinical Trial Protocol

Following 6 months of locomotor training (Harkema et al., 2011b) both participants were implanted with the Medtronic® Specify 5-6-5 spinal epidural electrode array (Medtronic, Fridley, MN) which was internally connected to the RestoreUltra SureScan MRI Neurostimulator (Model 97712, Medtronic, Fridley, MN). After recovering from surgery, ES-enabled task-specific training was performed over a period of ∼12 months (Gill et al., 2018). Following 12 months of ES-enabled task-specific training, participants returned for a data collection session aimed at comparing BWST stepping conditions (e.g., participant intent and varied BWS) with consistent ES parameters.

ES Parameter Selection

During initial sessions of ES-enabled task-specific training, stimulation parameters were adjusted incrementally while recording lower extremity EMG synchronized to delivery of each ES pulse in order to examine lower extremity muscle recruitment curves (Sayenko et al., 2014; Grahn et al., 2017; Calvert et al., 2019b). ES parameter usage at supra-motor threshold levels, defined as voltages that evoked observable activity in skin surface EMG recordings that were robust enough to generate movement of the lower extremities (Dimitrijevic et al., 1998), were utilized during the initial sessions of BWST training (Grahn et al., 2017; Calvert et al., 2019a). Subsequent refinement of these parameters occurred during each session of BWST training with an overarching goal of maximizing independent, volitional control over lower extremity movements comprised of stepping characteristics (e.g., initiation and/or termination of swing phase during contralateral weight bearing stance phase) (Gill et al., 2018). Refinement across BWST sessions resulted in a narrowed range of ES parameters with respect to voltage amplitude (2.0–4.1 V), pulse frequency (20–30 Hz), and pulse width (200–450 μs) applied continuously. During stepping experiments reported herein, ES parameters identified at the beginning of the data collection session were not adjusted across conditions.

Experimental Conditions

Multi-modal rehabilitation during the initial 12 months focused on standing and stepping utilizing a BWST system, along with a computer-controlled motorized treadmill, as well as a team of clinicians with expertise in assisting joint manipulation and tactile facilitation consistent with locomotor training principles (Behrman and Harkema, 2000; Beres-Jones and Harkema, 2004; Dolbow et al., 2015; Behrman et al., 2017). Participant-specific ES parameters and treadmill speeds, which were considered optimal for achieving the greatest independence during BWST stepping, remained unchanged during the data collection session. Participants were allowed to use parallel bars during BWST stepping to facilitate trunk stability and manipulation of weight shifts in an effort to maximize independence. However, participants were instructed to refrain from using their hands on parallel bars for weight-bearing. Changes in BWS were monitored using the treadmill software (Power Neuro Recovery, Louisville, KY, USA). Additionally, during passive conditions participants were asked to simply rest their arms on the bars and not engage in weight shifting. Stepping assistance was provided as needed at the hips, knees, and ankles. The order between intent and BWS conditions was standardized for both participants during each testing condition in the following manner: (1) 60% BWS, (2) 20% BWS, then (3) active stepping, and (4) passive stepping.

Intent Conditions (Active and Passive Stepping)

Here, intent describes descending commands and is defined as the intentional participation utilized during active stepping conditions. Methods to engage intentional participation included visual feedback while using mirrors and verbal feedback both between clinicians and to the participants for optimal kinematics during stepping bouts. Participants were instructed to fully concentrate on achieving both stance and swing phases of each gait cycle. Passive stepping occurred when the participants were instructed to have no intent while clinicians facilitated stepping movements as needed. Furthermore, participants were instructed to completely relax and allow the clinicians to assist with the stepping task. To compare motor outputs between active and passive stepping conditions, the participants were asked to complete 10 consecutive steps bilaterally for each

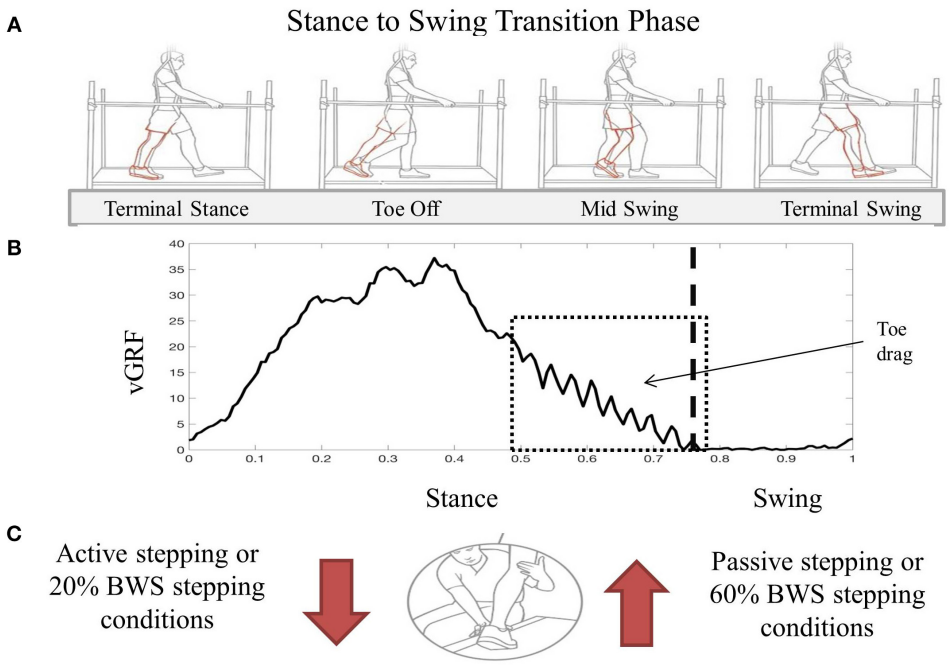

FIGURE 1 | Visual description of transition from stance to swing during BWST stepping **(A)**. Red limb indicates inadequate movement of the limb during swing phase demonstrating increased knee extension during toe off and toe drag during mid swing. An exemplary vGRF trace during one step cycle demonstrating increased difficulty transitioning from stance to swing with oscillatory force pattern representing toe drag **(B)**. Box represents the time during the gait cycle where assistance level increased as perceived by the clinicians assistance level increased as perceived by the clinicians. During the transition from stance to swing, clinician assistance facilitation technique increased during passive and 60% BWS stepping conditions compared to active and 20% BWS stepping **(C)**. Image used in Panel A was created by Mayo Clinic's Medical Illustration Department.

condition. ES parameters, BWS (20%), and treadmill speed (0.5 mph) remained unchanged during testing bouts. Clinician assistance was provided as needed to successfully complete each step.

BWS Conditions (60% and 20% Unloading)

BWS describes afferent proprioceptive input based on the percentage of the participant's body weight offloaded during BWST stepping. To compare motor output differences between two considerably different loading environments, 60% and 20% BWS levels were utilized. The participants were instructed to fully concentrate on achieving 10 consecutive steps bilaterally for each BWS condition, and actively focus on achieving appropriate stance and swing phases. ES parameters, participant intent (active stepping), and speed (0.5 mph) remained unchanged during testing bouts. Clinician assistance was provided as needed to successfully complete each step.

Data Collection

Stepping data was collected at a single time point following 12 months of ES-enabled task-specific training. Motor outputs for the 10 consecutive bilateral steps in each condition were collected using skin surface EMG recorded bilaterally on the rectus femoris (RF), vastus lateralis (VL), medial hamstring (MH), medial gastrocnemius (MG), soleus (SOL), and tibialis anterior (TA) muscles at a sampling rate of 4 kHz (PowerLab, AD Instruments, Inc., Colorado, USA). vGRF was recorded using shoe insole pressure sensors at a sampling rate of 50 Hz (FSCAN, Tekscan, Inc., South Boston, MA, USA). Data were synchronized with real time video capture using Labchart electrophysiological software.

Clinician Perceived Level of Assistance

During stepping, clinician assistance varied based on success in achieving each phase of the gait cycle. Assistance levels were reported by the clinicians and available reviewed through video recordings. Using locomotor training principles, clinician-assisted joint manipulation and tactile facilitation were used to activate appropriate muscles during specific gait phases for knee control, flexion vs. extension movements, and ankle control for toe clearance and foot placement (Harkema et al., 2011a). Knee control during stance requires facilitation at the anterior tibial crest with dual purpose of knee extension force and facilitation of the patellar tendon with the goal of engaging the knee extensor muscles. Knee control during swing phase responds to a quick stretch of the hamstring tendon to facilitate knee flexion. During stance phase, ankle control assistance is necessary for foot placement and to stabilize against rotation during loading. Clinicians performing the data collection were consistent but not blinded to the condition. Subjective reporting of either an increase or decrease in assist level, as well as identification of the phase of gait perceived to change, was not based on any scale and was verbally reported after data collection. These methods have not been validated and rely on the clinician's vast experience

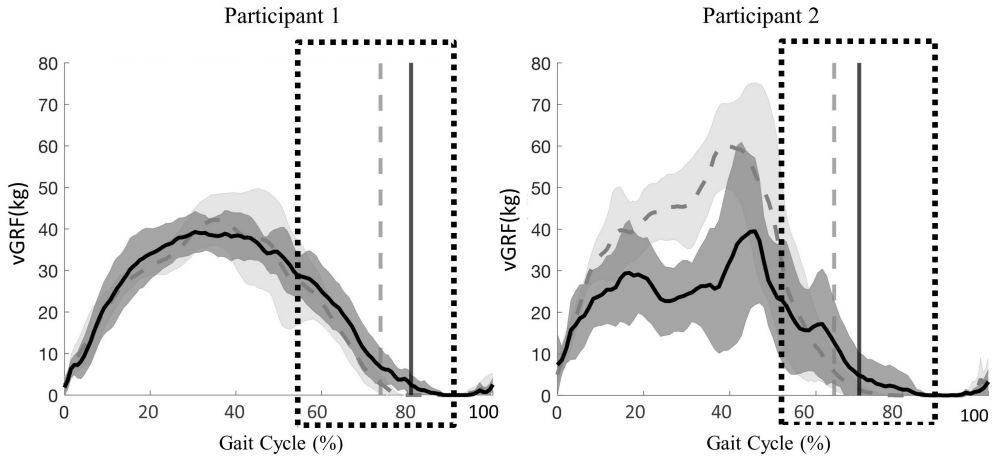

FIGURE 2 | Participant 1(right limb) and participant 2 (left limb), mean ± *SD* vGRF during passive (solid line) and active (dashed line) stepping across the gait cycle. Vertical lines represent transition from stance to swing for each respective condition. Boxes represent time during the gait cycle where assistance level increased as perceive by the clinicians.

following 12 months of multi-modal rehabilitation with each participant. Between conditions, the level of clinician assistance was most variable during the transition from stance to swing phase (**Figure 1**).

Data Analysis

Data was processed using a custom MATLAB algorithm (MATLAB, The MathWorks Inc., Natick, MA, USA). A total of 10 steps were collected from each participant in each condition. Five steps from participant 2 were excluded due to inconsistent use of the upper extremities. Data were averaged by participant, right or left limb, and stepping condition. Only the RF and/or the VL muscles were selected to be analyzed due to role of each during the stance phase of gait. EMG activation was also averaged by muscle. EMG data were full wave rectified and filtered with a second order zero-phase lag band-pass filter for frequencies between 59 and 61 Hz to remove any electrical noise. Subsequently, the linear envelope was created by low-pass filtering at 3 Hz using a zero-phase lag second order Butterworth filter (Olney and Winter, 1985; Arendt-nielsen, 1994; Heintz and Gutierrez-farewik, 2007; Danner et al., 2015; Lerner et al., 2017). The root mean square (RMS) was calculated from mean EMG responses of individual muscles in each condition for the stance and swing phases separately. A statistical analysis was performed using JMP (Cary, NC, USA) to determine if differences between RMS values were significant between conditions in each participant. Paired *t*-tests were performed on the VL and RF RMS values between passive and active stepping and 60% and 20% BWS stepping within each participant. Alpha was set to 0.05. Percent of the gait cycle was determined using a modified threshold equation on the vGRF signal (FSCAN, Tekscan) and verified though 2D video analysis. EMG and vGRF signals for each step were normalized from 0 to 100% of the gait cycle. The time of transition from stance to swing was calculated based on proprietary algorithms within the Tekscan software. A stance to swing transition phase was calculated as 60–90% of the gait cycle. Right and left sides were processed identically.

RESULTS

Influence of Intent on Stepping

Clinician Perceived Level of Assistance

The clinician perceived level of assistance for both participants was less during the transition phase from stance to swing during active stepping when compared to passive stepping. During active stepping, the transition from stance to swing was timely and purposeful, reducing the level of clinician assistance. When each participant was passively stepping, the stance to swing transition resulted in excessive lower extremity extension which requiring increased clinician assistance to facilitate flexion in order to minimize toe drag (**Figure 1**). Due to the decrease in trainer assistance, active stepping resulted in more independence than passive stepping.

vGRF

Peak vGRF timing over the entire gait cycle and vGRF magnitude during the transition phase of stance to swing were comparable between active and passive stepping conditions. For participant 1, the transition phase occurred on average 6% (right and left limb) later in the gait cycle in passive stepping when compared to active stepping (**Figure 2**). For participant 2, the transition phase occurred on average 2% and 6% (right and left limb) later in the gait cycle in passive stepping when compared to active stepping (**Figure 2**). Both participants exhibited toe drag in passive stepping as indicated by the oscillating mean curve from 70% to 100% of the gait cycle. Passive stepping toe drag was also verified with 2D video analysis. Active stepping did not result in toe drag.

Lower Extremity EMG

Significant differences were present in the knee extensor RMS values during passive stepping when compared to active stepping

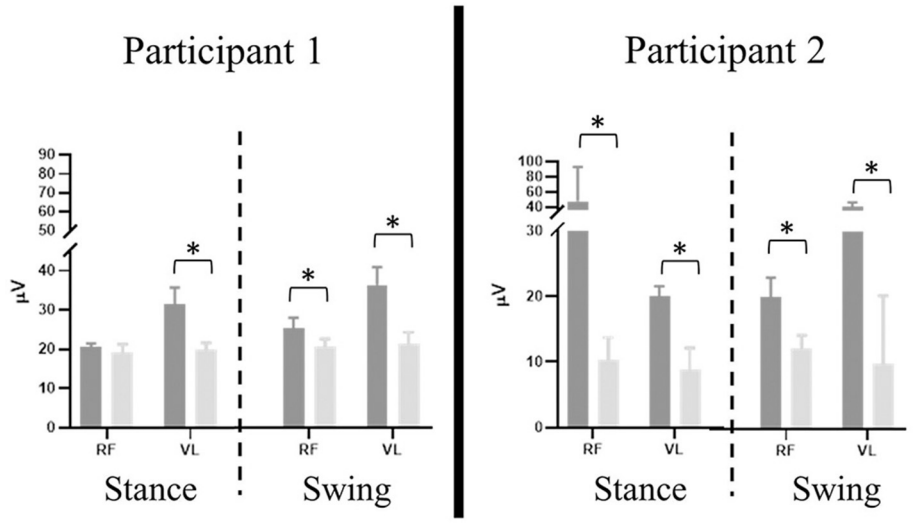

FIGURE 3 | Participant 1 (right limb) and participant 2 (left limb), mean ± *SD* RMS values of rectus femoris (RF) and vastus lateralis (VL) results separated by stance and swing phase (dashed line) during passive (dark gray) and active (light gray) stepping. Error bars represent one standard deviation. Asterisk denotes $P < 0.01$.

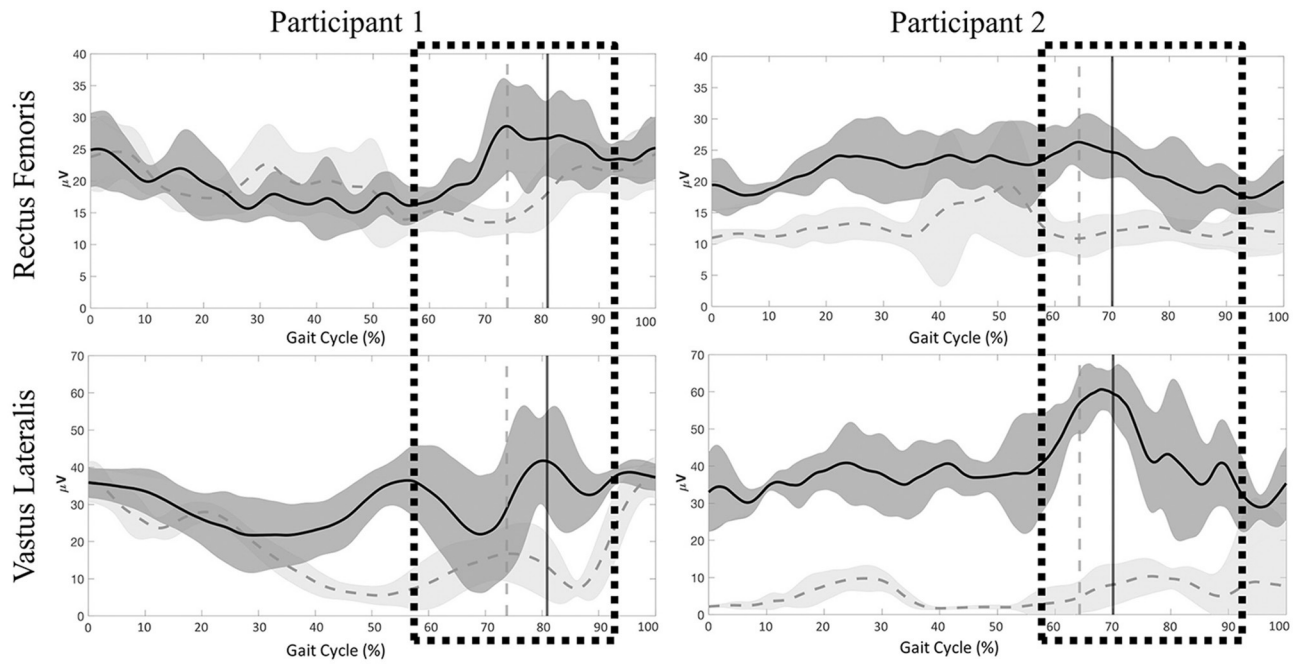

FIGURE 4 | Participant 1 (right limb) and participant 2 (left limb), mean ± *SD* electromyography activation of the rectus femoris (RF) and vastus lateralis (VL) for Participant 1 and Participant 2 during passive (dark gray) and active (light gray) stepping conditions. Vertical lines represent transition from stance to swing for each respective condition. Boxes represent time during the gait cycle were clinicians perceived an increase in the level of assistance.

during both stance and swing phase ($P < 0.01$) (**Figure 3**). RF RMS values during passive stepping were higher than in active stepping (participant 1: 1.81 μV higher in stance and 4.39 μV higher in swing; participant 2: 15.48 μV higher in stance and 13.6 μV higher in swing). VL RMS values during passive stepping were higher than in active stepping (participant 1: 10.8 μV higher in stance and 15.9 μV higher in swing; participant 2: 33.1 μV higher in stance and 36.7 μV higher in swing). Participant 1 demonstrated constant RF activation during the full gait cycle in both active and passive stepping (**Figure 4**). During the transition from stance to swing (60–90% of the gait cycle) passive stepping resulted in a larger increase in RF activation in comparison to active stepping. Similar activation patterns emerged in the VL; decreases in activation were larger during active stepping compared to passive stepping. The RF and VL for participant 2 also remained constant during stance to swing transition much

greater activation observed for passive stepping compared to active stepping. Overall, the RF and VL for both participants were greater during the transition from stance to swing during passive stepping compared to active. Changes between 20 and 60% BWS in the medial hamstring and distal muscles were minimal. Data can be viewed in the **Supplementary Material**.

Effect of Altering Body Weight Support During Stepping

Clinician Perceived Level of Assistance

Clinician perceived level of assistance for both participants during the transition from stance to swing phase was less during 20% BWS stepping than during 60% BWS stepping. For both participants, the transition from stance to swing was timely and purposeful, demonstrating appropriate lower extremity movement from extension during stance to flexion during swing (**Figure 1**). The clinicians reported less assistance required for stepping bouts during 20% BWS.

vGRF

The peak vGRF during 20% BWS stepping was at least twice the magnitude of that for 60% BWS stepping (**Figure 5**). Participant 1 exhibited a later transition from stance to swing in 20% BWS stepping when compared to 60% BWS stepping (2% of the gait cycle). Whereas, participant 2 demonstrated a transition phase 11% later in the gait cycle in 60% BWS stepping when compared to 20%. Toe drag was not visibly different in 60% and 20% BWS stepping conditions.

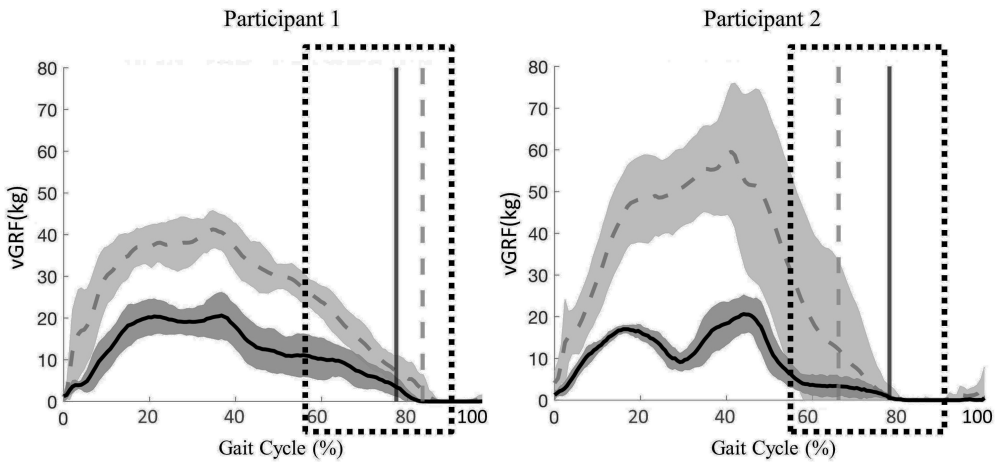

FIGURE 5 | Participant 1 (right limb) and participant 2 (left limb), mean ± *SD* vGRF during 60% (solid line) and 20% (dashed line) BWS stepping across the gait cycle. Vertical lines represent transition from stance to swing for each respective condition. Boxes represent time during the gait cycle where clinicians perceived an increase in the level of assistance.

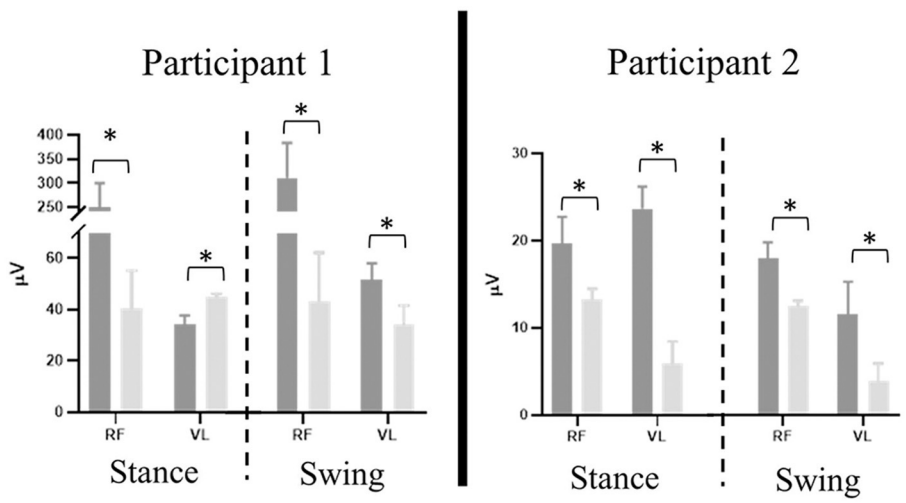

FIGURE 6 | Participant 1 (right limb) and participant 2 (left limb), mean ± *SD* RMS values of rectus femoris (RF) and vastus lateralis (VL) results separated by stance and swing phase (dashed line) during 60% (dark gray) and 20% (light gray) BWS stepping. Error bars represent one standard deviation. Asterisk denotes $P < 0.01$.

Lower Extremity EMG

Stepping at 20% BWS, when compared to 60% BWS, resulted in significantly lower RMS values during both stance and swing phases ($P < 0.01$) with the exception of the VL for participant 1 (**Figure 6**). The RF RMS values were significantly higher in 60% BWS stepping when compared to 20% BWS stepping (participant 1: 203.8 μV higher in stance and 261.9 μV higher in swing; P2: 6.36 μV higher in stance and 5.52 μV higher in swing; $P < 0.01$). During stance phase, participant 1 VL RMS was 8.7 μV less in 60% BWS stepping when compared to 20% BWS stepping. However, in swing phase VL RMS was 15.17 μV greater in 60% BWS stepping when compared to 20% BWS stepping. During both stance and swing phase, participant 2 demonstrated significantly higher VL RMS in 60% BWS stepping when compared to 20% (17.3 μV higher in stance and 6.52 μV higher in swing). Participant 1 RF demonstrated a sharp decreased in activation as toe off occurred during 60% BWS stepping whereas during 20% BWS stepping RF activation remained constant. Overall activation during 60% BWS stepping was much higher, especially during the transition from stance to swing phase compared to 20% BWS stepping (**Figure 7**). In participant 1 a large increase in VL activation was observed just before toe off and through swing phase in 60% BWS stepping, whereas during 20% BWS stepping, the VL activation decreased at mid swing phase. For participant 2, the RF activation remained constant through the transition from stance to swing in both 20% and 60% BWS stepping with activation higher during 60% BWS stepping. The VL activation increased prior to toe off and sharply decreased in swing phase, whereas in 20% BWS stepping VL activation decreased prior to toe off and remained decreased through swing phase. Overall, the activation of the RF and VL for both participants was greater during the transition from stance to swing phase during 60% BWS stepping compared to 20% BWS stepping, with the exception of the VL for participant 2. Changes between 20% and 60% BWS in the medial hamstring and distal muscles were minimal. Data can be viewed in the **Supplementary Material**.

DISCUSSION

During ES enabled BWST stepping in two participants with sensorimotor complete SCI, we demonstrate that descending intentional commands and afferent proprioceptive input result in varied modulation of the motor output identified through EMG and vGRF. Changes in stepping independence were described by the level of assistance perceived by the clinicians during BWST stepping, specifically during the transition from stance to swing. For both participants, optimal stepping performance requiring minimal trainer assistance was achieved when the participant was intentionally stepping (active stepping) and during trials when loaded with 80% of their body weight (20% BWS stepping). Conversely, when the participant was not intentionally stepping (passive stepping), or during trials when loaded with only 40% of their body weight (60% BWS stepping), the level of assistance increased during the transition from stance to swing. The increase in assistance was in response to an exaggerated lower extremity extension pattern demonstrated by a lack of lower extremity flexion necessary during the transition from stance to

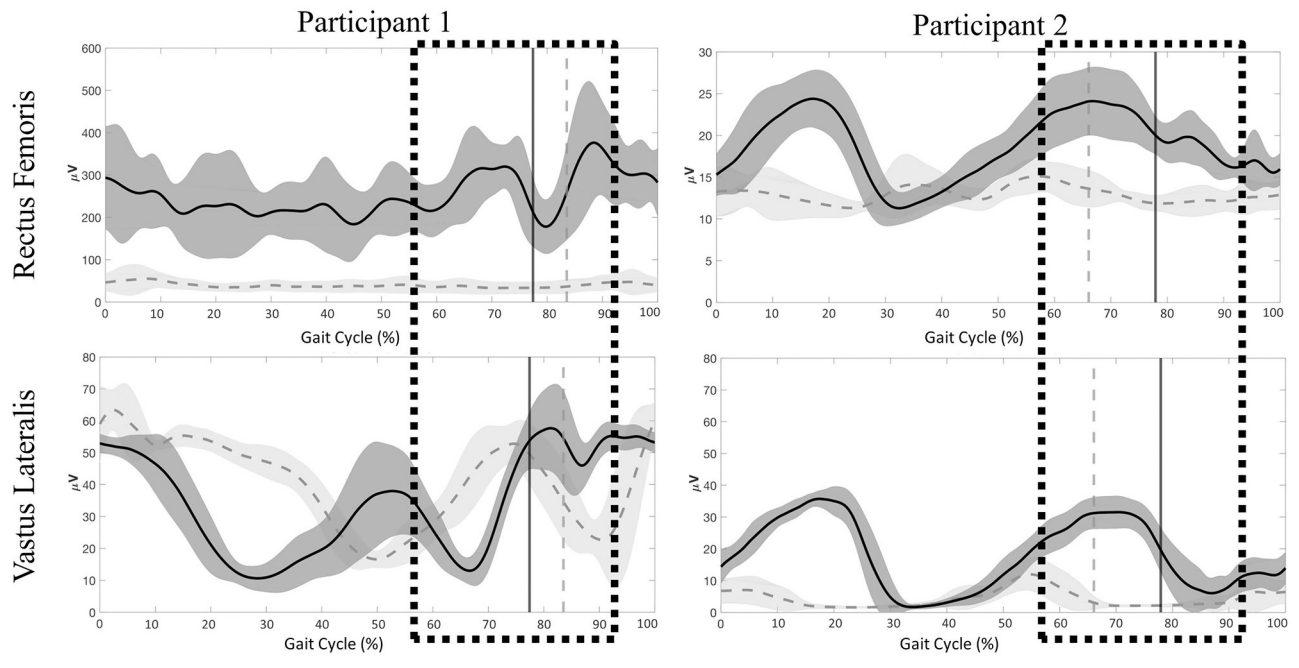

FIGURE 7 | Participant 1 (right limb) and participant (left limb), mean ± *SD* electromyography activation of the rectus femoris (RF) and vastus lateralis (VL) during 60% (dark gray) and 20% (light gray) BWS stepping conditions. Vertical lines represent transition from stance to swing for each respective condition. Boxes represent time during the gait cycle were clinicians perceived an increase in the level of assistance.

swing, likely caused by proximal extensor activation. In an effort to improve flexion of the lower extremity, substantial assistance from the clinician was needed at the posterior knee and the anterior ankle to facilitate swing phase.

Influence of Descending Intentional Commands

For individuals with discomplete SCI, such as the two participants enrolled in this clinical trial, intentional participation can facilitate residual descending supraspinal input and engage remaining non-functional pathways to spinal circuitry below the injury when ES is applied (Dimitrijevic, 1988; Sherwood et al., 1992). Previous experiments in animal models with completely transected spinal cords have indicated restoration of stepping function and modulation of motor outputs despite the absence of supraspinal input (Lavrov et al., 2006; Courtine et al., 2009; Brand et al., 2012; Gad et al., 2013). However, SCI in humans is rarely a complete transection, and therefore, study participants likely have some remaining descending supraspinal input (Calvert et al., 2019b). Previous studies with non-invasive stimulation have indicated augmentation of motor outputs with voluntary input in individuals with motor incomplete SCI (Gerasimenko et al., 2015; Hofstoetter et al., 2015). While intentional participation seems logical during rehabilitation sessions, some continuous activities, such as BWST stepping, can become mundane and extremely taxing for both the study participant and the assisting clinicians. The effect of intentional motor commands using ES in motor complete SCI has not been described to this detail. Describing clinician assist during a specific phase of gait allows clinical interpretation of stepping performance while determining insufficient portions of the gait cycle. Previously, regaining intentional control of the lower extremities during ES-enabled stepping was specifically observed in the flexor muscles during intentional stepping (Angeli et al., 2014), however, these initial studies failed to demonstrate independent ES-enabled stepping, whereas recent publications have detailed independence (Angeli et al., 2018; Gill et al., 2018; Wagner et al., 2018). Functional gait must incorporate lower extremity flexion and extension patterns to be successfully independent. Here, we are describing modulation of the lower extremity extensor muscles responding to the descending intentional command to allow flexion to occur purposefully and with greater independence.

ES-enabled passive stepping describes the lack of intent, which resulted in tonic motor activity in the proximal lower extremity extensors, mostly impacting the transition from stance to swing phase. Additionally, passive stepping resulted in an increase in clinician perceived level of assistance likely due to the sustained knee extensor activity during co-contraction of the RF and VL, which impaired lower extremity flexion necessary to initiate swing and resulted in a prolonged stance phase with toe drag for both participants. Interestingly, participant 2 demonstrated an increase in load (vGRF) through the lower extremities during the stance phase during active stepping when compared to passive stepping. Thus, utilization of the upper extremities to assist with weight shifting and posture support did not result in an unloading response. Overall, while ES parameters remain unchanged between conditions, tonic extension patterns emerged during passive stepping supporting the need for intent to facilitate necessary modulation of the lower extremity muscles to improve independence during ES enabled BWST stepping.

Influences of Afferent Proprioceptive Input

Afferent proprioceptive input during stepping has been shown to be critical to restore function in animal models of SCI (Lavrov et al., 2006). Additionally a meta-analysis of 54 studies of neurologically impaired and healthy human participants, investigating BWS adjustments and the effect on gait parameters including lower extremity motor activation, joint kinematics and kinetics, and vGRF, indicated afferent input had a strong influence on gait characteristics (Apte et al., 2018). The authors concluded that unloading (i.e., increasing BWS) of the lower extremities during BWST stepping reduced lower extremity motor activity; specifically, the mean activation of the lower extremity extensor muscles RF and SOL. Similar findings were reported by Harkema et al. (1997) with respect to motor output changes during alterations in loading as well as muscle-tendon stretches in the SCI population, which resulted in decreased motor activity of distal leg muscles, specifically the MG and the SOL, when unloading increased.

However, we report the opposite phenomenon, a decrease in motor output compared to an increase during supra-motor threshold ES-enabled BWST stepping with motor complete SCI individuals under conditions identified as ideal for promoting greater independence from clinician assist. Participant 1 exhibited increased motor activation of the RF muscles during stance at 60% BWS stepping compared to 20% BWS stepping and greater activation of the RF and VL during swing at 60% BWS stepping compared to 20% BWS stepping. Participant 2 experienced the same phenomenon in both the RF and VL, demonstrating greater motor activity during stance and swing under 60% BWS stepping conditions. Even when motor activity decreased during 20% BWS stepping, the level of assistance perceived by the clinician did not increase, implying the motor activation was sufficient to maintain knee extension for the load applied. Stepping with 20% BWS resulted in the greatest level of independence for both participants. Whereas, 60% BWS stepping resulted in greater clinician assistance during the transition from stance to swing transition phase due to the sustained activity of proximal knee extensor muscles. Demonstrated through vGRF, lower extremity loading was greater during 20% BWS stepping compared to 60% BWS stepping which is to be expected; however, during the transition from stance to swing, participant 2 had a considerably longer stance phase even with less loading through the limb. This exaggerated stance phase required an extreme increase in clinician assist, likely due to the amount of leg extension prohibiting flexion.

During ES-enabled BWST training, emphasis was placed on decreasing BWS while encouraging participants to use of their upper extremities, placed on rigid parallel bars, in order to maintain appropriate posture throughout their trunk and pelvis during stepping. More specifically, upper extremity use of the

parallel bars allowed manipulation of body positioning and weight shifting throughout the step cycle, such as facilitating hip and trunk extension in order to initiate stance and/or swing phases. We recognize that this compensatory strategy has the ability to impact lower extremity loading during stance, however, these changes in vGRF were not observed in the present study. Interestingly, we observed that use of the upper extremities may have positively impacted stepping independence by facilitating appropriate trunk and pelvic positioning, specifically during intent conditions. We surmise this observation may be due to changes in lower extremity and trunk afferent signaling such as kinematic muscle stretching at the hips. Likewise, in the absence of upper extremity-induced manipulation, specifically during the transition from stance to swing phase, the hip flexor muscles may have not received sufficient afferent input of a stretch, in turn, resulting in inadequate afferent signaling necessary to cue hip flexor activity.

Potential Strategies to Enhance Performance During ES-Enabled BWST Stepping

Based on the findings presented in this paper, we offer strategies to facilitate increased independence of performance for individuals with SCI during ES-enabled BWST stepping. ES-enabled BWST stepping performed in an environment that emphasizes intentional participant involvement, using real-time visual and verbal feedback regarding performance of stepping, enables greater independence. During training we recommend maximizing weight-bearing through the lower extremities by decreasing BWS as much as possible to promote convergence of the afferent proprioceptive input and descending intentional commands. Achieving optimal performance may require participants to compensate in other areas (e.g., use of arms on parallel bars) to allow afferent input from lower extremity loading and ES to converge facilitating adequate motor output necessary for stepping. Prior evidence generated in animal models of SCI (Gad et al., 2013; Wenger et al., 2014, 2016; Capogrosso et al., 2016; Islam et al., 2019; Chia et al., 2020), as well as in humans by our research team and others, indicates the importance that individualized ES parameters in order to enable intra-limb rhythmic motor activity of the lower extremities, and in turn restore stepping (Harkema et al., 2011b; Minassian et al., 2013; Hofstoetter et al., 2015; Grahn et al., 2017; Angeli et al., 2018; Gill et al., 2018; Wagner et al., 2018; Calvert et al., 2019a).

Limitations/Future Directions

Given the heterogeneity of severity of SCI, and limited sample size, we recognize that our results, along with previously reported literature, may not be generalizable to all individuals with SCI. A high degree of variability was seen between our two participants, signifying the necessity for further assessment of afferent proprioceptive input and descending intentional command changes across many individuals with various severities of SCI while using ES. Quantifying the clinician's level of assistance was subjective; however, utilizing quantitative measures to determine the level of assistance would add value to the interpretation of performance. Additional biomechanical assessments of BWST stepping would strengthen the understanding of motor coordination while a longitudinal comparison of EMG and vGRF may describe a training effect.

In conclusion, during ES-enabled BWST stepping participant intent and BWS modification can impact motor output, vGRF, as well as performance. ES-enabled motor activation facilitating independence of stepping requires input above and below the level of injury to facilitate modulation of specific muscle groups to improve performance, specifically during the transition from stance to swing during gait.

DATA AVAILABILITY STATEMENT

The raw data supporting the conclusions of this article will be made available by the authors, without undue reservation.

ETHICS STATEMENT

The studies involving human participants were reviewed and approved by Mayo Clinic IRB. The patients/participants provided their written informed consent to participate in this study. Written informed consent was obtained from the individual(s) for the publication of any potentially identifiable images or data included in this article.

AUTHOR CONTRIBUTIONS

MG, PG, DS, and KZ initiated the project. MG, PG, ML, and AT designed the experiments with contributions from all authors. LB, KG, MG, PG, IL, ML, and DV performed clinical assessments. LB, JC, MG, PG, ML, and DV designed and performed rehabilitation. LB, JC, MG, PG, ML, IL, and DV contributed to stimulation setting refinement. LB, JC, KF, MG, PG, RH, ML, CL, AT, DV, and KZ contributed to data collection, analysis, and interpretation. KF, MG, PG, RH, and ML drafted the manuscript with subsequent contribution from all authors. KZ supervised all aspects of the work. All authors contributed to the article and approved the submitted version.

FUNDING

This work was supported by The Grainger Foundation, Regenerative Medicine Minnesota, The Jack Jablonski Bel13ve in Miracles Foundation, Mayo Clinic Graduate School of Biomedical Sciences, Mayo Clinic Center for Regenerative Medicine, Mayo Clinic Rehabilitation Medicine Research Center, Mayo Clinic Transform the Practice, Minnesota Office of Higher Education's Spinal Cord Injury and Traumatic Brain Injury Research Grant, and Craig H. Neilsen Foundation.

KZ received funding from the Jack Jablonski Bel13ve in Miracles Foundation, Mayo Clinic Rehabilitation Medicine Research Center, Mayo Clinic Transform the Practice, and Craig H. Neilsen Foundation. Individual team members were also supported by Regenerative Medicine Minnesota, Mayo Clinic

Center for Regenerative Medicine and Mayo Clinic Graduate School of Biomedical Sciences.

ACKNOWLEDGMENTS

We thank the participants for their time, effort, and continuous feedback throughout the study. We also thank C. Blaha, J. Chen, B. Cloud, T. Gardner, D. Hare, Y. Li, K. Lee, A. Mendez, C. Mitrovich, A. Schmeling, T. Scrabeck, M. Shaft, C. Stoppel, J. Strommen, M. Van Straaten, B. Wessel, and L. Zoecklein, as well as the surgical team for their support during epidural electrical stimulation system implantation.

SUPPLEMENTARY MATERIAL

The Supplementary Material for this article can be found online at: https://www.frontiersin.org/articles/10.3389/fnsys.2020.590231/full#supplementary-material

REFERENCES

Angeli, C. A., Boakye, M., Morton, R. A., Vogt, J., Benton, K., Chen, Y., et al. (2018). Recovery of over-ground walking after chronic motor complete spinal cord injury. *N. Engl. J. Med.* 379, 1244–1250. doi: 10.1056/NEJMoa1803588

Angeli, C. A., Edgerton, V. R., Gerasimenko, Y. P., Harkema, S. J., and Way, A. F. (2014). Altering spinal cord excitability enables voluntary movements after chronic complete paralysis in humans. *Brain* 137, 1394–1409. doi: 10.1093/brain/awu038

Apte, S., Plooij, M., and Vallery, H. (2018). Influence of body weight unloading on human gait characteristics: a systematic review. *J. Neuroeng. Rehabil.* 15, 1–18. doi: 10.1186/s12984-018-0380-0

Arendt-nielsen, L. (1994). Power spectrum analysis of the rectified electromyogram during gait for normals and patients. *J. Electromyogr. Kinesiol.* 4, 105–115.

Barthélemy, D., Willerslev-Olsen, M., Lundell, H., Biering-Sørensen, F., and Nielsen, J. B. (2015). Assessment of transmission in specific descending pathways in relation to gait and balance following spinal cord injury. *Prog. Brain Res.* 218, 79–101. doi: 10.1016/bs.pbr.2014.12.012

Behrman, A. L., Ardolino, E. M., and Harkema, S. J. (2017). Activity-based therapy: from basic science to clinical application for recovery after spinal cord injury. *J. Neurol. Phys. Ther.* 41(Suppl.3), S39–S45. doi: 10.1097/npt.0000000000000184

Behrman, A. L., and Harkema, S. J. (2000). Spinal cord injury: a series of case studies. *Phys. Ther. Spinal Cord Inj. Spec. Ser.* 80, 688–700. doi: 10.1093/ptj/80.7.688

Beres-Jones, J. A., and Harkema, S. J. (2004). The human spinal cord interprets velocity-dependent afferent input during stepping. *Brain* 127, 2232–2246. doi: 10.1093/brain/awh252

Brand, Van Den R., Heutschi, J., Barraud, Q., Digiovanna, J., Bartholdi, K., Huerlimann, M., et al. (2012). Restoring voluntary control of locomotion after paralyzing spinal cord injury. *Science* 336, 1182–1185. doi: 10.1126/science.1217416

Burns, S., Biering-Sørensen, F., Donovan, W., Graves, D. E., Jha, A., Johansen, M., et al. (2012). International standards for neurological classification of spinal cord injury, revised 2011. *Top. Spinal Cord Inj. Rehabil.* 18, 85–99. doi: 10.1310/sci1801-85

Cai, L. L., Fong, A. J., Otoshi, C. K., Liang, Y., Burdick, J. W., Roy, R. R., et al. (2006). Implications of assist-as-needed robotic step training after a complete spinal cord injury on intrinsic strategies of motor learning. *J. Neurosci.* 26, 10564–10568. doi: 10.1523/JNEUROSCI.2266-06.2006

Calvert, J. S., Grahn, P. J., Strommen, J. A., Lavrov, I. A., Beck, L. A., Gill, M. L., et al. (2019a). Electrophysiological guidance of epidural electrode array implantation over the human lumbosacral spinal cord to enable motor function after chronic paralysis. *J. Neurotrauma* 36, 1451–1460. doi: 10.1089/neu.2018.5921

Calvert, J. S., Grahn, P. J., Zhao, K. D., and Lee, K. H. (2019b). Emergence of epidural electrical stimulation to facilitate sensorimotor network functionality after spinal cord injury. *Neuromodulation* 22, 244–252. doi: 10.1111/ner.12938

Capogrosso, M., Milekovic, T., Borton, D., Wagner, F., Moraud, E. M., Mignardot, J., et al. (2016). Spinal cord injury in primates. *Nature* 539, 284–288. doi: 10.1038/nature20118

Chia, R., Zhong, H., Vissel, B., Edgerton, V. R., and Gad, P. (2020). Novel activity detection algorithm to characterize spontaneous stepping during multimodal spinal neuromodulation after mid-thoracic spinal cord injury in rats. *Front. Syst. Neurosci.* 13:82. doi: 10.3389/fnsys.2019.00082

Courtine, G., Gerasimenko, Y., Van Den Brand, R., Yew, A., Musienko, P., Zhong, H., et al. (2009). Transformation of nonfunctional spinal circuits into functional states after the loss of brain input. *Nat. Neurosci.* 12, 1333–1342. doi: 10.1038/nn.2401

Danner, S. M., Hofstoetter, U. S., Freundl, B., Binder, H., Mayr, W., Rattay, F., et al. (2015). Human spinal locomotor control is based on flexibly organized burst generators. *Brain* 138, 577–588. doi: 10.1093/brain/awu372

Dietz, V., Colombo, G., Jensen, L., and Baumgartner, L. (1995). Locomotor capacity of spinal cord in paraplegic patients. *Ann. Neurol.* 37, 574–582. doi: 10.1002/ana.410370506

Dietz, V., Müller, R., and Colombo, G. (2002). Locomotor actiity in spinal man: significance of afferent input from joint and load receptors. *Brain* 125, 2626–2634. doi: 10.1093/brain/awf273

Dimitrijevic, M. R. (1988). Residual motor functions in spinal cord injury. *Adv. Neurol.* 47, 138–155.

Dimitrijevic, M. R., Gerasimenko, Y. P., Angeles, L., and Pinter, M. (1998). Evidence for a spinal central pattern generator in humans. *Ann. N. Y. Acad. Sci.* 16, 360–376.

Dobkin, B., Angeles, L., Requejo, P., Amigos, R. L., Edgerton, V., and Angeles, L. (1995). Modulation of locomotor-like EMG activity in subjects with complete and incomplete spinal cord injury. *J. Neuro Rehab.* 9, 183–190.

Dolbow, D. R., Gorgey, A. S., Recio, A. C., Stiens, S. A., Curry, A. C., Sadowsky, C. L., et al. (2015). Activity-based restorative therapies after spinal cord injury: inter-institutional conceptions and perceptions. *Aging Dis.* 6, 254–261. doi: 10.14336/AD.2014.1105

Edgerton, V. R., Courtine, G., Gerasimenko, Y. P., Lavrov, I., Ichiyama, R. M., Fong, A. J., et al. (2008). Training locomotor networks. *Brain Res. Rev.* 57, 241–254. doi: 10.1016/j.brainresrev.2007.09.002

Field-Fote, E. C., and Roach, K. E. (2011). Influence of a locomotor training approach on walking speed and distance in people with chronic spinal cord injury: a randomized clinical trial. *Phys. Ther.* 91, 48–60. doi: 10.2522/ptj.20090359

Forrest, G. F., Sisto, S., and Barbeau, H. (2008). Neuromotor and musculoskeletal responses to locomotor training for an individual with chronic motor complete AIS-B spinal cord injury. *J. Spinal Cord Med.* 31, 509–521. doi: 10.1080/10790268.2008.11753646

Gad, P., Lavrov, I., Shah, P., Zhong, H., Roy, R. R., Edgerton, V. R., et al. (2013). Neuromodulation of motor-evoked potentials during stepping in spinal rats. *J. Neurophysiol.* 110, 1311–1322. doi: 10.1152/jn.00169.2013

Galvez, J. A., Budovitch, A., Harkema, S. J., and Reinkensmeyer, D. J. (2011). Trainer variability during step training after spinal cord injury: Implications for robotic gait-training device design. *J. Rehab. Res. Dev.* 48, 147–160. doi: 10.1682/JRRD.2010.04.0067

Gerasimenko, Y. P., Lu, D. C., Modaber, M., Zdunowski, S., Gad, P., Sayenko, D. G., et al. (2015). Noninvasive reactivation of motor descending control after paralysis. *J. Neurotrauma* 32, 1968–1980. doi: 10.1089/neu.2015.4008

Gill, M. L., Grahn, P. J., Calvert, J. S., Linde, M. B., Lavrov, I. A., Strommen, J. A., et al. (2018). Neuromodulation of lumbosacral spinal networks enables independent stepping after complete paraplegia. *Nat. Med.* 24, 1677–1682. doi: 10.1038/s41591-018-0175-7

Grahn, P. J., Lavrov, I. A., Sayenko, D. G., Van Straaten, M. G., Gill, M. L., Strommen, J. A., et al. (2017). Enabling task-specific volitional motor functions via spinal cord neuromodulation in a human with paraplegia. *Mayo Clin. Proc.* 92, 544–554. doi: 10.1016/j.mayocp.2017.02.014

Harkema, S., Behrman, P. T., and Barbeau, H. (2011a). *Locomotor Training*. New York, NY: Oxford University Press. doi: 10.1093/acprof:oso/9780195342086.001.0001

Harkema, S., Gerasimenko, Y., Hodes, J., Burdick, J., Angeli, C., Chen, Y., et al. (2011b). Effect of epidural stimulation of the lumbosacral spinal cord on voluntary movement, standing, and assisted stepping after motor complete paraplegia: a case study. *Lancet* 377, 1938–1947. doi: 10.1016/S0140-6736(11)60547-3

Harkema, S. J., Hurley, S. L., Patel, U. K., Requejo, P. S., Dobkin, B. H., and Edgerton, V. R. (1997). Human lumbosacral spinal cord interprets loading during stepping. *J. Neurophysiol.* 77, 797–811. doi: 10.1152/jn.1997.77.2.797

Heintz, S., and Gutierrez-farewik, E. M. (2007). Static optimization of muscle forces during gait in comparison to EMG-to-force processing approach. *Gait Posture* 26, 279–288. doi: 10.1016/j.gaitpost.2006.09.074

Hofstoetter, U. S., Krenn, M., Danner, S. M., Hofer, C., Kern, H., McKay, W. B., et al. (2015). Augmentation of voluntary locomotor activity by transcutaneous spinal cord stimulation in motor-incomplete spinal cord-injured individuals. *Artif. Organs.* 39, E176–E186. doi: 10.1111/aor.12615

Huie, J. R., Morioka, K., Haefeli, J., and Ferguson, A. R. (2017). What is being trained? *How divergent forms of plasticity compete to shape locomotor recovery after spinal cord injury. J. Neurotrauma* 34, 1831–1840. doi: 10.1089/neu.2016.4562

Islam, R., Cuellar, C. A., Felmlee, B., Riccelli, T., Silvernail, J., Boschen, S. L., et al. (2019). Multifactorial motor behavior assessment for real-time evaluation of emerging therapeutics to treat neurologic impairments. *Sci. Rep.* 9:16503. doi: 10.1038/s41598-019-52806-1

Lavrov, I., Gerasimenko, Y. P., Ichiyama, R. M., Courtine, G., Zhong, H., Roy, R. R., et al. (2006). Plasticity of spinal cord reflexes after a complete transection in adult rats : relationship to stepping ability. *J. Neurol. Neurosurg. Psychiatry* 96, 1699–1710. doi: 10.1152/jn.00325.2006

Lerner, Z. F., Damiano, D. L., and Bulea, T. C. (2017). The effects of exoskeleton assisted knee extension on lower-extremity gait kinematics, kinetics, and muscle activity in children with cerebral palsy. *Sci. Rep.* 7:13512. doi: 10.1038/s41598-017-13554-2

Minassian, K., Jilge, B., Rattay, F., Pinter, M. M., Binder, H., Gerstenbrand, F., et al. (2004). Original article stepping-like movements in humans with complete spinal cord injury induced by epidural stimulation of the lumbar cord : electromyographic study of compound muscle action potentials. *Spinal Cord* 42, 401–416. doi: 10.1038/sj.sc.3101615

Minassian, K., Us, H., Sm, D., Mayr, W., Wb, M., and Tansey, K. (2013). Mechanisms of rhythm generation of the human lumbar spinal cord in response to tonic stimulation without and with step-related sensory feedback. *Biomed. Eng.* 58, 10–12. doi: 10.1515/bmt-2013-40

Olney, S. J., and Winter, D. (1985). Predictions of knee and ankle moments of force in walking from EMG and kinematic data. *J. Biomech.* 18, 9–20.

Petersen, T. H., Willerslev-Olsen, M., Conway, B. A., and Nielsen, J. B. (2012). The motor cortex drives the muscles during walking in human subjects. *J. Physiol.* 590, 2443–2452. doi: 10.1113/jphysiol.2012.227397

Rejc, E., Angeli, C., and Harkema, S. (2015). Effects of lumbosacral spinal cord epidural stimulation for standing after chronic complete paralysis in humans. *PLoS ONE* 10:e133998. doi: 10.1371/journal.pone.0133998

Rejc, E., Angeli, C. A., Atkinson, D., and Harkema, S. J. (2017). Motor recovery after activity-based training with spinal cord epidural stimulation in a chronic motor complete paraplegic. *Sci. Rep.* 7:13476. doi: 10.1038/s41598-017-14003-w

Sayenko, D. G., Angeli, C., Harkema, S. J., Reggie Edgerton, V., and Gerasimenko, Y. P. (2014). Neuromodulation of evoked muscle potentials induced by epidural spinal-cord stimulation in paralyzed individuals. *J. Neurophysiol.* 111, 1088–1099. doi: 10.1152/jn.00489.2013

Scivoletto, G., Tamburella, F., Laurenza, L., Torre, M., and Molinari, M. (2014). Who is going to walk? *A review of the factors influencing walking recovery after spinal cord injury. Front. Hum. Neurosci.* 8:141. doi: 10.3389/fnhum.2014.00141

Sherwood, A. M., Dimitrijevic, M. R., and McKay, W. B. (1992). Evidence of subclinical brain influence in clinically complete spinal cord injury : discomplete SCI. *J. Neurol. Sci.* 110, 90–98.

Thomas, S. L., Gorassini, M. A., Sarah, L., and Gorassini, M. A. (2005). Increases in corticospinal tract function by treadmill training after incomplete spinal cord injury before after. *J. Neurophysiol.* 94, 2844–2855. doi: 10.1152/jn.00532.2005

Wagner, F. B., Mignardot, J. B., Le Goff-Mignardot, C. G., Demesmaeker, R., Komi, S., Capogrosso, M., et al. (2018). Targeted neurotechnology restores walking in humans with spinal cord injury. *Nature* 563, 65–71. doi: 10.1038/s41586-018-0649-2

Wenger, N., Moraud, E. M., Gandar, J., Musienko, P., Capogrosso, M., Baud, L., et al. (2016). Articles spatiotemporal neuromodulation therapies engaging muscle synergies improve motor control after spinal cord injury. *Nat. Med.* 22, 5–7. doi: 10.1038/nm.4025

Wenger, N., Moraud, E. M., Raspopovic, S., Bonizzato, M., Digiovanna, J., Musienko, P., et al. (2014). Closed-loop neuromodulation of spinal sensorimotor circuits controls refined locomotion after complete spinal cord injury. *Sci. Transl. Med.* 6:255ra133. doi: 10.1126/scitranslmed.3008325

Winchester, P., Mccoll, R., Querry, R., Foreman, N., Mosby, J., Tansey, K., et al. (2005). Changes in supraspinal activation patterns following robotic locomotor therapy in motor-incomplete spinal cord injury. *Neurorehabil. Neural Repair.* 19, 313–324. doi: 10.1177/1545968305281515

Winstein, C., Pohl, P., and Lewthwaite, R. (1994). Effects of physical guidance and knowledge of results on motor learning: support for the guidance hypothesis. *Res. Q. Exerc. Sport* 65, 316–323. doi: 10.1080/02701367.1994.10607635

Wirz, M., Colombo, G., and Dietz, V. (2001). Long term effects of locomotor training in spinal humans. *J. Neurol. Neurosurg. Psychiatry* 71, 93–96. doi: 10.1136/jnnp.71.1.93

Conflict of Interest: The authors declare that the research was conducted in the absence of any commercial or financial relationships that could be construed as a potential conflict of interest.

frontiers in Neuroscience

HYPOTHESIS AND THEORY
published: 12 April 2021
doi: 10.3389/fnins.2021.643463

Engaging Spinal Networks to Mitigate Supraspinal Dysfunction After CP

V. Reggie Edgerton[1,2,3,4], *Susan Hastings*[5] *and Parag N. Gad*[1,6,7]*

[1] Department of Neurobiology, University of California, Los Angeles, Los Angeles, CA, United States, [2] Department of Neurosurgery, University of California, Los Angeles, Los Angeles, CA, United States, [3] Brain Research Institute, University of California, Los Angeles, Los Angeles, CA, United States, [4] Institut Guttmann, Hospital de Neurorehabilitació, Institut Universitari Adscrit a la Universitat Autònoma de Barcelona, Barcelona, Spain, [5] SH Pediatric Physical Therapy, San Jose, CA, United States, [6] Rancho Research Institute, Downey, CA, United States, [7] SpineX, Inc., Los Angeles, CA, United States

Although children with cerebral palsy seem to have the neural networks necessary to generate most movements, they are markedly dysfunctional, largely attributable to abnormal patterns of muscle activation, often characterized as spasticity, largely reflecting a functionally abnormal spinal-supraspinal connectivity. While it is generally assumed that the etiologies of the disruptive functions associated with cerebral palsy can be attributed primarily to supraspinal networks, we propose that the more normal connectivity that persists between peripheral proprioception-cutaneous input to the spinal networks can be used to guide the reorganization of a more normal spinal-supraspinal connectivity. The level of plasticity necessary to achieve the required reorganization within and among different neural networks can be achieved with a combination of spinal neuromodulation and specific activity-dependent mechanisms. By engaging these two concepts, we hypothesize that bidirectional reorganization of proprioception-spinal cord-brain connectivity to higher levels of functionality can be achieved without invasive surgery.

Keywords: cerebral palsy, spinal cord, brain, muscle, EMG

OPEN ACCESS

Edited by:
Enrico Rejc,
University of Louisville, United States

Reviewed by:
Lynn Bar-On,
Amsterdam University Medical Center, Netherlands
Andrew Gordon,
Columbia University, United States

***Correspondence:**
Parag N. Gad
paraggad@ucla.edu

Specialty section:
This article was submitted to Autonomic Neuroscience, a section of the journal Frontiers in Neuroscience

Received: *18 December 2020*
Accepted: *22 March 2021*
Published: *12 April 2021*

Citation:
Edgerton VR, Hastings S and Gad PN (2021) Engaging Spinal Networks to Mitigate Supraspinal Dysfunction After CP. Front. Neurosci. 15:643463. doi: 10.3389/fnins.2021.643463

THE PROBLEM

It is generally assumed that the primary pathology of the nervous system that leads to cerebral palsy (CP) is located within and among different combinations of supraspinal networks and these pathologies can be due to multiple etiologies. In most cases, however, it appears that these supraspinally occurring pathologies also will be necessarily manifested as spinally mediated dysfunctions, affecting multiple peripheral sensory-motor systems involving equilibrium posture, locomotion, and trunk and head control (Smith and Gorassini, 2018). Although a high level of functionally immature connections are normally formed early in development, the pruning of neurons and synaptic connections occur subsequently using multiple, largely unknown, guidance mechanisms that result in the more effective connections between spinal networks and descending axons and proprioceptive afferents. But, if functionally immature or abnormal connections persist at the end of the early developmental phase, the supraspinal and propriospinal connectivity will result in abnormal sensory-motor responses. Persistence of these functionally abnormal synaptic connections are reinforced postnatally throughout the critical period of development and into adulthood, resulting in the commonly recognized

neuromuscular disorders associated with CP, with the most common symptoms being collectively diagnosed as neuromuscular spasticity and stiffness of joints. More specifically, however, there is a persistent pervasiveness of poor coordination of the motor pools. Given the concept of coordination is so central to our basic hypothesis, it is important that the meaning of this concept be clearly defined. Often, a coordinated movement is one in which there is reciprocity of the dynamics of the temporal patterns of activation and deactivation of flexor and extensor motor pools that generate the movement. "Normal" movements, however, are generated with a continuum of differing degrees of overlap and changes in levels of activation and deactivation. It is useful to be aware that the motor task that is being generated is defined largely by the temporal patterns of activation of motor pools. For example, many of the same muscles are activated when stepping forward, backward and sideways, but the patterns of muscles activated differ substantially (Shah et al., 2012). The degree of reciprocity vs. co-activation varies considerably among the uninjured general population. In individuals with symptoms of spasticity, there is an unusually greater coincidence of co-contractions of flexor and extensor motor pools movements that would be considered poorly coordinated. Theoretically, the greater the number of connections that develop between the brain and spinal cord that are functionally aberrant, the fewer normal targets that remain accessible (Bennett et al., 1983; Callaway et al., 1989; Alexeeva et al., 1997; Maegele et al., 2002). A fundamental and essential driver in the biological design of our nervous systems, phylogenetically, ontogenetically and epigenetically in reaching the normal targets undoubtedly has been earth's gravitational vectors (Edgerton et al., 2000). We reason that this fundamental feature in the strategy of our sensory-motor design highlighted here is that the difficulty in accommodating gravity is consistently and pervasively revealed in individuals with CP, as children and in adults. So many of their sensory-motor challenges are linked to maintaining equilibrium while moving effectively in a 1G environment (Recktenwald et al., 1999). It is clearly evident in the motor behaviors of individuals with CP that the neural connectivity did not develop appropriately for this uniformly present fundamental gravitational challenge. For the reasons noted above our interventional strategy as presented has been focused functionally on the necessity of realigning the sensory-motor connectivity to accommodate to normal gravitational vectors. Theoretically, to regain a normal supraspinal-spinal connectivity to earth's gravitational forces, the earlier maladaptive state that was learned postnatally to sustain equilibrium while in an abnormal state, must be re-transformed to achieve a normal translation of sensory input in a 1G environment (Smith and Gorassini, 2018; Cappellini et al., 2020).

SOLUTION

Given our experience with spinal cord injury (Gerasimenko Y. et al., 2015; Reggie et al., 2018), which has similar, and in some ways more severe functional aberrations than in CP, we developed interventions designed to transform functionally aberrant brain-spinal connections to a greater prominence of functionally normal connections. We reasoned that we could do this by maximizing the dominance of proprioception and the spinal networks that translate this sensory input and minimizing the pathology of the brain, in controlling posture and locomotion. Cappellini et al. (2016, 2020) noted how much the dysfunction of gait in children with CP can be related to spinal neuronal networks vs. supraspinal dysfunction. A more thorough knowledge about pattern generation circuitries in infancy may improve our understanding of developmental motor disorders, highlighting the necessity for regulating the functional properties of abnormally developed neuronal locomotor networks as a target for early sensorimotor rehabilitation. Similarly a very tight link was described between the activity patterns of populations of pyramidal tract neurons and the biomechanics of unconstrained locomotion in cats (Prilutsky et al., 2005). Versteeg et al. (2021) reported that cuneate nucleus neurons have muscle-like properties that have a greater sensitivity to active than passive movements of the upper limb and that their receptive fields resemble single muscles. These observations suggest that muscle specific signals proprioceptive input could have an activity-dependent impact on supraspinal networks that could transform dysfunctional neural networks to a more functional state. There is extensive evidence that the neural networks of an individual with CP can learn more effective movement skills as it does after spinal injury (Dewar et al., 2015; Morgan et al., 2015; Reid et al., 2015). Thus, we hypothesize that spinal neuromodulation in concert with proprioceptive-driven activity-dependent mechanisms of spinal networks can transform the supraspinal-spinal dysfunctional connectivity of CP into highly functional connections, improving the functionality of networks. The result should be the recovery of motor tasks that are more forceful, powerful, efficient and display finer control as needed in a 1G environment. This hypothesis is counter to the predominant thinking that all of the "motor" functions, noted above are controlled largely by the brain, rather than the spinal cord. Ironically, proprioception is considered to be a major contributor to the spasticity in CP, and, therefore, is a primary target to reduce the tonic stiffness by performing selective dorsal root rhizotomy (Mortenson et al., 2021). However, selective rhizotomy minimizes the sensor input, which normally plays a prominent role in controlling movements and can disrupt autonomic functions.

Multiple clues led us to the logic applying a specialized neuromodulatory technique in combination with subject specific activity-dependent rehabilitation. First, our studies, and that of many other labs for decades clearly tell us that proprioception plays a more important role than occasionally correcting mistakes, as in tripping, when there is not enough time to adjust the planned movements (Gerasimenko et al., 2017). Proprioception plays a central role in the details of controlling posture, locomotion, and fine motor tasks, even when there is no connectivity between the spinal networks and the brain (Grillner and Zangger, 1975; de Leon et al., 1999). Some specific observations suggesting a possible crucial role for spinal networks in individuals with CP to facilitate functional recovery are: (1) After a complete, mid-thoracic spinal transection a mammal can step forward, backward or sideways and at speeds appropriate

to the speed of the treadmill belt. (2) Humans that have lost proprioception as an adult are essentially, functionally paralyzed, at least for months, even though all descending motor pathways remain intact. (3) Given that spinal networks can readily learn to perform a new motor task without help from the brain, we reasoned that the potential level of plasticity among spinal and supraspinal networks in the presence of spinal neuromodulation combined with skilled therapy can be robust enough to supplant the original supraspinal disruptive connectivity and reinforce more normal functional connections with a greater presence of normal sensory input associated with routine motor tasks via activity-dependent mechanisms. (4) Another clue, suggests that much of the aberrant connectivity is inextricably linked to skills associated with equilibrium, i.e., with gravity being of a constant presence in the evolution of all life on Earth (Wallard et al., 2014, 2018). It seems obvious that the network connectivity design of sensory motor functions that has evolved phylogenetically, has specifically accommodated to earth's gravity, and that there are numerous motor dysfunctions that reflect that this feature was not carried out normally, either ontogenetically or epigenetically in many CP cases. And finally, and (5) could the fact that CP being a developmental phenomenon be an advantage in using interventional strategies to take advantage of higher levels of neuroplasticity during the critical period of development of motor primitives as suggested by Bizzi and colleagues (Overduin et al., 2015) and hypothesized by Edelman (1993) as Neural Darwinism and Neuronal Group Selection, presumably of the brain, and Edgerton and colleagues as a similar phenomenon in the spinal cord (Edgerton et al., 2001).

TESTING THE HYPOTHESIS

While the biological bases of the underlying concepts may seem sound, there has not, however, been a single systems-level concept relevant to the etiology of CP as we have proposed. Technically it is now feasible to induce systems level changes in specific functional connectivity of networks patterns of sensory input that translates to a predictable motor output by repetitively activating specific proprioception patterns as occurs during stand training that enables standing ability but not stepping ability (de Leon et al., 1999), facilitates changes at the level of synapses and neural networks and changes the expression of genes that could mediate the synaptic adaptations to locomotor training after a spinal hemisection. More comprehensive, quantitative assays under clinically controlled conditions on a limited population of subjects could be performed with present-day technologies. Clear evidence of the validity of the proposed mechanisms at a systems level of understanding seems to be not only feasible with proper resources, but in addition a case can be made for the urgency of such an effort based on it's potential efficacy and safety as demonstrated from more than a decade of studies of human subjects with a similar non-invasive interventional strategy in recovering functions after SCI (Gerasimenko Y. P. et al., 2015; Rath et al., 2018; Sayenko et al., 2018; Gad et al., 2020; Kreydin et al., 2020).

Figure 1 illustrates the experimental outcomes that we hypothesize can be obtained with a patient with CP. We hypothesize that applying a combination of non-invasive spinal neuromodulation and specific activity-dependent mechanisms to an individual with CP can trigger a bidirectional reorganization of proprioception-spinal cord-brain connectivity to a functional state that can generate near normal postural and locomotor functions. An individual free of abnormalities are continuously signaling sensory-motor information bi-directionally between the brain and spinal cord and the kinetic and kinematic sensors (proprioception) in muscle, tendons, and skin (**Figure 1A**). CP is generally considered to be a cerebral pathology (**Figure 1B**) which will send abnormal motor signals due to the spinal networks which in turn will project abnormal signals to predominately flexor or extensor motor pools and muscles. As opposed to the spinal networks generating a highly coordinated agonist-antagonist pattern (**Figure 1A**), the disruptive, aberrant, descending commands from the brain generates abnormal levels of co-contraction signals among the spinal interneuronal networks that induces high levels of co-contractions of flexors and extensor muscles. The first key point here is that the disruptive signals from the brain, then spinal, then muscular, results in abnormal proprioceptive signal to the spinal networks which we now know sends muscle specific signals to multiple supraspinal nuclei. Thus, basically a continuous loop of abnormal signals imposes persistent abnormal sensory-motor signals that results in a reorganization of networks that reflect the initial supraspinal pathology. Fortunately, there is reason to predict that there are several key points that can be used to interrupt the abnormal sensory-motor loop to a much greater level of normality. These points are: (1) The disruptive spinal networks can be transformed to a more normal physiological state with newly developed electrical neuromodulation combined with activity-dependent modulation via a near normal pattern of proprioceptive ensembles project to the spinal networks. (2) Proprioceptive input has the potential to overcome the disruptive descending input and reorganize the connectivity into a state that generates coordinated movements. And, (3) There is strong evidence that a similar normalizing process can occur in the more normal ascending input to supraspinal centers can then form more normal networks in the descending motor signals. Experiments in which CP patients attempt to perform motor task in the presence and absence of neuromodulation while recording supraspinal and spinally evoked potentials and recording EMG activities of different combinations of muscles and kinematics and kinetics to characterize the motor task will provide the data that can determine whether the proposed hypothesis should be accepted, at least from a functional, systems level.

DISCLOSURE

VE holds shareholder interest in NeuroRecovery Technologies and hold certain inventorship rights on intellectual property licensed by the Regents of the University of California to NeuroRecovery Technologies and its subsidiaries. VE and PG

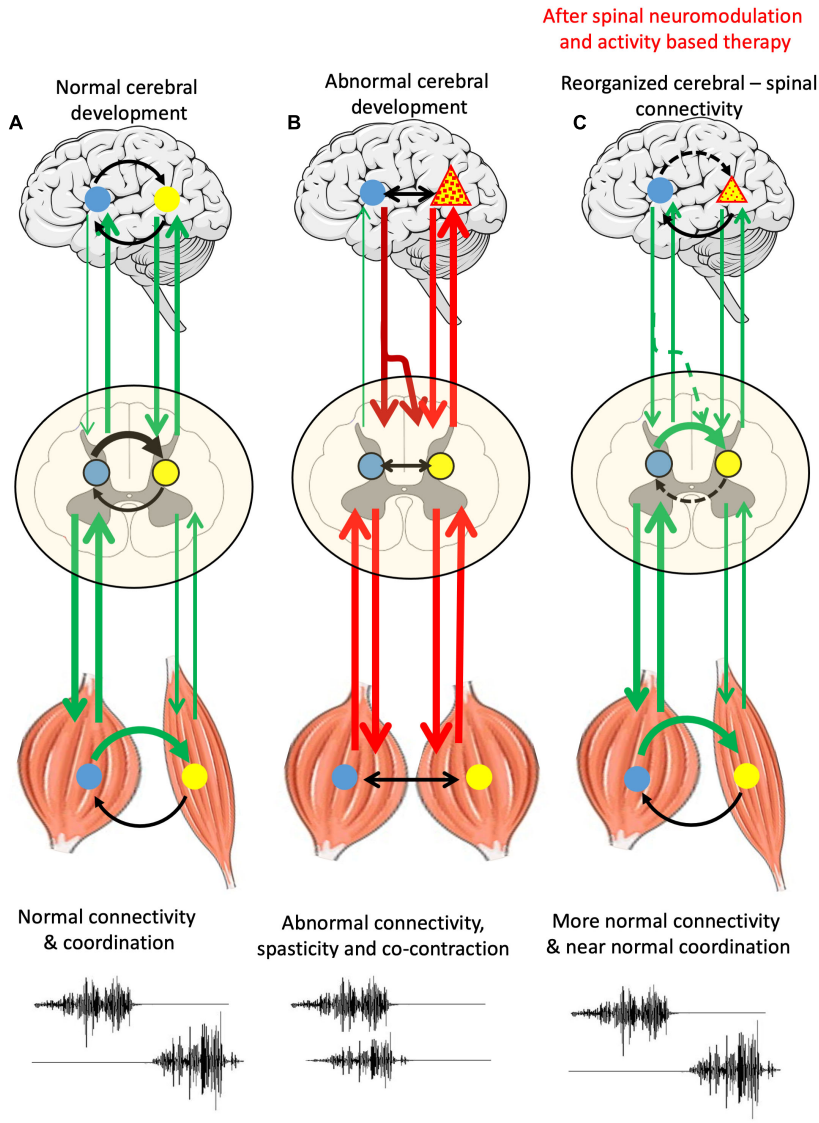

FIGURE 1 | Schematic representation of supraspinal-spinal-muscle connectivity in normal cerebral development, abnormal cerebral development and in abnormal cerebral development after spinal neuromodulation and activity-based therapy **(A)** normal brain-spinal networks and muscles with sensors, bidirectionally communicating input and output signals forming a complete loop, including reciprocal EMG of agonist and antagonist muscles, see two channels at the bottom. **(B)** A region of supraspinal pathology (triangle) resulting in aberrant descending signals causing disruptive degrees of co-contractions of flexor and extensor motor pools and muscles. **(C)** A remodeling process can of supraspinal and spinal networks can begin with a combination of a non-invasive electrical neuromodulation technique that empowers the spinal networks to begin to assume a dominating control of normalizing the coordination of flexor and extensor motor pools. With repetitive practice in the presence of neuromodulation, we propose that there will be significant reorganization toward a gradually occurring normalization of supraspinal and spinal networks.

holds shareholder interest in SpineX, Inc. and hold certain inventorship rights on intellectual property licensed by the Regents of the University of California to SpineX, Inc.

DATA AVAILABILITY STATEMENT

The original contributions presented in the study are included in the article/supplementary material, further inquiries can be directed to the corresponding author.

AUTHOR CONTRIBUTIONS

All authors listed have made a substantial, direct and intellectual contribution to the work, and approved it for publication.

FUNDING

The authors declare that this study received funding from by Walkabout Foundation, Dana & Albert R. Broccoli

Charitable Foundation and Nanette, Burt Forester, including matching by PwC LLP, Roberta Wilson, BEL13VE in Miracles Jack Jablonski Foundation, Brain Recovery Project, and The West Coast Consortium for Technology & Innovation in Pediatrics (CTIP). The funders were not involved in the study design, collection, analysis, interpretation of data, the writing of this article, or the decision to submit it for publication.

REFERENCES

Alexeeva, N., Broton, J. G., Suys, S., and Calancie, B. (1997). Central cord syndrome of cervical spinal cord injury: widespread changes in muscle recruitment studied by voluntary contractions and transcranial magnetic stimulation. *Exp. Neurol.* 148, 399–406. doi: 10.1006/exnr.1997.6689

Bennett, M. R., McGrath, P. A., Davey, D. F., and Hutchinson, I. (1983). Death of motorneurons during the postnatal loss of polyneuronal innervation of rat muscles. *J. Comp. Neurol.* 218, 351–363. doi: 10.1002/cne.902180311

Callaway, E. M., Soha, J. M., and Van Essen, D. C. (1989). Differential loss of neuromuscular connections according to activity level and spinal position of neonatal rabbit soleus motor neurons. *J. Neurosci.* 9, 1806–1824. doi: 10.1523/jneurosci.09-05-01806.1989

Cappellini, G., Ivanenko, Y. P., Martino, G., MacLellan, M. J., Sacco, A., Morelli, D., et al. (2016). Immature Spinal Locomotor Output in Children with Cerebral Palsy. *Front. Physiol.* 7:478. doi: 10.3389/fphys.2016.00478

Cappellini, G., Sylos-Labini, F., Dewolf, A. H., Solopova, I. A., Morelli, D., Lacquaniti, F., et al. (2020). Maturation of the Locomotor Circuitry in Children With Cerebral Palsy. *Front. Bioeng. Biotechnol.* 8:998. doi: 10.3389/fbioe.2020.00998

de Leon, R. D., Tamaki, H., Hodgson, J. A., Roy, R. R., and Edgerton, V. R. (1999). Hindlimb locomotor and postural training modulates glycinergic inhibition in the spinal cord of the adult spinal cat. *J. Neurophysiol.* 82, 359–369. doi: 10.1152/jn.1999.82.1.359

Dewar, R., Love, S., and Johnston, L. M. (2015). Exercise interventions improve postural control in children with cerebral palsy: a systematic review. *Dev. Med. Child Neurol.* 57, 504–520. doi: 10.1111/dmcn.12660

Edelman, G. M. (1993). Neural Darwinism: selection and reentrant signaling in higher brain function. *Neuron* 10, 115–125. doi: 10.1016/0896-6273(93)90304-a

Edgerton, V. R., Roy, R. R., and De Leon, R. D (2001). "Neural Darwinism in the mammalian spinal cord," in *Spinal Cord Plasticity: Alterations in Reflex Function*, eds M. M. Patterson and J. W. Graw (Boston: Kluwer Academic), 185–206. doi: 10.1007/978-1-4615-1437-4_8

Edgerton, V. R., Roy, R. R., Hodgson, J. A., Day, M. K., Weiss, J., Harkema, S. J., et al. (2000). How the science and engineering of spaceflight contribute to understanding the plasticity of spinal cord injury. *Acta Astronaut.* 47, 51–62. doi: 10.1016/s0094-5765(00)00009-6

Gad, P., Kreydin, E., Zhong, H., and Edgerton, V. R. (2020). Enabling respiratory control after severe chronic tetraplegia: an exploratory case study. *J. Neurophysiol.* 124, 774–780. doi: 10.1152/jn.00320.2020

Gerasimenko, Y., Gorodnichev, R., Moshonkina, T., Sayenko, D., Gad, P., and Reggie Edgerton, V. (2015). Transcutaneous electrical spinal-cord stimulation in humans. *Ann. Phys. Rehabil. Med.* 58, 225–231. doi: 10.1016/j.rehab.2015.05.003

Gerasimenko, Y. P., Lu, D. C., Modaber, M., Zdunowski, S., Gad, P., Sayenko, D. G., et al. (2015). Noninvasive Reactivation of Motor Descending Control after Paralysis. *J. Neurotrauma* 32, 1968–1980. doi: 10.1089/neu.2015.4008

Gerasimenko, Y., Sayenko, D., Gad, P., Liu, C. T., Tillakaratne, N. J. K., Roy, R. R., et al. (2017). Feed-Forwardness of Spinal Networks in Posture and Locomotion. *Neuroscientist* 23, 441–453. doi: 10.1177/1073858416683681

Grillner, S., and Zangger, P. (1975). How detailed is the central pattern generation for locomotion? *Brain Res.* 88, 367–371. doi: 10.1016/0006-8993(75)90401-1

Kreydin, E., Zhong, H., Latack, K., Ye, S., Edgerton, V. R., and Gad, P. (2020). Transcutaneous Electrical Spinal Cord Neuromodulator (TESCoN) Improves Symptoms of Overactive Bladder. *Front. Syst. Neurosci.* 14:1. doi: 10.3389/fnsys.2020.00001

Maegele, M., Muller, S., Wernig, A., Edgerton, V. R., and Harkema, S. J. (2002). Recruitment of spinal motor pools during voluntary movements versus stepping after human spinal cord injury. *J. Neurotrauma* 19, 1217–1229. doi: 10.1089/08977150260338010

Morgan, C., Novak, I., Dale, R. C., and Badawi, N. (2015). Optimising motor learning in infants at high risk of cerebral palsy: a pilot study. *BMC Pediatr.* 15:30. doi: 10.1186/s12887-015-0347-2

Mortenson, P., Sadashiva, N., Tamber, M. S., and Steinbok, P. (2021). Long-term upper extremity performance in children with cerebral palsy following selective dorsal rhizotomy. *Childs Nerv. Syst.* doi: 10.1007/s00381-020-05018-2 [Epub ahead of print].

Overduin, S. A., d'Avella, A., Roh, J., Carmena, J. M., and Bizzi, E. (2015). Representation of Muscle Synergies in the Primate Brain. *J. Neurosci.* 35, 12615–12624. doi: 10.1523/jneurosci.4302-14.2015

Prilutsky, B. I., Sirota, M. G., Gregor, R. J., and Beloozerova, I. N. (2005). Quantification of motor cortex activity and full-body biomechanics during unconstrained locomotion. *J. Neurophysiol.* 94, 2959–2969. doi: 10.1152/jn.00704.2004

Rath, M., Vette, A. H., Ramasubramaniam, S., Li, K., Burdick, J., Edgerton, V. R., et al. (2018). Trunk Stability Enabled by Noninvasive Spinal Electrical Stimulation after Spinal Cord Injury. *J. Nneurotrauma* 35, 2540–2553. doi: 10.1089/neu.2017.5584

Recktenwald, M. R., Hodgson, J. A., Roy, R. R., Riazanski, S., McCall, G. E., Kozlovskaya, I., et al. (1999). Effects of spaceflight on rhesus quadrupedal locomotion after return to 1G. *J. Neurophysiol.* 81, 2451–2463. doi: 10.1152/jn.1999.81.5.2451

Reggie, E. V., Yury, G., Parag, G., and Dimitry, S. (2018). Basic concepts underlying activity-dependent mechanisms in the rehabilitation of sensory-motor function after spinal cord injury. *Spinal Cord Med.* 54, 897–911.

Reid, L. B., Rose, S. E., and Boyd, R. N. (2015). Rehabilitation and neuroplasticity in children with unilateral cerebral palsy. *Nat. Rev. Neurol.* 11, 390–400. doi: 10.1038/nrneurol.2015.97

Sayenko, D. G., Rath, M., Ferguson, A. R., Burdick, J., Havton, L. A., Edgerton, V. R. et al. (2018). Self-assisted standing enabled by non-invasive spinal stimulation after spinal cord injury. *J. Neurotrauma.* 36, 1435–1450. doi: 10.1089/neu.2018.5956

Shah, P. K., Gerasimenko, Y., Shyu, A., Lavrov, I., Zhong, H., Roy, R. R., et al. (2012). Variability in step training enhances locomotor recovery after a spinal cord injury. *Eur. J. Neurosci.* 36, 2054–2062. doi: 10.1111/j.1460-9568.2012.08106.x

Smith, A. T., and Gorassini, M. A. (2018). Hyperexcitability of brain stem pathways in cerebral palsy. *J. Neurophysiol.* 120, 1428–1437. doi: 10.1152/jn.00185.2018

Versteeg, C., Chowdhury, R. H., and Miller, L. E. (2021). Cuneate nucleus: The somatosensory gateway to the brain. *Curr. Opin. Physiol.* 20, 206–215. doi: 10.1016/j.cophys.2021.02.004

Wallard, L., Dietrich, G., Kerlirzin, Y., and Bredin, J. (2014). Balance control in gait children with cerebral palsy. *Gait Posture* 40, 43–47. doi: 10.1016/j.gaitpost.2014.02.009

Wallard, L., Dietrich, G., Kerlirzin, Y., and Bredin, J. (2018). Effect of robotic-assisted gait rehabilitation on dynamic equilibrium control in the gait of children with cerebral palsy. *Gait Posture* 60, 55–60. doi: 10.1016/j.gaitpost.2017.11.007

Conflict of Interest: PG was employed by SpineX. SH was employed by Susan Hastings Pediatric Clinic.

The remaining author declares that the research was conducted in the absence of any commercial or financial relationships that could be construed as a potential conflict of interest.

Advantages of publishing in Frontiers

OPEN ACCESS
Articles are free to read for greatest visibility and readership

FAST PUBLICATION
Around 90 days from submission to decision

HIGH QUALITY PEER-REVIEW
Rigorous, collaborative, and constructive peer-review

TRANSPARENT PEER-REVIEW
Editors and reviewers acknowledged by name on published articles

Frontiers
Avenue du Tribunal-Fédéral 34
1005 Lausanne | Switzerland

Visit us: www.frontiersin.org
Contact us: frontiersin.org/about/contact

REPRODUCIBILITY OF RESEARCH
Support open data and methods to enhance research reproducibility

DIGITAL PUBLISHING
Articles designed for optimal readership across devices

FOLLOW US
@frontiersin

IMPACT METRICS
Advanced article metrics track visibility across digital media

EXTENSIVE PROMOTION
Marketing and promotion of impactful research

LOOP RESEARCH NETWORK
Our network increases your article's readership